



A University of Sussex PhD thesis

Available online via Sussex Research Online:

<http://sro.sussex.ac.uk/>

This thesis is protected by copyright which belongs to the author.

This thesis cannot be reproduced or quoted extensively from without first obtaining permission in writing from the Author

The content must not be changed in any way or sold commercially in any format or medium without the formal permission of the Author

When referring to this work, full bibliographic details including the author, title, awarding institution and date of the thesis must be given

Please visit Sussex Research Online for more information and further details

Defining the antigenic requirements for pan-lyssavirus neutralisation

Thesis submitted for the degree of
Doctor of Philosophy

Rebecca Ellen Shipley
B.Sc. (Hons)
September 2021



**UNIVERSITY
OF SUSSEX**

School of Life Sciences

University of Sussex



**Animal &
Plant Health
Agency**

Wildlife Zoonoses and Vector-Borne Diseases Research Group

Animal and Plant Health Agency

Thesis Summary

Rabies, the first zoonotic disease associated with bats, remains one of the most feared viruses known to man and causes approximately 59,000 deaths a year. With no medical intervention prior to symptom onset, rabies-induced encephalitis is invariably fatal. Alongside rabies virus, numerous related lyssaviruses exist. Also capable of causing fatal disease, these lyssaviruses pose a threat to human and animal health.

Since 2000, the genus has grown from eight fully characterised species to seventeen fully characterised species and two tentative species. These viruses are genetically and antigenically categorised into phylogroups according to the predicted level of vaccine protection, with protection from current vaccines and therapeutics afforded against phylogroup I but not II or III. The continued discovery of novel lyssaviruses globally, warrants an in-depth assessment of the cross-protection of current vaccines and the protective titre required, to inform occupationally high-risk groups (e.g., scientists, bat workers and speleologists).

Current evidence suggests that for a protective neutralising antibody response against rabies virus, a neutralising antibody titre of 0.5 IU/ml is sufficient. However, studies using cross protection assays have suggested that for protection against viruses in phylogroup I, 10-fold greater titres are required. Indeed, this study suggests that a minimum titre of 5 IU/ml is required for the neutralisation of all phylogroup I lyssaviruses *in vitro* and a minimum titre of 1 IU/ml is required for the neutralisation of novel phylogroup I viruses, Taiwan bat lyssavirus and Kotalahti bat lyssavirus, *in vivo*.

Additionally, experimental data in this study has shown that the antibody repertoire of lyssavirus-specific sera exhibits a strong level of intra-phylogroup neutralisation and very limited inter-phylogroup neutralisation. The data also suggests that a minimum of five distinct lyssavirus glycoproteins, rabies virus, Lagos bat virus lineage D, Ikoma lyssavirus, Lleida bat lyssavirus, and West Caucasian bat virus, would have to be included in any pan-lyssavirus vaccine. Promising cross-protective chimeric glycoproteins were designed and cloned into a rabies vaccine strain full length backbone. Reverse genetics techniques were used to enable virus rescue of these constructs. Where successful, the degree of vaccine-induced protection was assessed *in vivo*.

Acknowledgements

Firstly, I would like to thank my supervisors, Ashly Banyard, Edward Wright, and Tony Fooks for their roles as mentors, their direction, and for reading and commenting on my Thesis Chapters.

Ash, thank you for being an excellent supervisor and giving me the opportunity to pursue this PhD. Thank you for the constant enthusiasm and motivation in the harder times of my PhD (or as you might say, when it was 'a world of pain') and for the challenges and encouragement for when I needed to push myself out of my comfort zone. You have been a constant source of inspiration and a great mentor, for that I am eternally grateful!

To Ed, thank you for your help and guidance as my supervisor but also for your invaluable knowledge of pseudotype viruses. Thank you for providing some of your pseudotype constructs and sharing your pseudotyping skills.

To Tony, thank you for providing an insight into the world of rabies and for your continuous guidance and support through this journey. Thank you for providing numerous opportunities beyond the scope of my PhD.

To Dave, I am extremely grateful for your help with modified FAVNs in the earlier days of my PhD, the constant advice throughout my PhD, and the willingness to help with the animal element towards the end of my PhD. You have most certainly made my time at APHA much smoother, thank you for your patience!

To Dan, I am in awe of your antigenic cartography knowledge so thank you for going out of your way to teach me all things antigenic cartography. It has provided such a valuable aspect to my PhD and helped me understand my own data in a new and unique way.

To Hooman and Leigh, I am eternally grateful for the hours spent helping me with the animal element of my PhD and the invaluable technical assistance that comes with these experiments. I have so much appreciation for you both, taking the time to help me, thank you.

To Guanghai, thank you for your infinite advice, encouragement, and support. Thank you for sharing your insights and suggestions during my study and for the collaborative opportunities through external research projects.

To Fabian, I would like to extend my gratitude for your invaluable pathology expertise. Thank you for the time spent preparing slides for histology and immunohistochemistry. It was great to see the pathological features of the disease caused by infection with my recombinant viruses, thank you.

Whilst these past four years have been tough, there have been fun times too. For that, I have my PhD twin, Sam, to thank. Thank you for putting up with my frequent rants, and for providing me with a confidence that I failed to provide myself. I cannot express my gratitude enough for all the advice and knowledge you have imparted on me throughout my studies. I count myself incredibly lucky to have you as my friend and whilst we will eventually part ways through work, I know there's plenty of fun to be had yet.

To my family and those I consider family, especially my Mum, Dad, Daniella, Charlie, and Marie, thank you for your unwavering encouragement throughout this journey as it has allowed me to achieve more than I thought possible. Your support through weekly pep talks, enthusiasm, and around the clock care have been essential for my survival these past few years. I will never be able to thank you enough for everything.

Lastly, Kieran. I am truly grateful to have undertaken this endeavour with you in my life. Your overwhelming patience, support, and encouragement has never faltered. Thank you for not only having the most extraordinary ability to stop a meltdown in its tracks, but for believing in my eventual success when I couldn't. Your level of enthusiasm and motivation often surpassed my own and for that, I cannot thank you enough. Thank you for everything, I could not have completed this PhD without you.

Funding

This PhD was funded by Defra grant SE0431 and part funded by the European Union's Horizon 2020 research and innovation program under RABYD-VAX grant agreement no. 733176.

Statement

I hereby declare that this thesis has not been and will not be, submitted in whole or in part to another University for the award of any other degree.

Signature:

Parts of this thesis have been published by the author:

Shipley R, Wright E, Lean FZX, Selden D, Horton DL, Fooks AR, et al. Assessing Rabies Vaccine Protection against a Novel Lyssavirus, Kotalahti Bat Lyssavirus. *Viruses*. 2021;13(5).

Shipley R, Wright E, Selden D, Wu G, Aegerter J, Fooks AR, et al. Bats and Viruses: Emergence of Novel Lyssaviruses and Association of Bats with Viral Zoonoses in the EU. *Trop Med Infect Dis*. 2019;4(1).

Fooks AR, Shipley R, Markotter W, Tordo N, Freuling CM, Müller T, et al. Renewed Public Health Threat from Emerging Lyssaviruses. *Viruses*. 2021;13(9):1769.

Table of contents

Thesis Summary.....	2
Acknowledgements	3
Funding	4
Statement.....	5
Table of contents	6
List of Tables.....	17
List of Figures	18
Abbreviations used in the text.....	22
Chapter 1: Introduction	32
1.1 Lyssaviruses	32
1.1.1 Classification	33
1.1.2 Virion and genome organisation.....	44
1.1.2.1 The Nucleoprotein.....	47
1.1.2.2 The Phosphoprotein	48
1.1.2.3 The Matrix protein	50
1.1.2.4 The Glycoprotein	51
1.1.2.4.1 Antigenic sites on the glycoprotein	52
1.1.2.5 The Large Polymerase.....	56
1.1.2.6 Genomic Diversity	57
1.1.3 Life Cycle	58

1.1.3.1 Cell Entry	59
1.1.3.2 Transcription and Replication	60
1.1.3.3 Virus Egress and Migration	63
1.1.4 Epidemiology	65
1.1.4.1 Rabies epidemiology	65
1.1.4.2 Lyssavirus epidemiology	66
1.1.5 Infection	73
1.1.5.1 Transmission	73
1.1.5.2 Incubation Period	73
1.1.5.3 Immune response to RABV infection	74
1.1.5.3.1. Innate Immunity	74
1.1.5.3.2. Adaptive Immunity	77
1.1.5.3.3. Immune evasion	79
1.1.5.4 Human Infection.....	80
1.1.5.5 Terrestrial Carnivore Infection.....	82
1.1.5.6 Chiropteran Infection	82
1.2 Prophylactic and Therapeutic tools	84
1.2.1 Vaccines and Rabies Immunoglobulin	84
1.2.2 Milwaukee protocol	87
1.2.3. Possible non-antibody neutralisation mechanisms	88
1.2.4. Future perspectives and lyssavirus cross-neutralisation	92
1.3 Utilisation of lentiviral pseudotypes for glycoprotein expression.....	94

1.4 Reverse Genetics Techniques.....	97
1.5 Project Outline.....	100
Chapter 2: Materials and Methods	101
2.1. Cells.....	101
2.1.1. Cell lines and maintenance	101
2.1.2. Culturing cell lines.....	101
2.2. General Cloning and Molecular Biological Techniques	102
2.2.1. RNA Extraction	102
2.2.2. Polymerase Chain Reaction (PCR) Techniques	103
2.2.2.1. OneStep Reverse Transcription-PCR.....	103
2.2.2.2. Q5® PCR	104
2.2.2.3. GoTaq® Green PCR	104
2.2.2.4. iTaq™ Universal SYBR® Green One-Step Real Time RT-PCR.....	105
2.2.2.4.1. Quantitative PCR Technique.....	105
2.2.2.4.2. cDNA CVS standard curve generation	106
2.2.3. Agarose Gel Electrophoresis	107
2.2.4. Purification of extracted RNA for sequencing	108
2.2.5. Purification of DNA from agarose gel slices.....	108
2.2.6. Purification of DNA from PCR enzymatic reaction.....	108
2.2.7. Sequencing.....	109
2.2.7.1. Sanger Sequencing.....	109
2.2.7.2. Next Generation Sequencing (NGS).....	109

2.2.8. Primers	110
2.2.9. Large Scale Plasmid Preparations.....	110
2.2.10. Small Scale Plasmid Preparations.....	111
2.2.11. Spectrophotometry	112
2.2.12. Restriction digestion	112
2.2.12.1 Restriction digestion- preparative	112
2.2.12.2 Restriction digestion- analytical.....	112
2.2.13. Gibson Assembly	113
2.3. Bacterial Transformation and Culture	113
2.3.1. Bacterial Transformation	113
2.3.2. Culture on Agar	115
2.3.3. Culture on LB broth.....	115
2.3.4. Storage of Bacterial stocks	115
2.4. Virus Techniques.....	116
2.4.1. Virus Visualisation in Cells	116
2.4.2. Virus Propagation and Passage.....	116
2.4.2.1. Virus Propagation	116
2.4.2.2. Virus Passage	117
2.4.2.3. Virus Harvest	117
2.4.2.4. Virus Titration.....	118
2.4.2.5. Virus Back Titration.....	119
2.5. Generation of Specific Sera for each Lyssavirus	119

2.5.1. Preparation of Inocula.....	119
2.5.2. Confirmation of Inactivation of Inocula	121
2.5.3. Generation of Sera in Rabbits	121
2.5.4. Other test sera	122
2.5.5. Particle tracking	122
2.5.6 Concentrating Antibodies within serum samples	123
2.6. Serological Techniques	123
2.6.1. Fluorescent Antibody Virus Neutralisation (FAVN) Test.....	123
2.6.2. Modified Fluorescent Virus Neutralisation (mFAVN) Test.....	126
2.6.3. Enzyme-Linked Immunosorbent Assay (ELISA)	126
2.7. Pseudotype Techniques	127
2.7.1. Construction of Pseudotype Plasmids	127
2.7.2. Transient transfection	128
2.7.3. Pseudotype Titration	129
2.8. Recombinant virus generation	129
2.8.1. Manipulation of full length clones to insert wildtype and recombinant lyssavirus glycoproteins.....	129
2.8.2. Virus rescue	131
2.8.3. Assessing the Growth Kinetics of recombinant viruses	133
2.9. <i>In Vivo</i> Studies.....	133
2.9.1. Vaccination-Challenge in Mice	133
2.9.1.1. Mice	134

2.9.1.2. Vaccination of Mice	134
2.9.1.3. Blood Sampling by Tail Bleed	134
2.9.1.4. Intracranial Challenge with Virus	134
2.9.1.5. Serology	135
2.9.1.6. Tissue and Swab Sampling	135
2.9.1.7. Formalin fixation of mouse carcass	136
2.9.1.8. Virus Detection within Brain tissue	136
2.9.1.8.1. Direct Fluorescent Antibody Test (FAT)	136
2.9.1.8.2. Histopathology and Immunohistochemistry	137
2.10. Analytical Software	137
2.10.1. Benchling	137
2.10.2. NEB Tm Calculator	138
2.10.3. NEBuilder	138
2.10.4. Promega Tm for Oligos Calculator	138
2.10.5. DNASTAR Lasergene 14	138
2.10.6. MEGA 6	138
2.10.7. FigTree v1.4.2	139
2.10.8. SWISS-MODEL	139
2.10.9. Pymol	139
2.10.10. Acmacs Web Cherry - Antigenic Cartography	139
2.10.11. Mosaic Vaccine Tool Suite	139
2.11. Statistical Analysis	140

2.12. Gene Synthesis	140
2.13. Phylogenetics.....	140
2.14. Antigenic Cartography	141
Chapter 3: Defining the antigenic requirements for pan-lyssavirus neutralisation.....	143
3.1. Introduction	143
3.2. Viruses.....	145
3.2.1. Virus Isolates and Propagation	145
3.2.2. Molecular characterisation.....	147
3.2.3. Titration of virus stocks	150
3.2.4. Standardisation of Virus titre	150
3.3. Ability of sera derived from canine and human vaccinees to neutralise phylogroup I lyssaviruses	153
3.4. Generating Sera	155
3.4.1. Testing for Seroconversion.....	155
3.4.1.1. Binding antibody detection by ELISA.....	156
3.4.1.2. Neutralising antibody detection by mFAVN	156
3.4.1.3. Characterisation of BPL inactivated preparations.....	159
3.4.2. Other test Sera.....	161
3.5. Neutralisation within Phylogroup I	161
3.6. Neutralisation within Phylogroup II and III	163
3.7. Neutralisation across Phylogroup I, II, and III	166
3.8. Optimisation of Phylogroup II cross-neutralisation	169

3.9. Antigenic cartography	173
3.9.1. Phylogroup I	174
3.9.1.1. Lyssavirus antigenic variation.....	175
3.9.1.2. Predicting antigenic distance from evolutionary data.....	180
3.9.1.3. Predicting antigenic distance from amino acid sequence identity	180
3.9.2. Phylogroup II	182
3.9.2.1. Lyssavirus antigenic variation.....	182
3.9.2.2. Predicting antigenic distance from evolutionary data.....	186
3.9.2.3. Predicting antigenic distance from amino acid sequence identity	186
3.9.3. Phylogroup I, II, III.....	189
3.9.2.1. Cross-genus lyssavirus antigenic variation	189
3.9.2.2. Predicting antigenic distance from evolutionary data.....	194
3.9.2.3. Predicting antigenic distance from amino acid sequence identity	196
3.10. Determining the requirements for pan-lyssavirus neutralisation.....	198
3.11. Discussion	200
Chapter 4: Characterisation of novel lyssaviruses: Taiwan Bat Lyssavirus and putative lyssavirus, Kotalahti Bat Lyssavirus.....	214
4.1. Introduction	214
4.2. Generation of recombinant lyssavirus plasmids.....	216
4.3. Virus Rescue and Titration.....	219
4.4. Growth Kinetics	224
4.5. <i>In Vitro</i> Studies.....	226

4.5.1. Recombinant Viruses versus Vaccine Sera	227
4.5.2. Ability of phylogroup I specific sera to neutralise cSN-KBLV and cSN-TWBLV	229
4.5.3. Antigenic Cartography	232
4.6. In Vivo Vaccination Challenge Study	236
4.6.1 Vaccination of mice prior to ic challenge	236
4.6.2 Survival of vaccinated mice post ic challenge	238
4.6.3 Histology and Immunofluorescence	240
4.6.3.1 Histology	240
4.6.3.2 Immunofluorescence	241
4.6.4 Real time RT-PCR	243
4.6.5 Serological responses to infection and post-vaccination challenge	245
4.7. Discussion	250
Chapter 5: Construction and characterisation of recombinant viruses expressing chimeric glycoproteins	263
5.1. Introduction	263
5.2. Chimeric Glycoprotein rationale	265
5.2.1. Serological assessment of sera directed against a formulation of three BPL-inactivated viruses	265
5.2.2. Vaccine consisting of a single inactivated virus expressing multiple glycoproteins	267
5.3. <i>In silico</i> design of Chimeric Lyssavirus Glycoproteins	271

5.3.1. Hinge-based design.....	271
5.3.2. Mosaic-based design.....	274
5.3.3. Structure-based design.....	275
5.4. Generation of Chimeric and Mosaic clones	282
5.4.1. Cloning into pcDNA3.1(+).....	282
5.4.2. Cloning into cSN	282
5.5. Generation of Pseudotype Viruses expressing Chimeric Glycoprotein	284
5.6. Assessment of Live recombinant viruses expressing recombinant Glycoprotein	286
5.6.1. Virus Rescue and Titration	286
5.6.2. Growth Kinetics.....	288
5.6.3. In Vitro Studies.....	290
5.6.4. In Vivo Vaccination Challenge Study	292
5.6.4.1. Vaccination prior to challenge	292
5.6.4.2. Survival of vaccinated mice post challenge	295
5.6.5. Immunofluorescence.....	298
5.5.6. Serology	298
5.7. Discussion	304
Chapter 6: Discussion	313
6.1. Introduction	313
6.2. Implications of the degree of cross neutralisation across the genus.....	314

6.3. Benefits of using antigenic cartography to quantify lyssavirus antigenic variation	318
6.4. Strategies for chimeric glycoprotein development.....	321
6.5. Significance of <i>in vivo</i> vaccination-challenge experiments	322
6.6. Further work	325
6.7. Summary of conclusions	327
Bibliography.....	329
Appendix	356
Appendix 1: Reagents	356
A1.1. Tissue culture reagents.....	356
A1.2. Bacterial cell culture media	356
A1.3. Molecular biological buffers	357
A1.4. Fluorescent mAb	357
A1.5. Primers	358
Appendix 2: Cloning	360
A2.1. Cloning into cSN.....	360
Appendix 3: Chimeric Glycoprotein	361
A3.1. Table of isolates used for generation of Mosaic 2 G.	361
A3.2. Chimeric Glycoprotein sequences	362
Appendix 4: Generic scoring system for Mice inoculated ic with lyssaviruses.....	367
Appendix 5: Papers published as part of this thesis	367

List of Tables

Table 1.1.	Rhabdovirus taxonomy, species, hosts and vector species.
Table 1.2.	Nucleotide and amino acid identity of the lyssavirus G protein
Table 1.3.	Amino acid sequence of the lyssavirus antigenic sites.
Table 3.1.	Lyssavirus isolates used in this study.
Table 3.2.	Virus titre and dilution to achieve 100 TCID ₅₀ /50 µl.
Table 3.3.	Intergenotypic genetic and antigenic variation of phylogroup I viruses
Table 3.4.	Intergenotypic genetic and antigenic variation of phylogroup II viruses
Table 3.5.	Intergenotypic genetic and antigenic variation across the genus
Table 3.6.	Average antigenic distance in AU and equivalent fold difference in neutralisation titre within and between phylogroups
Table 4.1.	Post-mortem molecular testing on the brains of two mice from each group.
Table 5.1.	Lyssavirus Glycoprotein sequences used for chimeric glycoprotein design.
Table A1.5.	Primers
Table A3.1.	Table of isolates used for generation of mosaic2G
Table A3.2.	Chimeric Glycoprotein sequences
Table A4.	Generic scoring system for Mice inoculated ic with lyssaviruses

List of Figures

- Figure 1.1. Phylogenetic relationships of the lyssaviruses.
- Figure 1.2. Genome organisation of Rhabdoviruses and a pictorial representation of a mature RABV virion.
- Figure 1.3. Schematic representation of the lyssavirus G protein.
- Figure 1.4. Rabies life cycle in the cell.
- Figure 1.5. Schematic representation of suggested pathways for innate immune mechanisms following infection or vaccination.
- Figure 1.6. The process and outcome of generating pseudotype virus.
- Figure 1.7. The mechanism of reverse genetics and the rescue of lyssaviruses.
- Figure 2.1. Schematic showing the pre-assembly, assembly and post-assembly stages of cloning.
- Figure 2.2. Back titration protocol.
- Figure 2.3. Schematic of the FAVN test plate layout and protocol
- Figure 2.4. Pseudotype TCID₅₀ titration protocol.
- Figure 3.1. GBLV antigen stained with anti-N FITC mAb.
- Figure 3.2. Gel to show amplification of a 606bp section of the N gene of each of the lyssaviruses.
- Figure 3.3. The virus titre in ffu/ml for all of the lyssaviruses propagated.
- Figure 3.4. Heatmap to show the antibody titre required for the neutralisation of all phylogroup I viruses.
- Figure 3.5. Platelia Rabies II ELISA assay to show the RABV antigen-specific binding antibodies
- Figure 3.6. Modified FAVN to show the virus neutralising antibody titre of each lyssavirus-specific sera against the homologous virus.
- Figure 3.7. NanoSight measurement of virus particles

- Figure 3.8. Cross-neutralisation profiles within phylogroup I using a modified fluorescent antibody virus neutralisation (mFAVN) test.
- Figure 3.9. Cross-neutralisation profiles across phylogroup II and III using a modified fluorescent antibody virus neutralisation (mFAVN) test.
- Figure 3.10. Cross-neutralisation profiles across phylogroup I, II, and III using a modified fluorescent antibody virus neutralisation (mFAVN) test.
- Figure 3.11. Neutralisation profiles of concentrated phylogroup II-specific sera using a modified fluorescent antibody virus neutralisation (mFAVN) test.
- Figure 3.12. 3D antigenic map of phylogroup I viruses.
- Figure 3.13. Phylogenetic tree and Antigenic 2D map of phylogroup I viruses and antigenic clusters
- Figure 3.14. Plot of pair-wise antigenic and genetic distances between phylogroup I viruses.
- Figure 3.15. 3D antigenic map of phylogroup II viruses.
- Figure 3.16. Phylogenetic tree of the glycoprotein nucleotide sequences in phylogroup II.
- Figure 3.17. Plot of pair-wise antigenic and genetic distances between phylogroup II viruses.
- Figure 3.18. 3D antigenic map of phylogroup I, II, and III viruses.
- Figure 3.19. Phylogenetic tree of the glycoprotein nucleotide sequences across the lyssavirus genus.
- Figure 3.20. Plot of pair-wise antigenic and genetic distances between all lyssaviruses.
- Figure 3.21. The cross-neutralisation profile of a mix of two sera against all lyssaviruses.
- Figure 4.1. Cloning Strategy for the replacement of RABV glycoprotein with KBLV glycoprotein or TWBLV glycoprotein.
- Figure 4.2. Restriction digestion of cSN-KBLV and cSN-TWBLV
- Figure 4.3. Infection immunofluorescence

- Figure 4.4. Growth kinetics of cSN-KBLV, cSN-TWBLV, and the vaccine backbone, cSN, in vitro.
- Figure 4.5. Neutralisation profiles of cSN-KBLV, cSN-TWBLV, cSN and CVS against OIE and WHO standard sera mFAVN test.
- Figure 4.6. Cross-neutralisation profiles of cSN-KBLV, cSN-TWBLV, cSN and CVS against phylogroup I lyssavirus-specific sera using a mFAVN test.
- Figure 4.7. 3D antigenic map of phylogroup I viruses, cSN-KBLV, cSN-TWBLV, and cSN.
- Figure 4.8. Phylogenetic tree and Antigenic 2D map of phylogroup I viruses, cSN, cSN-KBLV, and cSN-TWBLV in antigenic clusters.
- Figure 4.9. Seroconversion and survivorship of the animals.
- Figure 4.10. In vivo survivorship following intracranial inoculation with cSN-KBLV or cSN-TWBLV
- Figure 4.11. Histopathology and immunohistochemistry against rabies nucleoprotein on cSN-KBLV and cSN-TWBLV-infected mouse brains.
- Figure 4.12. Direct FAT test.
- Figure 4.13. Quantitative SYBR real time RT-PCR.
- Figure 4.14. Assessment of serological status in mice following vaccination and challenge.
- Figure 4.15. Growth kinetics of the original codon optimised cSN-TWBLV, cSN-TWBLV 2017 isolate, cSN-TWBLV 2016 isolate, and cSN, in vitro.
- Figure 5.1. Modified FAVN to show the cross-neutralisation capability of IKOV/LLEBV/WCBV-specific sera against IKOV, LLEBV, WCBV virus.
- Figure 5.2. Genome organisation of ERA rabies virus with four glycoprotein genes (ERA-4G).
- Figure 5.3. Modified FAVN to show the cross-neutralisation capability of ERA-4G-specific sera against ERA-4G, RABV, LBV-B, MOKV, and WCBV virus.

- Figure 5.4. Linear schematic of a representative glycoprotein monomers designed using the hinge-based approach.
- Figure 5.5. Linear schematic of a representative glycoprotein monomer designed using the mosaic-based approach.
- Figure 5.6. Structural models of lyssavirus glycoprotein ectodomain monomers.
- Figure 5.7. Linear and structural schematic of representative glycoprotein monomers designed using the structure-based approach
- Figure 5.8. Restriction digestion of recombinant cSN plasmids
- Figure 5.9. Viral titres for luciferase pseudotypes.
- Figure 5.10. Infection immunofluorescence
- Figure 5.11. Growth kinetics of recombinant lyssavirus, cSN-Mosaic2; the vaccine backbone, cSN; and the wildtype viruses, LBV-A, LBV-B, LBV-C, LBV-D, MOKV, and SHIBV, in vitro.
- Figure 5.12. Cross-neutralisation of lyssavirus-specific sera and standard sera against cSN-Mosaic2 virus, using a mFAVN test.
- Figure 5.13. Post-vaccination serology on day 21 for mice vaccinated with inactivated LBV-D and mice mock-vaccinated with MEM.
- Figure 5.14. Post-vaccination serology on day 21 for mice vaccinated with inactivated cSN-Mosaic2 and mice mock-vaccinated with MEM.
- Figure 5.15. In vivo survivorship following intracranial inoculation with phylogroup II virus.
- Figure 5.16. Assessment of serological status in LBV-D infected mice following vaccination and challenge using modified FAVN.
- Figure 5.17. Assessment of serological status in cSN-Mosaic2 infected mice following vaccination and challenge using modified FAVN.
- Figure A2.1. Cloning into cSN.

Abbreviations used in the text

%	Percent
+ve	Positive
-ve	Negative
°C	Degrees Celsius
μl	Microliter
2D	2-Dimensional
3'	3 Prime
3D	3-Dimensional
5'	5 Prime
A	Adenine
aa	Amino Acid
ABLV	Australian bat lyssavirus
APC	Antigen Presenting Cell
APHA	Animal and Plant Health Agency
ARAV	Aravan virus
AU	Antigenic Unit
BBB	Blood Brain Barrier
BBLV	Bokeloh bat lyssavirus
BCR	B cell receptor
BHK	Baby Hamster Kidney
bp	Nucleotide Base Pair
BPL	Beta-propiolactone
BWA	Burrow-Wheeler Aligner

C	Cytosine
CD	C-Terminal Domain
cDNA	Copy DNA
cm	Centimetre
CNS	Central Nervous System
CO ₂	Carbon Dioxide
Cryo-EM	Cryogenic Electron Microscopy
cSN-EBLV-2-eGFP	cSN expressing enhanced Green Fluorescent Protein (eGFP) and EBLV-2 G instead of RABV G
cSN-KBLV	cSN Expressing KBLV G instead of RABV G
cSN-Mosaic2	cSN Expressing Mosaic2 G instead of RABV G
cSN-TWBLV	cSN Expressing TWBLV G instead of RABV G
Ct	Cycle Threshold
CVS	Challenge Virus Standard
DAMP	Damage-Associated Molecular Pattern
DC	Dendritic Cell
DI	Defective Interfering
DIC	Differential Interference Contrast
DMEM	Dulbecco's Modified Eagles Media
DNA	Deoxyribonucleic Acid
dNTP	Deoxyribonucleoside-5'-triphosphate
dpi	Days post infection
ds	Double stranded
DUVV	Duvenhage virus

EBLV-1	European bat lyssavirus type 1
EBLV-2	European bat lyssavirus type 2
EDTA	Ethylenediaminetetra-acetic acid
ELISA	Enzyme-linked Immunosorbent Assay
EM	Electron Microscopy
ER	Endoplasmic Reticulum
ERIG	Equine rabies immunoglobulin
ESCRT	Endosomal sorting complex required for transport
EU/ml	Equivalent Unit per millilitre
FAT	Fluorescent antibody test
FAVN	Fluorescent antibody virus neutralisation
FBS	Foetal bovine serum
FDC	Follicular Dendritic Cell
ffu/ml	Focus forming units per millilitre
FITC	Fluorescein Isothiocyanate
FMDV	Foot-And-Mouth Disease virus
For	Forward (primers)
G	Glycoprotein
G	Guanine
g	Gram
GBLV	Gannoruwa bat lyssavirus
GC	Germinal centre
GFP	Green fluorescent protein
GMEM	Glasgow Minimum Essential Media

h	Hour
H&E	Haematoxylin and Eosin
HCl	Hydrogen chloride
HDCV	Human diploid cell vaccine
HEK	Human Embryonic Kidney
HEP	High egg passage
HIV	Human immunodeficiency virus
hpi	Hours post infection
H ₂ O	Water
HRIG	Human rabies immunoglobulin
IB	Inclusion bodies
ic	Intracranial
ICTV	International Committee on the Taxonomy of Viruses
IFITM3	IFN-Induced Transmembrane Protein 4
IFN	Interferon
Ig	Immunoglobulin
IHC	Immunohistochemistry
IKOV	Ikoma lyssavirus
im	Intramuscular
IL	Interleukin
ip	Intraperitoneal
IRES	Internal ribosome entry site
IRF-3	IFN regulatory factor 3
IRKV	Irkut virus

IU/ml	International Units per millilitre
k.o	Knockout
KBLV	Kotalahti bat lyssavirus
kbp	Kilobase pairs
kDa	Kilodaltons
kg	Kilogram
KHUV	Khujand virus
k-mer	Constituent peptide
L	Large Polymerase
l	Litre
L domains	Late-budding domains
LB	Luria Bertani
LBV A–D	Lagos bat virus lineages A-D
LD ₅₀	50% Lethal dose
LLEBV	Lleida bat lyssavirus
LMCV	Lymphocytic choriomeningitis virus
LTR	Long terminal repeats
M	Matrix Protein
M	Molar
mAb	Monoclonal Antibody
MAST2	Microtubule-associated serine/threonine protein kinase 3
MBLV	Matlo bat lyssavirus
MDA-5	Melanoma differentiation-associated protein-5
MEM	Minimal Essential Media

mFAVN	Modified fluorescent antibody virus neutralisation
mg	Milligram
mGluR2	Metabotropic Glutamate Receptor 3
MHC	Major Histocompatibility Complex
min	Minute
ML	Maximum Composite Likelihood
ml	Millilitre
mm	Millimetre
mmol	Millimole
MOI	Multiplicity of infection
MOKV	Mokola virus
mRNA	Messenger ribonucleic acid
MSC	Microbiological safety cabinet
N	Nucleocapsid
N2a	Neuro-2a
nAChR	Nicotinic acetylcholine receptor
NaOH	Sodium hydroxide
NB	Negri inclusion bodies
NBF	Neutral buffered formalin
NCAM	Neural cell adhesion molecule
NCBI	National Center for Biotechnology Information
ND	N-Terminal Domain
NDV	Newcastle Disease virus
ng	Nanogram

ng/μl	Nanograms per microlitre
NGS	Next Generation Sequencing
NJ	Neighbour-Joining
NK	Natural Killer
nm	Nanometre
nmol	Nanomole
NMJ	Neuromuscular junction
nt	Nucleotide
OIE	World Organisation for Animal Health
ORF	Open reading frame
P	Passage
P	Phosphoprotein
p75NTR	P75 Neurotrophin Receptor
PAMP	Pathogen-Associated Molecular Pattern
PBS	Phosphate buffered saline
PCR	Polymerase chain reaction
PDB	Protein Data Bank
PEP	Post-exposure prophylaxis
PML	Promyelocytic Leukaemia
pmol	Picomole
PNA	Pseudotype neutralisation assay
PRR	Pattern Recognition Receptor
PT	Pseudotype
qPCR	Quantitative polymerase chain reaction

RABV	Rabies virus
RdRp	RNA dependent RNA polymerase
Rev	Reverse (primers)
RG	Reverse genetics
RIG	Rabies immunoglobulin
RIG-I	Retinoic-acid inducible protein-I
RLR	Retinoic-acid inducible gene like receptor
RLU	Relative Light Units
RNA	Ribonucleic Acid
RNAse	Ribonuclease
RNP	Ribonucleoprotein
rpm	Revolutions per minute
RT	Reverse transcription
RTCIT	Rabies tissue culture isolation test
SAD	Street Alabama Dufferin
SD	Standard deviation
SDS	Sodium dodecyl sulfate
SE	Standard error
Ser	Serine
SHIBV	Shimoni bat virus
si	Short inhibitory
SOC	Super optimal broth with catabolite repression
SP	Signal peptide
ss	Single stranded

SUMO	Small-ubiquitin like modifier
T	Thymine
TAE	Tris-Acetate EDTA
TCID ₅₀	50 % Tissue culture infective dose
TCSN	Tissue culture supernatant
T _{FH}	Follicular helper T Cell
Th1	T helper Type 1
Th17	Interleukin- 17 releasing T Helper
Th2	T helper Type 2
TLR	Toll-like receptor
T _m	Melting temperature
TM	Transmembrane domain
TMB	3,3',5,5'-Tetramethylbenzidine
TNF- α	Tumour necrosis factor- α
Tris	Trisaminomethane
TWBLV	Taiwan bat lyssavirus
U	Uracil
μg	Microgram
$\mu\text{g} / \mu\text{l}$	Micrograms per microlitre
μl	Microlitre
μmol	Micromole
UTR	Untranslated region
V	Volts
VNA	Virus neutralising antibody

VSV	Vesicular stomatitis virus
WCBV	West Caucasian bat virus
WHO	World Health Organization
wt	Wildtype
x g	Centrifugation force

Chapter 1: Introduction

1.1 Lyssaviruses

Rabies is caused by viruses classified within the *Lyssavirus* genus, family *Rhabdoviridae*, order *Mononegavirales* (1). These viruses are of importance to both human and animal health given the invariably fatal outcome from developing neurological disease (2). The genus *Lyssavirus* is divided into 17 species accepted by the International Committee on the Taxonomy of Viruses (ICTV) (3). The ancestral lyssavirus reservoir host species is universally accepted as being members of the Order *Chiroptera*, with all but two lyssaviruses, Mokola and Ikoma lyssaviruses, having been detected in different bat species (4-6).

Within the lyssavirus genus, the most broadly distributed and important for veterinary and public health is rabies virus (RABV). Though this virus has largely been eliminated throughout Western Europe, RABV is still the most commonly reported lyssavirus. RABV causes approximately 59,000 human deaths annually with the majority of these fatalities associated with dog-mediated transmission (7). The onset of clinical disease has been associated with the route of infection and hence the length of the incubation period. Factors such as: the location of the wound with respect to the brain, the viral dose transmitted, the genetics of infecting lyssavirus strain, and the immunocompetence of the infected host may all contribute to the incubation period (8). Regardless, where clinical disease develops, the outcome is invariably fatal (9). Consequently, rabies has the highest case-fatality rate of any infectious disease (7).

Surveillance is a critical component in disease elimination and control but in areas where rabies is endemic, countries often lack a good infrastructure to report cases and track vaccination programmes (10). Rabies is often considered a disease of poverty and

ignorance and of the total human fatalities that occur annually, 33,000 occur in Asia and 26,000 occur in Africa (11-13). In addition, these figures are believed to be a gross underestimate. It is estimated that only 3-5% of rabies cases are reported and rabies is often misdiagnosed as an alternative encephalitis such as malaria (10, 14, 15).

1.1.1 Classification

Lyssaviruses are classified within the family *Rhabdoviridae* within the order *Mononegavirales*. As well as the *Rhabdoviridae* family, the order *Mononegavirales* contains 10 other virus families including the *Bornaviridae*, *Paramyxoviridae* and *Filoviridae* families. With few exceptions, viruses within this order contain linear, non-segmented, negative-sense, single-stranded ribonucleic acid (RNA) genomes. Exceptions in the *Rhabdoviridae* family are the viruses classified in the *Dichorhavirus* genus and *Varicosavirus* genus which have bi-segmented, negative-sense genomes (3). For all the families within *Mononegavirales* except bornaviruses, nyavirus and the nucleorhabdoviruses, virus replication and transcription occur in the cytoplasm. The bornavirus, nyavirus and the nucleorhabdovirus families carry out transcription and replication of the viral genome in the host cell nucleus (16). Another shared property of members within the order *Mononegavirales* is the highly conserved gene order, where although the number of viral genes varies from 5 to 11, the core gene order (3'-N-P-M-G-L-5') is maintained throughout (17). Lyssaviruses, like other rhabdoviruses, encapsidate the virus genome in their entirety with the nucleocapsid protein. As such, genetic reassortment is thought to be a rare occurrence but has been reported (16).

The *Rhabdoviridae* family (Table 1.1) constitutes one of the most diverse virus families from the perspective of breadth of host infection, where viruses classified within the family can infect mammals, birds, reptiles, fish, plants and arthropods (18). However,

only lyssaviruses, ephemeroviruses, and vesiculoviruses are capable of causing clinical disease in both animals and humans, and rabies is the only significant human pathogen. Additionally, in contrast to all other rhabdoviruses, lyssaviruses have adapted to direct transmission and are not transmitted by arthropod vectors.

Within the lyssavirus genus, 17 different viral species are classified as separate entities according to their genomic sequence. This includes: Australian bat lyssavirus (ABLV), Aravan virus (ARAV), Bokeloh bat lyssavirus (BBLV), Duvenhage virus (DUVV), European bat lyssavirus type 1 (EBLV-1), European bat lyssavirus type 2 (EBLV-2), Gannoruwa bat lyssavirus (GBLV), Irkut virus (IRKV), Ikoma lyssavirus (IKOV), Khujand virus (KHUV), Lagos bat virus (LBV Lineages A–D), Lleida bat lyssavirus (LLEBV), Mokola virus (MOKV), Rabies virus (RABV), Shimoni bat virus (SHIBV), Taiwan bat lyssavirus (TWBLV), and West Caucasian bat virus (WCBV) accepted by the International Committee on Taxonomy of Viruses (3). Two further putative novel lyssaviruses, Kotalahti bat lyssavirus (KBLV), which was detected in a Brandt's bat (*Myotis brandtii*), and Matlo bat lyssavirus (MBLV), which was detected in two Natal long-fingered bats (*Miniopterus natalensis*), have been reported but remain as tentative species until fully characterised (19, 20). The genome lengths of each of the lyssavirus species vary, with the RABV species exhibiting the shortest genomes at 11,923-11,932 nucleotides and WCBV exhibiting the longest genome of 12,178 nucleotides (21).

Table 1.1: Rhabdovirus taxonomy, species, hosts and vector species as accepted by the ICTV (as of 04/07/2021) (1). Adapted from (22).

Genus	No. of Species	Species	Main hosts and vectors
Almendravirus	6	Arboretum almdravirus Balsa almdravirus Coot Bay almdravirus Puerto Almendras almdravirus Rio Chico almdravirus	Mosquito
Alphanemrhavirus	2	Xingshan alphanemrhavirus Xinzhou alphanemrhavirus	Nematode
Alphanucleorhabdovirus	11	Constricta yellow dwarf alphanucleorhabdovirus Eggplant mottled dwarf alphanucleorhabdovirus Maize Iranian mosaic alphanucleorhabdovirus Maize mosaic alphanucleorhabdovirus Morogoro maize-associated alphanucleorhabdovirus Peach alphanucleorhabdovirus Physostegia chlorotic mottle alphanucleorhabdovirus Potato yellow dwarf alphanucleorhabdovirus Rice yellow stunt alphanucleorhabdovirus Taro vein chlorosis alphanucleorhabdovirus Wheat yellow striate alphanucleorhabdovirus	Plants Planthoppers Aphids Leafhoppers
Arurhavirus	4	Aruac arurhavirus Inhangapi arurhavirus Santabarbara arurhavirus Xiburema arurhavirus	Mosquito Sandflies Mice
Barhavirus	2	Bahia barhavirus Muir barhavirus	Mosquito
Betanucleorhabdovirus	9	Alfalfa betanucleorhabdovirus Apple betanucleorhabdovirus Blackcurrant betanucleorhabdovirus Cardamom betanucleorhabdovirus Datura yellow vein betanucleorhabdovirus Pepper betanucleorhabdovirus Sonchus yellow net betanucleorhabdovirus Sowthistle yellow vein betanucleorhabdovirus Trefoil betanucleorhabdovirus	Plants Aphids
Caligrhavirus	3	Caligus caligrhavirus Lepeophtheirus caligrhavirus Salmonlouse caligrhavirus	Arthropods
Curiovirus	4	Curionopolis curiovirus Irii curiovirus Itacaiunas curiovirus	Midges Sandflies Mosquitoes

		Rochambeau curiovirus	
Cytorhabdovirus	28	Alfalfa dwarf cytorhabdovirus Barley yellow striate mosaic cytorhabdovirus Broccoli necrotic yellows cytorhabdovirus Cabbage cytorhabdovirus Colocasia bobone disease-associated cytorhabdovirus Festuca leaf streak cytorhabdovirus Lettuce necrotic yellows cytorhabdovirus Lettuce yellow mottle cytorhabdovirus Maize yellow striate cytorhabdovirus Maize-associated cytorhabdovirus Northern cereal mosaic cytorhabdovirus Papaya cytorhabdovirus Persimmon cytorhabdovirus Raspberry vein chlorosis cytorhabdovirus Rice stripe mosaic cytorhabdovirus Sonchus cytorhabdovirus 1 Strawberry crinkle cytorhabdovirus Strawberry cytorhabdovirus 1 Tomato yellow mottle-associated cytorhabdovirus Trichosanthes cytorhabdovirus Trifolium pratense cytorhabdovirus A Trifolium pratense cytorhabdovirus B Wheat American striate mosaic cytorhabdovirus Wuhan 4 insect cytorhabdovirus Wuhan 5 insect cytorhabdovirus Wuhan 6 insect cytorhabdovirus Yerba mate chlorosis-associated cytorhabdovirus Yerba mate cytorhabdovirus	Plants Aphids Planthoppers Leafhoppers
Dichorhavirus	5	Citrus chlorotic spot dichorhavirus Citrus leprosis N dichorhavirus Clerodendrum chlorotic spot dichorhavirus Coffee ringspot dichorhavirus Orchid fleck dichorhavirus	Arthropods Plants
Ephemerovirus	11	Adelaide River ephemerovirus Berrimah ephemerovirus Bovine fever ephemerovirus Hayes ephemerovirus Kent ephemerovirus Kimberley ephemerovirus Koolpinyah ephemerovirus Kotonkan ephemerovirus Obodhiang ephemerovirus Puchong ephemerovirus Yata ephemerovirus	Cattle Mosquitos Midges

Gammanucleorhabdovirus	1	Maize fine streak gammanucleorhabdovirus	
Hapavirus	16	Flanders hapavirus Gray Lodge hapavirus Hart Park hapavirus Holmes hapavirus Joinjakaka hapavirus Kamese hapavirus La Joya hapavirus Landjia hapavirus Manitoba hapavirus Marco hapavirus Mosqueiro hapavirus Mossuril hapavirus Ngaingan hapavirus Ord River hapavirus Parry Creek hapavirus Wongabel hapavirus	Birds Mosquitos
Ledantavirus	17	Barur ledantavirus Bughendera ledantavirus Fikirini ledantavirus Fukuoka ledantavirus Kanyawara ledantavirus Kern Canyon ledantavirus Keuraliba ledantavirus Kolente ledantavirus Kumasi ledantavirus Le Dantec ledantavirus Mount Elgon bat ledantavirus Nishimuro ledantavirus Nkolbisson ledantavirus Oita ledantavirus Vaprio ledantavirus Wuhan ledantavirus Yongjia ledantavirus	Arthropods Bats
Lostrhavirus	1	Hyalomma lostrhavirus Lonestar lostrhavirus	
Lyssavirus	17	Aravan lyssavirus Australian bat lyssavirus Bokeloh bat lyssavirus Duvnhage lyssavirus European bat 1 lyssavirus European bat 2 lyssavirus Gannoruwa bat lyssavirus Ikoma lyssavirus Irkut lyssavirus Khujand lyssavirus Taiwan bat lyssavirus Lagos bat lyssavirus Lleida bat lyssavirus Mokola lyssavirus Rabies lyssavirus Shimoni bat lyssavirus West Caucasian bat lyssavirus	Dogs Humans Bats
Mousrhavirus	1	Moussa mousrhavirus	Mosquito
Novirhabdovirus	4	Hirame novirhabdovirus Piscine novirhabdovirus Salmonid novirhabdovirus Snakehead novirhabdovirus	Fish
Ohlshavirus	8	Angeles ohlshavirus	Mosquito

		Culex ohlsrhavirus Lobeira ohlsrhavirus Northcreek ohlsrhavirus Ohlsdorf ohlsrhavirus Pseudovishnui ohlsrhavirus Riverside ohlsrhavirus Tongilchon ohlsrhavirus	
Perhabdovirus	3	Anguillid perhabdovirus Perch perhabdovirus Sea trout perhabdovirus	Fish
Sawgrhavirus	4	Connecticut sawgrhavirus Island sawgrhavirus Minto sawgrhavirus Sawgrass sawgrhavirus	Ticks
Sigmavirus	17	Capitata sigmavirus Domestica sigmavirus Drosophila affinis sigmavirus Drosophila ananassae sigmavirus Drosophila immigrans sigmavirus Drosophila melanogaster sigmavirus Drosophila obscura sigmavirus Drosophila tristis sigmavirus Hippoboscid sigmavirus Hubei sigmavirus Lousefly sigmavirus Muscina stabulans sigmavirus Myga sigmavirus Shayang sigmavirus Sturtevant sigmavirus Wuhan sigmavirus Ying sigmavirus	Fruitflies
Sprivirus	2	Carp sprivirus Pike fry sprivirus	Fish
Sripuvirus	8	Almpiwar sripuvirus Chaco sripuvirus Charleville sripuvirus Cuiaba sripuvirus Hainan sripuvirus Niakha sripuvirus Sena Madureira sripuvirus Sripur sripuvirus	Reptiles Sandflies
Sunrhavirus	7	Dillard sunrhavirus Garba sunrhavirus Harrison sunrhavirus Kwatta sunrhavirus Oakvale sunrhavirus Sunguru sunrhavirus Walkabout sunrhavirus	Mosquito Midges Birds
Tibrovirus	7	Bas-Congo tibrovirus Beatrice Hill tibrovirus Coastal Plains tibrovirus Ekpoma 1 tibrovirus Ekpoma 2 tibrovirus Sweetwater Branch tibrovirus Tibrogargan tibrovirus	Ticks Cattle
Tupavirus	3	Durham tupavirus Klamath tupavirus Tupaia tupavirus	Birds
Varicosavirus	3	Alopecurus varicosavirus	Plants

		Lettuce big-vein associated varicosavirus Trifolium varicosavirus	
Vesiculovirus	17	Alagoas vesiculovirus Carajas vesiculovirus Chandipura vesiculovirus Cocal vesiculovirus Eptesicus vesiculovirus Indiana vesiculovirus Isfahan vesiculovirus Jurona vesiculovirus Malpais Spring vesiculovirus Maraba vesiculovirus Morreton vesiculovirus New Jersey vesiculovirus Perinet vesiculovirus Piry vesiculovirus Radi vesiculovirus Rhinolophus vesiculovirus Yug Bogdanovac vesiculovirus	Cattle Arthropods Fish
Zarhavirus	1	Zahedan zarhavirus	Ticks

In addition to the genetic classification into species, the lyssaviruses have also been classified according to antigenic data into phylogroups (23-25). The trimeric lyssavirus glycoprotein, the surface antigen responsible for cell entry, is the sole target for neutralising antibodies (26). Whilst the crystal structures for RABV G and MOKV G were recently solved, meaningful assessment of these structures and the correlation to antigenicity still remains to be determined (27-29). Despite this, the divergence in G protein sequence data across the genus gives an indication of antigenic diversity (Table 1.2, Figure 1.1). The phylogroups generally dictate the degree of cross protection afforded by rabies vaccines. Rabies vaccines for human use are based on whole inactivated RABV particles.

Alongside administration of rabies immunoglobulin (RIG) and wound cleaning, vaccination, resulting in the production of virus neutralising antibodies (VNAs), is the only definitive way to prevent disease onset after contact with a rabid animal.

Individuals with an increased risk to exposure through high-risk occupations or domestic animals destined to travel are vaccinated pre-exposure and periodic antibody titre checks are used to evaluate the requirement for booster vaccinations. Because the production of VNAs affords protection against RABV, the use of serological assays to quantitate VNAs is recommended to assess immune response to vaccination in humans. No specific titre of VNAs has been determined to ensure complete protection against all RABV variants in all circumstances however statistical analysis of the survival rate against the VNA titre of challenged animals has enabled the definition of a conservative threshold for which protection against RABV is likely. In a previous report, the probability of survival increased as the titre of VNAs increased where 0.5 International Units (IU)/ml afforded a percentage survival rate of 99% (30). Further, specific working groups involved in several international human rabies vaccine trials provided

recommendations (31). Based on these reports of pre-exposure and post-exposure vaccination series and VNA titres achieved, 0.5 IU/ml was accepted as proof of seroconversion and the conservative threshold for which protection against RABV is likely (31, 32).

Alongside RABV, the current vaccines are understood to protect against all phylogroup I lyssaviruses; ARAV, ABLV, BBLV, DUVV, EBLV-1, EBLV-2, IRKV, KHUV, GBLV, and TWBLV although the level of neutralising antibody required to protect is undefined. Evidence has shown, however, that a titre higher than 0.5 IU/ml is required for protection for some phylogroup I lyssaviruses indicating an increased antigenic distance of the vaccine strains to the circulating lyssaviruses (33-35). For more divergent lyssaviruses such as those in phylogroup II and III, *in vivo* vaccination-challenge experiments have shown that the antibody response generated from the RABV vaccine is not sufficient for protection (36-38). Phylogroup II lyssaviruses include LBV (all lineages, A-D), MOKV and SHIBV. Three further lyssaviruses, WCBV, IKOV and LLEBV represent the most genetically and antigenically divergent lyssaviruses that have been tentatively assigned to a third phylogroup for the purposes of this study (37, 39).

Amino Acid % Identity																					
	ABLV	ARAV	BBLV	DUVV	EBLV-1	EBLV-2	GBLV	IRKV	KHUV	TWBLV	RABV	LBV-A	LBV-B	LBV-C	LBV-D	MOKV	SHIBV	IKOV	LLEBV	WCBV	
Nucleotide % Identity	ABLV		75.9	76.2	71.2	72.6	76.0	81.4	65.9	77.2	66.7	73.3	58.4	58.6	58.4	56.9	56.7	60.9	47.4	47.1	51.6
	ARAV	69.8		83.2	78.5	82.8	85.1	78.9	71.4	84.0	70.4	73.4	56.0	58.4	58.1	57.1	55.8	58.6	45.2	46.7	51.2
	BBLV	70.6	73.3		78.1	78.3	87.1	81.5	69.0	86.4	70.1	75.0	57.1	57.1	57.5	57.3	56.0	59.0	46.3	46.7	51.2
	DUVV	67.4	70.1	71.0		79.0	79.0	74.6	69.1	77.2	66.9	68.5	56.9	56.2	57.1	57.5	56.0	58.6	45.7	46.9	49.7
	EBLV-1	68.1	73.2	71.3	72.9		79.8	76.2	73.3	79.2	72.8	70.5	58.4	57.9	58.1	59.2	56.9	59.6	46.5	45.9	50.3
	EBLV-2	71.7	75.2	77.3	71.9	73.1		79.2	70.7	87.7	71.8	74.5	55.6	57.3	57.1	58.1	56.2	58.1	46.9	47.1	50.5
	GBLV	73.4	72.1	72.6	67.6	69.8	72.6		67.8	81.2	67.0	77.2	59.4	59.0	58.8	58.3	60.0	60.9	45.5	46.1	50.5
	IRKV	65.8	70.2	70.4	70.0	73.8	71.0	67.9		70.5	70.5	64.4	55.8	56.8	57.0	56.4	55.4	55.6	45.7	45.9	49.5
	KHUV	72.5	74.5	76.3	71.4	72.2	78.7	73.0	70.0		68.9	76.3	57.1	57.3	57.7	57.7	56.5	59.4	46.1	47.1	51.0
	TWBLV	64.0	66.5	66.6	65.3	68.6	66.7	66.4	67.7	67.0		65.7	55.3	55.6	54.7	55.1	54.5	56.4	48.3	46.8	48.9
	RABV	70.5	69.1	69.8	65.1	67.2	70.3	72.3	65.9	70.1	64.0		57.9	58.3	57.7	56.2	57.1	59.0	45.0	45.7	50.1
	LBV-A	59.3	58.3	58.4	57.7	60.5	57.2	58.6	59.3	58.6	56.7	58.9		80.5	82.0	81.2	76.1	78.4	48.8	44.0	52.9
	LBV-B	58.9	60.1	59.8	57.9	59.1	61.2	59.5	60.4	60.3	58.7	59.6	73.2		85.8	79.3	72.3	79.3	46.5	43.8	53.5
	LBV-C	57.7	60.0	59.6	58.1	60.0	60.9	59.0	60.7	59.0	57.2	59.0	72.6	77.1		81.6	73.4	79.7	47.8	44.6	52.4
LBV-D	58.5	61.1	60.2	60.2	61.4	60.7	60.1	60.4	59.8	59.7	58.8	72.8	73.6	73.9		75.1	76.9	47.4	44.2	51.4	
MOKV	58.9	59.5	60.6	59.8	59.9	60.4	60.4	59.0	60.2	58.2	59.1	69.1	68.6	68.6	70.1		70.6	47.1	43.8	51.8	
SHIBV	60.2	61.1	60.2	59.0	60.8	59.5	59.8	60.1	59.2	58.2	59.4	71.1	71.7	71.8	71.1	67.0		48.4	43.8	52.6	
IKOV	55.9	56.4	57.7	57.4	55.8	56.9	55.7	56.2	56.1	54.1	51.3	55.8	56.9	57.6	57.4	57.1	57.6		63.9	48.2	
LLEBV	52.8	54.1	53.6	52.8	53.4	51.7	53.9	53.0	54.2	54.3	52.1	52.9	52.7	54.0	53.4	51.1	54.1	54.8		47.1	
WCBV	52.9	53.2	53.5	51.2	53.0	53.5	51.7	53.4	52.7	53.1	56.2	53.8	52.3	53.9	53.2	52.5	54.6	54.7	65.2		

Table 1.2: Nucleotide and amino acid identity of the lyssavirus G protein. Percentage identities are shown. Where identity is more than or equal to 60% they are shaded blue. Viruses that have been classified into phylogroups are shaded accordingly.

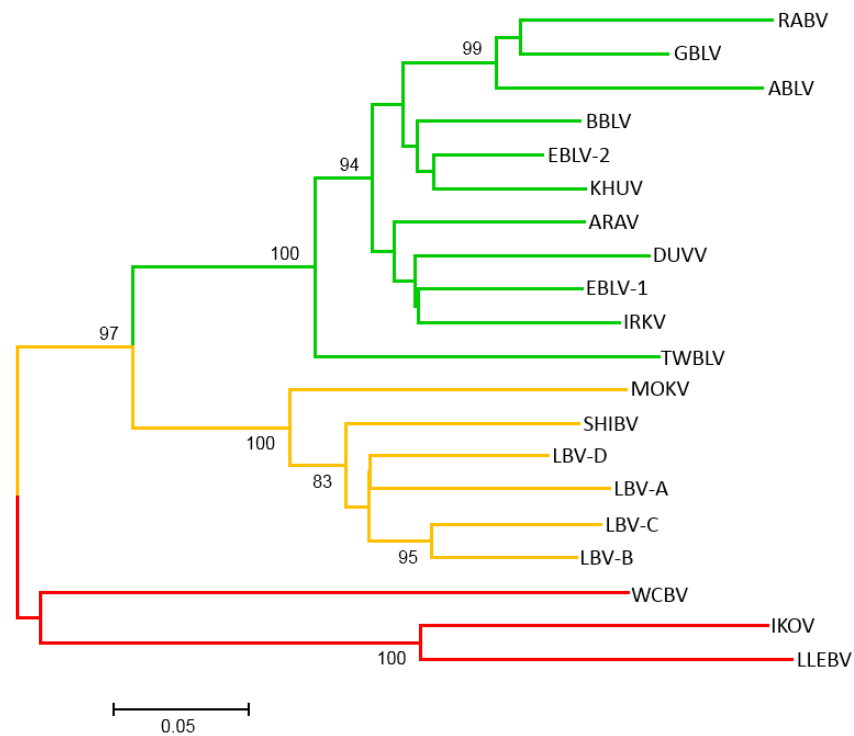


Figure 1.1: Phylogenetic relationships of the lyssaviruses with Phylogroup I lyssaviruses labelled in green, Phylogroup II in orange and Phylogroup III in red. The phylogenetic tree is based on an alignment of the complete lyssavirus glycoprotein gene. The analysis involved 20 lyssavirus glycoprotein nucleotide sequences. The evolutionary history was inferred using the Neighbour-Joining method and the evolutionary distances were computed using the Maximum Composite Likelihood method. A bootstrap analysis of 1000 replications was undertaken and are indicated at key nodes. Scale bar indicates the number of substitutions per site. Trees were generated in MEGA6 and edited in FigTree.

The following sequences were used for generation of the phylogenetic tree: ABLV, Australian bat lyssavirus, Genbank accession code: AF081020; ARAV, Aravan virus, Genbank accession code: EF614259; BBLV, Bokeloh bat lyssavirus, Genbank accession code: JF311903; DUVV, Duvenhage virus, Genbank accession code: GU936870 ; EBLV-1, European bat lyssavirus type 1, Genbank accession code: KF155003; EBLV-2, European bat lyssavirus type 2, Genbank accession code: KY688136; GBLV, Gannoruwa bat lyssavirus, Genbank accession code: KU244267; IRKV, Irkut virus, Genbank accession code: EF614260; KHUV, Khujand virus, Genbank accession code: EF614261; RABV, rabies virus, Genbank accession code: KF154997; TWBLV, Taiwan bat lyssavirus, Genbank accession code: MG763889 LBV-A, Lagos bat virus lineage A, Genbank accession code: EF547432; LBV-B, Lagos bat virus lineage B, Genbank accession code: EF547431; LBV-C, Lagos bat virus lineage C, Genbank accession code: EF547425; LBV-D, Lagos bat virus lineage D, Genbank accession code: GU170202; MOKV, Mokola virus, Genbank accession code: KF155005; SHIBV, Shimoni bat virus, Genbank accession code: GU170201; IKOV, Ikoma lyssavirus, Genbank accession code: JX193798; LLEBV, Lleida bat lyssavirus, Genbank accession code: NC031955; WCBV, West Caucasian bat virus, Genbank accession code: EF614258.

1.1.2 Virion and genome organisation

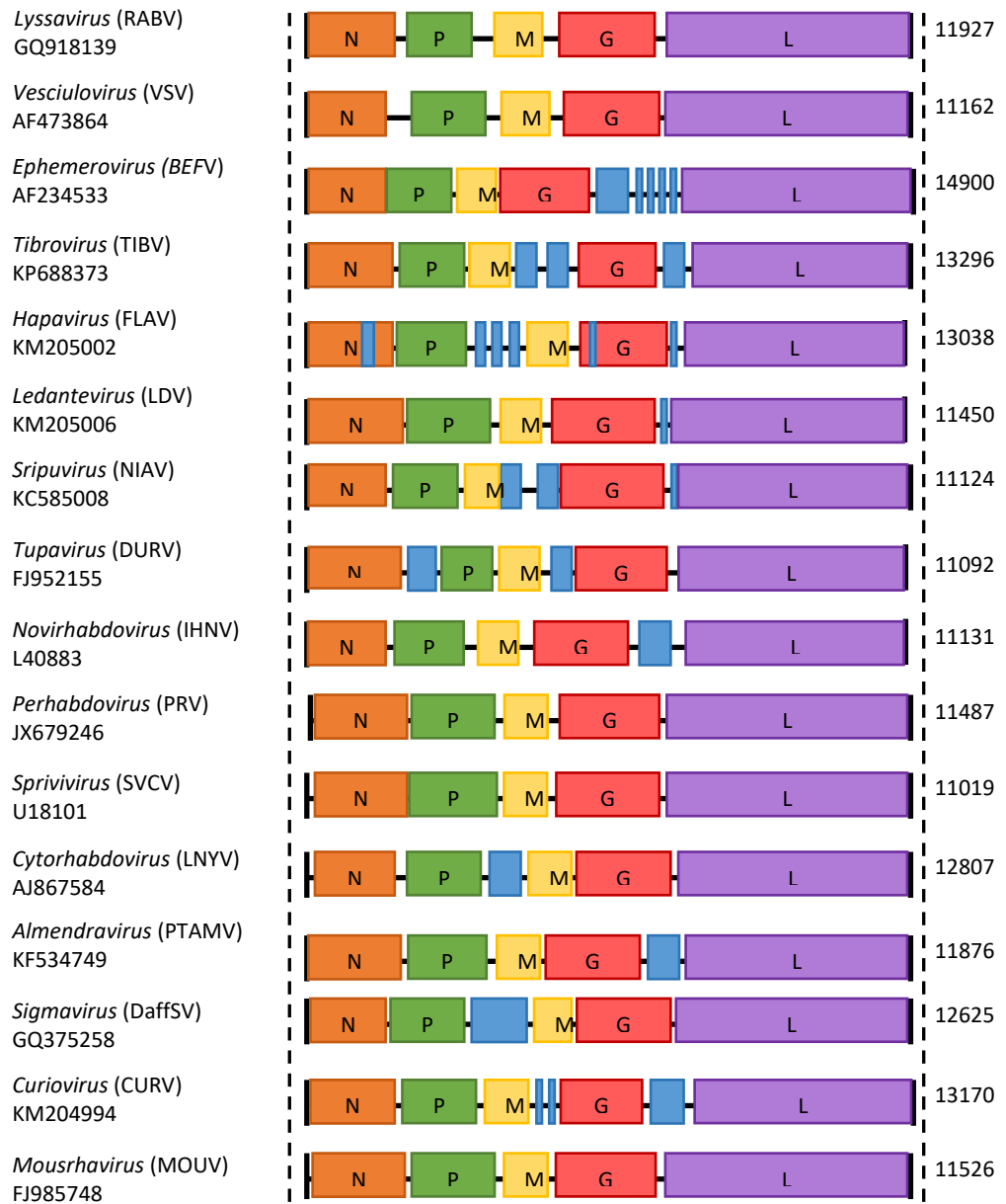
Lyssavirus species share many of the biological and physicochemical features that are associated with other viruses of the *Rhabdoviridae* family. This includes, a bullet-like virion morphology with an envelope derived from the plasma membrane of the infected host cell. One end of the bullet shape is conical (hemispherical), the other flat (planar) with approximate dimensions of ~75 nm and a length of ~180 nm, depending on the virus (40). Cryogenic Electron Microscopy (Cryo-EM) of RABV specifically indicates an average length of 198 nm and an average diameter of 75 nm (41). The lyssavirus genome consists of a single negative stranded RNA molecule consisting of about 12,000 nucleotides. Transcription of the viral genome gives rise to a short leader RNA and five monocistronic, capped, and polyadenylated messenger RNAs (mRNA) which encode five viral proteins; Nucleoprotein (N), Phosphoprotein (P), Matrix Protein (M), Glycoprotein (G) and Large polymerase (L). The N, M and L proteins are conserved in structure and length across each of the lyssaviruses, whilst the P and G proteins vary in length (42, 43). Lyssaviruses exhibit a conserved order of genes, with the N gene at the 3' end, followed by P, M, G, and finally L at the 5' end (Figure 1.2). This conserved order has been speculated to have a role in the control of protein expression (44). In terms of viral composition, the viral RNA genome forms the backbone of the ribonucleoprotein (RNP) core (tightly coiled RNA associated with proteins) and extends along the longitudinal axis of the bullet-shaped virus particle. The N, P, and L protein components are associated with the viral RNA and surrounded by the viral proteins, M and G, and lipoprotein components derived from the cell membrane that constitute the outer envelope of the virion. The most abundant protein in the RNP core is N (~1325 copies), followed by P (~691 copies), and L (~25 copies) (45).

A

Family *Rhabdoviridae*

Genome Organisation

Nucleotides



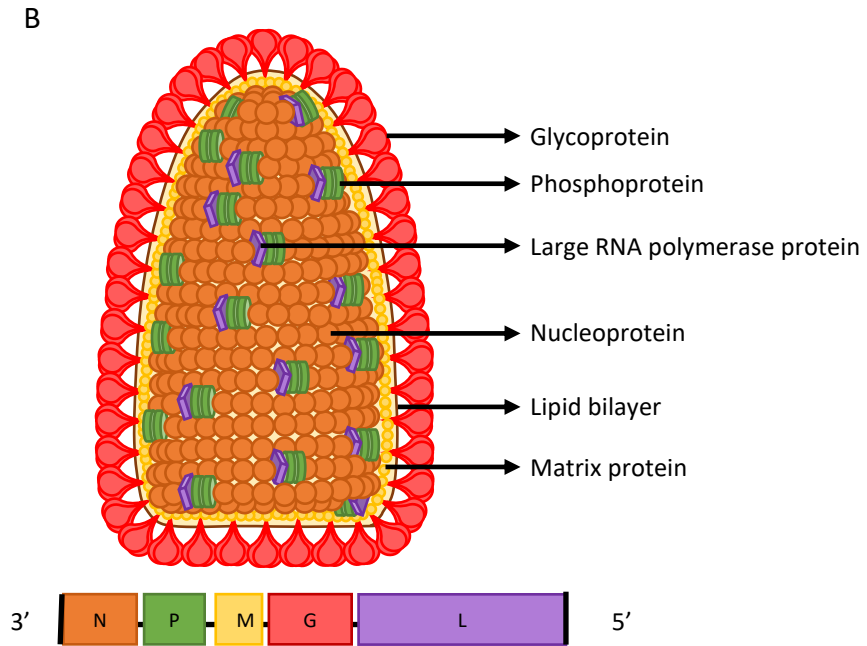


Figure 1.2: (A) Genome organisation of a selection of virus species within the family *Rhabdoviridae*. The total genome length and gene ORF sizes (N, P, M, G, L) are not shown to scale. Number of nucleotides and the accession number of an example virus are also stated next to genome schematics; extra genes are coloured blue. Adapted from (16). (B) A pictorial representation of a mature RABV virion. Adapted from (7).

Cryo-EM has also revealed the directionality of the virus RNA in the virion where the 3' end resides at the conical tip of the bullet and the 5' end resides at the planar end (41). However, it has been previously reported that low level incorporation (2% of all mature virions) of positive single stranded (ss) RNPs into mature virions does occur (46). Alongside standard bullet-shaped virions, truncated defective virions can also be produced *in vitro*. These defective virions are often cone-shaped and contain shorter RNA genomes as a result of internal sequence deletions or genome truncations (47-49). Some defective virions can interfere with the production of standard virions and become the dominant particle type in cell culture (50, 51). These are known as defective interfering (DI) virions (50, 52).

1.1.2.1 The Nucleoprotein

The amino acid sequence of the lyssavirus N protein is the most conserved of the of the lyssaviruses proteins (42, 53). Despite a high degree of genetic diversity of short segments of the N gene, a high level of amino acid sequence conservation of the N protein is required to retain key functions such as the specific protein-RNA genome interactions (54, 55). With an amino acid identity of 78-93% across the lyssavirus genus, N is an important diagnostic target for the laboratory diagnosis of rabies. In addition, the diversity of the N gene is the minimum criteria for lyssavirus species definition using polymerase chain reaction (PCR) and nucleotide sequencing techniques (55-58). Additionally, the quantity of N mRNA exceeds the quantity of the mRNA encoding other viral genes and consequently is more likely to be detected by PCR.

The lyssavirus N gene consists of 1421 nucleotides which encodes an open reading frame (ORF) of 450 amino acids (1350 nucleotides). These amino acids fold to form the N protein with a molecular weight of 50.5 kDa (59). In the cytoplasm, the P protein associates with the N-terminal domain of the N protein and acts as a chaperone to

maintain the soluble form of N (60). Whilst N is associated with P, the cleft between the N- and C-terminal domains of the N protein encapsidates the RNA genome into an RNase-resistant RNP core. Five basic residues of the RNA binding cavity associates with 9 nts of the viral RNA to coordinate the N-RNA interaction.

Phosphorylation of N at Ser389 by a cellular kinase promotes stabilisation of the interaction between N and P during the RABV replication cycle (61). Inside the virion, the L protein is also associated with RNP via binding to the P protein, to form the minimal essential replicative unit where the L protein acts as the viral RNA-dependent RNA polymerase (62).

The abundance of N in the infected cell plays a role in the regulation of transcription and replication by interacting with the leader RNA sequence of the lyssavirus. The leader RNA sequence is encapsidated when there is an abundance of N protein available in the cell, resulting in a switch from the transcription of monocistronic mRNA to the transcription of the full-length RNA antigenome (cRNA). Consequently, mRNA production is thought to halt and replication would begin using the full length positive sense antigenome strand as a template (7, 62, 63).

1.1.2.2 The Phosphoprotein

Conserved in all lyssaviruses, the P gene, located downstream of N, has at least five in-frame start codons, resulting in the translation of the full length P protein (P1) and four less-abundant isoforms (P2-5). The P protein is multifunctional and multifaceted. P consists of 297-303 amino acids, is the least conserved protein of the five viral proteins, and forms the non-catalytic subunit of the viral transcriptase complex (64, 65). The P2-5 isoforms do not interact with the L protein but instead are involved in immune evasion (66). Structural analysis shows that the P protein exists as either a dimer or tetramer in order to bind N and L (67, 68). The primary function of the P protein is as part of the

RNA polymerase complex, whereby P plays a pivotal role in stabilising the L protein to facilitate the interaction with the N-RNA template (69, 70). Additionally, the P protein interacts with N protein and acts as a chaperone to ensure N binds only genomic RNA, preventing N polymerisation and non-specific binding to cellular RNA (42, 71, 72). Like other negative sense RNA viruses, P exists in two forms depending on the degree of phosphorylation (73). The hypo-phosphorylated form has a molecular weight of 37 kDa whilst the hyper-phosphorylated form has a molecular weight of 40 kDa (61). The N-terminal domain of P is phosphorylated by two types of protein kinases: a unique protein kinase designated RABV protein kinase and protein kinase C (61, 73). Both RABV-protein kinase and the delta isoform of protein kinase C were found to be selectively packaged in mature rabies virions.

There is evidence to suggest that the P protein also interacts with host cell proteins to modulate cellular pathways. Previously, intracellular microtubule-dependent virus transport was suggested to occur through an interaction with the host dynein light chain LC8 and the P protein however more recently, deletion of the LC8 binding domain did not change RABV entry into the central nervous system (CNS) (74-76). Other host proteins that P associates with are the L9 component of the 60S ribosome, the mitochondrial complex I, and focal adhesion kinase; primarily to modulate or aid viral replication (77-79).

Finally, it is well established that the P protein also plays a critical role in counteracting the host-innate immune response, specifically the type I/III interferon system. The sensing of pathogen- or danger-associated molecular patterns (PAMPs and DAMPs) activates interferon (IFN) signalling cascades to stimulate the transcription of either antiviral and/or immune stimulatory genes. RABV P acts as an IFN antagonist by binding and retaining phosphorylated Signal transducer and activator of transcription 1

(STAT1) in the cytoplasm or preventing DNA binding STAT1 in the nucleus in order to prevent IFN induction and response (64, 80, 81). Additionally, P interferes with the phosphorylation of serine 386 of the IFN regulatory factor IRF-3, effectively counteracting IRF-3 activation (82).

1.1.2.3 The Matrix protein

The M protein is the smallest of the 5 proteins, with a molecular weight of 23-24 kDa. Across the genus, the M gene is relatively conserved with an amino acid percentage identity of 92.3% (59). The multifunctional M protein is able to interact with the N protein and the cell plasma membrane to form a layer between the RNP core and the G protein (83). This RNP-M protein complex not only holds the virion in its distinct bullet shaped form but it also mediates virus assembly and budding through interactions with the G protein tail at the cell membrane to produce progeny virions (84, 85). The first motif to be associated with virus budding was a proline-rich motif (PPEY) located at amino acids 35-38 near the N-terminus (86, 87). Other proline-rich motifs termed late-budding domains (L domains) are also found in the M protein of related rhabdovirus, vesicular stomatitis virus (VSV) (88). These domains interact with components contributing to the endosomal sorting complex required for transport (ESCRT) pathway to promote RNP recruitment and virus budding (89). Whilst the M protein is the only viral protein required for virus budding, the interaction of RNP-M with the G protein enhances virus budding efficiency and subsequently increases virion production (85, 90). Notably, heterologous G proteins of other lyssaviruses can replace the homologous G protein to produce mature virions, indicating that the interaction between M protein and G protein does not need to be optimal (23, 91-93).

It has also been suggested that the M protein, in addition to the N protein, may play a role in the switch from transcription to replication (94, 95). Whilst the molecular

mechanisms behind this phenomenon are still unresolved, the association of M with RNP would inhibit transcription of viral RNA and likely prompt contribute to the shift to replication (94). In addition, upon infection, the dissociation of M from the RNP, promoted by the host cellular protein V-type proton ATPase catalytic subunit, allows transcription to occur (96).

Like vesiculovirus, lyssavirus M is also speculated to play a role in inhibiting type 1 IFN signalling and may also be involved in the early induction of TRAIL-mediated apoptosis of infected neurons (97, 98).

1.1.2.4 The Glycoprotein

The fourth gene of the lyssavirus genome encodes the transmembrane envelope G protein. The G protein is comprised of 512-524 amino acids, including an N-terminal 19-amino acid signal peptide (SP) domain, and has a molecular weight of 65 kDa (42, 65). It has been estimated that there are approximately 1205 G molecules associated with 1148 M molecules per virion (45). The G protein is the sole protein present on the virion surface and predominantly exists as a trimer where it mediates viral assembly, cell attachment, and cell entry (99, 100).

After translation, the SP domain, a membrane insertion signal, facilitates the transport of the nascent G protein into the endoplasmic reticulum (ER) where the G protein trimerises and the SP domain is cleaved in the Golgi apparatus (101, 102). The trimeric conformation is then further stabilised by lateral interactions on the virion surface (103, 104). Additionally, the G protein is the only glycosylated protein and is glycosylated with branched-chain oligosaccharides, which account for 10-20% of the total mass of the protein. The resulting conformation of G on the virion surface is that of a type I membrane G protein, with an N-terminus ectodomain, a 22 amino acid transmembrane domain (TM), and a 44 amino acid cytoplasmic C-terminal domain (CD) (105).

The primary role of the G protein is to mediate virus-cell interaction (106). Initially, the G protein exists in a pre-fusion conformation, as either a monomer or a trimer, allowing it to readily attach to host cell receptors (107). In close proximity to the plasma membrane, the G protein adopts the activated hydrophobic conformation in response to a lower pH in the endosome, whereby G can directly fuse with the membrane to eventually form the post-fusion conformation (108, 109). The G protein, through its interactions with M, is studded throughout the virion envelope during the virus budding process (85).

Because the G protein sits on the surface of the virion, the pre-fusion conformation of G is the primary target for VNAs (26, 110). Unlike the other proteins which aid to evade the immune system, the G protein is the main immunogenic component of the virion as it is a major activator of the immune system resulting in the production of VNAs (111, 112). The G protein is of the most extensively studied lyssavirus protein in terms of its structure, immunogenicity, and antigenicity for VNAs because it is a potent immunogen capable of inducing the host immune response against virus infection.

Of the five proteins, the G protein is the one of the least conserved proteins and this is thought to cause the varying pathogenicity and neuroinvasiveness between specific RABV strains and across the lyssavirus genus (92, 113, 114).

[1.1.2.4.1 Antigenic sites on the glycoprotein](#)

The G protein is the sole inducer and the primary target of host neutralising antibodies.

The exact regions of the G protein responsible for the differences in antigenicity across the phylogroups is poorly defined. Not only is the G protein ORF relatively conserved across the genus but each lyssavirus G protein contains 14 conserved cysteine residues that contribute to its structure and 5 antigenic sites (Figure 1.3). Moreover, the G protein induces VNAs that recognise both conformational and linear epitope antigenic sites.

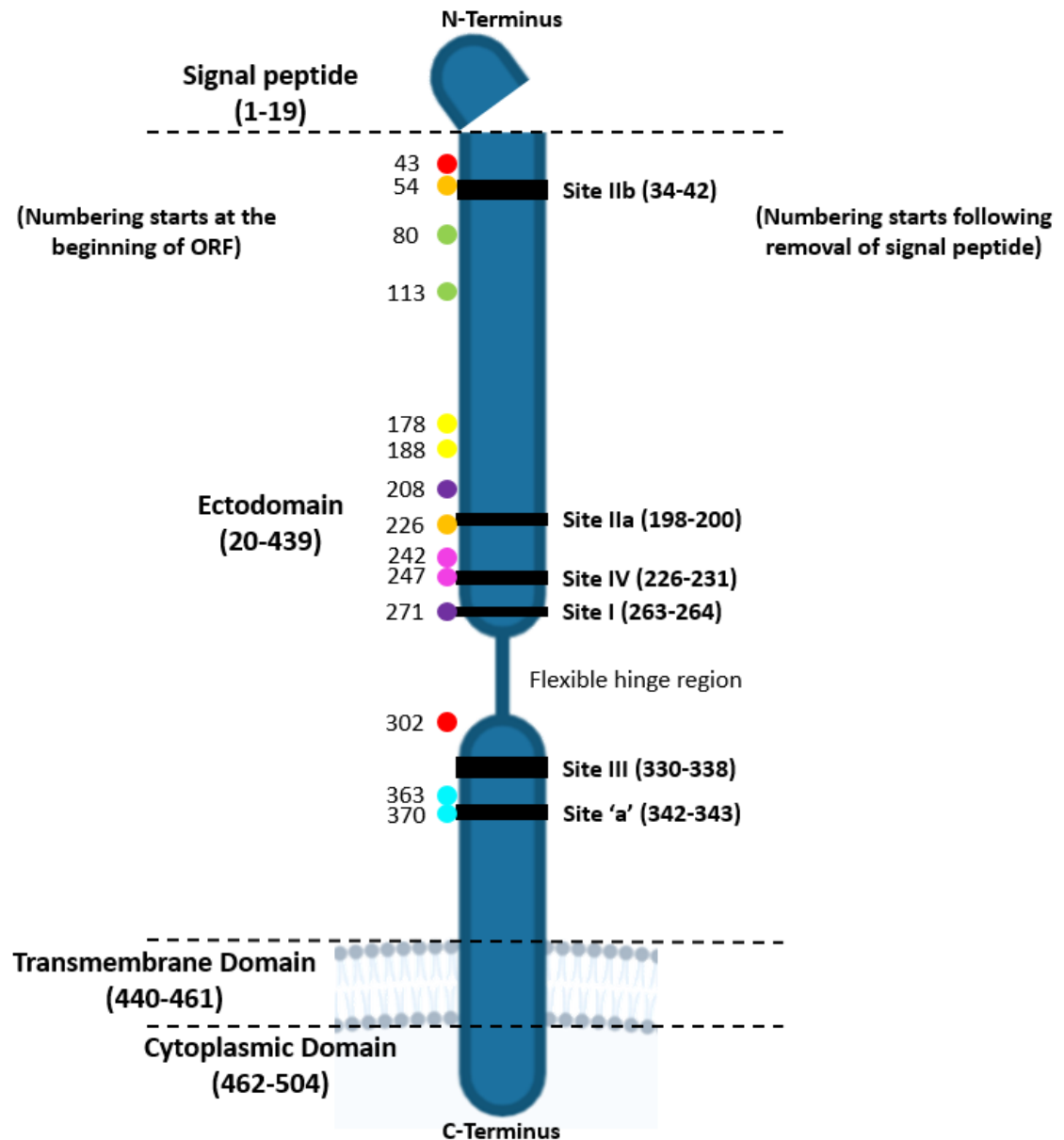


Figure 1.3: Schematic representation of the lyssavirus G protein. Defined antigenic sites and conserved cysteine residues are shown. Cysteine residues are coloured according to proposed disulphide linkages within the mature protein. TM: transmembrane; N-terminus: amino terminus (NH₂); C-terminus: Carboxyl-terminus (COOH). Adapted from (115).

Historically, monoclonal antibodies (mAb) have been used to map these antigenic sites (26, 116). This technique has identified four major antigenic sites, site I, II, III and IV and one minor antigenic site, site 'a' in the ectodomain of the G protein (Table 1.3).

Antigenic site I contains conformational epitopes as well as a linear epitopes. The mAb, CR57, recognises the linear epitope (26), whilst the mAb 509-6 can successfully delineate the conformational epitope found at amino acid position 226-231 (26). The potent neutralising antibody, 62-713, proposed as a potential candidate for use as a human rabies immunoglobulin (HRIG) alternative in post-exposure prophylaxis (PEP) when used as a cocktail with other potent neutralising antibodies, also specifically targets antigenic site I (117).

Antigenic site II is the discontinuous conformational epitope of the two major conformational antigenic sites. It extends from amino acids 34-42 (domain IIa) and from amino acids 198-200 (domain IIb) and is recognised by the neutralising antibody E559 (26, 117, 118).

The second major conformational epitope is antigenic site III. Antigenic site III is continuous and extends from amino acids 333-338, forming a loop on the surface of the protein (119). Whilst no mAbs that bind the unfolded antigenic site have been characterised, neutralising antibodies and neuronal receptors can bind the tertiary structure of the fully folded protein (26).

Table 1.3: Amino acid sequence of the lyssavirus antigenic sites. The amino acid sequences are given. The residues coloured in red are those that differ from the RABV sequence, given in the top row.

Virus	Phylogroup	Site IIb	Site IIa	Site I	Site IV	Site III	Site 'a'
RABV	I	GCTNLSGFS	KRA	KLCGVL	FR	KSVRTWNEI	KG
GBLV	I	GCTSLSGFS	KKA	KLCGIS	FH	KSVRAWNEI	KG
ABLV	I	GCTSLSGFS	KKA	KLCGIS	FN	KSVRTWDEI	KG
KHUV	I	GCTTLSGFT	KRA	KLCGVS	FH	KSIREWKEI	KG
ARAV	I	GCTTLTAFS	KKA	KLCGVM	FH	KSVREWTEV	KG
BBLV	I	GCTTLTVFS	KKA	KLCGVS	FH	KSIRQWTEI	KG
EBLV1	I	GCTTLTPFS	KKA	RLCGVP	FH	KSVREWKEV	KG
DUVV	I	GCTTLTPFS	KKA	RLCGIS	FH	KSVREWKEI	KG
IRKV	I	GCTTLTAFN	KKA	KLCGMA	FH	KSIREWSEI	KG
TWBLV	I	GCNTLSSF	KMA	KLCGIS	FR	RSIRNWTEV	KG
EBLV2	I	GCTTLTVFS	KKA	KLCGIS	FH	KSIREWTDV	KG
SHIBV	II	GCSSSTFS	KKS	TLCGKP	NR	KRVDRWEI	KG
MOKV	II	GCNAESSFT	KKA	TLCGRP	DR	KRVDKWADI	KG
LBV B	II	GCGTSSVFS	KKS	TLCGKP	NR	LRVDSWNDI	KG
LBV A	II	GCSETSSFT	RKA	TLCGKP	NR	KRVDNWVDI	KG
LBV C	II	GCSDTATFS	KKS	TLCGKP	NR	LRVDSWNDI	KG
LBV D	II	GCSTSTFS	RKA	TLCGKP	NR	RRVDNWTDI	KG
IKOV	III	GCNEGSKVS	ILL	IICGKS	VK	KSVDNWTDI	PI
WCBV	III	YCTTEQSIT	KLV	SICGRQ	IK	IKVENWSEV	KG
LLEBV	III	NCTDHGEIN	RLF	TICGKS	TK	KSVSNWSEI	PI

Antigenic site IV is poorly defined. Though it is widely defined as residues 263-264 and a continuous epitope; it has also been suggested that it contains overlapping linear epitopes at residues 251 and 264 (120, 121). Another study suggests that antigenic site IV comprises of solely amino acid 251 (122). This suggests that more conclusive evidence may be required to reveal the exact location of antigenic site IV.

Minor site 'a' includes amino acids 342-343 and is bound by several mAbs including mAb 40E1. Minor site 'a' is in close proximity (3 amino acids) to site III but does not have any overlapping epitopes (26).

1.1.2.5 The Large Polymerase

The largest gene within the lyssavirus genome encodes 2142 amino acid long protein known as the L protein (123). Alongside transcription as an RNA dependent RNA polymerase (RdRp), the large polymerase also functions as a mRNA methyltransferase and mRNA guanylyltransferase to cap and methylate the 5' end of the mRNA and a poly(A) synthetase to polyadenylate the 3' end (124-126). This process ensures that the viral mRNA is 'disguised' as host mRNA and subsequently recognised by host machinery. Despite the fact that 54% of the viral genome is solely responsible for encoding the L protein, the rhabdoviral L protein, is structurally homologous to other members of the mononegavirales, (123, 127). Based on similar identity to VSV and the Sendai virus, it is suggested that the L protein undergoes a vital conformational change when bound to the P protein for activation, thus reflecting an optimal shift in positioning of the L domains for efficient RNA synthesis (128).

1.1.2.6 Genomic Diversity

Whilst lyssaviruses are generally highly conserved, due to the error prone nature of the RNA dependent RNA polymerase, RNA virus populations can harbour a heterogeneous RNA populations within a single species (129). Historically, this phenomenon was referred to as ‘viral quasispecies’ but a more accurate term would be ‘viral heterogeneity’ (130-132). Viral heterogeneity, a nucleotide sequence variation of the viral genome, was initially suggested to confer some means of adaptation to a new host, particularly significant in host spillover events (133-135). Previous studies have suggested that due to viral heterogeneity, different variants of the same virus species have a more defined function in the pathogenesis of the species as a whole and determine cellular/host tropism. In this context, a study where mice were persistently infected with lymphocytic choriomeningitis virus (LCMV) showed that different variants of the same LCMV strain were responsible for the infection of different cells (136, 137). However, there is a lack of evidence that this is the case for lyssaviruses. Studies have shown that transmission between species, such as a dog and a fox, do not rely on host-specific residues in the RABV genome and therefore contributes to the lack of evidence for positive selection (135).

The differences in the non-coding regions of the lyssavirus species is a more plausible rationale for the adaption to particular host species. The untranslated regions represent 8.6-11.4% of the lyssavirus genome and although the lyssaviruses have highly conserved initiation and termination signals, the vast majority of the genome length variation between species is found in these non-coding regions (21, 42). Rich in adenine and uracil, the main function of these untranslated regions is to regulate transcription and replication. Leader RNA interacts with the N protein to activate the switch from transcription to replication as well as the complementary termini which also promote replication (138).

1.1.3 Life Cycle

Once the virus has been transmitted to a new host, the virus replicates at the wound site in muscle cells before entering motor and sensory neurons, predominantly by receptor-mediated endocytosis (139). Alongside neuromuscular junctions (NMJs), RABV has also been detected in sensory nerves and, *in vitro*, both retrograde and anterograde axonal transport have been observed (140, 141). Further, *in vivo* anterograde trans-synaptic transfer, in sensory neuronal circuits, has been shown (142). Following entry into neurons, the virus travels in a retrograde manner at a rate of approximately 50-100mm per day along axons via microtubules (74, 143, 144). Host factors including the dynein light chain, LC8, within the microtubule network are proposed to facilitate this transport (75). From replication sites, nascent viral RNP (the viral RNA associated with several essential viral proteins) is transported to post-synaptic membranes for virion assembly and trans-synaptic transmission to other neurons in a viral G protein dependent manner (145, 146). This process includes budding in the synaptic cleft and subsequent receptor mediated entry at pre-synaptic membranes. Once the virus reaches the brain, RNPs are released into the neuronal soma allowing primary transcription and replication to occur. Here, cytoplasmic inclusion bodies (IB) are formed and the virus spreads via cell-cell transmission or trans-synaptically throughout the brain (147). After CNS infection, the virus spreads centrifugally to other areas of the body such as the salivary glands for onward transmission (148). The sequence of events in the lyssavirus life cycle can be categorised into three phases. The first phase includes virus attachment and entry into host cells, the second phase includes transcription and replication of genomic RNA, and the third phase includes virus assembly and egress from the infected cell (Figure 1.4).

1.1.3.1 Cell Entry

The bite of rabid animal usually delivers the virus directly into striated muscles and connective tissue, though infection can still occur from a single abrasion of the skin. Following virus transmission into the host, the lyssavirus may enter a neuron directly or initially replicate in muscle cells before entering the neurons in larger quantities (149). This is speculated to be one of the factors that affects the duration of the incubation period. The lyssavirus G protein is exposed on the surface of the virus as a trimer and denotes neurotropism by playing a critical role in virion attachment and entry into host cells (150). Since the pathogenesis of lyssaviruses depends upon neuronal cell entry, the G protein is considered a major virulence factor (151). *In vitro*, there is evidence that the virus can enter peripheral motor neurons through NMJs and has also been reported in sensory spindles, stretch receptors and proprioceptors (152).

For entry into neurons four molecules have been proposed as receptors to the G protein: the Neural cell adhesion molecule (NCAM), present at NMJs; the Nicotinic acetylcholine receptor (nAChR), involved in peripheral nervous system (PNS) and CNS signalling; Metabotropic glutamate receptor 2 (mGluR2), an autoreceptor for glutamate in the brain; and the p75 Neurotrophin receptor (p75NTR), although, evidence for the latter is controversial and other undefined receptors are likely to be involved (149, 153-158). These receptors, with the exception of mGluR2, are not exclusive to neurons and can be expressed on cells in the skin dermis, suggesting a close proximity to infection sites, however the extent to which these receptors are used by lyssaviruses remains to be defined (159-161).

After binding receptors, the virus is internalised by receptor-mediated endocytosis (162). However, like VSV, multiple lyssavirus virions may enter through a single coated pit (viropexis) or uncoated vesicle (pinocytosis) (163). Fusion is activated in the

acidic environment (pH 6.3-6.5) of the endosomal compartment by a reversible change in G protein conformation (162). The G protein has been shown to adopt three different conformational states that each play a role in virus entry (108). The pre-fusion “native” state, due to a neutral environment (pH 7), allows the G protein to engage with the host cell receptor (164). Following initial acidification in the endosome, the G protein is “activated” to a hydrophobic state and adopts a structural conformation that exposes necessary hydrophobic residues (108). As part of the initial steps of fusion, this allows the virion to interact with the hydrophobic target endosomal membrane and expose the fusion domain. A fusion pore develops as a direct result of further rearrangements of the G protein and the close proximity of the viral and cell membrane (164). The transition from virus interaction to the generation of the fusion pore requires the correct folding of the G trimers and is a high-cost energy step. Additionally, more than one trimer is required to form a functioning fusion site (108). The G protein adopts the final, post-fusion (fusion-inactive) conformation once it’s been exposed to a low pH for a longer time period and appears longer than the other conformational states (108). Unlike other viruses, this conformational change is reversible when the pH is returned to a pH of 7 and above (165). Fusion initiates the release of the RNP into the cytoplasm which allows initiation of transcription (166, 167).

1.1.3.2 Transcription and Replication

The lyssavirus genome is a linear, negative-sense, single-stranded RNA which cannot be directly replicated using host machinery. As the tightly coiled RNP molecules are released into the cytoplasm, the M protein dissociates and they form a loosely coiled helix structure, conceivably to facilitate transcription and replication of the viral genome (168). With approximately 50 RNP-associated RNA polymerases (L protein), the L protein initiates the transcription of leader RNA and the 5 viral genes where 5'-capped and polyadenylated monocistronic viral mRNA transcripts are sequentially produced

(162). This process in the replication cycle is known as primary transcription. As the transcriptase recognises the start and stop codons, the protein transcripts are generated consecutively (169). The polymerase shutters back and forth on the poly-A signal (stop signal) which consists of a run of U's to form a 50-150nt poly-A tail (170). As shown for VSV, the polymerase then travels down to the next restart signal where it initiates transcription of the next protein by adding a 5'-m7G cap whilst releasing the previously transcribed mRNA (171). This results in the intergenic sequences being left untranscribed. The dissociation and re-association of the polymerase with the RNP can reflect a gradient effect of transcriptional efficiency (162). Consequently, this leads to the typical transcript gradient in which the 3' proximal genes are transcribed more abundantly than those of distal genes at the 5' end, resulting in different protein abundances. It is suggested that the conserved gene order reflects the relative protein amounts required in the replication process, with the intergenic sequences being a major factor in determining polymerase effectiveness. Lyssaviruses mostly have intergenic sequences of 2nt at the N/P border, 5nt at the P/M and M/G border and 19-28nt at the G/L border. As a consequence of this phenomenon, the L protein is the least expressed as the larger intergenic sequence (at the G/L border) promotes dissociation of the polymerase (94).

Following primary transcription, the viral mRNA is translated using the host cell machinery. The N, P, L and M proteins are translated on free ribosomes in the cytoplasm, whereas the G protein is translated on membrane bound ribosomes associated with the ER (65). The G protein is co-translationally imported into the ER lumen where chaperones mediate G monomer folding and modification at specific asparagine residues by core glycosylation and asparagine-glycan processing (172). Finally, the G protein has N-linked carbohydrate chains processed in the Rough ER and the Golgi before being transported to the cell membrane. The nascent G protein assumes

the fusion-inactive conformation, protecting the G post-translationally from fusing with the Golgi vesicles whilst it's being transported to the cell surface where it then assumes the "native" conformation and structure (173, 174). The G protein forms a trimer and exposes its glycosylated ectodomain on the exterior of the cell membrane (175).

A study also suggests that the M protein may interact with the eukaryotic translation initiation factor, eIF3h, to inhibit the translation of host cell mRNAs that have a Kozak-like 5'-UTR (98). This would make the host cell machinery more readily available for the translation of viral mRNAs, increasing the abundance of viral proteins. The accumulation of viral proteins forms inclusion bodies or Negri inclusion bodies (NB) in neurons, which grow larger over time and represent active viral factories (147, 176).

The IBs contain all components for replication (N, P, L, M proteins, viral RNA, complementary RNA, mRNA, and some cellular proteins) (79). IBs have been shown, by live-cell imaging processes, to eject viral nucleocapsids where they are later transported along microtubules to form either new virions or secondary IBs (177).

In later phases, there is a switch from transcription to replication. The exact mechanism responsible for this shift is unknown, though there are different hypotheses. Some studies suggest that the M protein is responsible for the shift of the L protein to a replicase (94). The association of M causes the L protein to become a RNP dependent RNP polymerase as it becomes associated with P-N heteromers, rather than a RNP dependent RNA polymerase which is associated with just P (69, 162, 178). The abundance and continued synthesis of N is also a factor affecting the switch to replication. Following the primer independent synthesis of the antigenome, the positive sense antigenome and the negative sense genome are encapsidated by N to form new RNPs. The P protein chaperones N in this process (162). Before, the accumulation of large quantities of N, this process is not possible.

The positive sense RNP is then used for templates for further synthesis of either, the genome, or more viral protein transcripts (secondary transcription). The negative sense RNP is encapsidated into progeny virions (7).

1.1.3.3 Virus Egress and Migration

The M protein is mainly responsible for virus assembly and budding and is found in the cytoplasm, nucleus and IBs (7). Virus assembly starts with the formation of RNP, which is closely followed by the association of M to the RNP. First, the association of M initiates promotes a shift from transcription to replication (162). It is possible that the differential conformational folding of the monomer M, M α and M β may provide the rationale for the multiple regulatory functions of M (179). RNP-M is localised to the cellular membrane where it accumulates. The RNP is then tightly coiled by M, halting the activity of L. For this particular function, M may exist as a dimer where it also bridges the RNP and the cytoplasmic tails of glycosylated trimeric G (85).

Once the mature virions bud through the cell membrane to acquire the lipid bilayer envelope, the M, G, and helical RNP interaction is thought to influence membrane curvature and the bullet morphology of the virus (7). As well as budding through the plasma membrane, virions can also egress through the normal secretory pathway by budding through ER or Golgi membranes into the lumen of the vesicles produced to produce mature virus particles (162). It is also possible that the M localises the RNP to a region of the cell membrane where the G protein trimers are not expressed, resulting in a spikeless, non-infectious particle (90).

Following CNS infection, RABV can spread in a G-dependent anterograde manner to peripheral organs or to the mandibular glands where RABV can spread to the salivary glands and be excreted into the oral cavity (140, 141, 180).

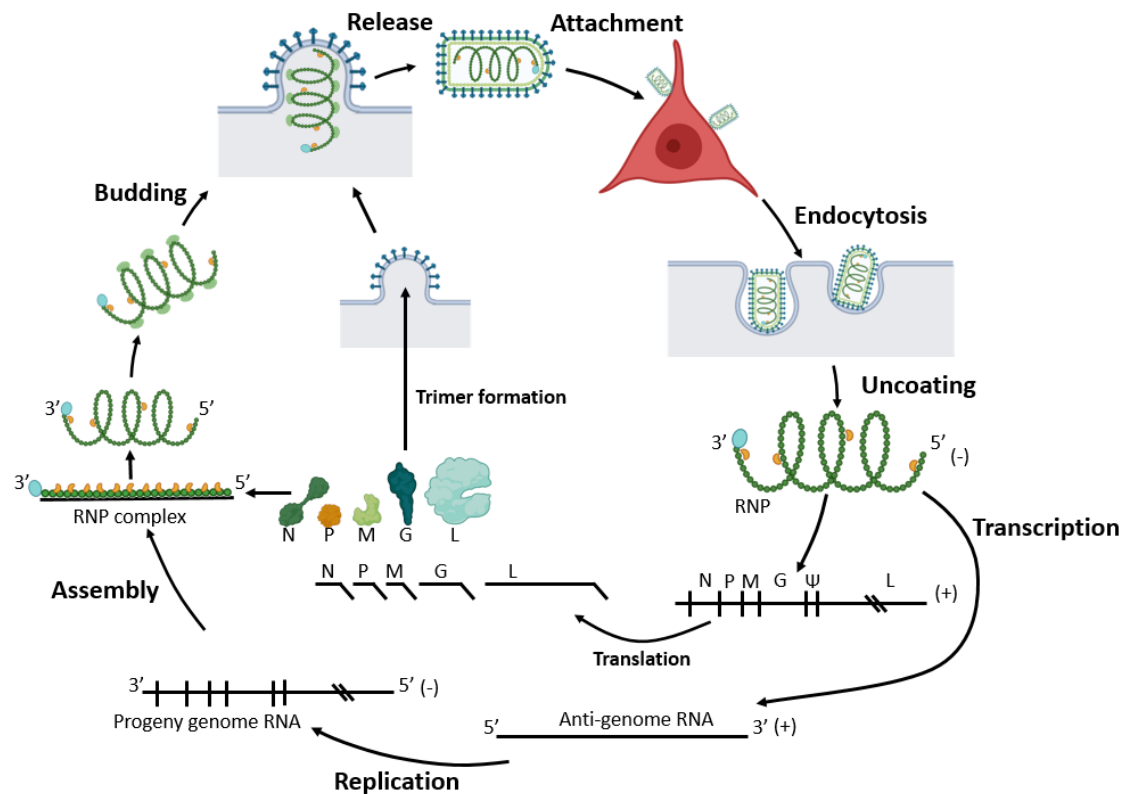


Figure 1.4: Rabies life cycle in the cell. Following attachment to cell surface receptors, mediated by the glycoprotein, the virus enters the cell through endocytosis. After internalisation, the virus is uncoated, releasing the helical nucleocapsid within the RNP core. From the viral genome, the five viral genes are transcribed into positive sense monocistronic mRNA and the positive sense antigenome is transcribed to act as a template for replication. The five viral proteins are translated from their respective mRNAs. After the negative sense progeny virus genome is generated, it is encapsidated by the N-P complex. L is then incorporated to form progeny RNP. M binds and condenses RNP and links to the trimeric G in the plasma membrane on the cells surface for assembly into virus particles (virions). Virions bud from the plasma membrane and are released from the infected cell. Adapted from (162).

1.1.4 Epidemiology

Fifteen of the 17 lyssaviruses are maintained by chiropteran hosts (bats). The geographical location and reservoir hosts are quite well documented for some lyssaviruses, however for some, information is lacking due to the recovery of only a small number of isolates. The infection of non-RABV lyssaviruses in other mammals, including humans and cattle, are cases of cross-species transmission (11). These cases usually result in dead end infections as a result of the fatal clinical disease outcome (7). Some studies have suggested that barriers to epizootic spread consist of mountain ranges and waterways whilst the human mediated movement of animals and mass human migrations can increase the rate of disease spread (181). Globally, the lyssaviruses remain abundant in chiropteran hosts and certain bats are protected under law (182). This, in part, supports the paradox that the complete eradication of lyssaviruses is an unattainable target.

1.1.4.1 Rabies epidemiology

In contrast to some lyssaviruses, RABV is reported globally and maintained in mesocarnivores (animals whose diet consists of 50-70% meat). This can include dogs, foxes, racoons, racoon dogs, skunks, mongooses and across the New World within multiple bat species (11). Vaccination in domesticated dog populations in parts of Western Europe and the USA has eliminated the presence of RABV in the domestic carnivore population. In Western Europe however, prolonged and widespread campaigns to vaccinate the wildlife population has led to the elimination of sylvatic rabies. Terrestrial RABV is maintained in populations of skunks, gray foxes, polar foxes and raccoons in North America and populations of marmoset and species of fox in South America (183). Rabies in the Americas is also associated with the infection of insectivorous; hematophagous; and, to a lesser extent, frugivorous bats. Interestingly, of

the 17 classified lyssaviruses, only classical RABV has been reported in the Americas, and the current bat population represents an omnipresent source of RABV infection, for which elimination options are very limited. Worldwide, there are seven main RABV lineages, each with multiple variants that are associated with a particular geographical location (184). The most widespread lineage circulates in Europe, Africa, Asia and the Americas in dog, fox, jackal and skunk populations (185).

1.1.4.2 *Lyssavirus epidemiology*

Along with RABV, four other lyssaviruses have been genetically characterised within Europe; European bat lyssavirus type-1 (EBLV-1), European bat lyssavirus type-2 (EBLV-2), Bokeloh bat lyssavirus (BBLV), Lleida bat lyssavirus (LLEBV), and West Caucasian bat virus (WCBV).

EBLV-1 is associated with the infection of *Eptesicus serotinus* and *Eptesicus serotinus isabellinus*, the Serotine bat. Early genomic sequencing revealed two distinct lineages of EBLV-1; EBLV-1a and EBLV-1b, which had different geographical regions. EBLV-1a is mostly found in northern Europe but has an extensive West-East geographic range, with detections in, France, the Netherlands, Denmark, northern Germany and Poland (186, 187). EBLV-1b is genetically more heterogeneous and exhibits a North-South distribution as it's located predominantly in France, South-western Germany, central Poland, and Spain (186, 187). The infection of a second bat species, *Eptesicus isabellinus*, the Meridional Serotine bat, may indicate the circulation of a third EBLV-1 lineage, EBLV-1c (188). Certainly, EBLV-1 continues to be discovered in new areas, including five detections in England among Serotine bats between 2018 and 2020 (unpublished data, APHA). Additionally, EBLV-1 has also been reported from a variety of bat species in Spain, including *Rhinolophus ferrumequinum*, the greater horseshoe bat, *Myotis myotis*, the greater mouse-eared bat, *Myotis nattereri*, Natterer's bat, and

Miniopterus schreibersii, the common bent-winged bat (189, 190). Spillover to terrestrial mammals and humans is very rare. There have only been a few isolated incidents of EBLV-1 in a Beech marten, sheep, domestic cats and three confirmed human casualties (25, 182, 191, 192). Moreover, terrestrial mammals such as foxes, ferrets, cat and dogs exhibit limited susceptibility to infection (191).

EBLV-2 was originally isolated from *Myotis dasycneme*, a Pond bat, in the Netherlands (193, 194). However, EBLV-2 is predominantly associated with the infection of *Myotis daubentonii*, Daubenton's bats, detected sporadically across Northern Europe and is considered enzootic within Daubenton's bat populations where detected. The virus has been detected in several countries including Switzerland, the United Kingdom, Germany, the Netherlands, and Finland; with the majority of the detections occurring in the UK (195-197). Like EBLV-1, an untreated EBLV-2 infection will result in a disease clinically indistinguishable from rabies caused by RABV infection. As for spillover events into humans, two fatal human infection cases have been reported (198, 199).

BBLV was first isolated in Germany from a Natterer's bat (*Myotis nattereri*) in November 2009 (200). BBLV has since been detected on nine further occasions, one from Poland, two from France and six from Germany, also within the Natterer's bat populations (201-204). In one case, BBLV was isolated from a common pipistrelle bat (*Pipistrellus pipistrellus*), however it is still unclear whether this was a spillover event or a cross-species transmission event. Antigenic cartography revealed that BBLV was antigenically distinct from all lyssaviruses but closely related to the phylogroup I lyssaviruses and genetic analysis of BBLV isolates indicate two different viral lineages of BBLV (33, 205).

As part of the rabies surveillance program in Spain, in 2012, a common bent winged bat (*Miniopterus schreibersii*) was reported to be positive for lyssavirus infection by the detection of nucleic acid alone (206). This genetic material was named Lleida bat lyssavirus (LLEBV) after it was shown to be genetically related to, but distinct from all the lyssaviruses and more closely related to IKOV and WCBV than to the lyssaviruses in phylogroups I and II (206, 207). Live virus was later isolated where it was determined that protection from existing vaccines was severely limited (39). LLEBV existed as a single detection until 2019 when a second isolate was reported from the same species of bat in France (208).

Lastly, evidence for another distinct lyssavirus in a Brandt's bat (*Myotis brandtii*) was reported following the detection of virus antigen and RNA in Finland in 2017 (19). Since the initial detection the full genome of Kotalahti bat lyssavirus (KBLV) has been determined although no live virus isolate has been recovered and consequently no virus isolate exists for KBLV (209). As a result, KBLV remains taxonomically unclassified.

In Eurasia, five further lyssaviruses have been isolated. This includes the Khujand virus (KHUV), isolated from a bat identified near Khujand, Tajikistan, in 2001 (21). It was initially believed that KHUV was found in whiskered bat (*Myotis mystacinus*) but following an update in the taxonomy of whiskered bats, it is suggested that KHUV may have in fact been isolated from a steppe whiskered bat (*Myotis auraszens*) (210).

Alongside KHUV, the Aravan virus (ARAV) was isolated in the Osh region of Kyrgyzstan in 1991 from a lesser mouse-eared bat (*Myotis blythi*) (211). Both ARAV and KHUV exist as single detections and as such there remains a significant lack of understanding regarding epidemiology and host range of the virus.

The Irkut virus (IRKV) was isolated from what was thought to be a greater tube-nosed bat (*Murina leucogaster*) in Irkutsk, Russia, in 2002 (211). These four lyssaviruses were shown to be genetically distinct from the current lyssaviruses but were closely related to the phylogroup I viruses. Following this detection, IRKV was isolated from a human rabies case reported in Russia, in 2009 (212). Also, following human deaths from bat-associated rabies, in 2012, bats of different species were collected in the Jilin Province of China (where the first bat-associated rabies case was reported). As a result, an Irkut lyssavirus was isolated from a greater tube-nosed bat and showed 92-99% nucleotide identity to the two isolates already available (213). Additionally, in 2018, a confirmed case of IRKV infection was documented in a rabid dog following after the dog had bitten a human (214). This event demonstrated the threat to animal and human health where a risk exists that non-RABV lyssaviruses may become established in a terrestrial carnivore host.

West Caucasian bat virus (WCBV) is a more divergent virus found in Eurasia. WCBV was isolated from a common bent wing bat (*Miniopterus schreibersi*) obtained from the Caucasus Mountains on the border between Russia and Georgia (211). In addition, *Miniopterus* bats, collected in Kenya, showed a prevalence of neutralising antibodies against WCBV, suggesting WCBV or a WCBV-related virus may be circulating in bats in parts of Africa. Approximately 17-26% of the bats collected in 4 of the 5 different locations were seropositive (215). Additionally, on the 23rd of June 2020, a cat from the Arezzo province, Italy was confirmed to have rabies. Sequencing of the virus showed 98.52 % identity with WCBV (216, 217).

Finally, Taiwan bat lyssavirus (TWBLV) was reported in 2016 and 2017 as part of an active surveillance program between 2014 and 2017. Both virus isolates were detected and isolated from Japanese house bats (*Pipistrellus abramus*) (218).

Whilst lyssaviruses have not been isolated in the South-East of Europe, numerous greater mouse-eared bats, *Myotis nattereri*, in Croatia were found to be seropositive against lyssaviruses. This suggests that lyssaviruses exist within this region of Europe and that further comprehensive analyses of lyssavirus distribution is required (219).

Due to the complete eradication of RABV in Australia, the lyssavirus burden comes from the Australian bat lyssavirus (ABLV). Found and isolated from five different bat species since initial isolation in 1996, ABLV is not restricted to a single host reservoir species (220). ABLV is associated with two distinct reservoir hosts, one insectivorous bat species, the yellow-bellied sheath-tailed bat (*Saccolaimus flaviventris*), and all four species of Pteropid bats found in Australia. In addition, early studies distinguished two distinct variants of ABLV, the pteropid variant that circulates in the Pteropid bats and the insectivorous variant that circulates in the yellow-bellied sheath-tailed bat (221-223). ABLV has also been the cause of three documented fatal human cases and has also been found in two horses in Queensland, raising concerns about the risk of transmission to humans (224-226).

In Asia, the Gannoruwa bat lyssavirus (GBLV) was detected in four Indian flying foxes (*Pteropus giganteus*) and isolated from three individual bat samples in Gannoruwa, Sri Lanka, in 2015 (227).

Across the African continent, five lyssaviruses have been detected. Arguably the most widespread of these lyssaviruses is the Lagos bat virus (LBV). This species is located across sub-Saharan Africa and has been isolated from a number of different bat species and is strongly associated with frugivorous bats (228). LBV was first detected in Lagos, Nigeria, in 1956 from a pool of African straw-coloured fruit bats (*Eidolon helvum*) brain samples (229). LBV has four genetically distinct lineages that are in some cases as

divergent as the other classified lyssaviruses (186). The ICTV dictates that isolates belong in the same species if they have identities higher than 80%, however, some LBV isolates are more divergent than this across the G gene, which may lead to re-classification in the future. Lineage A is strongly associated with the *Eidolon helvum* bat species and consists of the Senegalese (1985), French (imported from Africa) (1999), Kenyan (2007), and Ghanian (2013) isolates; lineage B is formed of just the Nigerian (1956) isolate (the first LBV isolate to be discovered); lineage C is strongly associated with the *Epomophorus wahlbergi* bat species has been detected in Central Africa Republic (1974), Ethiopia (1990), South Africa (1980, 2003-2006, 2008, 2013, 2014, 2017, 2018) and Zimbabwe (1986); and lineage D consists of a three isolates discovered in Kenya (2008 and 2010) and South Africa (2018) in Egyptian fruit bats (*Rousettus aegyptiacus*) (230-232). Additionally, LBV has been shown to exist in domestic animals such as cats and dogs as well as the terrestrial wildlife. LBV was isolated from a rabid African water mongoose (*Atilax paludinosus*) (233).

Duvenhage virus (DUVV) was initially discovered in 1970 after the fatal infection and subsequent death of a human following a bat bite in South Africa (234). Two further isolates were discovered in South Africa in a what was speculated to be a common bent-winged bat (*M. natalensis*) in 1981 and an Egyptian slit-faced bat (*Nycteris thebaica*) in 2012 (235). Moreover, another isolate was discovered in another Egyptian slit-faced bat in Zimbabwe, in 1986 (236, 237). Since the discovery of these isolates, there has been another two fatal cases of DUVV in humans; one was in 2006 in South Africa and the other occurred in 2007 in Kenya (238, 239). More recently, DUVV was detected in South Africa in an Egyptian slit-faced bat in 2012 (20).

Shimoni bat virus (SHIBV) was isolated in 2009 from a striped leaf-nosed bat (*Myonycteris vittatus* originally thought to be *H. commersoni*) in Kenya (230). Only a

single isolate of SHIBV has been detected. This detection and seroprevalence of *M. vittatus* to SHIBV suggests that *M. vittatus* is the reservoir host for SHIBV (240).

The Mokola virus (MOKV) is one of two lyssaviruses that have not been isolated from bats but other terrestrial mammals. MOKV was initially isolated from pooled organs from three shrews (*Crocidura flavescens manni*) in Nigeria in 1968. MOKV has since been isolated in domesticated dogs, cats, and one rodent but is yet to be detected in a bat species (5, 241, 242). Like DUVV, the majority of the isolates were discovered in South Africa (1970, 1995–1998, 2007, 2010, 2012, 2012, 2017) and Zimbabwe (1981–1982) but there have been intermittent cases in Ethiopia (1989–1990), Cameroon (1974), Nigeria (1968, 1969, 1972) and Central African (1983) Republic (243-246). Bats haven't been ruled out as the reservoir for the Mokola virus (6). More recently, serum samples were collected from *Gerbilliscus leucogaster* (Bushveld gerbils) rodents in South Africa and 87.80% were positive for the presence of MOKV neutralising antibodies, indicating a potential reservoir (242). There have been two recorded human cases of MOKV; in 1968 a 3-year-old girl survived MOKV and in 1971 a 6-year-old girl died from a MOKV infection. (247, 248).

Ikoma lyssavirus is the second lyssavirus that has not been isolated from a bat. Like Mokola, a Chiropteran host cannot be discounted, despite the only isolate originating from an African Civet (*Civettictis civetta*), detected in 2009 (4).

Lastly, evidence for another distinct lyssavirus in two Natal long-fingered bats (*Miniopterus natalensis*) was reported following the detection of viral RNA in South Africa in 2015 and 2016 (20). Until Matlo bat lyssavirus (MBLV) is characterised, it will remain taxonomically unclassified. The findings of the study suggested that a

shared N protein nucleotide identity of 80.9–81% with WCBV could result in MLBV being classified as a distinct lineage of WCBV rather than a new lyssavirus species.

1.1.5 Infection

1.1.5.1 *Transmission*

Rabies is most commonly transmitted via infected saliva transfer following a bite from an infected animal. However, exposure that facilitates virus infection can vary from deep bite wounds to superficial skin penetration following contact with an infected animal (249). Small lesions in the skin following contact with an infected animal can go unrecognised, resulting in cryptic infections that usually go unreported (250). Studies show that the virus cannot pass the dermal barrier preventing virus infection. Therefore, where breaches of this barrier occur, or through contact with mucous membranes, there is opportunity for infection. Rare instance of infection via aerosol exposure have been reported but not scientifically corroborated and entry via this mechanism is considered to be likely through exposed mucous membranes (251-253). The transmission from preclinical organ donors to recipients can also facilitate virus entry into a host leading to productive infection (254-256). In 2004 and 2005, two organ donors with undiagnosed rabies caused the deaths of six individuals (257, 258). Another individual also contracted rabies following a corneal transplant (259). Furthermore, the handling and skinning of infected carcasses and consumption of raw infected meat have resulted in the transmission of RABV (260).

1.1.5.2 *Incubation Period*

The incubation period for rabies can be highly variable. Typical incubation periods are in the range of 21-90 days, however individual cases have presented more extreme incubation periods. In the UK an incubation period of 2 and a half years was reported in a human case of rabies (261)

Non-RABV lyssavirus incubation periods are even harder to define because often, bat bites go unnoticed. The length of the incubation period can vary drastically from case to case because it depends on a number of factors. One of the biggest factors is where the transmission occurs and the part of the body on the victim's torso with the bite wound. If the bite is located in a highly innervated area (e.g. head and hands), the incubation period can be considerably shorter. This is due to the neurotropic nature of the virus so easy access to the peripheral nervous system would facilitate disease progression. Another factor affecting virus migration is how readily available specific G protein receptors are in the vicinity of the infected site.

The dose transmitted also influences the incubation period as well as the health status and age of an individual. An immunocompromised individual and a younger individual, due to their smaller stature, may have a much shorter incubation period (262, 263).

1.1.5.3 Immune response to RABV infection

1.1.5.3.1. Innate Immunity

Following exposure to RABV, natural killer (NK) cells and antigen presenting cells (APCs) such as dendritic cells (DCs) and macrophages are recruited and activated as part of the innate immune response (Figure 1.5). NK cells are innate immune effectors that, by cytokine production, help to contain an infection until the effective adaptive immune response is mounted (264). Activated NK cells produce cytokines such as Interferon gamma (IFN- γ) and tumour necrosis factor- α (TNF- α) which cause further NK cell proliferation and activation whilst also activating macrophages and causing naïve T cells to differentiate. NK cells also degranulate to release perforins and granzymes (265). Perforins aid in delivering the contents of the granules into the cytoplasm of the target cell by punching holes into the cell membrane (266). Granzymes such as granzyme B promote apoptosis of the target cell. TNF- α targets the TNF- α receptor (TNFR) which also promotes apoptosis in attempt to clear infection (266).

APCs recognise PAMPS/DAMPS via pattern recognition receptors (PRRs) and initiate a type I IFN response (267). Following stimulation by PAMPS/DAMPS or phagocytosis of RABV virions, DCs are activated to initiate changes in expression levels of major histocompatibility complex (MHC) molecules and co-stimulatory molecules (267). PAMPs, from the RABV virion, are presented by the DCs via MHC class II. Alternatively, DAMPs, such as endogenous or viral proteins from the infected cellular proteome are processed and presented via MHC class I. Following this, the DC chemokine receptor expression facilitates the migration of DCs to lymph nodes where these antigens are presented. Upon antigen encounter, the naïve CD4 T cells may differentiate into a Type 1 cytokine T helper cell (Th1), Type 2 cytokine T helper cell (Th2), an interleukin- 17 (IL-17) releasing T helper cell (Th17) or a follicular helper T cell (T_{FH}) (267, 268). Bias towards a Th1 immune response is required for viral clearance following RABV infection (269). This is primarily due to the subsequent antibody production by B cells but also the further maturation of DCs and inflammatory M1 macrophages (270-272).

Interferons, cytokines, and chemokines are released after detection of PAMPS/DAMPS by PRRs (265). With respect to RABV infection, PRRs include toll-like receptors (TLRs) and retinoic-acid inducible gene like receptors (RLRs). These PRRs recognise different targets and are located in different cell compartments. TLR3, 7-9, and 13 reside in endosomes whilst RLRs reside in the cytoplasm. PRRs typically detect viral RNA where RLRs and TLR3 recognise double stranded (ds) RNA and TLR7 recognises ssRNA (273-276). Typically, due to the ssRNA genome of RABV, TLR7 recognises RABV infection. TLR7 is also found to be expressed in B cells and is essential for the formation of germinal centres (GCs) for antibody production.

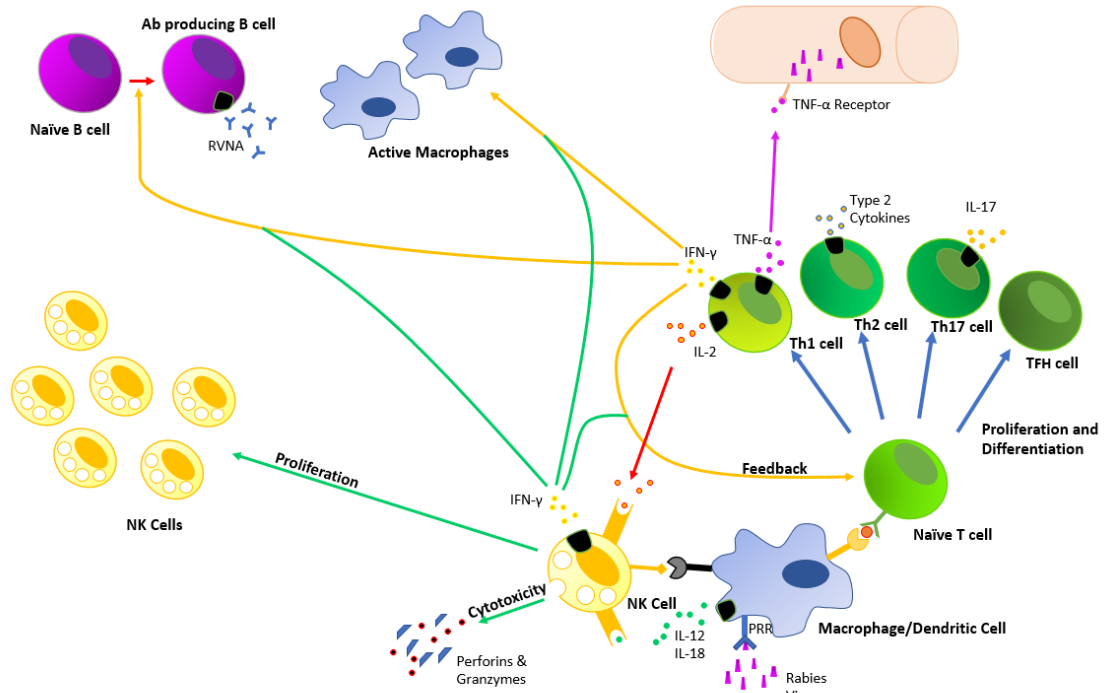


Figure 1.5: Schematic representation of suggested pathways for innate immune mechanisms following infection or vaccination. Pathogen binds Macrophages/Dendritic cell Pattern Recognition Receptor (PRR) either on the surface or intracellularly (265). This leads to cytokine secretion and upregulation of costimulatory molecules. Naïve T cells are primed by DC following antigen exposure. Naïve T cells undergo differentiation and proliferation. Type I cytokine (Th1) cell produces IFN- γ , TNF- α , IL-2, and other type I cytokines (269). TNF- α binds TNFR and induces apoptosis. IFN- γ induces B cell differentiation into antibody producing B cells, activates more macrophages, and induces further T cell proliferation and differentiation as part of a feedback loop (267, 268). IL-2 from Th1 cell and IL-12, IL-18 and costimulatory molecules from macrophage/DC activates Natural killer (NK) cells. NK cells then release further IFN- γ as well as perforins and granzymes, whilst also inducing proliferation and activation of more NK cells (265).

Recognition by TLR3 also may occur in response to RABV and the exact mechanism behind this phenomenon is unclear however dsRNA may arise from replication errors (277).

In response to binding PAMPS, TLRs dimerise and initiate downstream pathways which activate transcription factors, IFN-regulatory factor 7 and nuclear factor- κ B. Transcription of IFN-stimulated genes involved in type I/III IFN responses occurs in response to these signalling cascades (278-280).

RLRs, such as retinoic-acid inducible protein-I (RIG-I) and melanoma differentiation-associated protein-5 (MDA-5), also initiate transcription of IFN-stimulated genes involved in type I/III IFN responses (278, 281). RABV is known to trigger the RIG-I mediated innate immune response by detecting the 5'-triphosphate base pairing of the viral genome (282).

Innate immune response is not exclusive to the site of infection. CNS resident APCs, microglia, express TLRs 1-9 whilst astrocytes express TLRs 1-5 and 9 (283, 284).

Within the CNS and in response to RABV infection, TLR3 is the dominant TLR and demonstrates the greatest fold-increase. This initiates a type I/III IFN response (285).

1.1.5.3.2. Adaptive Immunity

As mentioned in section 1.1.5.3.1, DCs initiate T cell maturation. CD4⁺ T cells that differentiate into Th1 cells produce IFN γ , TNF- α , and IL-2 which facilitates IgG2a class switching of B cells and promotes CD8⁺ T cell interaction with DCs (269). The type 2 cytokines released by Th2 cells are known for their aid in the B cell humoral response but can also contribute to the immunopathology exhibited in some viral infections (286-288). Activated DCs can also generate high-affinity B-cell responses directly. Antigen presenting DCs pass antigen to follicular DCs (FDCs) which present the antigen to naïve B cells (289). Activated B cells then present the antigen to CD4⁺ T cells at the

T:B border and subsequently differentiate into extrafollicular plasma cells or divide to form GCs (290).

GCs are composed of two main components: a dark zone and a light zone. In the dark zone, B cells divide rapidly and undergo somatic hypermutation (291). Following somatic hypermutation, which alters the B cell receptor (BCR) specificity, B cells migrate to the light zone (291). In the light zone, B cells are exposed to antigens present on FDCs and B cells with high affinity BCRs are selected for survival. T_{FH} cells aid further division of these B cells which are either maintained in the GC or exit the GC to become high affinity memory B cells or plasma cells (292).

Whilst influenza virus clearance predominantly relies on CD8⁺ T cell responses, B cell responses are essential for RABV clearance (293, 294). This was demonstrated in previous studies where knockout (ko) mice lacking B cells exhibited 100% mortality (295, 296). However, ko mice lacking both T and B cells succumbed to infection sooner (295, 296).

After RABV infection in the CNS, chemokines secreted by microglia and neuronal cells recruit CD4⁺ T cells that subsequently differentiate into IL-17 producing Th17 cells or IFN γ -producing Th1 cells. IL-17 promotes downregulation of tight junctions within the blood brain barrier (BBB) whilst signalling cascades involving IFN γ recruits more CD4⁺ T cells (297-299). BBB permeability and production of RABV-specific antibodies are vital for viral clearance and survival (294). Whilst RABV-specific antibodies are usually detected in the blood of lethally infected animals, many studies have demonstrated that relatively low levels of RABV-specific antibodies cross the BBB (294, 299-302). This is likely due to the delay in BBB permeabilisation relative to disease progression (294, 300). Previous studies have demonstrated that promotion of

CNS inflammation and BBB permeabilisation facilitated antibody producing B-cell infiltration resulting in viral clearance (294, 296, 297, 303).

1.1.5.3.3. Immune evasion

Traditional immune response pathways have been described, however RABV uses multiple mechanisms to evade or interfere with immune response processes. Immune evasion mechanisms used by RABV are determined by comparing apathogenic and pathogenic strains. A feature of pathogenic lyssavirus virulence is its ability to evade the host's immune response whilst keeping the infected neurons viable. In comparison to attenuated strains of RABV, pathogenic strains show reduced levels of virus clearance from the brain as a result of lower APC activation, lower expression of chemokines and cytokines, a lack of BBB permeabilisation, and a weakened humoral response (294, 304-306).

RABV is also a poor inducer of the type 1 IFN response, a response that mediates and activates further antiviral responses (307). This means that the type 1 IFN response that does occur is not sufficient to prevent virus replication. The activation of the Fas ligand to induce apoptosis in activated T-cells and the upregulation of the programmed cell death ligand 1 to inhibit T-cell proliferation have also been proposed as mechanisms to counteract host defence strategies (308, 309).

Though the clinical symptoms of a lyssavirus infection can be severe, there is often very little morphological damage and the neurons are mostly viable until the very last stages of infection. Specific RABV protein mechanisms have been previously described in section 1.1.2. Briefly, RABV can self-limit its replication process by activating molecular switches to inhibit L protein expression and therefore maintain the integrity of the neuron. This supports the maintenance of the CNS which allows the rabies infection to spread by the intraneuronal transport mechanisms (310). One cellular stress

response, proposed to also be a mechanism mediated by RABV to limit cellular damage, is the storage of viral and host transcripts into stress granules to inhibit translation (311). Finally, in order to prevent neuronal apoptosis and the inadvertent recruitment of immune cells to the vicinity of the virus, the cytoplasmic end of the G protein has a PDZ-binding domain capable of binding to microtubule-associated serine/threonine protein kinase 2 (MAST2). When the G protein binds a MAST2 complex it inactivates its pro-apoptotic function (312).

The virus neutralising antibodies present in the acute neurological phase of infection are insufficient to prevent the fatal endpoint of the clinical disease due to the virulence factors highlighted (7).

As a result, it is crucial that pre-exposure vaccinations are available in areas at high risk of exposure. Following vaccination, immunoglobulin (Ig) M is detectable four days post vaccination, followed by IgG seven days post vaccination; providing an effective level of protection that persists for two years (313).

1.1.5.4 Human Infection

In the prodromal phase, non-specific symptoms of a lyssavirus infection, such as fever, malaise, headaches, weakness, pruritus and paraesthesia at the site of infection, may last up to 10 days before neurological symptom begin. If not already diagnosed, this phase of the disease is often misdiagnosed; commonly mistaken for Guillain-Barre syndrome (314).

Notably, it is estimated that 80% of these cases develop into the encephalitic or ‘furious’ form of rabies whereby patients experience periods of hyperexcitability, agitation, hallucinations, and confusion (315, 316). Patients may also experience hypersalivation, sweating and dilated pupils, signs of autonomic dysfunction. Before the later stages of the clinical disease, seizures and convulsions may occur, however these

symptoms are less common. Impaired swallowing and tongue weakness indicate cranial nerve dysfunction. Typically, 50-80% of cases develop hydrophobia (fear of water), unique to rabies, and some cases also exhibit aerophobia (fear of air on the patient's skin).

Eventual ataxic breathing manifests as a symptom when the patient loses consciousness and in furious rabies, there is often progression to paralysis, coma, and multiple organ failure. Death often occurs within 14 days of symptom onset and experimental studies have suggested that disruption of the sleep-wake cycle causes brain death prior to cardiac arrest (317, 318).

The other 20% of cases develop paralytic rabies or 'dumb' rabies. In contrast to furious rabies, patients usually exhibit a normal mental status but exhibit extensive muscle weakness (319, 320). Weakness tends to originate at the bitten extremity and spreads to other areas of the body. The paralytic form of rabies is often misdiagnosed as other diseases due to the non-specific symptoms. To distinguish paralytic rabies from Guillain-Barre syndrome, urinary incontinence is commonly seen in paralytic rabies (321).

The reason that the clinical disease can manifest itself in two different ways has not been determined. Electrophysiologic studies have indicated that demyelination of peripheral nerves likely contributes to weakness, typical of paralytic rabies. In addition, genetic traits, such as a compromised immune system may influence these two clinical phenomena (322). Patients with the furious form of rabies typically exhibit an earlier serum-neutralising antibody response than those with paralytic rabies (323). Further, paralytic rabies patients have been determined to have a lack of lymphocyte

proliferation and reduced levels of interleukin-6 and soluble interleukin-2 receptor, than furious rabies patients (324, 325).

1.1.5.5 *Terrestrial Carnivore Infection*

Initial symptoms of the clinical disease are similar to the human infection whereby the animal will experience weakness and lethargy. Whilst in humans the clinical disease manifests as either solely furious or solely paralytic forms, an animal may present symptoms of both. Like humans, the incubation period and rate of clinical progression can be linked to the site of the infection and the dose of virus transmitted (326). The first clinical signs manifest as behavioural changes, such as loss of appetite, hyperexcitability, and irritability, indicating signs of CNS disturbance. Animals with furious rabies have a short prodromal phase of increased alertness and neurological symptoms comparable to human furious rabies. Like humans, animals can exhibit aggressiveness and tend to attack other humans or animals as well as inanimate objects when given the opportunity. Grooming or scratching can lead to eventual mutilation at the site of infection in response to the paraesthesia or pruritus experienced by the animal. Like humans, paralytic rabies presents with less symptoms and usually starts with lack of coordination and weakness. Progressive paralysis impacts the mandible and halts the swallowing reflex before the animal dies (34). Eventual organ failure and respiratory arrest results in death.

1.1.5.6 *Chiropteran Infection*

Since the discovery of insectivorous bat rabies in the 1950s in the United States, experimental efforts have been undertaken to understand lyssavirus infection in bats.

An early pathogenesis study involved intracerebral (ic) or intramuscular (im) inoculation of little brown bats (*Myotis lucifugus*), big brown bats (*Eptesicus fuscus*), and tricoloured bats (*Pipistrellus subflavus*) with virus isolates from either a bat or a

canine as inoculum (327). All bats inoculated ic with virus, regardless of dose, succumbed to infection. In addition, of the bats inoculated ic with the bat-derived virus isolate, 20% had detectable virus in saliva, demonstrating the bat-bat transmission potential (327). Similarly viral shedding in saliva has been demonstrated for Brazilian free tail bats (*Tadarida brasiliensis*), silver haired bats (*Lasionycteris noctivagans*), hoary bats (*Lasiurus cinereus*), and big brown bats following ic inoculation with homologous RABV (328-330). For peripheral inoculation (im or subcutaneous (sc)), survival was inversely proportional to dose of virus inoculated. In one study, only 20% (n=9/46) of Mexican free tailed bats died following peripheral inoculation of up to 2000 times the lethal dose 5 (LD50) (331). This study and numerous others have demonstrated that bats are less susceptible to disease following virus inoculation and infection that likely simulates a natural infection in bats. Similar mortality rates were observed for vampire bats both ic and im (332, 333). For non-RABV lyssaviruses, ic inoculation typically results in 100% mortality whereas im inoculation results in varied mortality rates, comparable to RABV (334-339).(232)

Bat surveillance initiatives have routinely detected healthy, seropositive bats. Steece and Altenbach showed that 69% of the Brazilian free-tailed bats they tested had seroconverted to rabies virus and only 0.5% had an active rabies virus infection (340). In another study, seronegative bats developed a strong VNA response to an administered virus, indicating that the presence of antibodies in bats may be too low to detect using current methods (341). Non-RABV lyssavirus neutralising antibodies have also been detected such as EBLV-1, LBV, WCBV, and KHUV (20, 215, 219, 232, 342, 343).

Detection of virus neutralising antibodies (VNAs) does not always correlate with virus antigen or nucleic acid detection in the saliva or brain. The cause of this phenomenon is

still unclear. One hypothesis suggests that passive transfer of maternal antibodies to juvenile bats may afford protection against initial exposure to a lyssavirus (344).

Another hypothesis is ‘abortive infections’ whereby some lyssavirus exposures lead to the production of virus neutralizing antibodies that clear viral infection prior to the invasion of the CNS (345). Experimental observations indicate varying levels of susceptibility to disease following infection with a bat-derived lyssavirus isolate. As a result, defining the cause of susceptibility has been difficult to theorise. Factors such as exposure to novel virus variants, transmitted dose, site of exposure, and immune suppression or advanced age of the bat have all been suggested as possible causes (186).

Where clinical disease develops, regardless of bat species, general symptoms include loss of appetite, alteration of reflexes, tremors, and onset of paralysis. Aggressive behaviour has also been reported.

1.2 Prophylactic and Therapeutic tools

1.2.1 Vaccines and Rabies Immunoglobulin

With no known cure for the clinical disease of rabies, the only tools of protection following potential exposure to rabies virus are vaccines and RIG. In 1885, the first rabies vaccine was developed by Louis Pasteur. The vaccine formulation consisted of dried spinal cord tissue taken from rabbits infected with rabies virus (346). With further modifications, this vaccination formulation remained in use until vaccines consisting of chemically inactivated virus were developed. In 1911, a vaccine containing phenol inactivated rabies virus from the brains of infected rabbits was developed. Whilst these nerve tissue-based vaccines prevented rabies, neuroallergenic reactions caused fatal neurological disease in 0.5-1.25% of vaccine recipients. Subsequently, these harsh side effects were reduced when rabies vaccines were generated from the brains of suckling

mice and β -propiolactone (BPL) was used for virus inactivation (347). Despite this, the WHO advises against the use of these vaccines, however similar nerve tissue-based vaccines are used in poor endemic countries due to their cheap production.

Tissue cell culture advancement paved way for the human diploid cell vaccine (HDCV), developed by virus inactivation of adapted RABV grown in human diploid cells (348). This vaccine was licensed for use in 1976 in Europe and 1980 in the US. Currently, the HDCV and similar vaccines, the purified chick embryo cell vaccine (PCECV) and purified Vero cell rabies vaccine (PVRV), are used for pre-exposure prophylaxis (PrEP) and PEP (349). PrEP consists of the appropriate administration of a rabies vaccine, whilst PEP is a combination of passive immunisation with RIG and active immunisation with a rabies vaccine.

PrEP is recommended to those with continual or increased risk of exposure to lyssaviruses as a result of activity or occupation (350). This includes travellers to high-risk areas, veterinarians, and laboratory workers (115). In contrast, PEP is required after potential exposure to a lyssavirus to prevent the onset of rabies. The type of treatment required is determined by the type of exposure. The WHO classifies rabies exposure into three categories: Category I which is touching or receiving licks from an animal on intact skin, category II which includes minor scratching or bites that do not result in bleeding, and category III which includes bites or licks of broken skin or mucosal membranes. All potential exposures to bats even if a bite/scratch are not easily observed are classed as category III. No PEP treatment is recommended for category I exposures, wound cleaning and vaccination is recommended for category II exposures, and thorough wound cleaning, administration of RIG at the wound site, and vaccination is recommended for category III exposures. Vaccination at a site distant to the wound is administered to stimulate the production of virus neutralising antibodies. This aims to

provide protection against any infecting virus not neutralised by the RIG (351).

Following rigorous wound cleaning and the application of antiseptics (iodine), RIG is added to the wound site to neutralise any local live virus (352). Wound cleaning has been suggested as a major factor in clinical disease prevention and arguably increases survival rates by 50% (106). There are two types of RIG available, Human RIG (HRIG) or Equine RIG (ERIG). The WHO states that per kg of body weight, 20 IU of HRIG or 40 IU of ERIG must be administered (353). RIG has a high manufacturing cost and this prohibits accessibility in endemic countries, however, cheaper alternatives such as mAbs are being explored (121, 354). Rabies is preventable with prompt PEP, however in some cases where incubation times are very short (due to bites on highly innervated areas) or even where there's a delay in seeking PEP, failure to prevent the clinical disease can occur (355, 356). After the onset of clinical disease, PEP is not effective.

Most human and animal rabies vaccines consist of whole inactivated RABV particles as they are highly immunogenic, however some animal rabies vaccines are based on attenuated live RABV or recombinant viral vectors. The WHO does not endorse a particular strain of RABV for vaccine development, however 'fixed' virus strains such as Pitmann Moore (PM), Pasteur Virus (PV), Kelev, Vnukovo-32, Evelyn Rokitniki Abelseth (ERA), Street Alabama Dufferin (SAD), Flury low egg passage (LEP), Flury high egg passage (HEP), and Challenge Virus Standard (CVS) are recommended.

The most effective method for controlling and eliminating rabies is the mass vaccination of animals with vaccines that are safe, potent, affordable, and induce long-lasting immunity. Affordable vaccine formulations as a result of inexpensive upstream processes in vaccine development are crucial for resource-poor countries where rabies is endemic. The various upstream processes of rabies vaccine development such as cell

line, formulation, and potency testing varies based on the vaccine and each of these factors influence the cost of production.

The cell lines used for vaccine production consist of primary cells (Chicken embryo fibroblasts for the production of the PCECV, Rabipur, GSK), diploid cells (normal human foetal fibroblasts for the production of the HDCV, Imovax, Sanofi) and continuous cell lines (African Green Monkey kidney cells for the production the PVRV, Verorab, Sanofi). Primary cells tend to have a number of limitations such as the need for continuous harvesting, risk of contamination, and cell-to-cell variation in cell permissiveness to RABV. Diploid cells have a limited lifespan *in vitro* however the WHO endorses human diploid cells for vaccine production as the one of the safest cell lines. High costs associated with the generation of HDCV limits its use worldwide however (349, 357). The use of continuous cell lines in vaccine production facilitates large scale propagation at lower costs (349). The Vero cell line, established from the kidney of an African Green monkey, generates high virus yields and is a more suitable cell line for industrial scale-up than a diploid cell line. One major limitation of rabies vaccines is that they fail to protect against all lyssaviruses. Whilst protection is afforded against the lyssavirus that causes the highest burden (RABV), there is limited cross-reactivity with lyssaviruses outside phylogroup I.

1.2.2 Milwaukee protocol

The Milwaukee protocol was developed following the treatment of an unvaccinated girl who developed clinical symptoms but survived (358). The protocol involves inducing a therapeutic coma whilst administering antiviral drugs to, hypothetically, prevent brain dysfunction and allow the immune system to neutralise the lyssavirus (359).

The Milwaukee protocol was initially proclaimed as being a huge advancement in the battle against rabies however the procedure has had a very low survival rate despite the initial success. At least 53 failures have been documented, and of the 10 successes reported from India, the only component implemented from the protocol was critical care. As a result, critical care is likely the only effective component of the protocol.

The Milwaukee protocol has been deemed ineffective and an impediment to the development of new therapies. Consequently, it is speculated to be more beneficial if it were discontinued (360).

1.2.3. Possible non-antibody neutralisation mechanisms

Historically, a wealth of studies have documented the seroprevalence of animals (bats, raccoons, foxes) to lyssaviruses and some studies have described the same for humans (361-363). Seropositivity in these cases had occurred in absence of vaccine exposure and the development of fatal clinical disease suggesting exposure to antigen or an abortive infection (361). Evidence of seropositivity in unvaccinated respondents in an area endemic for vampire bat rabies, suggests RABV exposure is not always fatal to humans (361). Genetic predisposition to rabies resistance has been previously described in mice, consequently deeming it possible that isolated communities may have evolved to be immunologically unique (364-366).

Innate immunity is the first line of defence following transmission, making it an important component in the clearance of viral infections (367). A key feature of lyssavirus virulence is to avoid the induction of the host innate immune response, particularly the induction of IFN mechanisms (307). Highly neuroinvasive strains of street rabies are thought to avoid these mechanisms by limiting the viral replication that occurs in the periphery. This subsequently limits G protein accumulation and prevents

activation of apoptotic signalling cascades in infected cells (368, 369). In the event that the infection fails to evade the immune system whilst still in the periphery, the immune system possesses the capabilities to clear the infection before the virus reaches the CNS and becomes fatal.

Timely detection of lyssavirus infection is vital. In mammalian cells, TLRs and RLRs detect the non-self pattern of negative stranded viruses such as ssRNA and 5'-triphosphate base pairing of the viral genome. RIG-I activates IFNs and IFN-inducible genes, namely the type 1 IFN pathway (282, 370). RIG-I activates caspase 1 rather than caspase 3 and 9. This results in the formation of the pyroptosome and leads to pyroptosis as an attempt to clear the infection rather than apoptosis. This pathway is responsible for the prevalence of neuronal dysfunction, typical of lyssavirus infection, instead of neuronal cell death (371). The anti-inflammatory JAK-STAT pathway is also upregulated following viral transmission as a result of activated type I IFN pathways. Typically, following RABV infection, the type I IFN response is activated, however the virus uses multiple immune evading strategies (described in section 1.1.5.3.3) to counteract this initial antiviral response.

How certain populations of people and animals have seroconverted in absence of vaccine exposure is unknown, though the immune processes mounted in response to attenuated strains or the vaccines themselves could reveal the pathways activated in response to the viral exposure in these cases.

In response to vaccination, a neutralising antibody titre of ≥ 0.5 IU/ml is accepted as proof of seroconversion and the conservative threshold for which protection against RABV is likely (30, 31). Nevertheless, the role of cellular mediated immunity in the protection against rabies is less clear. One study reported that individuals who generated

a high antibody titre in response to vaccination had very low levels of IFN- γ and those with low neutralising antibody responses exhibited very high levels of IFN- γ thereby affirming that one mechanism of immunity may compensate or be more dominant than the other depending on the individual (32).

As previously covered in section 1.1.5.3, on first exposure to the rabies vaccine, DCs/macrophages bind the antigen through their PRRs, consequently leading to cytokine secretion and the upregulation of co-stimulatory signals. This mechanism has been speculated to be key for RABV clearance in the CNS because whilst high egg passage (HEP)-Flury (a highly attenuated strain where survival is likely) activated the MHC-class II/CD4⁺ T cell interaction, challenge virus standard (CVS)-11 (a highly virulent strain where the outcome is usually fatal) did not (372).

IFN- γ activates several pathways to increase cell lysis and inhibit viral replication. It also promotes antibody production, activates macrophages and contributes to further T cell proliferation and differentiation, creating a feedback mechanism. IFNs also induce transmembrane proteins such as IFN-induced transmembrane protein 3 (IFITM3), a restriction factor that blocks the cytosolic entry of viruses that use the acidic endosomal entry pathways (373, 374). IFITMs specifically localise to the endosome and lysosomes to do this. Once within the membrane, IFITMs form multimers to increase membrane rigidity and causes the accumulation of cholesterol in the membrane, via VAPA protein interaction (375). As a result, the IFITMs either physically resist deformation of the membrane or hinder the lateral mobility of virus proteins and host membrane proteins, inhibiting pore formation (373-376). Lyssaviruses are pH-dependent for entry into cells; the G protein, the sole viral protein required for membrane fusion, must assume multiple conformations throughout the process. Benfield et al., used A549 basal epithelial cells that stably expressed IFITM3 and a bat IFITM3 orthologue to assess the

effect on lyssavirus entry (373). The cells were transfected with pseudotyped lentivirus that expressed the G proteins of RABV, MOKV, LBV and WCBV. The A549 cells expressing IFITM3 exhibited reduced infectivity by almost 2 log₁₀ relative to the control cells. Benfield et al., also reported that siRNA inhibition of IFITM3 lead to a significant increase in virus replication (373).

Also in response to antigen encounter, namely detection of dsRNA, small-ubiquitin like modifier (SUMO) proteins are activated (377). Post translational modification with SUMO is a reversible reaction that can control localisation stabilisation, gene transcription, innate immunity modulation and antiviral response (378-380). The SUMOylation (a form of covalent modification) of promyelocytic leukaemia (PML) protein has been shown to inhibit secondary RABV transcription, increasing the RABV resistance of the cell (381). SUMO can also conjugate to double-stranded RNA-dependent protein kinase (PKR) promoting apoptosis of the virus infected cell (382). Conversely, upon RABV infection, SUMO3 conjugates to IFN regulatory factor 3 (IRF3) reducing its activation and consequently IFN production, rendering the cells more susceptible (377). As a result, the overall effect of the SUMO pathway on the effectiveness of the innate immune system's ability to clear infection is unclear.

Second exposure to RABV antigens produces a cellular mediated immune response four times greater than the primary exposure response (288). For the humoral immune response, a second exposure to rabies antigen results in faster production of VNAs due to the B memory cells generated following the primary exposure. Specific mAbs are more readily generated, and the rabies antigen is rapidly neutralised. For cell-mediated immunity, NK cells are speculated to be responsible for generating a "re-call" response upon re-exposure to rabies antigen (383). Once primed, CD45RO⁺ CD4⁺ T cells produce and secrete IL-2 which, along with IL-12 and IL-18, activate NK cells (264,

383). The purpose of vaccinations is to cause immune cell populations to differentiate from naïve T and B lymphocytes into larger populations of memory cells with enhanced effector function. One study showed that the NK cell “re-call” response was accountable for over 70% of all IFN- γ -secreting and degranulating cells in the first 12-18 hours after RABV re-challenge (383). These findings justify the need for a course of rabies vaccinations as not only are T and B lymphocytes more specific through differentiation, but type 1 and type 2 cytokine production is also greatly enhanced. The contribution of cell-mediated mechanisms to the overall quality of protective immunity and the extent to which it is relied upon in the fight against a rabies infection needs to be further investigated. Though, the assessment of cell mediated immunity should be considered when designing new schedules for vaccinations or developing new rabies vaccines.

1.2.4. Future perspectives and lyssavirus cross-neutralisation

With no medical intervention prior to symptom onset in humans, rabies-induced encephalitis is invariably fatal. Alongside infection attributed to RABV, all other lyssaviruses in the genus pose a threat to human and animal health as, whilst less studied, each virus is capable of causing rabies (25). The lyssavirus species are divided into phylogroups based on the degree of cross protection afforded by rabies vaccines (24, 42) (Figure 1). This is a reflection of the antigenic relationship between the lyssaviruses, allowing characterisation into distinct phylogroups. Although the genetic distance of the G genes across the lyssaviruses can give a good indication of vaccine protection, there are discrepancies on how antigenically related lyssaviruses are. Thirty percent of antigenic distance could not be predicted by genetic distance alone (115). Serological data, although often considered to have low resolution, is invaluable to assess neutralisation and generate knowledge of antigenic relationships.

Currently, there is one recognised phylogroup which correlates to the protection afforded by the vaccine derived antibodies generated by available vaccines. Vaccination and challenge experiments have shown that current rabies vaccines induced VNA production that elicited protection against RABV, EBLV-1, EBLV-2, BBLV, ABLV, DUVV, ARAV, KHUV, IRKV and GBLV (227, 384-386). Antigenically, a number of lyssavirus species are sufficiently divergent from RABV to escape virus neutralisation antibodies generated following vaccination with current vaccines (23). The reports of fatal LBV and MOKV disease in rabies vaccinated companion animals highlighted the lack of protection against these two lyssaviruses. However, sera from LBV infected bats has been shown to neutralise MOKV indicating some cross neutralisation within these viruses, subsequently assigning them to a second phylogroup along with SHIBV (24, 387). The rabies vaccine also confers no protection against the genetically highly divergent lyssaviruses, WCBV, IKOV and LLEBV, and further these lyssaviruses are not thought to be able to cross neutralise each other. This may lead to the characterisation of more phylogroups (39).

The burden of each lyssavirus is not entirely known but the advancement in diagnostic evaluation using molecular techniques in endemic areas may indicate the overall threat to human life from other lyssaviruses in the future. In addition, recent non-RABV lyssavirus spillover events into terrestrial species have highlighted the risk for cross-species transmission in a newly infected species and the subsequent establishment of a terrestrial transmission chain (388-390). With no protection afforded for phylogroup II and III, these factors suggest that more cross protective vaccine formulations may be necessary where non-RABV lyssaviruses pose a threat to human populations (115, 391).

Currently, there is no treatment for clinical rabies. An effective antiviral would have to cross the BBB and interfere with lyssavirus replication whilst maintaining neuronal

integrity. Neurodegenerative disease treatments have been extensively researched and may be applied to rabies as therapeutic tools. The physical barrier of the BBB conveys a difficulty in drug penetration, but the transport mechanisms on the BBB provide a window of opportunity for drug delivery.

1.3 Utilisation of lentiviral pseudotypes for glycoprotein expression

Lentiviral vectors, derived from the human immunodeficiency virus (HIV), have been extensively studied and developed in the last decade. Their ability to transduce non-proliferating cells meant that lentiviral vectors were initially used for gene therapy (392, 393). More recently, lentiviral vectors, termed pseudotype (PT) viruses, have been used to express different viral envelope proteins. Many of the earlier vectors expressed the VSV G protein to increase PT stability and to broaden the range of cells that could be targeted for infection. Due to the sole target for neutralisation being the lyssavirus G protein, pseudotype viruses expressing lyssavirus G proteins were developed as a way of mimicking live virus (110, 387). As a result, these pseudotype viruses are used as an alternative to live virus in serological assays so that such assays could be undertaken outside of high containment facilities. Lentiviruses are also capable of reverse transcribing their genomic RNA into dsDNA which can then be integrated into the host genome. This mechanism has been used to stably introduce reporter genes such as luciferase, green fluorescent protein (GFP), and β -galactosidase (LacZ) into infected cells, allowing quantification of PT particles by reporter gene expression (394).

Pseudotype viruses are generated by the triple transfection of three plasmids (Figure 1.6). The lentiviral core plasmid (gag-pol plasmid) encodes the protective core and matrix proteins (GAG), for viral assembly and infection, as well as the enzymatic proteins, such as the reverse transcriptase, RNase H and integrase (POL), for reverse

transcription and genomic integration. The envelope plasmid encodes the envelope protein such as the lyssavirus G protein, which dictates cell tropism and cell entry. The reporter plasmid, which encodes as reporter gene such as luciferase, contains a packaging signal as well as two long terminal repeats (LTR) at the 5' and 3' end of the gene. The packaging signal upstream of the reporter gene ensures that this gene is packaged into the produced PT by interacting with GAG. The LTR regions within this plasmid enables integration into the host genome and subsequent transcription of the PT RNA genome, allowing for detection of pseudotype infection. Each of these three plasmids are transfected into producer cells such as human embryonic kidney (HEK) 293T cells.

Following transfection, the PT viruses are generated by the host cell machinery. The transfected plasmids are transcribed and translated to produce the lentiviral proteins (GAG and POL) and the PT genome (the reporter gene). The lyssavirus G protein is also produced and glycosylated before being trafficked to the cell plasma membrane. This allows the PT capsid to arrive at the cell membrane and bud out of the cell. The resulting PT virions have a lentiviral core, consisting of the GAG and POL proteins associated with the reporter gene. This capsid is surrounded by the plasma membrane studded with multiple lyssavirus G proteins. The PTs within the cell culture supernatant is harvested 48 and 72 hours after transfection.

These PT particles contain only the reporter gene, allowing quantification of PT entry into target cells. This prohibits further PT propagation as no viral proteins are generated in an infected cell. As a result, the PTs can only undergo one round of infection rendering the PTs non-replication competent.

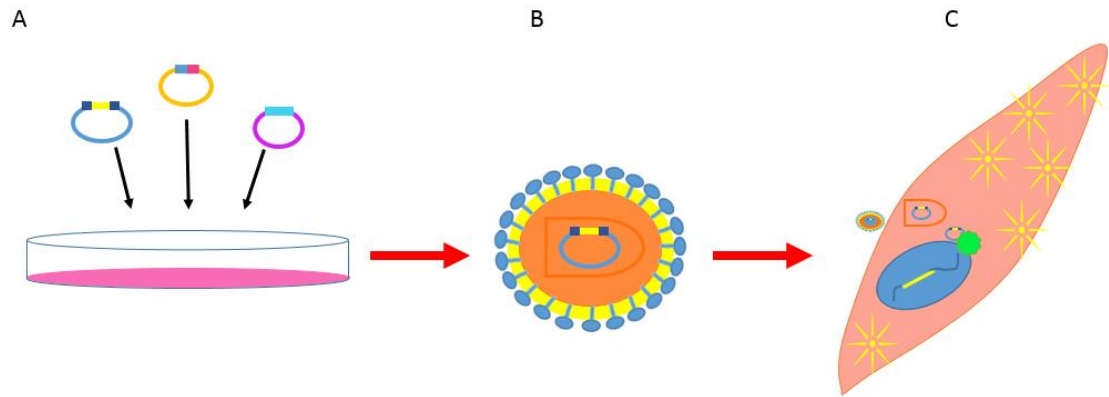


Figure 1.6: The process and outcome of generating pseudotype virus.

- (A) Transfection of three plasmids; the reporter gene flanked by LTRs, the gag-pol plasmid and the envelope plasmid into a permissive cell line (HEK 293T).
- (B) The Pseudotype virus generated. The lentiviral proteins are found at the core interacting with the PT genome (the reporter gene) and the envelope protein is found at the surface of the PT.
- (C) Pseudotype viruses infecting a target cell (baby hamster kidney (BHK) -21). Integrase recognises the LTRs on the reporter gene and integrates it into the host genome for expression. In this example, luciferase is expressed as a way of measuring pseudotype transfection.

As a result, one advantage of PTs is that they can be used at a lower containment levels than the live virus (395). Lyssavirus PTs have previously been used to study the neutralisation profiles of a range of lyssavirus specific sera in a pseudotype neutralisation assay (PNA) but also to assess recombinant G protein function (38, 387, 394).

More recently, PTs expressing recombinant G proteins have been generated and inoculated into rabbits to generate sera specific for each recombinant PT. The lyssavirus G proteins expressed by these PTs had defined antigenic epitopes swapped between a phylogroup I virus (CVS) and a phylogroup II virus (LBV lineage B) (38). Results showed varying degrees of cross-neutralisation of the recombinant PT specific sera against the wildtype CVS and LBV PTs. This demonstrated that swapping antigenic sites between G proteins can increase the neutralisation profile of a PT virus (38).

1.4 Reverse Genetics Techniques

Specific mutations can be engineered into viral genomes by a technique known as reverse genetics. This process involves recovering infectious virus from complimentary DNA (cDNA). Due to the nature of the process, the first genome manipulations were performed on DNA viruses either by transfecting cells with plasmids encoding the viral genome or via heterologous recombination between plasmids with specific viral sequences and the viral genome (396, 397). Positive sense RNA viruses were the next group of viruses with a reverse genetics system as the viral genome is mRNA sense. Infectious poliovirus was first recovered by transfecting plasmids or RNA transcribed from plasmid, containing the poliovirus genome into susceptible cells (398).

Lyssaviruses have single-stranded RNA genomes of a negative polarity. The negative sense ssRNA viruses have been less amenable to manipulate artificially due to a number

of reasons: specific 5' and 3' ends are required for the replication and packaging of genomic RNA; the viral RdRp is required for transcribing mRNA; and the anti-genome template RNA and both the genomic and anti-genomic RNA exist as RNP complexes (399). For viral replication within the cell, the viral RdRp (the L protein) must first transcribe the genome into positive sense mRNA to generate proteins. Transcription of the genomic RNA then follows once there is an abundance of the N protein present to form the RNP complex with the newly transcribed genomes. These specific requirements have paved way for a reverse genetics system that recovers live virus from cDNA (Figure 1.7).

The reverse genetics system has revolutionised the study of lyssaviruses and their interactions with host cells and organisms. The function of individual genes or gene segments has been investigated via truncation or epitope mutation. Genes such as fluorescent markers have also been incorporated into viral genomes. Reverse genetics is a key element in the development of novel vaccines against lyssaviruses. Attenuated RABVs have been generated in a number of ways as potential vaccine formulations. The P protein is an essential cofactor of the large polymerase and acts as an IFN antagonist by inhibiting IRF3 and the STATs (82). Moving the P gene after the L gene or the introduction of an internal ribosome entry site (IRES) elements minimises protein expression and the resulting recombinant viruses have proven to be highly attenuated in mice (400-402). Another successful complete attenuation of RABV was a result of introducing a mutant form of P (W265G/M287V) resulting in the inability to inactivate STAT1 (81). Due to the G protein being the sole target of neutralising antibodies, it is also possible to swap G genes between different lyssaviruses to study neutralisation and G protein function (403).

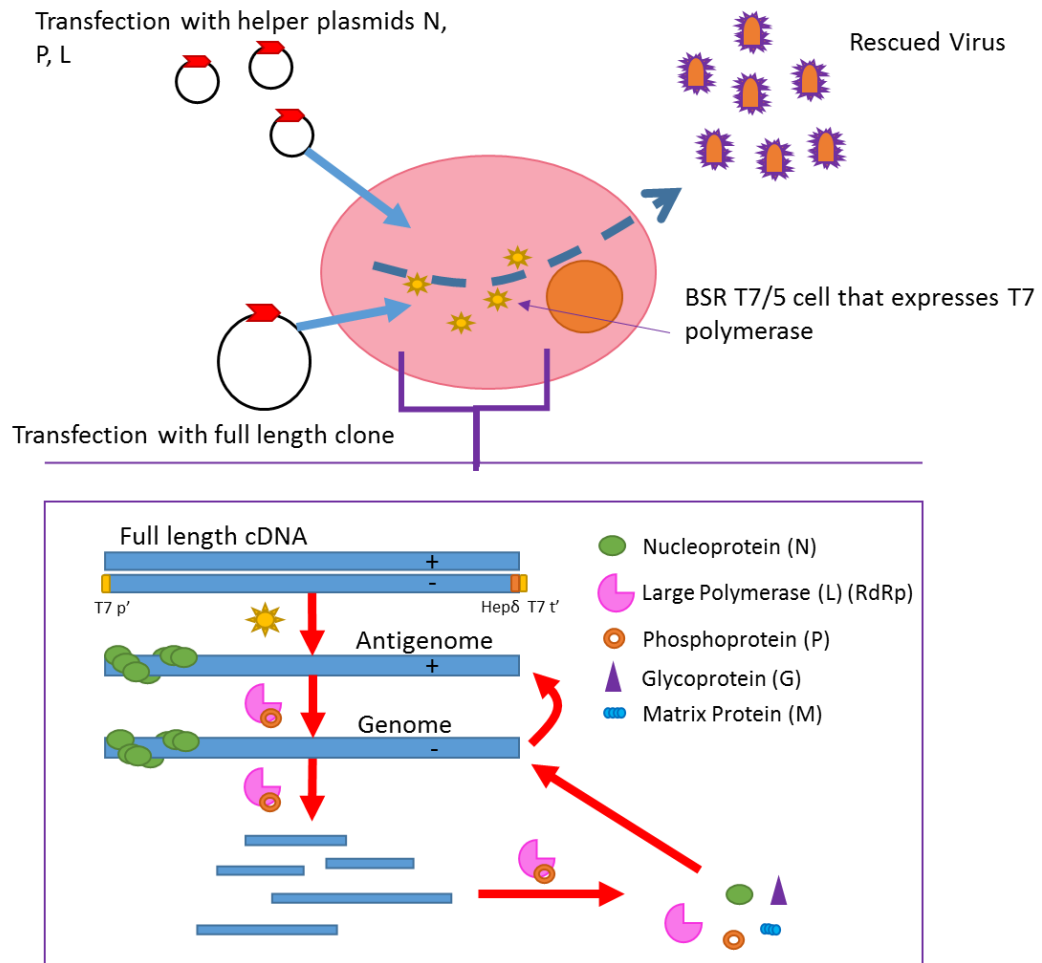


Figure 1.7: The mechanism of reverse genetics and the rescue of lyssaviruses. The cDNA full length clone and the helper plasmids each expressing a different viral protein required for transcription and replication (N, P, L and G) are under the transcriptional control of the T7 RNA promoter. These plasmids are transfected into BSR T7/5 cells that stably express the T7 RNA polymerase. The T7 derived primary transcripts consist of the antigenome (positive sense) which are encapsidated by the N protein. The antigenome is then replicated into the negative genomes which are also subsequently encapsidated by the N protein. The Hepatitis Delta (Hepδ) ribozyme sequence generates the correct 3' end of the RNA which serve as a template for the expression of the five viral proteins and viral transcription. This process begins a virus infectious cycle resulting in the release of live virus from the cell.

Marston et al., demonstrated that it was possible to incorporate a heterologous lyssavirus G protein in place of the homologous G protein within a vaccine strain (93). Studies have also shown that it is possible to generate G proteins with its two halves originating from two different lyssaviruses or swapping individual antigenic sites between different lyssaviruses and assessing the cross-neutralisation capabilities of the resulting recombinant viruses (23, 38).

1.5 Project Outline

The continued discovery of novel lyssaviruses warrants an in depth assessment of the antibody titre required to protect against each of the lyssaviruses. A further review of which lyssaviruses cross-neutralisation would indicate which lyssaviruses would need to be included in a pan-lyssavirus vaccine. This vaccine formulation would consist of the minimal G proteins required to induce an effective antibody response. This would pave way for a future vaccine capable of affording protection against all lyssaviruses and potentially undiscovered lyssaviruses.

The project will utilise live virus assays and sera specific for each lyssavirus species to determine a cut-off value for protection against each of the lyssaviruses. Alongside assessing serological cut off for testing of vaccine efficacy against all lyssaviruses, outputs may indicate where cross reactivity exists within the genus. The observation that current vaccines do not confer any protection against viruses from phylogroups II and III suggest that more cross-reactive vaccine formulations would be highly beneficial for those at risk of potential exposure. The study will essentially guide the development of novel vaccines by screening all the lyssaviruses and associated sera to determine which G proteins could confer the greatest cross-neutralisation consequently determining what could be used as minimal requirements in a pan-lyssavirus vaccine.

Chapter 2: Materials and Methods

2.1. Cells

2.1.1. Cell lines and maintenance

Baby hamster kidney cells (BHK-21), an adherent fibroblastic cell line isolated from the kidneys of 1-day old Syrian golden hamsters, were propagated in Glasgow Minimum Essential Media (GMEM; Gibco) with added 10 % foetal bovine serum (FBS; Gibco), streptomycin (100 µl/ml) (Gibco), penicillin (100 U/ml) (Gibco) and 10 % tryptose phosphate (Gibco). Human embryonic kidney cells (HEK 293T/17), an endothelial cell line established from the kidney of a human foetus, were grown in Dulbecco's Modified Eagles Media (DMEM; Gibco) supplemented with 10 % FBS, 4 g/L of D (+) glucose (Sigma Aldrich), penicillin (100 U/ml) (Gibco) and streptomycin (100 µg/ml) (Gibco). BSR T7/5 cells, a BHK-derived cell line stably expressing T7 RNA polymerase, were grown in GMEM with added 5-10 % FBS, streptomycin (100 µl/ml) (Gibco), penicillin (100 U/ml) (Gibco) and 10 % tryptose phosphate (Gibco). Neuro-2a (N2a) cells, a mouse neuroblastoma cell line, were propagated in DMEM 10 % FBS, penicillin (100 U/ml) (Gibco) and streptomycin (100 µl/ml) (Gibco). The tissue culture flasks (Sarstedt) containing the media and cells were incubated at 37 °C in a 5 % CO₂ incubator (Binder).

2.1.2. Culturing cell lines

Media was discarded and cells washed briefly with 3 ml of 0.05% Antibiotic-Trypsin-Versene (ATV; Sigma-Aldrich). The ATV was removed from the cell monolayer and a further 3 ml aliquot of ATV was added and incubated for 2-5 minutes at 37 °C until the cells had started to detach from the flask. Once the cells had fully detached from the flask, the cells were reconstituted in a further 7 ml of media, to a total volume of 10 ml.

Cells were either split 1:10 directly for regeneration of cell stocks or were counted using a haemocytometer (Improved Neubauer) before being utilised further (in virus titrations, virus propagation etc.). To count cells, 10 µl of cell suspension was added to a haemocytometer and viewed under the microscope. The cells were counted in their respective grids to calculate an average.

2.2. General Cloning and Molecular Biological Techniques

2.2.1. RNA Extraction

Total cellular RNA was extracted from virus infected cells, virus infected tissues, and oral/rectal swab solutions using a solution of phenol and guanidine isothiocyanate, TRIzol® or TRIzol® LS reagent (Life Technologies) as described previously (404). For liquid samples, 0.72 ml TRIzol LS was mixed with the 0.25 ml of the sample to be extracted and incubated at room temperature for at least 5 minutes. For tissue samples, 1 ml of TRIzol was mixed per 50-100 mg of tissue to be extracted and completely homogenised. Following homogenisation, the sample was incubated for at least 5 minutes. Following incubation, 0.2 ml of chloroform was added to the sample before shaking vigorously for 15 seconds. Following another incubation at room temperature for 2-3 minutes, the samples were centrifuged at 10,000 rpm (2500 x g) at 4 °C for 15 minutes. The upper aqueous phase was aspirated into a new tube containing 0.5 ml isopropanol, mixed by inverting and incubated at room temperature for a further 10 minutes. Samples were then centrifuged at 10,000 rpm (2500 x g) at 4 °C for 10 minutes. The supernatant was aspirated and discarded, without disturbing the pellet. The pellet was then washed with 20 µl of 75 % ethanol and left to air dry for 5-10 minutes before being re-suspended in a minimum of 15 µl RNase free water. Extracted RNA was stored at -80 °C.

2.2.2. Polymerase Chain Reaction (PCR) Techniques

All primer sequences and their uses are available in Appendix 1.

2.2.2.1. OneStep Reverse Transcription-PCR

For the reverse transcription (RT) of RNA extracts and subsequent amplification of a 606 bp region of the lyssavirus nucleoprotein gene or entire G gene (~1.5 kbp), the OneStep RT-PCR kit (Qiagen) was used according to manufacturers instructions and as previously described (405). The one-step RT-PCR assay generates cDNA from RNA by combining RT and first round PCR in a single tube as it includes both a reverse transcriptase and a DNA polymerase within the master mix. Following the first strand cDNA synthesis reaction, downstream PCR was performed with using the single stranded (ss) cDNA as a template and gene specific primers (Appendix 1) for amplification. Each reaction used 29 µl of molecular grade water, 10 µl of 5x buffer, 2 µl (10 mM) deoxynucleotide triphosphates (dNTPs), 3 µl of each primer at 7.5 pmol/µl, 2 µl of enzyme mix (as supplied) and 1 µl of extracted RNA at 1-2 µg/µl to constitute the 50 µl required for each reaction. The PCR was run on a PE2720/9700 thermocycler (Applied Biosystems) using the following cycling conditions:

Step 1: 50 °C for 30 minutes

Step 2: 95 °C for 15 minutes

Step 3: 95 °C for 20 seconds

Step 4: 5 °C below Primer T_m for 20 seconds

Step 5: 70 °C for 1 minute per kb of cDNA to be amplified

Step 6: repeat steps 3-5; 45 times

Step 7: 70 °C for 10 minutes

Step 8: hold at 4°C

The PCR products were visualised by gel electrophoresis as described in section 2.2.3.

2.2.2.2. Q5® PCR

PCR amplifications were completed using Q5® High-fidelity 2X Master Mix from New England Biolabs (NEB) according to the manufacturers protocol. The PCR was run on a PE2720/9700 thermocycler (Applied Biosystems) using the following cycling conditions according to the manufacturers protocol:

Step 1: 98 °C for 30 seconds

Step 2: 98 °C for 10 seconds

Step 3: Primer T_m dependent temperature for 30 seconds

Step 4: 72 °C for 30 seconds per kb of DNA to be amplified

Step 5: repeat steps 2-4; 30 times

Step 6: 72 °C for 5 minutes

Step 8: hold at 4 °C

The PCR products were visualised by gel electrophoresis as described in section 2.2.3.

2.2.2.3. GoTaq® Green PCR

Colony PCR amplifications were completed using GoTaq® Green Master Mix

(Promega) according to the manufacturers protocol. This master mix contains

bacterially derived Taq DNA polymerase, dNTPs, MgCl₂ and Green GoTaq® Reaction buffer which consists of yellow and blue dyes for direct loading onto agarose gels post PCR. The PCR was run on a PE2720/9700 thermocycler (Applied Biosystems) using the following cycling conditions according to the recommended protocol:

Step 1: 95 °C for 2 minutes

Step 2: 95 °C for 30 seconds

Step 3: 5 °C below Primer T_m for 30 seconds

Step 4: 72 °C for 1 minute per kb of DNA to be amplified

Step 5: repeat steps 2-4; 30 times

Step 6: 72 °C for 5 minutes

Step 8: hold at 4 °C

The PCR products were visualised by electrophoresis as described in section 2.2.3.

2.2.2.4. iTaq™ Universal SYBR® Green One-Step Real Time RT-PCR

2.2.2.4.1. Quantitative PCR Technique

For the reverse transcription of RNA extracts from mouse samples and subsequent quantitative analysis by real time qPCR, the iTaq Universal SYBR Green One-Step kit (Bio-Rad) was used as previously described (406, 407). The one-step real time RT-PCR assay generates cDNA from RNA by combining reverse transcription and PCR amplification in a single tube (includes both a reverse transcriptase and a DNA polymerase within the master mix). Each reaction used 7.55 µl of molecular grade water, 10 µl of 2x iTaq Universal SYBR Green reaction mix (as supplied), 0.6 µl of each primer at 20 pmol/ml, 0.25 µl of iScript RT enzyme mix (as supplied) and 1 µl of viral RNA extract at 1 µg/µl to constitute the 20 µl required for each reaction. The primers used were either rabies N gene primers: JW12 RT/PCR primer (5'-ATGTAACACCYCTACAATG-3') and the N1650146 PCR primer (5'-GCAGGGTAYTTTTRACTATA-3') to detect the presence of lyssavirus N gene in the RNA sample; or multispecies beta-actin primers: BatRat beta-actin intronic primer (5'-CGATGAAGATCAAGATCATTG-3') and the BatRat beta-actin reverse primer (5'-AAGCATTTGCGGTGGAC-3') to detect the beta-actin housekeeping gene, as described previously (408). Alongside RNA samples, a RABV strain, challenge virus standard (CVS), RNA positive control, a no template negative control, and a cDNA CVS standard curve (described in 2.2.2.4.2) were included in triplicate on the PCR

plate. The PCR was run on the Mx3000P Real Time PCR system (Stratagene) using the MxPro Software (Stratagene) using the following cycling conditions:

Step 1: 50 °C for 10 minutes

Step 2: 95 °C for 5 minutes

Step 3: 95 °C for 10 seconds

Step 4: 60 °C for 30 seconds

Step 5: repeat steps 3-4; 40 times *

Step 6: 95 °C for 1 minute

Step 7: 55 °C for 1 minute **

Step 8: 95 °C for 10 seconds

* Fluorescence data collected at end of 60 °C (step 4) after each repeated cycle using the Endpoints Data Collection Marker within the MxPro software.

** Fluorescence data collected between 55 °C and 95 °C (step 6 and 7) using the All Data Collection Marker within the MxPro software.

2.2.2.4.2. cDNA CVS standard curve generation

RNA was extracted from CVS infected tissue culture supernatant as described in section 2.2.1 and reverse transcribed and amplified using the previously described RT-PCR technique (section 2.2.2.1). The following specific primers were used to amplify a 606 bp region of the CVS N gene: JW12 RT/PCR primer (5'-ATGTAACACCYCTACAATG-3') and JW6UNI primer (5'-CARTTVGCRCACATYTTTRTG-3'). The PCR products were visualised by agarose gel electrophoresis and DNA amplicons were extracted and purified from the agarose gel (described in section 2.2.5).

After quantification of the purified dsDNA, the copy number was calculated using the following formula:

$$\text{Number of copies} = \frac{\text{Concentration (ng/}\mu\text{l) of DNA} \times \text{Avogadro's constant}}{\text{Length (bp)} \times \text{Conversion factor} \times \text{Average mass of DNA (Daltons)}}$$

$$\text{Number of copies} = \frac{\text{Concentration (ng/}\mu\text{l) of DNA} \times (6.022 \times 10^{23})}{606 \text{ (bp)} \times (1 \times 10^9) \times 650 \text{ (Daltons)}}$$

A ten-fold dilution series of the CVS (dsDNA) in nuclease free water was then prepared to produce the cDNA CVS standards with a range of 10^8 - 10^1 copies. These standards were run in triplicate on the sample plate for quantitative analysis of samples.

2.2.3. Agarose Gel Electrophoresis

Agarose powder (Helena Biosciences Europe) was used to make 1-1.8 % agarose gels in 1 x TAE buffer. 5 μ l of SYBR safe DNA gel stain (Invitrogen) was added per 100 ml of cooled dissolved gel. Gels were left to set for 30 minutes at room temperature prior to loading. 2 μ l 6X loading dye (Promega) was used along with 10 μ l of DNA. A number of DNA ladders were used depending on the length of the PCR product: 1kb DNA ladder (Promega), Φ X174 DNA/HaeIII Ladder (Promega), and Quick-Load 1 kb Extend DNA ladder (NEB). Gels were run in 1 x TAE at 120 V for 50 minutes.

The Bio-Rad GelDoc XR transilluminator was used to visualise the gel.

2.2.4. Purification of extracted RNA for sequencing

RNA was purified following RNA extraction using the RNeasy® Mini Kit was used according to the manufacturer's instructions (Qiagen) for RNA Clean up. Briefly, 350 µl of buffer and 250 µl of ethanol (96-100 %) were added to 100 µl of RNA sample. The sample was then loaded into a column before optional on-column DNase digestion was also performed. Following this, the column was washed twice and eluted.

2.2.5. Purification of DNA from agarose gel slices

DNA was purified from agarose gel slices using the Monarch PCR & DNA Clean-up Kit (5 µg) according to manufacturer's instructions (NEB). Briefly, the DNA fragment of the correct size was excised using a scalpel and transferred to a 1.5 ml microcentrifuge tube. Monarch Gel Dissolving Buffer was added to the agarose gel slice at a ratio of 4:1. The sample was incubated at 50 °C for 10 minutes, vortexing periodically. The sample containing the DNA was then loaded into a column and centrifuged. The column containing the adsorbed DNA was then washed twice before being eluted with the elution buffer.

2.2.6. Purification of DNA from PCR enzymatic reaction

DNA was purified from the PCR reaction using the Monarch PCR & DNA Clean-up Kit (5 µg) according to manufacturer's instructions (NEB). Briefly, DNA binding buffer was added to the post-PCR sample at a ratio of 2:1 if the dsDNA fragment was bigger than 2 kb or 5:1 if the fragment was smaller than 2kb. The sample was then loaded into a column before being washed twice and eluted with the elution buffer.

2.2.7. Sequencing

2.2.7.1. Sanger Sequencing

PCR products were sequenced by the Central Sequencing Unit (CSU) at APHA as described previously (409). Briefly, undiluted PCR product was sent to CSU along with primers at 0.8-1 pmol/μl. At CSU the samples were cleaned and quantified. Dye-terminated products were obtained from purified amplicon DNA using the BigDye Terminator v3.1 Cycle sequencing kit (Applied Biosystems). The products were precipitated and run on ABI 3130xl (16 capillary) and ABI 3730 (48 capillary) Genetic Analysers to obtain sequence reads.

2.2.7.2. Next Generation Sequencing (NGS)

Whole Genome Sequencing of RNA was performed by the CSU at APHA as described previously (410). Briefly, purified RNA extracts were sent to CSU where the samples were converted to double stranded cDNA using the cDNA Synthesis System (Roche). Samples were then cleaned, and concentrated using AMPure XP magnetic beads (Beckman Coulter). For NGS, 1 ng was used in the Nextera XT DNA sample preparation kit (Illumina) and a sequencing library was prepared according to manufacturer's instructions. The generated library was then sequenced using Illumina MiSeq with 2 x 150 bp paired-end reads, according to Illumina protocols. Using the Burrow-Wheeler Aligner (BWA) (version 0.7.17-r1188) (411), the sequence reads were mapped to a reference sequence. SAMtools v1.10 (412) and a modified vcfutils script (vcf2consensus.pl script available at: https://github.com/ellisrichardj/csu_scripts/blob/master/vcf2consensus.pl) was used to generate an intermediate consensus, whereby any indels relative to the reference sequence were appropriately termed.

2.2.8. Primers

Primers were designed manually or by the NEBuilder software (described in 2.10.3) against previously published sequences or sequences designed in this study. With the exception of the primers used for Gibson Assembly, primers were approximately 18-22 nucleotides in length and the G:C:A:T ratio was approximately equal. Primers sequences were assessed for secondary structures, primer dimers, and hairpin loops using the OligoEvaluator (<http://www.oligoevaluator.com>) web tool. Primers were synthesised by Sigma-Aldrich. They were delivered lyophilised and re-suspended in nuclease free water to give 100 pmol/μl solution, which was then diluted to the appropriate working dilution. Primer sequences are available in Appendix 1.

2.2.9. Large Scale Plasmid Preparations

Plasmid constructs were cloned and grown in *E. coli* (DH5α derivative cells) (NEB). For large scale plasmid preparations (maxipreps), the GeneJET Plasmid Maxiprep Kit (Thermo Fisher) was used according to the manufacturer's instructions. Plasmid DNA was transformed into DH5α derivative cells by heat shock and transformed as described in section 2.3.1. Approximately 50 μl of the transformed cells were then cultured on Luria-Bertani (LB)-agar containing the appropriate antibiotic (e.g. ampicillin (Sigma-Aldrich) in this study) and left overnight at 37 °C. Following colony PCR to identify positive colonies, a single colony was picked and re-cultured on a fresh LB agar-antibiotic plate for another 24 hour incubation at 37 °C (as described in 2.3.2.). After incubation, a single colony was cultured overnight in 25 ml of LB-broth and ampicillin at 37 °C and shaking (as described in 2.3.3). After 18-24 hours, the 25 ml of LB-broth and *E.coli* suspension was added to 225 ml of fresh LB-broth and antibiotic and left overnight at 37 °C and shaking. After incubation, the LB-broth and *E.coli* suspension were centrifuged at 5000 rpm (4696 x g) with a Heraeus Megafuge 16R

(Thermoscientific) for 40 minutes to pellet the cells. Cells were re-suspended with an RNase buffer and mixed with a sodium dodecyl sulfate (SDS)/alkaline lysis buffer. The resulting lysate was neutralised to precipitate proteins and chromosomal DNA and an endotoxin binding reagent was added to bind bacterial endotoxins. Cell debris and chromosomal DNA was pelleted by centrifugation for 40 minutes at 5000 rpm (4696 x g). The supernatant containing the plasmid DNA was loaded and captured in the spin column. The adsorbed DNA in the silica-based column was washed with two wash solutions (ethanol and isopropanol based) to remove contaminants and eluted with the elution buffer. The DNA was then stored in the elution buffer in 1 ml aliquots at -20 °C.

2.2.10. Small Scale Plasmid Preparations

Plasmid constructs were cloned and grown in *E. coli* (DH5 α derivative cells) (NEB). For small scale plasmid preparations (minipreps), the Monarch[®] Plasmid Miniprep Kit (NEB) was used according to the manufacturer's instructions. Plasmid DNA was transformed into DH5 α by the heat shock method described in 2.3.1 and left to grow overnight at 37 °C on a LB agar plate containing the ampicillin (as described in 2.3.2). Following colony PCR, a single positive colony was picked the following day and re-cultured on a fresh LB agar-antibiotic plate for another 24 hour incubation at 37 °C. After incubation, a single colony was cultured overnight in 20 ml of LB-broth and ampicillin at 37 °C and shaking (as described in 2.3.3). Following this, *E. coli* cells were pelleted following centrifugation at 5000 rpm (4696 x g) with a Heraeus Megafuge 16R (Thermoscientific) for 5 minutes. Pellets were re-suspended and bacterial cells were lysed with a sodium hydroxide (NaOH)/SDS buffer containing RNase A. This was followed with quick neutralisation and centrifugation at 14000 rpm (21,000 x g) at 4 °C for 5 minutes using a Sigma 2-5 microcentrifuge (Sigma) to separate plasmid DNA from denatured proteins, debris, chromosomal DNA. Supernatant was added to the

silica membrane where plasmid DNA was tightly bound and subsequently washed before being eluted with a low-salt high-pH buffer (10 mM Tris·HCl, pH 8.5).

2.2.11. Spectrophotometry

In order to measure the concentration and purity of DNA in a solution, the Nanodrop ND-2000 machine was used (Thermo Scientific). Before any measurements, a blank of solely the elution buffer or nuclease free water was used to set the zero readings.

Following this 1.5µl of each sample was measured and the concentration and the absorbance ratio value (A260:A280) to assess the purity of the sample was recorded.

Between each sample the nanodrop was cleaned with a non-scratching wipe and deionised water.

2.2.12. Restriction digestion

2.2.12.1 Restriction digestion- preparative

Preparative digests were performed on post-PCR plasmid DNA preparations, to prepare the DNA for ligation by Gibson Assembly. The restriction enzyme *DpnI* (NEB) was used according to manufacturer's instructions and as previously described (413).

Briefly, 1-2 µl of *DpnI* (NEB) was added to 50 µl of post PCR mix and incubated at 37 °C for 1 hour and heat inactivated at 80 °C for 20 minutes. *DpnI* cleaves methylated DNA. Without methyltransferases in a PCR reaction, DNA PCR products will not be methylated and so only template DNA will be cleaved.

2.2.12.2 Restriction digestion- analytical

Analytical digests were performed on plasmid DNA preparations to ensure plasmids were of the correct size before virus rescue was attempted. The High-Fidelity (HF) restriction enzymes *NheI*-HF and *MluI*-HF (NEB) were used according to manufacturer's instructions. Briefly, 1-2 µl of restriction enzyme was added to 5 µl of CutSmart Buffer (NEB) and 1 µg of plasmid DNA for a total volume of 25 µl. The

plasmid DNA and enzymes were then incubated at 37 °C for 1 hour and heat inactivated at 80 °C for 20 minutes.

2.2.13. Gibson Assembly

Primers were designed to incorporate 19-20 bp overlapping sequences directed at the 5' and 3' ends of the insert sequences. The reaction conditions to obtain the insert and vector sequences are described in 2.2.2.2. Once the overlapping fragments had been obtained they were assembled using the Gibson Assembly Master Mix (NEB) according to manufacturer's instructions. Approximately, 1-5 µl of the PCR fragments and 5 µl of Gibson assembly master mix was incubated at 50 °C for 15-60 minutes depending on the number and length of fragments being assembled (Figure 2.1).

2.3. Bacterial Transformation and Culture

Plasmid constructs were cloned and grown in *E. coli* (Max Efficiency NEB® 5-alpha Competent *E.coli* (NEB); JM109 competent cell (Promega)). All bacterial preparations were cultured in Luria Bertani (LB) broth at 37 °C.

2.3.1. Bacterial Transformation

Approximately 3 µl containing 10-100 ng of plasmid DNA was incubated with 50 µl of *E. coli* on ice for a minimum of 1 hour, before incubation at 42°C for 30 seconds. Cells were placed back on ice for 5 minutes and 450 µl of sterile Super Optimal broth with Catabolite repression (SOC) outgrowth media (NEB) was added. Cells were incubated at in a KS 4000 I control shaking incubator (IKA) at 37°C and 225 rpm for 1 hour.

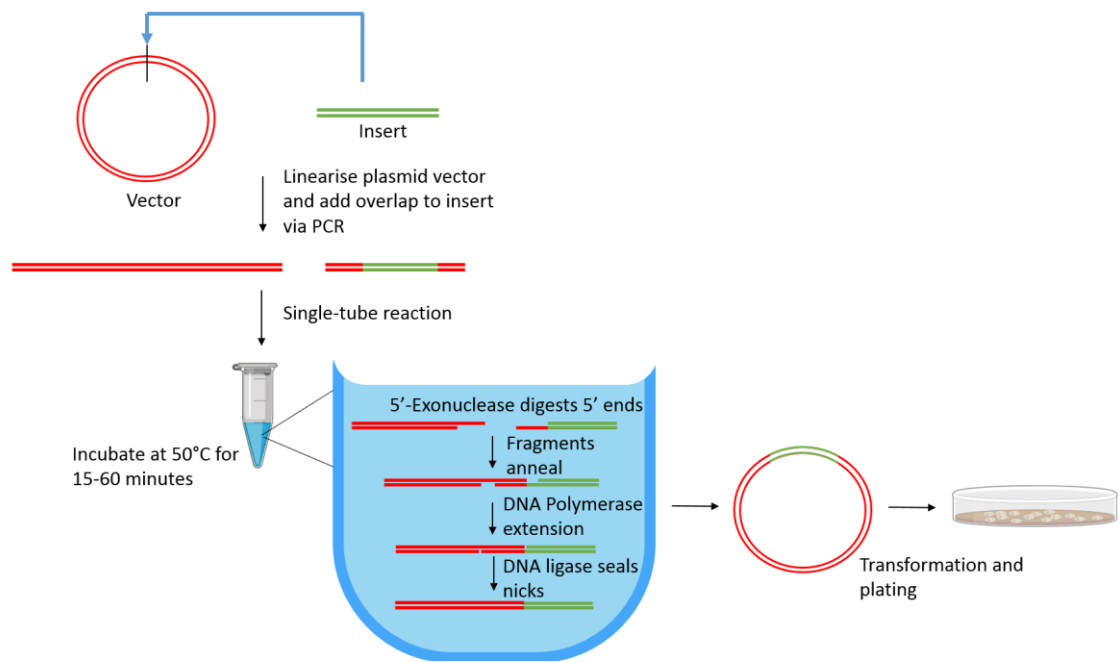


Figure 2.1: Schematic showing the pre-assembly, assembly and post-assembly stages of cloning.

2.3.2. Culture on Agar

For bacterial cell culture on agar, LB agar was used throughout this study following bacterial transformation or for the further propagation of a single colony. Stock LB agar was melted and cooled to ~60 °C before ampicillin (Sigma-Aldrich) was added to a final concentration of 500 µg/ml. Approximately 20 ml of the LB agar was then poured into a 10 cm culture dish before being left at room temperature to solidify for 30 minutes. Following this, a previously propagated colony or 50 µl of the transformed bacterial cell suspension was streaked across the agar plate. The agar plate was then incubated agar-side up at 37 °C for 18-24 hours using a SI60D incubator (Stuart).

2.3.3. Culture on LB broth

For bacterial cell propagation in a liquid cell culture, LB broth was used throughout this study to propagate single bacterial colonies. Ampicillin was added to LB broth to a final concentration of 500 µg/ml. A single colony was selected and a sterile pipette tip was used to inoculate the LB broth. The LB broth was mixed by swirling the conical flask and sterile aluminium foil was used to loosely cover the culture. The conical flask containing the culture was then incubated at 37 °C and 225 rpm using a KS 4000 I control shaking incubator (IKA) for 18-24 hours.

2.3.4. Storage of Bacterial stocks

Fresh bacterial stocks were stored at -80 °C. Transformed bacterial cells in a culture were stored in 500µl of 15% Glycerol (Sigma-Aldrich) at a 1:1 ratio at -80 °C for long term storage. For short term storage, agar plates containing colonies or bacterial suspensions were stored at 4 °C.

2.4. Virus Techniques

2.4.1. Virus Visualisation in Cells

Cell monolayers were fixed in acetone before being stained with a fluorescent mAb to detect the presence of virus within cell culture as described previously (414). Media from the cell culture plate was removed and the plate was washed before being submerged in 80 % acetone (Fisher Chemicals) for 20 minutes at room temperature. After incubation, the acetone was removed and plates were blotted and left to air dry. Once all wells were dry, 50 µl of a 1:50 dilution (for phylogroup II and III) or 1:100 dilution (for phylogroup I) of anti-N fluorescein isothiocyanate (FITC) conjugated mAb (Fujirebio Diagnostics Inc.) was added to every well and the plates were incubated at 37 °C with 5 % CO₂ for 30 minutes. This fluorescent mAb was used to indicate whether virus was present by binding cytoplasmic nucleocapsid aggregates. After, the unbound mAb was removed, the cells were washed 2-3 times with 0.1 M phosphate buffered saline (PBS). The cells were then visualised using a fluorescence Leica L5 microscope at wavelength 475-490 nm. The presence of distinct bright 'apple' green fluorescence, usually in the perinuclear area of cells confirmed presence of the lyssavirus nucleoprotein.

2.4.2. Virus Propagation and Passage

2.4.2.1. Virus Propagation

Virus propagation of all lyssaviruses (phylogroup I, II and III) were undertaken in BHK-21 cells. Approximately 1.2 ml of cells in suspension, at a 2.5×10^5 cells/ml dilution, were added to tissue culture flasks (T75 flasks; Sarstedt), containing 20 ml of GMEM (Gibco). Either immediately or the following day, 1 ml of each virus was added to its corresponding flask in a microbiological safety cabinet (MSC) in either class I or class III mode to achieve an approximate multiplicity of infection (MOI) of 0.1 (415).

MSCs in Class I mode were used for manipulation of phylogroup I viruses whilst for increased operator protection, cabinets were used in class III mode for phylogroup II and III lyssaviruses within the ACDP3/SAPO4 biocontainment facility. Alongside the T75 flasks (Sarstedt), 200 µl was taken in triplicate and added to a 96-well plate (Corning) to allow for future assessment of the percentage of cells infected in the T75 flasks.

2.4.2.2. Virus Passage

To allow for sufficient virus infection and approximately 90-100% cell confluency, infected cells were incubated for 96 hours at 37 °C and 5 % CO₂. Following incubation, virus passage was undertaken to increase virus stock as necessary. First, the 96-well control plate was fixed and stained (as described in 2.4.1) to assess the percentage of cell monolayer infection. Once the percentage of infection had been determined, 10 ml of fresh GMEM (Gibco) and 10 ml of infected supernatant were added to two T75 flasks (Sarstedt) per virus. If the infected flask was at 100 % infection following direct immunofluorescent assessment, 0.5 ml of the infected cells were added to each flask with 1.5 ml of uninfected fresh cells. If the infected flask was sub-confluent for cell infection, a larger ratio of infected cells to uninfected cells was added to the flasks. Flasks were left for 72 hours before harvesting to allow time for cell infection and for cells to achieve 100 % confluency.

2.4.2.3. Virus Harvest

The tissue culture supernatant (TCSN) of each lyssavirus infected flask was pipetted off into two falcon tubes (Sarstedt). The cells in their respective tissue culture flasks (Sarstedt) were frozen at -80 °C for 10 minutes. Following this, 5 ml of fresh media was added to the tissue culture flasks and the cell monolayer was left to thaw completely.

The contents of the flask with the media and suspended thawed cells were decanted into the falcon tube. The falcon tubes containing the infected TCSN and the infected cells were then centrifuged (Beckman Allegra 25R Centrifuge) for 10 minutes at 1500 rpm (800 x g) to pellet the cells and any cells debris. The TCSN was then aspirated off into 500 µl aliquots and stored at -80°C. The pellet was aliquoted into a separate tube and stored at -80°C. The total cellular RNA was extracted from the cell pellet and the G protein or N protein genes were amplified by RT-PCR (as described in 2.2.1 and 2.2.2). This allowed the sample to be sequenced for confirmation as described in section 2.2.7.

2.4.2.4. Virus Titration

Harvested virus titres were defined in focus forming units per ml (ffu/ml) as well as 50 % tissue culture infective dose (TCID₅₀) as described previously (416). Each virus was titrated in 6 columns of a 96-well flat bottomed tissue culture plate (Corning). Per well, 90 µl of GMEM (Gibco) 10 % FBS was added. Along row A of the plate 10 µl of virus was added. Eight serial 10-fold dilutions of virus were made down the plate to row H, discarding the pipette tip each time. BHK-21 cells were split and diluted to 3-4 x 10⁶ cells/ml and 15 µl of cells in suspension was then added to each well. After a 48 hour incubation, the cells were 100% confluent and the titration plates were fixed and stained as described in 2.4.1. The number of foci in each well was recorded and the average number of foci in the row where the concentration showed less than 10 ffu was used to determine the presence of virus in ffu/ml. The TCID₅₀ titre of the virus stock was calculated using the Spearman-Kärber equation from the dilution at which 50% of wells contained any fluorescence (417). In this case, wells were deemed positive if they had one or more positive cells.

2.4.2.5. Virus Back Titration

From the stock titration of each virus, an estimate was made of the TCSN dilution required to achieve a virus titre of 100 TCID₅₀ per well for use as the ‘working strength’ dilution in the fluorescent antibody virus neutralisation (FAVN) test and the modified FAVN (mFAVN) test (as described in 2.6.1 and 2.6.2, respectively). Before the FAVN and mFAVN tests were performed, the estimated working strength dilution was checked using the back titration technique routinely used as part of the FAVN test as described previously (414). BHK-21 media was added to rows A-D of a 96-well plate, according to Figure 2.2, before 50 µl of the working strength dilution was added to column 1 and 2. From the second column, 50 µl was serially transferred across columns 3-6, with thorough mixing and a change of pipette tips between each dilution. At the final dilution factor, 50 µl was discarded. Before the plates were incubated for 48 hours at 37 °C and 5 % CO₂, 50 µl of a 5 x 10⁵ cells/ml BHK-21 cell suspension was added to each well. As per section 2.4.1, plates were then fixed and stained before being visualised. The titre of the working strength dilution was then calculated using an adaption of the Spearman Kärber technique (417).

2.5. Generation of Specific Sera for each Lyssavirus

2.5.1. Preparation of Inocula

For the generation of specific sera to each lyssavirus species inoculation of rabbits with beta-propiolactone inactivated virus was undertaken. Each virus was BPL inactivated by mixing live virus with BPL at a 1/4000 dilution as described previously (418). The virus and BPL mix was incubated overnight (or a minimum of 6 hours) at 4 °C and then incubated for 1 hour at 37 °C.

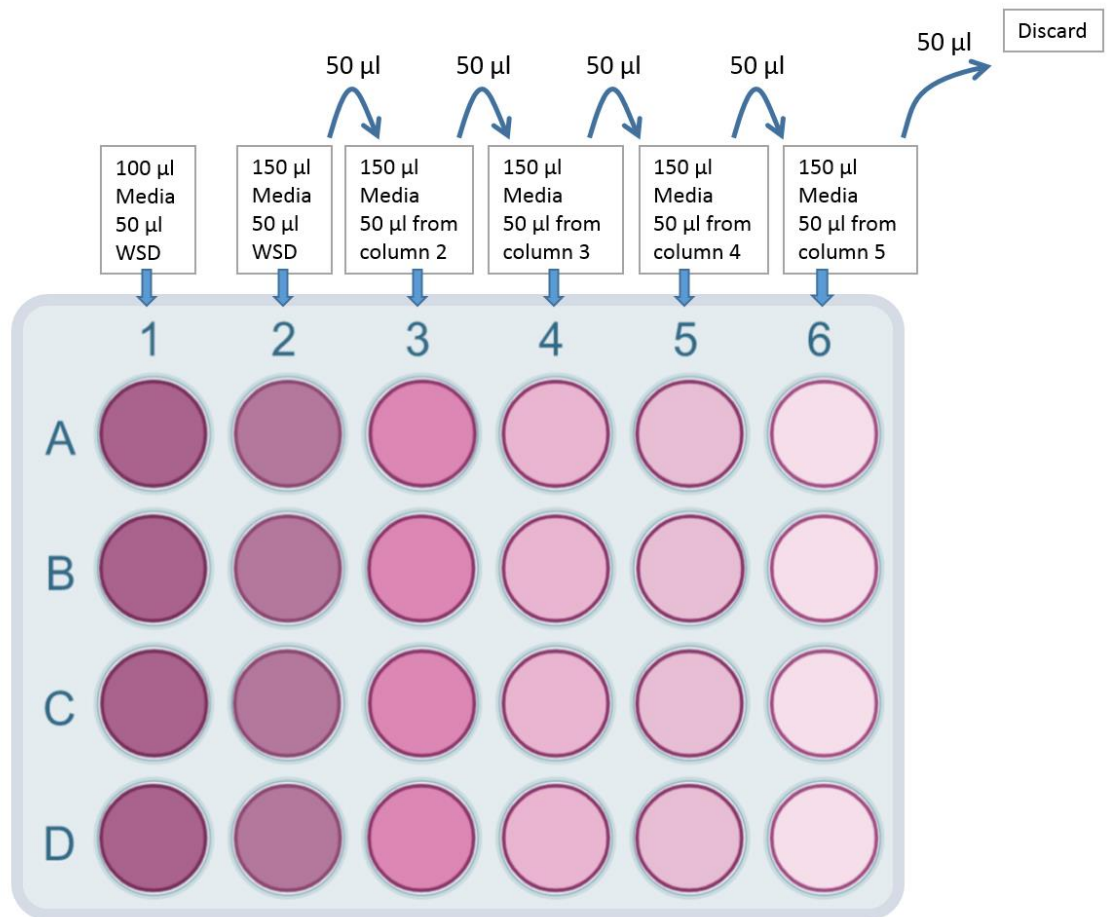


Figure 2.2: Back titration protocol. The working strength dilution (WSD), 100 TCID₅₀, is indicated by fluorescent cells in wells up to and including column 4.

A neutral pH was then obtained by adding drops of NaOH (1 M) indicated by the media colour change to orange. All BPL inactivated material was tested using a validated and accredited rabies tissue culture isolation test (RTCIT) prior to removal of BPL inactivated material from the high containment facility. Montanide™ ISA 50 V2 (Seppic) was used as an adjuvant at a 1:1 dilution with the inactivated viruses prepared to form an emulsion on the day of inoculation.

2.5.2. Confirmation of Inactivation of Inocula

Prior to inoculation of inactivated tissue culture supernatant, inactivation was confirmed using the RTCIT as described previously (419). Briefly, 200 µl of N2A cells of a 2×10^5 cells/ml cell suspension was added to each well of a 96-well plate. Cells were then incubated for 30 minutes at 37 °C and 5 % CO₂ to allow cell attachment. Following this, 100 µl of the inocula to be tested was added to 4 wells of the 96-well plate. On a separate plate, a positive control of CVS TCSN and a negative control of uninfected TCSN were added to 4 wells each. After 24 hours incubation at 37 °C and 5 % CO₂, all supernatant was aspirated off, pooled, and stored. Before a further 72 hour incubation at 37 °C and 5 % CO₂, 200 µl of fresh media was added to each of the wells. Following incubation, supernatant was again aspirated, pooled and stored before plates were fixed and stained as described in 2.4.1. Supernatant from the initial RTCIT was re-inoculated onto fresh cells and the RTCIT repeated to further ensure all virus in the inocula was inactivated.

2.5.3. Generation of Sera in Rabbits

All *in vivo* experimentation was undertaken in ACDP3/SAPO4 biocontainment facilities at the Animal and Plant Health Agency (APHA), Weybridge, UK and complied with UK Home Office regulations under the Animals in Scientific Procedures Act (1986) and

Home Office license P7A668AF8. All studies were assessed internally by the APHA ethics and statistical committee and carried out following ARRIVE guidelines (420).

One rabbit was used per lyssavirus species to generate species specific antisera as described previously (38). One year old New Zealand White rabbits (Envigo) were housed according to UK Home Office regulations for a 10 day acclimatisation period onsite at the APHA before the initial inoculation. Sufficient and appropriate enrichment was supplied and food and water was supplied *ad libitum*. Before inoculation, rabbits were correctly identified and shaved at the sites where sub-cutaneous injections would be carried out. Emla cream was applied liberally to the inoculation site as a local anaesthetic. The inocula was administered at four sites subcutaneously and two sites intramuscularly at days 0, 21, 28 and 35. On day 43 all rabbits were anaesthetised and a maximal volume of blood was removed by cardiac puncture under terminal anaesthesia.

2.5.4. Other test sera

Occasionally, where rabbit sera was unavailable, specific lyssavirus sera was acquired from experimentally infected bats generated on other projects. Where standardised control sera were required, the following three RABV-specific polyclonal sera were obtained: i) WHO serum, an international standard human serum used as control sera for WHO gold standard serological assays; ii) the World Organisation for Animal Health (OIE) serum, a diagnostic control serum obtained from a pool of sera from vaccinated dogs used in serological diagnostic tests; and iii) hyperimmune human sera from a HDCV (Rabies Vaccine BP, Pasteur Merieux) recipient.

2.5.5. Particle tracking

Where rabbits showed no immune response to inoculation with BPL inactivated preparations, antigen preparations were analysed using a NanoSight LM10 Machine

(Malvern). BPL-inactivated virus particles were tracked in suspension according to the manufacturer's protocols. Briefly, a 1/100 dilution of 100 nm latex standard beads (Malvern) were used to calibrate the machine. Approximately, 300 µl of the beads were aseptically injected into the machine's specimen chamber until there were no air bubbles. Once the machine was calibrated, the specimen chamber was washed with fresh 0.1 M PBS. Inactivated virus preparations were diluted 1/30 in 0.1 M PBS and injected into the machine. Standards and specimens were tracked and measured for 30 seconds at room temperature using the NanoSight LM10 NTA software (version 3.00).

2.5.6 Concentrating Antibodies within serum samples

Amicon Ultra-4 Centrifugal Filter Units (Millipore) were used to concentrate antibodies within serum according to the manufacturer's protocol. The centrifugal filter units were first washed with molecular grade water and spun at 5000 rpm (4696 x g) with a Heraeus Megafuge 16R (Thermoscientific) for 10 minutes. Following this, approximately 4-15 ml of lyssavirus specific-sera was added to the Amicon Ultra-4 Centrifugal Filter Unit (Millipore) and spun at 5000 rpm (4696 x g) with a Heraeus Megafuge 16R (Thermoscientific) for a minimum of 45 minutes. The concentrated serum was extracted from the top of the filter and aliquoted into a separate tube. The sample that had passed the filter was also aliquoted into a separate 2ml tube. Both samples were tested on FAVN to determine whether the micro-concentrator had indeed concentrated the sample.

2.6. Serological Techniques

2.6.1. Fluorescent Antibody Virus Neutralisation (FAVN) Test

The FAVN was used, as described previously (414), to determine the extent to which sera can neutralise CVS, and in doing so, generate a serological value for neutralisation

(Figure 2.3). In 100 µl of BHK-21 media, serial 3-fold dilutions of the serum to be tested was carried out on a 96 well plate (Corning) across 2-4 rows. Following this, 50 µl of CVS at 100TCID₅₀ was added to each well containing BHK-21 media and diluted sera and left to incubate for one hour at 37 °C and 5 % CO₂. After incubation, 50 µl of BHK-21 cells at a concentration of 5×10^5 cells/ml were added to every well and the plates were incubated for a further 48 hours at 37°C and 5 % CO₂. Alongside the FAVN, a virus back titration plate was prepared to ensure the virus was at the correct concentration. Four-fold serial dilutions of CVS were carried out in BHK-21 media across four rows as described in 2.4.2.5. This plate was also incubated for 48 hours at 37 °C and 5 % CO₂. Following incubation, the supernatant was discarded from the FAVN plates and virus titration control plates and plates were subsequently fixed and stained as described in section 2.4.1. Following incubation, the plates were washed twice with 0.1 M PBS and dried on absorbent paper before being visualised on a fluorescent microscope. The 50 % endpoint dilution (where complete neutralisation stopped in 50 % of wells) was calculated using the Spearman-Kärber method (417). Controls included media-only, cell-only wells and negative rabbit serum and the standard OIE control at 0.5 IU/ml. Only FAVN tests where back titration showed the working strength dilution to be above 64 TCID₅₀ and below 362 TCID₅₀ were considered. A neutralising antibody titre of 0.5 IU/ml was considered the cut off for proof of seroconversion and the conservative threshold for which protection against RABV is likely (30, 31).

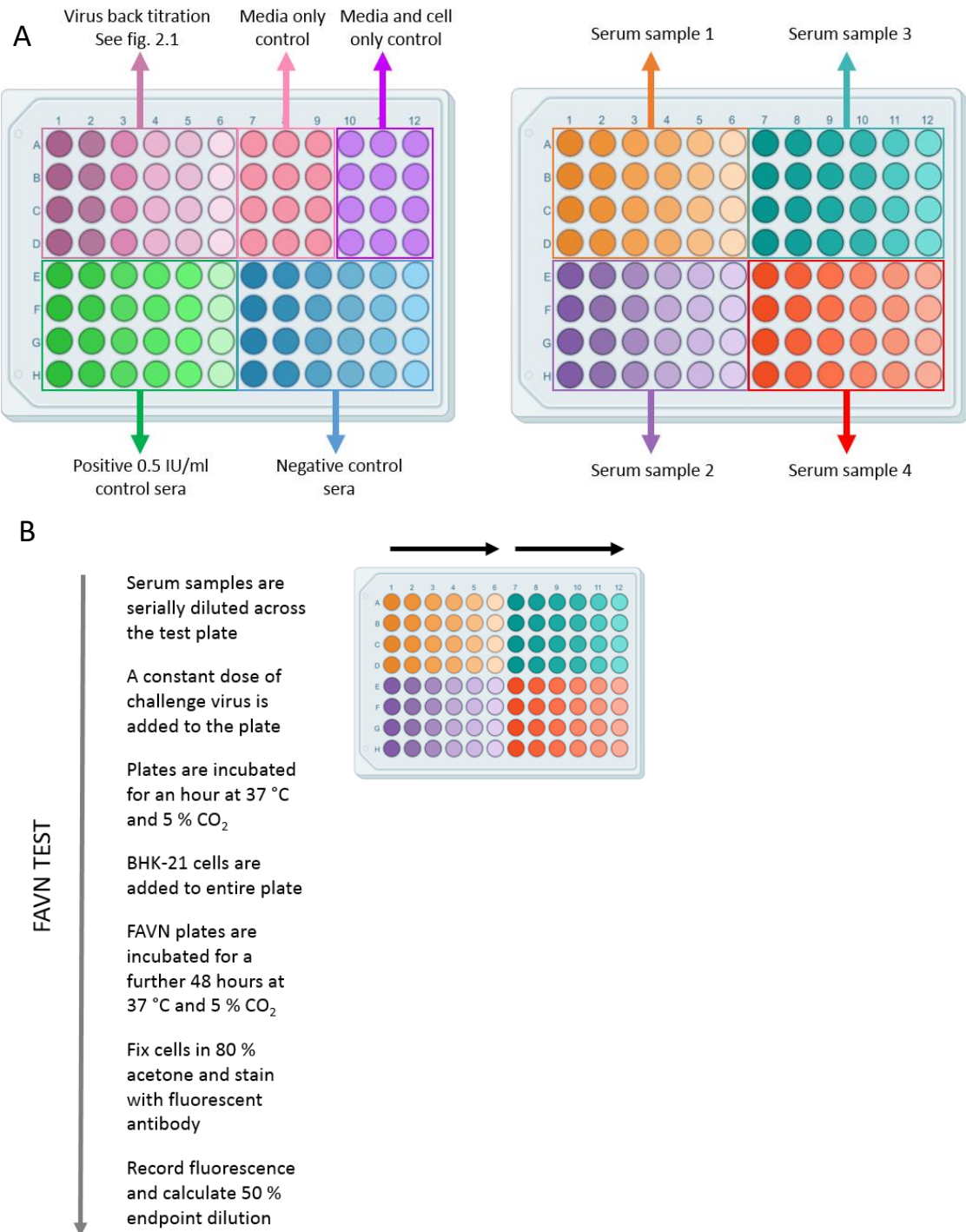


Figure 2.3: A) Schematic of the FAVN test 96-well plate layout. B) FAVN test protocol schematic.

2.6.2. Modified Fluorescent Virus Neutralisation (mFAVN) Test

The modified FAVN is a modified version of the standard FAVN as described previously (421). The principal modification is the use of any lyssavirus-specific sera vs any lyssavirus rather than testing standardised vaccine sera against CVS. This allows for the testing of sera to neutralise a range of lyssaviruses rather than just the CVS strain of RABV. The OIE standard control at 0.5 IU/ml did not routinely neutralise all viruses, so titres were not converted to IU/ml as they would be for diagnostic FAVN tests.

Consequently, the readout of these assays is the reciprocal titre at which neutralisation is observed in comparison to control sera. Therefore, the 0.5 IU/ml neutralisation cut-off is dictated by standardised vaccine sera vs CVS. This translates to a serum dilution of 1/9 as the threshold for detecting specific neutralisation.

2.6.3. Enzyme-Linked Immunosorbent Assay (ELISA)

Using the Platelia Rabies Kit II (Bio-Rad), an enzyme-linked immunosorbent assay (ELISA) was performed on each of the lyssavirus species-specific polyclonal serum sample to evaluate the presence of all binding, neutralising and non-neutralising, antibodies. The ELISA test was performed as per the manufacturer's instructions. Reagents were stored at 4 °C and placed at room temperature for a minimum of 30 minutes prior to use. A negative (R3) and two positive (R4a and R4b) controls were also tested in each run after being diluted 1:100 in sample buffer. The negative control is composed of synthetic material and the positive controls are composed of rabies immunoglobulin in synthetic material. The positive controls are calibrated against WHO international standard for rabies immunoglobulin. R4b was used to establish a reference curve after serial two-fold dilutions (S6 = 4 Equivalent units per ml (EU/ml), S5 = 2 EU/ml, S4 = 1 EU/ml, S3 = 0.5 EU/ml, S2 = 0.25 EU/ml, S1 = 0.125 EU/ml). 100 µl of each of the samples and negative (R3) and positive controls (R4a and S6-1) were added

in duplicate to the microplate wells coated with the rabies virus G protein for 60 ± 5 minutes at 37°C . The microplate was then washed three times with washing solution before adding 100 μl horseradish peroxidase-conjugated protein A to each well. The microplate was incubated for a further 60 ± 5 minutes at 37°C . Following five more wash cycles, the linked peroxidase conjugate was visualised by adding 3,3',5,5'-tetramethylbenzidine (TMB) and incubated for 30 ± 5 min at room temperature before the reaction was stopped with 1 N sulphuric acid solution. Absorbance was measured at 450 nm with the use of a Multiskan Ascent microplate reader (Thermolab Systems). The standard curve dictated by the positive quantification standards allowed for interpolation of the titre of each sample run in equivalent unit per ml (EU/ml).

2.7. Pseudotype Techniques

2.7.1. Construction of Pseudotype Plasmids

The backbone plasmid used for pseudotype (PT) expression were the mammalian expression vectors, pcDNA3.1 (+) (Invitrogen) or pI.18 (described previously (387, 422)). The pcDNA3.1(+) plasmid was linearised using the PCR reaction and enzyme mix described in 2.2.2.2 and the following primers: pcDNA(+)fwd (5'-GAGCTCGGATCCACTAGTC-3') and pcDNA(+)rev (5'-GGTACCAAGCTTAAGTTTAAACG-5') (Figure 2.1). Methylated template DNA was removed by *DpnI* digestion restriction digested as described in 2.2.12.1. Lyssavirus G genes were synthesised (as described in 2.12) with complementary 19-20 bp overlapping sequences directed at the 5' and 3' ends of the vector which enabled directional cloning into the prepared linearised plasmid. Gibson assembly was then performed to ligate the vector and insert sequences (as described in 2.2.13.) and the resulting plasmids were then transformed into DH5 α *E.coli* cells (as described in 2.3.1). Small scale DNA preparations then followed to ensure successful ligation, using

confirmatory primers and the PCR reaction and enzyme mix described in 2.2.2.2. Once plasmids were sequenced, attempts to transfect plasmids containing the correct insert then followed.

2.7.2. Transient transfection

Transfection was performed as described previously (387). HEK 293T/17 cells were seeded in a 6-well plate (Corning), 24 hours prior to transfection at a concentration of $1.6 \times 10^6/\text{ml}$ in DMEM 10 % FBS. After an 18 hour incubation, cells were supplemented with fresh DMEM 10 % FBS. For each PT, transfections were carried out 6 hours later with FuGENE® 6 Transfection Reagent (Promega) according to the manufacturer's instructions. Per well, 0.6 µg of env (wildtype or recombinant lyssavirus G protein), 0.6 µg of lentiviral Gag-Pol (p8.91) (423) and 0.9 µg of reporter plasmid (pCSFLW) (387) were combined in a sterile Eppendorf. In a separate tube, 6.1 µl of Fugene (DNA:Fugene ratio of 1:2.9) was added to an appropriate volume of OptiMEM (Gibco) such that the total transfection mix equalled 100 µl. Both tubes were left for 5 minutes before they were mixed together. After a further 20 minutes incubation at room temperature, the contents of the tube was added dropwise to the corresponding wells of the 60-80% confluent HEK 293T/17 cells. Following a 24 hour incubation at 37 °C and 5 % CO₂, media in each well was changed for fresh DMEM 10% FBS. At 48 and 72 hours post-transfection, the supernatant containing PT virus was harvested. At the 48 hour time-point, the media was replenished. The supernatant was filtered through a Millipore Sigma Millex Sterile syringe filter with a 0.45 µm pore size MCE membrane (Merck) and stored at -80 °C.

2.7.3. Pseudotype Titration

The titres of harvested PT viruses were determined by relative light units (RLU) as described previously (394). Each PT was titrated in four replicates in a 96-well tissue culture plate (Figure 2.4). In each well, 100 µl of BHK-21 media was first distributed. Following this, 10 serial 5-fold dilutions of the PT stock were made across the plate; 25 µl of PT stock was added to the first column of the 96-well plate and 25 µl was serially diluted down the plate to column 11. Column 12 was left as a cell only/uninfected control. From a stock of BHK-21 cells at a concentration of 2×10^5 , 50 µl was added to each well. The plates were then incubated for 48 hours at 37 °C and 5 % CO₂. Following incubation, media was removed and replaced with 50 µl of fresh BHK-21 media and 50 µl of Bright-Glo reagent (Promega). Luciferase activity was measured 3-5 minutes later on an Infinite® 200 PRO microplate reader (Tecan). The negative cut off value was defined by the average cells alone luminescence multiplied by 2.5.

2.8. Recombinant virus generation

2.8.1. Manipulation of full length clones to insert wildtype and recombinant lyssavirus glycoproteins

The backbone plasmid used for full length expression contains the full genome of a phylogroup I RABV. The rabies vaccine strain used is based on the street Alabama Dufferin (SAD) B19 vaccine strain and is derived from the SAD B19 cDNA clone with additional restriction sites upstream of the G gene (SmaI) and Ψ gene (NheI) (cSN) (23, 93, 416, 424, 425). The cSN RABV G was removed from cSN in preparation for ligation of lyssavirus G proteins by Gibson Assembly according to the manufacturer's instructions.

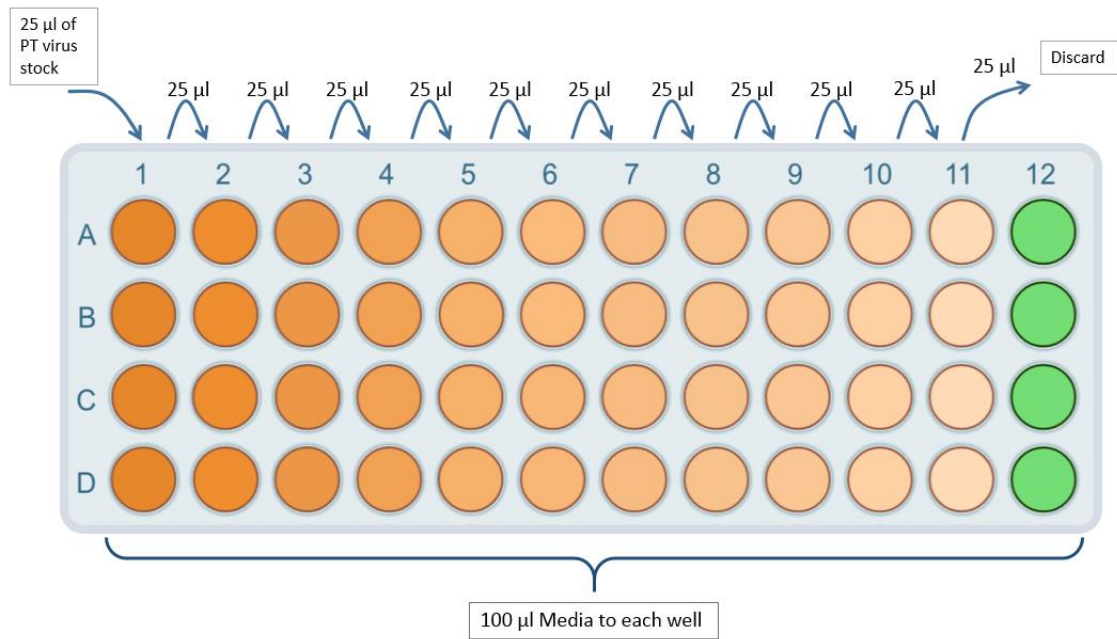


Figure 2.4: Pseudotype TCID₅₀ titration schematic illustrating a dilution series of the pseudotype virus (orange) and cell only control (green).

To linearise cSN into two fragments and remove the RABV G, the PCR reaction and enzyme mix described in section 2.2.2.2 and the following sets of primers were used: cSNfragment1A (5'- GGACTGGCTAGCCTTTCAAC-3') with cSNfragment1B (5'- TTTCACACAGGAAACAGCTATGACCATGATTACGCC-3') and cSNfragment2A (5'- CTTTCCCGGGGTCTTTTG-3') with cSNfragment2B (5'- TCATGGTCATAGCTGTTTCCTGTGTGAAATTGTTATC-3').

The output of these PCR reactions is two cSN fragments of 7284 bp and 6888 bp in length, consequently excluding the RABV G. Each representative wildtype and recombinant lyssavirus G gene ORF was amplified using primers that incorporated 19-20 bp overlapping sequences directed at the 5' and 3' ends of the vector and insert sequences for downstream cloning into cSN.

G genes were synthesised within or cloned into pUC19 or pcDNA3.1(+) plasmids for long term storage at -20 °C. These plasmids were then used as the template DNA using Q5® High-fidelity PCR for further cloning. The PCR products consisted of the lyssavirus G gene flanked by the correct incorporated overhangs complementary to cSN which enabled directional cloning into the prepared cSN plasmid. Methylated template DNA was restriction digested as described in 2.2.12.1 before Gibson assembly was performed. Following ligation through the Gibson assembly method (as described in 2.2.13) and transformation into DH5α *E.coli* cells (as described in 2.3.1), small scale DNA preparations were made and successful ligation was checked using confirmatory primers and the same PCR conditions. Once, plasmids were sequenced (as described in section 2.2.7.1), attempts to rescue plasmids containing the correct insert then followed.

2.8.2. Virus rescue

In a SAPO4/ACDP3 biocontainment facility, rescue of full-length clones of recombinant lyssaviruses were carried out in BSR T7/5 cells using FuGENE® 6

Transfection Reagent (Promega) according to the manufacturer's protocol. Virus rescue involved the simultaneous transfection of three RABV helper plasmids (pTIT-N, pTIT-P, pTIT-L) alongside a full-length RABV plasmid under the transcriptional control of the T7 polymerase (424). In classical RABV rescue, a T7 polymerase-encoding plasmid is transfected alongside the helper and full length RABV plasmids because BHK-21 cells are used. However, in this study, cells which stably express T7 polymerase, BSR T7/5 cells, were used. This eliminated the need for transfection of a fifth plasmid, thereby making this protocol more efficient (426). Cells were plated in a 96-well plate at 3×10^4 cells per well in 100 μ l of GMEM (10% FCS) and incubated overnight at 37 °C, 5 % CO₂, to give 60-70 % confluence the following day.

DNA was defrosted on ice 40 minutes prior to transfection. Each well was transfected with 40 ng of pTIT-N, 40 ng of pTIT-P, 40 ng of pTIT-L, and 200 ng of genome plasmid at a DNA:Fugene ratio of 1:3.5 in a total of 10 μ l transfection mix. After warming to room temperature, the appropriate volume of Fugene 6 was incubated with OptiMEM (Gibco) for 5 minutes. During this time, helper plasmids and the full-genome plasmid were combined in separate tube. Additionally, existing media was removed from incubated cells and 90 μ l of fresh GMEM media (5% FCS) was added. The DNA mix was then added to the OptiMEM-Fugene mix and incubated for 30 minutes at room temperature. This transfection mix was added dropwise to each well. Plates were gently agitated and incubated for 72-96 hours until 100 % cell confluency. Due to the fact that the N gene is transfected into cells and expressed as N protein and the FITC-conjugated mAb used to detect lyssavirus antigen binds the N-protein, cells were passaged two to three times to ensure no residual transfected N protein remained before a proportion of the transfected cells were fixed and stained as described in section 2.4.1. This would ensure that any fluorescence would indicate lyssavirus infection, rather than just

transient expression of the N protein following transfection. If cells were positive for lyssavirus infection, indicated by fluorescent foci, the remaining cells were harvested or passaged further into larger quantities.

2.8.3. Assessing the Growth Kinetics of recombinant viruses

Virus growth was assessed using a multi-step growth curve of rescued recombinant viruses and cSN as described previously (93). BHK cells were seeded in a 12-well plate (Corning) at 1.5×10^5 /ml and incubated for 24 hours at 37 °C. Cells were then infected with each virus at a MOI of either 0.1 and incubated for 1 hour at 37 °C before being washed three times with 0.1 M PBS (Gibco). At set time points (0 hours, 6 hours, 12 hours, 24 hours, 48 hours, 72 hours, 96 hours, 120 hours) 150 µl of media was aspirated off and frozen at -80 °C until required and 150 µl of fresh GMEM was added back onto each of the wells to maintain a total volume of 2 ml. After the course of the experiment, each of the time point aliquots were defrosted and titrated in triplicate on fresh BHK-21 cells as three independent titration experiments (as described in section 2.4.2.4). The log₁₀ values of the final virus titres were taken and the means of the rescued viruses against cSN were compared.

2.9. *In Vivo* Studies

2.9.1. Vaccination-Challenge in Mice

All *in vivo* experimentation was undertaken in ACDP3/SAPO4 biocontainment facilities at the Animal and Plant Health Agency (APHA), Weybridge, UK and complied with UK Home Office regulations under the Animals in Scientific Procedures Act (1986) and Home Office license PCA17EA73. All studies were assessed internally by the APHA ethics and statistical committee and carried out following ARRIVE guidelines (420).

2.9.1.1. Mice

Three to four week old BALB/c mice were purchased from a licensed and registered breeder within the UK (Charles River) and microchipped (Trovan) to enable identification. Mice were grouped according to random selection using a random number generator. All mice were given food and water *ad libitum* along with appropriate environmental enrichment and checked twice a day throughout the course of the experiment.

2.9.1.2. Vaccination of Mice

Mice were vaccinated with the human rabies vaccine VeroRab (Novartis), reconstituted as per the manufacturer's instructions and diluted 1/20 in Minimal Essential Media (MEM) as described previously (39). Mice were vaccinated with 0.5 ml of diluted vaccine via the intraperitoneal (ip) route at days 0 and 7 to ensure high serological response to vaccination. Mock vaccinated mice were inoculated with MEM alone to act as a positive control group and ensure the pathogenicity of the challenge virus.

2.9.1.3. Blood Sampling by Tail Bleed

The dorsal vein of each mouse was nicked using a scalpel blade and blood was collected in CB300 tubes (Sarstedt) at 21 days post vaccination to assess seroconversion as described previously (39). Blood samples were stored at 4 °C for 24 hours prior to centrifugation at 2500 rpm (860 x g) for 10 minutes to separate the serum. The serum was aspirated off the blood pellet and heat inactivated at 56 °C for 30-40 minutes prior to being stored at 4 °C for short term storage or -20 °C for long term storage. Blood samples were assessed for virus neutralising antibody detection by a standard FAVN or mFAVN test (described in 2.6.1 and 2.6.2).

2.9.1.4. Intracranial Challenge with Virus

At day 28-29 post vaccination, mice were challenged intracranially (ic) with 100 ffu 30/μl of virus as described previously (39). Post challenge, mice were observed twice daily for 22-28 days and clinical signs were scored using a scale of 0-5 (where 0, no

effect; 1, hunched body/ruffled fur; 2, limb twitching; 3 hindquarter paralysis; 4, progressive paralysis; 5, terminal recumbency/death) (Appendix 4) (326). The humane endpoint for termination was a clinical score of 1-2 where mice were bled under terminal anaesthesia followed by cervical dislocation. Kaplan-Meier survival curves and the log-rank Mantel-Cox test were used to analyse survivorship rates.

2.9.1.5. Serology

Mice were tail bled 21 days post vaccination to assess seroconversion to the VeroRab vaccine as described previously (39). Each serum sample was tested on a standard FAVN test or mFAVN test (described in 2.6.1 and 2.6.2). Serum was tested at a 1/9 starting dilution due to the limited volume of serum and run alongside OIE diagnostic standard 0.5 IU/ml serum in order to determine the antibody titre generated as a result of seroconversion. Mice that showed a clinical disease score of 1-2 and mice that survived until the termination of the experiment were terminally anaesthetised with isofluorane. During terminal anaesthesia, mice were cardiac bled. A needle was inserted into the chest cavity and blood was removed directly from the heart into a syringe. Immediate cervical dislocation followed. The blood was processed to generate sera as described in 2.9.1.3 and subsequently assessed by FAVN against CVS and mFAVN against other lyssavirus species. Mock vaccinated mouse sera was tested against all lyssaviruses by mFAVN to assess cross-neutralisation ability of the rescued virus.

2.9.1.6. Tissue and Swab Sampling

During post-mortem, for each mouse being tested, the skin at the back of the skull was cut into and the base of the skull was cut using sharp, curved scissors. Three incisions were made towards the nose of each mouse to open the top of the skull. A small amount of brain tissue was taken from the hindbrain and placed on blotting paper to be used on the direct fluorescent antibody test or placed in a 2 ml tube for RNA extraction (as

described in section 2.2.1). At this stage, any remaining brain was kept in a 2 ml tube and frozen at -80 °C for future use.

Oral and rectal swabs were also obtained from mock vaccinated mice and placed in a 2 ml tube with 100 µl of 0.1 M PBS for RNA extraction or frozen at -80 °C for future use. Swabs to be RNA extracted were vortexed in the 2 ml tubes for 5 minutes before the swab was removed and discarded. Of the 100 µl remaining solution, 25 µl was then utilised for RNA extraction using TRIzol LS. The remaining mouse carcasses were kept in a 50 ml falcon tube and frozen at -80 °C for future use.

2.9.1.7. Formalin fixation of mouse carcass

For immunohistochemistry (IHC) and histopathology examination, whole mouse carcasses were fixed in 10% neutral buffered formalin (NBF) after displaying signs of clinical disease and subsequent termination. Briefly, whole mice were cut from the lower abdomen, through the rib cage, to the neck, to open the body cavity. Additionally, a cross section through the atlanto-occipital joint was cut to open the skull. The whole mouse was then placed in 100 ml of 10% buffered formalin and left for a minimum fixation period of 7 days.

2.9.1.8. Virus Detection within Brain tissue

2.9.1.8.1. Direct Fluorescent Antibody Test (FAT)

The FAT was performed as described previously (427). A small amount of mouse brain tissue was taken from the hindbrain and placed on blotting paper. For a positive control, previously extracted CVS infected mouse brain was used. A small amount of positive control material was taken from the 2 ml tube and placed on blotting paper. A microscope slide was then inverted onto the brain tissue to make two impression smears and excess brain was blotted if necessary. Slides were left to air dry for 2-3 minutes before being fixed in 99-100 % acetone for 20 minutes. Following incubation, a drop of anti-N FITC conjugated mAb (Fujirebio) at working strength dilution (1:20) was added

to each of the smears and incubated for a further 30 minutes at 37 °C. Microscope slides were then washed twice in PBS and once in distilled water before being dried using blotting paper. The slides were then visualised using a fluorescence Leica L5 microscope at wavelength 475-490 nm. Virus antigen was denoted by bright ‘apple’ green fluorescence generally in the peri-nuclear area of cells, or longer ‘string-like’ neurons.

2.9.1.8.2. Histopathology and Immunohistochemistry

Histology was performed by the Histology unit at APHA. Fixed tissues were sent to histology following a 7-day fixation in 10 % buffered formalin. Histopathology and immunohistochemistry methods were performed on lyssavirus infected mouse brains using a Ventana automated stainer as described previously (428). Briefly, serial sections (4 µm) were cut and stained with haematoxylin and eosin (H&E) for brain morphology examination or labelled immunohistochemically for viral antigen using a rabies virus mAb, mAb 5B12 (MyBioSource).

2.10. Analytical Software

2.10.1. Benchling

The online Benchling program (<https://www.benchling.com/>) was used to align ABI Sanger sequencing produced sequence reads as well as next generation sequencing reads after they had been aligned to a reference sequence. The reads were aligned against an appropriate known G protein sequence in order to confirm the sample’s sequence. It was also used to map and design constructs and primers for other routine molecular biology applications including Gibson Assembly and sequence annotation.

2.10.2. NEB Tm Calculator

The NEB Tm Calculator (<https://tmcalculator.neb.com/#!/main>) was used to estimate the appropriate annealing temperature when using NEB PCR reaction mixes.

2.10.3. NEBuilder

The NEBuilder tool (<https://nebuilder.neb.com/#!/>) was used to design primers for Gibson Assembly reactions. The vector and insert sequences were uploaded to the software and the coordinates for insertion of the insert sequence were selected. The output was a set of two primers with 19-20 bp complementary overhangs to be used in a PCR reaction as described in 2.2.2.2 and Gibson Assembly as described in 2.2.13.

2.10.4. Promega Tm for Oligos Calculator

The Promega Tm for Oligos Calculator (<https://www.promega.co.uk/resources/tools/biomath/tm-calculator/>) was used to estimate the appropriate annealing temperature when using Promega PCR reaction mixes.

2.10.5. DNASTAR Lasergene 14

The DNASTAR Lasergene suite v.14 (DNASTAR Inc., Madison, USA) was used to visualise and align sequences, as well as produce percentage sequence identity values for both nucleotide and amino acid sequences.

2.10.6. MEGA 6

MEGA version 6 was used to produce phylogenetic trees from a multitude of lyssavirus G protein sequences (429).

2.10.7. FigTree v1.4.2

FigTree v1.4.2 (430) was used to edit phylogenetic trees produced from MEGA 6.

2.10.8. SWISS-MODEL

SWISS-MODEL (<https://swissmodel.expasy.org/interactive>) is an automated protein structure identity-modelling software whereby the amino acid sequence of one lyssavirus G protein could be modelled onto a previously published crystal structure of a similar G protein (431-433). Due to a lack in the published crystal structure of all lyssavirus G proteins, this method was used to assess possible lyssavirus G protein structures and amino acid interactions for those without a published crystal structure.

2.10.9. Pymol

Pymol v2.3 was used to manipulate the protein structures from either the Protein database (PDB) or the SWISS-MODEL outputs (434). Antigenic sites were mapped onto protein structures and key features of the lyssavirus G proteins were outlined using this software.

2.10.10. Acmacs Web Cherry - Antigenic Cartography

The Acmacs Web Cherry software (<https://acmacs-web.antigenic-cartography.org/>) was used to produce antigenic maps based on neutralisation data as previously described (24, 435).

2.10.11. Mosaic Vaccine Tool Suite

The Mosaic Vaccine Tool

Suite (<https://www.hiv.lanl.gov/content/sequence/MOSAIC/makeVaccine.html>) was used to produce mosaic recombinant lyssavirus G proteins as previously described (436). Mosaic proteins are assembled *in silico* using a genetic algorithm that chooses

the most frequent epitopes from a number of natural proteins and combines them to form a synthetic antigen representative of all the input proteins. This is unlike a consensus sequence as it takes epitope amino acid lengths of 12-mer rather than picking the most frequent amino acid at each position. The parameter options were set as follows: 1) the cocktail size was set to one so that a single peptide was generated, 2) the rare threshold was set to 3 for optimal value and where this failed, set to 2 or 1, and 3) the epitope length was set to an amino acid length of 12-mer in an attempt to encapsulate each of the antigenic sites targeted by neutralising antibodies and to also match the length of natural T helper cell epitopes.

2.11. Statistical Analysis

All statistical analysis was performed within the software GraphPad Prism v8.4.2 (GraphPad Software, San Diego, USA). For each data set, the appropriate statistical analysis function was selected.

2.12. Gene Synthesis

Recombinant lyssavirus G proteins as well as novel lyssavirus G proteins where no live virus isolate existed were synthesised using GeneArt (Thermo Fisher). Genes were synthesised as DNA Fragments with a 19-20 bp overhang complementary to pcDNA3.1(+). Upon receipt, the DNA fragments were re-suspended in nuclease free water and cloned into pcDNA3.1(+) by Gibson Assembly for long term storage and use.

2.13. Phylogenetics

Phylograms were constructed in MEGA6 using the Neighbour joining (NJ) algorithm after sequences were aligned. The sequences were bootstrap re-sampled 1000 times to assess robustness of each tree node. The evolutionary distances were computed using

the Maximum Composite Likelihood (ML) method and are in the units of the number of base substitutions per site. The resulting tree was viewed in FigTree (v1.4.2).

2.14. Antigenic Cartography

Antigenic characterisation was derived from mFAVN data. The mFAVN is based on the ability of the lyssavirus to infect cells and of specific antisera to neutralise and prevent cell infection. A fixed quantity of virus was tested against a panel of lyssavirus-specific antisera. Three-fold serial dilutions of the antisera were used to determine the highest dilution able to neutralise the virus and prevent cell infection. This dilution was the reciprocal neutralisation titre and ranges between <10 (lower dilutions are not used due to no neutralisation/limitation of the mFAVN test) and 1263 (reciprocal maximum titre achieved in the dataset). A target distance from a serum to each virus was derived by calculating the difference between the \log_2 reciprocal neutralisation titre for that particular virus and the \log_2 reciprocal maximum titre achieved by that serum against any virus. Thus, the higher the reciprocal titre value, the greater the antigenic relationship between virus and antiserum, and the shorter the target antigenic distance. As the logarithm (\log_2) of the reciprocal titres were used, a two-fold change in titre equates to a fixed difference in target distance (denoted as 1 antigenic unit (AU)).

The Acmacs Web Cherry software was used to generate these antigenic maps. Metric and ordinal multidimensional scaling techniques were used to optimise the positions of viruses and antisera relative to each other on a 3D or 2D map, minimising sum-squared error (E) between the map distance and target distance (435) (supplementary online material). The position of each virus was dictated by the distance to multiple antisera and the position of the antisera was dictated by the distance to multiple viruses. Consequently, sera with different neutralisation profiles to the homologous virus

appeared in separate locations on the map but could still all contribute to the positioning of the viruses.

When generating the maps in the Acmacs Web Cherry software, 100 random restart optimisations were carried out to generate a map that obtained the best fit of map distances to the neutralisation data (24). Maps could then be visualised in different dimensions (D), 2D or 3D, with the 3D maps allowing fewer constraints on the virus and serum positioning. Viruses (spheres) and sera (cubes) were then colour coded according to phylogroup and maps were orientated such that each virus/serum could be viewed in relation to each other.

Chapter 3: Defining the antigenic requirements for pan-lyssavirus neutralisation

3.1. Introduction

Since the 1950s, many non-RABV lyssaviruses capable of causing rabies have been identified, including six highly genetically-divergent viruses, MOKV, LBV, SHIBV, IKOV, LLEBV, and WCBV. In over 50 years, each of the non-RABV lyssaviruses were identified in separate geographical locations either as single or multiple detections. With all but two lyssavirus species originating from Chiropteran species, bats are widely considered to be the global reservoir for lyssaviruses (437). This reservoir presents a ‘spillover’ risk to both animals and humans and cross-species transmission events have occurred previously into multiple species (described in section 1.1.4.2).

PrEP or PEP using vaccination and RIG is universally accepted to prevent rabies after infection with RABV (438). All rabies vaccines licensed for human use are based on whole inactivated RABV particles. For humans and domestic animals, it has been established that a neutralising antibody titre of equal to or greater than 0.5 IU/ml is generally considered a conservative threshold, above which protection from classical RABV strains is likely, however, for more divergent phylogroup I lyssaviruses this value is yet to be defined (438). Brookes, Healy (35) determined that an antibody titre of 4.5 IU/ml and above was required for complete neutralisation of EBLV-1, EBLV-2 and ABLV *in vitro*. Nolden, Banyard (33) suggested that an antibody titre of ≥ 10 IU/ml was required for protection against BBLV *in vivo*. Protection against phylogroup II and III lyssaviruses remains problematic as several studies have demonstrated that the existing RABV vaccines do not confer any protection against these more diverse lyssaviruses (34, 37, 39), regardless of neutralising titre against RABV isolates. In phylogroup II, limited studies have shown some cross-reactivity between LBV, MOKV,

and SHIBV (5, 36, 38). This suggests that only one antigen may be needed in a cross-protective formulation for use as a vaccine to induce antibodies against phylogroup II.

The efficacy of rabies vaccines is determined by the genetic differences and the resulting antigenic differences between the lyssaviruses and the rabies vaccine strains.

The lyssavirus trimeric G protein is the sole target for neutralising antibodies and several antigenic sites on the lyssavirus G proteins have been described previously (see section 1.1.2.4.1) (26, 439). The effect of antigenic site differences cannot be accurately determined without a reliable method to quantitatively test antigenic data.

The FAVN test and ELISA (Platelia Rabies II Kit, Bio-Rad) are two serological methods to detect antibodies to assess seroconversion against RABV (414, 440). In addition to the qualitative detection of antibodies, serological assays can also be used to detect antigenic differences in antibody titres to different viruses. These serological assays, however, have low resolution due to the different sera and viruses used. Whilst some studies have shown a linear correlation between the G protein amino acid identity and neutralisation titres, other studies have demonstrated variable serological cross reactivity and paradoxical relationships (24, 36). It has been previously suggested that the antigenic relationship between different RABV isolates and the antigenic relationship between EBLV-1 and EBLV-2 may not be reflected in the genetic data (24, 441). Additionally, mouse anti-ARAV antibodies neutralised KHUV and ARAV equally, however mouse anti-KHUV antibodies were less effective at neutralising ARAV than KHUV (34). This could be a result of a different presentation of epitopes on the virus G protein surface where antibodies selected in affinity maturation against ARAV target epitopes shared by both ARAV and KHUV but antibodies selected against KHUV target epitopes specific to KHUV. In this chapter, lyssavirus species were generated, titrated, and genetically characterised. The sixteen individual lyssavirus

species, including LBV lineages A-D and three RABV isolates, were then assessed antigenically using standard sera and lyssavirus-specific hyperimmune sera on serological assays, with the aim of defining the potential antigenic requirements for any future pan-lyssavirus vaccine preparation. To interpret this data quantitatively, antigenic cartography, a theory and associated computational method that resolves the resolution and visualisation of antigenic data, was used.

3.2. Viruses

3.2.1. Virus Isolates and Propagation

A total of 21 lyssaviruses were selected for inclusion in this study, spanning the entire genus and wide geographical origin (Table 3.1). All isolates used in this study were from an archive of lyssaviruses held at APHA, Weybridge. Three RABV isolates were used for comparison; a wild or street RABV isolate (designated RABV in this study), the rabies challenge virus standard-11 isolate (designated CVS in this study), and the cDNA clone of the SN strain of RABV (designated cSN in this study).

Of the 21 viruses studied, 19 were grown in cell culture specifically for this study and the remaining two were previously cultured. Lyssaviruses were propagated and grown as described in section 2.4. For each virus, a suspension of BHK-21 cells in T75 flasks were infected to achieve a MOI of 0.1. Due to the lack of visible cytopathic effect following a lyssavirus infection, a 200 µl aliquot of infected material from each flask was added in triplicate to a 96-well plate as a control. After a 72-96 hour incubation at 37°C, depending on cell confluency, the 96-well control plate was fixed in 80% acetone and subsequently stained with an anti-N FITC conjugated mAb (Fujirebio) (as described in section 2.4.1) to assess the proportion of cells that were positive for lyssavirus antigen.

Table 3.1. Lyssavirus isolates used in this study.

Designation	Species	Phylogroup	RV Number *	Isolated From	Year	Country	Genbank accession code ^{\$}	Reference
CVS	RABV	I	Challenge Virus Standard-11 strain				EU352767	(387, 442)
cSN	RABV	I	Recombinant virus; Street Alabama Dufferin (SADB19) backbone + SADB19 Glycoprotein				M31046.1 [^]	(424)
RABV	RABV	I	RV437	Raccoon Dog	-	Estonia	KF154997	(404)
ABLV	ABLV	I	RV634	Bat	1996	Australia	AF081020	(221)
ARAV	ARAV	I	RV3379	Bat	1991	Kyrgyzstan	EF614259	(443)
BBLV	BBLV	I	RV2507	Bat	2009	Germany	JF311903	(200)
DUVV	DUVV	I	RV131	Bat	1986	Zimbabwe	GU936870 (G)	(24, 54)
EBLV-1	EBLV-1	I	RV20	Bat	1986	Denmark	KF155003	(404)
EBLV-2	EBLV-2	I	RV628	Bat	1996	UK	KY688136	(444)
GBLV	GBLV	I	RV3267	Bat	2015	Sri Lanka	KU244267	(227)
IRKV	IRKV	I	RV3382	Bat	2002	Siberia	EF614260	(55)
KHUV	KHUV	I	RV3380	Bat	2001	Tajikistan	EF614261	(443)
LBV A	LBV	II	RV767	Bat	1999	France (ex-Egypt)	EF547432 (G)	(231, 445)
LBV B	LBV	II	RV1	Bat	1956	Nigeria	EF547431 (G)	(231)
LBV C	LBV	II	RV134	Bat	1982	South Africa	EF547425 (G)	(231)
LBV D	LBV	II	RV3383	Bat	2008	Kenya	GU170202	(230)
MOKV	MOKV	II	RV4	Shrew	1968	Nigeria	KF155005	(404)
SHIBV	SHIBV	II	RV3381	Bat	2009	Kenya	GU170201	(230)
IKOV	IKOV	III	RV2508	Civet	2009	Tanzania	JX193798	(446)
LLEBV	LLEBV	III	RV3208	Bat	2011	Spain	NC031955	(447)
WCBV	WCBV	III	RV3384	Bat	2002	Russia	EF614258	(55)

Abbreviations: ABLV, Australian bat lyssavirus; ARAV, Aravan virus; BBLV, Bokeloh bat lyssavirus;

DUVV, Duvenhage virus; EBLV, European bat lyssavirus; GBLV, Gannoruwa bat lyssavirus; IRKV,

Irkut virus; KHUV, Khujand virus; RABV, rabies virus; LBV, Lagos bat virus; MOKV, Mokola virus;

SHIBV, Shimoni bat virus; IKOV, Ikoma lyssavirus; LLEBV, Lleida bat lyssavirus; WCBV, West

Caucasian bat virus.

* Animal and Plant Health Agency lab identification number

^{\$} Where full genome sequence accession numbers cannot be found, G gene sequence accession numbers have been included instead and are highlighted by (G).

[^] SADB19 GenBank accession number

- Data not known

After passage 1, all lyssavirus infected cell cultures showed a varied percentage of infection, but all ranged from 70-100% infection. Infection was identified by the presence of individual cells with bright green, perinuclear granular fluorescence, or a larger foci of infected cells (Figure 3.1).

Infected cells were passaged with fresh cells (ratio dependent on percentage of cell infection) to increase the stocks of each lyssavirus as before, and a further 96-well control plate was used to assess infection.

Following a further 72 hour incubation, the 96-well control plates were fixed and stained. At this stage, antibody staining of control wells in a 96-well plate, suggested that each lyssavirus flask was likely to be 100% infected.

Supernatant from each virus culture was aspirated off and aliquoted into 500 µl aliquots and stored at -80°C. The cell monolayers were frozen at -80°C and subsequently thawed to lyse the cells. The cells and debris were then pelleted by centrifugation as described in section 2.4.2.3.

3.2.2. Molecular characterisation

To ensure that each virus preparation was the correct isolate, extracted RNA (described in 2.2.1) from each cell pellet was used in a one-step RT-PCR to amplify the lyssavirus nucleoprotein gene (described in section 2.2.2.1 with primers described in Appendix 1). Nuclease free water was used as a negative control and previously propagated and characterised EBLV-2 was used as a positive control. The resulting amplicons were all of the expected size (606bp) when analysed by gel electrophoresis (Figure 3.2) and the PCR products were subsequently sequenced with N gene-specific primers by Sanger sequencing (as described in 2.2.7.1).

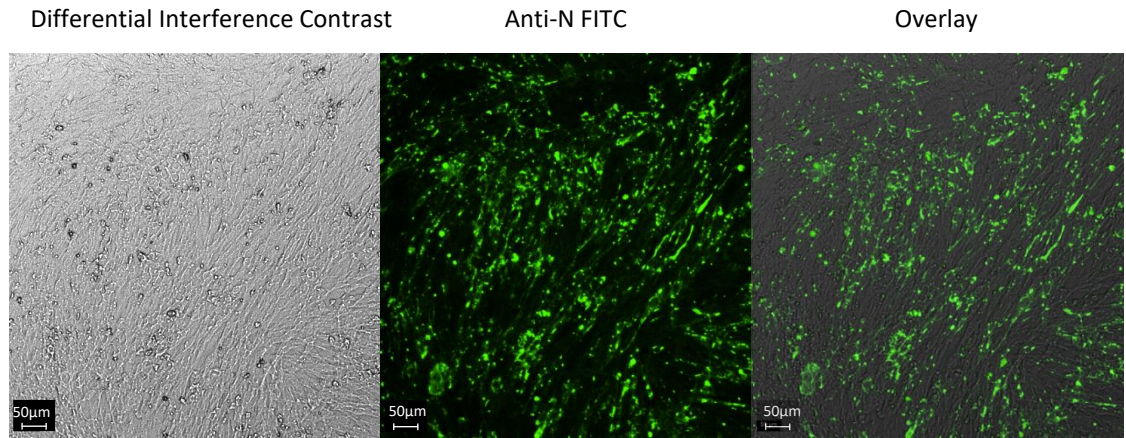


Figure 3.1: GBLV antigen stained with anti-N FITC mAb. Scale represents 50µm.

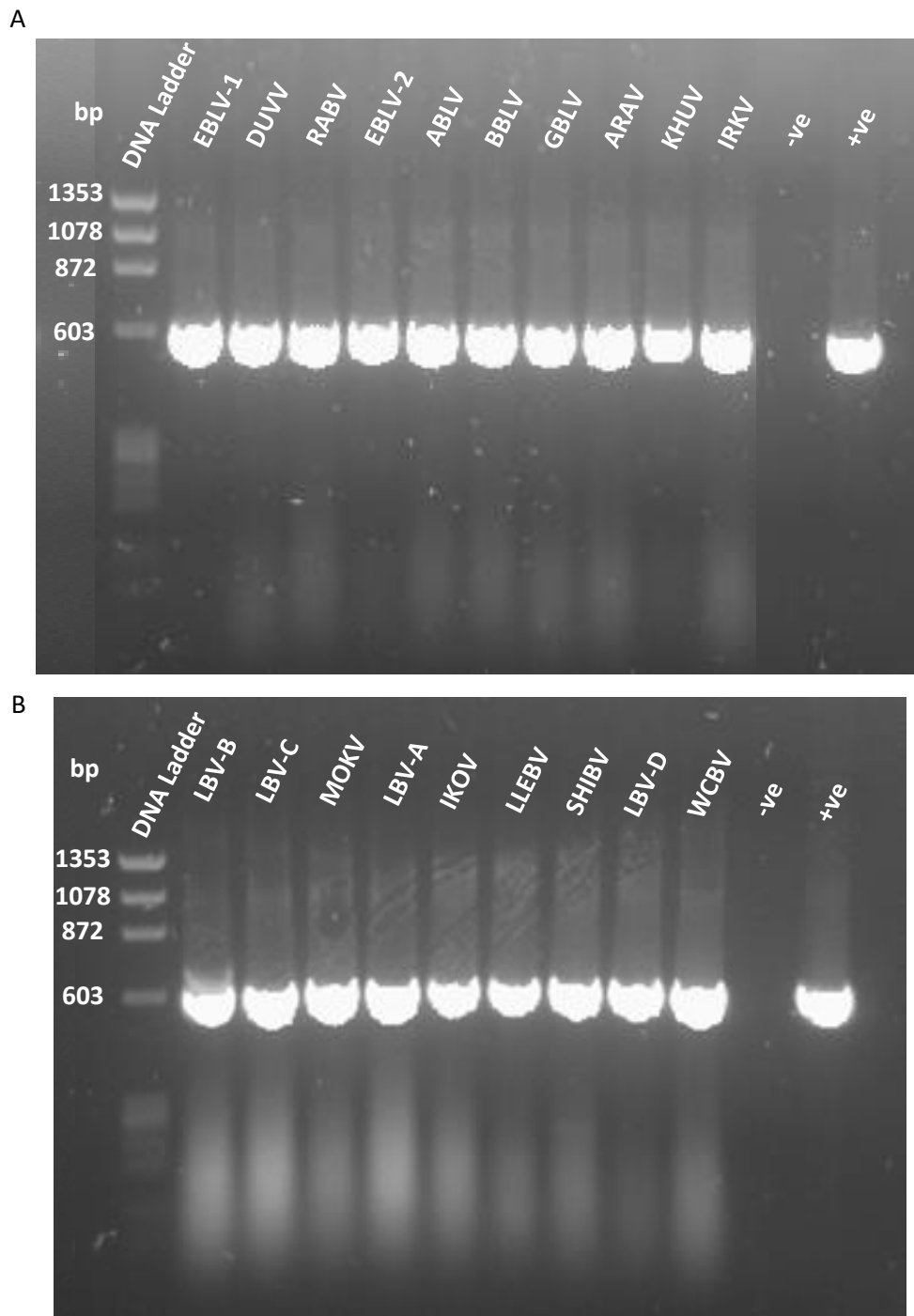


Figure 3.2: Agarose gel to show amplification of a 606bp section of the N gene of each of the lyssaviruses. The DNA ladder used was the Φ X174 DNA/HaeIII Ladder (Promega). (A) Phylogroup I lyssaviruses. (B) Phylogroup II and III lyssaviruses.

3.2.3. Titration of virus stocks

Viruses were titrated via a 10-fold dilution series (as described previously 2.4.2.4) to determine the virus titre in ffu/ml (Figure 3.3). Viruses varied in their final titre, despite requiring the same number of passages for 100% cell infection. The titres of the phylogroup I lyssaviruses exhibited a range between 10^4 and 10^6 ffu/ml, with EBLV-1 exhibiting the highest titre of 4×10^6 ffu/ml, with DUVV exhibiting the second highest and BBLV the third highest. The mode titre among the phylogroup I lyssaviruses was 10^5 ffu/ml, with EBLV-2 exhibiting the lowest titre at 4.3×10^4 ffu/ml.

The titres of the phylogroup II lyssaviruses showed more variability, with titres between 10^3 and 10^8 ffu/ml. SHIBV exhibited the highest titre of 5.3×10^8 ffu/ml, and LBV-D exhibited the second highest titre at 4.1×10^7 ffu/ml. The virus with the lowest titre was LBV-A with a titre of 3.7×10^3 ffu/ml. The titres of phylogroup III were less variable between 10^4 and 10^5 ffu/ml, with WCBV growing to the highest titre of 4.3×10^5 ffu/ml. Whilst the titres vary between lyssaviruses, all lyssaviruses grew to measurable and sufficient titres for future use.

3.2.4. Standardisation of Virus titre

To determine where cross-neutralisation occurs in the genus, a virus titre of 100 TCID₅₀/50 µl had to be established to ensure each virus was tested at the same concentration. This dilution is required for a modified version of the OIE recommended FAVN test that assesses the ability of suspect sera to neutralise 100 TCID₅₀/50 µl of live virus and thus determine a serological titre of neutralising antibodies present in a sample. To determine the optimal dilution for 100 TCID₅₀/50 µl, each virus was diluted and checked by back-titration (as described in section 2.4.2.5); concurrent with the back titration performed as part of the FAVN test. The optimal dilutions of each virus stock to achieve a concentration of 100 TCID₅₀/50 µl are detailed in Table 3.2.

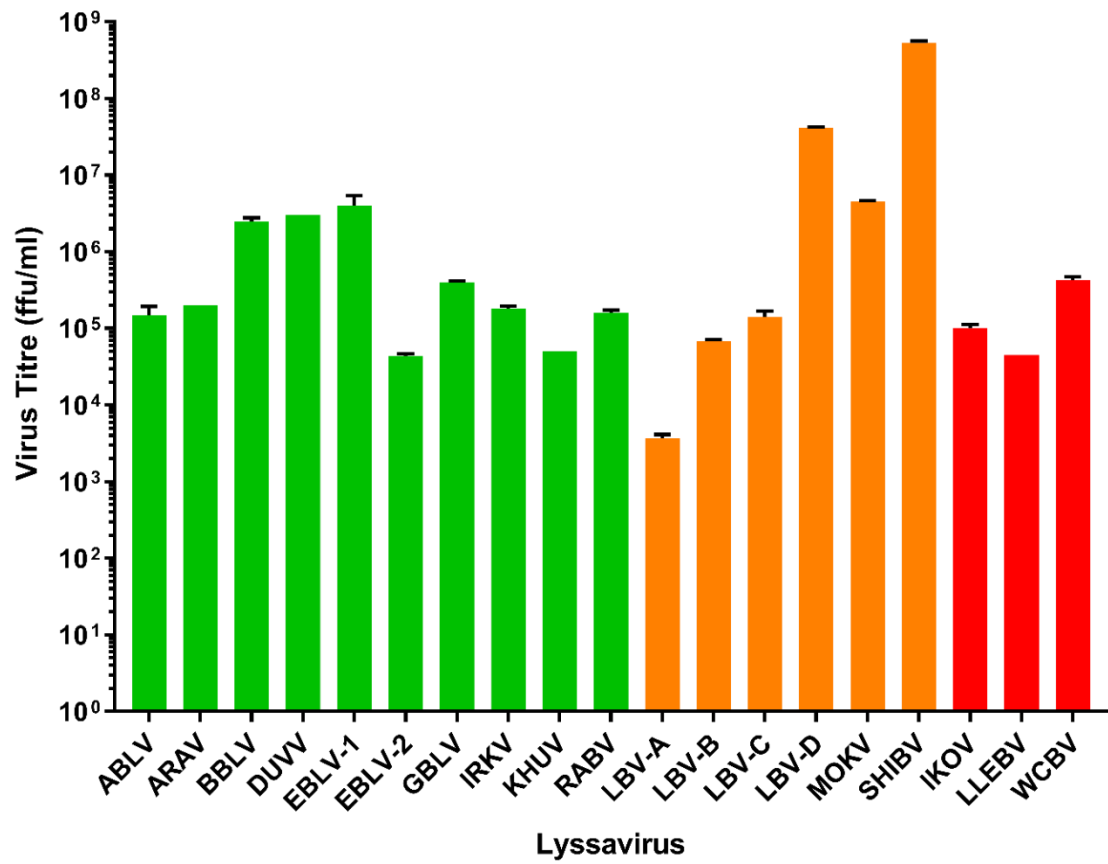


Figure 3.3: The virus titre in ffu/ml for all of the lyssaviruses propagated, plotted on a logarithmic scale. The mean and SD are displayed as each titration was performed in triplicate. The phylogroups are coloured to represent the different phylogroups; with phylogroup I in green, phylogroup II in orange, and phylogroup III in red.

Table 3.2: Virus titre and dilution to achieve 100 TCID₅₀/50 µl for this study.

Virus	Number of passages required for 100% infection from pre-passaged material	Stock titre (ffu/ml)	Dilution required for 100 TCID₅₀/50µl
ABLV	2	1.5×10^5	1:20
ARAV	2	2.0×10^5	1:40
BBLV	2	2.5×10^6	1:30
DUVV	2	3.0×10^6	1:400
EBLV-1	2	4.0×10^6	1:90
EBLV-2	2	4.3×10^4	1:20
GBLV	2	4.0×10^5	1:60
IRKV	2	1.8×10^5	1:15
KHUV	2	5.0×10^4	1:15
RABV	2	1.6×10^5	1:70
LBV A	2	3.7×10^3	1:15
LBV B	2	6.8×10^4	1:20
LBV C	2	1.4×10^5	1:40
LBV D	2	4.1×10^7	1:5000
MOKV	2	4.5×10^6	1:1500
SHIBV	2	5.3×10^8	1:25000
IKOV	2	1.0×10^5	1:20
LLEBV	2	4.5×10^4	1:40
WCBV	2	4.3×10^5	1:10
CVS	-	4.3×10^6	1:3500
cSN	-	1.2×10^6	1:700

- Data not known or data was not generated by the author

3.3. Ability of sera derived from canine and human vaccinees to neutralise phylogroup I lyssaviruses

In order to assess the ability of sera derived from vaccinated humans and animals to neutralise all viruses within phylogroup I, three types of hyperimmune sera were tested at increasing titres. The three sera used (described in section 2.5.4) were WHO serum, OIE serum, and HDCV recipient serum. WHO and OIE serum were diluted to and tested at antibody titres of 0.5 IU/ml, 1 IU/ml, 2.5 IU/ml and 5 IU/ml, and HDCV recipient serum was tested at 0.5 IU/ml, 1 IU/ml, 2.5 IU/ml, 5 IU/ml, and 7.5 IU/ml. A higher antibody titre was tested for the HDCV recipient serum because sufficient serum was available at a high enough titre to do so. All phylogroup I lyssaviruses including two rabies isolates, CVS and RABV, were diluted to 100 TCID₅₀/50 µl and tested on an mFAVN. This involved incubating 50 µl of virus with 50 µl of serially diluted sera at each antibody concentration and assayed according to Section 2.6.1 and 2.6.2. The results of this assay can be seen in Figure 3.4.

All phylogroup I lyssaviruses were neutralised above the cut off titre (≥ 0.5 IU/ml) at 5 IU/ml or less by OIE serum. Despite showing a similar pattern of neutralisation, each of the sera showed varying degrees of neutralisation; qualitatively through the neutralising antibody titre against each of the phylogroup I viruses, and quantitatively through the ability to cross-neutralise phylogroup I lyssaviruses. Between the sera, using the antibody concentrations of 1 IU/ml and 2.5 IU/ml showed the biggest disparity in neutralisation. At 1 IU/ml, 54 % (n=6/11) of the phylogroup I viruses tested were neutralised by OIE sera, whereas only 36 % (n=4/11) were neutralised at this concentration for WHO and HDCV recipient sera.

At 2.5 IU/ml, 91 % (n=10/11) of the phylogroup I lyssaviruses were neutralised by the OIE sera, and 73 % (n=8/11) were neutralised by WHO and HDCV recipient sera.

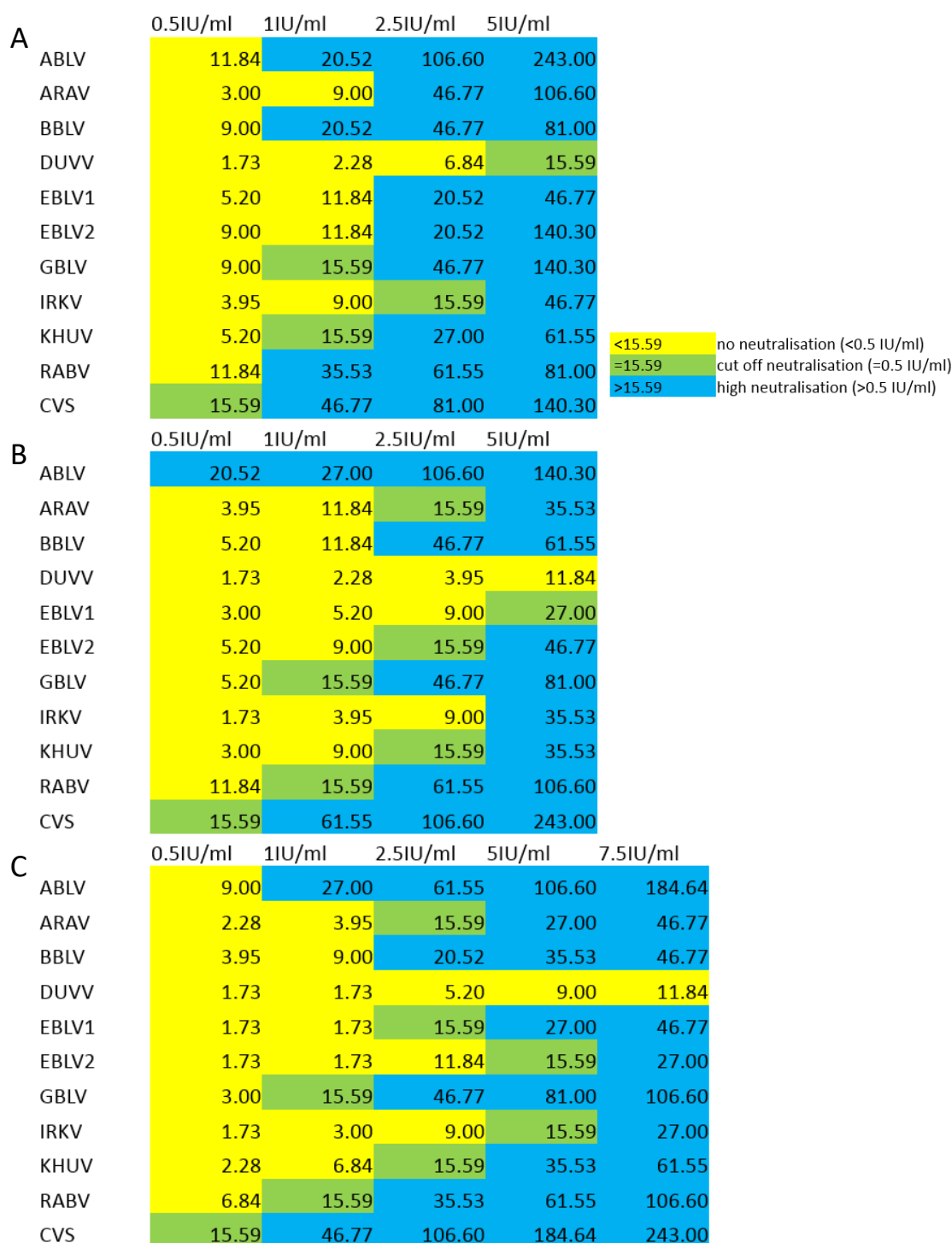


Figure 3.4: Heatmap to show the antibody titre required for the neutralisation of all phylogroup I viruses. Sera of increasing titre (0.5 IU/ml-7.5 IU/ml) was tested against all phylogroup I lyssaviruses. Each dataset is in reciprocal titre (1/x). In this case, a reciprocal titre of 1/15.59 represents 0.5 IU/ml. Yellow represents no neutralisation above or equal to the pre-defined 0.5 IU/ml cut-off (<0.5 IU/ml), green represents neutralisation at the 0.5 IU/ml cut-off titre (=0.5 IU/ml) and blue represents neutralisation exceeding the 0.5 IU/ml cut off titre (>0.5IU/ml). A) OIE sera B) WHO sera C) HDCV vaccine recipient sera.

Despite belonging to the same lyssavirus species of RABV, all sera showed a lower titre of neutralising antibodies against RABV than CVS. This suggests possible antigenic divergence of wild/street RABV strains from the cell culture adapted RABV strain, CVS, used regularly in diagnostic assays.

The pattern of neutralisation of each of the vaccine sera against the phylogroup I viruses is most likely a reflection of genetic distance between each lyssavirus species (shown in Figure 1.1). With licensed rabies vaccines for human use based on whole inactivated RABV particles, the neutralising antibodies present in vaccine sera are most specific to the RABV species. All sera showed the lowest titre of neutralising antibodies against DUVV and IRKV, reflective of the fact that these lyssavirus species are the most genetically-divergent members to RABV within phylogroup I. The viruses with the same or similar pattern of neutralisation to RABV were ABLV, BBLV and GBLV. This correlates with the evolutionary relationship between these viruses as they are the least genetically distant to RABV.

3.4. Generating Sera

3.4.1. Testing for Seroconversion

For a full assessment of cross-neutralisation across the genus, specific sera had to be generated against each lyssavirus. As described in section 2.5, each lyssavirus was inactivated by beta-propiolactone (BPL) and inoculated into 1 year old New Zealand white rabbits. Before sera cross-neutralisation could be assessed, seroconversion was first determined by ELISA using the Platelia Rabies Kit II (Bio-Rad) (as described in section 2.6.3) and then by mFAVN against the homologous virus (as described in 2.6.2).

3.4.1.1. *Binding antibody detection by ELISA*

Lyssavirus specific sera, generated in rabbits, was first assessed using the Platelia Rabies II Kit ELISA described in section 2.6.3. All hyperimmune sera tested positively for RABV antigen-specific binding antibodies above 0.5 EU/ml, units equivalent to the international units (IU/ml) defined by seroneutralisation (Figure 3.5). Unsurprisingly, RABV-specific sera showed the highest titre of binding antibodies at 8.64 EU/ml. BBLV-specific sera showed the second highest titre of binding antibodies at 2.66 EU/ml, and ARAV-specific sera the third highest titre of binding antibodies at 1.97 EU/ml. LBV-C-specific sera showed the lowest titre of binding antibodies at 1.05 EU/ml. Additionally, the binding antibody titres were more variable in phylogroup I than phylogroup II and III; with titres ranging from 1.19 EU/ml to 8.64 EU/ml in phylogroup I and 1.05 EU/ml to 1.58 EU/ml in phylogroup II and III. This demonstrated that all rabbits seroconverted in response to the BPL inactivated preparations of inactivated lyssavirus.

3.4.1.2. *Neutralising antibody detection by mFAVN*

A mFAVN assay was undertaken with each lyssavirus-specific serum, against the homologous virus. All lyssavirus-specific sera, except IRKV and LBV-A specific sera, exhibited sufficient neutralising antibody titres against the homologous virus for use in future serological assays (Figure 3.6). Of the sera that exceeded the cut off for neutralisation, mean reciprocal titres ranged from 1/26 to 1/1263 with EBLV-2-specific sera exhibiting the highest titre. Phylogroup I lyssavirus-specific sera showed the greatest range in neutralising antibody titres and phylogroup III lyssavirus-specific sera showed the least.

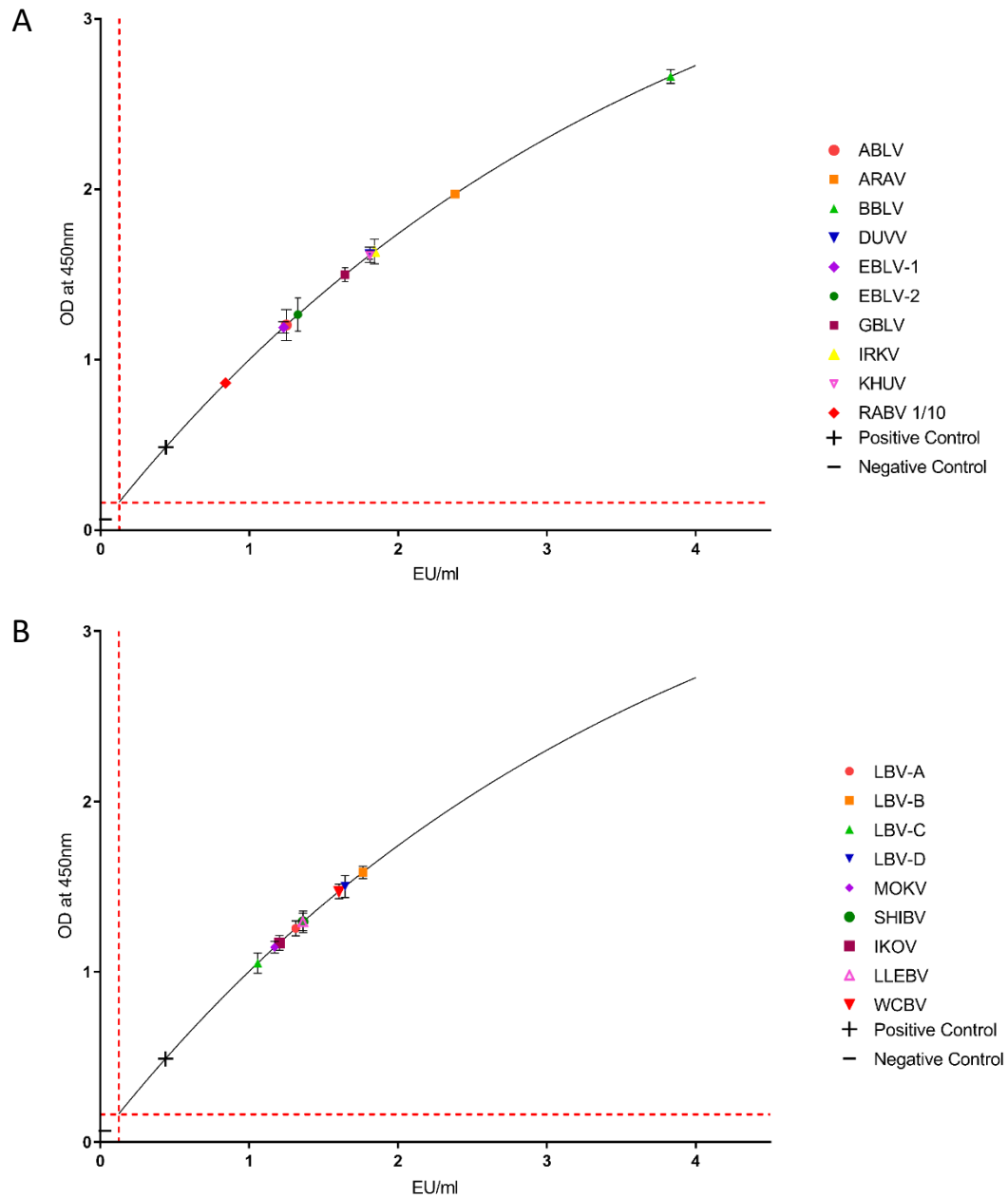


Figure 3.5: Platelia Rabies II ELISA assay to show the RABV antigen-specific binding antibodies in (A) Phylogroup I lyssavirus-specific sera and (B) Phylogroup II and III lyssavirus-specific sera. The test was performed in triplicate and the mean and standard deviation (SD) of the results displayed. The red lines indicate the test's limit of detection. For interpolation using the ELISA standards, a 1/10 dilution of RABV-specific sera had to be used to accurately determine the binding antibody titre in EU/ml.

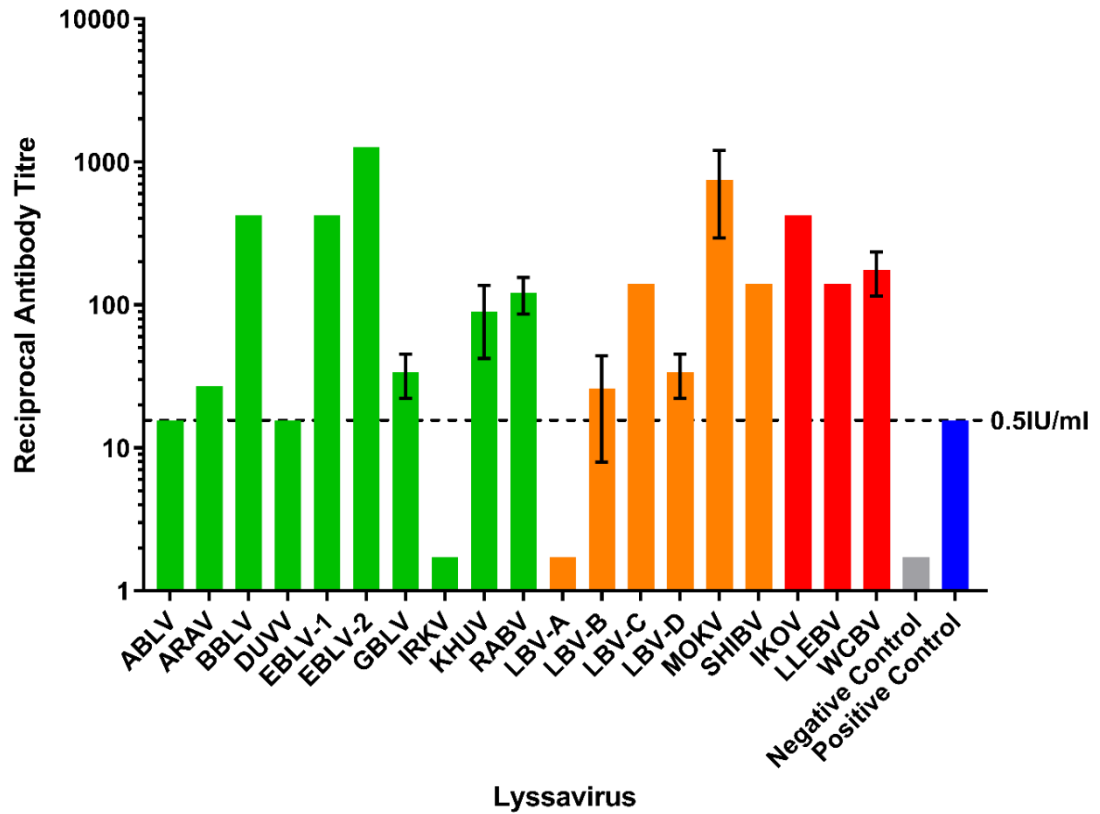


Figure 3.6: Modified FAVN to show the virus neutralising antibody titre of each lyssavirus-specific sera against the homologous virus. The test was performed in triplicate and the mean and standard deviation of the results displayed on a logarithmic scale. The 0.5 IU/ml neutralisation cut off is dictated by the OIE sera against CVS (indicated by the dashed line and positive control). Naïve canine sera was used as the negative control.

3.4.1.3. Characterisation of BPL inactivated preparations

To investigate why the rabbits seroconverted in response to inoculation with inactivated IRKV or inactivated LBV-A, but did not produce neutralising antibodies, the LBV-A inoculum was visualised using a NanoSight instrument (Malvern) and compared to inocula that did induce the production of neutralising antibodies. The IRKV inocula could not be tested as there was an insufficient volume left after inoculation. The NanoSight instrument enables visualisation of particles present in a sample based on the light scatter of a laser. Using the assumption of Brownian motion in a liquid, the particle size is calculated from the tracked frames of scattered light. The BPL inactivated preparations of MOKV, LBV-C, and LBV-A were measured on the NanoSight and compared as described in section 2.5.5. The size distribution of the particles within these preparations is shown in Figure 3.7.

In the inactivated MOKV virus suspension, the mean particle size was 172.3 nm and the mode particle size was 140.9 nm, with a SD of 50.5 nm. The inactivated LBV-C virus suspension showed a similar result, with the mean particle size measuring 162.4 nm and the mode measuring 148.8 nm, with a SD of 43.2 nm. Finally, in the inactivated LBV-A virus suspension, the mean particle size was 178.4 nm and the mode was 136.9 nm, with a SD of 58.2 nm.

Whilst these sizes are comparable, the size of the particles within the inactivated LBV-A virus suspension are more variable, with two clear peaks indicating particles sizes of 182.0 nm and 270.0 nm.

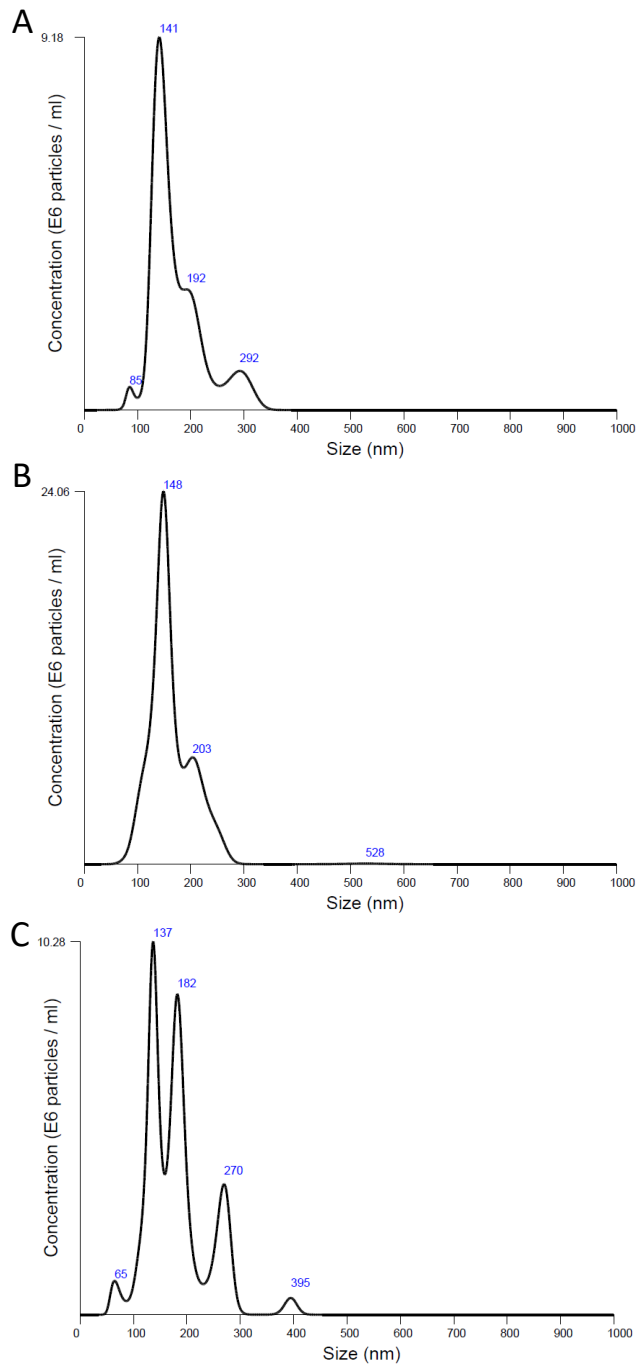


Figure 3.7: NanoSight measurement of A) MOKV virus particles B) LBV-C virus particles and C) LBV-A virus particles. The range of particle sizes is shown.

3.4.2. Other test Sera

Where rabbit sera were unavailable, LBV-A lyssavirus-specific sera was acquired from experimentally infected bats, and IRKV lyssavirus-specific sera was excluded from the dataset.

3.5. Neutralisation within Phylogroup I

Having observed a high degree of cross phylogroup I neutralisation with standard vaccine recipient sera (Figure 3.4) the next stage was to assess the ability of phylogroup I-specific sera to neutralise phylogroup I viruses. This was investigated using a mFAVN where phylogroup I lyssaviruses (a panel of 10 lyssaviruses) were tested against all phylogroup I lyssavirus-specific sera except IRKV-specific sera (a panel of 9 hyperimmune lyssavirus-specific rabbit sera). In addition, CVS and OIE standard sera at 0.5 IU/ml were used as the positive control and naïve canine sera as a negative control. The result of this assay is detailed in Figure 3.8. Whilst varying levels of cross-neutralisation was observed within phylogroup I, each phylogroup I lyssavirus was neutralised by three or more phylogroup I lyssavirus-specific sera to a level above or equal to the predefined cut off at the reciprocal titre equivalent to 0.5 IU/ml. The sera demonstrating the greatest degree of cross-neutralisation was BBLV-specific sera (orange) which exhibited neutralising antibody titres above 0.5 IU/ml against all phylogroup I lyssaviruses. This was closely followed by EBLV-1-specific sera (dark blue) which exhibited neutralising antibody titres above or equal to 0.5 IU/ml against eight of the ten phylogroup I lyssaviruses tested, with detectable neutralising antibody titres against the two viruses that were not neutralised above the cut off. The sera that showed the least cross-neutralisation was DUVV (purple), KHUV (grey), and ABLV-specific sera (yellow) where only the homologous viruses were neutralised.

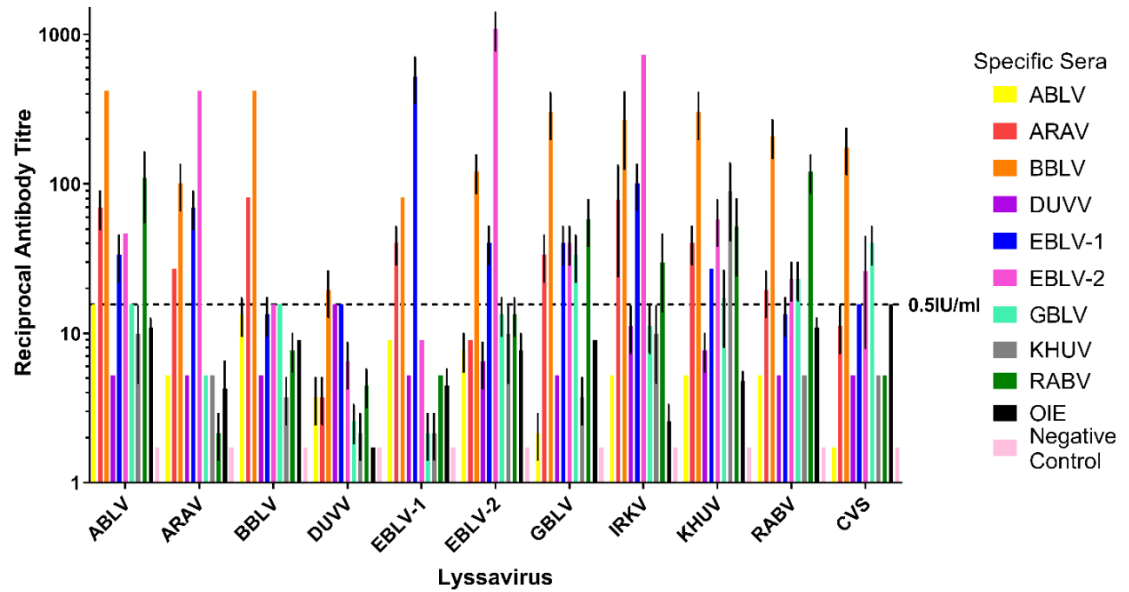


Figure 3.8: Cross-neutralisation profiles within phylogroup I using a modified fluorescent antibody virus neutralisation (mFAVN) test. The test was performed in triplicate and the mean and SD of the results plotted on a logarithmic scale. The 0.5 IU/ml neutralisation cut off is dictated by the OIE sera against CVS (indicated by the dashed line and positive control). Naïve canine sera was used as the negative control. IRKV-specific sera not shown.

Whilst below the cut-off for neutralisation, DUVV-specific sera, showed detectable neutralising antibody titres against IRKV, and KHUV-specific sera exhibited detectable neutralising antibody titres against ABLV, EBLV-2, and IRKV.

Interestingly, whilst ABLV-specific sera exhibited no cross-neutralisation and KHUV-specific sera exhibited little cross-neutralisation against the phylogroup I lyssaviruses, ABLV virus and KHUV virus were most readily neutralised by phylogroup I-specific sera. Both ABLV and KHUV were neutralised by seven phylogroup I-specific sera, and GBLV was neutralised by six phylogroup I-specific sera. DUVV and EBLV-1 were least readily neutralised with only three phylogroup I-specific sera exhibiting neutralising antibody titres above or equal to the 0.5 IU/ml cut off.

Overall, within this group of antigenically and genetically similar viruses, there was a strong degree of cross neutralisation. On average, each phylogroup I lyssavirus was neutralised by five phylogroup I-specific sera.

3.6. Neutralisation within Phylogroup II and III

Based on the extensive cross-neutralisation observed for phylogroup I lyssaviruses using standard vaccine sera and lyssavirus-specific sera, the next stage was to assess cross-neutralisation within phylogroup II and III. In general, the cross-neutralisation observed for the phylogroup I viruses in this study may be a result of the genetic distances between these viruses; pairwise G protein amino acid identities within phylogroup I show identities of $\geq 64\%$. Therefore, with G protein amino acid identities of $>70\%$ within phylogroup II, it was hypothesised that cross-neutralisation would also occur. Additionally, it was hypothesised that phylogroup III lyssavirus-specific sera would be highly specific to the homologous virus based on the low amino acid identity with all other viruses within and outside phylogroup III ($<64\%$).

For phylogroup II, virus isolates and virus-specific sera representative of the four lineages of LBV (A-D) were included due to the antigenic divergence between these isolates, along with the other characterised African lyssaviruses (MOKV and SHIBV). For phylogroup III, virus isolates and virus-specific sera for IKOV, LLEBV and WCBV were included for the full panel. The panel of phylogroup II and III viruses were run against phylogroup II and III-specific rabbit/bat derived polyclonal serum using a mFAVN assay to determine the degree of cross neutralisation. The results of this assay can be seen in Figure 3.9.

Whilst varying levels of cross-neutralisation was observed within phylogroup II, each phylogroup II lyssavirus was neutralised by two or more phylogroup II-specific sera above the predefined cut off. The sera demonstrating the greatest degree of cross-neutralisation were LBV-C-specific sera (orange) and LBV-D-specific sera (purple) which exhibited neutralising antibody titres above or equal to 0.5 IU/ml against five of the six phylogroup II lyssaviruses. Whilst below the cut-off for neutralisation, LBV-C-specific sera showed detectable neutralising antibody titres against LBV-D, and LBV-D-specific sera exhibited detectable neutralising antibody titres against SHIBV. Interestingly, LBV-D-specific sera showed higher neutralising antibodies against LBV-C than the homologous virus LBV-D. The sera that showed the least cross-neutralisation was SHIBV (magenta) and LBV-B (red) which only neutralised the homologous viruses above the 0.5 IU/ml cut off. This data differs from the results of a previous study which showed that phylogroup II pseudotype viruses were more than 90% neutralised by LBV-B-specific sera (38). Whilst below the pre-defined cut-off for neutralisation, SHIBV-specific sera did, however, exhibit detectable neutralising antibody titres against LBV-B.

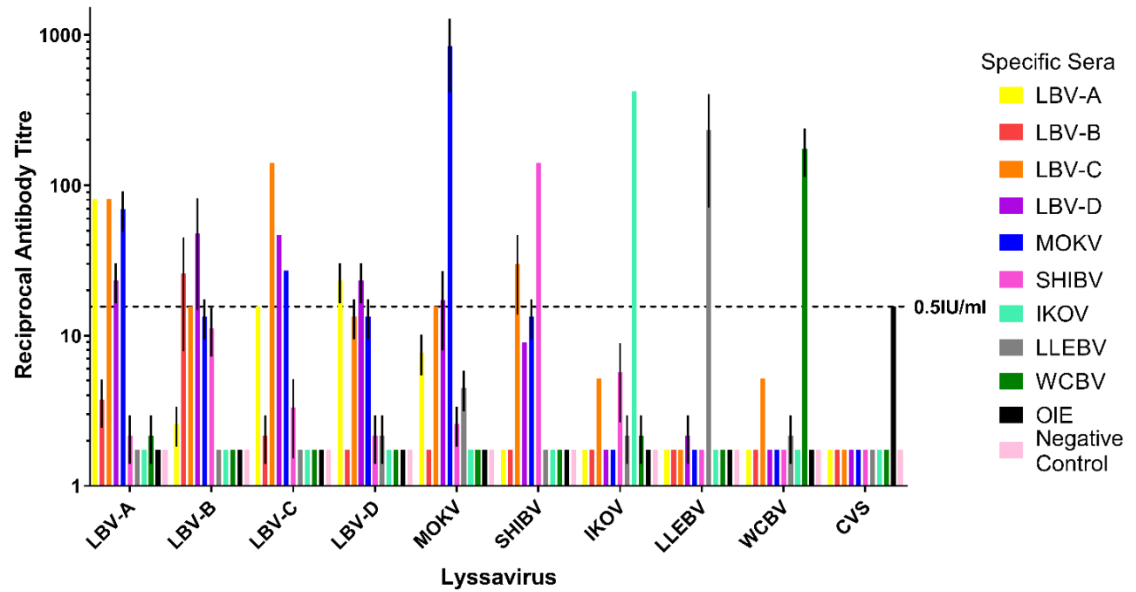


Figure 3.9: Cross-neutralisation profiles across phylogroup II and III using a modified fluorescent antibody virus neutralisation (mFAVN) test. The test was performed in triplicate and the mean and SD of the results plotted on a logarithmic scale. The 0.5 IU/ml neutralisation cut off is dictated by the OIE sera against CVS (indicated by the dashed line and positive control). Naïve canine sera was used as the negative control.

LBV-A virus and LBV-C virus were most readily neutralised by phylogroup II-specific sera. Both viruses were neutralised by four of the six phylogroup II-specific sera. This was closely followed by MOKV and LBV-B as they were neutralised by three phylogroup-II specific sera. SHIBV and LBV-D were the least readily neutralised with only two phylogroup II-specific sera exhibiting neutralising antibody titres above the cut off.

Overall, within this group of antigenically and genetically similar viruses, there was a varied degree of cross neutralisation. On average, each phylogroup II lyssavirus was neutralised by three phylogroup II-specific sera above the cut off for neutralisation.

For phylogroup III, each phylogroup III-specific sera was highly specific to the homologous virus and exhibited no cross-neutralisation above the cut-off with any other virus in phylogroup II or III. LLEBV-specific sera exhibited a neutralising antibody titre against MOKV, however this was below the cut-off.

3.7. Neutralisation across Phylogroup I, II, and III

Following establishment of the level of cross-neutralisation within phylogroup I and between phylogroup II and III, it was of interest to determine the level of cross-neutralisation across phylogroups I, II, and III. It has long been established that rabies vaccines are unable to induce the production of virus neutralising antibodies against viruses from other phylogroups. Most recently with the discovery of LLEBV, a complete lack of cross-neutralisation of human and dog hyperimmune sera for LLEBV has been demonstrated (39). Additionally, mice vaccinated with the rabies vaccine Rabipur had a 40% survival rate following LLEBV challenge although outcome did appear challenge virus dose dependent (39). In order to make an in-depth assessment of

cross-neutralisation across phylogroups, the panel of 18 hyperimmune lyssavirus-specific sera was tested against 19 lyssaviruses, representative of the lyssavirus genus.

Data in Figure 3.10A suggest little to no cross neutralisation of phylogroup I-specific sera against phylogroup II and III viruses. Of the phylogroup I-specific sera, RABV-specific sera (dark green) exhibited neutralising antibody titres against MOKV at the 0.5 IU/ml cut off. This was the first instance of inter-phylogroup neutralisation. Whilst below the cut off, DUVV-specific sera (purple) exhibited a detectable neutralising antibody titre against MOKV, SHIBV, and WCBV; notable due to the fact that DUVV-specific sera showed little to no neutralisation against other phylogroup I viruses.

Data in Figure 3.10B suggest little to no cross neutralisation of phylogroup II and III-specific sera against phylogroup I viruses. Of the phylogroup II and III-specific sera, none exhibited neutralising antibody titres against any phylogroup I virus above the 0.5 IU/ml cut off. Interestingly, LBV-B sera (red) showed a mean reciprocal titre of 1/11 against DUVV, just below the predefined cut off. This was a notable phenomenon as LBV-B sera showed no neutralising antibodies against other phylogroup II viruses.

To conclude, cross-neutralisation across phylogroups was minimal. The only evidence of inter-phylogroup cross-neutralisation above the cut off for neutralisation was RABV-specific sera against MOKV virus. Interestingly, MOKV-specific sera (blue) exhibited no cross-neutralisation against RABV virus.

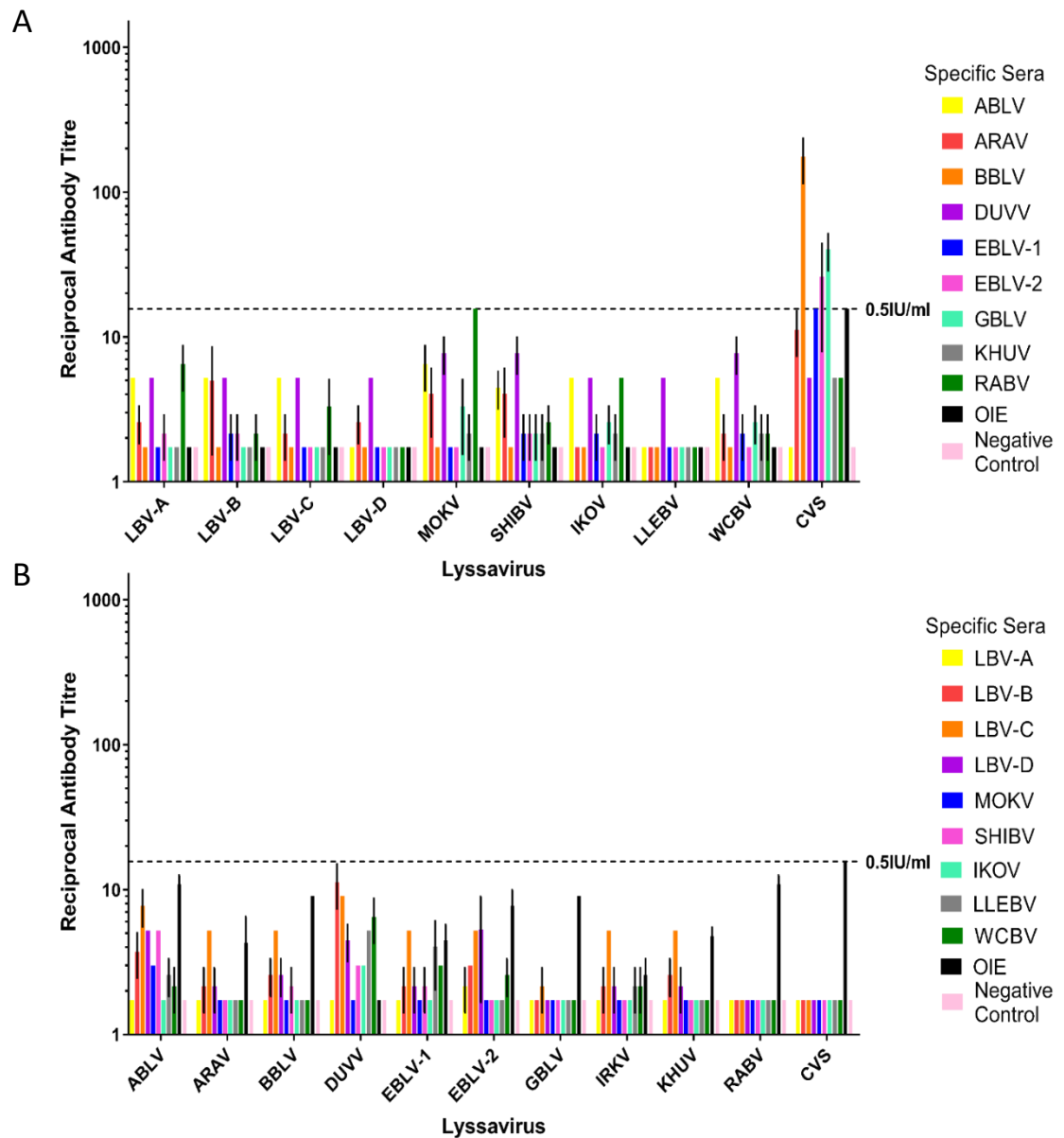


Figure 3.10: Cross-neutralisation profiles across phylogroup I, II, and III using a modified fluorescent antibody virus neutralisation (mFAVN) test. The test was performed in triplicate and the mean and SD of the results plotted on a logarithmic scale. The 0.5 IU/ml neutralisation cut off is dictated by the OIE sera against CVS (indicated by the dashed line and positive control). Naïve canine sera was used as the negative control. A) Phylogroup I-specific sera against phylogroup II and III viruses. B) Phylogroup II and III-specific sera against phylogroup I viruses.

3.8. Optimisation of Phylogroup II cross-neutralisation

Initial data in Figure 3.4 show that OIE sera at 5 IU/ml was sufficient to neutralise all phylogroup I lyssaviruses above the cut-off, however, OIE sera at 0.5 IU/ml only neutralised CVS. Within phylogroup II, LBV-B and LBV-D -specific sera showed low neutralising antibody titres against the homologous virus, albeit exceeding the 0.5 IU/ml cut off (Figure 3.6). Despite this, LBV-D-specific sera exhibited sufficient neutralising antibodies against five of the six phylogroup II lyssaviruses, LBV-A, LBV-B, LBV-C, LBV-D, and MOKV. As a result, it was hypothesised that higher neutralising antibody titres of phylogroup II-specific sera would elicit complete cross-neutralisation across phylogroup II. For this reason, phylogroup II hyperimmune sera was concentrated using an Amicon Ultra-4 Centrifugal Filter Unit (Millipore) as described in section 2.5.6 and tested against the homologous virus to assess the increase in reciprocal titre (Figure 3.11A).

Whilst all neutralising antibody titres of the concentrated phylogroup II sera increased, the proportion to which the titre increased varied between sera when compared to the original titres. With a 12-fold increase, concentrated LBV-A-specific sera exhibited the largest increase in neutralising antibody titre, whilst MOKV-specific sera exhibited the smallest with a 1.2-fold increase. The phylogroup II-specific sera with lowest neutralising antibody titre after concentration was LBV-D-specific sera and the sera exhibiting the highest neutralising antibody titre was SHIBV-specific sera. Using the Kruskal-Wallis test and a level of significance (alpha value) of 0.05, LBV-A and SHIBV-specific sera were the only hyperimmune sera to significantly increase in neutralising antibody titre after concentration ($P=0.002$, $P<0.031$).

All titres of the concentrated sera were within a range that would be considered possible by natural immunity with a range equivalent to ~1.05-40.50 IU/ml (448).

Once concentrated stocks of phylogroup II-specific sera had been established, cross-neutralisation across phylogroup II and III was re-assessed. The results of this assay can be seen in Figure 3.11B.

The degree of cross-neutralisation across phylogroup II increased, as each phylogroup II lyssavirus was neutralised by three or more phylogroup II-specific sera above or equal to the pre-defined cut off. A 2-way ANOVA test was used to compare the degree of neutralisation of each of the phylogroup II-specific sera before and after concentration. It was determined that LBV-A, LBV-B, LBV-D, and SHIBV-specific sera all exhibited a significant increase in cross-neutralisation ($P < 0.001$). The sera demonstrating the greatest degree of cross-neutralisation within phylogroup II was now LBV-B-specific sera (red) and LBV-D-specific sera (purple) which exhibited neutralising antibody titres above or equal to 0.5 IU/ml against all six phylogroup II lyssaviruses. This is notable since LBV-B-specific sera did not neutralise any phylogroup II viruses prior to concentration. LBV-B-specific sera increased 5.4 fold in titre after concentration, sufficient for cross-neutralisation compared to the lower titre.

Additionally, SHIBV-specific sera (magenta) also exhibited sufficient neutralising antibody titres against six lyssaviruses; five viruses within phylogroup II and IKOV virus within phylogroup III. This was the second instance of inter-phylogroup cross-neutralisation. In a previous study, IKOV pseudotyped virus was shown to be 60% neutralised by LBV-B specific sera, indicating that IKOV was more antigenically similar to phylogroup II lyssaviruses than the other phylogroup III lyssaviruses are to phylogroup II (38). Interestingly, LBV-D-specific sera showed a higher titre of neutralising antibodies against four phylogroup II lyssaviruses than against the homologous virus, LBV-D.

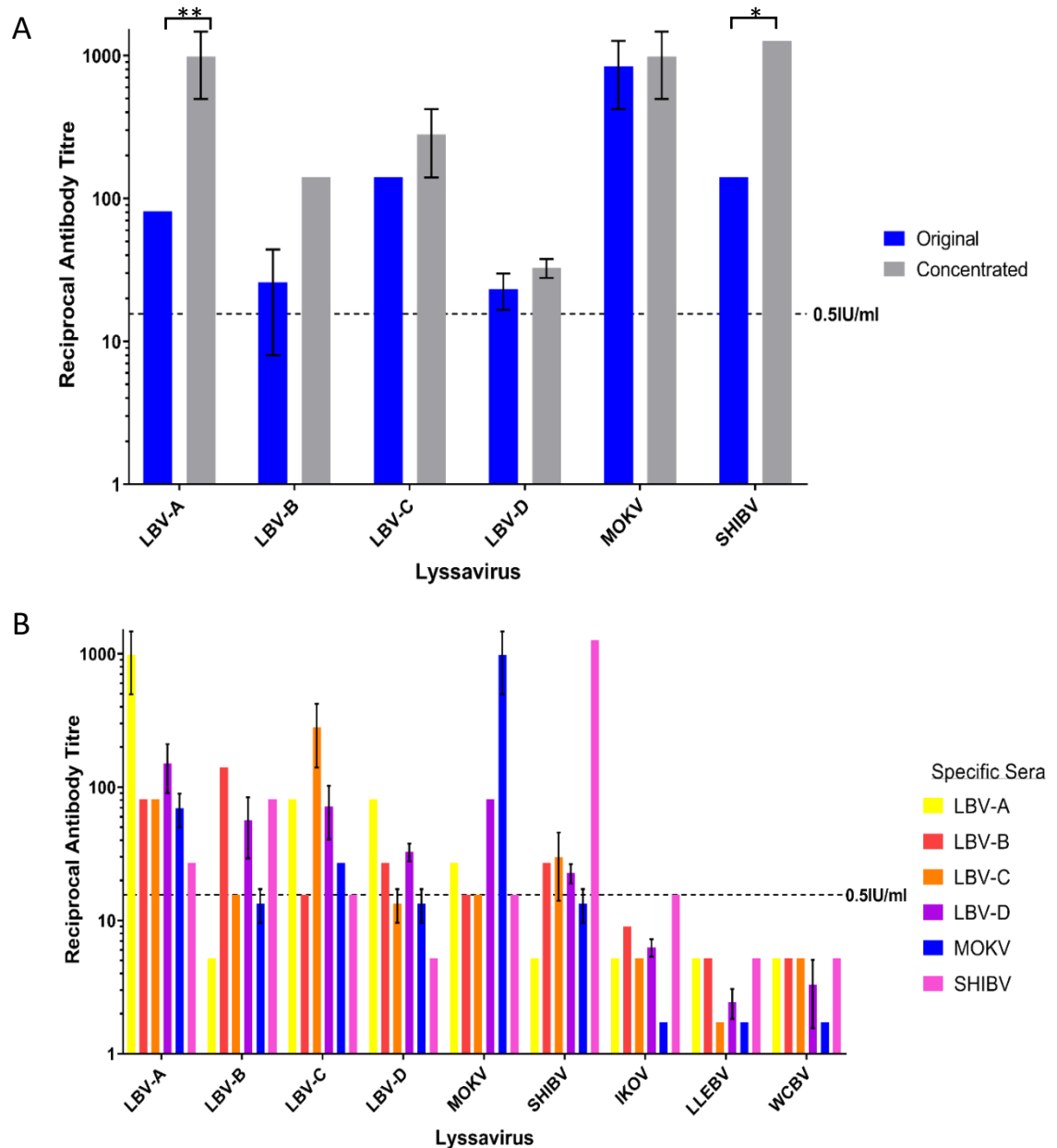


Figure 3.11: Neutralisation profiles of concentrated phylogroup II-specific sera using a modified fluorescent antibody virus neutralisation (mFAVN) test. (A) Phylogroup II-specific sera before (blue) and after (grey) concentration against the homologous virus. Asterisks indicate significant differences between the original and concentrated sera calculated using the Kruskal-Wallis test (** $P < 0.01$, * $P < 0.05$). (B) The cross-neutralisation profiles of concentrated phylogroup II-specific sera against phylogroup II and III viruses. The mFAVN tests were performed in triplicate and the mean and SD of the results plotted on a logarithmic scale. The 0.5 IU/ml neutralisation cut off is dictated by the OIE sera against CVS (indicated by the dashed line).

Concentrated LBV-C-specific sera (orange), exhibited neutralising antibody titres, exceeding or equal to the 0.5 IU/ml cut off, against five phylogroup II lyssaviruses and showed detectable neutralising antibody titres against LBV-D.

The sera that showed the least cross-neutralisation was MOKV-specific sera (dark blue) which neutralised three phylogroup II lyssaviruses above the 0.5 IU/ml cut off.

LBV-A virus, LBV-C virus, and MOKV virus were most readily neutralised by phylogroup II-specific sera as all three viruses were neutralised by each of the six phylogroup II-specific sera. This was followed by SHIBV and LBV-B as they were neutralised by four phylogroup-II specific sera. LBV-D was the least readily neutralised with only three phylogroup II-specific sera exhibiting neutralising antibody titres above or equal to the cut off against this virus.

Overall, as observed between the viruses in phylogroup I, there was a high degree of cross neutralisation between the viruses in phylogroup II. On average, each phylogroup II lyssavirus was neutralised by approximately five phylogroup II-specific sera.

Crucially, of the phylogroup II-specific sera tested, two sufficiently neutralised all six phylogroup II lyssaviruses. This supports the concept of including only one phylogroup I and one phylogroup II lyssavirus G protein in any cross protective antigen formulation. These antigens should be able to provide sufficient cross neutralisation between all viruses in phylogroups I and II. One caveat to this hypothesis is that the phylogroup II-specific sera was concentrated to elicit cross-neutralisation across the phylogroup. However, the neutralisation titres for the concentrated phylogroup II-specific sera were all within a range considered possible by natural immunity. To investigate this more samples of phylogroup II-specific sera would have to be tested.

For cross-neutralisation across the entire genus, it is likely that each of the phylogroup III lyssaviruses would have to be included.

3.9. Antigenic cartography

The antigenic difference between isolates dictates the degree to which neutralising antibodies induced by one isolate are effective against another. Consequently, the analysis of antigenic differences and cross neutralisation is vital for vaccine strain selection. FAVN and mFAVN data gives an approximation of antigenic differences, but reciprocal titres alone are generally considered unsuitable for quantitative analyses.

In order to quantitatively assess the cross-neutralisation assay data by facilitating visualisation and interpretation of antigenic data, lyssavirus antigenic maps were generated from the mFAVN neutralisation data using antigenic cartography techniques described in section 2.14.

Briefly, each antigen and antiserum are assigned a point on an antigenic map such that the distance between the antigen and the antiserum directly corresponds to the reciprocal neutralisation titre from the mFAVN assays. The target distance is derived by calculating the difference between the \log_2 reciprocal neutralisation titre for that particular virus and the \log_2 reciprocal maximum titre achieved by that serum against any virus within the dataset. As a result, the higher the reciprocal titre, the shorter the antigenic distance. As antigenic distance, denoted in antigenic units (AU), is linearly related to the \log_2 of the reciprocal titres, a two-fold change in reciprocal titre would equal 1 AU, a four-fold change would equal 2 AU, and an eight-fold change would equal 3 AU, and so on.

To optimise the relative positions of the viruses and sera on a map, metric and ordinal multidimensional scaling techniques are used. Additionally, multiple random restart

optimisations (100) were completed to reduce the chance of maps getting trapped in local optima. The maps selected for analysis were those that exhibited the highest coefficient of determination (R^2) for the variables: antigenic cartography map distance (AU), and reciprocal titre from the neutralisation assay data. Whilst resolution increases with each increasing dimension, 3D maps were used to determine antigenic distance and visualisation as the incremental increase in precision becomes negligible beyond three dimensions (24). In some cases 2D maps were included for clarity.

Where neutralisation occurs, each virus is positioned by multiple sera, and vice versa. Hence, antisera with different neutralisation profiles to the homologous viruses can be in separate locations on the map but still contribute to the viruses' position.

Consequently, the resolution of the antigenic maps can be greater than the mFAVN assay resolution because the location of a point on the map is fixed by multiple measurements to other points; thereby averaging out error.

3.9.1. Phylogroup I

All phylogroup I lyssaviruses were neutralised above the cut off titre (≥ 0.5 IU/ml) at 5 IU/ml or less by the standard OIE serum (Figure 3.4). Whilst a vaccine strain has already been established for RABV and OIE serum neutralised other members of phylogroup I, it was critical to quantitatively assess the mFAVN assay data (Figure 3.8) as antigenicity is a significant factor for predicting vaccine protection against novel lyssaviruses. Additionally, retrospective quantitative analyses of lyssavirus genetic data have revealed important insights into the evolution of lyssaviruses and have highlighted three distinct phylogroups within the genus. By quantitatively assessing the antigenic differences among phylogroup I lyssaviruses, the antigenic effect of G protein amino acid sequence identity can be predicted.

3.9.1.1. *Lyssavirus antigenic variation*

Figure 3.12 shows a three-dimensional antigenic map, displaying the antigenic relationships among the panel of 11 phylogroup I lyssaviruses; represented by the coloured spheres. Sera are represented by coloured translucent boxes, and are omitted from Figure 3.12B and D for clarity.

Consistent with genetic data (Table 3.3), the antigenic map derived from phylogroup I cross-neutralisation data revealed that RABV and CVS are antigenically indistinguishable. In addition, GBLV was positioned closest to RABV and CVS, closely followed by ABLV. Previously, ABLV has been reported as being antigenically indistinguishable from wt-RABV (24). Whilst consistent with the findings in this report that ABLV is antigenically close to RABV in comparison to the other phylogroup I lyssaviruses, the discovery of GBLV and the added constraints of additional phylogroup I-specific sera may have identified distinct antigenic differences between these viruses. As a result, it could be hypothesised that a larger and more diverse panel of viruses and hyperimmune sera increased the accuracy of these antigenic maps.

Between lyssavirus species, ABLV and GBLV positioned closest to each other antigenically, closely followed by ARAV and EBLV-2, and ARAV and IRKV. Previously it has been suggested that that EBLV-1 and EBLV-2 may be equally antigenically distinct from RABV (441). This is concurrent with the findings of this study where the distance between RABV and EBLV-1 was 3.58 AU and the distance between RABV and EBLV-2 was 3.12 AU, equivalent to a 12 fold change in reciprocal titre and a 9 fold change in reciprocal titre, respectively (Table 3.3).

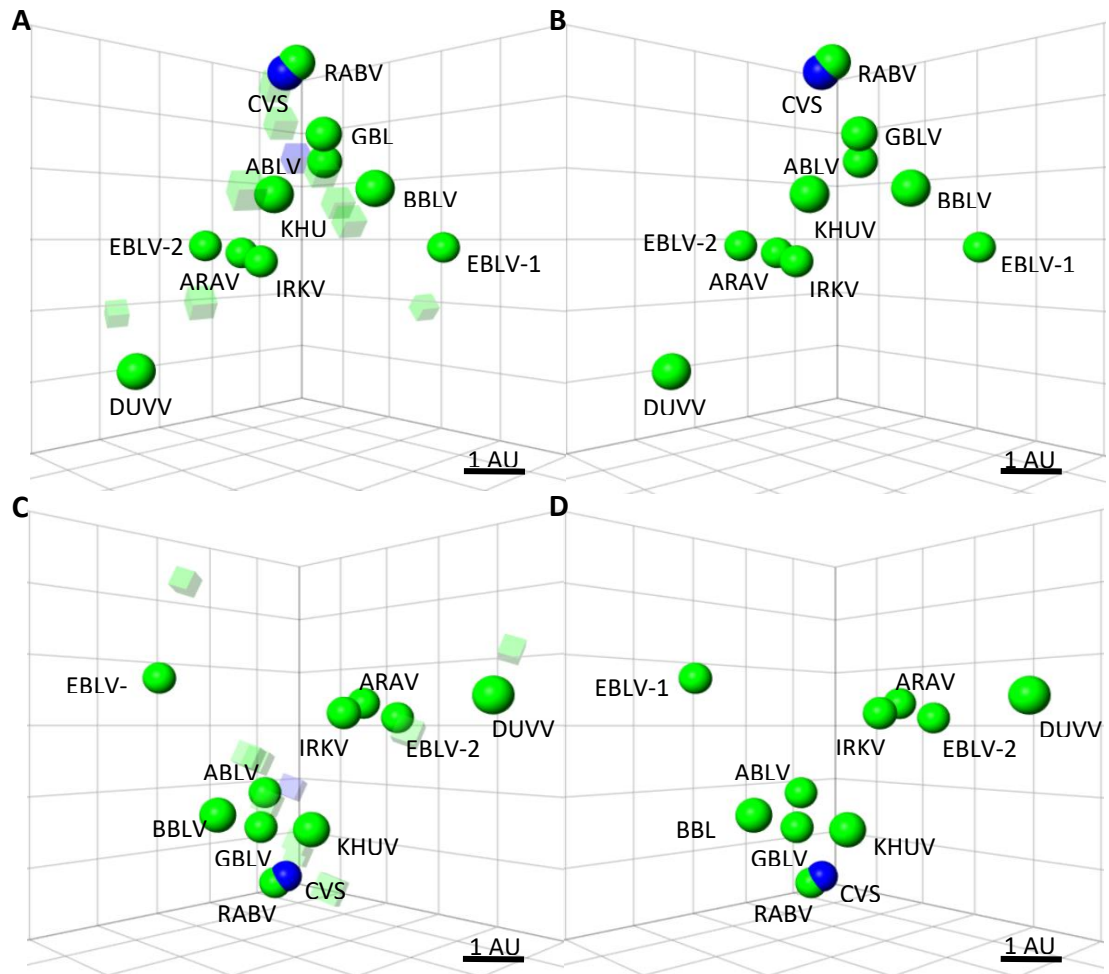


Figure 3.12: (A) 3D antigenic map of phylogroup I viruses. Viruses (spheres, coloured green to represent phylogroup I with CVS in dark blue) and sera (coloured translucent boxes) are positioned such that the distance from each serum to each virus is determined by the neutralisation titre. Multidimensional scaling is used to position both sera and viruses relative to each other, so orientation of the map within the axes is free. Scale bar shows one antigenic unit (AU), equivalent to a two-fold dilution in antibody titre. (B) The same map with sera removed for clarity. (C) The same map but inverted and rotated $\sim 180^\circ$. (D) The same view as C removed for clarity.

Table 3.3: Intergenotypic genetic (below diagonal) and antigenic variation (above diagonal) of phylogroup I viruses

		Antigenic Distance										
		ABLV	ARAV	BBLV	DUVV	EBLV-1	EBLV-2	GBLV	IRKV	KHUV	RABV	CVS
Amino Acid difference (%)	ABLV		1.96	1.34	3.78	2.29	2.22	0.53	1.71	1.48	1.45	1.37
	ARAV	19		2.77	2.56	2.94	0.54	2.38	0.61	2.28	3.07	2.91
	BBLV	19	13		3.77	2.40	3.04	1.22	2.27	1.22	2.02	2.00
	DUVV	22	16	18		4.71	2.39	3.95	2.36	2.88	4.54	4.38
	EBLV-1	23	12	18	17		3.46	2.67	2.68	3.22	3.58	3.56
	EBLV-2	19	12	10	16	16		2.56	0.96	2.35	3.12	2.95
	GBLV	13	16	14	20	19	16		2.10	1.34	1.01	0.95
	IRKV	25	18	22	21	16	20	22		1.81	2.90	2.75
	KHUV	18	12	10	18	16	9	14	19		1.91	1.81
	RABV	19	19	18	23	22	19	15	25	17		0.19
	CVS	20	19	18	23	23	19	15	25	18	7	

Above diagonal: Map antigenic distances measured in antigenic units. Below diagonal: Amino acid percentage difference in glycoprotein ectodomain.

On average however, EBLV-1 is approximately 0.5 AU further from CVS and RABV than EBLV-2 is to CVS and RABV. This is reflected in other studies that suggest EBLV-2 is antigenically closer to CVS and Pasteur virus than EBLV-1 is to CVS and Pasteur virus (24, 449).

For other members of phylogroup I, ARAV and IRKV are antigenically closer to EBLV-2 than EBLV-1, and KHUV is closer to RABV than either of the EBLVs. EBLV-1 and DUVV are positioned furthest from all phylogroup I lyssaviruses on the antigenic map, indicating that they are the most antigenically divergent members within phylogroup I. The findings of the phylogroup I data in this study concurs with a previous study (24).

Rather than forming a continuous antigenic lineage, the phylogroup I viruses tend to group in clusters (Figure 3.13A). Within this map, viruses have been grouped into clusters based on the antigenic distance to the cluster centre.

The resolution of these antigenic maps in the average prediction error has been previously determined to be 1.22 (SE, 0.17) AU in 3D and 1.36 (SE, 0.16) AU in 2D (24). Therefore, viruses that are positioned ≤ 1.4 AU from the cluster centre are included in the cluster. In this case, two clusters have been identified and the viruses occupying the centre of each cluster are GBLV and ARAV. CVS, RABV, ABLV, GBLV, BBLV, and KHUV form one cluster, and ARAV, IRKV, and EBLV-2 form a second cluster. EBLV-1 and DUVV do not reside in either clusters because they are the most antigenically divergent members within phylogroup I and are positioned >1.4 AU from the other viruses. In this sense, EBLV-1 and DUVV could form a third and fourth cluster.

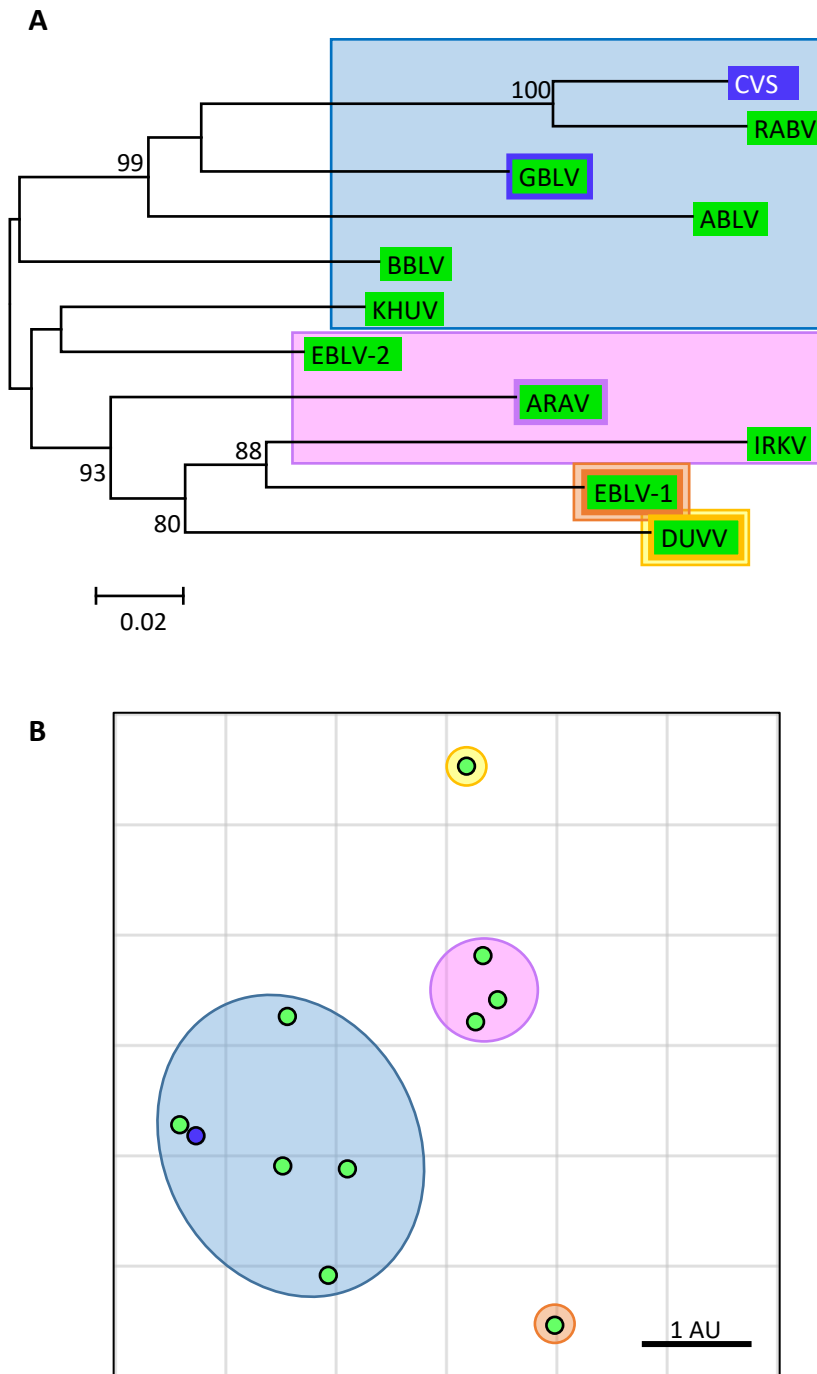


Figure 3.13: (A) Phylogenetic tree of the phylogroup I glycoprotein nucleotide sequences (described in Table 3.1), colour coded based on Fig 3.12. Antigenic clusters have been identified in relation to GBLV, ARAV, EBLV-1, and DUVV and are shown through transparent differentially coloured rectangles. The evolutionary history was inferred using the Neighbor-Joining method and the evolutionary distances were computed using the Maximum Composite Likelihood (ML) method and are in the units of the number of base substitutions per site. Trees were generated in MEGA6 and edited in FigTree. (B): Antigenic 2D map of phylogroup I viruses. The relative positions of the viruses coloured as before (Fig. 3.13A). Antigenic clusters have been identified in relation to GBLV, ARAV, EBLV-1, and DUVV and are shown through transparent differentially coloured ovals. Scale bar represents 1 AU.

3.9.1.2. Predicting antigenic distance from evolutionary data

Quantitatively visualising antigenic data allows direct comparison to the genetic data.

To further investigate the genetic basis of the antigenic distances, the G protein nucleotide sequences of each phylogroup I lyssavirus are quantitatively displayed as a phylogenetic tree and colour-coded according to the clusters identified in the antigenic map of Figures 3.12 and 3.13A (Figure 3.13B).

Pairwise comparison of the antigenic distances to the genetic distances was undertaken using the Pearson product-moment correlation coefficient (Figure 3.14A). Whilst the data is statistically significant ($P=0.005$), the linear relationship between the antigenic distance and evolutionary distance indicate that the variables have low correlation ($r=0.37$ (95%CI 0.12 to 0.58), $R^2=0.14$).

3.9.1.3. Predicting antigenic distance from amino acid sequence identity

Pairwise comparisons of the antigenic distances with the amino acid sequence identity of the entire G protein sequence, the G protein ectodomain, and the identified G protein antigenic sites were undertaken using the Pearson product-moment correlation coefficient. The antigenic site amino acid identity showed an even lower correlation to the antigenic distances ($r=0.32$ (95%CI 0.06 to 0.54), $R^2=0.10$, $P=0.019$) (Figure 3.14B). Whilst the correlation between the antigenic distance and the amino acid identity of the entire G protein ($r=0.44$ (95%CI 0.21 to 0.64), $R^2=0.20$, $P<0.001$) or the ectodomain ($r=0.39$ (95%CI 0.14 to 0.60), $R^2=0.15$, $P=0.003$) showed a better correlation than the evolutionary genetic distances, the correlation coefficient (r) is still below 0.5, indicating low correlation (Figure 3.14C and D).

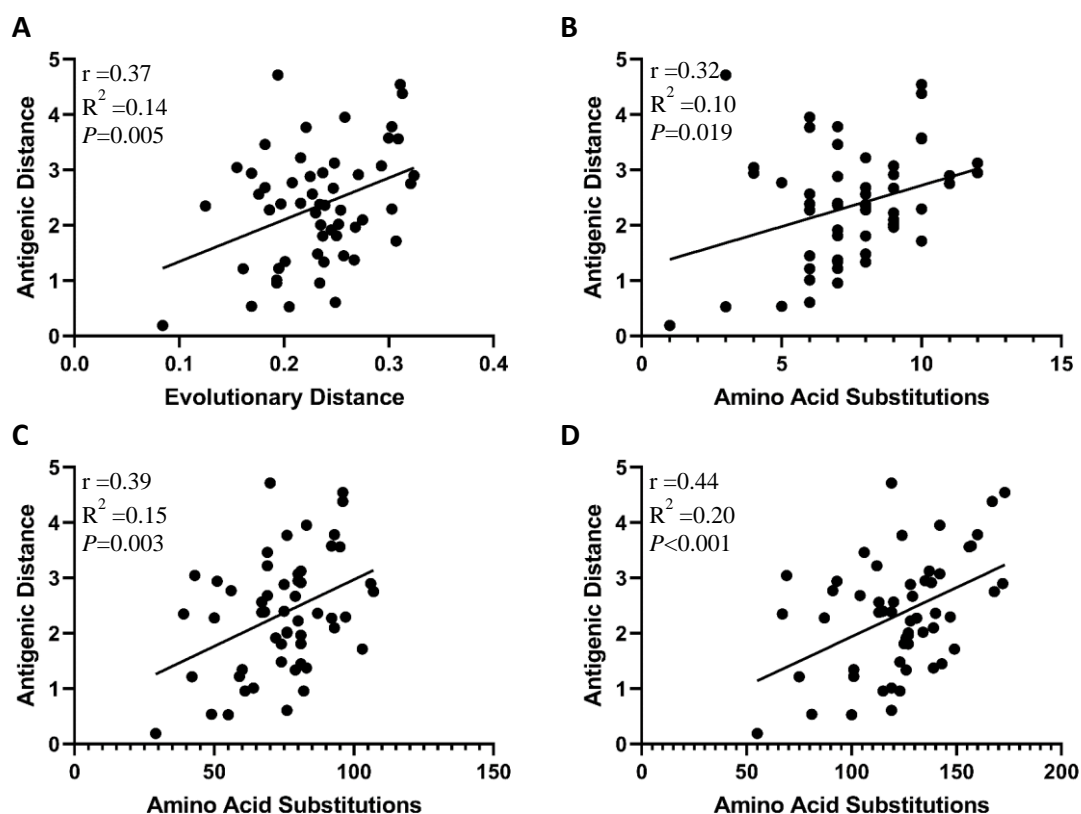


Figure 3.14: Plot of pair-wise antigenic and genetic distances between phylogroup I viruses. Antigenic distances are measured from the antigenic map, in antigenic units. (A) Genetic distances are represented as the pair-wise Maximum likelihood distance of the glycoprotein. (B-D) Genetic distances are represented as the number of pair-wise amino acid substitutions in the antigenic sites (B), glycoprotein ectodomain (C), and the entire glycoprotein (D). The line represents a linear regression model.

3.9.2. Phylogroup II

Whilst there was limited inter-phylogroup cross neutralisation, a high degree of cross neutralisation between viruses in phylogroup II could identify a vaccine strain candidate for neutralisation of all phylogroup II viruses. The concept of generating any cross protective antigen formulation for use as a pan-lyssavirus vaccine would require a combination of antigens representative of the lyssavirus genus. Antigenic cartography was used to quantitatively assess the phylogroup II antigenic data to identify a single antigen that could be representative of all phylogroup II viruses in a cross protective vaccine.

3.9.2.1. *Lyssavirus antigenic variation*

Figure 3.15 shows three-dimensional antigenic maps, displaying the antigenic relationships among a panel of six phylogroup II lyssaviruses (LBV lineages A-D); represented by the coloured spheres. Sera are represented by coloured translucent boxes, and are omitted from Figures 3.15B and D for clarity.

Despite belonging to the same lyssavirus species, the LBV viruses are antigenically distinct. The antigenic distances within phylogroup II range from 1.56-5.59 AU, with an average of 3.74 AU between viruses (Table 3.4). Between each lyssavirus, LBV-A and LBV-C were the most antigenically similar of all phylogroup II lyssaviruses, followed by LBV-A and LBV-D. As a result, LBV-A, LBV-C, and LBV-D cluster together on the 3D map. LBV-B is more antigenically divergent than the other LBVs and most antigenically similar to SHIBV; with an antigenic distance of 2.55 AU. MOKV is the most antigenically divergent phylogroup II lyssavirus with an average distance of 4.22 AU from each of the phylogroup II lyssavirus.

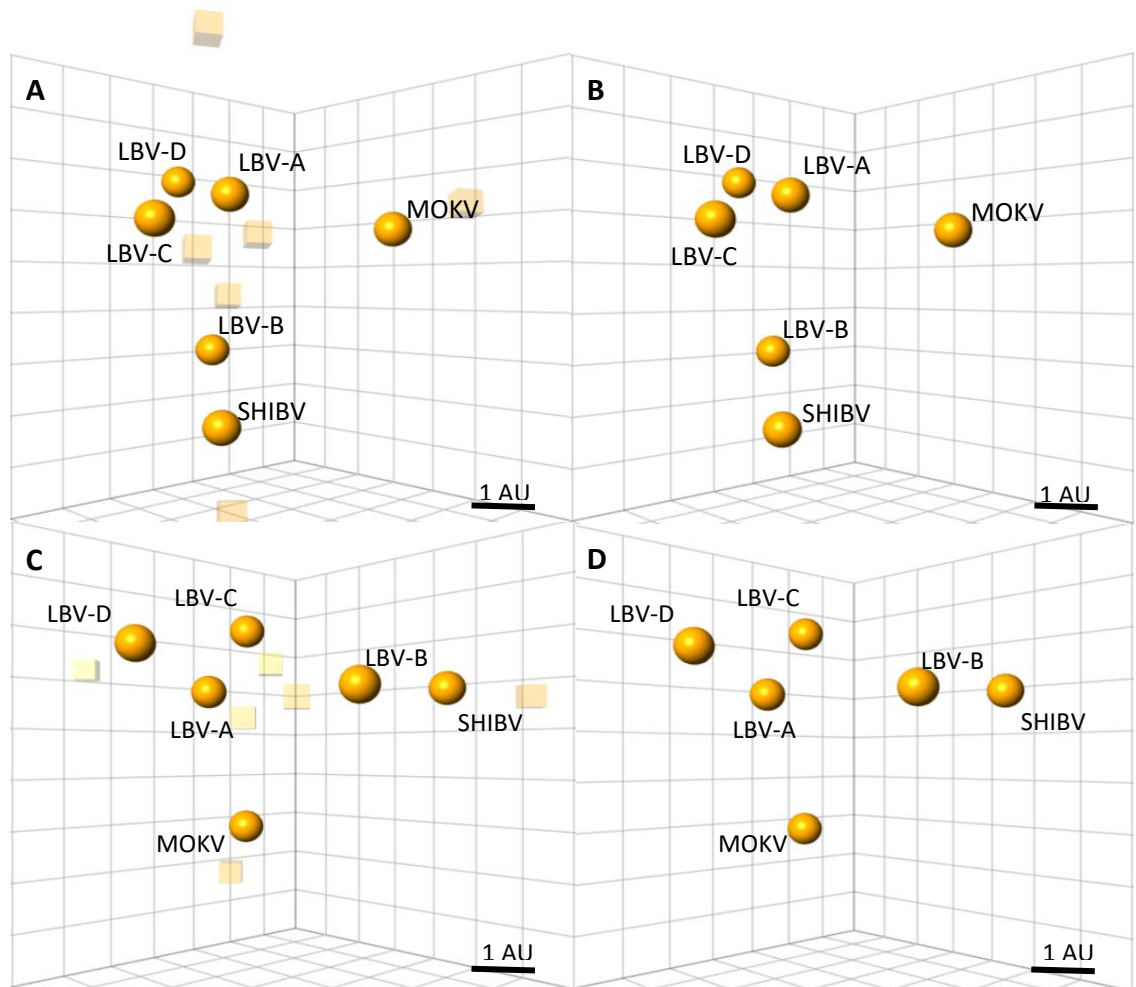


Figure 3.15: (A) 3D antigenic map. Viruses (spheres, coloured orange to represent phylogroup II) and sera (coloured translucent boxes) are positioned such that the distance from each serum to each virus is determined by the neutralisation titre. Multidimensional scaling is used to position both sera and viruses relative to each other, so orientation of the map within the axes is free. Scale bar shows one antigenic unit (AU), equivalent to a two-fold dilution in antibody titre. (B) The same map with sera removed for clarity. (C) The same map but inverted and rotated $\sim 90^\circ$. (D) The same view as C removed for clarity.

Table 3.4: Intergenotypic genetic (below diagonal) and antigenic variation (above diagonal) of phylogroup II viruses

	Antigenic Distance						
Amino Acid difference (%)		LBV-A	LBV-B	LBV-C	LBV-D	MOKV	SHIBV
	LBV-A		3.69	1.56	2.44	2.94	4.44
	LBV-B	15		3.84	3.74	4.54	2.55
	LBV-C	13	12		3.12	4.14	4.07
	LBV-D	11	14	13		4.67	5.59
	MOKV	18	21	21	18		4.82
	SHIBV	16	15	14	16	24	

Above diagonal: Map antigenic distances measured in antigenic units. Below diagonal: Amino acid percentage difference in glycoprotein ectodomain.

A common phenomenon that occurred in phylogroup II was that the antisera had different neutralisation profiles to the homologous viruses. Consequently, when this data was translated to a 3D antigenic map, the antisera and homologous viruses were in separate locations. This has been documented previously for foot-and-mouth disease virus (FMDV), adding to the complexity of antigenicity analysis and vaccine strain selection (450). The position of antisera in relation to the viruses tested is arguably more appropriate when determining whether a virus is a good vaccine strain candidate as it represents the effect of the virus neutralising antibodies produced in response to the virus. Therefore, as well as the antigenic differences between lyssaviruses, the analysis of antigenic differences between lyssaviruses-specific sera was vital for vaccine strain selection. Both LBV-D and LBV-B specific sera were capable of neutralising all phylogroup II viruses above or equal to the pre-defined cut off. The homologous viruses, LBV-D and LBV-B, however, were only neutralised by 50% and 67% of the phylogroup II-specific sera, respectively. As a result, on the antigenic map, the antisera are more central than the homologous viruses and are antigenically closer to the phylogroup II viruses than the other phylogroup II-specific sera. The LBV-D specific sera has an average antigenic distance of 2.48 AU from each of the phylogroup II lyssaviruses, whilst LBV-B specific sera exhibited an average distance of 2.60 AU.

Based on evolutionary data, LBV-D exhibited the shortest genetic distance to the phylogroup II lyssaviruses with an average Maximum Likelihood (ML) distance of 0.210 (Figure 3.16). Additionally, based on the G protein ectodomain, LBV-D has the highest average amino acid identity with the other phylogroup II viruses (Table 3.4). The average number of amino acid substitutions between LBV-D and each of the phylogroup II lyssaviruses was 60 amino acid substitutions (14.2% difference in amino acids).

In this case, amino acid identity and genetic distance showed a linear relationship to the antigenic distances between LBV-D specific sera and phylogroup II lyssaviruses.

3.9.2.2. Predicting antigenic distance from evolutionary data

Pairwise comparison of the antigenic distances with the genetic distances was undertaken using the Pearson product-moment correlation coefficient (Figure 3.17A). The linear relationship between the antigenic distance and evolutionary distance indicate that the variables have low correlation and were not significant ($r=0.35$ (95%CI -0.1976 to 0.7312), $R^2=0.12$, $P=0.201$).

3.9.2.3. Predicting antigenic distance from amino acid sequence identity

Pairwise comparisons of the antigenic distances with the amino acid sequence identity of the entire G protein sequence, the G protein ectodomain, and the known G protein antigenic sites were undertaken using the Pearson product-moment correlation coefficient (Figure 3.17B-D).

The correlation between the antigenic distance and the amino acid identity of the entire G protein ($r=0.53$ (95%CI 0.02 to 0.82), $R^2=0.28$, $P=0.044$) and the ectodomain ($r=0.55$ (95%CI 0.05 to 0.93), $R^2=0.30$, $P=0.035$) showed a moderate correlation however, due to the small sample size, the 95% confidence interval is broad. The antigenic site amino acid identity showed an even lower correlation to the antigenic distances and the data was not statistically significant ($r=0.43$ (95%CI -0.11 to 0.77), $R^2=0.18$, $P=0.110$).

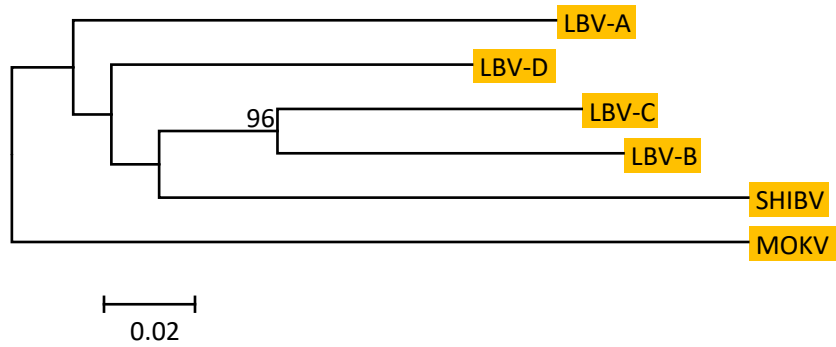


Figure 3.16: Phylogenetic tree of the phylogroup II glycoprotein nucleotide sequences in (described in Table 3.1). The evolutionary history was inferred using the Neighbor-Joining method and the evolutionary distances were computed using the Maximum Composite Likelihood method and are in the units of the number of base substitutions per site. Trees were generated in MEGA6 and edited in FigTree.

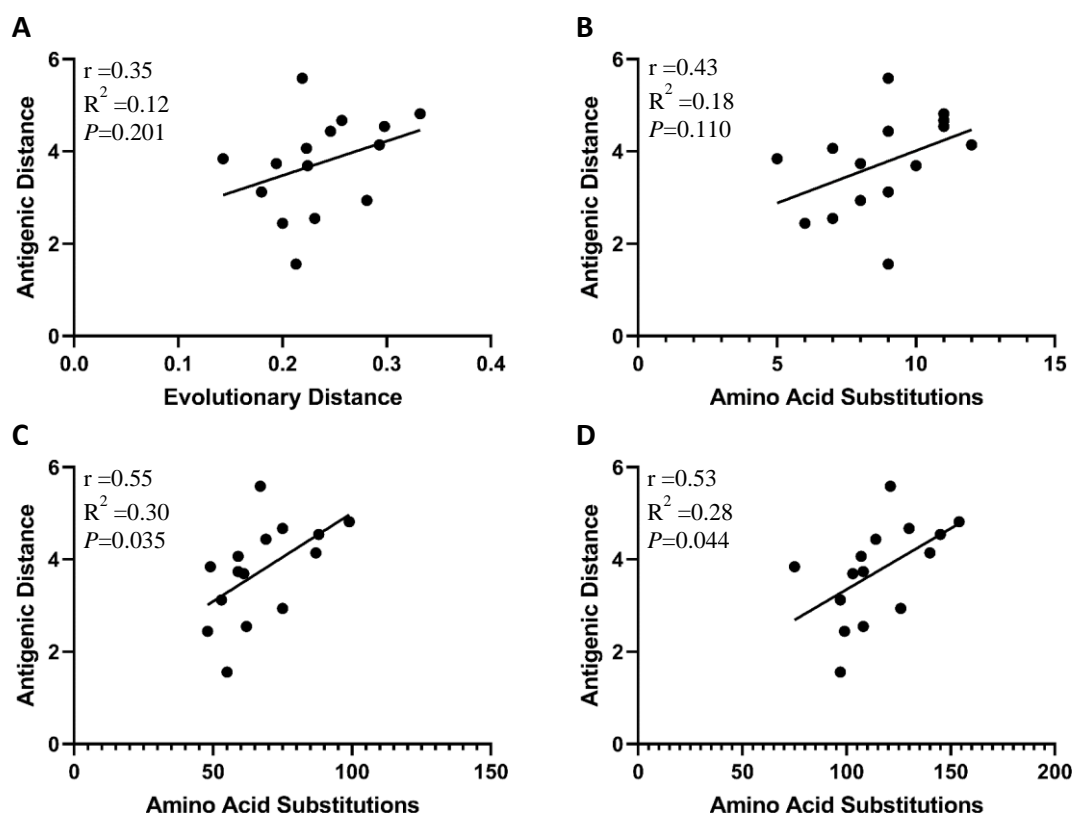


Figure 3.17: Plot of pair-wise antigenic and genetic distances between phylogroup II viruses. Antigenic distances are measured from the antigenic map, in antigenic units. (A) Genetic distances are represented as the pair-wise Maximum likelihood distance of the glycoprotein. (B-D) Genetic distances are represented as the number of pair-wise amino acid substitutions in the antigenic sites (B), glycoprotein ectodomain (C), and the entire glycoprotein (D). The line represents a linear regression model.

3.9.3. Phylogroup I, II, III

Although the data for phylogroup I and II indicate moderate to low correlation between antigenic distance and genetic distance, it could be hypothesised that these maps have a lower resolution due to the lack of antigenic variation as a result of extensive cross-neutralisation within phylogroups. Additionally, within phylogroups, viruses are genetically closely related. In this case, the difficulties with antigenic interpretation of genetic data within phylogroups could be due to the variation in antigenic effect of specific amino acid substitutions. The type of amino acid substitution, the location of the substitution, or the resulting interaction of the substitution cannot be considered or quantified when interpreting the linear relationship between the antigenic and genetic data (435). As already demonstrated with ABLV, a larger and more diverse panel of viruses and hyperimmune sera may increase the accuracy of these antigenic maps by adding more constraints to each point on the map. In this study, as in others, low but detectable degrees of cross reactivity were observed between phylogroups I, II, and III; hence enabling the positioning of all lyssaviruses relative to others on the antigenic map (24, 34, 37, 39).

3.9.2.1. Cross-genus lyssavirus antigenic variation

Figure 3.18 shows three-dimensional antigenic maps, displaying the antigenic relationships among a panel of 20 lyssaviruses; represented by the coloured spheres.

Sera are represented by coloured translucent boxes, and are omitted from Figure 3.18B and D for clarity. Similar to the evolutionary data (Figure 3.19), on the map, three phylogroups can clearly be identified. Phylogroup I viruses cluster together, phylogroup II viruses cluster together and phylogroup III viruses are shown to be the most antigenically divergent. Neutralisation of the phylogroup III lyssaviruses was very weak, indicating that these viruses are distinct from all other viruses assessed.

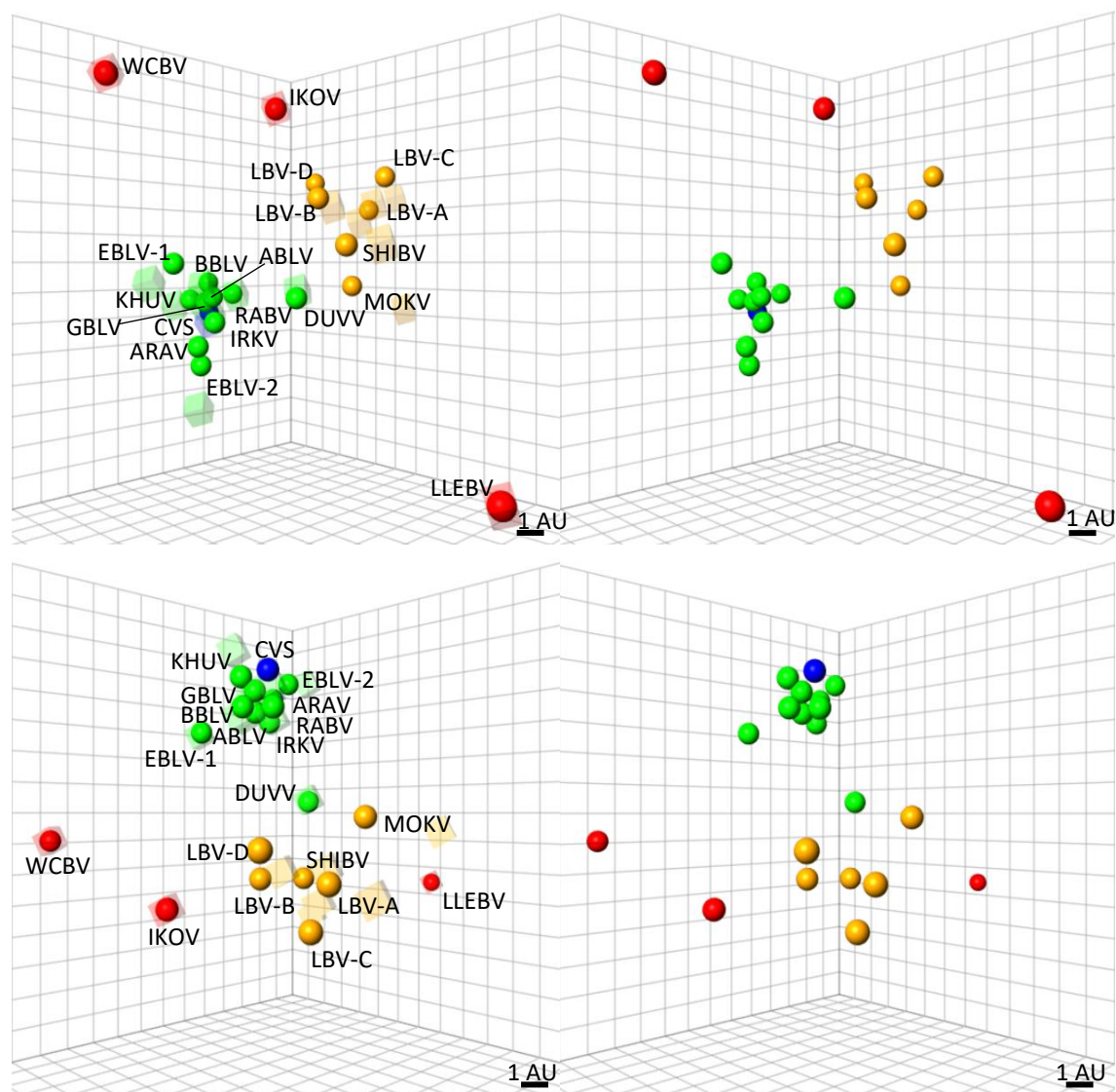


Figure 3.18: (A) 3D antigenic map. Viruses (spheres, coloured green to represent phylogroup I, CVS in dark blue, orange to represent phylogroup II, and red to represent phylogroup III) and sera (coloured translucent boxes) are positioned such that the distance from each serum to each virus is determined by the neutralisation titre. Multidimensional scaling is used to position both sera and viruses relative to each other, so orientation of the map within the axes is free. Scale bar shows one antigenic unit (AU), equivalent to a two-fold dilution in antibody titre. (B) The same map with sera and labels removed for clarity. (C) Rotated and inverted view. (D) Rotated view with sera and labels removed for clarity.

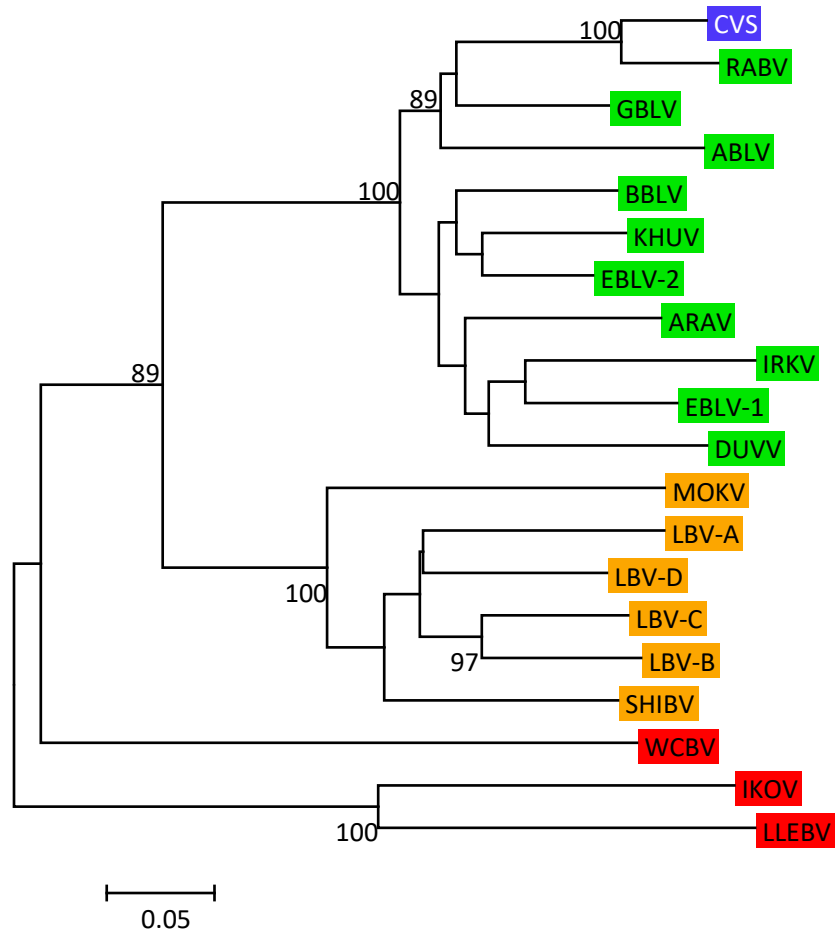


Figure 3.19: Phylogenetic tree of the glycoprotein nucleotide sequences (described in Ttable 3.1) across the lyssavirus genus. The evolutionary history was inferred using the Neighbor-Joining method and the evolutionary distances were computed using the Maximum Composite Likelihood method and are in the units of the number of base substitutions per site. Trees were generated in MEGA6 and edited in FigTree.

On average, IKOV exhibited a distance of 8.10 AU from the RABV isolates, WCBV a distance of 9.85 AU, and LLEBV a distance of 13.66 AU (Table 3.5). This is reflected in the findings of a previous study reporting that WCBV exhibited an antigenic distance of 9 AU from the RABV isolates tested (24). Overall, LLEBV was the most divergent lyssavirus, exhibiting an average antigenic distance of 12.77 AU from the other lyssaviruses in the genus, equivalent to a 7000-fold difference in neutralising antibody titre. WCBV was the second most divergent with an average distance of 9.68 AU, equivalent to an 820-fold difference in neutralising antibody titre, and IKOV was the third most divergent with an average distance of 7.12 AU, equivalent to a 139-fold difference in neutralising antibody titre.

Rarely, a virus from one phylogroup positioned closer to a virus in a different phylogroup. Interestingly, DUVV was antigenically closer to SHIBV than any of the phylogroup I viruses with a distance of 2.69 AU. As well as SHIBV, DUVV exhibited an antigenic distance of 3.26 AU to MOKV, indicating divergence within phylogroup I. Additionally, WCBV and the phylogroup II lyssaviruses were equally antigenically distinct to EBLV-1.

Finally, IKOV and phylogroup II lyssaviruses were equally antigenically distinct from LBV-B. This gives an indication that IKOV may be more antigenically similar to phylogroup II viruses than it is to phylogroup I lyssaviruses and LLEBV.

Table 3.5: Inter-genotypic genetic (below diagonal) and antigenic variation (above diagonal) across the genus.

	Antigenic Distance																			
	ABL	ABV	ABL	ABV	ABL	ABV	ABL	ABV	ABL	ABV	ABL	ABV	ABL	ABV	ABL	ABV	ABL	ABV	ABL	ABV
ABL																				
ABV	2.12																			
ABL	2.83	4.01																		
ABV	4.25	2.38	3.23																	
ABL	18	18	18	17																
ABV	12	10	10	16	16															
ABL	16	14	20	19	16	2.06														
ABV	18	22	21	16	20	22	2.49													
ABL	12	10	18	16	16	9	14	19												
ABV	19	18	23	22	19	15	25	17	7											
ABL	20	19	18	23	23	19	15	26	18	7										
ABV	36	39	39	38	37	39	35	37	38	36	47									
ABL	35	36	38	38	37	37	34	36	37	36	37	15								
ABV	35	36	38	38	36	38	35	35	37	36	37	13	12							
ABL	36	36	38	37	36	36	36	36	37	38	39	11	14	13						
ABV	38	39	39	39	37	39	36	37	39	37	38	18	21	21	18					
ABL	32	36	37	37	36	37	33	36	36	35	36	16	15	14	16	24				
ABV	47	49	48	48	48	47	49	48	48	49	48	45	47	47	47	47	47			
ABL	48	48	48	48	48	48	49	47	47	48	48	51	51	51	51	51	51	31		
ABV	45	45	44	46	45	45	46	46	45	45	44	42	42	42	43	44	42	48	49	

Above diagonal: Map antigenic distances measured in antigenic units. Below diagonal: Amino acid percentage difference in glycoprotein ectodomain.

The average antigenic distances between phylogroups and the approximate difference in neutralising antibody titre have been described in Table 3.6. Phylogroup I viruses are the most antigenically similar, followed by phylogroup II. The antigenic distance between phylogroup I and phylogroup II viruses is approximately double the distance between viruses in phylogroup II. Phylogroup I viruses are on average more than 0.8 AU further from phylogroup III lyssaviruses than phylogroup II viruses are from phylogroup III. The average distance between the phylogroup III viruses is 12.28 AU, indicating divergence within the phylogroup. On average, IKOV is 1.44 AU closer to phylogroup II than phylogroup I are to phylogroup II. On the other hand, WCBV and LLEBV are 3.42 AU and 5.26 AU further from phylogroup II than phylogroup I are to phylogroup II. The distance between the phylogroup III viruses could be justification for the separation of the phylogroup III viruses into several distinct phylogroups.

Certainly, based on the antigenic maps, the concept of generating a cross protective antigen formulation for use as a pan-lyssavirus vaccine would require a combination of antigens representative of each of the phylogroup III viruses.

3.9.2.2. Predicting antigenic distance from evolutionary data

Pairwise comparison of the antigenic distances to the genetic distances was undertaken using the Pearson product-moment correlation coefficient (Figure 3.20). Whilst the data is statistically significant ($P < 0.001$), the linear relationship between the antigenic distance and evolutionary distance indicate that the variables have low correlation ($r = 0.43$ (95%CI 0.31 to 0.54), $R^2 = 0.19$).

Table 3.6: Average antigenic distance in AU and equivalent fold difference in neutralisation titre within and between phylogroups

Phylogroups	Average antigenic distance (AU)	Fold difference in neutralisation titre
Phylogroup I to Phylogroup I	2.48	6
Phylogroup I to Phylogroup II	6.62	98
Phylogroup I to Phylogroup III	9.86	929
Phylogroup II to Phylogroup II	3.58	12
Phylogroup II to Phylogroup III	9.03	523
Phylogroup III to Phylogroup III	12.28	4973

3.9.2.3. Predicting antigenic distance from amino acid sequence identity

Pairwise comparisons of the antigenic distances with the amino acid sequence identity of the entire G protein sequence, the G protein ectodomain, and the known G protein antigenic sites were undertaken using the Pearson product-moment correlation coefficient (Figure 3.20 B-D).

Whilst the correlation between the antigenic distance and amino acid sequence identity of the antigenic sites showed the highest correlation, the correlation with the amino acid sequence identity of the G protein ectodomain and the entire G protein was also high.

Pair-wise comparison of antigenic distances with antigenic site genetic distances shows a statistically significant correlation ($r=0.82$ (95%CI 0.76 to 0.86), $R^2=0.66$, $P<0.001$) (Figure 3.20B). Pair-wise comparison of antigenic distances with G protein and G protein ectodomain genetic distances also show a statistically significant correlation ($r=0.80$ (95%CI 0.74 to 0.84), $R^2=0.64$, $P<0.001$; $r=0.81$ (95%CI 0.75 to 0.85), $R^2=0.65$, $P<0.001$) (Figure 3.20C and D). Moreover, a linear regression model demonstrates that, on average, one unit of antigenic change (95%CI 0.89-1.10, $P<0.001$), equivalent to a two-fold change in antibody titre, is linearly correlated to 25 amino acid substitutions (~6 %) in the G protein ectodomain. This is similar to previous reports that determined that one unit of antigenic change linearly correlated to 21 amino acid substitutions (4.8 %) in the G protein ectodomain (24).

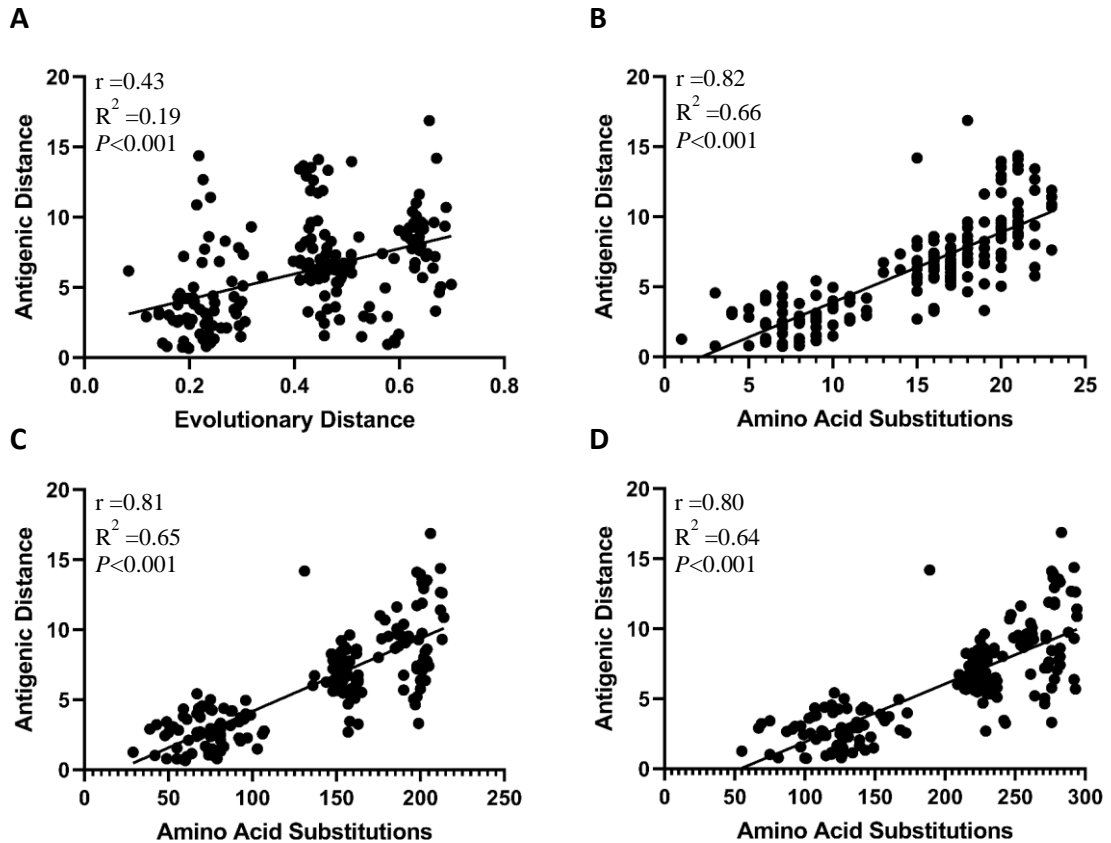


Figure 3.20: Plot of pair-wise antigenic and genetic distances between all lyssaviruses.

Antigenic distances are measured from the antigenic map, in antigenic units. (A) Genetic distances are represented as the pair-wise Maximum likelihood distance of the glycoprotein. (B-D) Genetic distances are represented as the number of pair-wise amino acid substitutions in the antigenic sites (B), glycoprotein ectodomain (C), and the entire glycoprotein (D). The line represents a linear regression model.

3.10. Determining the requirements for pan-lyssavirus neutralisation

Within phylogroup I and II, a high degree of cross neutralisation was observed.

Crucially, LBV-D-specific sera exhibited sufficient virus neutralising antibodies against all phylogroup II viruses. Based on the antigenic divergence of the phylogroup III viruses, it was hypothesised that antigens representative of each of the phylogroup III viruses would need to be included for neutralisation of each of the phylogroup III viruses. As a result, it was determined that five lyssavirus antigens would have to be included in a pan-lyssavirus vaccine to afford cross protection across the entire lyssavirus genus: RABV as rabies vaccines marketed for human use are based on whole inactivated RABV particles and OIE standard vaccine sera exhibited sufficient neutralising antibody titres against phylogroup I; LBV-D as LBV-D-specific sera exhibited neutralising antibody titres against phylogroup II viruses above the 0.5 IU/ml cut off; and each of the phylogroup III lyssaviruses (IKOV, LLEBV, WCBV).

As a proof of concept, concentrated LBV-D specific sera was mixed 1:1 with OIE sera at a concentration of 10 IU/ml to give a final concentration of 5 IU/ml, and tested against all lyssaviruses on a mFAVN (Figure 3.21). It was hypothesised that the sera mix would neutralise all phylogroup I and II viruses above the pre-defined cut-off, but due to antigenic divergence, would not be able to neutralise the phylogroup III viruses. Certainly, reciprocal titres of virus neutralising antibodies against phylogroup I and II viruses were all high and exceeded the neutralisation cut-off, however, the titre of virus neutralising antibodies against IKOV demonstrated titres at the cut-off; concurrent with the previous findings of this study (Figure 3.11) and a previous study that shows moderate cross-neutralisation between phylogroup II and IKOV (38).

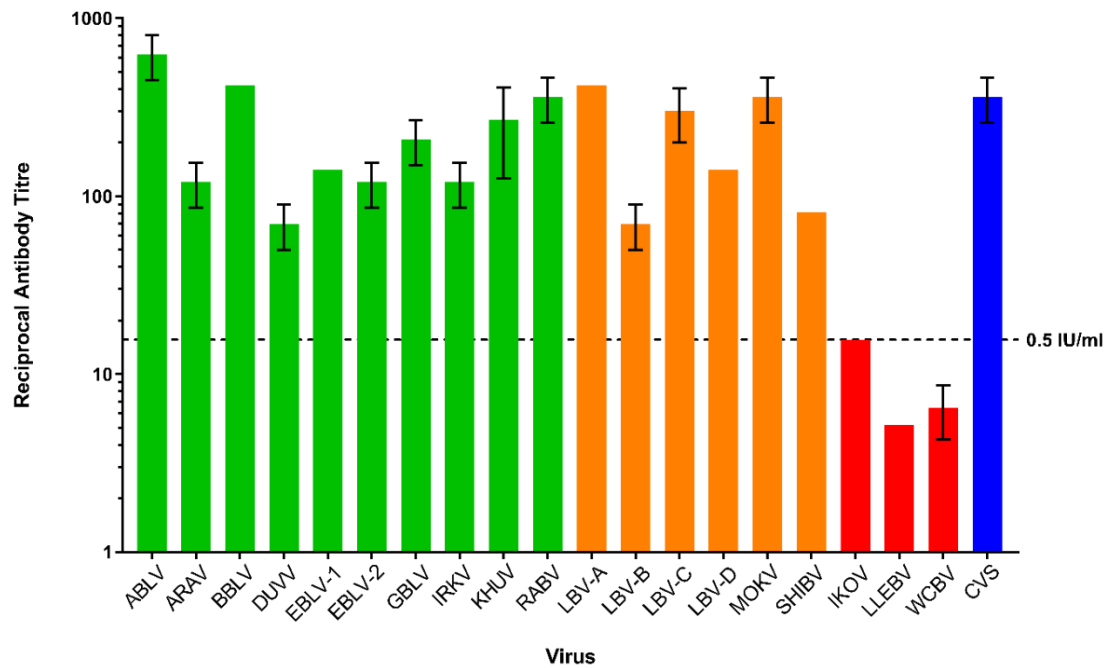


Figure 3.21: The cross-neutralisation profile of a mix of two sera (concentrated LBV-D specific sera mixed 1:1 with OIE sera to give a final concentration of 5 IU/ml) against all lyssaviruses. The mFAVN tests were performed in triplicate and the mean and SD of the results plotted on a logarithmic scale. The 0.5 IU/ml neutralisation cut off is dictated by the OIE sera against CVS (indicated by the dashed line).

3.11. Discussion

In the absence of extensive assessment of innate immune responses to divergent lyssaviruses, it is understood that the primary method of protection against lyssaviruses is conferred through virus neutralising antibodies (448). Following vaccination, the humoral response produced is directed against the virus surface G protein. An antibody titre of 0.5 IU/ml is generally considered as a conservative threshold, above which protection from classical rabies virus strains is likely (451). Whilst the ability of rabies vaccines, based on classical RABV strains, to cross-protect against other lyssaviruses has been widely studied, the titre of neutralising antibodies required to confer protection against non-RABV lyssaviruses has not been established. Additionally, RABV based vaccines have not been shown to provide cross-protection for lyssaviruses in phylogroup II and III. This warrants a balanced assessment of the antigenic requirements for a cross-protective formulation for use as a pan-lyssavirus vaccine.

A large panel of 21 lyssaviruses were generated and titres achieved were adequate for use throughout this study. Whilst each of the lyssaviruses being propagated were harvested when the cells used for virus propagation showed 100% infection, stock titres varied between each isolate. The variability of stock viral titres generated for each virus could be due to a number of factors including virus adaption to allow certain lyssaviruses to propagate within a specific cell line more rapidly than others. Viruses were obtained from original material, which for divergent lyssaviruses can mean small quantities of bat brain and as such passage in cell culture is required to generate stocks. Whilst genetic adaptation is thought to be minimal, it cannot be discounted. Certainly, further investigation into potential cell culture adaptation of lyssaviruses would be of value; RABV strains such as CVS-11 have been shown to adapt to BHK-21 cells through serial passages (452) although serial passage to generate stocks of other

lyssaviruses have suggested minimal adaptation at consensus level (37). The ability to achieve high titres however, may be a consequence of virus adaptation to cell culture.

The phenomenon behind viral adaptation to cell culture in the case of lyssaviruses is not entirely clear. One suggestion is based on the fact that RNA viruses are especially prone to mutation, and after multiple passages, a mutation that benefits the lyssavirus is selected for, consequently increasing virus titre (113, 453). However, this example of positive selection has been disputed (135). Viral heterogeneity has been proposed as the mechanism driving RABV adaption to new environments or hosts (135). It has been suggested that for each lyssavirus a mutant spectrum or quasispecies exists that, when a selection pressure such as replication within cell culture is applied, selects for quasispecies with advantageous mutations. This example of purifying selection allows for viral adaptation to cell culture after multiple passages (454, 455).

In addition, discrepancies between the virus stock titres, the dilution to achieve 100TCID₅₀/50µl, and the back titration at the time of the mFAVNs could have been due to several factors. Whilst varied virus adaption to replicate and spread in cell culture could be the cause of these discrepancies, the tests also could not be performed on the same day. Inevitably, day-to-day variations in cells and media could be a factor.

Additionally, the precision of the back titration technique may differ to the standard titration technique. The back titration method was performed using four-fold dilutions, with four replicates, whereas the standard method for stock virus titration was performed with ten-fold dilutions with twelve replicates. Another critical difference between the two methods is the amount of cells added to the wells. The standard titration method is performed with two-fold more cells than the FAVN and mFAVN back titration method. Any of these differences could be responsible for the variation seen.

As a way to mediate these variations, for the purposes of this study, the FAVN/mFAVN back titration method was used as the sole determinant of the amount of virus used for each assay as it provides a way to ensure 100 TCID₅₀ of each virus was added. It also determined the acceptable titre range (64-256 TCID₅₀) for each test to establish consistency between tests. This ensured that the titre of virus used in the FAVN/mFAVN assay for each lyssavirus was the same.

Complete neutralisation of phylogroup I lyssaviruses, apart from DUVV, at 5 IU/ml of OIE standard sera was confirmed by mFAVNs in figure 3.4. The disparity between the different standardised sera is inexplicable, though pooled canine sera from dogs vaccinated with different RABV vaccines (OIE) could have a more diverse population of neutralising polyclonal antibodies compared to sera derived from humans (WHO and HDCV recipient sera). In addition, OIE, WHO, and HDCV recipient sera all showed lower titres of neutralising antibodies against the wild/street strain of RABV (wRABV) compared to CVS a cell-culture adapted RABV strain used regularly in diagnostic assays, suggesting possible divergence of these RABV isolates. This is likely due to the history of these viruses and the antigenic relatedness to vaccine strains. CVS, and two vaccine strains Pitmann Moore RABV strain and Pasteur virus RABV strain are all derivatives of the same virus (456). This is likely the rationale for the phenomenon observed. Regardless, these data are supported by the knowledge of phylogroup I viruses. Previously, 0.5 IU/ml of WHO and OIE sera was sufficient to neutralise pseudotype viruses representative of each of the phylogroup I viruses used in the study (38). Additionally, another study showed that 96% (n=48/50) of human sera from HDCV recipients exhibited neutralising antibodies against non-RABV phylogroup I viruses, ABLV, EBLV-1, and EBLV-2 (35). Similar to this study, other studies have reported varying levels of the cross neutralisation within phylogroup I (457, 458). It was

previously demonstrated that 100% of human sera from PCEV recipients exhibited sufficient neutralising antibodies against CVS, ABLV, EBLV-1, EBLV-2, and DUVV; and 94% of the human sera exhibited sufficient neutralising antibodies against BBLV, however the titre of neutralising antibodies varied and were less than the titre against CVS (457, 458). The titre of neutralising antibodies against these non-RABV phylogroup I lyssaviruses could be ranked in the following order: highest titre ABLV>EBLV-2>DUVV>EBLV-1>BBLV lowest titre (457, 458). ABLV was the most readily neutralised non-RABV phylogroup I lyssavirus in this study, whilst DUVV was the least readily neutralised by WHO, OIE, and HDCV recipient sera, concurrent with a previous study that determined 80% human sera from vaccinated personnel exhibited neutralising antibodies against DUVV whilst other phylogroup I lyssaviruses (ARAV, KHUV, IRKV, EBLV-1) were neutralised by 90-100% of the sera (34). The same trend was evident in all studies however, where higher reported neutralising antibody titres against CVS coincided with higher neutralising antibody titres against phylogroup I viruses.

For a full assessment of cross-neutralisation across the lyssavirus genus, specific sera had to be generated against each lyssavirus. The presence of an antibody response in harvested rabbit sera was assessed by ELISA (Figure 3.5) and neutralising antibody titre was assessed by mFAVN (Figure 3.6). This revealed discrepancies between the humoral responses produced in rabbits against BPL-inactivated lyssaviruses. LBV-A-specific sera and IRKV-specific sera exhibited binding antibodies on the ELISA but did not exhibit neutralising antibodies against the homologous virus on the mFAVN. Additionally, phylogroup II and III-specific sera exhibited binding antibody titres against RABV antigen on the ELISA and did not exhibit neutralising antibody titres against RABV on the mFAVN assay (Figure 3.10B). This highlights the fundamental

differences between the two serological assays, and the rationale that the two tests cannot be easily compared. ELISA's detect antibodies able to bind virus (or purified virus antigen in the case of the ELISA used in this study). Neutralisation tests will detect antibodies able to prevent viral entry into a cell, therefore measuring antibodies important for protection against infection. For the purpose of investigating antigenic differences between the lyssaviruses to define the minimum antigenic requirements for pan-lyssavirus neutralisation, the mFAVN was determined the most appropriate test.

The mechanism behind the phenomenon seen in the case of LBV-A-specific sera and IRKV-specific sera is unclear. However, it could be hypothesised that the process of virus inactivation could be responsible. *In vitro* visualisation of inactivated LBV-A virus particles was attempted using NanoSight technology. Multiple peaks were observed for each of the inactivated virus stocks tested, with the stock of inactivated LBV-A exhibiting the most variation in particle size. The multiple peaks could be a result of testing an unpurified sample or could represent DI particles or virions that have cross-linked after BPL inactivation. Despite this, the NanoSight data suggested that there was no significant difference in the sizes of the inactivated LBV-A particles when compared with inactivated virus particles that initiated a neutralising humoral response (Figure 3.7). This would indicate that the effect of virus inactivation, in relation to the production of a neutralising humoral response, occurred at the amino acid/protein level.

The mechanism of neutralisation is determined by the properties of both the antibody and the virus epitope it binds to. One factor contributing to virus neutralisation is the inhibition of virus-cell attachment, where the binding antibody occludes or interferes with the G protein binding site (459). One factor that could be responsible for antibody-mediated virus neutralisation is antibody occupancy (460). This hypothesis assumes that virus neutralisation is due to antibodies coating the virion surface; subsequently

inactivating a significant number of functional G proteins to prevent virus attachment or entry (461, 462). Essentially, this theory is not entirely based on the total number of antibodies bound for neutralisation but rather the total area they occupy, thereby acknowledging the effects of antibody orientation, the ability of an antibody to interfere with neighbouring G proteins, or the effect of multiple antibodies binding to a single G protein in different locations. This model acknowledges that whilst antibodies may be bound, below a minimum threshold of occupancy, neutralisation will not occur. Thus, a virion partially coated with antibodies can establish an infection provided there is enough functional G protein to interact with the target cell (459). Hence, viruses possessing more functional epitopes will require more bound antibodies for neutralisation. Certainly, studies have shown that neutralisation of RABV requires more than 200 IgG molecules per virion, however, it has been shown that some binding antibodies do not inhibit attachment even in saturating amounts; up to 1000 IgG (Mab 30AA5) molecules bound one RABV mutant without exhibiting a neutralising effect (45). As a result, it could be hypothesised that the ‘critical binding site’ concept is also responsible for virus neutralisation (463). This theory proposes that antibody binding of specific epitopes is another requisite for neutralisation. This model acknowledges the existence of high affinity, non-neutralising antibodies as it recognises that neutralisation requires more than just binding of antibodies to functional G proteins. Certainly, in this study, phylogroup II and III-specific sera exhibited binding antibody titres against the RABV antigen used for the ELISA test but did not exhibit neutralising antibody titres against the live RABV virus used in the mFAVN assay.

For the LBV-A-specific sera and IRKV-specific sera, it could be hypothesised that BPL-inactivation modified these critical epitopes. Consequently, the humoral response produced following inoculation with these inactivated viruses may not have been

specific to the critical epitopes pre-modification, resulting in the generation of binding but non-neutralising antibodies against the live homologous viruses. BPL is an organic compound with an electrophilic nature, thus giving it the ability to readily react with nucleophiles (464). The mechanism of action by which BPL inactivates viruses is thought to lie with the direct effect on nucleic acids (465-467). BPL primarily reacts with the nitrogen-7 atom of guanosine and the nitrogen-1 atom of adenosine, resulting in nicks and cross-links between RNA and viral proteins (468). Consequently, the genomes are rendered dysfunctional and the virus replication incompetent. Whilst it was initially believed that BPL primarily reacts with nucleic acids and the immunogenic epitopes of viral proteins would remain intact, amino acids also display nucleophilic moieties. A previous study defined nine amino acids that reacted with BPL, which implies BPL inactivation could result in the modification of important immunogenic epitopes and induce conformational changes to viral surface proteins (469).

Additionally, in a separate study looking at the effect of BPL and formaldehyde inactivation on influenza virions, the alterations caused by BPL inactivation were strain dependent and it was determined that inactivation procedures should be tailored to the virus strain (470). As a result, the differences in glycoprotein amino acid sequence between viruses from different lyssavirus species such as LBV-A and IRKV may result in increased modification of the glycoprotein compared to the other species.

Once lyssavirus-specific sera was established for all lyssaviruses except IRKV, cross neutralisation within and across phylogroups was assessed. The mFAVN assays in this chapter identified a strong level of intra-phylogroup neutralisation within phylogroup I and II (Figure 3.8 and 3.9) concurrent with previous studies (34, 36, 38, 391).

Additionally, the cross-neutralisation results also suggest a small degree of inter-phylogroup neutralisation as RABV-specific sera neutralised MOKV, however VNA

titres were 8 fold lower against MOKV than against RABV (Figure 3.10). Cross-neutralisation between RABV and phylogroup II viruses has been documented previously where 40% (n=4/10) of human sera from vaccinated personnel demonstrated neutralising antibody titres against MOKV and LBV-B, however VNA titres were 10-140 fold lower against MOKV and LBV-B than against CVS-11. Conversely and more similar to the findings of this study, a separate study demonstrated that 16% (n=15/94) of human sera from PCEV vaccinated personnel exhibited neutralising antibody titres against MOKV but 0% exhibited neutralising antibody titres against LBV-B (457). Additionally, a separate study demonstrated that human mAb RVC20 neutralised RABV and MOKV but did not neutralise LBV-B (471).

In some cases, variable cross reactivity was observed where the lyssavirus-specific sera was broadly cross-neutralising but the homologous virus was neutralised by few lyssavirus-specific sera, such as LBV-D. Previously, ARAV-specific sera was shown to readily neutralise ARAV and KHUV, however KHUV-specific sera was shown to only readily neutralise KHUV (34), a finding also reflected in the results of this study. Additionally, RABV-specific sera exhibited sufficient neutralising antibody titres against MOKV but MOKV-specific did not exhibit sufficient neutralising antibody titres against RABV.

The sera used in these assays were obtained from rabbits inoculated with inactivated virus preparations, meaning that the sera were polyclonal. Despite this, the results of this study are limited by the fact that only one rabbit was used per lyssavirus. This may result in functional differences in the cross-neutralisation activity or of rabbit polyclonal antibodies against heterologous viruses and limitations where the titre generated was weak. This phenomenon could be rectified in the future by assessing the cross-neutralisation activity of lyssavirus-specific sera from multiple rabbits. One way to test

more samples would be to assess the serum response in animals used in previous experiments. Typically, mice are used in these experiments and yield a low blood volume, therefore getting enough serum to assess cross-neutralisation would be problematic. The pseudotype neutralisation assay, however, requires a fraction of the serum and has been shown to be comparable to the FAVN (394). Future work generating lyssavirus pseudotypes and extensive cross-neutralisation pseudotype assays with more sera would be of interest.

As expected, higher concentrations of lyssavirus-specific sera increased cross-neutralisation within and between phylogroups where, upon concentration, LBV-B-specific sera and LBV-D-specific sera exhibited sufficient neutralising antibody titres against all phylogroup II viruses and SHIBV-specific sera exhibited sufficient neutralising antibody titres against IKOV (Figure 3.11). Whilst LBV-B-specific sera did not exhibit cross-neutralisation against IKOV in this study, previously LBV-B-specific sera was shown to neutralise IKOV pseudotype virus by 60% (38). Consequently, it is possible that phylogroup II-specific sera may elicit cross-neutralising activity against IKOV depending on the humoral response produced.

The overall finding of this study is that whilst extensive intra-phylogroup neutralisation occurs in phylogroup I and II, there is little neutralisation using lyssavirus-specific sera at the equivalent reciprocal titre of 0.5 IU/ml. Typically, higher concentrations of lyssavirus-specific sera and vaccine sera correlated to increased cross-neutralisation across the genus. It would be of value to investigate cross-neutralisation using more than one lyssavirus isolate and more than one lyssavirus-specific sera for each lyssavirus species, where multiple isolates exist.

Following the assessment of cross-neutralisation, antigenic cartography techniques were used to quantify and visualise antigenic relationships among all lyssaviruses. Analysing the antigenic data in this way allows comparison to the genetic data, which, in the case of this study, was dictated as ML distance or G protein amino acid sequence identity. The antigenic sites, ectodomain, and whole G protein amino acid identity was assessed. The correlation between phylogroup I and II antigenic data with genetic data was low (Figure 3.14 and 3.17), likely due to the limitations of the map resolution when interpreting shorter antigenic distances and the inability to account for specific amino acid substitutions where sequence similarity is high. This has been demonstrated for human influenza A (H3N2) viruses, where on average 13 amino acid substitutions resulted in an antigenically distinct virus, but in some cases only one amino acid substitution had caused a similar effect on antigenic drift (435). This has also been demonstrated for FMDV serotype A, where viruses were able to sustain a number of amino acid substitutions without inducing a change in antigenicity however one critical amino acid was able to significantly affect antigenicity as a result of structural change in one of the three surface proteins (450).

Antigenic cartography maps generated from the antigenic data across recognised phylogroups provided a more precise estimate of the correlation between genetic and antigenic relationships (Figure 3.20). In this case, using the antigenic site amino acid sequence identity as a predictor of antigenic difference showed the highest correlation (95% CI for $r = 0.76$ to 0.86) and using the ML distance showed the lowest (95% CI for $r = 0.31$ to 0.54). Using the G protein ectodomain amino acid sequence identity and the entire G protein amino acid sequence identity as predictors of antigenic difference also showed a high correlation (95% CI for $r = 0.75$ to 0.85 ; 95% CI for $r = 0.74$ to 0.84). A

previous study using different lyssavirus isolates also showed a correlation between genetic and antigenic data for lyssaviruses (95% CI for $r = 0.81$ to 0.88) (24).

For the purposes of this study, the G protein ectodomain amino acid sequence identity was used as the predictor of antigenic difference because it is possible that other immunogenic epitopes may reside outside the previously defined antigenic sites for RABV. Fitting a linear regression model to this data revealed that, on average, one AU (95% CI 0.89-1.10 AU, $P < 0.001$), equivalent to a two-fold change in reciprocal titre was linearly equal to a 5.7% change in the G protein ectodomain amino acid sequence. This data is remarkably similar to previous reports where a 4.8% change and a 5.5% change in G protein ectodomain amino acid sequence identity was reported to equate to a two-fold change in antibody titre, albeit with slightly different confidence intervals (95% CI 0.93-1.07 AU, $p < 0.001$; 95% CI -0.8 to 4.4 two- fold dilutions, $P = 0.296$) (24, 36).

Discrepancies between genetic and antigenic relationships were common but have possible clinical relevance, particularly for lyssaviruses where infection can only be prevented by vaccination. The data from this study indicates that genetic relationships do not always correlate well with antigenic relationships, and comparison of the two enables complete characterisation of each of the lyssaviruses.

Within phylogroup I (Figure 3.12), the close antigenic relationship between the wild strain of RABV and CVS corroborates previous work suggesting low levels of antigenic variation (472). However, a separate study showed that CVS was antigenically distinct to the other wild strains of RABV viruses despite being closely related genetically (24). Additionally, ABLV was antigenically distinct from RABV in this study, a contrast to a previous study where ABLV was determined to be antigenically indistinguishable from

RABV (24). The reason for discrepancy between these studies is not clear but might, in part, be due to the different isolates used in each study; specifically, the differences between number of RABV isolates and non-RABV phylogroup I lyssavirus isolates used. Further analyses are required using multiple virus isolates and multiple virus-specific sera per lyssavirus to increase the robustness of genetic and antigenic studies. Discrepancies of the antigenic and genetic data between KHUV, ARAV, and IRKV has also been documented previously (24) and are reflected in the results of this study. Antigenically, ARAV and IRKV are close to EBLV-2, and KHUV is close to RABV. Phylogenetic analyses using the G gene here and similar to that using the N gene elsewhere (20), suggests that KHUV is more closely related to EBLV-2 than ARAV or IRKV are to EBLV-2. Additionally, IRKV is the most genetically divergent to the other phylogroup I viruses but is less antigenically divergent from phylogroup I viruses than DUVV and EBLV-1 are to phylogroup I.

Within phylogroup II (Figure 3.15), the close but distinct antigenic relationship among LBV-A, LBV-C, and LBV-D corroborates previous phylogenetic analyses and the phylogenetic analyses undertaken here (231). Contrary to the genetic data, however, LBV-B was antigenically closer to SHIBV than LBV-B was to the rest of the LBVs, despite being closest genetically to the other LBVs. The reason for the antigenic difference between LBV-B and the rest of the LBV viruses is not clear but may, in part, be related to the natural history of the viruses. The LBV-B lineage is formed of just one isolate and was the first LBV isolate to be discovered in 1956 (231). In contrast, the LBV-A and LBV-C lineages consist of multiple isolates, detected between 1980 and 2007, and whilst the LBV-D lineage is also formed of a single isolate, it was discovered more recently (230, 231). Overall, the data from this study supports the concept of four distinct lineages for the LBV lyssavirus species.

Within phylogroup III, IKOV, WCBV, and LLEBV are all antigenically diverse from each other and other lyssaviruses in the genus, directly proportional to the genetic data (Table 3.5). One caveat to antigenic cartography and the positioning of these viruses is that there is less confidence in their position on the map as a result of no or low cross-neutralising titres.

Evidence suggests there is a cut-off threshold for antigenic relatedness for which vaccines will be ineffective and fail to provide cross-protection (24, 36, 473). Certainly, the reported variable efficacy of RABV-specific sera and sera from vaccine recipients against more divergent phylogroup I viruses such as DUVV and IRKV, and evidence that few lyssavirus-specific sera are able to neutralise across phylogroups, suggests there is a gradual loss of protection as the antigenic distance between these viruses and RABV increases.

In this study, the confirmation of intra-phylogroup cross-neutralisation within phylogroup I and II is essential to the remainder of this investigation as it indicates that a formulation containing the antigenic epitopes representative of RABV and LBV-D would be sufficient to neutralise phylogroup I and II viruses. According to the results in Figure 3.11 and 3.21, the formulation may also induce a degree of neutralisation against IKOV. Despite this, the cross-neutralisation data and antigenic cartography data suggest that, if a pan-lyssavirus candidate vaccine was to be developed, it would likely also require antigenic epitopes representative of each of the phylogroup III viruses in order to produce strongly neutralising antibodies against all of the characterised lyssaviruses. The classification of WCBV, IKOV, and LLEBV into phylogroups is still under review, however the data from this study supports the concept that each of the phylogroup III lyssaviruses should separate into three distinct phylogroups (39). This is due to the complete lack of sufficient neutralising antibody titres between WCBV, LLEBV, and

IKOV, a contrast to the extensive intra-phylogroup neutralisation seen within phylogroup I and II. The basis for the cross-neutralisation of IKOV by the SHIBV-specific sera and the LBVD/OIE-specific sera is unknown, however both IKOV and the phylogroup II viruses are African lyssaviruses so there may be specific immunogenic epitopes shared by these viruses (6, 474).

Chapter 4: Characterisation of novel lyssaviruses: Taiwan Bat Lyssavirus and putative lyssavirus, Kotalahti Bat Lyssavirus.

4.1. Introduction

Whilst RABV is the most commonly detected lyssavirus in terrestrial species, the epidemiology of non-RABV lyssaviruses is less well understood. ARAV, KHUV, SHIBV, and IKOV, specifically, exist as single viral detections. Consequently, gaps in our knowledge of the epidemiological distribution, host range, and broader ranging characteristics of these viruses remain. The continual discovery of novel lyssaviruses in bats has warranted an increasing interest in the degree of vaccine cross protection afforded by rabies vaccines (475).

In 2016 and 2017, a novel lyssavirus was detected in two Japanese Pipistrelles (*Pipistrellus Abramus*) in Tainan City and Yunlin County, respectively (218). These isolates were named Taiwan bat lyssavirus (TWBLV) after live virus was successfully isolated and genomic sequences for each of the viral genes showed that it was a distinct lyssavirus species (218). Genetically, TWBLV is closely related to EBLV-1 (75%) and IRKV (74%) when comparing the concatenated coding genes, however, no attempts to characterise this virus antigenically *in vivo* or *in vitro* have been attempted (218).

Similarly, in 2017, nucleic acid from a putative lyssavirus, termed Kotalahti bat lyssavirus (KBLV), was detected in a Brandt's bat (*Myotis brandtii*) in Kotalahti, Finland (19). Attempts to isolate the virus were unsuccessful, likely because the bat was in a considerable stage of decomposition on arrival to the Finnish Food Safety Authority Evira. Initial genetic assessment enabled amplification of small fragment of the genome and sequencing of the N gene demonstrated that KBLV was most closely related to KHUV (81%), followed by ARAV (79.7%), BBLV (79.5%) and EBLV-2 (79.4%) at

the nucleotide level (19). A follow-up investigation using deep sequencing successfully obtained the full KBLV genome sequence consisting of 11,878 nucleotides encoding for the five genes N, P, M, G, and L. (209). Consequently, it was determined that KBLV is phylogenetically closely related to EBLV-2 and clusters with KHUV and BBLV. It was also determined that sera, derived from humans vaccinated against RABV, demonstrated cross-neutralising activity against KBLV G pseudotyped RABV particles (209). Despite the preliminary findings, attempts to isolate a live replication-competent KBLV virus or recombinant virus were unsuccessful. This has prevented the *in vivo* evaluation of vaccine efficacy as well as full antigenic characterisation. For this reason, KBLV remains taxonomically unclassified.

It is well understood that the lyssavirus G protein is the sole viral surface protein and is the sole target for neutralising antibodies (23, 92). A lack of live virus isolate for KBLV and inaccessibility of the TWBLV live isolates has meant that assessment of vaccine protection has not been determined. However, previous studies have utilised reverse genetics (RG) techniques to exchange the gene encoding the G proteins derived from other lyssavirus species into a RABV vaccine RG backbone to enable assessment of vaccine protection against recombinant viruses (23, 105, 403). Since the initial detection of KBLV nucleic acid and the two TWBLV live isolates, the full genome sequences have been published (GenBank accession no. LR994545, no. MF472710.1, and no. MF472709.1, respectively).

This chapter describes the development of a live recombinant RABV where the RABV G gene has been replaced by KBLV G or TWBLV G. *In vitro* and *in vivo* studies were undertaken to define the ability of vaccine derived sera and vaccine induced antibodies (anti-RABV) to neutralise and protect against a recombinant virus containing the KBLV G or the TWBLV G in a murine model. Further *in vitro* studies were used to assess the

cross-neutralisation potential of lyssavirus-specific sera against these recombinant viruses.

4.2. Generation of recombinant lyssavirus plasmids

Recombinant lyssavirus plasmids were generated through PCR and Gibson Assembly (476). Gibson Assembly (NEB) involves the generation of overlapping PCR products in order to construct the clones (Figure 2.1). The cloning strategy was the same for all produced G constructs (Figure 4.1). The cDNA clone of the SN strain of RABV (cSN) was derived from the SAD B19 cDNA clone as described previously (92, 416, 477). Subsequently, the full length cSN clone was used as the backbone plasmid for the recombinant lyssavirus plasmids. The cSN plasmid was amplified by PCR and cSN specific primers, as described in section 2.8, to generate two fragments whilst also excluding the homologous RABV G. Splitting the cSN plasmid into two fragments decreased PCR extension times and improved Gibson Assembly outputs. The linearised cSN plasmid was assessed by gel electrophoresis to ensure products were the correct size and subsequently purified using the Monarch® PCR & DNA Cleanup Kit (NEB) to remove enzymes, nucleotides, primers and buffer components for downstream use.

KBLV G was synthesised as a DNA fragment (GeneArt, Thermo Fisher) and initially cloned into the vector, pcDNA3.1(+) for long term storage. The plasmid vector pcDNA3.1(+) was linearised and amplified by PCR. KBLV was synthesised with incorporated overhangs complementary to pcDNA3.1(+) to allow immediate assembly into the multiple cloning site of pcDNA3.1(+) and ligation using the Gibson assembly method.

The resulting plasmids were then transformed into Max Efficiency NEB® 5-alpha Competent E.coli (NEB) in the presence of the selective antibiotic, ampicillin. Positive

colonies were identified using colony PCR and from 4 separate positive colonies, small scale plasmid mini preparations were generated. The plasmid DNA sequence from the small scale preparations was then confirmed by Sanger sequence analysis. This plasmid vector with KBLV G gene was used in subsequent PCR reactions rather than the DNA fragment that was synthesised.

The TWBLV G from the 2016 TWBLV isolate was codon optimised for expression in humans and cloned into the pI.18 expression vector. This was kindly gifted by Dr Ed Wright at the University of Sussex, UK.

For insertion into cSN, KBLV G and TWBLV G ORFs were amplified with 20 bp overhangs directed at the 5' and 3' end of cSN using a PCR reaction (described in 2.2.2.2.) and the following primers; KBLVfwd (5'-

CTCAAAAGACCCCGGGAAAGATGCCATTTCAAGCGGTTC-3') and KBLVRev (5'- GTTGAAAGGCTAGCCAGTCCCTAGGCCTGAGACTGATC-3') for KBLV G and TWBLVfwd (5'-CTCAAAAGACCCCGGGAAAGATGCCCAATTACACACTG-3') and TWBLVrev (5'-

GTTGAAAGGCTAGCCAGTCCCTACGTATGGATTCGGGAC-3') for TWBLV.

The underlined sequence within the primers are the incorporated overhangs complementary to cSN. Primers were designed using an online tool provided by NEB (NEBuilder).

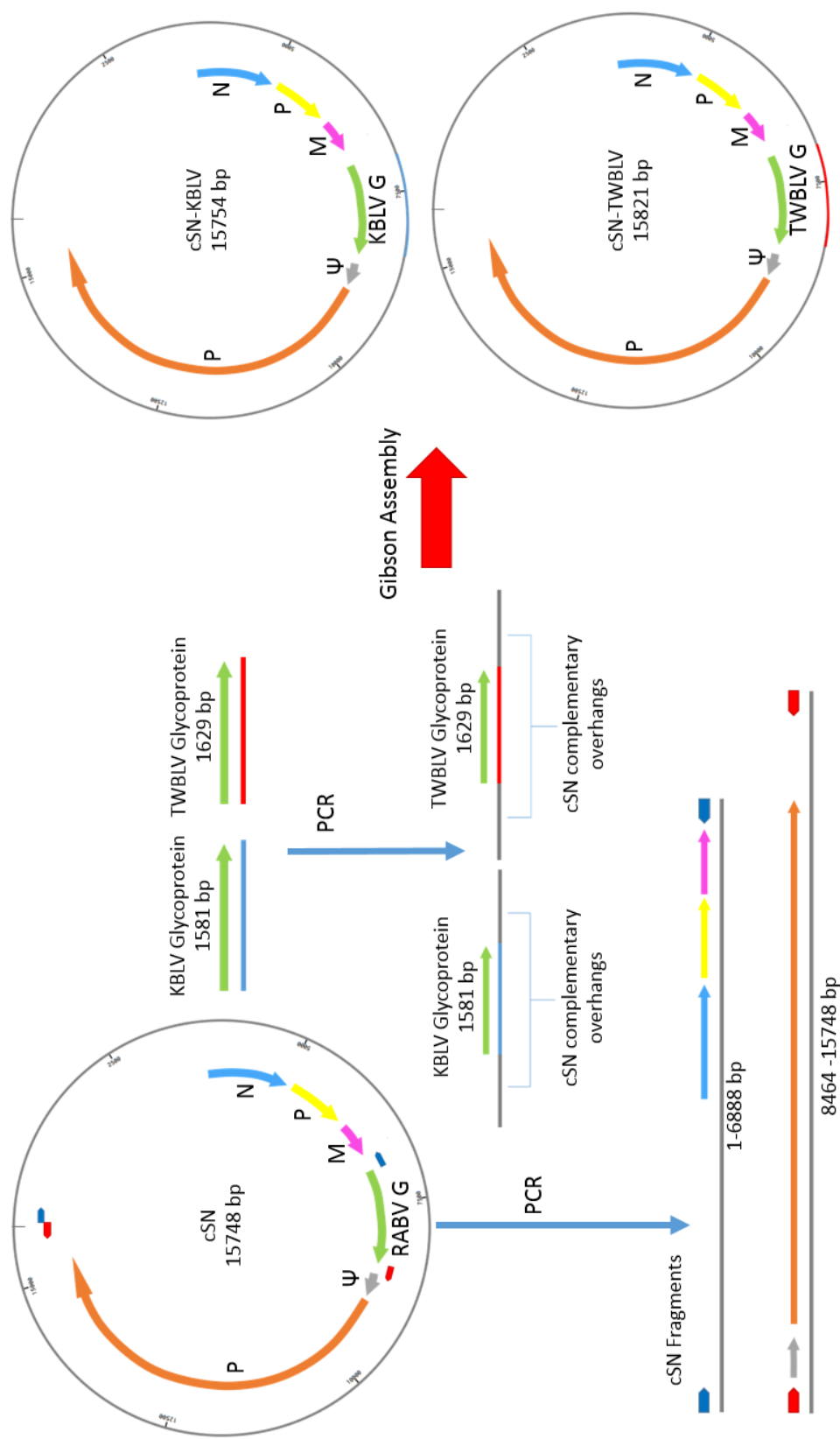


Figure 4.1: Cloning Strategy for the replacement of RABV glycoprotein with KBLV glycoprotein or TWBLV glycoprotein. Two cSN fragments were generated using specific primers (Blue and Red arrows) to exclude RABV G. In a separate PCR reaction, 19-20bp overhangs complementary to cSN were added to the 5' and 3' ends of KBLV G and TWBLV G. The two cSN fragments and one glycoprotein with cSN complementary overhangs were assembled by Gibson Assembly to produce the cSN-KBLV and cSN-TWBLV recombinant plasmids.

To confirm the presence of PCR amplicons at the appropriate size, reaction products were assessed by agarose gel electrophoresis. Like the cSN fragments, the PCR products were then purified using the Monarch® PCR & DNA Cleanup Kit (NEB). Following this, all purified PCR products were restriction digested by *DpnI* to cleave any residual template DNA as described in section 2.2.12.2. The two cSN vector fragments and one of the G gene inserts with cSN complementary overhangs were assembled by Gibson Assembly to produce the recombinant plasmids that expressed either KBLV G or TWBLV G genes (henceforth referred to as cSN-KBLV and cSN-TWBLV). Each of the full length clones were then transformed and colonies were screened as previously described for KBLV G in the pcDNA3.1(+) plasmid vector. Once positive colonies were identified, plasmid DNA, from four separate positive colonies, was then produced in large amounts using the GeneJET Plasmid Maxiprep Kit (Thermo Fisher). The purity and concentration of the large scale DNA preparations were measured on the Nanodrop ND-2000 spectrophotometer (Thermo Scientific) absorbance ratio value (A260:A280). The sequence of each was determined by Sanger sequence analysis. In addition, restriction digestion of the plasmids was performed using restriction enzymes *NheI* and *MluI*, as described in section 2.2.12.2, to ensure the plasmids were of the correct size (Figure 4.2).

4.3. Virus Rescue and Titration

The reverse genetics technique was used to rescue the full length clones as live virus. Each full length clone was selected, along with the wildtype cSN full length clone as a positive control, and cSN expressing enhanced Green Fluorescent Protein (eGFP) and EBLV-2 G instead of RABV G (cSN-EBLV-2-eGFP) as an early indicator as to whether the virus rescue method had worked.

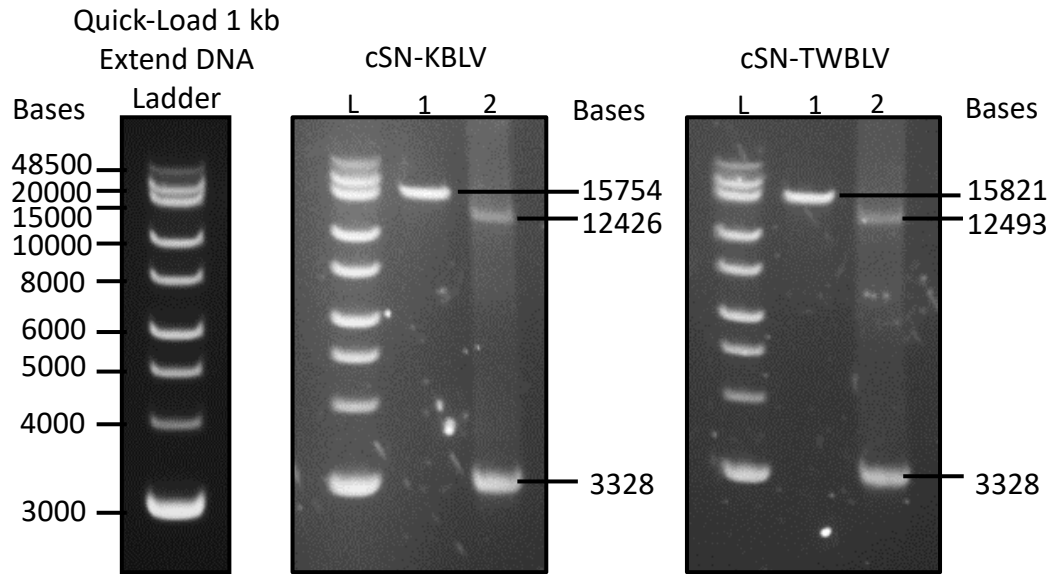


Figure 4.2: Restriction digestion of cSN-KBLV and cSN-TWBLV. Digestion of the intact cSN-KBLV plasmid and cSN-TWBLV plasmid with *NheI*, to generate one full length fragment (Lane 1), and with *NheI* and *MluI* to generate two fragments (Lane 2). The ladder is Quick-Load 1 kb Extend DNA ladder (NEB).

In 96 well plates, these plasmids were transfected at a concentration of 200 ng along with four helper plasmids: pTIT-N (40 ng), pTIT-P (40 ng), and pTIT-L (40 ng) into BSR T7/5 cells, cells that express T7 RNA polymerase, using FuGENE 6 (Promega). This was designated as passage 1 (P1). After 96 hours, the wells with transfected cSN-EBLV2 expressing eGFP were first visualised to give an indication as to whether the virus rescue had occurred without the need for fixing in acetone and staining with a fluorescent antibody. Cells showing bright green fluorescence throughout the cell under UV were an indication of cSN-EBLV-2-eGFP infection, determining that the virus rescue had been successful. Further passage of this control rescue was stopped at this point. Following this, the cells and supernatant for the cSN, cSN-KBLV and cSN-TWBLV clones were harvested and supplemented with fresh BHK -21 cells and transferred to 12 well plates (P2). Following a further 72 hour incubation, the P2 cells and supernatant were supplemented with more fresh BHK-21 cells and transferred to a 6 well plate (P3). At this stage, prior to incubation, an aliquot of 200 μ l from each of the 6 well plates was transferred to a 96 well plate in triplicate. Due to the lack of visible cytopathic effect as a result of lyssavirus infection and the depleted transfected N at this passage, the cells and TCSN transferred to the 96 well plate would act as the control plate.

After a further 72 hour incubation, the 96 well plates were fixed in 80% acetone and subsequently stained with an anti-N FITC conjugated mAb (Fujirebio) to assess the proportion of cells that were positive for N antigen. All rescues at this stage showed positive cells showing bright green, perinuclear granular fluorescence as well as multiple foci, indicative of infection.

At P3, the cSN rescues suggested approximately 100% of the cells were positive for antigen whereas cSN-KBLV showed approximately 60% infection and cSN-TWBLV

showed approximately 30% infection. In order to increase the volume of each virus stock, the cells and supernatants were harvested and transferred to a T75 flask along with fresh BHK-21 cells (P4).

After a further 72 hour incubation, cSN was again 100% positive for N antigen, cSN-KBLV approximately 80-90% positive and cSN-TWBLV approximately 60% positive. At this stage, the cells and supernatant from the cSN infected T75 flask was split in half across two fresh T75 flasks and supplemented with fresh BHK-21 cells. For cSN-KBLV and cSN-TWBLV, a proportion of cells and supernatant were transferred to a single T75 flask with fresh media and BHK-21 cells in an attempt to increase the percentage infectivity. This was repeated until 100% infectivity was observed. After six passages, cSN-TWBLV reached 100 % infectivity whereas cSN-KBLV only required five passages (Figure 4.3).

Following the final passage to achieve 100 % infectivity, the virus TCSNs were harvested and the RNA was extracted from the remaining cell pellets as described in section 2.2.1. The RNA was used to generate cDNA which was then used as the template in confirmatory RT-PCRs.

The resulting products were all of the expected size; 1.5-1.6 kb so were confirmed by amplicon sequencing using G specific primers. In addition to Sanger sequencing, Next generation sequencing was also performed on the entire construct, using the purified RNA extracted material as the template. Sequencing data enabled comparison of the rescued viruses to the original construct and it was determined that throughout the full genomes of both viruses, no mutations had been acquired following multiple passages and that KBLV G and TWBLV G had been inserted correctly with no frame shifts. This also confirmed no contamination had occurred.

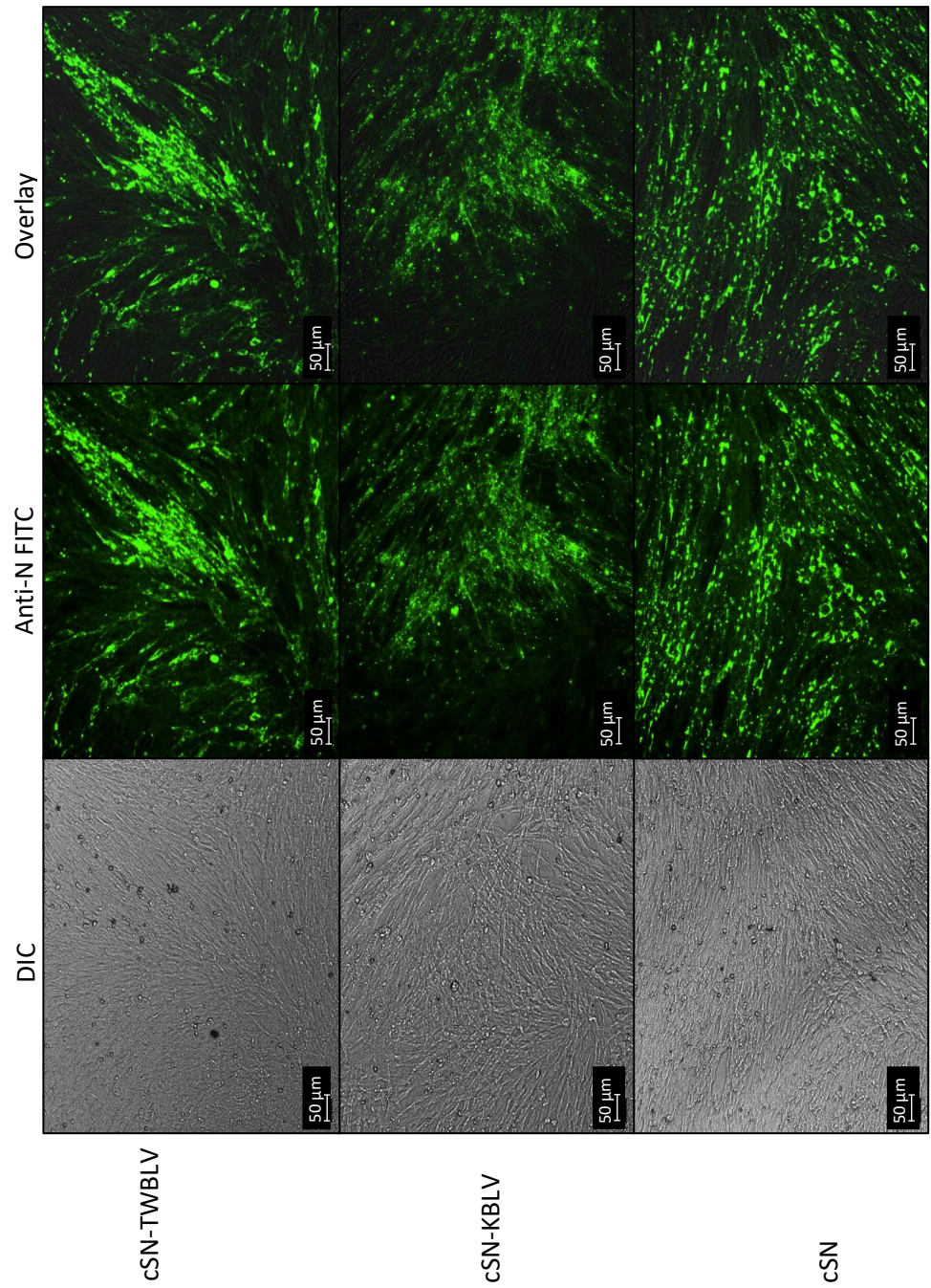


Figure 4.3: Infection immunofluorescence. BHK cells infected with either cSN-TWBVLV (first row), cSN-KBLV (second row), cSN (third row) were fix and stained with a FITC Anti-rabies nucleoprotein monoclonal globulin (Fujirebio) (green). Scale bars represent 50 µm.

Harvested virus was titrated as described in section 2.4.2.4 and showed that cSN-KBLV grew to a titre of 2.5×10^4 ffu/ml and cSN-TWBLV grew to a titre of 1.5×10^4 ffu/ml, almost 2 \log_{10} lower than cSN with a titre of 1.6×10^6 ffu/ml. Both values, however, are comparable to similar studies using EBLV-1 G, EBLV-2 G, IKOV G, and WCBV G within a cSN vector (23, 403).

4.4. Growth Kinetics

Following the calculation of the viral titres of each of the rescued viruses, growth kinetics could be determined *in vitro*. To determine the growth kinetics of cSN-KBLV and cSN-TWBLV, multi-step growth curves were performed with cSN, cSN-TWBLV, and cSN-KBLV in BHK cells (Figure 4.4). Performing single step growth curves was not possible due to the low titres of both cSN-KBLV and cSN-TWBLV, consequently a multiple step growth curve using a MOI of 0.1 was performed. Due to the fact that the wildtype virus for KBLV had not been successfully isolated and TWBLV was unavailable, the growth kinetics of cSN-KBLV and cSN-TWBLV were compared to that of the vaccine backbone, cSN.

By 24 hours post infection (hpi), all viruses were detected at around 10^3 ffu/ml, however cSN-KBLV and cSN-TWBLV were first detected 12 hours earlier. cSN grew to the highest peak titre of 7.6×10^7 ffu/ml at around 96 hpi, cSN-KBLV grew to a peak titre of 1.55×10^7 ffu/ml at 72 hpi, over four times less than the peak titre of cSN, and cSN-TWBLV grew to a peak titre of 1.13×10^5 ffu/ml at 48 hpi, almost 700 times lower than cSN.

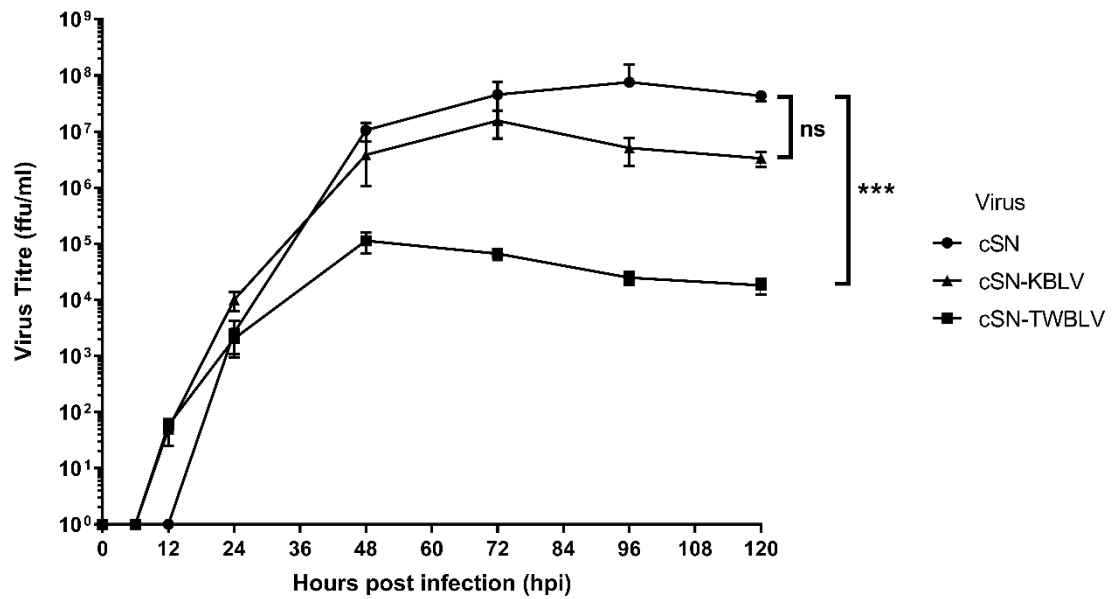


Figure 4.4: Growth kinetics of cSN-KBLV, cSN-TWBLV, and the vaccine backbone, cSN, *in vitro*. For each virus, BHK-21 cells were infected with an MOI of 0.1 to produce a multiple step growth curve over the course of 120 hours. The test was performed in triplicate and the mean and standard deviation of the results plotted on a logarithmic scale. Asterisks indicate significant differences between the groups calculated using the Kruskal-Wallis test with Dunn's multiple comparisons (***, $P < 0.001$; ns, not significant).

The endpoint titres showed varying significant differences between the viruses, with cSN-KBLV exhibiting a titre of 3.33×10^6 ffu/ml compared to cSN at 4.3×10^7 ffu/ml ($P=0.190$) and cSN-TWBLV exhibiting a titre of 1.81×10^4 ffu/ml ($P<0.001$). This difference in titre for cSN-TWBLV was over 3 \log_{10} lower than that of cSN and over 2 \log_{10} lower than cSN-KBLV.

The growth kinetics show a similar curve for cSN-KBLV and cSN however cSN increases in titre until 96 hpi and plateaus. In contrast, cSN-KBLV plateaus and drops in titre after 72 hpi. For cSN-TWBLV, as well as significant different viral titres at each time point, the growth pattern also differed. At 48 hpi, cSN-TWBLV reached peak titre and plateaued and decreased in titre from that point onwards. This indicates a retarded growth rate of cSN-TWBLV.

The titres of the viruses roughly indicated the trend seen in the growth kinetics of each rescued virus. The virus with the highest overall titre was cSN and this virus grew to the highest titre when assessing growth kinetics. Surprisingly, despite cSN-KBLV having a similar but lower initial titre than cSN-TWBLV, it grew to much higher titres in the growth kinetics experiment, unlike cSN-TWBLV which did not grow to high titres and remained around 10^4 ffu/ml.

4.5. *In Vitro* Studies

Two experimental approaches were taken to assess cSN-KBLV antigenically: i) to determine the titre of standard sera sufficient to neutralise cSN-KBLV over the 0.5 IU/ml value assigned as the cut-off for protection and; ii) to evaluate the ability of other lyssavirus sera to neutralise this virus in the absence of a wildtype isolate.

4.5.1. Recombinant Viruses versus Vaccine Sera

In the first assay, a mFAVN was used to test the comparative neutralisation of cSN-KBLV, cSN-TWBLV, cSN, and CVS against increasing titres of two standard sera, OIE and WHO. In Chapter 3, a variable degree of neutralisation from standard sera was observed within phylogroup I, demonstrating that different titres were required for the complete neutralisation of different phylogroup I lyssaviruses.

The current rabies vaccines confer protection against phylogroup I lyssaviruses so vaccines are generally considered to be effective against novel lyssaviruses genetically classified within phylogroup I. As a result, it was of interest to investigate the neutralisation ability of standardised vaccinated animal and human derived sera.

CVS, cSN, cSN-KBLV, and cSN-TWBLV were standardised to a concentration of 100 TCID₅₀ and 50 µl was incubated with WHO serum, an international standard human serum and OIE serum, a diagnostic control canine serum, at 0.5 IU/ml, 1 IU/ml, 2.5 IU/ml, and 5 IU/ml (as described in section 2.5) (Figure 4.5).

Both the OIE and WHO sera neutralised all three viruses at 1IU/ml and at 2.5IU/ml.

Both CVS and cSN were neutralised by both OIE and WHO sera with complete neutralisation at 0.5 IU/ml. However, cSN was the most readily neutralised where OIE sera exhibited a reciprocal titre of 1/64 and WHO sera exhibited a titre of 1/37, higher than that of CVS where OIE sera exhibited a reciprocal titre of 1/24 and WHO sera exhibited a reciprocal titre of 1/22.

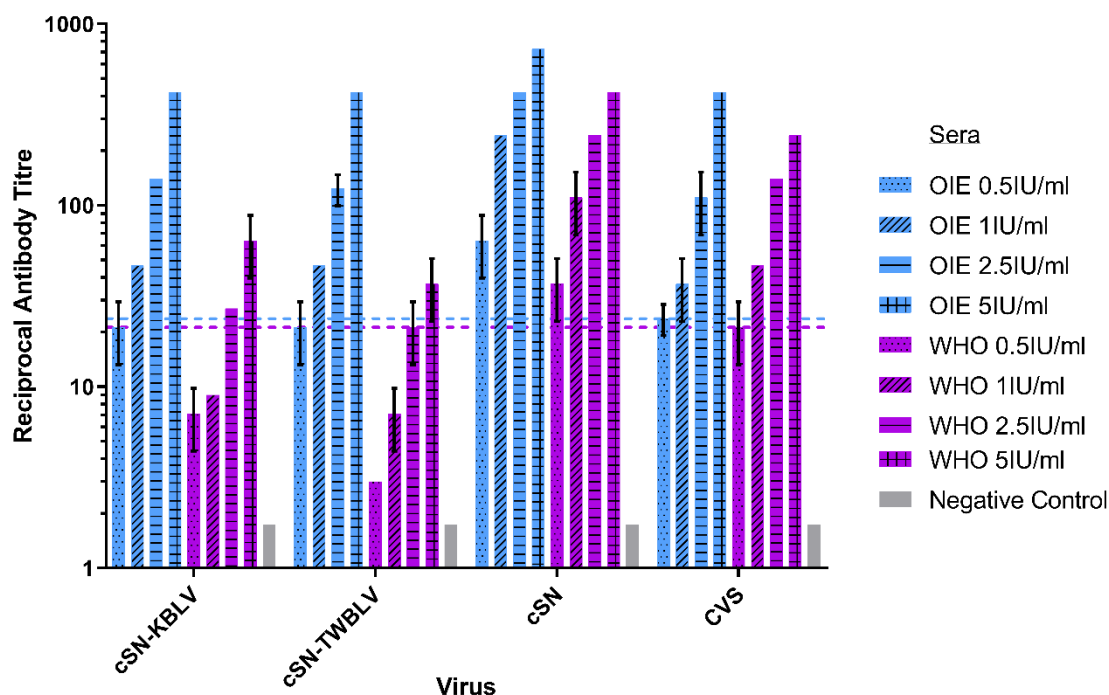


Figure 4.5: Neutralisation profiles of cSN-KBLV, cSN-TWBLV, cSN and CVS against OIE and WHO standard sera using a modified fluorescent antibody virus neutralisation (mFAVN) test. The test was performed in triplicate and the mean and standard deviation of the results plotted on a logarithmic scale. The 0.5 IU/ml neutralisation cut-off is dictated by the serological standards against CVS (indicated by the coloured dashed lines – OIE=blue, WHO=purple). Naïve canine sera was used as the negative control.

Both serological standards demonstrated the lowest level of neutralising antibodies against cSN-TWBLV and cSN-KBLV as 1 IU/ml of OIE sera and 2.5 IU/ml of WHO sera was required to neutralise both viruses above the 0.5 IU/ml threshold for WHO and OIE sera against CVS. Additionally, the trend in neutralising antibody levels differed between each of the standard sera used. OIE sera consistently showed higher levels of neutralising antibodies than WHO sera when tested against each of the viruses, though the greatest difference was observed with cSN-KBLV and cSN-TWBLV.

At 5 IU/ml, OIE sera shows almost \log_{10} higher neutralising antibodies against cSN-KBLV than WHO, and almost double for CVS and cSN. Against cSN-TWBLV, 0.5 IU/ml of the OIE sera exhibited a similar titre of neutralising antibodies to 2.5 IU/ml of the WHO sera. Based on these results, it is likely that rabies vaccines confer protection against KBLV and TWBLV *in vivo*.

4.5.2. Ability of phylogroup I specific sera to neutralise cSN-KBLV and cSN-TWBLV

A mFAVN was used to assess cross-neutralisation of lyssavirus-specific sera against cSN-KBLV and cSN-TWBLV, in addition to CVS and cSN (Figure 4.6).

Whilst varying levels of cross-neutralisation were observed within phylogroup I lyssavirus-specific sera, phylogroup II and III-specific sera showed no/little neutralising antibodies against each of the viruses. The virus cSN was most readily neutralised by the phylogroup I sera panel, with seven lyssavirus-specific sera showing levels of neutralising antibodies above 0.5 IU/ml, whereas cSN-KBLV was neutralised by five lyssavirus-specific sera. For cSN-KBLV, ARAV, BBLV, EBLV-1, EBLV-2, and GBLV-specific sera exhibited a titre of neutralising antibodies above the 0.5 IU/ml cut off, whilst ABLV, DUVV, KHUV, and RABV-specific sera did not.

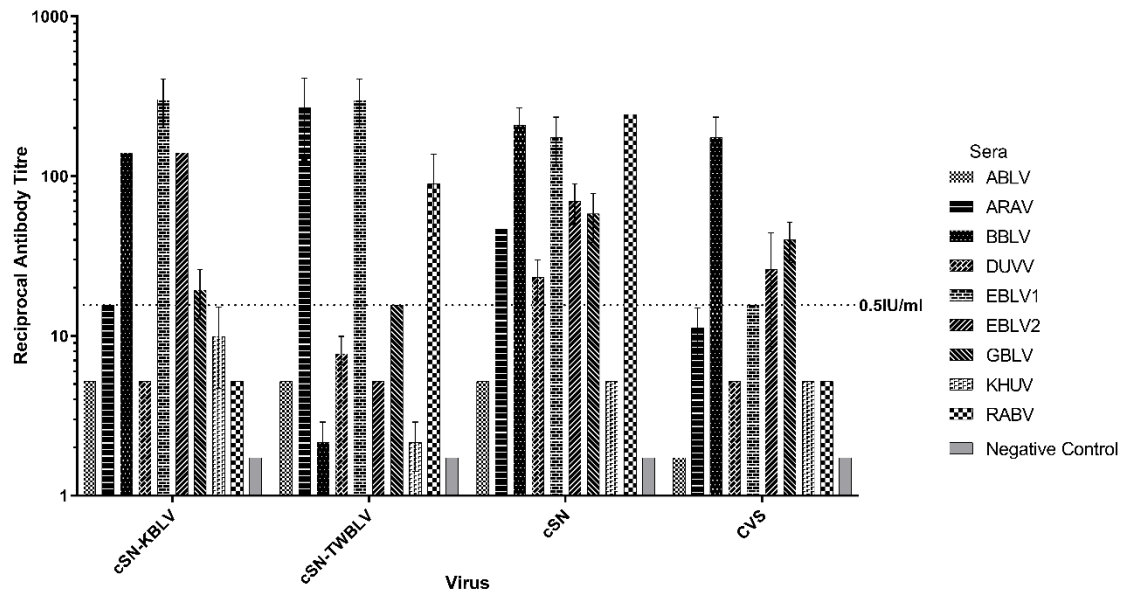


Figure 4.6: Cross-neutralisation profiles of each phylogroup I lyssavirus-specific sera using a modified fluorescent antibody virus neutralisation (mFAVN) test. The test was performed in triplicate and the mean and standard deviation of the results plotted on a logarithmic scale. The 0.5 IU/ml neutralisation cut off is dictated by the OIE sera against CVS (indicated by the dashed line). IRKV sera not shown. Naïve canine sera was used as the negative control.

CVS and cSN-TWBLV were neutralised by the least number of lyssavirus specific sera, with only four lyssavirus sera exhibiting titres of neutralising antibodies above the cut-off. For cSN-TWBLV, only ARAV, EBLV-1, and RABV-specific sera exhibited a titre of neutralising antibodies above the 0.5 IU/ml cut off.

In addition, the ability of each sera to cross-neutralise each virus varied. For cSN-KBLV, EBLV-1-specific sera exhibited the highest titre of neutralising antibodies with a reciprocal titre of 1/302. For cSN-TWBLV, EBLV-1 and ARAV-specific sera exhibited the highest titre of neutralising antibodies at 1/302 and 1/268, respectively. BBLV-specific sera exhibited the greatest reciprocal titre of neutralising antibodies against CVS at 1/174.

Specific sera for a wild/street RABV strain showed the highest reciprocal titre of neutralising antibodies against cSN at 1/243, closely followed by BBLV and EBLV-1-specific sera. Interestingly, the wild/street RABV-specific sera was only capable of neutralising cSN and cSN-TWBLV and not CVS, indicating possible antigenic divergence of wild/street strains to the cell culture adapted CVS, used regularly in diagnostic assays. Further, EBLV-1-specific sera neutralised cSN, cSN-KBLV, and cSN-TWBLV but not CVS. Finally, cSN-TWBLV was the only virus not neutralised by BBLV.

4.5.3. Antigenic Cartography

Whilst the antigenic distance has been reported for phylogroup I lyssaviruses in Chapter 3, the antigenic distances for novel lyssaviruses, KBLV and TWBLV, were not included. Similarly, to the cross-neutralisation data in Chapter 3, antigenic cartography maps were generated in order to quantify antigenic relationships between phylogroup I viruses and cSN-TWBLV and cSN-KBLV and enable comparison to the evolutionary relationships facilitated by phylogenetic nucleotide analysis.

Both cSN-KBLV and cSN-TWBLV are antigenically distinct from the other phylogroup I lyssaviruses (Figure 4.7). Based on the antigenic distances on the 3D map, cSN-KBLV is antigenically closest to cSN (1.00 AU), ARAV (1.21 AU), IRKV (1.45 AU) and EBLV-2 (1.65 AU). Whereas, cSN-TWBLV is antigenically closest to ABLV (1.11 AU), cSN (1.58 AU), KBLV (1.59 AU) and EBLV-1 (1.63 AU). Whilst cSN-TWBLV is closely located to other phylogroup I lyssaviruses, on average, cSN-KBLV is antigenically closer to the phylogroup I lyssaviruses than cSN-TWBLV. This is also reflected in the 2D antigenic map with cSN located at the centre of the map (Figure 4.8A).

It has been suggested that vaccine candidates obtain a central position within antigenic clusters, which is certainly the case for this antigenic map where cSN (RABV vaccine strain SAD-B19) obtains a central position within the phylogroup I viruses (435). The phylogroup I viruses have been grouped into the clusters described previously in Chapter 3. In this case, the clusters are defined by the viruses that occupy a point on the map that is <1.4 AU from the most centrally located viruses.

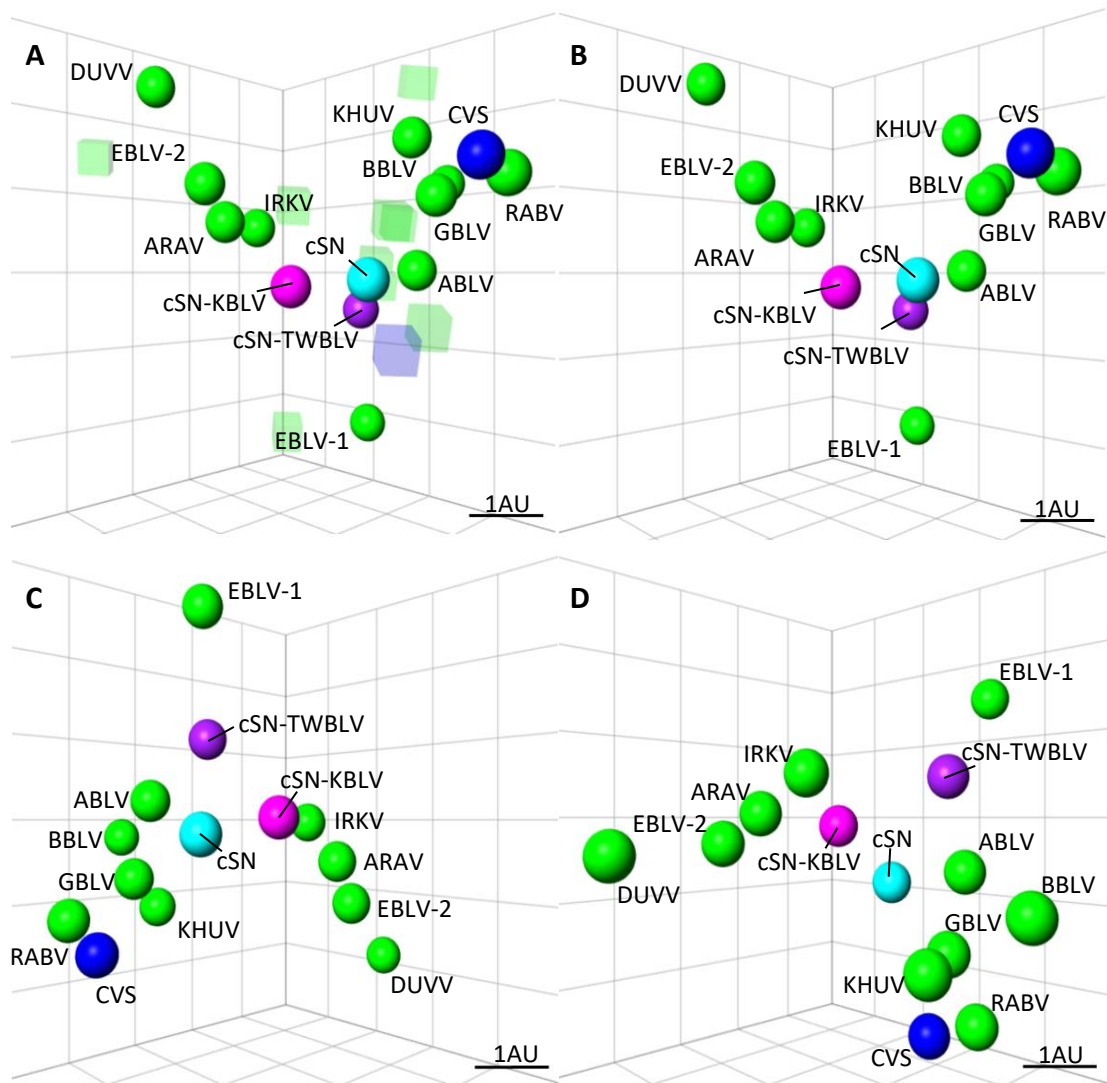


Figure 4.7: (A) 3D antigenic map. Viruses (spheres, coloured according to genetic relationships and sera (translucent coloured boxes) are positioned such that the distance from each serum to each virus is determined by the neutralisation titre. Multidimensional scaling is used to position both sera and viruses relative to each other, so orientation of the map within the axes is free. Phylogroup I lyssaviruses are coloured green, challenge virus standard coloured dark blue and the viruses discussed in this Chapter coloured differently for clarity. Scale bar shows one antigenic unit (AU). (B) The same view and orientation with sera removed for clarity. (C) Rotated to a different orientation and sera removed for clarity. (D) Rotated to a different orientation for clarity

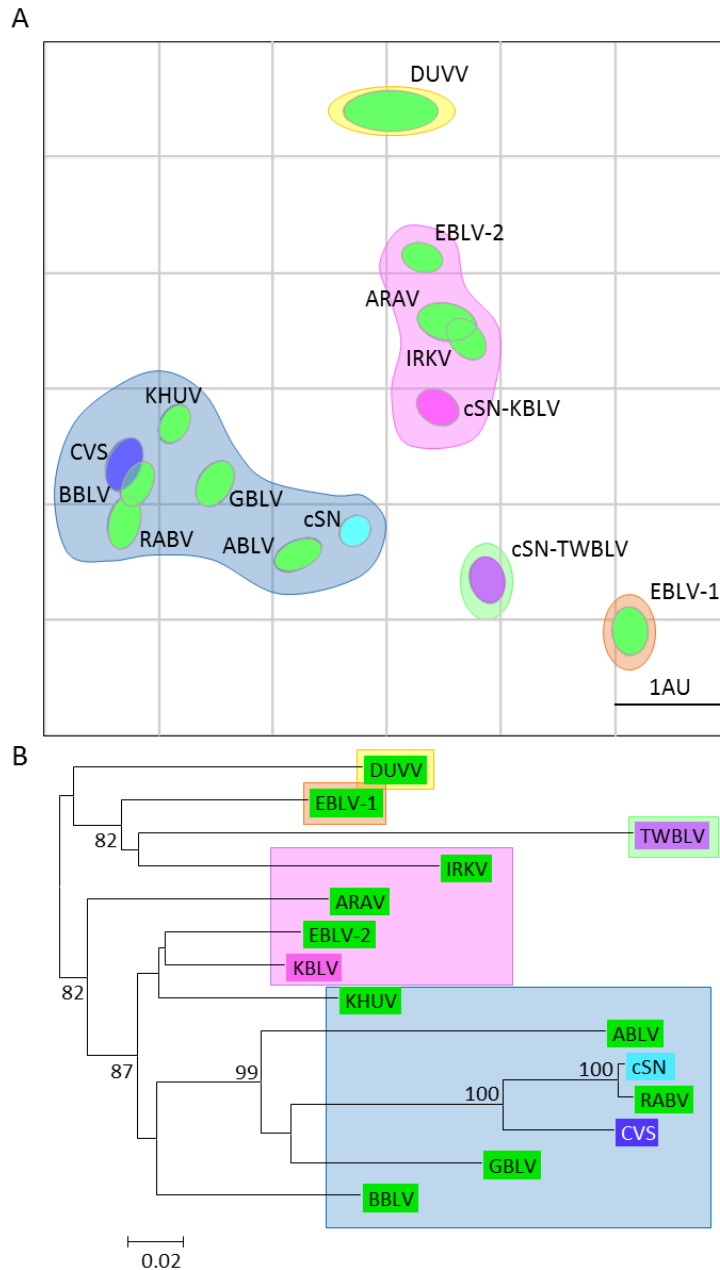


Figure 4.8: (A) 2D antigenic map of Phylogroup I viruses, cSN, cSN-KBLV and cSN-TWBLV. The relative positions of the viruses (coloured ovals) were plotted such that the size and shape represent the confidence area in placement of the virus. Viruses are coloured as before (Fig. 5.6). Antigenic clusters have been identified in relation to cSN, cSN-KBLV and cSN-TWBLV and are shown through transparent differentially coloured shapes. Scale bar shows 1 antigenic unit with both horizontal and vertical axis representing antigenic distance so orientation within this map is free. (B) Phylogenetic tree of the glycoprotein nucleotide sequences (described in Figure 1.1 and Table 3.1), colour coded based on Figure 4.8A. The evolutionary history was inferred using the Neighbor-Joining method and the evolutionary distances were computed using the Maximum Composite Likelihood method and are in the units of the number of base substitutions per site. Trees were generated in MEGA6 and edited in FigTree.

Interestingly, cSN-KBLV is located within a cluster with ARAV, IRKV and EBLV-2, and cSN-TWBLV, being >1.4AU from GBLV, ARAV, EBLV-1, and DUVV is more antigenically divergent and so does not belong to a cluster using this cut off. As before in Chapter 3, DUVV and EBLV-1 are antigenic outliers, as they are antigenically distant from other viruses.

This method of visualising and quantifying antigenic data allows direct comparison to the genetic data. To further investigate the genetic basis of the antigenic distances and antigenic clusters, the evolutionary history of the G protein nucleotide sequences of the of each phylogroup I lyssaviruses were quantitatively inferred using the Neighbor-Joining method and the evolutionary distances were computed using the Maximum Composite Likelihood (ML) method and displayed as a phylogenetic tree. The tree was colour-coded according to the clusters identified in the antigenic map of Figure 4.8A (Figure 4.8B).

Direct comparison shows a rough correspondence between the relative positions of clusters in the antigenic map and the phylogenetic tree, but this was seen more clearly across all phylogroups in Chapter 3. To accurately compare the data, the correlation between antigenic distance and ML phylogenetic tree distance could be inferred by comparing the distances between cSN and each of the viruses.

Based on this data, 1 AU was equal to a ML distance of 0.235 ($r=0.58$ (95%CI 0.20 to 0.81), $R^2=0.34$, $P=0.007$) when RABV, CVS, and cSN-TWBLV were excluded from the dataset.

This highlights that it is not always possible to infer antigenic distance based on genetic data alone as RABV G and CVS G are highly genetically similar to cSN G but show vastly different cross-neutralisation profiles. In contrast, TWBLV G is more genetically

distinct from cSN G but shows a smaller antigenic distance to cSN when compared to a virus of similar genetic diversity as TWBLV G such as DUVV G.

It could be hypothesised that the difficulties with antigenic interpretation of genetic data could be due to the variation in antigenic effect of specific amino acid substitutions as proposed in chapter 3, due to the type of amino acid substitution, the location of the substitution or the resulting interaction of the substitution (435).

4.6. In Vivo Vaccination Challenge Study

4.6.1 Vaccination of mice prior to ic challenge

To assess the ability of vaccine induced neutralising antibodies to protect mice from challenge with cSN-KBLV and cSN-TWBLV, mice were vaccinated with a current human rabies vaccine; VeroRab (Sanofi Pasteur) as described in chapter 2, section 2.9. Four week old BALB/c mice were vaccinated via the ip route with 500 µl of vaccine. The vaccine was reconstituted as per the manufacturer's instructions and then diluted 1 in 20 in serum free media (MEM). Mice were vaccinated on day 0 and again on day 7 with the same dose. The mock vaccinated mice were inoculated with 500 µl of MEM only on the same days. On day 21, blood samples were collected from the dorsal vein as described in 2.9.1.3. The sera were recovered from these samples and a standard FAVN test was used to determine serological response. This enabled comparison to the OIE standard 0.5 IU/ml.

All mice seroconverted to a titre above the internationally assigned cut-off for neutralisation of RABV, 0.5 IU/ml. The serological responses ranged from 0.87 IU/ml and 23.38 IU/ml for cSN-KBLV mice and 1.5 IU/ml and 23.38 IU/ml for cSN-TWBLV mice, 21 days after vaccination (Figure 4.9).

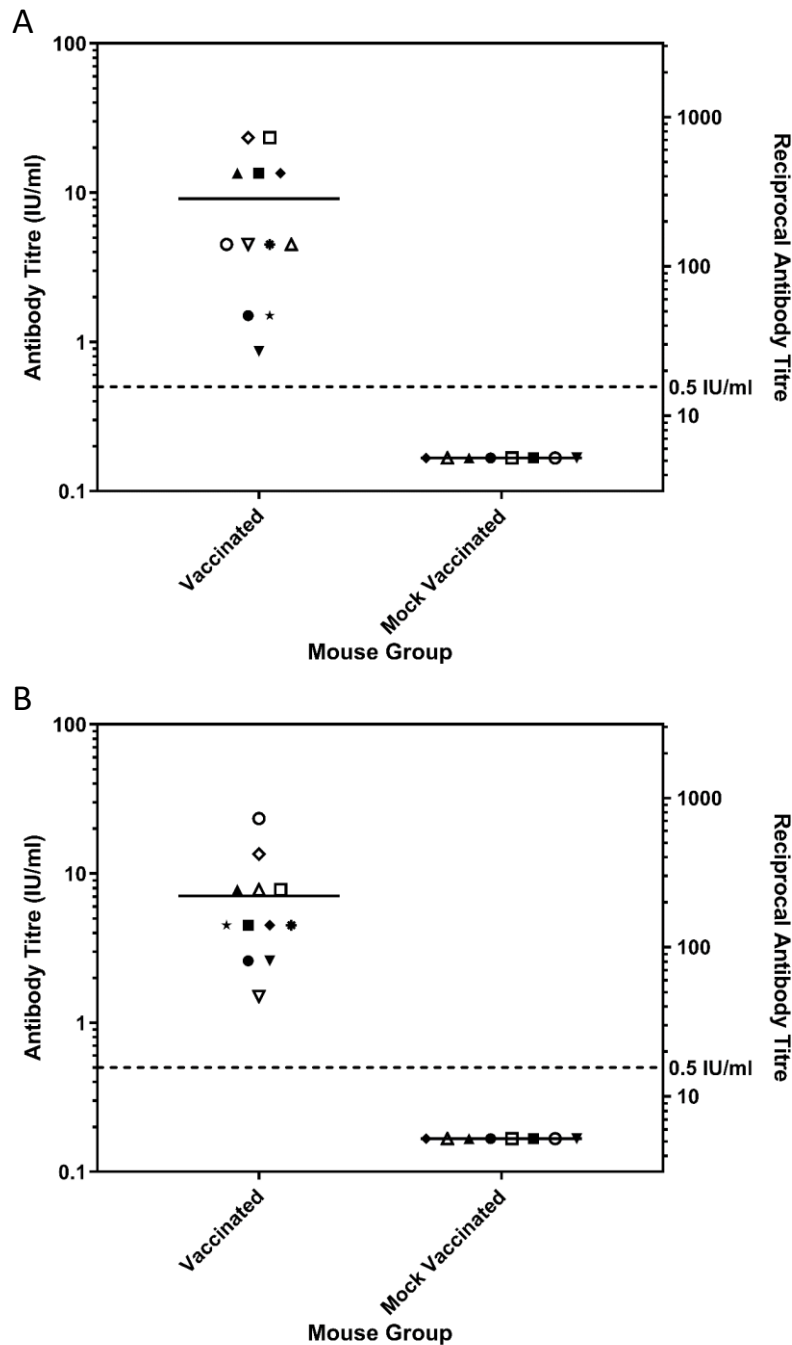


Figure 4.9: Seroconversion and survivorship of the animals. Post-vaccination serology on day 21 for mice vaccinated with VeroRab and mice mock vaccinated with MEM on days 0 and 7. All sera, each assigned a different symbol on the graph, was assessed for neutralising antibodies by FAVN and plotted on a logarithmic scale where A) To be challenged with cSN-KBLV and B) To be challenged with cSN-TWBLV. The Y1 axis represents the Antibody titre (IU/ml) and the Y2 axis represents the equivalent reciprocal antibody titre.

4.6.2 Survival of vaccinated mice post ic challenge

Following the assessment of seroconversion, both mock vaccinated and vaccinated groups were challenged ic on day 29 post-vaccination with 100 ffu/30µl of cSN-KBLV or cSN-TWBLV. Twelve vaccinated mice were compared to eight mock-vaccinated mice given the same dose of virus.

A statistically significant difference ($P < 0.001$) in survival was observed between the vaccinated and mock-vaccinated groups in cSN-KBLV (Figure 4.10A). However, this was not the case for cSN-TWBLV challenged mice where there was no difference in survival between mock vaccinated and vaccinated mice (Figure 4.10B).

All mice in the cSN-KBLV mock-vaccinated group ($n=8$) reached clinical endpoint by seven days post-challenge, one day after onset of clinical disease. Throughout the course of the experiment, mice were assessed for clinical disease according to a clinical score sheet and humanely terminated at a clinical score of 2 or below (Appendix 4). The first sign of clinical disease was ruffled fur. Subsequent clinical signs observed included piloerection, tail-biting, intermittent hyperactivity and hunched stance.

In the cSN-KBLV vaccinated group ($n=12$), one mouse was terminated after developing score 2 clinical signs, which included an extreme hunched stance and limb twitching. The time from initiation of disease to termination in line with humane endpoints was however protracted, with the mouse reaching clinical endpoint at day 13 post-challenge, three days after the onset of clinical disease.

In addition, the vaccinated mouse that succumbed to infection had the lowest neutralising antibody titre of 0.87 IU/ml prior to challenge. From a serological perspective, all mice with virus neutralising antibody titres of 1.5 IU/ml and above survived ic challenge.

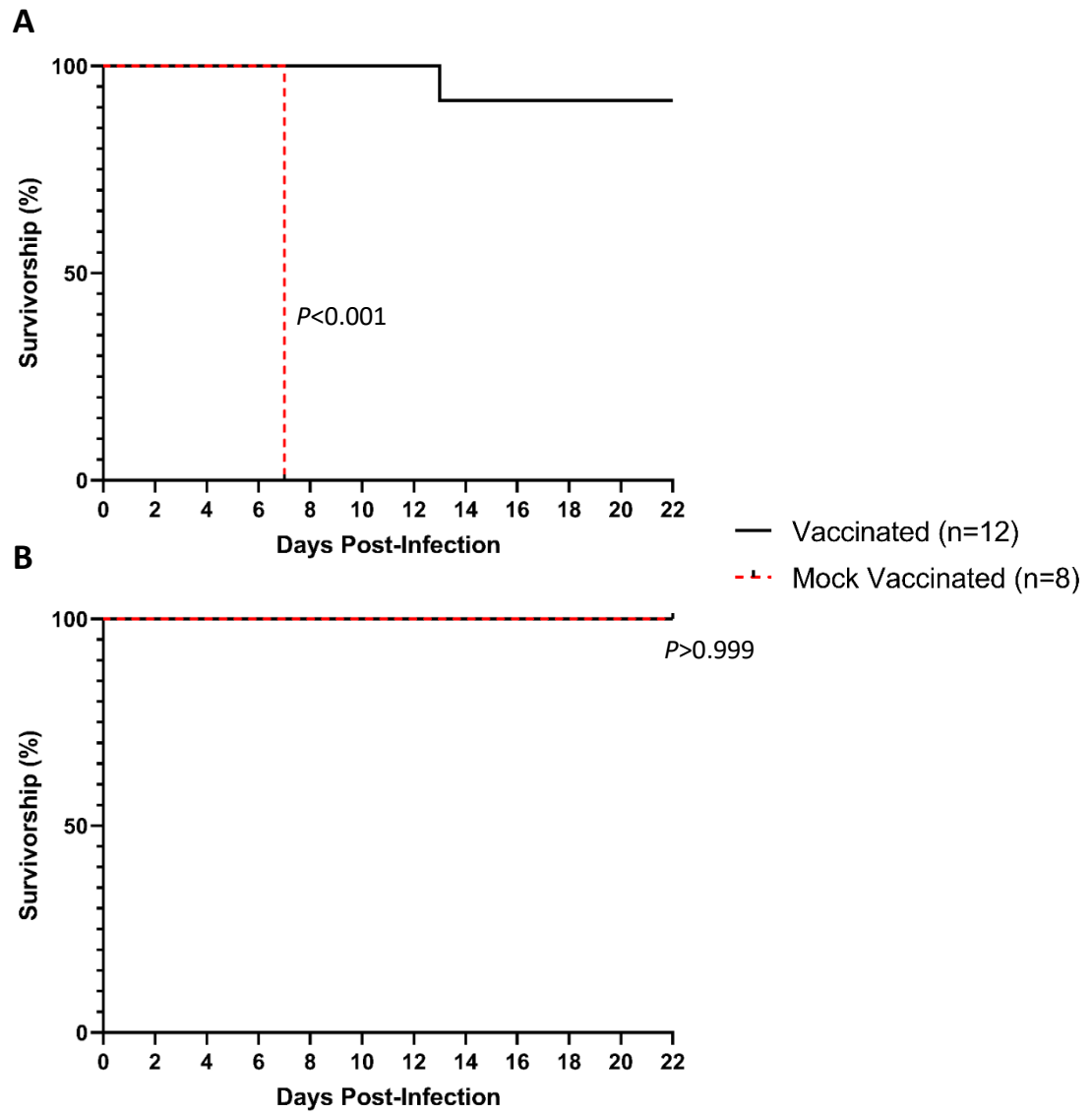


Figure 4.10: *In vivo* survivorship following intracranial inoculation with A) 100 ffu/30 μ l of cSN-KBLV and B) cSN-TWBLV. Mice were vaccinated 29 days before challenge and day 0 on the graph is the day of challenge. Survival was analysed using the log rank Mantel-Cox test.

For the mice challenged with cSN-TWBLV, zero mice from the vaccinated group (n=12) and zero mice from the mock vaccinated group (n=8) succumbed to infection, despite the mock vaccinated mice exhibiting no neutralising antibody titres post mock vaccination. However, on days 10, 11, 13 and 15 post challenge, mock vaccinated mice exhibited a slightly rough coated and hunched appearance but were not severe enough to be classified as a clinical score of 1 or 2 so were not terminated. These mice, however, recovered and show no further clinical signs for the remainder of the experimental period.

4.6.3 Histology and Immunofluorescence

4.6.3.1 Histology

To demonstrate the pathogenicity of cSN-KBLV in the mouse model, naïve mice that succumbed to disease were evaluated by histopathology and immunohistochemistry. In the cSN-KBLV mock vaccinated group, one mouse that developed clinical disease and succumbed to infection was humanely terminated and fixed in 10 % NBF (as described in 2.9.1.7) for a 14 day period. Two mice in the mock vaccinated cSN-TWBLV group, despite surviving to the end of the experiment, were also fixed in 10 % NBF upon termination. Brains were removed and coronally cross-sectioned before being processed to paraffin wax. Serial sections (4 µm) were cut and either stained with haematoxylin and eosin (H&E) for morphological examination or labelled immunohistochemically for viral antigen using a RABV mAb, mAb 5B12 (MyBioSource) (as described in 2.9.1.8.2).

For the mock vaccinated cSN-KBLV challenged mice, infection via the ic route resulted in mild to moderate, multifocal, neuronal necrosis in the cerebral cortex, thalamic (Figure 10A) and hippocampal regions (Figure 10B) of the forebrain with the association of abundant amounts of viral antigen. More specifically, the anti-rabies N

antibody staining (brown-orange staining) in Figure 4.11B reveals viral antigen in the neuronal cell bodies and dissemination down the neuronal axons, indicated by the hair-like projections across the hippocampus cross-section. In the thalamus (third ventricular region), dense aggregations of lyssavirus antigen were also observed (Figure 4.11A). Moderate to minimal amounts of virus antigen were also present multifocally within the neuroparenchyma of the thalamus, cerebellum, brain stem, and rare antigen labelling was detected in neuronal cell bodies within the spinal cord but histological changes were not present in these areas.

For the mock vaccinated cSN-TWBLV mice, neither neuronal necrosis nor viral antigen was detected in the hippocampus or third ventricle (Figure 4.11 C and D). The minimal brown-orange staining surrounding the blood vessels in the immunohistochemistry (IHC) stain was non-specific staining due to the anti-mouse secondary antibody used.

4.6.3.2 Immunofluorescence

Aggregations of lyssavirus antigen were also detected in brain smears subjected to the direct fluorescent antibody test (FAT) as described in 2.9.1.8.1. Briefly, two mice from each group; cSN-KBLV vaccinated, cSN-KBLV mock vaccinated, cSN-TWBLV vaccinated, and cSN-TWBLV mock vaccinated were selected for the FAT. Due to different termination dates, these mice were frozen at -80 °C post termination until the FAT was performed. Prior to the FAT, mice were left to defrost for 24 hours. For each mouse being tested, the brain was extracted from the carcass (as described in 2.9.1.6) and impression smears were made on microscope slides using a small amount of hindbrain.

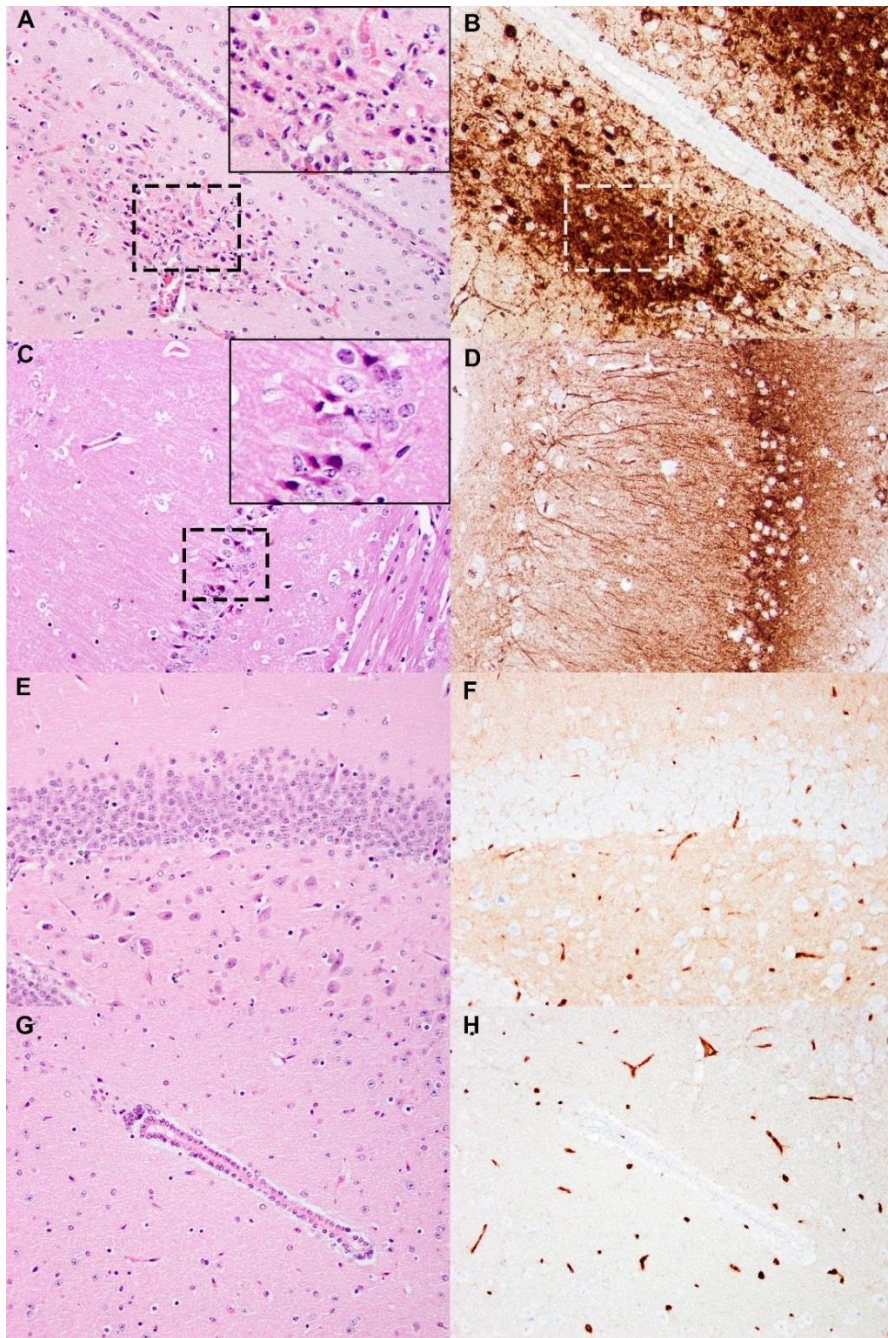


Figure 4.11: Histopathology and immunohistochemistry (IHC) against rabies nucleoprotein (N) on cSN-KBLV and cSN-TWBLV-infected mouse brains. (A, B) A cSN-KBLV ic challenged mouse brain. Areas of neuronal necrosis with pyknotic nuclei and karyorrhectic cellular debris (outlined with black dashed-line box) observed in the thalamic region adjacent to the third ventricle (left, H&E stain) and serial-stained sections for N protein revealed abundant intralesional virus antigens (right, IHC, white dashed line box for region of interest co-localised with H&E section). (C, D) A cSN-KBLV ic challenged mouse brain. Areas of neuronal necrosis characterised by red, angular and shrunken neurons (outlined with dashed-line box) in the hippocampus (left, H&E) where IHC-stained serial tissue section revealed abundant intralesional virus antigens (right, IHC). (E, F) A cSN-TWBLV ic challenged mouse brain. Representative sections showing no histological changes or virus antigens in the hippocampus or (G, H) third ventricle. Images taken at 200x magnification. Insets show digitally magnified region of interest.

The cSN-KBLV mock vaccinated mice that succumbed to infection were the only brains to test positive for viral N antigen (Figure 4.12 A and B). The mice in this group showed differing levels of viral N antigen with one smear showing more fluorescence than the other, however, both were comparable to the CVS positive control (Figure 4.12 D).

For the cSN-KBLV vaccinated mice, cSN-TWBLV mock vaccinated mice, and cSN-TWBLV vaccinated mice, no viral antigen was observed as indicated by no fluorescence (Figure 4.12 C).

4.6.4 Real time RT-PCR

Alongside FAT analysis, RNA was extracted from the same mouse brains described, and used for SYBR real time RT-PCR analysis. RNA was extracted from brain homogenate using the Trizol method described in 2.2.1 and run on the real-time RT-PCR assay with 8 positive control standards as described in 2.2.2.4.2.

All samples except the cSN-TWBLV vaccinated mouse brains tested positive by the real-time PCR assay (Table 4.1). The mouse group showing the lowest mean Ct value, 19.05 ± 0.10 and 19.37 ± 0.11 , were the mice that succumbed to clinical disease in the cSN-KBLV mock vaccinated group, therefore indicating that this group had much higher viral RNA levels in the brain.

The mouse group with the second lowest Ct value was the cSN-TWBLV mock vaccinated group, with Ct values of 30.41 ± 0.57 and 32.57 ± 0.34 , indicating that whilst clinical disease did not develop and FAT/IHC were negative, viral RNA was still present in the brain.

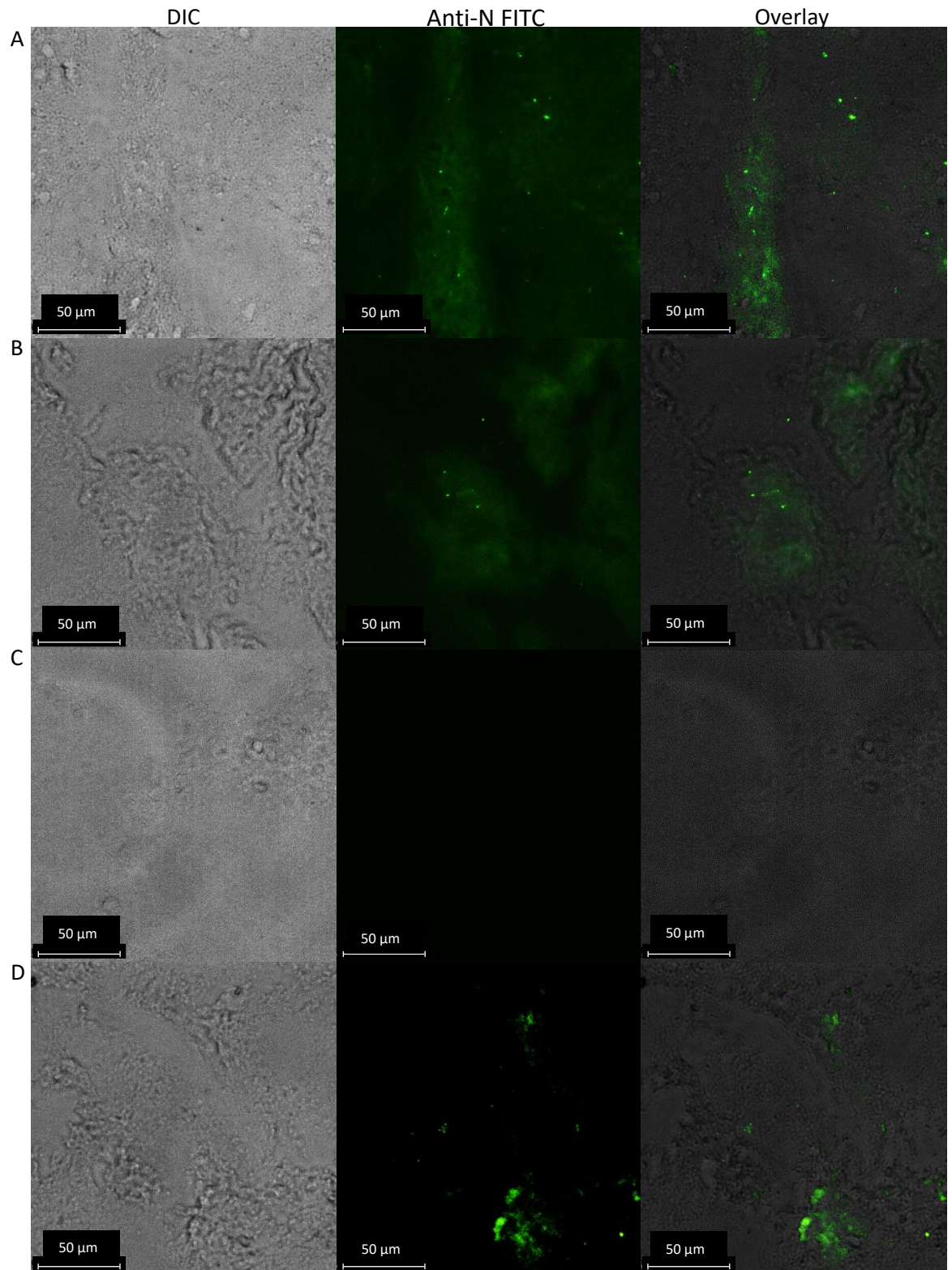


Figure 4.12: Direct FAT test. Green fluorescence indicative of lyssavirus nucleoprotein in a brain smear subjected to a direct fluorescent antibody test with fluorescein isothiocyanate–conjugated monoclonal antibody (Fujirebio). A and B show the positive brain smears from two mice in the cSN-KBLV mock vaccinated group. C shows a negative smear, representative of all other brain smears tested in the cSN-KBLV vaccinated group (n=11), cSN-TWBLV vaccinated group (n=12) and cSN-TWBLV mock vaccinated group (n=8). D shows the CVS positive control smear. Scale bars represent 50 μm.

Lastly, the survivors of the cSN-KBLV vaccinated mouse group showed the highest mean Ct values, with Ct values of 33.14 ± 0.53 and 36.06 ± 0.55 . Similar to the cSN-TWBLV mock vaccinated group, whilst the mice were FAT/IHC were negative, negligible viral RNA loads were present in the brain at the time of termination.

For comparison of initial quantity in copy number, cDNA of CVS-11, at a known concentration (copies/g), was serially diluted from 10^{-1} to 10^{-8} and used alongside the mouse brain RNA extracts as a standard curve on the real time RT-PCR assay (Figure 4.13). This standard curve was used to interpolate the initial quantity (copy number) of each sample tested, using the Ct-values.

Using two mice from each group, cSN-KBLV mock vaccinated mice had the highest copy numbers per gram with 1.07×10^6 copies/g and 8.53×10^5 copies/g. The cSN-TWBLV mock vaccinated mice had 763.70 copies/g and 188.00 copies/g and the cSN-KBLV vaccinated mice had 133.30 copies/g and 20.68 copies/g.

4.6.5 Serological responses to infection and post-vaccination challenge

All animals, that succumbed to clinical disease or survived until the end of the experiment, were cardiac bled before being humanely terminated. Sera was assessed for seroconversion using both FAVN against CVS and modified FAVN against the challenge virus. Mean titres were compared using the Kruskal-Wallis test with Dunn's multiple comparisons test.

In the cSN-KBLV mock vaccinated group (n=8), 63% (n=5/8) of the animals had an antibody response capable of neutralising cSN-KBLV using the modified FAVN.

Reciprocal titres ranged from 1/16 to 1/421. In contrast, no neutralising antibody against CVS was detected with the standard FAVN (Figure 4.14A).

Table 4.1: Post-mortem molecular testing on the brains of two mice from each group

Mouse Group	SYBR real time RT-PCR Assay	
	Lyssavirus Nucleoprotein	β -actin
	Ct-value Mean \pm SD	Ct-value Mean \pm SD
cSN-KBLV vaccinated	33.14 \pm 0.53	23.23 \pm 0.11
	36.06 \pm 0.55	23.87 \pm 0.12
cSN-KBLV mock vaccinated	19.37 \pm 0.11	21.93 \pm 0.08
	19.03 \pm 0.10	21.82 \pm 0.14
cSN-TWBLV vaccinated	No Ct	24.24 \pm 0.10
	No Ct	22.95 \pm 0.46
cSN-TWBLV mock vaccinated	30.41 \pm 0.57	22.96 \pm 0.08
	32.57 \pm 0.34	23.42 \pm 0.10

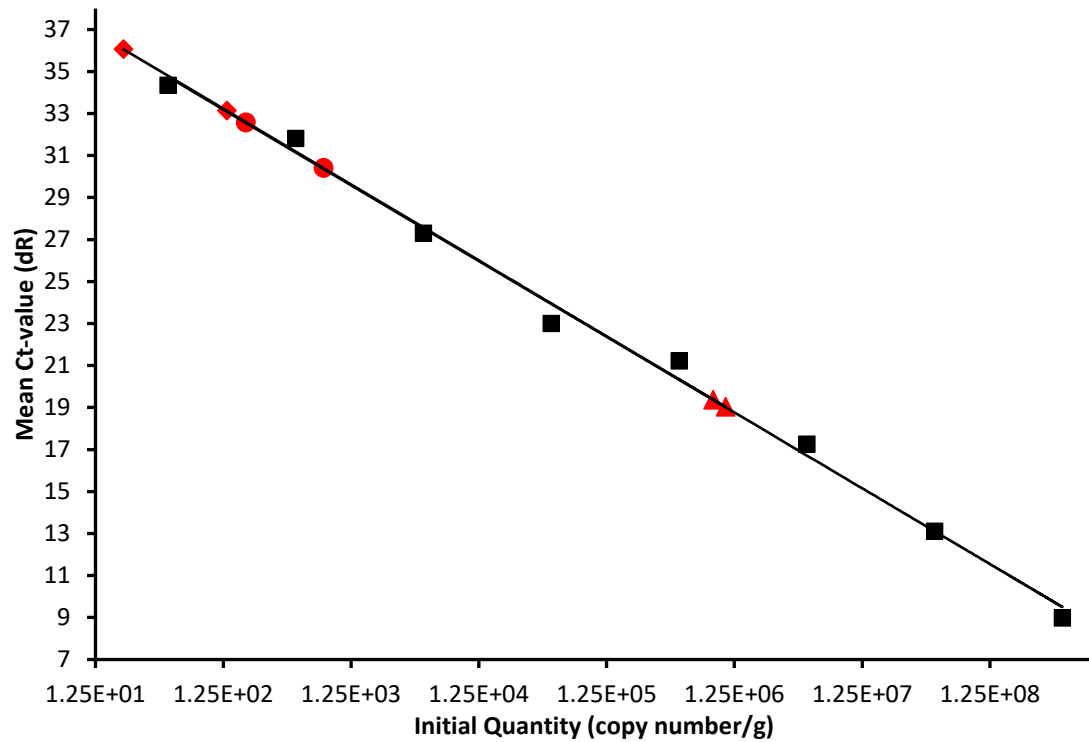


Figure 4.13: Quantitative SYBR real time RT-PCR. Standard curve and standards are shown in black. SYBR sample values (indicated by the red symbols) are plotted and interpolated using the standard curve regression line ($Y = -3.607 \cdot \text{LOG}(X) + 40.76$) and the mean Ct-values. Triangles represent cSN-KBLV mock vaccinated mice, circles represent cSN-TWBLV mock vaccinated mice and diamonds represent cSN-KBLV vaccinated mice.

Despite the difference in mean reciprocal titres against CVS in the standard FAVN ($1/4 \pm 1/2$) and cSN-KBLV in the modified FAVN ($1/87 \pm 1/134$), the difference was not statistically significant ($P>0.99$).

For the vaccinated group, all surviving mice developed neutralising antibody titres. In the standard FAVN against CVS, sera showed neutralising antibody titres ranging from $1/243$ to $1/59049$. In the modified FAVN against cSN-KBLV, sera showed less variability with neutralising antibody titres ranging from $1/729$ to $1/34092$. On average however, the titre of neutralising antibodies against CVS and cSN-KBLV were not significantly different ($P>0.99$).

When comparing the serology post-challenge to serology following vaccination and prior to challenge (using the standard FAVN), the titre of neutralising antibodies in the vaccinated group increased 50 fold from an average reciprocal titre of $1/284$ to $1/14400$ (Figure 4.9A and Figure 4.14A)

Interestingly, the one mouse that succumbed to infection on day 13 post-infection showed high reciprocal titres of $1/1262$ against CVS and $1/2187$ against cSN-KBLV (as indicated by ▼ in both Figure 4.9A and 5.13A).

Despite this, sera from the vaccinated group showed a statistically significant difference in neutralising antibody titres against CVS and cSN-KBLV than the sera derived from the mock vaccinated group ($P<0.001$; $P=0.01$).

In contrast, when sera from cSN-TWBLV mock vaccinated mice ($n=8$) was assessed using FAVN and modified FAVN, 75% ($n=6/8$) had developed CVS neutralising antibody titres and 100% ($n=8$) developed significant cSN-TWBLV neutralising antibody titres, demonstrating exposure and immune response to cSN-TWBLV (Figure 4.14B).

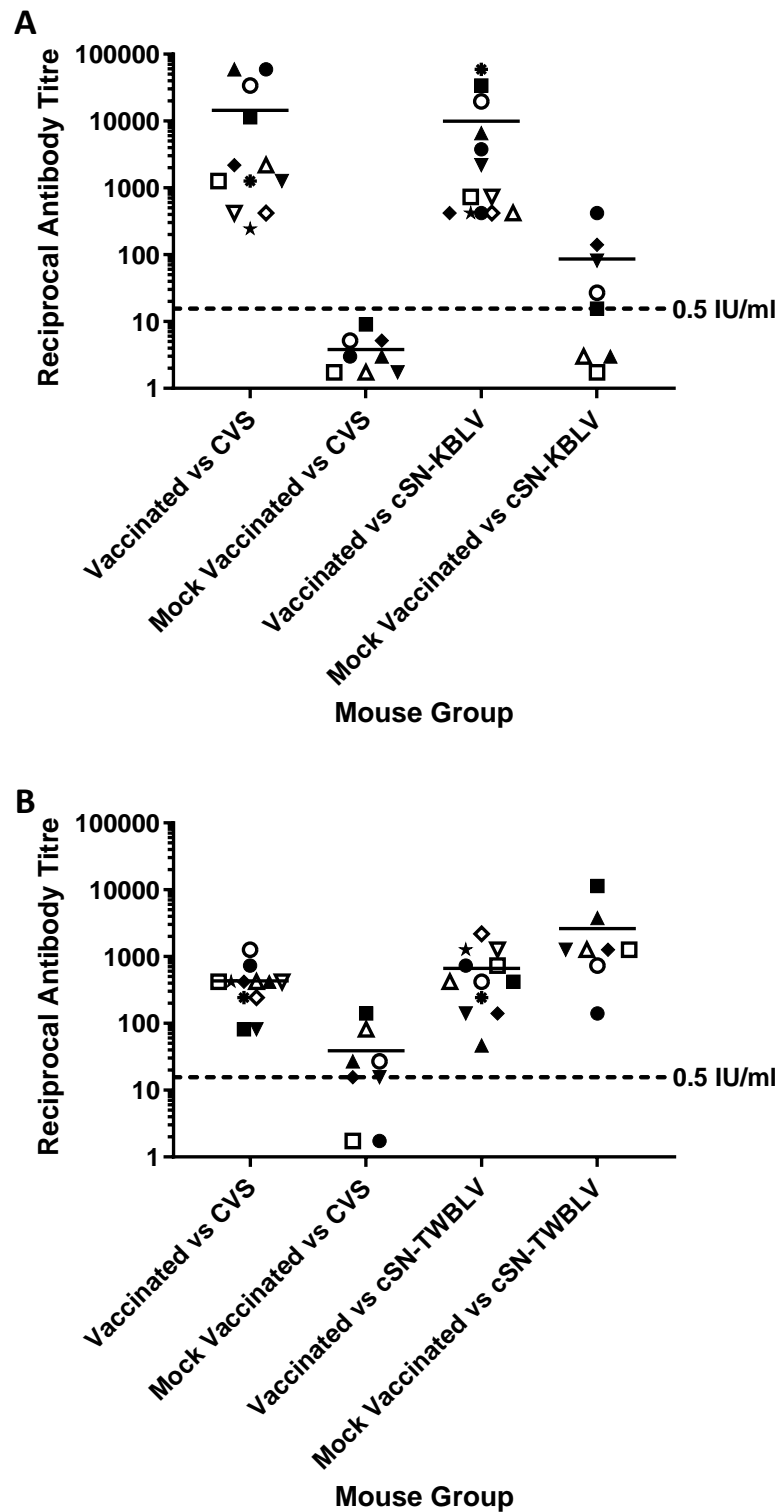


Figure 4.14: Assessment of serological status in mice following vaccination and challenge. A, cSN-KBLV challenged mice were serologically assessed against CVS and cSN-KBLV using FAVN and modified FAVN assays. B, cSN-TWBLV challenged mice were serologically assessed against CVS and cSN-TWBLV using FAVN and modified FAVN assays. Dotted line represents 0.5 IU/ml neutralisation cut off, dictated by OIE sera against CVS.

Additionally, the average neutralising antibody titres against cSN-TWBLV were significantly higher than the neutralising antibody titres against CVS at 1/2622 and 1/39 respectively ($P < 0.001$).

In the cSN-TWBLV challenged vaccinated group, the cSN-TWBLV challenge did not have a statistically significant effect on the serological titre when assessed for the ability to neutralise CVS versus cSN-TWBLV. Despite no significant difference in contrast to the cSN-KBLV vaccinated group, the average neutralising antibody titres against cSN-TWBLV were higher than CVS at 1/667 and 1/430 respectively.

Of the cSN-TWBLV challenged mice, it was the mock vaccinated mice that showed the highest neutralising antibodies against cSN-TWBLV with no significant difference from the vaccinated group ($P = 0.734$).

4.7. Discussion

Although the current rabies vaccines confer protection against phylogroup I lyssaviruses, the discovery of novel lyssaviruses warrants investigation into vaccine efficacy as infection with lyssaviruses still results in a clinically incurable encephalitis.

KBLV, first detected in 2017, has not been successfully isolated, nor has it been formally classified within the lyssavirus genus as a virus isolate despite being genetically related to other members of the genus (19). In contrast, TWBLV was detected in 2016 and 2017 and isolates were successfully isolated, however inaccessibility to the live virus isolates meant that TWBLV has not been assessed *in vitro* and *in vivo*. However, the availability of the KBLV and TWBLV genome data enabled synthesis of the G gene open reading frames and generation of recombinant viruses expressing the KBLV G or TWBLV G. This in turn enabled further antigenic characterisation of these viruses. The full-length RABV vaccine DNA backbone, cSN,

was manipulated such that the homologous RABV G gene was replaced with the KBLV G gene or TWBLV G gene. These recombinant clones containing the heterologous G gene were successfully rescued as live virus and were both able to replicate *in vitro*. Additionally, cSN-KBLV was able to productively infect mice to cause rabies. This confirms the ability of the viruses to infect, replicate and spread between cells. This further enabled the antigenic characterisation of KBLV and TWBLV, in the absence of the wildtype KBLV and TWBLV viruses, through *in vitro* cross-neutralisation assays and *in vivo* vaccination-challenge studies using the representative cSN-KBLV and cSN-TWBLV recombinant viruses.

Growth kinetic assessment of these viruses revealed that despite a successful virus rescue, endpoint titres achieved were significantly different with cSN-KBLV and cSN-TWBLV reaching lower final titres compared to the parent cSN virus (Figure 4.4). Whilst both cSN-KBLV and cSN virus titres peaked with titres $>10^7$ ffu/ml, cSN-KBLV peaked 24 hours earlier than cSN and the endpoint titres were significantly different, albeit still high. cSN-TWBLV peaked at 48 hpi with a titre of 1.13×10^5 ffu/ml and the endpoint titre when compared to cSN was significantly different. This reduction in titre compared to the parent cSN may reflect sub-optimal protein interactions following interspecies G protein substitution. This is most likely due to impartial or incomplete interaction with heterologous M protein, leading to sub-optimal assembly of G protein on the viral surface, although the hypothesis requires testing. A decreased viral fitness of recombinant lyssaviruses has been linked to how divergent the vaccine backbone strain is to the lyssavirus the G gene originates from. In a similar study, cSN expressing IKOV G and WCBV G have been shown to grow to viral titres around 10^5 - 10^6 , almost $2 \log_{10}$ lower than cSN-KBLV (23). Due to a greater degree of amino acid sequence identity of the KBLV G protein to cSN G protein, the KBLV G might interact more

optimally with the cSN M protein than other more divergent lyssavirus G proteins.

IKOV and WCBV are among the most divergent lyssaviruses within the genus, leading to the hypothesis that these would interact least optimally with cSN M protein. KBLV G has ~74.0 % amino acid sequence identity to cSN G, whereas TWBLV G has ~63.8 % sequence identity to cSN G so these cross-species protein interactions may indeed interact less optimally. Whilst the sequence identity of TWBLV G to cSN G is more than 11 % less than the sequence identity of KBLV G and cSN, it is still 13 % more than cSN-WCBV and cSN, with a sequence identity of 50.1 %. It would be expected that if this hypothesis was the sole determinant for the viability of these recombinant viruses, cSN-TWBLV would grow to higher titres than cSN-WCBV but lower than cSN-KBLV, however only the latter is true.

Another hypothesis for decreased viral fitness is that the novel parent viruses (KBLV and TWBLV) have even lower viral fitness within cell culture than the recombinant cSN-KBLV and cSN-TWBLV viruses. This cannot be assessed as a wildtype virus isolate does not exist for KBLV and is not available for TWBLV, although similar examples have been proposed previously. Certainly, in a previous study, wildtype EBLV-1 and -2 isolates grew to a lower titre than the recombinant cSN-EBLVs (referred to as SN-1 and SN-2 in the study), indicating that the low titres observed were not a result of the G protein-dependent processes such as receptor binding and viral entry, but rather poor adaption for *in vitro* viral replication and assembly (93).

Regardless, for a recombinant lyssavirus expressing a heterologous G protein, the viral titre achieved for cSN-KBLV was comparable to cSN and the cSN-EBLVs, indicating little to no effect on growth.

A further difference, between cSN-TWBLV and the other viruses discussed previously, was that cSN-TWBLV was the only virus where the G gene was codon optimised for human expression. In previous studies, codon optimisation/de-optimisation of the RABV G gene decreased/ slowed virus growth *in vitro* (478, 479). The combination of the lower sequence similarity to cSN and the effect of codon optimisation/de-optimisation on viral growth, may greatly affect the growth of cSN-TWBLV *in vitro* and *in vivo*.

To assess the antigenicity of the KBLV- G protein and the TWBLV-G protein, mFAVNs were undertaken with a panel of sera specific for different lyssavirus G proteins.

Previous phylogenetic assessment determined that KBLV would be classified within phylogroup I given the nucleotide identity of 81 %, 79.7 %, 79.5 % and 79.4 % with KHUV, ARAV, BBLV and EBLV-2 N proteins, respectively (19). It was concluded, following the analysis of the whole genome sequence in a second study, that KBLV is genetically most closely related to EBLV-2, KHUV and BBLV (209). In the neutralisation assays performed in this study, cSN-KBLV grouped within phylogroup I based on reactivity with phylogroup specific sera, with EBLV-1, BBLV and EBLV-2 specific sera exhibiting the highest titres of neutralising antibodies against cSN-KBLV (Figure 4.6).

Additionally, antigenic cartography was also used to quantitatively analyse antigenic data. As previously mentioned in Chapter 4, antigenic cartography involves geometric interpretation of binding assay data by assigning each antigen and serum a point on a 3D map, such that the distance between the antigen and antiserum directly corresponds to the reciprocal titres in the cross-neutralisation assay (24). Due to the extensive cross-

neutralisation between phylogroup I species and novel lyssaviruses, cSN-KBLV and cSN-TWBLV, the location of these antigens on the map is fixed by multiple measurements to other antigens/antisera. Consequently, the resolution of the antigenic maps can be greater than the mFAVN assay resolution (435). On the antigenic map, cSN-KBLV was closest to cSN, ARAV, IRKV and EBLV-2 with an antigenic distance of 1.00 AU, 1.21 AU, 1.45 AU, and 1.65 AU respectively (Figure 4.7).

It has been previously suggested that the genetic difference in the G protein ectodomain correlates to neutralising antibody titre of lyssavirus specific sera (24). In terms of G protein amino acid sequence identities, KBLV G is most closely related to the G proteins of EBLV-2 (AGG81486), KHUV (YP_009094330), ARAV (YP_007641395), BBLV (AMR44685) and EBLV-1 (AAX62854) with identities of 89.12 %, 87.26 %, 83.84 %, 83.02 % and 79.39 %, respectively.

Whilst this does not match the antigenic data completely, it shows a better correlation than the N protein genetic data published by other workers, including Nokireki (19) and full-genome data by Calvelage (209). Whilst EBLV-1 specific sera was most able to neutralise cSN-KBLV, being more potent than sera raised against EBLV-2, BBLV and KHUV, this phenomenon was not visually translated in the antigenic maps, with EBLV-1 showing an antigenic distance of 2.68 AU from cSN-KBLV.

The amino acid sequence identities of TWBLV G protein and other lyssaviruses determined that EBLV-1 (AAX62856), EBLV-2 (AGG81481), KBLV (LR994545), ARAV (YP_007641395), and IRKV (YP_007641400) were the most closely related to TWBLV G with identities of 74.65 %, 72.28 %, 71.67 %, 71.32 %, and 70.61 %, correlating with the data published by Hu et al., 2018. This also roughly correlates to the cross-neutralisation assays (Figure 4.6) as EBLV-1-specific sera showed the highest

titre of neutralising antibodies against cSN-TWBLV, and ARAV-specific sera showed the second highest titre of neutralising antibodies. However, RABV-specific sera showed the third highest titre of neutralising antibodies and despite high sequence identity, EBLV-2 specific sera did not neutralise cSN-TWBLV above the 0.5 IU/ml cut off. However, as reported in chapter 3, these genetic data support the concept that there is not always a correlation to the antigenic data.

Antigenic cartography also showed similar results and cSN-TWBLV was positioned closest to ABLV, cSN, cSN-KBLV, EBLV-1, and IRKV with antigenic distances of 1.12 AU, 1.58 AU, 1.59 AU, 1.68 AU, and 1.85 AU, respectively (Figure 4.7). With the exception of ABLV and cSN, cSN-TWBLV positions closest to cSN-KBLV, EBLV-1, and IRKV and these viruses are closely related to TWBLV based on amino acid percentage identity.

Interestingly, cSN was antigenically distinct from RABV which conflicts with the findings of previous a study (93). However, a single wild type RABV was used in this study (RV437) and further assessment against a panel of RABVs would be needed to reliably infer antigenic differences between KBLV, TWBLV, cSN, and circulating street RABV strains.

Due to the close antigenic and genetic relationship of EBLV-2 and ARAV to KBLV, and EBLV-1 and IRKV to TWBLV, it was predicted that existing rabies vaccines would be able to afford protection against these viruses (343). Previously it was reported that rabies vaccines protect against BBLV *in vivo* and an antibody titre of ≥ 10 IU/ml was required for protection. For EBLV-1 and EBLV-2, *in vitro* analyses have suggested that titres ≥ 4.5 IU/ml are required for neutralisation (33, 385). Additionally, sera from human vaccinees has been shown to exhibit neutralisation activity against a

KBLV-G pseudotyped RABV particle, 1.8 fold lower neutralisation activity against CVS (209).

In the present study, *in vitro* neutralisation assays demonstrated that an antibody titre of 1.0 IU/ml of OIE sera or 2.5 IU/ml of WHO sera was sufficient for neutralisation of cSN-KBLV and cSN-TWBLV above the serological cut off (Figure 4.5). In comparison to CVS, OIE standard sera showed 1.1 fold lower neutralisation activity against cSN-KBLV and cSN-TWBLV. The difference in the neutralising antibody titres against cSN, cSN-KBLV, and cSN-TWBLV confirms that G is the dominant target for neutralising antibodies. These values, however, predict the conservative threshold for which *in vivo* protection against either cSN-KBLV or cSN-TWBLV is likely

Indeed, the *in vivo* vaccination-challenge experiments revealed that VeroRab, a commercially available rabies vaccine, afforded almost complete protection against intracranial challenge of cSN-KBLV (Figure 4.10A). One vaccinated mouse succumbed to infection at day 13 but interestingly demonstrated the lowest post-vaccination antibody response as assessed by FAVN at 0.87 IU/ml. Whilst above the cut off 0.5 IU/ml value, the nature of the ‘severe’ virus challenge through the introduction of virus *ic* may have been too invasive to prevent productive infection in this single animal. Regardless, with this sample size, it is speculated that for protection against KBLV, a higher neutralising antibody titre may be needed than that required to give complete protection against RABV in this *in vivo* model, in which, all mice with antibody titres above 1.5 IU/ml survived *ic* challenge (33, 115, 385). Future work with larger sample sizes would need to be undertaken to generate conclusive evidence-based data.

In contrast, mock vaccinated mice challenged with cSN-TWBLV did not succumb to infection. Due to the *in vitro* growth kinetics of this virus and the post-experiment

serology neutralisation data, it could be hypothesised that cSN-TWBLV did not grow sufficiently *in vivo* to produce a fatal infection or is more immunogenic and consequently apathogenic.

Apathogenicity *in vivo* could be a result of the codon-optimisation of the TWBLV G. Previous studies have shown that codon-optimised/codon de-optimised lyssavirus G genes have reduced pathogenicity *in vivo* (478, 479). Codon bias occurs in all organisms, resulting in the use of one or two synonymous codons during translation. Therefore, changing codons or codon-pair usage can alter gene expression within these organisms or specific cell lines (480).

Viruses containing the codon-optimised G genes has reported to induce increased apoptosis and result in the recruitment of more inflammatory cells in the brain (479). This resulted in reduced pathogenicity when compared with the same virus without a codon optimised G gene. Additionally, in a second study, it was reported that codon optimisation and codon de-optimisation of the G gene resulted in less pathogenic viruses than the wildtype virus. As a result, it was concluded that the expression level of the G gene had an impact on pathogenicity but is not necessarily the sole factor that determines pathogenicity (478). Finally, the effect of codon de-optimisation of the M gene was investigated and it was determined that de-optimisation led to the attenuation of M protein expression and consequently decreased virus replication in the early stages of infection (480). *In vitro*, codon de-optimisation of the M gene increased G protein expression and induced stronger apoptosis of mouse neuroblastoma (NA) cells.

In this study, codon de-optimisation, paired with the observation that recombinant viruses traditionally show a decreased viral fitness than wildtype viruses, could form the hypothesis that the combination of these factors has resulted in reduced growth and

decreased pathogenicity of cSN-TWBLV. However, without access to the live virus isolate, this remains a supposition and needs to be determined in future studies.

In an attempt to partially determine the cause of this phenomenon, two more constructs were cloned and assessed. The non-codon optimised G genes from both TWBLV 2017 and TWBLV 2016 isolates were synthesised and inserted in place of the cSN RABV G gene as described in section 4.2. These clones were then rescued as live virus as described in section 4.3. Following the calculation of the viral titres of each of the rescued viruses, growth kinetics could be determined *in vitro*. Multiple step growth curves using a MOI of 0.01 were then performed with cSN, the original codon optimised cSN-TWBLV, and the new clones, cSN-TWBLV2016 and cSN-TWBLV2017, in BHK cells (Figure 4.15).

By 24 hpi, all viruses were detected, however cSN, cSN-TWBLV2016 and cSN-TWBLV2017 were all detected 12 hours earlier. At 96 hpi, cSN-TWBLV reached a viral titre of 1.57×10^3 ffu/ml, whereas cSN-TWBLV2016, cSN-TWBLV2017, and cSN grew to a titre of 1.05×10^5 ffu/ml, 1.67×10^5 ffu/ml, and 5.83×10^6 ffu/ml, respectively. As seen previously in section 4.4, cSN grew to the highest peak titre at 96 hpi and cSN-TWBLV grew to the lowest titre, with a peak titre of 2.33×10^3 ffu/ml at 120 hpi. At 144 hpi, there was a significant difference between the endpoint titres of the codon optimised cSN-TWBLV and the two non codon-optimised isolates, cSN-TWBLV2016 ($P=0.006$) and cSN-TWBLV2017 ($P<0.001$).

At each time point, the non codon-optimised recombinant viruses showed a significant increase in viral fitness than the codon optimised cSN-TWBLV. However, further *in vivo* studies are required to determine the full effect of codon optimisation on pathogenicity.

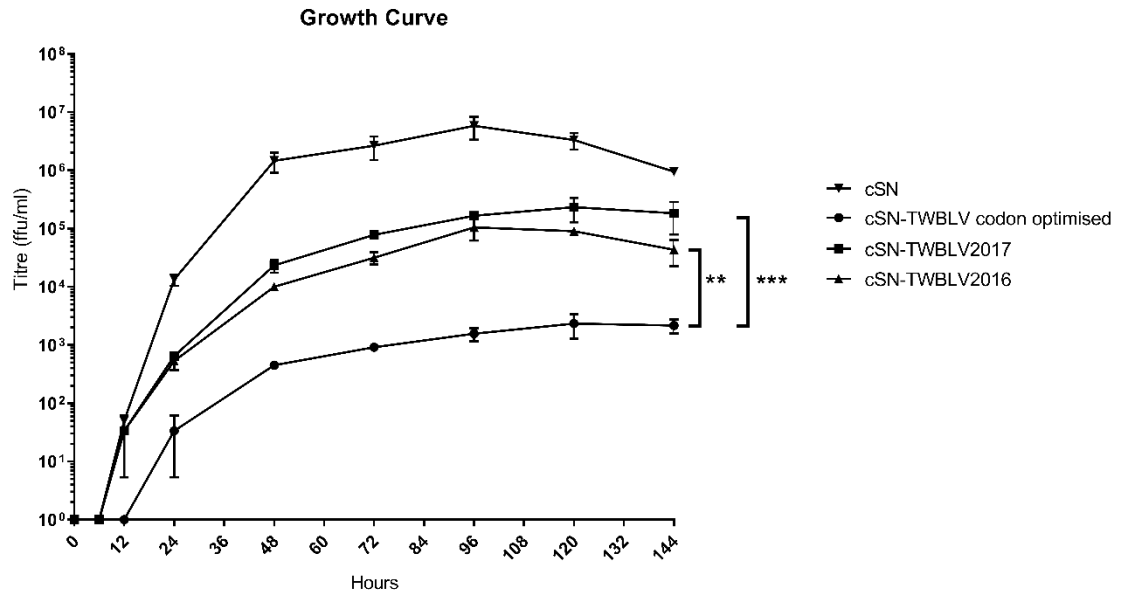


Figure 4.15: Growth kinetics of recombinant lyssaviruses; the original codon optimised cSN-TWBLV, cSN-TWVLV 2017 isolate, cSN-TWBLV 2016 isolate and the vaccine backbone, cSN, *in vitro*. For each virus, cells were infected with an MOI of 0.01 to produce a multiple step growth curve. Asterisks indicate significant differences between the groups calculated using the Kruskal-Wallis test with Dunn's multiple comparisons (***, $P < 0.001$; **, $P < 0.01$).

Following the *in vivo* experiments in this study, the analyses of samples taken by necropsy revealed that a lyssavirus-specific antigen could not be detected in the brains of the cSN-TWBLV infected mice by using FAT and IHC methods (Figure 4.11 and 4.12). However, viral RNA was detected in the cSN-TWBLV mock vaccinated mice by SYBR real time RT-PCR (Table 4.1) indicating virus infection and subsequent clearance. In the cSN-TWBLV vaccinated mice, neither viral antigen nor viral RNA was detected in the brains of mice. Previous studies have shown that, post-infection, viral RNA levels are inversely proportional to virus neutralising antibodies. In one study, mice were intranasally (in) inoculated with an apathogenic RABV strain, HEP-Flury, or pathogenic RABV strain, CVS-11 and subsequently tested at multiple time points, for viral RNA, spanning 25 days. Three mice from each group were euthanised at each time point, and the quantity of viral RNA was measured by RT-PCR. The results from this study showed that viral RNA was readily detected in the brain tissue of HEP-Flury and CVS-11 infected mice at 4 dpi and had significantly increased by 10 dpi.

All CVS-11 infected mice subsequently succumbed to clinical disease whereas HEP-Flury infected mice did not. In the brain tissue of the HEP-Flury infected mice, viral RNA had significantly decreased by 18 dpi, whilst virus neutralising antibodies had increased and continued to increase until the end of the experiment. The CVS-11 infected mice showed no virus neutralising antibodies. It was determined that the attenuated HEP-Flury strain replicated more slowly, triggered the innate immunity earlier and achieved sufficient adaptive immunity (372).

A second study assessed the viral RNA levels of CVS-F3 in 8 mouse strains. By 13 dpi, all viral RNA had been cleared in from the brains in 75% of the mouse strains tested, and by 37 dpi, all viral DNA had been cleared from the remaining 25%. This study also showed that as viral RNA levels decreased, VNA levels increased (296). Certainly, the

mock vaccinated cSN-TWBLV infected mice that survived infection showed high levels of neutralising antibodies at the end of the experiment. Additionally, the cSN-TWBLV vaccinated mouse group had strong neutralising antibodies post-vaccination but pre-challenge which would have led to earlier viral clearance than the mock vaccinated control. This is likely responsible for the differences observed in the real time RT-PCR results as viral RNA in the cSN-TWBLV vaccinated group would have been cleared by 28 dpi. The serological assessment in this study also indicated that the cSN-TWBLV vaccinated group showed no increase in neutralising antibody titres against the challenge virus versus the vaccine virus, whereas the cSN-TWBLV mock vaccinated group showed significantly higher neutralising antibody titres against the challenge virus versus the vaccine virus, indicating lyssavirus infection and subsequent clearance in the mock vaccinated mice.

In the case of cSN-KBLV, the vaccinated mice that survived to the end of the experiment (22 days, n=11/12) were negative for lyssavirus antigen in the brain by the gold standard FAT method, but very low levels of viral RNA copies could be detected in the brain using SYBR real time RT-PCR. The lethal outcome of infection with wildtype RABV is usually a result of various mechanisms to evade and delay the host immune response (265). Due to the severe nature of an ic challenge, it was hypothesised that circulating vaccine-induced antibodies delayed escalation of infection and subsequent neuronal damage, allowing sufficient time for the recruitment of immune effector cells and complete infiltration of the CNS for viral clearance.

As a result, it is predicted that the RNA detected is remnant non-infectious viral RNA from this event, a phenomenon reported previously (481). Viral RNA levels were the lowest in this group (with the exception of the vaccinated cSN-TWBLV mice that were negative) and serological assessment showed no significant difference in serological

titre against the challenge virus and vaccine virus. The mock vaccinated mice in this group succumbed to infection, were positive for lyssavirus antigen via FAT and IHC, and had the highest levels of viral RNA in the brain. These findings are consistent with the hypothesis that the vaccinated mice would have cleared the infection earlier than the mock vaccinated controls, leading to increased depletion of viral RNA levels in the brain by the end of the experiment.

In conclusion, whilst the wildtype KBLV is yet to be isolated, the data presented has demonstrated that current rabies vaccines do afford protection against this lyssavirus in mice. As a result, it can be extrapolated that vaccination with approved WHO rabies vaccines will probably confer protective immunity in human subjects. Notably, a neutralising antibody titre of 1.5 IU/ml or above was required. Genetically, KBLV G is closely related to EBLV-2, BBLV, KHUV, and EBLV-1. Cross-neutralisation assays revealed that EBLV-1, BBLV and EBLV-2 lyssavirus-specific sera showed the highest neutralising antibodies against cSN-KBLV and antigenic map data revealed that cSN-KBLV clusters with cSN, ARAV, EBLV-2, and IRKV.

In contrast, the cSN-TWBLV construct was apathogenic in the *in vivo* experiment conducted in these studies. In this sense, it is still possible that the novel parent virus has increased viral fitness within cell culture and increased pathogenicity *in vivo*.

Despite this, *in vitro* experiments indicated vaccine protection with a minimum of 1 IU/ml is required for neutralisation. Genetically, TWBLV G is closely related to EBLV-1, EBLV-2, KBLV, ARAV, and IRKV. Cross-neutralisation assays revealed that EBLV-1, ARAV and RABV lyssavirus-specific sera showed the highest neutralising antibodies against cSN-TWBLV and antigenic map data revealed that cSN-TWBLV clusters with ABLV, cSN, cSN-KBLV, EBLV-1, and IRKV.

Chapter 5: Construction and characterisation of recombinant viruses expressing chimeric glycoproteins

5.1. Introduction

The data presented in Chapter 3 highlighted the minimal inter-phylogroup cross-neutralisation between all lyssaviruses and further antigenic analyses determined that phylogroup II and III lyssaviruses were antigenically distant to RABV and phylogroup I. However, the assessment of serological cross-neutralisation across the entire genus highlighted the minimum antigenic requirements for pan-lyssavirus neutralisation. It was determined that a minimum of five G proteins from the following lyssavirus species would need to be included: RABV, LBV-D, IKOV, LLEBV, and WCBV. For broader cross-neutralisation and likely cross-protection, more antigens from phylogroup I (e.g. DUVV) and II (e.g. SHIBV) would be preferred, however, for the purposes of this study, the minimum number of G proteins were assessed. This is due to the caveats, explored in this chapter, to using more antigens in a single vaccine formulation.

In recent decades, the diversity of known lyssaviruses has expanded and spillover events have been continually documented (134, 135). Since 2000, the genus has increased from eight fully characterised species to 17 fully characterised species and two tentative species (3, 19, 20). Of the 11 novel lyssavirus species, five represent divergent lyssaviruses and belong to either phylogroup II or III, or as suggested in chapter 3, phylogroups IV and V. Since 2017, highly divergent LLEBV has been detected in a second European country and a novel, highly divergent lyssavirus, tentatively assigned the name MBLV, was detected in two bats in South Africa (20, 208). In addition, notable spillover events included: the detection of IRKV in a dog in China; the detection of highly divergent WCBV in a cat in Italy; and a confirmed human rabies case from infection with EBLV-1 in France (182, 214). Certainly, the

development of a pan-lyssavirus vaccine may have significant utility in humans if or when divergent lyssavirus spillover events occur in the future.

Consequently, the primary focus of this study was to assess the antigenicity of inactivated virions of recombinant viruses; as proof of concept for future pan-lyssavirus vaccine formulations. As mentioned in Chapter 4, the G protein is the sole protein on the lyssavirus surface and is therefore the sole target for virus neutralising antibodies. As a result, the focus for this chapter was G protein engineering, such that a single G protein contained immunological epitopes representative of a range of lyssaviruses across the genus.

Previously, one method for generating chimeric G proteins was the ‘epitope-based’ approach where antigenic sites were swapped and antigenicity of the site-swap mutants assessed (38, 91). Whilst this revealed immunodominant epitopes for LBV, the assessment of the immunological potential for use as a cross-neutralising vaccine was inconclusive (38). This is possibly due to the fact that the antigenic sites for non-RABV lyssaviruses are undefined and swapping these short regions may exclude other important sites.

In this chapter, three approaches were assessed for the design and generation of chimeric recombinant lyssavirus G proteins. The first approach used was the well-established ‘hinge-based’ approach as described previously (482). This approach divides the G protein into two parts separated by a flexible hinge region, whereby, the N-terminus sequence originates from one lyssavirus species and the C-terminus sequence originates from a different lyssavirus species. The second approach used was the ‘mosaic’ approach as described previously (436). This approach utilises an *in silico* antigen designer tool, as described in section 2.10.11, to create a mosaic G protein

representative of the wildtype input proteins. The third and final approach used was a novel approach utilising the recently published MOKV G protein crystal structure (27). For the purposes of this study, this approach was designated the ‘structure-based’ approach and involved designing chimeras based on the G protein structure. During the course of this study, a similar approach was published, whereby the vesicular stomatitis virus (VSV) pre-fusion G was used as a structural model for the basis of chimeric G protein engineering (483).

5.2. Chimeric Glycoprotein rationale

5.2.1. Serological assessment of sera directed against a formulation of three BPL-inactivated viruses

There are a variety of ways to broaden the immune response to a vaccine, and hence its ability to induce cross-protective antibodies, including the simplistic approach to inactivate all viruses required for neutralisation across the genus and combine into a single vaccine. One predicted caveat of this approach was that one lyssavirus G protein may be more immunodominant than others. To test this hypothesis, all phylogroup III lyssaviruses were propagated and titrated. The virus stock of IKOV had a titre of 3.9×10^4 ffu/ml, the stock of LLEBV had a titre of 3.25×10^4 ffu/ml, and the stock of WCBV had a titre of 1.4×10^4 ffu/ml. Following this, IKOV and LLEBV were diluted to the same concentration as WCBV and the virus stocks were combined and inactivated. Specific serum for this inactivated virus mix was then generated as described in section 2.5. To test the immunogenicity of the IKOV/LLEBV/WCBV-specific sera, an mFAVN was performed against IKOV, LLEBV, and WCBV (Figure 5.1).

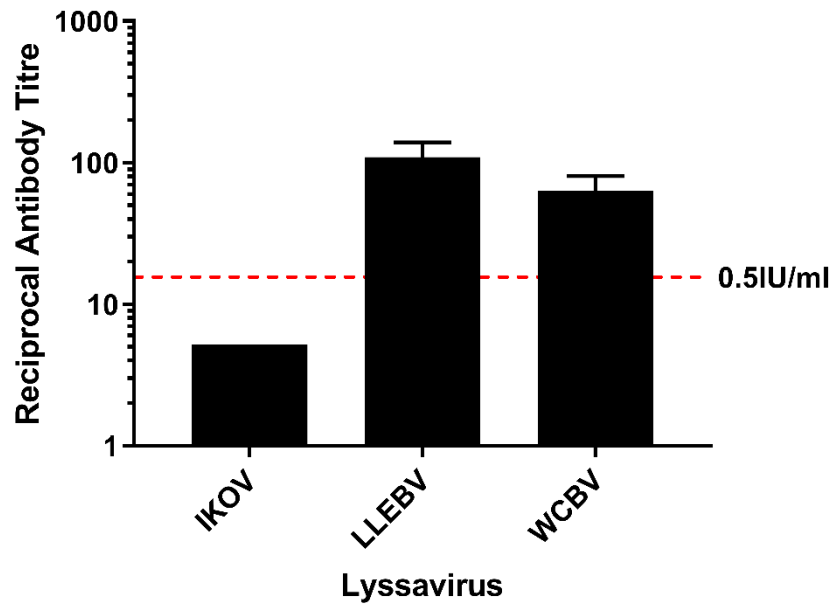


Figure 5.1: Modified FAVN to show the cross-neutralisation capability of IKOV/LLEBV/WCBV-specific sera against IKOV, LLEBV, WCBV viruses. The test was performed in triplicate and the mean of the results displayed on a logarithmic scale. The 0.5 IU ml⁻¹ neutralisation cut off is dictated by the OIE sera against CVS (indicated by the dashed line).

The IKOV/LLEBV/WCBV-specific sera exhibited the highest titre of neutralising antibodies against LLEBV, followed by WCBV. However, the sera did not exhibit a titre of neutralising antibodies against IKOV above 0.5 IU/ml. A future direction for this work would be to modify the expression of this antigen within the formulation to improve the immunological response against IKOV. Further, vaccines for human use are based on whole inactivated RABV particles where the RABV strains are ‘fixed’ and attenuated for safety purposes (8, 484, 485). For this reason, this approach was not considered for the generation of a cross-protective antigen in this study.

5.2.2. Vaccine consisting of a single inactivated virus expressing multiple glycoproteins

Another approach is to create a single vaccine construct with multiple glycoproteins from different lyssavirus species. Foreign viral glycoproteins have been added to a RABV backbone and assessed for expression (486-489). However, the stability of these constructs expressing multiple glycoproteins is yet to be determined and the cross-neutralisation potential across the lyssavirus genus has not been rigorously tested.

To test this approach, a live recombinant virus, ERA-4G, encoding rabies glycoprotein and three heterologous glycoproteins from other lyssavirus species was assessed *in vitro*. The construct in the form of DNA plasmid and live virus were kindly gifted by Dr Xianfu Wu from the Centers of Disease Control and Prevention (CDC). The genome of ERA-4G virus had four glycoprotein genes (LBV-B, MOKV, RABV, WCBV) (Figure 5.2).



Figure 5.2: Genome organisation of ERA rabies virus with four glycoprotein genes (ERA-4G). The LBV G gene was cloned between N and P genes, the MOKV G gene was cloned between P and M genes and the WCBV G gene was cloned between the psi region after the RABV G gene and before the L gene.

Consequently, ERA-4G-specific sera was generated, as described in section 2.5, and tested using a mFAVN against ERA-4G, RABV, LBV-D, MOKV, and WCBV (Figure 5.3).

The ERA-4G-specific sera showed the highest titre of neutralising antibodies against ERA-4G, followed by RABV. However, the same sera did not exhibit a titre of neutralising antibodies against LBV-B, MOKV, and WCBV. Certainly, preliminary data suggests that when multiple glycoproteins are combined in a single vector, the virus loses expression of the heterologous glycoproteins. This may be because these glycoproteins confer a disadvantage to the virus and propagation in cell culture applies a selective pressure resulting in the loss of expression of the glycoprotein(s) conferring slower growth (483). A future direction for this work would be to assess the expression of each glycoprotein after serial passage in cell culture. As a result, only constructs expressing a single glycoprotein were considered when designing a pan-lyssavirus vaccine.

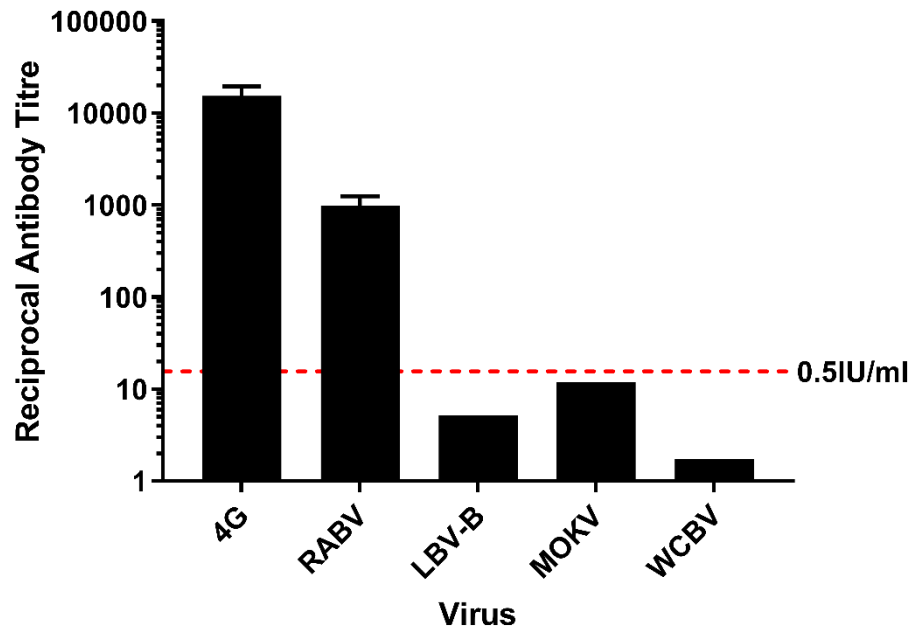


Figure 5.3: Modified FAVN to show the cross-neutralisation capability of ERA-4G-specific sera against ERA-4G, RABV, LBV-B, MOKV, and WCBV virus. The test was performed in triplicate and the mean of the results displayed on a logarithmic scale. The 0.5 IU ml⁻¹ neutralisation cut off is dictated by the OIE sera against CVS (indicated by the dashed line).

5.3. *In silico* design of Chimeric Lyssavirus Glycoproteins

5.3.1. Hinge-based design

Previously, it has been determined that the region (amino acids 253 to 275) is less structurally constrained than other areas of the lyssavirus G protein, however, this region contains the non-conformational epitope IV located at amino acids 263-264 (26, 490).

To conserve the IV epitope and avoid the hinge region of the G protein, the chimeric G proteins containing the coding sequence from two different lyssaviruses were designed using a previous method (482). The accession numbers for each lyssavirus G gene are described in Table 5.1.

For the chimeric G proteins where either the N-terminus or C-terminus originated from a phylogroup I or II virus (RABV/LBV-D G and LBV-D/RABV G), the coding sequence at the N-terminus was defined as amino acids 1 to 257, and the coding sequence at the C-terminus was defined as amino acids 258 to 504/506 (Figure 5.4). For the chimeric G proteins where the N-terminus originated from a phylogroup III virus and the C-terminus originated from a different phylogroup III virus (IKOV/LLEBV G, IKOV/WCBV G, LLEBV/IKOV G, LLEBV/WCBV G, WCBV/IKOV G, and WCBV/LLEBV G), the coding sequence at the N-terminus was defined as amino acids 1 to 255, and the coding sequence at the C-terminus was defined as amino acids 256 to 506/507 (Figure 5.4) (Appendix 3).

Table 5.1: Lyssavirus Glycoprotein sequences used for chimeric glycoprotein design.

Lyssavirus	Year	Genbank accession code
RABV (ERA)	-	GQ406342
LBV-D	2008	GU170202
IKOV	2009	JX193798
LLEBV	2011	NC031955
WCBV	2002	EF614258

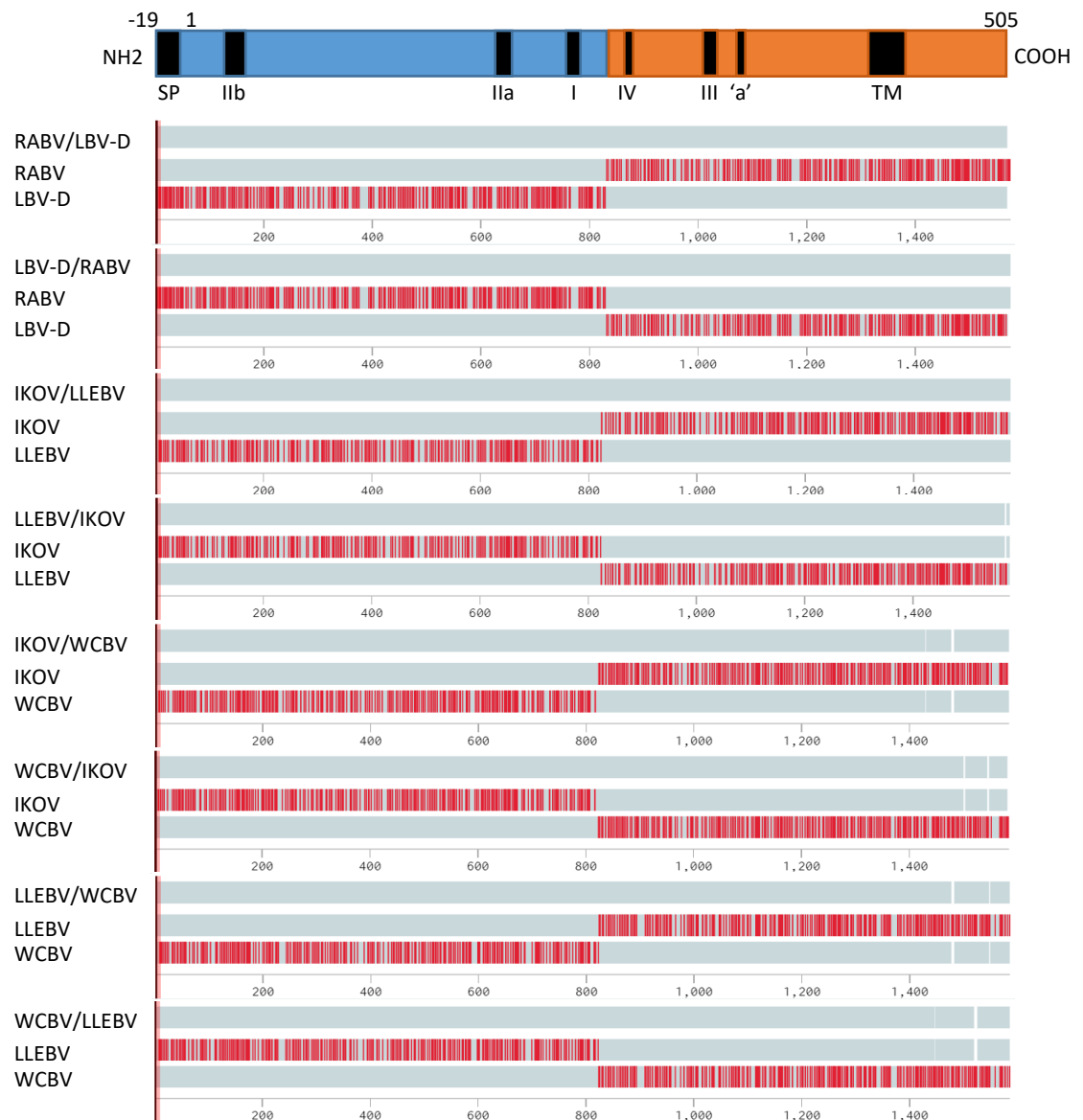


Figure 5.4: Linear schematic of a representative glycoprotein monomers designed using the hinge-based approach and multiple alignments of chimeric glycoprotein nucleotide sequences with the wildtype glycoprotein nucleotide sequences. On the glycoprotein schematic, numbers give the positions of amino acid residues and proposed domains originating from different lyssaviruses are noted (N-terminus sequence in blue and C-terminus is orange), as are the antigenic sites, signal peptide, and transmembrane domain as they are known to exist on the RABV G. Under the glycoprotein schematic are the multiple alignments of the chimeric glycoproteins. The wildtype glycoprotein sequences that constitute the chimeric glycoprotein sequences are aligned to the chimeric glycoproteins where grey indicates matching nucleotides and red indicates mismatched nucleotides.

5.3.2. Mosaic-based design

The Mosaic Vaccine Tool Suite was used to produce mosaic recombinant lyssavirus G proteins as previously described (436). Using a genetic algorithm, the mosaic G proteins were assembled *in silico* from fragments of the natural proteins. This software not only aims to prevent the formation of new epitopes but also chooses the most frequent epitopes and combines them to form a recombinant protein representative of the natural protein.

For each of the mosaics, the cocktail size was set to one so the output would consist of a single protein. To obtain a protein that had the fewest infrequently occurring epitopes, the rare threshold was initially set to 3.

This meant that the algorithm required there be at least three copies of a given constituent peptide (k-mer) in order for the k-mer to be considered for optimisation. However, due to the diversity and low number of lyssavirus G proteins used in the dataset, the algorithm stalled. Consequently, the rare threshold was set to one, meaning that every k-mer was considered in optimisation. As previously mentioned in section 2.10.11., the k-mer length was set to 12 amino acids in an attempt to encapsulate the length of the antigenic sites, the conserved regions contributing to the G protein structure, and to also match the length of natural T-helper cell epitopes. It was hypothesised that this method would generate a functional chimeric G protein that, when cloned into a rabies virus backbone and used as a virus vaccine strain, would induce a strong cross-neutralising immune response.

The G protein sequences included as the wildtype input proteins were the same sequences described for the hinge-based design in Table 5.1. A mosaic representative of LBV-D and RABV was generated and termed Mosaic 1 & 2; a mosaic representative of IKOV, LLEBV, and WCBV was generated and termed Mosaic 3; and a mosaic representative of RABV, LBV-D, IKOV, LLEBV, and WCBV was generated and termed Mosaic All (Figure 5.5) (Appendix 3).

The Mosaic 2 G protein, however, was designed slightly differently. All available G protein sequences for phylogroup II lyssaviruses were obtained from the National Center for Biotechnology Information (NCBI) (Appendix 3). Complete G protein sequences for the LBV viruses (16 sequences) and MOKV viruses (16 sequences) were submitted to the Mosaic Vaccine Tool Suite. Using a rare threshold of 3, and a cocktail size of 1, two G protein sequences were obtained: one representative of the LBVs and one representative of MOKV. This process was not performed for SHIBV as it exists as a single detection. Following this, the two sequences generated for LBV and MOKV were submitted to the Mosaic Vaccine Tool Suite for a second time alongside the SHIBV G protein sequence to generate the Mosaic 2 G protein (Figure 5.5) (Appendix 3).

5.3.3. Structure-based design

Chimeric G genes using the RABV and LBV-D sequences from NCBI (accession numbers defined in Table 5.1) were also designed using a structure-based approach. Using the structural modelling program, SWISS-MODEL, structural models of LBV-D G protein and RABV G protein were generated by modelling their amino acid sequences onto the closest related G protein structure available on the Protein Data Bank (PDB); the MOKV post-fusion G (PDB ID: 6tmr) (27, 431, 491).

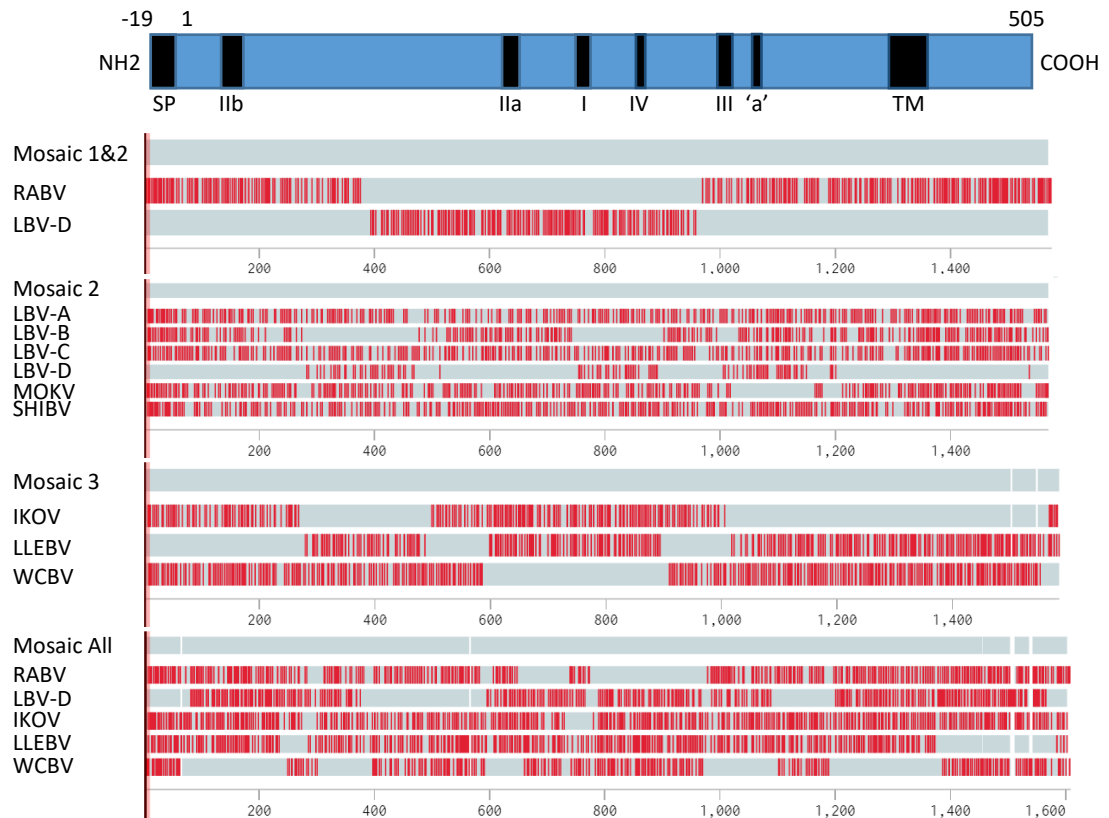


Figure 5.5: Linear schematic of a representative glycoprotein monomer designed using the mosaic-based approach and multiple alignments of chimeric glycoprotein nucleotide sequences with the wildtype glycoprotein nucleotide sequences. On the glycoprotein schematic, numbers give the positions of amino acid residues and the antigenic sites, signal peptide, and transmembrane domain are noted as before. Under the glycoprotein schematic are the multiple alignments of the chimeric glycoproteins. The wildtype glycoprotein sequences that constitute the chimeric glycoprotein sequences are aligned to the chimeric glycoproteins where grey indicates matching nucleotides and red indicates mismatched nucleotides.

However, during the course of this study, the structure of RABV G was also solved at both acidic and basic pH (28). With new information available, well known features of the RABV G protein ectodomain were highlighted on both RABV and LBV-D models. Extensive studies have mapped five antigenic sites for RABV (described in section 1.1.2.4.1) as well as the positions of structural elements such as putative glycosylation consensus sequences and highly conserved cysteine residues (492). In both LBV-D and RABV models, the antigenic sites, cysteine residues, and glycosylation motifs were mapped and considered when designing the chimeric G proteins (Figure 5.6).

In addition to the well-established structural elements, the structural modelling of both the LBV-D and RABV G protein monomers revealed three subdomains (Figure 5.7). Excluding the signal peptide, the subdomain closest to the N-terminus defined by amino acids 1-32, exhibited a small hairpin conformation and was closely associated with the third subdomain defined by amino acids 262-401, located near the transmembrane domain. These two subdomains form the trimerisation/central domain of the G protein (27, 28). The second domain defined by amino acids 33-261, constitutes the fusion domain and the pleckstrin identity domain (27, 28). From this structural analysis, it was determined that the amino acid sequence for subdomain one and three would have to derive from the same lyssavirus species in order to conserve bonding interactions and promote optimal protein folding of these chimeric G proteins. To assume the post-fusion conformation, subdomains one and three move independently of subdomain two as segments (R1 to R5) refold when exposed to an acidic pH (27). Consequently, it was hypothesised that the amino acid sequence that constitutes subdomain two could derive from a different lyssavirus species to the amino acid sequences that constitute subdomain one and three. As a result, the chimeric G proteins designed were RABV/LBV-D/RABV and LBV-D/RABV/LBV-D where subdomain one was defined

as amino acids 1-32, subdomain two was defined as amino acids 33-261, and subdomain three, the transmembrane domain, and the cytoplasmic domain at the c-terminus were defined as amino acids 262-504/506 (Figure 5.7) (Appendix 3).

A further chimeric G protein, LBV-D/RABV/LBV-D/RABV was designed to include all putative glycosylation sites mapped for LBV-D and RABV and to ensure optimal interaction with the M protein of the RABV vector. Subdomain one was defined as amino acids 1-32 (LBV-D), subdomain two was defined as amino acids 33-261 (RABV), and subdomain three, the transmembrane domain, and a proportion of the cytoplasmic domain were defined as amino acids 262-464 (LBV-D), and the final portion of the G protein sequence at the C-terminus was defined as amino acids 465-506 (RABV). Using this approach, the chimeric G proteins should also have a balanced immunogenicity as antigenic sites I and II are derived from one lyssavirus species, and antigenic sites III, IV, and 'a' are derived from a different lyssavirus species. Certainly, a separate study published recently using the VSV pre-fusion G protein as the structural model, also described three subdomains as the 'clip', 'core', and 'flap' domains of the G protein, and designed chimeric G proteins using sequences derived from MOKV and RABV (483). This justifies the use of this structural method as two independent studies, this study and the study described, used similar methods and hypotheses when designing chimeric G proteins.



Figure 5.6: Structural models of lyssavirus glycoprotein ectodomain monomers. For the RABV model, antigenic sites have been coloured in magenta, putative glycosylation sites have been coloured blue and cysteine residues have been coloured green. For the LBV-D model, antigenic sites have been coloured in magenta, putative glycosylation sites have been coloured orange and cysteine residues have been coloured green.

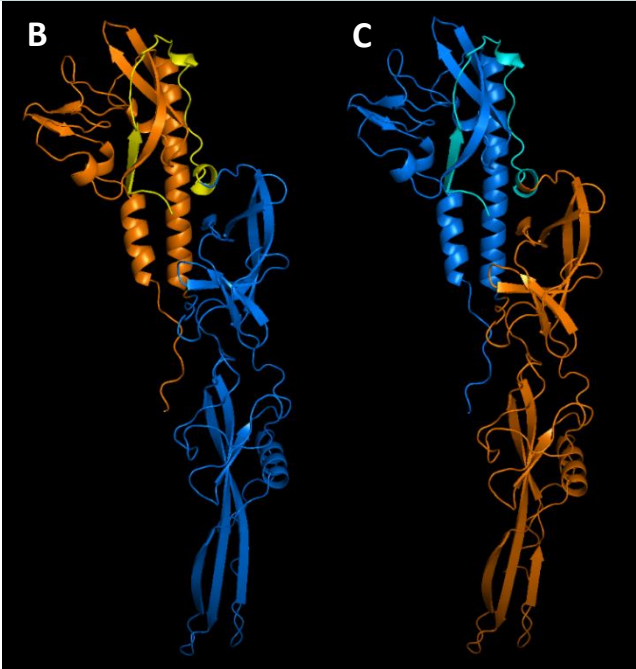
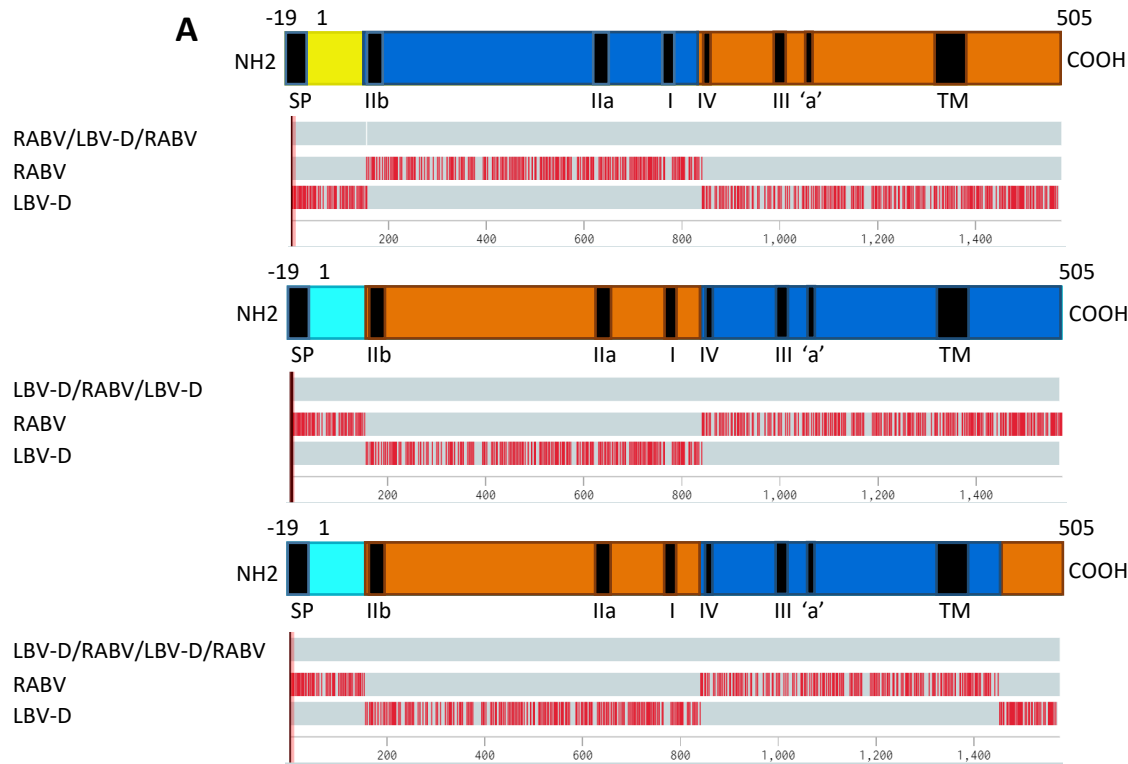


Figure 5.7: (A) Linear schematic of representative glycoprotein monomers designed using the structure-based approach with multiple alignments of chimeric glycoprotein nucleotide sequences with the wildtype glycoprotein nucleotide sequences. On the glycoprotein schematic, numbers give the positions of amino acid residues and the antigenic sites, signal peptide, and transmembrane domain are noted as before. Under the glycoprotein schematic are the multiple alignments of the chimeric glycoproteins. The wildtype glycoprotein sequences that constitute the chimeric glycoprotein sequences are aligned to the chimeric glycoproteins where grey indicates matching nucleotides and red indicates mismatched nucleotides. Structural models of these chimeric glycoprotein ectodomain monomers are also displayed where (B) is a model of RABV/LBV-D/RABV G and (C) is a model of LBV-D/RABV/LBV-D G and LBV-D/RABV/LBV-D/RABV G. On the glycoprotein linear schematics and the structural glycoprotein models, proposed structural domains are highlighted. For RABV/LBV-D/RABV G, subdomain 1 is coloured yellow, subdomain 2 is coloured blue and subdomain 3 is coloured orange. For LBV-D/RABV/LBV-D G and LBV-D/RABV/LBV-D/RABV G, subdomain 1 is coloured cyan, subdomain 2 is coloured orange, and subdomain 3 is coloured blue. The subdomains coloured yellow and orange derive their sequence from RABV G and the subdomains coloured cyan and blue derive their sequence from LBV-D.

5.4. Generation of Chimeric and Mosaic clones

5.4.1. Cloning into pcDNA3.1(+)

The chimeric G gene sequences were synthesised as DNA fragments (GeneArt, Thermo Fisher) and initially cloned into the vector, pcDNA3.1(+) for long term storage and pseudotype virus generation. The plasmid vector pcDNA3.1(+) was linearised and amplified by PCR as described in section 2.7.1. The chimeric G genes were synthesised with incorporated overhangs complementary to pcDNA3.1(+) to allow immediate assembly into the multiple cloning site of pcDNA3.1(+) and ligation using the Gibson assembly method, as previously described for KBLV G and TWBLV G in Chapter 4. Plasmid constructs were then grown in *E. coli* (DH5 α derivative cells; NEB), to generate larger stocks, as previously described in section 4.2 and 2.2.9.

5.4.2. Cloning into cSN

For insertion into cSN, the chimeric G gene ORFs were amplified with 20 bp overhangs directed at the 5' and 3' end of cSN using a PCR reaction (described in 2.2.2.2.) and the primers listed in Appendix 1. The cSN vector was linearised into two fragments to remove the RABV G sequence as described in section 2.8.1. The two cSN vector fragments and one of the G protein inserts with cSN complementary overhangs were assembled by Gibson Assembly to produce the recombinant plasmids containing a chimeric G (Appendix 2). The full length clones were transformed and grown in *E. coli* (DH5 α derivative cells; NEB), to generate larger stocks, as previously described in section 4.2 and 2.2.9. The sequence of each was determined by Sanger sequence analysis. In addition, restriction digestion of the plasmids was performed using restriction enzymes *NheI* and *MluI*, as described in section 2.2.12.2, to ensure the plasmids were of the correct size (Figure 5.8).

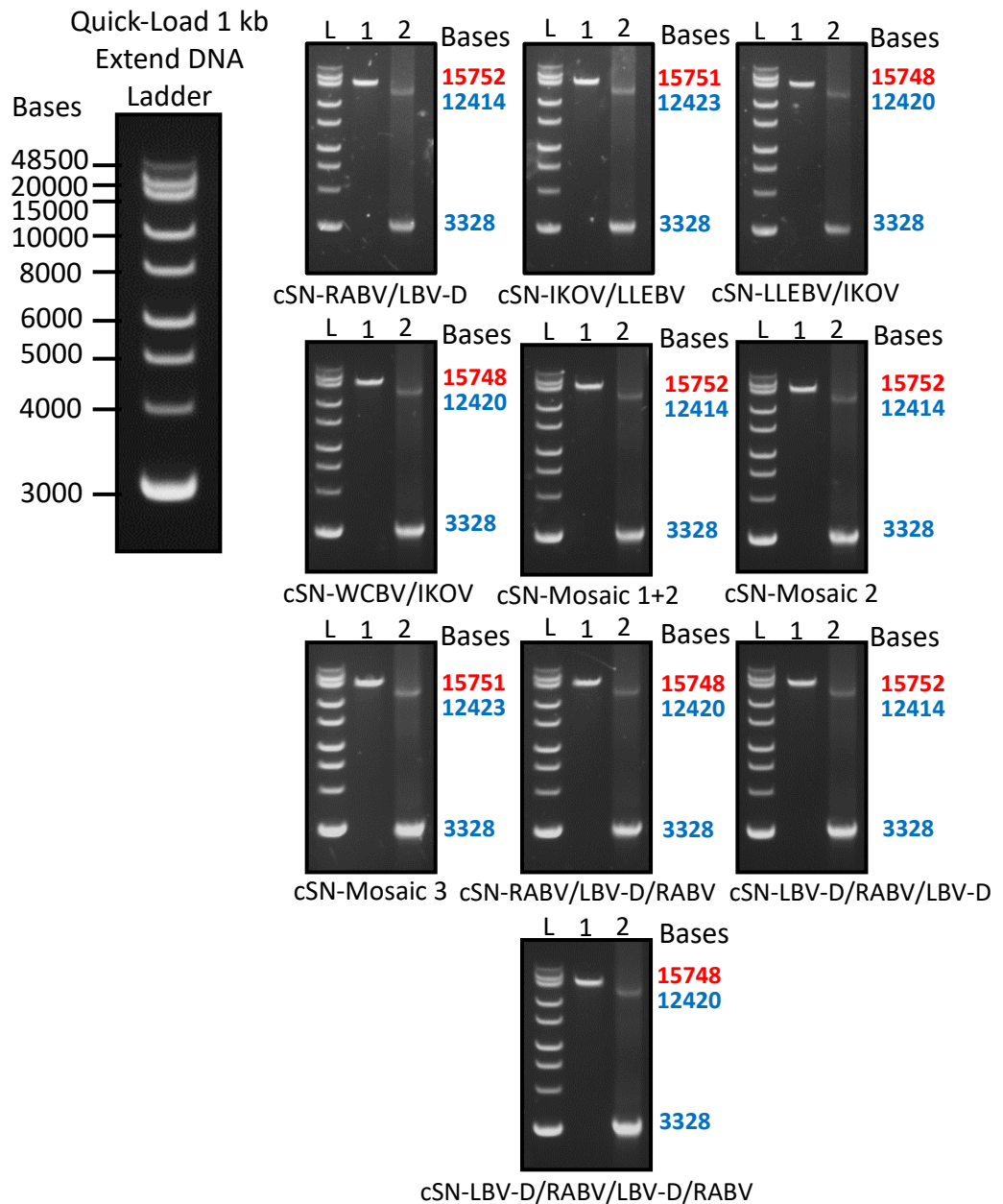


Figure 5.8: Restriction digestion of recombinant cSN plasmids. Digestion of the intact plasmids with *NheI*, to generate one full length fragment (Lane 1; red), and with *NheI* and *MluI* to generate two fragments (Lane 2; blue). The ladder is Quick-Load 1 kb Extend DNA ladder (NEB).

5.5. Generation of Pseudotype Viruses expressing Chimeric Glycoprotein

The adaption of pseudotype viruses to express lyssavirus G proteins was used in this study to assess the functionality of the engineered chimeric G proteins. Plasmids containing both the wildtype G and mutant chimeric G genes were constructed to compare the functionality of the wildtype and chimeric Gs through the generation and titration of lyssavirus pseudotypes. The lyssaviruses included on the wildtype G panel were RABV, LBV-D, IKOV, LLEBV, and WCBV. The harvested pseudotypes were titrated via a 5-fold dilution series to obtain a titre in relative light units per ml (RLU/ml). The results of this titration assay are detailed in Figure 5.9. The titres of the wildtype lyssavirus pseudotypes ranged from 10^8 to 10^{11} RLU/ml with WCBV exhibiting the highest titre and IKOV the lowest titre. These titres were in the range expected for a pseudotype virus expressing a functional G protein.

The titres of the chimeric lyssavirus pseudotypes using the hinge-based approach varied considerably. Four of the eight constructs failed to produce detectable pseudotype titres indicating that the chimeric G proteins were not functional.

The pseudotype expressing the LLEBV/IKOV G exhibited the highest titre at 7.8×10^7 RLU/ml, however the other three generated pseudotypes expressing RABV/LBV-D G, IKOV/LLEBV G, and WCBV/IKOV, exhibited low titres at 10^5 to 10^6 RLU/ml. The titres of the chimeric lyssavirus pseudotypes using the mosaic-based approach also varied considerably. Of the four constructs, three produced detectable pseudotype titres. The pseudotype virus expressing Mosaic 3 G exhibited the lowest titre at 1.1×10^6 RLU/ml, and the pseudotype virus expressing the Mosaic 2 G exhibited the highest titre at 6.3×10^8 RLU/ml.

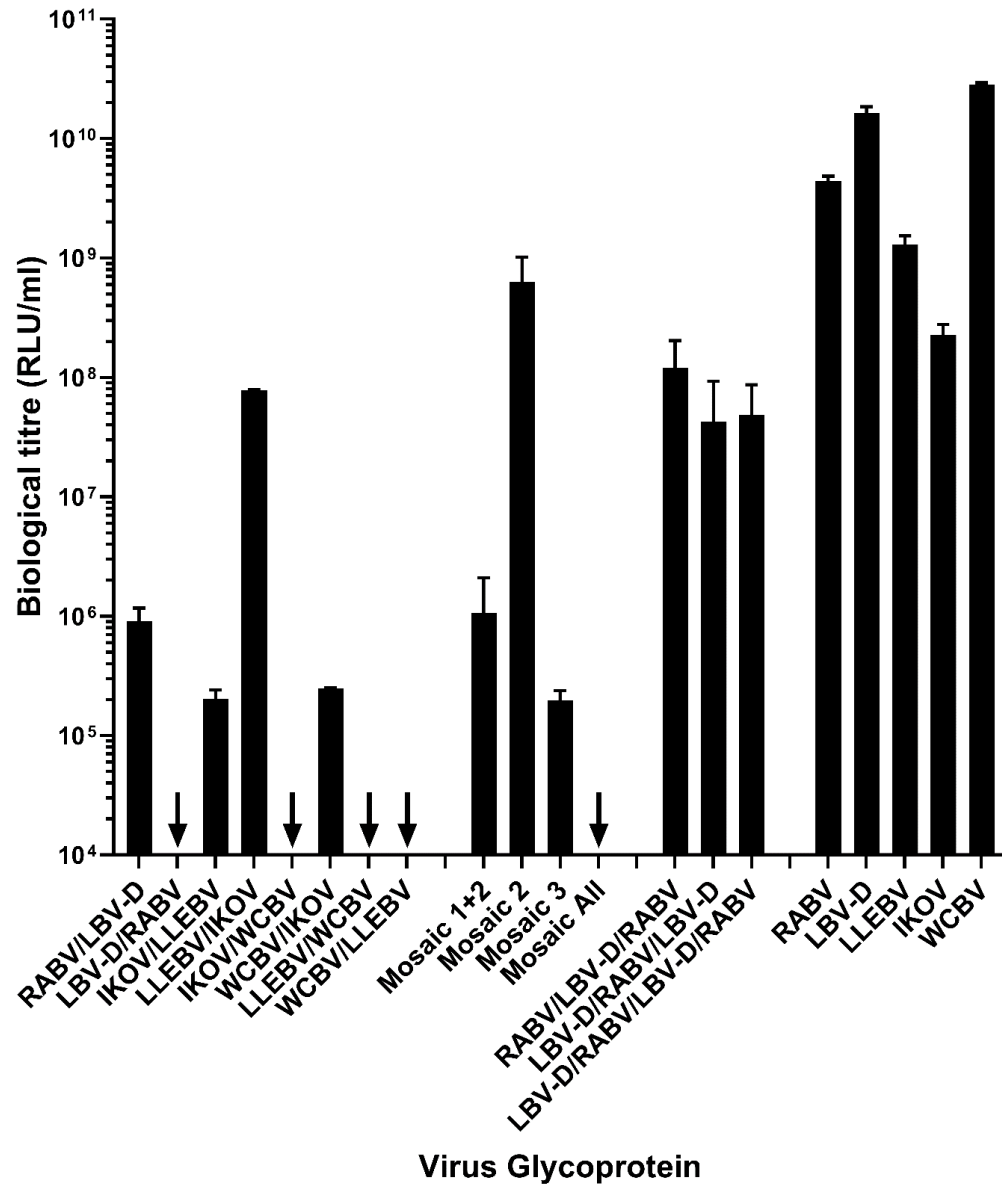


Figure 5.9: Viral titres for luciferase pseudotypes are given in RLU and the mean and standard deviation are displayed on a logarithmic scale. Titres reported are after deduction of the non-specific background luciferase activity.

The high titre of Mosaic 2 G gives the indication that the G protein is as functional as the wildtype Gs as the titre is not significantly different to the titres of the pseudotypes expressing IKOV G ($P= 0.817$) and LLEBV G ($P=0.466$) when the Brown-Forsythe and Welch's ANOVA test with Dunnett's T3 multiple comparisons test was used. The titres of the chimeric lyssavirus pseudotypes using the structure-based approach were the most consistent. The lowest titre was the pseudotype virus expressing LBV-D/RABV/LBV-D G at 4.2×10^7 RLU/ml and the highest titre was the pseudotype virus expressing RABV/LBV-D/RABV at 1.2×10^8 RLU/ml. These titres were not significantly different from the pseudotype expressing IKOV G ($P= 0.059$ and $P=0.783$, respectively) indicating that these chimeric G proteins could be functional.

5.6. Assessment of Live recombinant viruses expressing recombinant Glycoprotein

The reverse genetics technique was used to rescue the full length clones as live virus, as described for TWBLV and KBLV in section 4.3.

5.6.1. Virus Rescue and Titration

After the third passage, the only construct successfully rescued was cSN-Mosaic2 (Figure 5.10). Approximately 50% of the cells were positive for antigen whereas for cSN, 100% of the cells were positive for antigen. After five passages of the cells infected with cSN-Mosaic2, 100% of the cells were positive for antigen. Following this, the virus TCSN of cSN-Mosaic2 was harvested and RNA was extracted from the cell pellet. The RNA was used to generate cDNA which was used as the template in confirmatory PCRs. The resulting product was of the expected size, 1.5-1.6 kb, and subsequently sequenced with cSN specific primers. As well as Sanger sequencing of the G protein, whole genome sequencing was performed on the entire construct, using the purified RNA as the template as described in section 2.2.7.

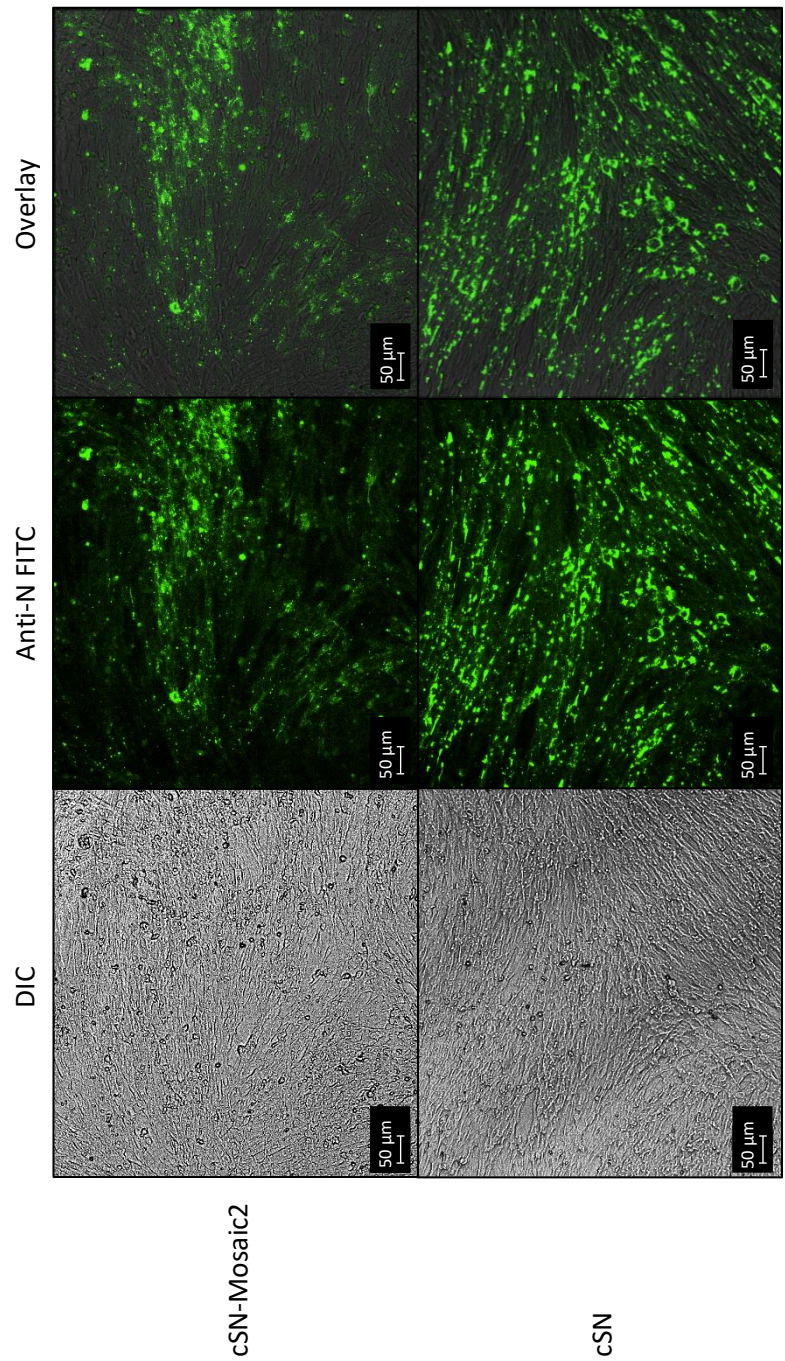


Figure 5.10: Infection immunofluorescence. BHK cells infected with either cSN-Mosaic2 (first row) or cSN (second row) were fix and stained with a FITC Anti-Rabies Nucleoprotein Monoclonal Globulin (Fujirebio) (green). Scale bars represent 50 µm.

Sequence data enabled comparison of the rescued virus to the original construct and it was determined that no mutations had been acquired following multiple passages and that Mosaic 2 G had been inserted correctly with no frame shifts. This also confirmed no contamination had occurred. The harvested cSN-Mosaic2 virus was then titrated and had a stock titre of 1.4×10^5 ffu/ml, higher than the stock titres of cSN-KBLV and cSN-TWBLV described in Chapter 4.

5.6.2. Growth Kinetics

Once the stock titre of cSN-Mosaic2 had been determined, the growth kinetics of the virus was determined *in vitro*. To determine the growth kinetics of cSN-Mosaic2, multi-step growth curves using a MOI of 0.1 was performed with cSN, cSN-Mosaic2, LBV-A, LBV-B, LBV-C, LBV-D, MOKV, and SHIBV in BHK-21 cells (Figure 5.11). Performing single step growth curves was not possible due to the low titres of cSN-Mosaic2, LBV-A, LBV-B, and LBV-C. Comparison of growth kinetics was made between cSN-Mosaic2, the phylogroup II viruses and the vaccine backbone used, cSN. By 24 hpi, all viruses were detected at around 10^2 to 10^4 ffu/ml, however all viruses except cSN were first detected 12 hours earlier. Using the Brown-Forsythe and Welch's ANOVA test with Dunnett's T3 multiple comparisons test, whilst there was a significant difference in endpoint titres between cSN-Mosaic2 and cSN ($P < 0.001$), cSN-Mosaic2 grew significantly more than four of the wildtype phylogroup II viruses. cSN-Mosaic2 grew to an endpoint titre of 4.1×10^5 ffu/ml, most similar to LBV-D which exhibited an endpoint titre of 1.5×10^5 ffu/ml, whereas, cSN grew to the highest endpoint titre at 3.1×10^7 ffu/ml. As well as endpoint titre, LBV-D and cSN-Mosaic2 showed a similar growth pattern. Both viruses were first detected at 12hpi at 10^1 ffu/ml and exhibited peak titres at 96 hpi at 10^5 ffu/ml.

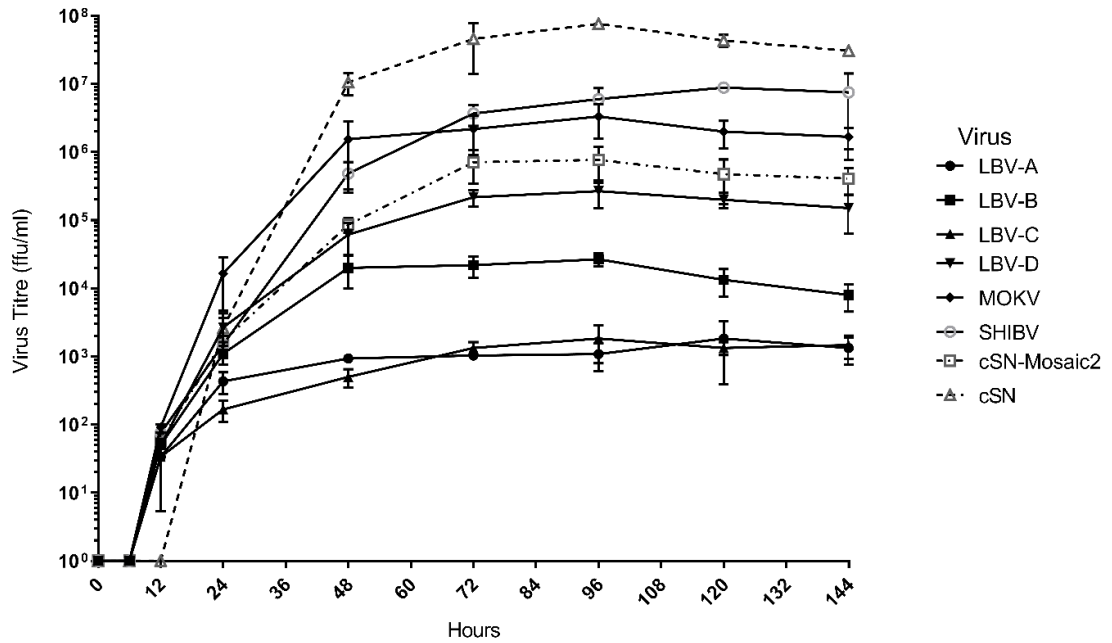


Figure 5.11: Growth kinetics of recombinant lyssavirus, cSN-Mosaic2; the vaccine backbone, cSN; and the wildtype viruses, LBV-A, LBV-B, LBV-C, LBV-D, MOKV, and SHIBV, *in vitro*. For each virus, cells were infected with an MOI of 0.1 to produce a multiple step growth curve.

5.6.3. In Vitro Studies

A mFAVN was performed to assess cSN-Mosaic2 antigenically by determining where cross-neutralisation may occur with a panel of 18 lyssavirus-specific sera and two standard sera (Figure 5.12).

Whilst varying levels of cross-neutralisation were observed with phylogroup I and phylogroup II lyssavirus-specific sera, phylogroup III-specific sera showed no detectable neutralising antibodies against cSN-Mosaic2. Phylogroup II-specific sera exhibited the most cross-neutralisation with four of the six sera showing neutralising antibody titres against cSN-Mosaic2 above or equal to the 0.5 IU/ml cut-off. Within phylogroup II, MOKV-specific sera and LBV-D-specific sera showed the highest titres against cSN-Mosaic2, whilst SHIBV-specific sera showed the lowest. Phylogroup I-specific sera exhibited detectable neutralising antibodies against cSN-Mosaic2, however these titres were below the 0.5 IU/ml cut off. EBLV-2-specific sera showed the highest titre of neutralising antibodies against cSN-Mosaic2 which was just below the serological cut-off. For other members of phylogroup I, the BBLV, DUVV, GBLV, RABV-specific sera, and standard sera, WHO and OIE, showed undetectable levels of neutralising antibodies against cSN-Mosaic2.

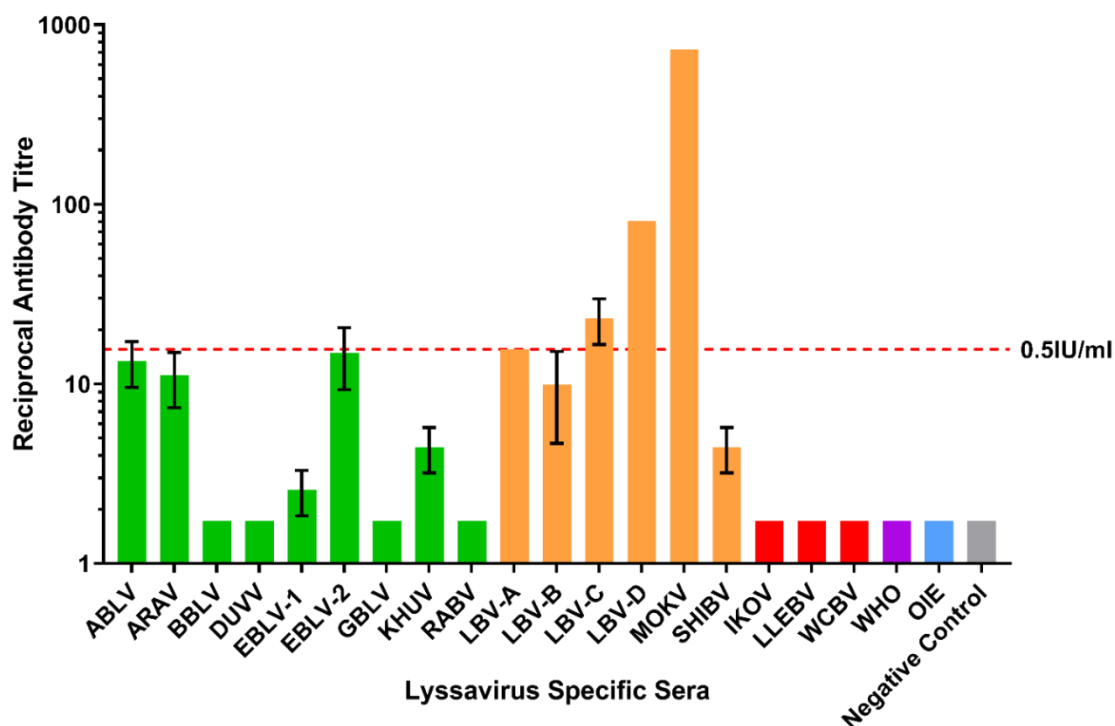


Figure 5.12: Modified FAVN to show the cross-neutralisation of each of the lyssavirus-specific sera and the standard OIE and WHO sera against cSN-Mosaic2 virus. The test was performed in triplicate and the mean of the results displayed on a logarithmic scale. The 0.5 IU ml⁻¹ neutralisation cut off is dictated by the OIE sera against CVS (indicated by the dashed line). IRKV sera not shown. Naïve dog sera was used as the negative control.

5.6.4. In Vivo Vaccination Challenge Study

5.6.4.1. Vaccination prior to challenge

In Chapter 3, the assessment of cross-neutralisation within phylogroup II determined LBV-D-specific sera was most effective at eliciting sufficient cross-neutralisation against all phylogroup II viruses. To assess the immunogenicity of LBV-D and the recombinant virus cSN-Mosaic2 and to determine which elicits the most cross-protection against phylogroup II viruses, inactivated LBV-D and cSN-Mosaic2 were administered to groups of 12 mice.

Large stocks of LBV-D and cSN-Mosaic2 were grown and titrated. Approximately 180 ml of each virus was propagated and the virus stock of cSN-Mosaic2 had a titre of 5.5×10^5 ffu/ml and LBV-D had a titre of 5×10^6 ffu/ml. Subsequently, LBV-D was diluted to 5.5×10^5 ffu/ml. Virus stocks were then BPL-inactivated using the technique described in section 2.5.1. Four week old BALB/c mice were vaccinated via the ip route with 500 μ l of either inactivated LBV-D or cSN-Mosaic2 on day 0, day 7, and day 14. The mock vaccinated mice were inoculated with 500 μ l of MEM only on the same days. On day 21, blood samples were collected from the dorsal vein as described in 2.9.1.3. The sera from these samples were then used in a mFAVN against the homologous virus to determine serological response and compared to CVS against the OIE standard sera at 0.5 IU/ml. All vaccinated mice seroconverted to a reciprocal titre above the internationally assigned cut-off, 0.5 IU/ml, and mock vaccinated mice did not. However, on average, mice vaccinated with inactivated cSN-Mosaic2 seroconverted to a reciprocal titre 1/3800, almost 7-fold higher than the mice vaccinated with inactivated LBV-D with an average reciprocal titre of 1/582. The reciprocal titres ranged from 1/47 and 1/1263 for LBV-D vaccinated mice (Figure 5.13) and 1/421 and 1/34092 for cSN-Mosaic2 vaccinated mice (Figure 5.14).

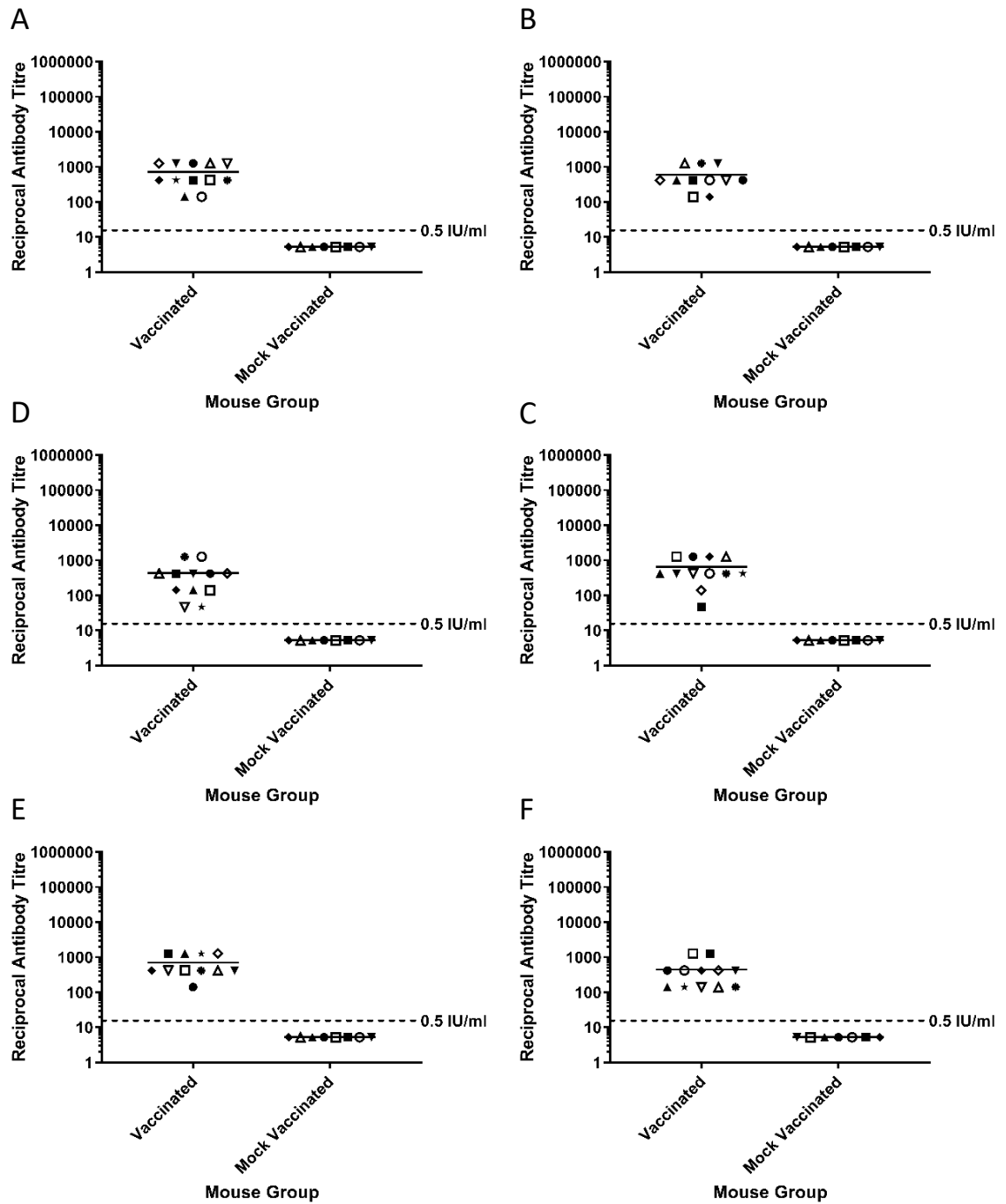


Figure 5.13: Post-vaccination serology on day 21 for mice vaccinated with inactivated LBV-D and mice mock-vaccinated with MEM on days 0, 7, and 14. All sera was assessed for neutralising antibodies against LBV-D by mFAVN where (A) were to be challenged with LBV-A, (B) were to be challenged with LBV-B, (C) were to be challenged with LBV-C, (D) were to be challenged with LBV-D, (E) were to be challenged with MOKV, and (F) were to be challenged with SHIBV.

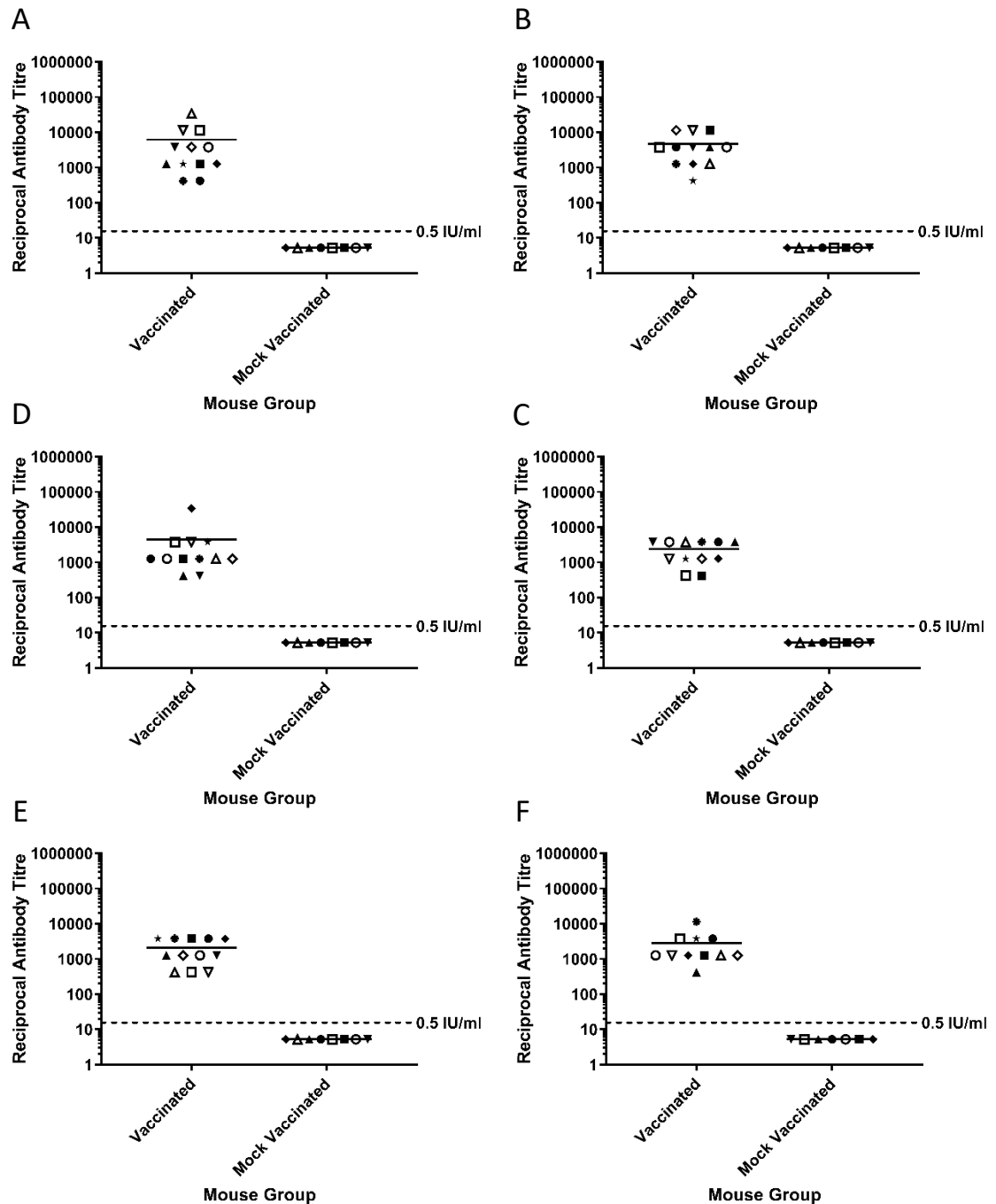


Figure 5.14: Post-vaccination serology on day 21 for mice vaccinated with inactivated cSN-Mosaic2 and mice mock-vaccinated with MEM on days 0, 7, and 14. All sera was assessed for neutralising antibodies against cSN-Mosaic2 by mFAVN where (A) were to be challenged with LBV-A, (B) were to be challenged with LBV-B, (C) were to be challenged with LBV-C, (D) were to be challenged with LBV-D, (E) were to be challenged with MOKV, and (F) were to be challenged with SHIBV.

5.6.4.2. *Survival of vaccinated mice post challenge*

Following the assessment of seroconversion, both mock vaccinated and vaccinated groups were challenged on day 28 post-vaccination with 100 ffu/30µl of either LBV-A, LBV-B, LBV-C, LBV-D, MOKV, or SHIBV where 12 vaccinated mice were compared to 8 mock vaccinated mice. Throughout the course of the experiment, mice were assessed for clinical disease according to a clinical score sheet and humanely terminated at a clinical score of 2 (493) (Appendix 4). Clinical disease included ruffled fur, tail-biting, hyperactivity and a hunched stance.

On average, the cSN-Mosaic2 vaccine promoted a higher percentage survival rate at 26% survival compared to the LBV-D vaccine with an average survival rate of 17%. For cSN-Mosaic2 vaccinated mice, survival rates ranged from 0% to 83% in each challenge group, whereas for LBV-D vaccinated mice, survival rates ranged from 0% to 25% (Figure 5.15). None of the mock vaccinated mice survived to the end of the experiment following challenge. Survival curves were compared using the log-rank Mantel-Cox test.

In the LBV-A challenged mouse groups, the LBV-D vaccine promoted a survival rate of 25% (n=3/12) whereas the cSN-Mosaic2 vaccine promoted a survival rate of just 8% (n=1/12), however the survival curves were not significantly different ($P=0.094$).

In the LBV-B challenged mouse groups, the LBV-D vaccine promoted a survival rate of 0% (n=0/12) whereas the cSN-Mosaic2 vaccine promoted a survival rate of 33% (n=4/12). Whilst the LBV-D vaccinated mice all succumbed to infection, the survival curve was significantly different from the mock vaccinated mice ($P<0.001$). The survival curve of the cSN-Mosaic2 vaccinated mice was also significantly different from the survival curves of the mock vaccinated mice ($P<0.001$) and LBV-D vaccinated mice ($P=0.007$).

In the LBV-C challenged mouse groups, both the LBV-D vaccine and cSN-Mosaic2 vaccine promoted a survival rate of 25% ($n=3/12$) and both were significantly different from the mock vaccinated mouse group (LBV-D vaccine, $P=0.004$; cSN-Mosaic2 vaccine, $P<0.001$). The survival curves of the LBV-D and cSN-Mosaic2 vaccinated mice were not significantly different ($P=0.859$).

In the LBV-D challenged mouse groups, the LBV-D vaccine promoted a survival rate of 25% ($n=3/12$) whereas the cSN-Mosaic2 vaccine promoted a survival rate of 8% ($n=1/12$), however the survival curves were not significantly different ($P=0.545$).

Whilst the cSN-Mosaic2 vaccinated mice nearly all succumbed to infection, the survival curve was significantly different from the mock vaccinated mice ($P<0.001$). The survival curve of the LBV-D vaccinated mice was also significantly different from the survival curves of the mock vaccinated mice ($P<0.001$).

In the MOKV challenged mouse groups, the LBV-D vaccine promoted a survival rate of 25% ($n=3/12$) whereas the cSN-Mosaic2 vaccine promoted the highest survival rate of the experiment at 83% ($n=10/12$), and both were significantly different from the mock vaccinated mouse group (LBV-D vaccine, $P<0.001$; cSN-Mosaic2 vaccine, $P<0.001$). The survival curves of the LBV-D and cSN-Mosaic2 vaccinated mice were also significantly different ($P=0.003$).

In the SHIBV challenged mice, all mice in each group succumbed to infection.

However, the time to development of disease was prolonged in the vaccinated groups, resulting in significantly different survival curves of both the LBV-D vaccinated and cSN-Mosaic2 vaccinated mice to the mock vaccinated mice ($P<0.001$).

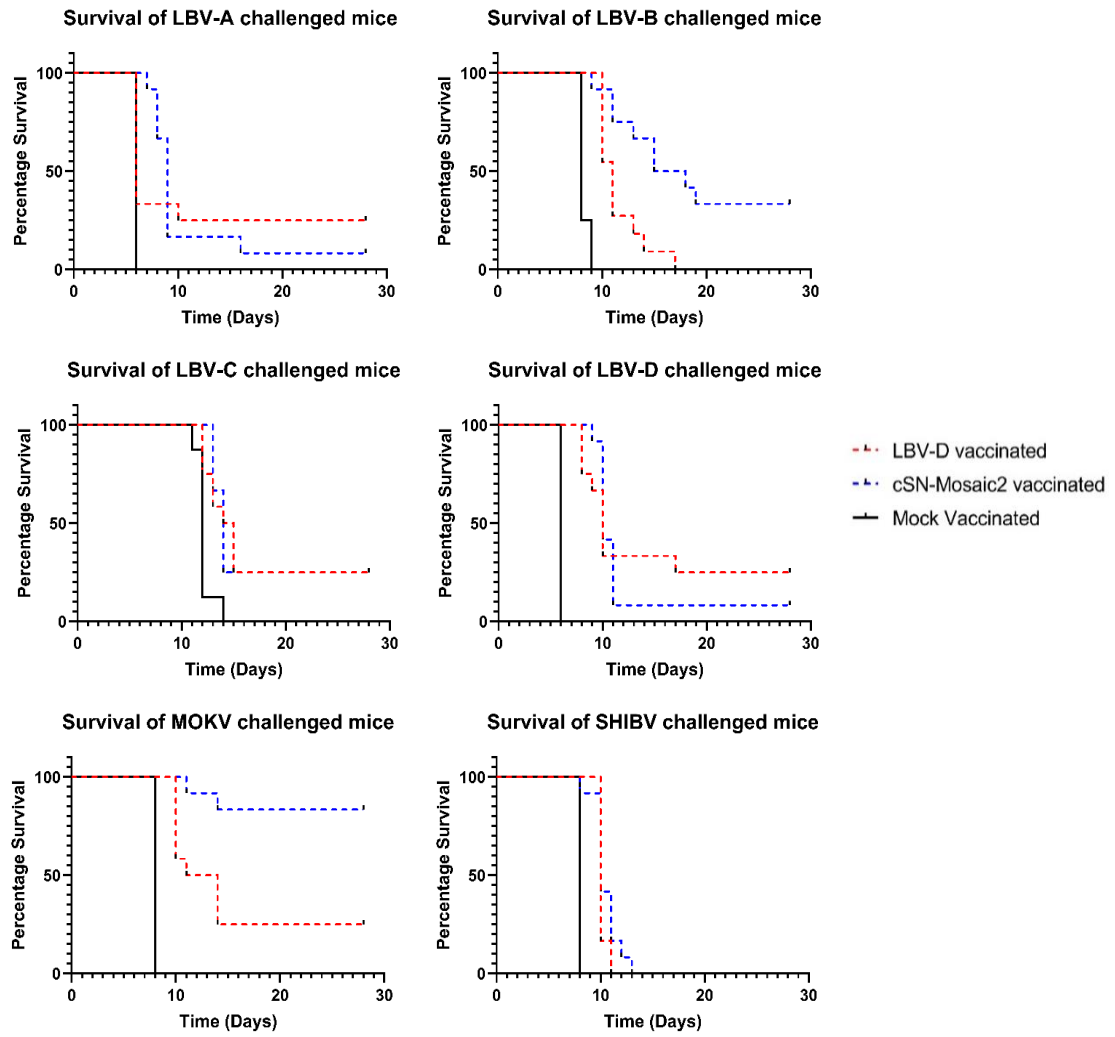


Figure 5.15: *In vivo* survivorship following intracranial inoculation with 100 ffu/30µl of phylogroup II virus. Mice were vaccinated 28 days before challenge and day 0 on the graph is the day of challenge.

5.6.5. Immunofluorescence

Numerous aggregations of lyssavirus antigen were also detected in brain smears subject to the direct Fluorescent Antibody Test (FAT) as described in section 2.9.1.8.1 and 4.6.3.2. Two mice that had been terminated from each group and all the surviving mice were selected for the FAT.

All mice that were tested and had succumbed to infection tested positive for viral antigen. All mice that survived to the end of the experiment tested negative for viral antigen as indicated by no fluorescence indicative of viral antigen not being present.

5.5.6. Serology

All animals that succumbed to clinical disease and were humanely terminated, and all animals that survived until the end of the experiment, were cardiac bled before termination. Sera was assessed for seroconversion using a mFAVN against the vaccine virus as well as a modified FAVN against the challenge virus (Figure 5.16 and Figure 5.17). Mean serological titres were compared using the Mann-Whitney test.

From the mock vaccinated groups ($n=8$), whilst all of the animals developed clinical disease, in some cases the animal generated a measurable antibody response against the challenge virus. In the case of all mock vaccinated mouse groups, titres increased significantly post challenge in LBV-A ($P<0.001$), LBV-B ($P<0.001$), LBV-D ($P=0.001$), MOKV ($P=0.007$), and SHIBV ($P=0.048$).

In addition, in the LBV-A, LBV-B, LBV-D, and SHIBV challenged mice, the average antibody titre exceeded the 0.5 IU/ml serological cut off. In both vaccinated groups, the antibody titres against the vaccine virus were higher than the antibody titres against the challenge virus.

For the LBV-D vaccinated/LBV-A challenge group, the virus challenge did not have a statistically significant effect on the serological titre ($P=0.200$). On average the animals in this group had a significantly higher level of neutralising antibodies against LBV-D than LBV-A at 1/11390 and 1/243, respectively ($P<0.001$).

For the LBV-D vaccinated/LBV-B challenge group, the virus challenge did not have a statistically significant effect on the serological titre ($P=0.316$). On average the animals in this group had a significantly higher level of neutralising antibodies against LBV-D than LBV-B at 1/1219 and 1/81 respectively ($P<0.001$).

For the LBV-D vaccinated/LBV-C challenge group, the virus challenge did not have a statistically significant effect on the serological titre ($P=0.366$). In contrast, on average, the animals in this group did exhibit a significantly higher level of neutralising antibodies against LBV-D than LBV-C at 1/11210 and 1/1323, respectively ($P=0.003$).

For the LBV-D vaccinated/LBV-D challenge group, the virus challenge did not have a statistically significant effect on the serological titre ($P=0.489$). Due to the same vaccine and challenge virus, the neutralising antibody titre was the same, with an average reciprocal titre of 1/8541.

For the LBV-D vaccinated/MOKV challenge group, the virus challenge did not have a statistically significant effect on the serological titre ($P=0.677$). On average the animals in this group had a significantly higher level of neutralising antibodies against LBV-D than MOKV with reciprocal titres of 1/1472 and 1/415 respectively ($P=0.003$).

For the LBV-D vaccinated/SHIBV challenge group, the virus challenge did not have a statistically significant effect on the serological titre ($P=0.875$). On average, the animals in this group had a significantly higher level of neutralising antibodies against LBV-D than SHIBV with reciprocal titres of 1/467 and 1/89 respectively ($P<0.001$).

For the cSN-Mosaic vaccinated/LBV-A challenge group, the virus challenge did not have a statistically significant effect on the serological titre ($P=0.225$). On average, the animals in this group had a significantly higher level of neutralising antibodies against cSN-Mosaic than LBV-A with reciprocal titres of 1/2306 and 1/248 respectively ($P<0.001$).

For the cSN-Mosaic vaccinated/LBV-B challenge group, the virus challenge did not have a statistically significant effect on the serological titre ($P=0.395$). On average, the animals in this group had a significantly higher level of neutralising antibodies against cSN-Mosaic than LBV-B with reciprocal titres of 1/22628 and 1/856 respectively ($P<0.001$).

For the cSN-Mosaic vaccinated/LBV-C challenge group, the virus challenge did not have a statistically significant effect on the serological titre ($P=0.322$). On average, the animals in this group did exhibit a significantly higher level of neutralising antibodies against cSN-Mosaic than LBV-C with reciprocal titres of 1/4891 and 1/281 respectively ($P<0.001$).

For the cSN-Mosaic vaccinated/LBV-D challenge group, the virus challenge did not have a statistically significant effect on the serological titre ($P=0.726$). On average, the animals in this group did exhibit a significantly higher level of neutralising antibodies against cSN-Mosaic than LBV-D with reciprocal titres of 1/33018 and 1/1074 respectively ($P=0.012$).

For the cSN-Mosaic vaccinated/MOKV challenge group, the virus challenge did not have a statistically significant effect on the serological titre ($P=0.772$). On average, the animals in this group did exhibit a significantly higher level of neutralising antibodies against cSN-Mosaic than MOKV with reciprocal titres of 1/3518 and 1/491 respectively ($P=0.002$).

For the cSN-Mosaic vaccinated/SHIBV challenge group, the virus challenge did have a statistically significant effect on the serological titre ($P=0.015$). On average, the animals in this group had a significantly higher level of neutralising antibodies against cSN-Mosaic than SHIBV with reciprocal titres of 1/1765 and 1/176 respectively ($P<0.001$).

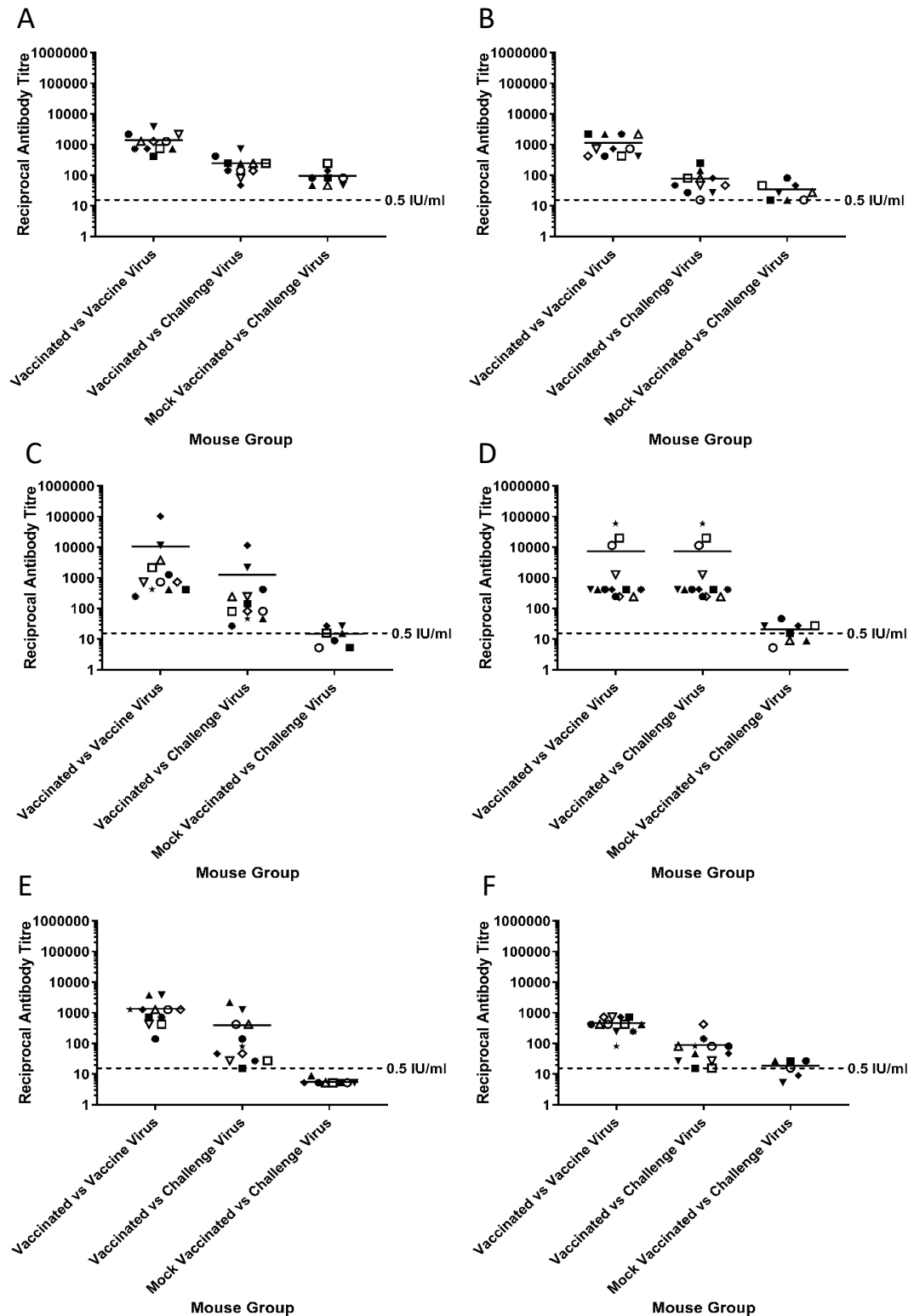


Figure 5.16: Assessment of serological status in mice following vaccination and challenge using modified FAVN. Mice were serologically assessed against the LBV-D (vaccine virus) and the challenge virus where (A) were challenged with LBV-A, (B) were challenged with LBV-B, (C) were challenged with LBV-C, (D) were challenged with LBV-D, (E) were challenged with MOKV, and (F) were challenged with SHIBV.

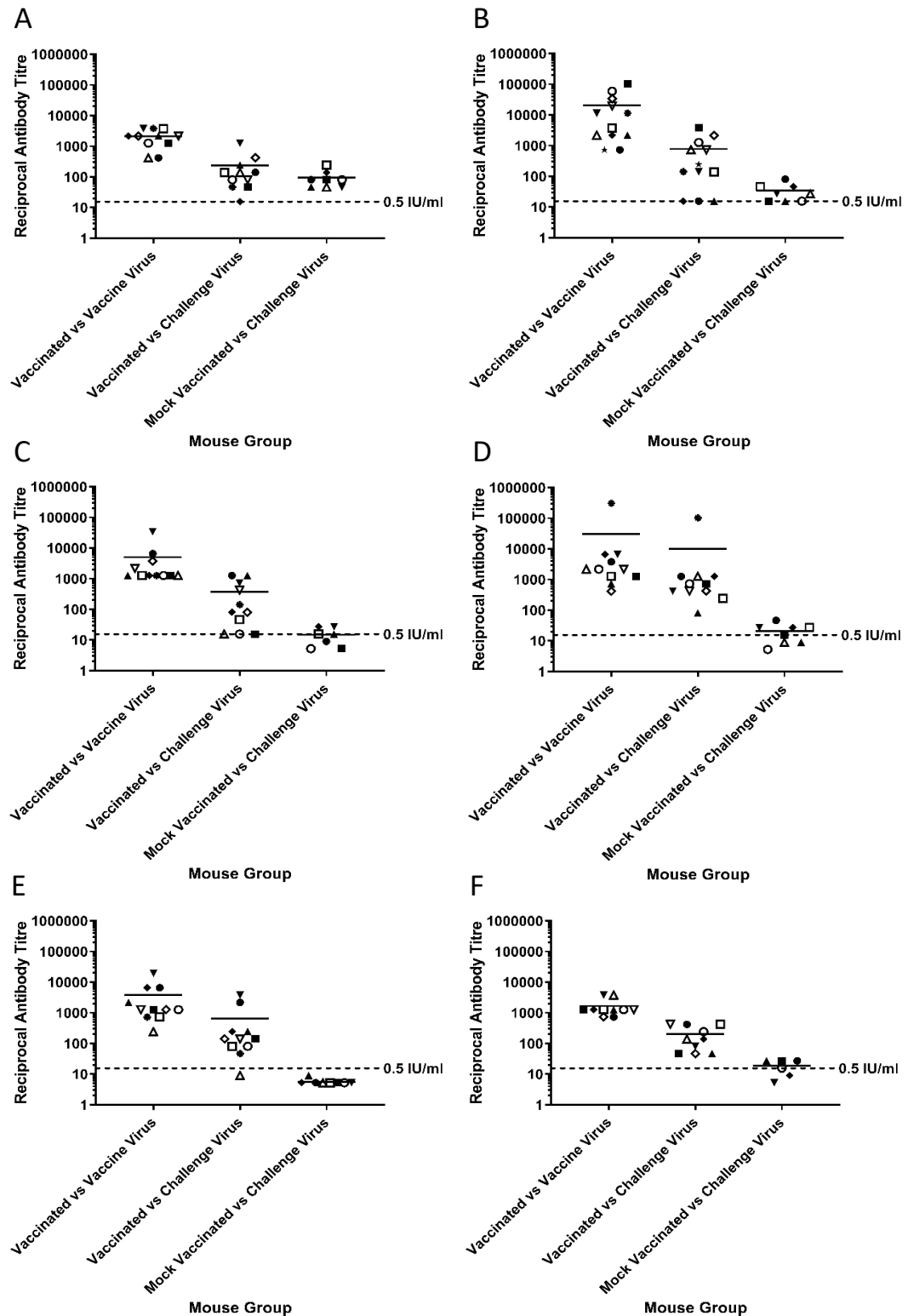


Figure 5.17: Assessment of serological status in mice following vaccination and challenge using modified FAVN. Mice were serologically assessed against the cSN-Mosaic2 (vaccine virus) and the challenge virus where (A) were challenged with LBV-A, (B) were challenged with LBV-B, (C) were challenged with LBV-C, (D) were challenged with LBV-D, (E) were challenged with MOKV, and (F) were challenged with SHIBV.

5.7. Discussion

A variety of approaches to create a broadly cross-protective vaccine were assessed, and it was determined that the primary focus was to generate vaccine formulations consisting of inactivated virions of a single virus that expressed a single chimeric G protein. Initially, the straightforward approach to create a vaccine of multiple inactivated viruses was explored. Specific sera generated in response to inoculation of inactivated LLEBV, IKOV, and WCBV was unable to neutralise IKOV virus *in vitro* (Figure 5.1). In addition, it appeared that LLEBV was more immunodominant than WCBV and IKOV as the specific sera exhibited the highest neutralising antibody titre against LLEBV. Simultaneous administration (mixing multiple vaccines with a rabies vaccine and injecting at the same site), has been previously shown to inhibit the development of the immune response to rabies, particularly *leptospira* (494). Immunological interference in adaptive immunity to simultaneously administered vaccines is not well understood. The magnitude of the adaptive immune response may involve complex innate immunity mechanisms that limit initial exposure to the inactivated virus/vaccine (495). Alternatively, within the formulation of the three BPL-inactivated viruses, the concentration of G protein for each lyssavirus was not quantified. Whilst virus titre gives an indication of the number of viruses per ml, the number of viable G proteins for each virus was not quantified, which could ultimately affect seroconversion to a particular antigen.

Three approaches were adopted for the generation of chimeric G proteins. The hinge-based approach and the mosaic-based approach were revisited and the methodology from previous studies was adapted (436, 482). Whereas, the novel structure-based approach utilised the recently published post-fusion MOKV G crystal structure as a basis for chimeric G protein design (27).

For the hinge-based design, a linear region of the ectodomain was used as a divide on the G protein whereby the N-terminus and the C-terminus sequence originated from different lyssavirus species (Figure 5.4). Like the structure-based approach, chimeric G proteins were designed such that the antigenic sites were ‘balanced’ between the two domains from different lyssavirus species (Figure 5.7). In both models, antigenic sites I and II derived their sequence from one lyssavirus and antigenic sites III, IV, and ‘a’ derived their sequence from a different lyssavirus. Antigenic site II is widely considered the most immunogenic as a large number of G protein-specific mAbs bind site II, and site II is involved in the binding of one of the putative RABV cellular receptors, nAChR (26, 149, 496). However, site III shares the binding site for the low affinity neurotrophin receptor (p75^{NTR}) and mAbs targeting site I and III have been developed to replace HRIG in PEP, indicating that these sites could be equally immunogenic (121, 149, 497).

The mosaic-based design did not follow the same approach as the regions of the chimeric G protein sequences were selected in lengths of 12-mers by an algorithm. In all cases, however, the antigenic sites were as ‘balanced’ as possible across the majority of the input proteins (Figure 5.5).

Appropriate glycosylation of the lyssavirus G protein is critical for protein expression and function (498). The oligosaccharides associated with the lyssavirus G protein are linked to asparagine residues in the tripeptide motif asparagine-X-serine/threonine (NXS/T) where X is any amino acid other than proline (N-linked glycosylation) (499). Depending on the strain, the RABV G protein can have one to four putative glycosylation sites (492). In the case of the RABV ERA strain, the G protein has four putative glycosylation sites: N37, N247, N319, and N465, where N465 is the only site located in the cytoplasmic domain (Figure 5.6). Glycosylation sites differ between different lyssavirus species and in the case of LBV-D, the G protein has four putative

glycosylation sites: N184, N202, N319, and N334 (Figure 5.6), whilst MOKV has just two: N202 and N319. Typically, however, even if a glycosylation site is present, it may not be glycosylated sufficiently or at all (500-502). The N319 site is well defined, however, as it is conserved across all lyssavirus species and is suggested to be essential for correct and complete folding of the nascent G protein and subsequent transport to the infected cell surface for virion assembly (503, 504). Whilst other glycosylation sites of the lyssaviruses are not well defined, a recent study determined that in the case of MOKV G protein, the N202 site is glycosylated (27). The molecular mass of the protein was 56.5 ± 0.2 kDa, consistent with the mass of a monomer of the G protein ectodomain with two glycosylated sites (27). As LBV-D shares these two glycosylation sites with MOKV, it is likely that LBV-D would be glycosylated in the same way.

Using the novel structure-based approach to design the chimeric G proteins, as many glycosylation sites as possible were conserved in the resulting chimeric G protein sequences. A recently published study which utilised the VSV crystal structure to design similar RABV/MOKV chimeras determined that there was no evidence of glycosylation or lack of glycosylation affecting chimeric G protein functionality (483).

Pseudotype viruses were generated to assess the functionality of the chimeric G proteins (Figure 5.9). The constructs designed using the structure based approach generated consistent results where all three constructs were successful at producing detectable pseudotype virus titres above 10^7 RLU/ml. These titres were not significantly different from the IKOV wildtype G pseudotype titres and indicated that these recombinant G proteins were functional. The pseudotype virus expressing the Mosaic 2 G exhibited the highest titre, however this was not entirely unexpected since the input proteins that constitute Mosaic 2 G all belong to phylogroup II. The viruses in phylogroup II have a

G protein amino acid sequence identity of $\geq 70\%$, considerably more than the G protein sequence identity of the lyssavirus species constituting the other chimeric G proteins.

In general, successful pseudotype virus generation and pseudotype virus titre correlated with the sequence identity of the lyssavirus species that the chimeric G protein sequence derived from. However, for the hinge-based designed chimeric G proteins, it was unclear why some chimeric G proteins enabled pseudotype generation, but the reciprocal chimera did not. For example, the pseudotype virus expressing RABV/LBV-D G exhibited a titre of 9.1×10^5 RLU/ml, whilst the LBV-D/RABV G construct failed to produce pseudotype virus. In addition, the pseudotype virus expressing LLEBV/IKOV G exhibited a titre of 7.8×10^7 RLU/ml, whilst the pseudotype virus expressing IKOV/ LLEBV G exhibited a titre of 2.0×10^5 RLU/ml. One hypothesis for this phenomenon is that one chimera might form a structure that is able to interact well with a receptor or the HIV matrix protein and the reciprocal chimera does not.

Through a reverse genetics system, live virus rescue was attempted from full length constructs with the chimeric G genes. The only construct that resulted in successful live virus rescue was cSN-Mosaic2 (Figure 5.10). Whilst the Mosaic 2 G resulted in the highest titre of pseudotype virus and subsequently indicated that the recombinant G protein was functional, it is unclear why constructs with similarly high titres of pseudotype virus did not. As the single surface protein, the G protein is involved in trimerisation, receptor binding, and membrane fusion. The successful generation of pseudotype virus, subsequent cell infection, and reporter gene expression suggests that the chimeric G proteins are successfully expressed, trafficked to the cell surface, and facilitate pseudotype virus infection through cell receptor binding. In addition, a previous study which described the design and rescue of similar viruses expressing either RABV/MOKV/RABV G or MOKV/RABV/MOKV G found that whilst both G

proteins were trafficked to the cell surface, only RABV/MOKV/RABV G facilitated the rescue of live virus (483). Consequently, it is unclear why the RABV/LBV-D/RABV G construct in this study did not produce virus.

The evidence suggests that functional implications prevented viral recovery of these constructs and the subsequent production of virus particles expressing chimeric Gs such as the RABV/LBV-D/RABV G. However, whilst the rabies virus G protein has been demonstrated to enhance the production of virus particles through intrinsic and independent exocytosis activity, the matrix protein is the main determinant for virus assembly and budding (85, 90). Consequently, it could be hypothesised that chimeric G proteins that were functional in the pseudotype system formed a structure that is able to interact with the HIV matrix (p24) but unable to interact optimally with the cSN matrix protein. Alternatively, optimisation of the virus rescue protocol could facilitate more efficient virus rescue. Certainly, recovery of rabies virus mutants deficient for the G protein (pSAD Δ G) or the G protein cytoplasmic domain (pSAD Δ CD) failed (90). However, virus rescue of these constructs was successful if the constructs were initially transfected into cells transiently expressing wildtype RABV G protein. Further, whilst transient cell expression of wildtype G was an absolute requirement for the propagation of pSAD Δ G, transient cell expression of wildtype G was only required for initial virus rescue and not necessary for further propagation of pSAD Δ CD (90). Alternatively, in the case of Newcastle Disease Virus (NDV), a 2-plasmid reverse genetics system was adapted to replace the conventional 4-plasmid system to increase transfection efficiency and facilitate the virus rescue of attenuated strains that previously failed using the conventional approach (505). Similarly to rabies virus rescue, NDV requires the co-transfection of three helper plasmids that deliver the minimum elements required for virus replication. These three viral genes were combined into one plasmid and

consequently co-transfection of this combined plasmid and the full length genome plasmid facilitated efficient virus recovery (505). Future avenues of this work could involve optimisation of the virus rescue protocol, in an attempt to increase virus rescue efficiency, to rescue the other full length constructs as live virus.

Nevertheless, after establishing sufficient stocks of cSN-Mosaic2, the recombinant virus was assessed *in vitro*. It was first determined that the growth kinetics of the virus was most similar to LBV-D and grew to higher titres than four of the six phylogroup II wildtype lyssaviruses (Figure 5.11). Whilst Mosaic 2 G shares the highest sequence similarity to LBV-D, cSN-Mosaic2 grew to higher titres than LBV-D. This could suggest that the cSN backbone or other regions of the Mosaic 2 G facilitated increased fitness within cell culture.

Following growth kinetic analyses, a mFAVN assay using lyssavirus-specific sera determined that phylogroup II-specific sera, particularly MOKV-specific sera and LBV-D-specific sera, demonstrated the highest titres of neutralising antibodies against cSN-Mosaic2 (Figure 5.12). Whilst the antibody concentration of the lyssavirus-specific sera used in this study was variable, the neutralisation by MOKV-specific sera and LBV-D-specific sera could highlight the highly antigenic regions on the cSN-Mosaic2 G protein. Certainly, the sequence of MOKV constitutes a small section of the Mosaic2 G sequence but cSN-Mosaic2 was highly susceptible to neutralisation by MOKV-specific sera.

An *in vivo* vaccination-challenge experiment enabled a thorough assessment of the immunogenicity of cSN-Mosaic2 and LBV-D to determine which antigen elicits the most cross-protection against phylogroup II viruses. Whilst both inactivated viruses elicited high titres of neutralising antibodies, inactivated cSN-Mosaic2 induced higher

titres of neutralising antibodies than LBV-D (Figure 5.13 and 5.16). At day 21 post vaccination, titres of cSN-Mosaic2-specific sera against cSN-Mosaic2 virus averaged >250-fold higher than the 0.5 IU/ml threshold for protection, whereas titres of LBV-D-specific sera against LBV-D virus averaged >38-fold higher than the 0.5 IU/ml threshold. This demonstrated the robust functionality of the VNAs induced by inactivated cSN-Mosaic2 and inactivated LBV-D. The data also suggest that the Mosaic G protein may be more effective at activating adaptive immune responses such as priming T helper cells, which stimulate B cell activation, necessary for the clearance of lyssaviruses (296, 436, 506, 507).

Following vaccination and seroconversion assessment, mouse groups were challenged with one of the six phylogroup II lyssaviruses. Based on the high titres of VNAs produced against either cSN-Mosaic2 or LBV-D and the cross-neutralisation observed within phylogroup II in Chapter 3, cross-protection against phylogroup II virus challenge was anticipated. However, the results of this *in vivo* experiment had a lower survival rate than expected (Figure 5.15).

Among the control groups, the data from the survival curves indicated that LBV-A virus and LBV-D virus appeared to be the most pathogenic when inoculated intracranially in naïve mice. All mock vaccinated mice challenged with either LBV-A or LBV-D exhibited the shortest incubation period with 0% survival at day 6 post challenge. Mock vaccinated mice challenged intracranially with LBV-C exhibited the longest average time to 0% survival at 12 days post challenge. Whilst this is longer than for the other phylogroup II viruses, virus challenge of naïve mice is traditionally considered successful if mice succumb to infection between day 5 and day 14 post challenge, based on previous methodologies for RABV (508).

Whilst survival rates of vaccinated mice were low, the data from the survival curves indicated significant differences between survivorship and disease onset in vaccinated and mock vaccinated mice. Overall, the engineered cSN-Mosaic2 virus was a better vaccine candidate than wildtype LBV-D, concurrent with previous studies that have shown that mosaic proteins induce greater cross-reactivity than consensus sequence and wildtype antigens (436, 509). However, the higher average survival rate could also have been a result of higher VNA titres post vaccination.

For both vaccinated groups, all mice succumbed to SHIBV infection, reflected in the previous findings in Chapter 3 where SHIBV was the most antigenically divergent lyssavirus within phylogroup II. In addition, the survival of LBV-D vaccinated mice against LBV-B challenge also supports existing data in Chapter 3, where LBV-B positioned closest to SHIBV on the 3D antigenic cartography map, indicating possible antigenic divergence of this virus. Whilst significantly different to the mock vaccinated group due to delayed symptom onset, the survival rate for mice vaccinated with LBV-D and challenged with LBV-B was 0%.

For the cSN-Mosaic2 vaccinated mice, the survivorship following MOKV challenge and LBV-B challenge exhibited the highest percentage survival at 83% and 33% survival respectively. For the LBV-D vaccinated mice, the survivorship following LBV-A, LBV-C, LBV-D, and MOKV challenge exhibited the joint highest percentage survival rate at 25% for each group. Whilst this data corroborates with the serological data performed previous to the vaccination-challenge experiment where LBV-D and MOKV-specific sera demonstrated the highest titres of neutralising antibodies against cSN-Mosaic2, the low survival rate of mice immunised and challenged with LBV-D indicates that the lethal dose used in this experiment could be too high. In general, for the titres measured post-vaccination against LBV-D in the mFAVN, percentage survival

after challenge with the homologous virus was expected to be more than 70% based on previous methodologies for RABV (508). Future avenues for this work would be to define the 50% lethal dose (LD₅₀) to establish a lethal model for each of the phylogroup II viruses, followed by an investigation into vaccine protection in mice against virus challenge with the minimum dose required for 0% survival in naïve mice.

Post-experiment serology determined that VNA titres did not significantly increase after virus challenge, however for most mouse groups the VNA titres against the vaccine virus (LBV-D or cSN-Mosaic2) was significantly higher than against the challenge virus, similar to what was documented for cSN-KBLV challenged mice in Chapter 4.

To conclude, the development of an antigen that induces the production of broadly neutralising antibodies against lyssaviruses warrants further investigation. A previous study described the successful generation of a phylogroup I/phylogroup II chimeric virus (Lyssavax) that protected against wildtype RABV and recombinant MOKV *in vivo* but protection against other phylogroup I and II viruses was not assessed and only intranasal challenge was investigated (483). In this study, vaccination with inactivated LBV-D induced the production of high titres of virus neutralising antibodies but failed to afford protection against LBV-D challenge in 75% of mice. Whilst in this case the challenge dose may have been too high, the survival proportions of LBV-D vaccinated mice challenged with LBV-A, LBV-C, LBV-D, and MOKV were the same. This suggests that inactivated LBV-D as a vaccine affords similar cross-protection against LBV-A, LBV-C, and MOKV to the homologous virus LBV-D, similar to the cross-neutralisation data in Chapter 3.

Chapter 6: Discussion

6.1. Introduction

The term ‘rabies’ has induced terror throughout human history, as rabies virus is the only viral pathogen that is associated with 100% fatality following the onset of the clinical disease in humans (11). Whilst rabies is predominantly circulating within domestic and feral dog populations globally, the presence of lyssaviruses in bats is well established (475). Bats, abundant and geographically widespread, have been increasingly associated as the reservoir host for infectious zoonotic diseases (510, 511). Historically, the association of rabies with hematophagous bats (*Desmodus* sp., although primarily *Desmodus rotundus*) across the Caribbean, and Central and South America, has both embedded a fear of rabies into human populations, as well as driven an irrational and unjustified fear of bats across many cultures. Certainly, bat transmitted human RABV is rare, however bat rabies remains a constant threat, as exemplified by continued human cases of bat rabies across North America (512). As well as RABV transmission, recent human deaths due to IRKV, ABLV, and EBLV-1 highlight the rare spillover events of non-RABV lyssaviruses into humans (513-515). A larger threat to animal and human populations would be a host switching event whereby a bat lyssavirus adapts to a terrestrial host resulting in inter-host transmission. Certainly, phylogenetic evidence suggests that the emergence of carnivoran rabies, resulting in the ongoing global RABV epidemic, originated from spillover events from bats approximately 888-1459 years ago (504). Whilst non-RABV lyssaviruses are yet to be established in terrestrial hosts, complete knowledge of lyssavirus antigenicity in relation to current biologicals and other lyssaviruses would be invaluable. This study has demonstrated that there is antigenic variation across all lyssaviruses that is associated with genetic variation, providing a rationale for the assignment of lyssaviruses within

phylogroups. Here, the implications of antigenic differences between recognised, novel, and putative lyssaviruses, and the antigenicity of viruses expressing chimeric G proteins is discussed.

6.2. Implications of the degree of cross neutralisation across the genus

It is widely accepted that the key immune defence and the principal modality of protection against rabies is virus neutralising antibodies (296, 303). However, cell-mediated responses during lyssavirus infection are less well defined (516). The level of neutralising antibodies in serum samples are routinely assessed to determine the response to rabies vaccination in humans and animals or to determine exposure to lyssaviruses in bats (34, 385, 517). Infiltration of B cells and the production of neutralising antibodies are required for the clearance of RABV from the CNS however the relationship between neutralising antibody titre and degree of protection against a non-phylogroup I lyssavirus has been difficult to define (34, 35, 294, 296, 518). In general, the presence of neutralising antibodies to a particular virus correlates well with protection and absence of neutralising antibodies correlates well with susceptibility to experimental virus challenge.

In comparison to influenza virus and other RNA viruses, lyssaviruses are antigenically conserved, however sufficient variation across the genus has given rise to a lack of cross protection of rabies vaccines against the most divergent viruses. Viruses in phylogroup II (LBV, MOKV, and SHIBV) and viruses tentatively assigned to phylogroup III (IKOV, LLEBV, and WCBV), are genetically and antigenically divergent from RABV vaccine strains and other viruses in phylogroup I.

In this study, a high degree of intra-phylogroup I cross-neutralisation was observed, corroborating data from previous studies (34, 35, 38, 457). With the exception of

DUVV, all phylogroup I viruses including cSN- TWBLV and cSN-KBLV, were neutralised by 2.5 IU/ml of OIE international standard sera. In contrast, DUVV was neutralised by 5 IU/ml, indicating divergence within the phylogroup. In addition to OIE sera, BBLV-specific sera also cross-neutralised all phylogroup I viruses except cSN- TWBLV, whilst other phylogroup I-specific sera showed variable cross-neutralisation against the same viruses.

An important finding from this study was that OIE, WHO, and HDCV recipient sera all showed lower titres of neutralising antibodies against the wild/street strain of RABV (wRABV) compared to CVS, suggesting possible divergence of these RABV isolates. The neutralising antibody titre calculated by a neutralisation test is dependent on the challenge virus used, as demonstrated here and reported previously (24, 519). CVS is used regularly in diagnostic assays to determine humoral response to rabies vaccination. However, exposure to CVS (a laboratory derived isolate) is highly unlikely, and rather exposure to a wRABV strain is much more probable. The standard sera used here and in diagnostic assays neutralise CVS at 0.5 IU/ml, whereas the same sera neutralise wRABV at 1 IU/ml. In the future, should wRABV isolates become more antigenically divergent to the laboratory isolates used in diagnostic assays, false positive results may occur where a serum neutralises CVS but might not neutralise wRABV. Testing sera against appropriate wRABV strains would reduce the likelihood of an unprotected human or domestic animal being considered protected.

For people in certain high-risk occupations, such as laboratory workers that handle live lyssaviruses, a titre of ≥ 5 IU/ml would be preferable to ensure protection against all viruses in phylogroup I. However, this may impact dosing regimens and be less economically viable. In the UK, the current official guidance for personnel in high-risk occupations recommends a titre of ≥ 0.5 IU/ml (520). In addition, since DUVV is the

most divergent within phylogroup I, it could be considered for inclusion in a pan-Africa vaccine where fatal human DUVV infections have been documented (238, 239, 521).

Previous to this study, the degree of cross-neutralisation within phylogroup II and III had not been investigated in the same depth as for phylogroup I. As shown in this study, there was a high degree of cross-neutralisation within phylogroup II and a complete lack of cross-neutralisation within phylogroup III. At low neutralising antibody titres against the homologous virus, LBV-D-specific sera cross-neutralised five of the six phylogroup II viruses. Similar to the standard sera used against phylogroup I, at higher neutralising antibody titres phylogroup II-specific sera cross-neutralised a broader range of viruses where LBV-D and LBV-B-specific sera neutralised all phylogroup II viruses. On average, each phylogroup II virus was neutralised by five phylogroup II-specific sera, indicating the extensive intra-phylogroup II cross-neutralisation. The increased genetic diversity of viruses in phylogroup III was likely the cause of no cross-neutralisation within phylogroup III and the antigenic diversity highlighted by the antigenic cartography maps.

Finally, inter-phylogroup cross-neutralisation was minimal; RABV-specific sera neutralised MOKV virus and SHIBV-specific sera neutralised IKOV virus. This could indicate specific antigenic epitopes shared between these viruses. Certainly, mAb RVC20, targeting antigenic site I, has been shown to neutralise both MOKV and RABV *in vitro* (29, 471). In addition, both IKOV and the phylogroup II viruses are African lyssaviruses so there may be specific immunogenic epitopes shared by these viruses (6, 474).

Standardised RABV-specific sera, OIE sera, was shown to neutralise all phylogroup I lyssaviruses, and LBV-D-specific sera was shown to neutralise all phylogroup II

viruses. As a result, it was hypothesised that sera specific to RABV and LBV-D would neutralise all viruses within phylogroup I and II. As a proof of concept, LBV-D-specific sera was mixed 1:1 with 10 IU/ml OIE sera for a final concentration of 5 IU/ml. This sera mix was subsequently tested against all lyssaviruses by mFAVN. All viruses except WCBV and LLEBV were cross-neutralised. Interestingly, the sera mix neutralised IKOV, whilst LBV-D-specific sera and OIE-specific sera alone did not. This could indicate that the requirements for neutralisation included a combination of specific antibody populations within both the OIE and LBV-D-specific sera. Despite this, the cross-neutralisation data and antigenic cartography data suggest that, if a pan-lyssavirus candidate vaccine was to be developed, it would likely require antigenic epitopes representative of each of the phylogroup III viruses in order to produce strongly neutralising antibodies against all of the characterised lyssaviruses. Additionally, the classification of WCBV, IKOV, and LLEBV into phylogroups requires further review, however these data from this study supports the concept that each of the phylogroup III lyssaviruses should separate into three distinct phylogroups; WCBV in phylogroup III, IKOV in phylogroup IV and LLEBV in phylogroup V. The proposed novel lyssavirus, MBLV, shares a nucleotide identity of 80.9-81% with the WCBV nucleoprotein gene. If MBLV is not pronounced a novel species, it would represent a distinct lineage of WCBV. In addition, the detection of WCBV neutralising antibodies in *Miniopterus* bats in Kenya caused speculation that WCBV or a WCBV-related virus was circulating in Africa. Consequently, it could be hypothesised that MBLV may also be classified within phylogroup III following further antigenic analyses (20).

Globally, active and passive surveillance for bat lyssaviruses reveals serological evidence for their circulation in bat species. The results generated in Chapter 3 have significant implications to the interpretation of serological surveillance data. The

extensive cross-neutralisation within phylogroup I and II and the type of serological assay used must be considered. Based on the data generated in Chapter 3, a neutralisation assay method would be required to detect the presence of neutralising antibodies in test sera against a particular lyssavirus species. Neutralisation assays distinguish antibodies from binding antibodies and are therefore more specific as explored previously (32). To the contrary, an ELISA based method would be useful for initial serological screening. The ELISA method used in this study detected broadly cross-reactive binding antibodies, such that all lyssavirus-specific antibodies bound the RABV antigen. Where a neutralisation assay is used, cross-neutralisation within phylogroup I and II must be considered when interpreting results. Consequently, the choice of challenge virus(es) used in the assay should be considered. It is advised that more than one challenge virus is used to determine the cross-neutralising potential of the test sera as described previously (232).

6.3. Benefits of using antigenic cartography to quantify lyssavirus antigenic variation

Antigenic relationships among lyssaviruses are difficult to quantify from genetic data or raw neutralising antibody titres alone as the antigenic data is limited by variation in antibody concentrations and populations present in sera. Antigenic cartography resolves this limitation by plotting sera and viruses relative to each other on an antigenic map; where the neutralisation profiles of sera with different antibody concentrations contribute to the viruses' position (24, 435).

Due to the interphylogroup cross-neutralisation detected between RABV (phylogroup I) and MOKV (phylogroup II), DUVV (phylogroup I) and SHIBV (phylogroup II), and SHIBV (phylogroup II) and IKOV (phylogroup III), the antibody titre required for neutralisation of diverse viruses can be extrapolated. In phylogroup III, IKOV exhibited

an average distance of 8.10 AU from the RABV isolates, WCBV a distance of 9.85 AU, and LLEBV a distance of 13.66 AU (Table 3.5). This would be equivalent to a 274-fold, 923-fold, an 12944-fold difference in neutralising antibody titre meaning approximately a 140 IU/ml, 4500 IU/ml, and 66300 IU/ml antibody titre in response to rabies vaccination would be required for neutralisation of these viruses, respectively. Phylogroup II viruses exhibited an antigenic distance range of 4.69-8.59 AU from RABV isolates, where MOKV exhibited the closest distance and LBV-C the furthest. This would be equivalent to a 26-fold and 385-fold difference in neutralising antibody titre meaning approximately a 26 IU/ml and 385 IU/ml antibody titre in response to rabies vaccination would be required for neutralisation of these viruses, respectively. Typically humans exhibit a range of 0.5 IU/ml to 40 IU/ml antibody titre in response to vaccination (522, 523). Therefore, vaccine protection against diverse viruses in phylogroup II and III, with the exception of MOKV, would be unlikely.

In addition, quantifying antigenic relationships enables an estimate of correlation between antigenicity and G protein amino acid sequence identity. In this study, the correlation between amino acid differences in the G protein ectodomain and the antigenic distances from the cartography maps was estimated ($r=0.81$, 95% CI 0.75 to 0.85, $P<0.001$) (Figure 3.20C) compared to previous studies investigating the correlation between amino acid differences in the G protein ectodomain and lyssavirus antigenic data ($r=0.85$, 95% CI 0.81 to 0.88, $P=0.001$; $r=92$, 95% CI -0.39 to 1.00, $p=0.08$) (24, 36).

Fitting a linear regression model to the data in this study determined that, on average, a 6% change in G protein ectodomain amino acid sequence identity (~25 amino acid substitutions) caused a one-unit change in antigenic difference. This is comparable to previous studies investigating lyssavirus antigenic diversity where a 4.8% change and a

5.5% change in amino acid sequence identity was reported to equate to a 1 AU change (24, 36). Whilst for FMDV serotype A viruses, correlation between antigenic distance and amino acid sequence identity of the P1 domain was low ($r=0.42$), it was also reported that a 5.7% amino acid change (42 amino acid substitutions) occurred for every change in antigenic unit (450). In contrast, studies of human influenza H3N2 viruses showed that a <1% change in amino acid sequence identity (2.9 amino acid substitutions) occurred for every change in antigenic unit (435).

The implication of the close antigenic relationships of the lyssaviruses in comparison to influenza viruses has prevented identification of specific amino acid substitutions common to closely antigenically-related lyssaviruses, such as those in the same antigenic cluster. These amino acid substitutions are known as cluster defining substitutions and have been defined for FMDV serotype A and various influenza H3N2 viruses (435, 450).

Specific cluster defining amino acid substitutions (or epitopes) may be identified in the future if a larger dataset including multiple isolates of the same lyssavirus species were included. However, it is also likely that the close antigenic relationship of the lyssaviruses, despite sufficient genetic variation relative to influenza viruses, is due to a low degree of positive selection in the lyssavirus G gene (135). For RABV, one hypothesis for low positive selection and the relative lack of non-synonymous variation is the genetic constraints imposed for broad cell tropism, analogous to the lack of non-synonymous variation of vector-borne RNA viruses that replicate in both vertebrate and invertebrate hosts (524). An alternative hypothesis is that RABV is not subject to the strong immune pressures that characterise other RNA viruses due to host immune evasion, the CNS being an immune privileged site, and a fatal disease outcome (524, 525). Finally, the evolution of RABV is also likely affected by stochastic effects, such

as population bottlenecks, which can affect the host species post transmission (524, 525). In fact, previous data has suggested that purifying selection is the main driving force for RABV viral adaption (135). It is questionable, however, whether these hypotheses for RABV can be applied to non-RABV lyssaviruses where restriction to a single host species is observed and infection does not always lead to death (134). This has been highlighted by recent evidence of seroprevalence against LBV, EBLV, DUVV, and potentially WCBV in healthy hosts (215, 219, 232, 526, 527).

6.4. Strategies for chimeric glycoprotein development

Cross neutralisation data and antigenic data support the concept of including RABV, LBV-D, IKOV, WCBV, and LLEBV in a pan-lyssavirus vaccine. This study explored the rational design and construction of chimeric G proteins with sequences derived from these five lyssaviruses. Three approaches were adopted for the generation of chimeric G proteins: the hinge-based approach, the mosaic-based approach, and the structure-based approach. Chimeric G proteins were designed such that antigenic sites were ‘balanced’ between the domains from different lyssavirus species.

One strategy not explored in this study was the antigenic site swap approach. First adapted by Evans and colleagues in 2018, chimeric RABV G proteins with antigenic site swapped singly and in combination with cognate sequences of LBV-B G protein were generated (38). Additionally, the reciprocal chimeras were generated with chimeric LBV-B G proteins with RABV antigenic sites swapped singly or all together. Previously, this strategy would have been an attractive approach given the considerable knowledge surrounding RABV antigenic sites at the time. However, two recent studies describing the co-crystallisation of two mAbs with RABV indicate that the current knowledge of the antigenic sites of RABV is limited (28, 29). Antigenic site III, defined

by amino acids 330-338, forms a loop on the protein surface and is the immunogenic epitope of mAb 523-11 (303, 439). Initially, it was hypothesised that mAb 523-11 binding was isolated to just these residues however co-crystallisation of this mAb with RABV G protein identified other antibody contacts with amino acid residues within and outside the predefined antigenic site III: 333, 336, 339-342, 346, 350, 368, 370, 376, and 384 (28). In addition, antigenic site I defined by amino acids 226-231 was previously determined to be the target for mAb RVC20 (471). Similarly, the antibody was shown to make contact with amino acid residues 42, 44, 47, 186-192, 194, and 225-231 on the RABV G protein (29). Whilst it is unlikely that every residue is required for antibody binding, these findings highlight the limited understanding of the RABV antigenic sites. Future avenues for antigenic site characterisation could involve re-examination of mAb binding in the new context of the RABV and MOKV crystallised structures. The assessment of mAbs with clinical significance, such as mAb 17C7 (RAB1), would provide new information surrounding RABV epitopes and antigenic sites (528, 529). These findings suggest that a critical epitope encoded on the RABV genome may span across multiple domains in the chimeric G proteins described in this study, however it is less likely than with the antigenic site swap chimeric G proteins.

6.5. Significance of *in vivo* vaccination-challenge experiments

Each approach resulted in successful pseudotype generation of at least one chimeric G protein construct and typically correlated with the sequence identity of the lyssavirus species that the chimeric G protein sequence was derived. However, of these chimeric G proteins, only one live virus was rescued. Whilst the Mosaic 2 G resulted in the highest titre of pseudotype virus and subsequently indicated that the recombinant G protein was functional, it is unclear why constructs with similarly high titres of pseudotype virus did not show biological function. As the single surface protein, the G protein is involved in

trimerisation, receptor binding, and membrane fusion. The successful generation of pseudotype virus, subsequent cell infection, and reporter gene expression suggests that the chimeric G proteins are successfully expressed, trafficked to the cell surface, and facilitate pseudotype virus infection through cell receptor binding. In addition, a previous study which described the design and rescue of similar viruses expressing either RABV/MOKV/RABV G or MOKV/RABV/MOKV G showed that whilst both G proteins were trafficked to the cell surface, only RABV/MOKV/RABV G (Lyssavax) facilitated the rescue of live virus (483).

The evidence suggests that functional rather than structural implications prevented viral recovery of these constructs and the subsequent production of virus particles expressing chimeric G proteins. It is possible that the chimeric G proteins that did not facilitate virus rescue formed a structure that is able to be efficiently expressed on the cell surface and interact with the HIV matrix (p24) but unable to interact optimally with the cSN matrix protein. Alternatively, optimisation of the virus rescue protocol could facilitate virus rescue as discussed previously in section 5.7.

In addition, constructs expressing chimeric G proteins could be cloned to express an epitope tag (28, 530, 531). This would enable staining of transfected cells to assess the cellular location of G proteins. Alternatively, to accurately determine whether a G protein is functional, future work could involve assessment using a cell-based syncytia formation assay where cells would be transfected with a plasmid encoding a chimeric G protein and incubated for 18-24 hours to allow time for protein expression. Following incubation, functional G proteins would induce syncytia formation, visible under a light microscope, after incubation with a low pH buffer (28, 532, 533).

After extensively testing LBV-D and cSN-Mosaic2 on serological assays, vaccine-challenge experiments were designed to determine whether these antigens elicited cross-protection against *in vivo* challenge with phylogroup II viruses.

Post-vaccination serology demonstrated the robust functionality of the VNAs induced by inactivated cSN-Mosaic2 and inactivated LBV-D as titres, on average, were ≥ 250 -fold higher and ≥ 38 -fold higher than the 0.5 IU/ml cut off, respectively. However, despite high titres, survival was not as high as predicted. Survival proportions were low against the homologous virus, potentially indicating too high a lethal dose for the virus challenge. *In vivo* vaccination-challenge experiments are limited in this way as the correct challenge dose would ensure adequate challenge for vaccinated mice but also ensure controls succumb to infection. However, the data from the survival curves indicated notable differences between survivorship and disease onset in vaccinated and mock vaccinated mice. Overall, based on the results from Chapter 5, the engineered cSN-Mosaic2 virus was a more efficacious vaccine candidate than wildtype LBV-D, analogous to previous studies that have shown that mosaic proteins induce greater cross-reactivity than consensus sequence and wildtype antigens (436, 509). Whilst in this case the challenge dose may have been too high, the survival proportions of LBV-D vaccinated mice challenged with LBV-A, LBV-C, LBV-D, and MOKV were the same. This suggests that inactivated LBV-D affords similar cross-protection against LBV-A, LBV-C, and MOKV to the homologous virus LBV-D, similar to the cross-neutralisation data in Chapter 3.

6.6. Further work

Further work involving cross-neutralisation assays and antigenic cartography would include more virus isolates per lyssavirus species and more lyssavirus-specific sera per virus. This would enable production of antigenic maps with increased accuracy as more data would contribute to the positioning of the virus isolates and sera. Previously, antigenic relationships between diverse RABV strains and other lyssavirus species have been explored (24), however since 2010 more lyssavirus species have been detected. As a result, it would be of interest to assess diverse RABV strains against the panel of lyssaviruses used in this study. Additionally, specific regions or specific amino acid residues on the virus G protein could be identified to cause antigenic variation between lyssaviruses.

Further, building on previous research describing mAb escape mutants (117), using the reverse genetics system to rescue live recombinant viruses, cross-neutralisation and antigenic cartography could test the antigenic effect of recombinant viruses with specific amino acid substitutions. This approach could test assumptions and identify/map specific epitopes contributing to increased and disproportionate variation across the genus.

In addition, further work investigating the pathogenicity of TWBLV *in vivo* would be warranted as a naturally occurring apathogenic virus has not been documented for the lyssavirus species. The non codon-optimised clone generated in section 4.7 or the wildtype isolates would be good candidates for investigation.

Finally, comparison of serological responses from species of clinical interest would be of value. As the host reservoir species for the majority of lyssaviruses are bat species and spillover events commonly involve cats, assessing the serological response from

these species would provide invaluable insight into seroprevalence and antigenic variation of circulating lyssaviruses (6, 236, 534-536). Due to the low blood volume of bats and the likely scarce source of sera from cats suspected to be infected with a lyssavirus, microneutralisation assays or pseudotype virus neutralisation assays would provide a viable alternative to FAVN or mFAVN assays (394).

In addition to the assessment of sera from clinically significant species, chimeric G protein constructs that facilitated pseudotype virus generation could also be assessed using a pseudotype virus neutralisation assay (38, 394). This would facilitate the assessment of chimeric G protein constructs that failed to produce viable virus in this study. Additionally, pseudotype viruses can be inactivated and used as inocula for the production of specific sera. Specific sera generated against pseudotype viruses expressing chimeric G proteins would enable assessment of cross-neutralisation.

Nevertheless, virus rescue of more recombinant viruses expressing chimeric G proteins would be of value. Further work involving virus rescue protocol optimisation or the use of alternative systems to cSN, such as pHEP-1.0, pHEP-3.0 or pRC-HL(+) , could facilitate this (537, 538). Alternatively, where chimeric G protein constructs facilitated pseudotype virus generation but not live virus rescue, subunit vaccines, viral vector vaccines, or mRNA vaccines could provide an economically viable alternative (539-543).

Finally, to fully assess cross-protection among wildtype and recombinant lyssaviruses, the lethal challenge dose for phylogroup II and III viruses would need to be defined. This would enable reliable *in vivo* vaccination-challenge experiments, allowing the identification of pan-lyssavirus vaccine candidates in animal models.

6.7. Summary of conclusions

In conclusion, cross-neutralisation data and antigenic cartography have provided further rationale for classification into phylogroups based on antigenic and genetic variation. The results of this study suggest that, due to the complete lack of cross-neutralisation, divergent lyssaviruses, WCBV, IKOV, and LLEBV be assigned to phylogroup III, IV, and V, respectively. In addition, the rabies vaccine, Verorab, induces a cross-neutralising antibody response against phylogroup I, including cSN-TWBLV *in vitro*, and confers protection against cSN-KBLV *in vivo*. Serological cut-offs were defined for each of the phylogroup I viruses, indicating the titre of neutralising antibodies required for neutralisation. For personnel in high-risk occupations, these cut-offs may be accepted as proof of seroconversion against non-RABV phylogroup I lyssaviruses.

LBV-D-specific sera cross-neutralises all members of phylogroup II and survival proportions of LBV-D vaccinated mice were the same against challenge with LBV-A, LBV-C, LBV-D, and MOKV. Consequently, based on the results of this study, five lyssavirus G proteins (RABV, LBV-D, IKOV, LLEBV, and WCBV) would need to be included in a universal pan-lyssavirus vaccine for human use.

Finally, a panel of chimeric G protein constructs were meticulously designed using a range of approaches. A number of these constructs facilitated the generation of pseudotype viruses and one construct facilitated the generation of a live recombinant virus. When inactivated and used as a vaccine as part of an *in vivo* vaccination-challenge experiment, cSN-Mosaic2 induced a strong neutralising response post vaccination however survival proportions were variable following virus challenge with phylogroup II viruses.

Studies with lyssavirus-specific sera and chimeric G proteins presented here have highlighted the antigenic complexities across the lyssavirus genus and provide an insight into the future development of pan-lyssavirus biologicals.

Bibliography

1. Kuhn JH, Adkins S, Alioto D, Alkhovsky SV, Amarasinghe GK, Anthony SJ, et al. 2020 taxonomic update for phylum Negarnaviricota (Riboviria: Orthornavirae), including the large orders Bunyavirales and Mononegavirales. *Archives of Virology*. 2020;165(12):3023-72.
2. Rupprecht C, Kuzmin I, Meslin F. Lyssaviruses and rabies: current conundrums, concerns, contradictions and controversies. *F1000Res*. 2017;6:184.
3. Walker PJ, Siddell SG, Lefkowitz EJ, Mushegian AR, Adriaenssens EM, Dempsey DM, et al. Changes to virus taxonomy and the Statutes ratified by the International Committee on Taxonomy of Viruses (2020). *Archives of Virology*. 2020;165(11):2737-48.
4. Marston DA, Horton DL, Ngeleja C, Hampson K, McElhinney LM, Banyard AC, et al. Ikoma lyssavirus, highly divergent novel lyssavirus in an African civet. *Emerg Infect Dis*. 2012;18(4):664-7.
5. Shope RE, Murphy FA, Harrison AK, Causey OR, Kemp GE, Simpson DI, et al. Two African viruses serologically and morphologically related to rabies virus. *J Virol*. 1970;6(5):690-2.
6. Kgaladi J, Wright N, Coertse J, Markotter W, Marston D, Fooks AR, et al. Diversity and epidemiology of Mokola virus. *PLoS neglected tropical diseases*. 2013;7(10):e2511.
7. Fooks AR, Cliquet F, Finke S, Freuling C, Hemachudha T, Mani RS, et al. Rabies. *Nat Rev Dis Primers*. 2017;3:17091.
8. Jackson AC, Fu, Z.F. Scientific basis of the disease and its management. In: A.C. J, editor. *Rabies*. San Diego: Elsevier-Academic Press; 2013. p. 299-349.
9. Jackson AC. Rabies pathogenesis. *J Neurovirol*. 2002;8(4):267-9.
10. Townsend SE, Lembo T, Cleaveland S, Meslin FX, Miranda ME, Putra AA, et al. Surveillance guidelines for disease elimination: a case study of canine rabies. *Comp Immunol Microbiol Infect Dis*. 2013;36(3):249-61.
11. Fooks AR, Banyard AC, Horton DL, Johnson N, McElhinney LM, Jackson AC. Current status of rabies and prospects for elimination. *Lancet*. 2014;384(9951):1389-99.
12. World Health O. WHO Expert Consultation on Rabies. Second report. World Health Organ Tech Rep Ser. 2013(982):1-139, back cover.
13. Warrell MJ. The dilemma of managing human rabies encephalitis. *Trop Med Int Health*. 2016;21(4):456-7.
14. Mallewa M, Fooks AR, Banda D, Chikungwa P, Mankhambo L, Molyneux E, et al. Rabies encephalitis in malaria-endemic area, Malawi, Africa. *Emerg Infect Dis*. 2007;13(1):136-9.
15. Knobel DL, Cleaveland S, Coleman PG, Fevre EM, Meltzer MI, Miranda ME, et al. Re-evaluating the burden of rabies in Africa and Asia. *Bull World Health Organ*. 2005;83(5):360-8.
16. Jennings D, Marston, D., Banyard, A. and Fooks, A. *Rhabdoviruses* 2017.
17. Banerjee AK, Barik S, De BP. Gene expression of nonsegmented negative strand RNA viruses. *Pharmacol Ther*. 1991;51(1):47-70.
18. Dietzgen RG, Kondo H, Goodin MM, Kurath G, Vasilakis N. The family Rhabdoviridae: mono- and bipartite negative-sense RNA viruses with diverse genome organization and common evolutionary origins. *Virus Res*. 2017;227:158-70.
19. Nokireki T, Tammiranta N, Kokkonen UM, Kantala T, Gadd T. Tentative novel lyssavirus in a bat in Finland. *Transbound Emerg Dis*. 2018;65(3):593-6.
20. Coertse J, Grobler CS, Sabeta CT, Seamark ECJ, Kearney T, Paweska JT, et al. Lyssaviruses in Insectivorous Bats, South Africa, 2003-2018. *Emerg Infect Dis*. 2020;26(12):3056-60.
21. Kuzmin IV, Wu X, Tordo N, Rupprecht CE. Complete genomes of Aravan, Khujand, Irkut and West Caucasian bat viruses, with special attention to the polymerase gene and non-coding regions. *Virus research*. 2008;136(1-2):81-90.
22. Healy D, Banyard A, Fooks A. *Rhabdoviruses*. In eLS. Chichester: John Wiley & Sons Ltd. [http://doi.org/10.1002/9780470015902 ...](http://doi.org/10.1002/9780470015902...); 2013.

23. Evans JS, Wu G, Selden D, Buczkowski H, Thorne L, Fooks AR, et al. Utilisation of Chimeric Lyssaviruses to Assess Vaccine Protection against Highly Divergent Lyssaviruses. *Viruses*. 2018;10(3).
24. Horton DL, McElhinney LM, Marston DA, Wood JLN, Russell CA, Lewis N, et al. Quantifying Antigenic Relationships among the Lyssaviruses. *Journal of Virology*. 2010;84(22):11841-8.
25. Fooks A. The challenge of new and emerging lyssaviruses. Taylor & Francis; 2004.
26. Benmansour A, Leblois H, Coulon P, Tuffereau C, Gaudin Y, Flamand A, et al. Antigenicity of rabies virus glycoprotein. *J Virol*. 1991;65(8):4198-203.
27. Belot L, Ouldali M, Roche S, Legrand P, Gaudin Y, Albertini AA. Crystal structure of Mokola virus glycoprotein in its post-fusion conformation. *PLoS Pathog*. 2020;16(3):e1008383.
28. Yang F, Lin S, Ye F, Yang J, Qi J, Chen Z, et al. Structural Analysis of Rabies Virus Glycoprotein Reveals pH-Dependent Conformational Changes and Interactions with a Neutralizing Antibody. *Cell Host Microbe*. 2020;27(3):441-53 e7.
29. Hellert J, Buchrieser J, Larrous F, Minola A, de Melo GD, Soriaga L, et al. Structure of the prefusion-locking broadly neutralizing antibody RVC20 bound to the rabies virus glycoprotein. *Nat Commun*. 2020;11(1):596.
30. Bunn TO, Ridpath HD. The relationship between rabies antibody titres in dogs and cats and protection from challenge. No. 11, U. S. Department of Health, Education and Welfare, Public Health.1984. p. 43-5.
31. Bogel K, editor Proposed International Reference Rabies Vaccine (HDC-Origin) and the potency tests used to test these products. Joint WHO/IABS Symposium on the Standardization of Rabies Vaccines for Human Use Produced in Tissue Culture [Rabies III] Karger; 1978.
32. Moore SM, Hanlon CA. Rabies-specific antibodies: measuring surrogates of protection against a fatal disease. *PLoS Negl Trop Dis*. 2010;4(3):e595.
33. Nolden T, Banyard AC, Finke S, Fooks AR, Hanke D, Hoper D, et al. Comparative studies on the genetic, antigenic and pathogenic characteristics of Bokeloh bat lyssavirus. *J Gen Virol*. 2014;95(Pt 8):1647-53.
34. Hanlon CA, Kuzmin IV, Blanton JD, Weldon WC, Manangan JS, Rupprecht CE. Efficacy of rabies biologics against new lyssaviruses from Eurasia. *Virus Res*. 2005;111(1):44-54.
35. Brookes SM, Healy DM, Fooks AR. Ability of rabies vaccine strains to elicit cross-neutralising antibodies. *Dev Biol (Basel)*. 2006;125:185-93.
36. Badrane H, Bahloul C, Perrin P, Tordo N. Evidence of two Lyssavirus phylogroups with distinct pathogenicity and immunogenicity. *J Virol*. 2001;75(7):3268-76.
37. Horton DL, Banyard AC, Marston DA, Wise E, Selden D, Nunez A, et al. Antigenic and genetic characterization of a divergent African virus, Ikoma lyssavirus. *J Gen Virol*. 2014;95(Pt 5):1025-32.
38. Evans JS, Selden D, Wu G, Wright E, Horton DL, Fooks AR, et al. Antigenic site changes in the rabies virus glycoprotein dictates functionality and neutralizing capability against divergent lyssaviruses. *J Gen Virol*. 2018;99(2):169-80.
39. Banyard AC, Selden D, Wu G, Thorne L, Jennings D, Marston D, et al. Isolation, antigenicity and immunogenicity of Lleida bat lyssavirus. *J Gen Virol*. 2018.
40. Warrell MJ, Warrell DA. Rabies and other lyssavirus diseases. *Lancet*. 2004;363(9413):959-69.
41. Riedel C, Vasishtan D, Prazak V, Ghanem A, Conzelmann KK, Rumenapf T. Cryo EM structure of the rabies virus ribonucleoprotein complex. *Sci Rep*. 2019;9(1):9639.
42. Marston DA, McElhinney LM, Johnson N, Muller T, Conzelmann KK, Tordo N, et al. Comparative analysis of the full genome sequence of European bat lyssavirus type 1 and type 2 with other lyssaviruses and evidence for a conserved transcription termination and polyadenylation motif in the G-L 3' non-translated region. *J Gen Virol*. 2007;88(Pt 4):1302-14.
43. Banerjee AK. Transcription and replication of rhabdoviruses. *Microbiol Rev*. 1987;51(1):66-87.

44. Hodges EN, Heinrich BS, Connor JH. A Vesiculovirus Showing a Steepened Transcription Gradient and Dominant trans-Repression of Virus Transcription. *Journal of Virology*. 2012;86(16):8884-9.
45. Flamand A, Raux H, Gaudin Y, Ruigrok RW. Mechanisms of rabies virus neutralization. *Virology*. 1993;194(1):302-13.
46. Finke S, Conzelmann KK. Ambisense gene expression from recombinant rabies virus: random packaging of positive- and negative-strand ribonucleoprotein complexes into rabies virions. *J Virol*. 1997;71(10):7281-8.
47. Conzelmann KK, Cox JH, Thiel HJ. An L (polymerase)-deficient rabies virus defective interfering particle RNA is replicated and transcribed by heterologous helper virus L proteins. *Virology*. 1991;184(2):655-63.
48. Marriott AC, Dimmock NJ. Defective interfering viruses and their potential as antiviral agents. *Reviews in Medical Virology*. 2010;20(1):51-62.
49. Lazzarini RA, Keene JD, Schubert M. The origins of defective interfering particles of the negative-strand RNA viruses. *Cell*. 1981;26(2, Part 2):145-54.
50. Clark HF, Parks NF, Wunner WH. Defective interfering particles of fixed rabies viruses: lack of correlation with attenuation or auto-interference in mice. *J Gen Virol*. 1981;52(Pt 2):245-58.
51. Wunner WH, Clark HF. Regeneration of DI particles of virulent and attenuated rabies virus: genome characterization and lack of correlation with virulence phenotype. *J Gen Virol*. 1980;51(Pt 1):69-81.
52. Wiktor TJ, Dietzschold B, Leamson RN, Koprowski H. Induction and biological properties of defective interfering particles of rabies virus. *J Virol*. 1977;21(2):626-35.
53. Mannen K, Hiramatsu K, Mifune K, Sakamoto S. Conserved nucleotide sequence of rabies virus cDNA encoding the nucleoprotein. *Virus Genes*. 1991;5(1):69-73.
54. Johnson N, McElhinney LM, Smith J, Lowings P, Fooks AR. Phylogenetic comparison of the genus *Lyssavirus* using distal coding sequences of the glycoprotein and nucleoprotein genes. *Arch Virol*. 2002;147(11):2111-23.
55. Kuzmin IV, Hughes GJ, Botvinkin AD, Orciari LA, Rupprecht CE. Phylogenetic relationships of Irkut and West Caucasian bat viruses within the *Lyssavirus* genus and suggested quantitative criteria based on the N gene sequence for *lyssavirus* genotype definition. *Virus Res*. 2005;111(1):28-43.
56. Kissi B, Tordo N, Bourhy H. Genetic polymorphism in the rabies virus nucleoprotein gene. *Virology*. 1995;209(2):526-37.
57. Bourhy H, Kissi B, Tordo N. Molecular diversity of the *Lyssavirus* genus. *Virology*. 1993;194(1):70-81.
58. Sacramento D, Bourhy H, Tordo N. PCR technique as an alternative method for diagnosis and molecular epidemiology of rabies virus. *Mol Cell Probes*. 1991;5(3):229-40.
59. Delmas O, Holmes EC, Talbi C, Larrous F, Dacheux L, Bouchier C, et al. Genomic Diversity and Evolution of the *Lyssaviruses*. *PLOS ONE*. 2008;3(4):e2057.
60. Majumder A, Basak S, Raha T, Chowdhury SP, Chattopadhyay D, Roy S. Effect of osmolytes and chaperone-like action of P-protein on folding of nucleocapsid protein of Chandipura virus. *J Biol Chem*. 2001;276(33):30948-55.
61. Toriumi H, Kawai A. Association of rabies virus nominal phosphoprotein (P) with viral nucleocapsid (NC) is enhanced by phosphorylation of the viral nucleoprotein (N). *Microbiol Immunol*. 2004;48(5):399-409.
62. Schnell MJ, McGettigan JP, Wirblich C, Papaneri A. The cell biology of rabies virus: using stealth to reach the brain. *Nat Rev Microbiol*. 2010;8(1):51-61.
63. Whelan SP, Barr JN, Wertz GW. Transcription and replication of nonsegmented negative-strand RNA viruses. *Curr Top Microbiol Immunol*. 2004;283:61-119.
64. Faul EJ, Lyles DS, Schnell MJ. Interferon response and viral evasion by members of the family *rhabdoviridae*. *Viruses*. 2009;1(3):832-51.

65. Tordo N. Characteristics and molecular biology of the rabies virus. *Laboratory techniques in rabies*. 1996;40.
66. Okada K, Ito N, Yamaoka S, Masatani T, Ebihara H, Goto H, et al. Roles of the Rabies Virus Phosphoprotein Isoforms in Pathogenesis. *J Virol*. 2016;90(18):8226-37.
67. Ding H, Green TJ, Lu S, Luo M. Crystal structure of the oligomerization domain of the phosphoprotein of vesicular stomatitis virus. *Journal of virology*. 2006;80(6):2808-14.
68. Gerard FC, Ribeiro Ede A, Jr., Leyrat C, Ivanov I, Blondel D, Longhi S, et al. Modular organization of rabies virus phosphoprotein. *J Mol Biol*. 2009;388(5):978-96.
69. Chenik M, Chebli K, Gaudin Y, Blondel D. In vivo interaction of rabies virus phosphoprotein (P) and nucleoprotein (N): existence of two N-binding sites on P protein. *J Gen Virol*. 1994;75 (Pt 11):2889-96.
70. Fu ZF, Zheng Y, Wunner WH, Koprowski H, Dietzschold B. Both the N- and the C-terminal domains of the nominal phosphoprotein of rabies virus are involved in binding to the nucleoprotein. *Virology*. 1994;200(2):590-7.
71. Tan GS, Preuss MA, Williams JC, Schnell MJ. The dynein light chain 8 binding motif of rabies virus phosphoprotein promotes efficient viral transcription. *Proc Natl Acad Sci U S A*. 2007;104(17):7229-34.
72. Gigant B, Iseni F, Gaudin Y, Knossow M, Blondel D. Neither phosphorylation nor the amino-terminal part of rabies virus phosphoprotein is required for its oligomerization. *J Gen Virol*. 2000;81(Pt 7):1757-61.
73. Gupta AK, Blondel D, Choudhary S, Banerjee AK. The phosphoprotein of rabies virus is phosphorylated by a unique cellular protein kinase and specific isomers of protein kinase C. *J Virol*. 2000;74(1):91-8.
74. Gillet JP, Derer P, Tsiang H. Axonal transport of rabies virus in the central nervous system of the rat. *J Neuropathol Exp Neurol*. 1986;45(6):619-34.
75. Jacob Y, Badrane H, Ceccaldi PE, Tordo N. Cytoplasmic dynein LC8 interacts with lyssavirus phosphoprotein. *J Virol*. 2000;74(21):10217-22.
76. Rasalingam P, Rossiter JP, Mebatsion T, Jackson AC. Comparative pathogenesis of the SAD-L16 strain of rabies virus and a mutant modifying the dynein light chain binding site of the rabies virus phosphoprotein in young mice. *Virus Res*. 2005;111(1):55-60.
77. Li Y, Dong W, Shi Y, Deng F, Chen X, Wan C, et al. Rabies virus phosphoprotein interacts with ribosomal protein L9 and affects rabies virus replication. *Virology*. 2016;488:216-24.
78. Kammouni W, Wood H, Saleh A, Appolinario CM, Fernyhough P, Jackson AC. Rabies virus phosphoprotein interacts with mitochondrial Complex I and induces mitochondrial dysfunction and oxidative stress. *J Neurovirol*. 2015;21(4):370-82.
79. Fouquet B, Nikolic J, Larrous F, Bourhy H, Wirblich C, Lagaudriere-Gesbert C, et al. Focal adhesion kinase is involved in rabies virus infection through its interaction with viral phosphoprotein P. *J Virol*. 2015;89(3):1640-51.
80. Wiltzer L, Larrous F, Oksayan S, Ito N, Marsh GA, Wang LF, et al. Conservation of a unique mechanism of immune evasion across the Lyssavirus genus. *J Virol*. 2012;86(18):10194-9.
81. Wiltzer L, Okada K, Yamaoka S, Larrous F, Kuusisto HV, Sugiyama M, et al. Interaction of Rabies Virus P-Protein With STAT Proteins is Critical to Lethal Rabies Disease. *The Journal of Infectious Diseases*. 2014;209(11):1744-53.
82. Brzozka K, Finke S, Conzelmann KK. Inhibition of interferon signaling by rabies virus phosphoprotein P: activation-dependent binding of STAT1 and STAT2. *J Virol*. 2006;80(6):2675-83.
83. Lenard J. Negative-strand virus M and retrovirus MA proteins: all in a family? *Virology*. 1996;216(2):289-98.
84. Graham SC, Assenberg R, Delmas O, Verma A, Gholami A, Talbi C, et al. Rhabdovirus matrix protein structures reveal a novel mode of self-association. *PLoS pathogens*. 2008;4(12):e1000251.

85. Mebatsion T, Weiland F, Conzelmann KK. Matrix protein of rabies virus is responsible for the assembly and budding of bullet-shaped particles and interacts with the transmembrane spike glycoprotein G. *J Virol.* 1999;73(1):242-50.
86. Harty RN, Brown ME, McGettigan JP, Wang G, Jayakar HR, Huibregtse JM, et al. Rhabdoviruses and the cellular ubiquitin-proteasome system: a budding interaction. *J Virol.* 2001;75(22):10623-9.
87. Harty RN, Paragas J, Sudol M, Palese P. A proline-rich motif within the matrix protein of vesicular stomatitis virus and rabies virus interacts with WW domains of cellular proteins: implications for viral budding. *J Virol.* 1999;73(4):2921-9.
88. Irie T, Licata JM, Jayakar HR, Whitt MA, Bell P, Harty RN. Functional analysis of late-budding domain activity associated with the PSAP motif within the vesicular stomatitis virus M protein. *Journal of virology.* 2004;78(14):7823-7.
89. Schöneberg J, Lee I-H, Iwasa JH, Hurley JH. Reverse-topology membrane scission by the ESCRT proteins. *Nature Reviews Molecular Cell Biology.* 2017;18(1):5-17.
90. Mebatsion T, König M, Conzelmann KK. Budding of rabies virus particles in the absence of the spike glycoprotein. *Cell.* 1996;84(6):941-51.
91. Mebatsion T, Schnell MJ, Conzelmann KK. Mokola virus glycoprotein and chimeric proteins can replace rabies virus glycoprotein in the rescue of infectious defective rabies virus particles. *J Virol.* 1995;69(3):1444-51.
92. Morimoto K, Foley HD, McGettigan JP, Schnell MJ, Dietzschold B. Reinvestigation of the role of the rabies virus glycoprotein in viral pathogenesis using a reverse genetics approach. *J Neurovirol.* 2000;6(5):373-81.
93. Marston DA, McElhinney LM, Banyard AC, Horton DL, Nunez A, Koser ML, et al. Interspecies protein substitution to investigate the role of the lyssavirus glycoprotein. *J Gen Virol.* 2013;94(Pt 2):284-92.
94. Finke S, Mueller-Waldeck R, Conzelmann KK. Rabies virus matrix protein regulates the balance of virus transcription and replication. *J Gen Virol.* 2003;84(Pt 6):1613-21.
95. Clinton GM, Little SP, Hagen FS, Huang AS. The matrix (M) protein of vesicular stomatitis virus regulates transcription. *Cell.* 1978;15(4):1455-62.
96. Liu X, Li F, Zhang J, Wang L, Wang J, Wen Z, et al. The ATPase ATP6V1A facilitates rabies virus replication by promoting virion uncoating and interacting with the viral matrix protein. *The Journal of biological chemistry.* 2020;296:100096.
97. Kassis R, Larrous F, Estaquier J, Bourhy H. Lyssavirus matrix protein induces apoptosis by a TRAIL-dependent mechanism involving caspase-8 activation. *J Virol.* 2004;78(12):6543-55.
98. Komarova AV, Real E, Borman AM, Brocard M, England P, Tordo N, et al. Rabies virus matrix protein interplay with eIF3, new insights into rabies virus pathogenesis. *Nucleic Acids Res.* 2007;35(5):1522-32.
99. Klepfer SR, Debouck C, Uffelman J, Jacobs P, Bollen A, Jones EV. Characterization of rabies glycoprotein expressed in yeast. *Arch Virol.* 1993;128(3-4):269-86.
100. Langevin C, Jaaro H, Bressanelli S, Fainzilber M, Tuffereau C. Rabies virus glycoprotein (RVG) is a trimeric ligand for the N-terminal cysteine-rich domain of the mammalian p75 neurotrophin receptor. *J Biol Chem.* 2002;277(40):37655-62.
101. Conzelmann KK, Cox JH, Schneider LG, Thiel HJ. Molecular cloning and complete nucleotide sequence of the attenuated rabies virus SAD B19. *Virology.* 1990;175(2):485-99.
102. Tordo N, Poch O, Ermine A, Keith G, Rougeon F. Completion of the rabies virus genome sequence determination: highly conserved domains among the L (polymerase) proteins of unsegmented negative-strand RNA viruses. *Virology.* 1988;165(2):565-76.
103. Zagouras P, Ruusala A, Rose JK. Dissociation and reassociation of oligomeric viral glycoprotein subunits in the endoplasmic reticulum. *Journal of virology.* 1991;65(4):1976-84.
104. Lyles DS, McKenzie M, Parce JW. Subunit interactions of vesicular stomatitis virus envelope glycoprotein stabilized by binding to viral matrix protein. *Journal of virology.* 1992;66(1):349-58.

105. Gaudin Y, Ruigrok RW, Tuffereau C, Knossow M, Flamand A. Rabies virus glycoprotein is a trimer. *Virology*. 1992;187(2):627-32.
106. Rupprecht CE, Gibbons RV. Clinical practice. Prophylaxis against rabies. *N Engl J Med*. 2004;351(25):2626-35.
107. Yousaf MZ, Qasim M, Zia S, Khan M, Ashfaq UA, Khan S. Rabies molecular virology, diagnosis, prevention and treatment. *Virol J*. 2012;9:50.
108. Gaudin Y, Ruigrok RW, Knossow M, Flamand A. Low-pH conformational changes of rabies virus glycoprotein and their role in membrane fusion. *J Virol*. 1993;67(3):1365-72.
109. Durrer P, Gaudin Y, Ruigrok RW, Graf R, Brunner J. Photolabeling identifies a putative fusion domain in the envelope glycoprotein of rabies and vesicular stomatitis viruses. *J Biol Chem*. 1995;270(29):17575-81.
110. Dietzschold B, Wiktor TJ, Macfarlan R, Varrichio A. Antigenic structure of rabies virus glycoprotein: ordering and immunological characterization of the large CNBr cleavage fragments. *J Virol*. 1982;44(2):595-602.
111. Wiktor TJ. Historical aspects of rabies treatment. *World's debt to Pasteur*. 1985.
112. Macfarlan RI, Dietzschold B, Koprowski H. Stimulation of cytotoxic T-lymphocyte responses by rabies virus glycoprotein and identification of an immunodominant domain. *Mol Immunol*. 1986;23(7):733-41.
113. Faber M, Faber ML, Papaneri A, Bette M, Weihe E, Dietzschold B, et al. A single amino acid change in rabies virus glycoprotein increases virus spread and enhances virus pathogenicity. *J Virol*. 2005;79(22):14141-8.
114. Yan X, Mohankumar PS, Dietzschold B, Schnell MJ, Fu ZF. The rabies virus glycoprotein determines the distribution of different rabies virus strains in the brain. *J Neurovirol*. 2002;8(4):345-52.
115. Evans JS, Horton DL, Easton AJ, Fooks AR, Banyard AC. Rabies virus vaccines: is there a need for a pan-lyssavirus vaccine? *Vaccine*. 2012;30(52):7447-54.
116. Lafon M, Wiktor TJ, Macfarlan RI. Antigenic sites on the CVS rabies virus glycoprotein: analysis with monoclonal antibodies. *J Gen Virol*. 1983;64 (Pt 4):843-51.
117. Muller T, Dietzschold B, Ertl H, Fooks AR, Freuling C, Fehlner-Gardiner C, et al. Development of a mouse monoclonal antibody cocktail for post-exposure rabies prophylaxis in humans. *PLoS Negl Trop Dis*. 2009;3(11):e542.
118. Prehaud C, Coulon P, LaFay F, Thiers C, Flamand A. Antigenic site II of the rabies virus glycoprotein: structure and role in viral virulence. *J Virol*. 1988;62(1):1-7.
119. Seif I, Coulon P, Rollin PE, Flamand A. Rabies virulence: effect on pathogenicity and sequence characterization of rabies virus mutations affecting antigenic site III of the glycoprotein. *J Virol*. 1985;53(3):926-34.
120. Ni Y, Tominaga Y, Honda Y, Morimoto K, Sakamoto S, Kawai A. Mapping and characterization of a sequential epitope on the rabies virus glycoprotein which is recognized by a neutralizing monoclonal antibody, RG719. *Microbiol Immunol*. 1995;39(9):693-702.
121. Both L, van Dolleweerd C, Wright E, Banyard AC, Bulmer-Thomas B, Selden D, et al. Production, characterization, and antigen specificity of recombinant 62-71-3, a candidate monoclonal antibody for rabies prophylaxis in humans. *FASEB J*. 2013;27(5):2055-65.
122. Liu Y, Chen Q, Zhang F, Zhang S, Li N, Lian H, et al. Evaluation of rabies biologics against Irkut virus isolated in China. *J Clin Microbiol*. 2013;51(11):3499-504.
123. Koser ML, McGettigan JP, Tan GS, Smith ME, Koprowski H, Dietzschold B, et al. Rabies virus nucleoprotein as a carrier for foreign antigens. *Proc Natl Acad Sci U S A*. 2004;101(25):9405-10.
124. Morin B, Liang B, Gardner E, Ross RA, Whelan SP. An In Vitro RNA Synthesis Assay for Rabies Virus Defines Ribonucleoprotein Interactions Critical for Polymerase Activity. *J Virol*. 2017;91(1).
125. Ogino M, Ito N, Sugiyama M, Ogino T. The Rabies Virus L Protein Catalyzes mRNA Capping with GDP Polyribonucleotidyltransferase Activity. *Viruses*. 2016;8(5).

126. Abraham G, Rhodes DP, Banerjee AK. The 5' terminal structure of the methylated mRNA synthesized in vitro by vesicular stomatitis virus. *Cell*. 1975;5(1):51-8.
127. Poch O, Blumberg BM, Bougueleret L, Tordo N. Sequence comparison of five polymerases (L proteins) of unsegmented negative-strand RNA viruses: theoretical assignment of functional domains. *Journal of General Virology*. 1990;71(5):1153-62.
128. Rahmeh AA, Schenk AD, Danek EI, Kranzusch PJ, Liang B, Walz T, et al. Molecular architecture of the vesicular stomatitis virus RNA polymerase. *Proceedings of the National Academy of Sciences of the United States of America*. 2010;107(46):20075-80.
129. Vignuzzi M, Stone JK, Arnold JJ, Cameron CE, Andino R. Quasispecies diversity determines pathogenesis through cooperative interactions within a viral population. *Nature*. 2006;439(7074):344-8.
130. Holmes EC, Moya A. Is the quasispecies concept relevant to RNA viruses? *Journal of Virology*. 2002;76(1):460-2.
131. Domingo E. Genetic variation and quasi-species. *Current Opinion in Genetics & Development*. 1992;2(1):61-3.
132. Morimoto K, Hooper DC, Carbaugh H, Fu ZF, Koprowski H, Dietzschold B. Rabies virus quasispecies: Implications for pathogenesis. *Proceedings of the National Academy of Sciences*. 1998;95(6):3152-6.
133. Benmansour A, Brahimi M, Tuffereau C, Coulon P, Lafay F, Flamand A. Rapid sequence evolution of street rabies glycoprotein is related to the highly heterogeneous nature of the viral population. *Virology*. 1992;187(1):33-45.
134. Marston DA, Banyard AC, McElhinney LM, Freuling CM, Finke S, de Lamballerie X, et al. The lyssavirus host-specificity conundrum-rabies virus-the exception not the rule. *Curr Opin Virol*. 2018;28:68-73.
135. Marston DA, Horton DL, Nunez J, Ellis RJ, Orton RJ, Johnson N, et al. Genetic analysis of a rabies virus host shift event reveals within-host viral dynamics in a new host. *Virus Evol*. 2017;3(2):vex038.
136. Dockter J, Evans CF, Tishon A, Oldstone M. Competitive selection in vivo by a cell for one variant over another: implications for RNA virus quasispecies in vivo. *Journal of virology*. 1996;70(3):1799-803.
137. Villarete L, Somasundaram T, Ahmed R. Tissue-mediated selection of viral variants: correlation between glycoprotein mutation and growth in neuronal cells. *Journal of virology*. 1994;68(11):7490-6.
138. Finke S, Conzelmann K-K. Virus promoters determine interference by defective RNAs: selective amplification of mini-RNA vectors and rescue from cDNA by a 3' copy-back ambisense rabies virus. *Journal of virology*. 1999;73(5):3818-25.
139. Bellinger DA, Chang J, Bunn TO, Pick JR, Murphy M, Rahija R. Rabies induced in a cat by high-egg-passage Flury strain vaccine. *J Am Vet Med Assoc*. 1983;183(9):997-8, 65.
140. Velandia-Romero ML, Castellanos JE, Martinez-Gutierrez M. In vivo differential susceptibility of sensory neurons to rabies virus infection. *J Neurovirol*. 2013.
141. Bauer A, Nolden T, Schroter J, Romer-Oberdorfer A, Gluska S, Perlson E, et al. Anterograde glycoprotein-dependent transport of newly generated rabies virus in dorsal root ganglion neurons. *J Virol*. 2014;88(24):14172-83.
142. Zampieri N, Jessell TM, Murray AJ. Mapping sensory circuits by anterograde transsynaptic transfer of recombinant rabies virus. *Neuron*. 2014;81(4):766-78.
143. Tsiang H. Evidence for an intraaxonal transport of fixed and street rabies virus. *J Neuropathol Exp Neurol*. 1979;38(3):286-99.
144. Ceccaldi PE, Gillet JP, Tsiang H. Inhibition of the transport of rabies virus in the central nervous system. *J Neuropathol Exp Neurol*. 1989;48(6):620-30.
145. Charlton KM, Casey GA. Experimental rabies in skunks: immunofluorescence light and electron microscopic studies. *Lab Invest*. 1979;41(1):36-44.

146. Etessami R, Conzelmann KK, Fadai-Ghotbi B, Natelson B, Tsiang H, Ceccaldi PE. Spread and pathogenic characteristics of a G-deficient rabies virus recombinant: an in vitro and in vivo study. *J Gen Virol*. 2000;81(Pt 9):2147-53.
147. Lahaye X, Vidy A, Pomier C, Obiang L, Harper F, Gaudin Y, et al. Functional characterization of Negri bodies (NBs) in rabies virus-infected cells: Evidence that NBs are sites of viral transcription and replication. *J Virol*. 2009;83(16):7948-58.
148. Jackson AC. Human Rabies: a 2016 Update. *Curr Infect Dis Rep*. 2016;18(11):38.
149. Lafon M. Rabies virus receptors. *J Neurovirol*. 2005;11(1):82-7.
150. Dietzschold B, Schnell M, Koprowski H. Pathogenesis of rabies. *Curr Top Microbiol Immunol*. 2005;292:45-56.
151. Piccinotti S, Kirchhausen T, Whelan SP. Uptake of rabies virus into epithelial cells by clathrin-mediated endocytosis depends upon actin. *J Virol*. 2013;87(21):11637-47.
152. Lewis P, Fu Y, Lentz TL. Rabies virus entry at the neuromuscular junction in nerve-muscle cocultures. *Muscle Nerve*. 2000;23(5):720-30.
153. Thoulouze MI, Lafage M, Schachner M, Hartmann U, Cremer H, Lafon M. The neural cell adhesion molecule is a receptor for rabies virus. *J Virol*. 1998;72(9):7181-90.
154. Gastka M, Horvath J, Lentz TL. Rabies virus binding to the nicotinic acetylcholine receptor alpha subunit demonstrated by virus overlay protein binding assay. *J Gen Virol*. 1996;77 (Pt 10):2437-40.
155. Dechant G, Barde Y-A. The neurotrophin receptor p75 NTR: novel functions and implications for diseases of the nervous system. *Nature neuroscience*. 2002;5(11):1131.
156. Tuffereau C, Schmidt K, Langevin C, Lafay F, Dechant G, Koltzenburg M. The rabies virus glycoprotein receptor p75NTR is not essential for rabies virus infection. *J Virol*. 2007;81(24):13622-30.
157. Tuffereau C, Benejean J, Blondel D, Kieffer B, Flamand A. Low-affinity nerve-growth factor receptor (P75NTR) can serve as a receptor for rabies virus. *EMBO J*. 1998;17(24):7250-9.
158. Wang J, Wang Z, Liu R, Shuai L, Wang X, Luo J, et al. Metabotropic glutamate receptor subtype 2 is a cellular receptor for rabies virus. *PLoS Pathog*. 2018;14(7):e1007189.
159. Arredondo J, Nguyen VT, Chernyavsky AI, Bercovich D, Orr-Urtreger A, Kummer W, et al. Central role of $\alpha 7$ nicotinic receptor in differentiation of the stratified squamous epithelium. *The Journal of cell biology*. 2002;159(2):325-36.
160. Botchkareva NV, Botchkarev VA, Chen L-H, Lindner G, Paus R. A role for p75 neurotrophin receptor in the control of hair follicle morphogenesis. *Developmental biology*. 1999;216(1):135-53.
161. Müller-Röver S, Peters EJ, Botchkarev VA, Panteleyev A, Paus R. Distinct patterns of NCAM expression are associated with defined stages of murine hair follicle morphogenesis and regression. *Journal of Histochemistry & Cytochemistry*. 1998;46(12):1401-9.
162. Wunner WH, Conzelmann K-K. Chapter 2 - Rabies Virus. In: Jackson AC, editor. *Rabies* (Third Edition). Boston: Academic Press; 2013. p. 17-60.
163. Tsiang H. Pathophysiology of rabies virus infection of the nervous system. *Adv Virus Res*. 1993;42:375-412.
164. Albertini AA, Baquero E, Ferlin A, Gaudin Y. Molecular and cellular aspects of rhabdovirus entry. *Viruses*. 2012;4(1):117-39.
165. Gaudin Y. Rabies virus-induced membrane fusion pathway. *J Cell Biol*. 2000;150(3):601-12.
166. Gosztanyi G. Reproduction of lyssaviruses: ultrastructural composition of lyssavirus and functional aspects of pathogenesis. *Curr Top Microbiol Immunol*. 1994;187:43-68.
167. Finke S, Conzelmann KK. Replication strategies of rabies virus. *Virus Res*. 2005;111(2):120-31.
168. Iseni F, Barge A, Baudin F, Blondel D, Ruigrok RW. Characterization of rabies virus nucleocapsids and recombinant nucleocapsid-like structures. *J Gen Virol*. 1998;79 (Pt 12):2909-19.

169. Holloway BP, Obijeski JF. Rabies virus-induced RNA synthesis in BHK21 cells. *J Gen Virol.* 1980;49(1):181-95.
170. Barr JN, Whelan S, Wertz GW. cis-Acting signals involved in termination of vesicular stomatitis virus mRNA synthesis include the conserved AUAC and the U7 signal for polyadenylation. *Journal of virology.* 1997;71(11):8718-25.
171. Li J, Rahmeh A, Morelli M, Whelan SP. A conserved motif in region v of the large polymerase proteins of nonsegmented negative-sense RNA viruses that is essential for mRNA capping. *Journal of virology.* 2008;82(2):775-84.
172. Gaudin Y. Folding of rabies virus glycoprotein: epitope acquisition and interaction with endoplasmic reticulum chaperones. *J Virol.* 1997;71(5):3742-50.
173. Gaudin Y, Moreira S, Benejean J, Blondel D, Flamand A, Tuffereau C. Soluble ectodomain of rabies virus glycoprotein expressed in eukaryotic cells folds in a monomeric conformation that is antigenically distinct from the native state of the complete, membrane-anchored glycoprotein. *J Gen Virol.* 1999;80 (Pt 7):1647-56.
174. Gaudin Y, Tuffereau C, Durrer P, Flamand A, Ruigrok RW. Biological function of the low-pH, fusion-inactive conformation of rabies virus glycoprotein (G): G is transported in a fusion-inactive state-like conformation. *J Virol.* 1995;69(9):5528-34.
175. Whitt MA, Buonocore L, Prehaud C, Rose JK. Membrane fusion activity, oligomerization, and assembly of the rabies virus glycoprotein. *Virology.* 1991;185(2):681-8.
176. Menager P, Roux P, Megret F, Bourgeois JP, Le Sourd AM, Danckaert A, et al. Toll-like receptor 3 (TLR3) plays a major role in the formation of rabies virus Negri Bodies. *PLoS Pathog.* 2009;5(2):e1000315.
177. Nikolic J, Le Bars R, Lama Z, Scrima N, Lagaudrière-Gesbert C, Gaudin Y, et al. Negri bodies are viral factories with properties of liquid organelles. *Nature Communications.* 2017;8(1):58.
178. Schoehn G, Iseni F, Mavrakis M, Blondel D, Ruigrok RW. Structure of recombinant rabies virus nucleoprotein-RNA complex and identification of the phosphoprotein binding site. *J Virol.* 2001;75(1):490-8.
179. Ameyama S, Toriumi H, Takahashi T, Shimura Y, Nakahara T, Honda Y, et al. Monoclonal antibody #3-9-16 recognizes one of the two isoforms of rabies virus matrix protein that exposes its N-terminus on the virion surface. *Microbiol Immunol.* 2003;47(9):639-51.
180. Potratz M, Zaack LM, Weigel C, Klein A, Freuling CM, Müller T, et al. Neuroglia Infection by Rabies Virus after Anterograde Virus Spread in Peripheral Neurons. *bioRxiv.* 2020:2020.09.20.305078.
181. Horton DL, McElhinney LM, Freuling CM, Marston DA, Banyard AC, Goharriz H, et al. Complex epidemiology of a zoonotic disease in a culturally diverse region: phylogeography of rabies virus in the Middle East. *PLoS Negl Trop Dis.* 2015;9(3):e0003569.
182. Freuling CM, Kloss D, Schroder R, Kliemt A, Muller T. The WHO Rabies Bulletin Europe: a key source of information on rabies and a pivotal tool for surveillance and epidemiology. *Rev Sci Tech.* 2012;31(3):799-807.
183. Müller T, Freuling CM. Rabies in terrestrial animals. *Rabies: Elsevier;* 2020. p. 195-230.
184. Nadin-Davis SA. Chapter 4 - Molecular Epidemiology. In: Jackson AC, editor. *Rabies (Third Edition).* Boston: Academic Press; 2013. p. 123-77.
185. Bernardi F, Nadin-Davis SA, Wandeler AI, Armstrong J, Gomes AA, Lima FS, et al. Antigenic and genetic characterization of rabies viruses isolated from domestic and wild animals of Brazil identifies the hoary fox as a rabies reservoir. *J Gen Virol.* 2005;86(Pt 11):3153-62.
186. Banyard AC, Davis A, Gilbert AT, Markotter W. Chapter 7 - Bat rabies. In: Fooks AR, Jackson AC, editors. *Rabies (Fourth Edition).* Boston: Academic Press; 2020. p. 231-76.
187. Schatz J, Ohlendorf B, Busse P, Pelz G, Dolch D, Teubner J, et al. Twenty years of active bat rabies surveillance in Germany: a detailed analysis and future perspectives. *Epidemiol Infect.* 2014;142(6):1155-66.

188. Vazquez-Moron S, Juste J, Ibanez C, Berciano JM, Echevarria JE. Phylogeny of European bat Lyssavirus 1 in *Eptesicus isabellinus* bats, Spain. *Emerg Infect Dis.* 2011;17(3):520-3.
189. Amengual B, Bourhy H, Lopez-Roig M, Serra-Cobo J. Temporal dynamics of European bat Lyssavirus type 1 and survival of *Myotis myotis* bats in natural colonies. *PLoS One.* 2007;2(6):e566.
190. Serra-Cobo J, Amengual B, Abellan C, Bourhy H. European bat lyssavirus infection in Spanish bat populations. *Emerg Infect Dis.* 2002;8(4):413-20.
191. Vos A, Muller T, Cox J, Neubert L, Fooks AR. Susceptibility of ferrets (*Mustela putorius furo*) to experimentally induced rabies with European Bat Lyssaviruses (EBLV). *J Vet Med B Infect Dis Vet Public Health.* 2004;51(2):55-60.
192. Cliquet F, Picard-Meyer E, Barrat J, Brookes SM, Healy DM, Wasniewski M, et al. Experimental infection of foxes with European Bat Lyssaviruses type-1 and 2. *BMC veterinary research.* 2009;5(1):19.
193. Nieuwenhuijs J, Haagsma J, Lina P. Epidemiology and control of rabies in bats in The Netherlands. *Rev Sci Tech.* 1992;11(4):1155-61.
194. Nieuwenhuijs JH. [Veterinary Chief Inspection for Public Health. Rabies in bats]. *Tijdschr Diergeneeskde.* 1987;112(20):1193-7.
195. Jakava-Viljanen M, Lilley T, Kyheroinen EM, Huovilainen A. First encounter of European bat lyssavirus type 2 (EBLV-2) in a bat in Finland. *Epidemiol Infect.* 2010;138(11):1581-5.
196. Wise EL, Marston DA, Banyard AC, Goharriz H, Selden D, Maclaren N, et al. Passive surveillance of United Kingdom bats for lyssaviruses (2005–2015). *Epidemiology and Infection.* 2017;145(12):2445-57.
197. Freuling C, Grossmann E, Conraths FJ, Schameitat A, Kliemt J, Auer E, et al. First Isolation of EBLV-2 in Germany. *Veterinary Microbiology.* 2008;131(1):26-34.
198. Fooks AR, McElhinney LM, Pounder DJ, Finnegan CJ, Mansfield K, Johnson N, et al. Case report: isolation of a European bat lyssavirus type 2a from a fatal human case of rabies encephalitis. *J Med Virol.* 2003;71(2):281-9.
199. Lumio J, Hillbom M, Roine R, Ketonen L, Haltia M, Valle M, et al. Human rabies of bat origin in Europe. *Lancet.* 1986;1(8477):378.
200. Freuling CM, Beer M, Conraths FJ, Finke S, Hoffmann B, Keller B, et al. Novel lyssavirus in Natterer's bat, Germany. *Emerg Infect Dis.* 2011;17(8):1519-22.
201. Freuling CM, Abendroth B, Beer M, Fischer M, Hanke D, Hoffmann B, et al. Molecular diagnostics for the detection of Bokeloh bat lyssavirus in a bat from Bavaria, Germany. *Virus Res.* 2013;177(2):201-4.
202. Picard-Meyer E, Servat A, Robardet E, Moinet M, Borel C, Cliquet F. Isolation of Bokeloh bat lyssavirus in *Myotis nattereri* in France. *Arch Virol.* 2013;158(11):2333-40.
203. Smreczak M, Orłowska A, Marzec A, Trebas P, Muller T, Freuling CM, et al. Bokeloh bat lyssavirus isolation in a Natterer's bat, Poland. *Zoonoses Public Health.* 2018;65(8):1015-9.
204. Klein A, Calvelage S, Schlottau K, Hoffmann B, Eggerbauer E, Müller T, et al. Retrospective Enhanced Bat Lyssavirus Surveillance in Germany between 2018-2020. *Viruses.* 2021;13(8):1538.
205. Eggerbauer E, Troupin C, Passior K, Pfaff F, Hoper D, Neubauer-Juric A, et al. The Recently Discovered Bokeloh Bat Lyssavirus: Insights Into Its Genetic Heterogeneity and Spatial Distribution in Europe and the Population Genetics of Its Primary Host. *Adv Virus Res.* 2017;99:199-232.
206. Ceballos NA, Morón SV, Berciano JM, Nicolás O, López CA, Juste J, et al. Novel lyssavirus in bat, Spain. *Emerging infectious diseases.* 2013;19(5):793.
207. Echevarria JE, Banyard AC, McElhinney LM, Fooks AR. Current Rabies Vaccines Do Not Confer Protective Immunity against Divergent Lyssaviruses Circulating in Europe. *Viruses.* 2019;11(10).

208. Picard-Meyer E, Beven V, Hirchaud E, Guillaume C, Larcher G, Robardet E, et al. Lleida Bat Lyssavirus isolation in *Miniopterus schreibersii* in France. *Zoonoses Public Health*. 2019;66(2):254-8.
209. Calvelage S, Tammiranta N, Nokireki T, Gadd T, Eggerbauer E, Zaack LM, et al. Genetic and Antigenetic Characterization of the Novel Kotalahti Bat Lyssavirus (KBLV). *Viruses*. 2021;13(1).
210. Benda P, Gazaryan S, Vallo P. On the distribution and taxonomy of bats of the *Myotis mystacinus* morphogroup from the Caucasus region (Chiroptera: Vespertilionidae). *Turkish Journal of Zoology*. 2015;2016.
211. Botvinkin AD, Poleschuk EM, Kuzmin IV, Borisova TI, Gazaryan SV, Yager P, et al. Novel lyssaviruses isolated from bats in Russia. *Emerging infectious diseases*. 2003;9(12):1623.
212. Belikov S, Leonova G, Kondratov I, Romanova E, Pavlenko E. Isolation and genetic characterisation of a new lyssavirus strain in the Primorskiy kray. *East Siberian J Infect Pathol*. 2009;16(3):68-9.
213. Liu Y, Zhang S, Zhao J, Zhang F, Hu R. Isolation of Irkut virus from a *Murina leucogaster* bat in China. *PLoS neglected tropical diseases*. 2013;7(3):e2097.
214. Chen T, Miao FM, Liu Y, Zhang SF, Zhang F, Li N, et al. Possible Transmission of Irkut Virus from Dogs to Humans. *Biomed Environ Sci*. 2018;31(2):146-8.
215. Kuzmin IV, Niezgoda M, Franka R, Agwanda B, Markotter W, Beagley JC, et al. Possible emergence of West Caucasian bat virus in Africa. *Emerging infectious diseases*. 2008;14(12):1887.
216. Coxon C, McElhinney L, Pacey A, Gauntlett F, Holland S. Preliminary Outbreak Assessment: Rabies in a Cat in Italy 2020 [Available from: <https://www.who-rabies-bulletin.org/site-page/classification>].
217. Vega S, Lorenzo-Rebenaque L, Marin C, Domingo R, Fariñas F. Tackling the Threat of Rabies Reintroduction in Europe. *Frontiers in Veterinary Science*. 2021;7(1196).
218. Hu SC, Hsu CL, Lee MS, Tu YC, Chang JC, Wu CH, et al. Lyssavirus in Japanese Pipistrelle, Taiwan. *Emerg Infect Dis*. 2018;24(4):782-5.
219. Šimić I, Lojkić I, Krešić N, Cliquet F, Picard-Meyer E, Wasniewski M, et al. Molecular and serological survey of lyssaviruses in Croatian bat populations. *BMC Veterinary Research*. 2018;14(1):274.
220. McCall BJ, Epstein JH, Neill AS, Heel K, Field H, Barrett J, et al. Potential exposure to Australian bat lyssavirus, Queensland, 1996-1999. *Emerg Infect Dis*. 2000;6(3):259-64.
221. Gould AR, Kattenbelt JA, Gumley SG, Lunt RA. Characterisation of an Australian bat lyssavirus variant isolated from an insectivorous bat. *Virus Res*. 2002;89(1):1-28.
222. Gould AR, Hyatt AD, Lunt R, Kattenbelt JA, Hengstberger S, Blacksell SD. Characterisation of a novel lyssavirus isolated from Pteropid bats in Australia. *Virus Res*. 1998;54(2):165-87.
223. Prada D, Boyd V, Baker M, Jackson B, O'Dea M. Insights into Australian Bat Lyssavirus in Insectivorous Bats of Western Australia. *Trop Med Infect Dis*. 2019;4(1).
224. Allworth A, Murray K, Morgan J. A human case of encephalitis due to a lyssavirus recently identified in fruit bats. *Communicable diseases intelligence*. 1996;20:504-.
225. Hanna JN, Carney IK, Smith GA, Tannenberg AE, Deverill JE, Botha JA, et al. Australian bat lyssavirus infection: a second human case, with a long incubation period. *Med J Aust*. 2000;172(12):597-9.
226. Weir DL, Smith IL, Bossart KN, Wang LF, Broder CC. Host cell tropism mediated by Australian bat lyssavirus envelope glycoproteins. *Virology*. 2013;444(1-2):21-30.
227. Gunawardena PS, Marston DA, Ellis RJ, Wise EL, Karawita AC, Breed AC, et al. Lyssavirus in Indian Flying Foxes, Sri Lanka. *Emerg Infect Dis*. 2016;22(8):1456-9.
228. Hayman DT, Fooks AR, Horton D, Suu-Ire R, Breed AC, Cunningham AA, et al. Antibodies against Lagos bat virus in megachiroptera from West Africa. *Emerging infectious diseases*. 2008;14(6):926.

229. Boulger LR, Porterfield JS. Isolation of a virus from Nigerian fruit bats. *Transactions of the Royal Society of Tropical Medicine and Hygiene*. 1958;52(5):421-4.
230. Kuzmin IV, Mayer AE, Niezgoda M, Markotter W, Agwanda B, Breiman RF, et al. Shimoni bat virus, a new representative of the *Lyssavirus* genus. *Virus Res*. 2010;149(2):197-210.
231. Markotter W, Kuzmin I, Rupprecht CE, Nel LH. Phylogeny of Lagos bat virus: challenges for *lyssavirus* taxonomy. *Virus Res*. 2008;135(1):10-21.
232. Coertse J, Geldenhuys M, le Roux K, Markotter W. Lagos Bat Virus, an Under-Reported Rabies-Related *Lyssavirus*. *Viruses*. 2021;13(4):576.
233. Markotter W, Randles J, Rupprecht CE, Sabeta CT, Taylor PJ, Wandeler AI, et al. Lagos bat virus, South Africa. *Emerging infectious diseases*. 2006;12(3):504.
234. Meredith CD, Prossouw AP, Koch H. An unusual case of human rabies thought to be of chiropteran origin. *S Afr Med J*. 1971;45(28):767-9.
235. King AA, Meredith CD, Thomson GR. The biology of southern African *lyssavirus* variants. *Curr Top Microbiol Immunol*. 1994;187:267-95.
236. King A, Crick J. Rabies-related viruses. *Rabies: Springer*; 1988. p. 177-99.
237. Foggin C. Rabies and rabies-related viruses in Zimbabwe: historical, virological and ecological aspects 1988.
238. Paweska JT, Blumberg LH, Liebenberg C, Hewlett RH, Grobbelaar AA, Leman PA, et al. Fatal human infection with rabies-related Duvenhage virus, South Africa. *Emerg Infect Dis*. 2006;12(12):1965-7.
239. van Thiel PP, van den Hoek JA, Eftimov F, Tepaske R, Zaaijer HJ, Spanjaard L, et al. Fatal case of human rabies (Duvenhage virus) from a bat in Kenya: The Netherlands, December 2007. *Euro Surveill*. 2008;13(2).
240. Kuzmin IV, Bozick B, Guagliardo SA, Kunkel R, Shak JR, Tong S, et al. Bats, emerging infectious diseases, and the rabies paradigm revisited. *Emerg Health Threats J*. 2011;4:7159.
241. Coertse J, Markotter W, le Roux K, Stewart D, Sabeta CT, Nel LH. New isolations of the rabies-related Mokola virus from South Africa. *BMC Vet Res*. 2017;13(1):37.
242. McMahon WC, Coertse J, Kearney T, Keith M, Swanepoel LH, Markotter W. Surveillance of the rabies-related *lyssavirus*, Mokola in non-volant small mammals in South Africa. *Onderstepoort J Vet Res*. 2021;88(1):e1-e13.
243. Foggin C. Mokola virus infection in cats and a dog in Zimbabwe. *Veterinary Record*. 1983;113(5):115-.
244. Le-Gonideg G, Rickenbach A, Robin Y, Heme G. Isolation of a strain of Mokola virus in Cameroun. *Ann Microbiol(Inst Pasteur)*. 1978(2):245-9.
245. Mebatsion T, Cox JH, Frost JW. Isolation and characterization of 115 street rabies virus isolates from Ethiopia by using monoclonal antibodies: identification of 2 isolates as Mokola and Lagos bat viruses. *J Infect Dis*. 1992;166(5):972-7.
246. Saluzzo J-F, Rollin P, Daguette C, Digoutte J-P, Georges A-J, Sureau P, editors. Premier isolement du virus Mokola à partir d'un rongeur (*Lophuromys sikapusi*). *Annales de l'Institut Pasteur/Virologie*; 1984: Elsevier.
247. Familusi JB, Moore DL. Isolation of a rabies related virus from the cerebrospinal fluid of a child with 'aseptic meningitis'. *Afr J Med Sci*. 1972;3(1):93-6.
248. Familusi J, Osunkoya B, Moore D, Kemp G, Fabiyi A. A fatal human infection with Mokola virus. *The American journal of tropical medicine and hygiene*. 1972;21(6):959-63.
249. Messenger SL, Smith JS, Orciari LA, Yager PA, Rupprecht CE. Emerging pattern of rabies deaths and increased viral infectivity. *Emerg Infect Dis*. 2003;9(2):151-4.
250. Messenger SL, Smith JS, Rupprecht CE. Emerging epidemiology of bat-associated cryptic cases of rabies in humans in the United States. *Clin Infect Dis*. 2002;35(6):738-47.
251. Winkler WG. Airborne rabies virus isolation. *Wildl Dis*. 1968;4(2):37-40.
252. Winkler WG, Fashinell TR, Leffingwell L, Howard P, Conomy P. Airborne rabies transmission in a laboratory worker. *JAMA*. 1973;226(10):1219-21.

253. Johnson N, Phillpotts R, Fooks A. Airborne transmission of lyssaviruses. *Journal of medical microbiology*. 2006;55(6):785-90.
254. Zhou H, Zhu W, Zeng J, He J, Liu K, Li Y, et al. Probable Rabies Virus Transmission through Organ Transplantation, China, 2015. *Emerg Infect Dis*. 2016;22(8):1348-52.
255. Vora NM, Orciari LA, Niezgoda M, Selvaggi G, Stosor V, Lyon GM, 3rd, et al. Clinical management and humoral immune responses to rabies post-exposure prophylaxis among three patients who received solid organs from a donor with rabies. *Transpl Infect Dis*. 2015;17(3):389-95.
256. Maier T, Schwarting A, Mauer D, Ross RS, Martens A, Kliem V, et al. Management and outcomes after multiple corneal and solid organ transplantations from a donor infected with rabies virus. *Clin Infect Dis*. 2010;50(8):1112-9.
257. Burton EC, Burns DK, Opatowsky MJ, El-Feky WH, Fischbach B, Melton L, et al. Rabies encephalomyelitis: clinical, neuroradiological, and pathological findings in 4 transplant recipients. *Arch Neurol*. 2005;62(6):873-82.
258. Johnson N, Brookes SM, Fooks AR, Ross RS. Review of human rabies cases in the UK and in Germany. *Vet Rec*. 2005;157(22):715.
259. Javadi MA, Fayaz A, Mirdehghan SA, Ainollahi B. Transmission of rabies by corneal graft. *Cornea*. 1996;15(4):431-3.
260. Wallerstein C. Rabies cases increase in the Philippines. *BMJ*. 1999;318(7194):1306.
261. Hunter M, Johnson N, Hedderwick S, McCaughey C, Lowry K, McConville J, et al. Immunovirological correlates in human rabies treated with therapeutic coma. *J Med Virol*. 2010;82(7):1255-65.
262. Ugolini G. Use of rabies virus as a transneuronal tracer of neuronal connections: implications for the understanding of rabies pathogenesis. *Dev Biol (Basel)*. 2008;131:493-506.
263. Warrell MJ. Emerging aspects of rabies infection: with a special emphasis on children. *Curr Opin Infect Dis*. 2008;21(3):251-7.
264. Newman KC, Riley EM. Whatever turns you on: accessory-cell-dependent activation of NK cells by pathogens. *Nature Reviews Immunology*. 2007;7:279.
265. Katz ISS, Guedes F, Fernandes ER, Dos Ramos Silva S. Immunological aspects of rabies: a literature review. *Arch Virol*. 2017;162(11):3251-68.
266. Rosendahl Huber S, van Beek J, de Jonge J, Luytjes W, van Baarle D. T cell responses to viral infections - opportunities for Peptide vaccination. *Frontiers in immunology*. 2014;5:171-.
267. Constantino J, Gomes C, Falcão A, Neves BM, Cruz MT. Dendritic cell-based immunotherapy: a basic review and recent advances. *Immunologic research*. 2017;65(4):798-810.
268. Lei T-Y, Ye Y-Z, Zhu X-Q, Smerin D, Gu L-J, Xiong X-X, et al. The immune response of T cells and therapeutic targets related to regulating the levels of T helper cells after ischaemic stroke. *Journal of Neuroinflammation*. 2021;18(1):25.
269. Lebrun A, Portocarrero C, Kean RB, Barkhouse DA, Faber M, Hooper DC. T-bet Is Required for the Rapid Clearance of Attenuated Rabies Virus from Central Nervous System Tissue. *J Immunol*. 2015;195(9):4358-68.
270. Embregts CWE, Begeman L, Voesenek CJ, Martina BEE, Koopmans MPG, Kuiken T, et al. Street RABV Induces the Cholinergic Anti-inflammatory Pathway in Human Monocyte-Derived Macrophages by Binding to nAChR $\alpha 7$. *Frontiers in Immunology*. 2021;12(378).
271. Pan J, Zhang M, Wang J, Wang Q, Xia D, Sun W, et al. Interferon-gamma is an autocrine mediator for dendritic cell maturation. *Immunol Lett*. 2004;94(1-2):141-51.
272. Nguyen-Pham TN, Lim MS, Nguyen TA, Lee YK, Jin CJ, Lee HJ, et al. Type I and II interferons enhance dendritic cell maturation and migration capacity by regulating CD38 and CD74 that have synergistic effects with TLR agonists. *Cell Mol Immunol*. 2011;8(4):341-7.
273. Lester SN, Li K. Toll-like receptors in antiviral innate immunity. *J Mol Biol*. 2014;426(6):1246-64.

274. Uehata T, Takeuchi O. RNA Recognition and Immunity-Innate Immune Sensing and Its Posttranscriptional Regulation Mechanisms. *Cells*. 2020;9(7).
275. Gantier MP, Tong S, Behlke MA, Xu D, Phipps S, Foster PS, et al. TLR7 is involved in sequence-specific sensing of single-stranded RNAs in human macrophages. *J Immunol*. 2008;180(4):2117-24.
276. Petes C, Odoardi N, Gee K. The Toll for Trafficking: Toll-Like Receptor 7 Delivery to the Endosome. *Front Immunol*. 2017;8:1075.
277. Ostertag D, Hoblitzell-Ostertag TM, Perrault J. Overproduction of double-stranded RNA in vesicular stomatitis virus-infected cells activates a constitutive cell-type-specific antiviral response. *J Virol*. 2007;81(2):503-13.
278. Bowie AG, Unterholzner L. Viral evasion and subversion of pattern-recognition receptor signalling. *Nat Rev Immunol*. 2008;8(12):911-22.
279. Stanifer ML, Guo C, Doldan P, Boulant S. Importance of Type I and III Interferons at Respiratory and Intestinal Barrier Surfaces. *Front Immunol*. 2020;11:608645.
280. Hemann EA, Gale M, Jr., Savan R. Interferon Lambda Genetics and Biology in Regulation of Viral Control. *Front Immunol*. 2017;8:1707.
281. Rehwinkel J, Gack MU. RIG-I-like receptors: their regulation and roles in RNA sensing. *Nature Reviews Immunology*. 2020;20(9):537-51.
282. Hornung V, Ellegast J, Kim S, Brzozka K, Jung A, Kato H, et al. 5'-Triphosphate RNA is the ligand for RIG-I. *Science*. 2006;314(5801):994-7.
283. Trudler D, Farfara D, Frenkel D. Toll-like receptors expression and signaling in glia cells in neuro-amyloidogenic diseases: towards future therapeutic application. *Mediators of inflammation*. 2010;2010.
284. Bsibsi M, Ravid R, Gveric D, van Noort JM. Broad expression of Toll-like receptors in the human central nervous system. *J Neuropathol Exp Neurol*. 2002;61(11):1013-21.
285. Jackson AC, Rossiter JP, Lafon M. Expression of Toll-like receptor 3 in the human cerebellar cortex in rabies, herpes simplex encephalitis, and other neurological diseases. *J Neurovirol*. 2006;12(3):229-34.
286. Nair S, Bayer W, Ploquin MJ, Kassiotis G, Hasenkrug KJ, Dittmer U. Distinct roles of CD4+ T cell subpopulations in retroviral immunity: lessons from the Friend virus mouse model. *Retrovirology*. 2011;8:76.
287. Swain SL, McKinstry KK, Strutt TM. Expanding roles for CD4(+) T cells in immunity to viruses. *Nat Rev Immunol*. 2012;12(2):136-48.
288. Venkataswamy MM, Madhusudana SN, Sanyal SS, Taj S, Belludi AY, Mani RS, et al. Cellular immune response following pre-exposure and postexposure rabies vaccination by intradermal and intramuscular routes. *Clin Exp Vaccine Res*. 2015;4(1):68-74.
289. Luo Z, Lv L, Li Y, Sui B, Wu Q, Zhang Y, et al. The dual role of TLR7 in the pathogenesis of rabies virus in a mouse model. *J Virol*. 2020.
290. MacLennan IC, Toellner KM, Cunningham AF, Serre K, Sze DM, Zúñiga E, et al. Extrafollicular antibody responses. *Immunological reviews*. 2003;194:8-18.
291. Stebegg M, Kumar SD, Silva-Cayetano A, Fonseca VR, Linterman MA, Graca L. Regulation of the Germinal Center Response. *Frontiers in Immunology*. 2018;9(2469).
292. Allen CD, Okada T, Cyster JG. Germinal-center organization and cellular dynamics. *Immunity*. 2007;27(2):190-202.
293. Schmidt ME, Varga SM. The CD8 T Cell Response to Respiratory Virus Infections. *Front Immunol*. 2018;9:678.
294. Hooper DC, Phares TW, Fabis MJ, Roy A. The production of antibody by invading B cells is required for the clearance of rabies virus from the central nervous system. *PLoS Negl Trop Dis*. 2009;3(10):e535.
295. Hooper DC, Roy A, Kean RB, Phares TW, Barkhouse DA. Therapeutic immune clearance of rabies virus from the CNS. *Future Virol*. 2011;6(3):387-97.

296. Hooper DC, Morimoto K, Bette M, Weihe E, Koprowski H, Dietzschold B. Collaboration of antibody and inflammation in clearance of rabies virus from the central nervous system. *J Virol.* 1998;72(5):3711-9.
297. Phares TW, Kean RB, Mikheeva T, Hooper DC. Regional Differences in Blood-Brain Barrier Permeability Changes and Inflammation in the Apathogenic Clearance of Virus from the Central Nervous System. *The Journal of Immunology.* 2006;176(12):7666-75.
298. Chai Q, He WQ, Zhou M, Lu H, Fu ZF. Enhancement of blood-brain barrier permeability and reduction of tight junction protein expression are modulated by chemokines/cytokines induced by rabies virus infection. *J Virol.* 2014;88(9):4698-710.
299. Qin Y, Smith TG, Jackson F, Gallardo-Romero NF, Morgan CN, Olson V, et al. Revisiting rabies virus neutralizing antibodies through infecting BALB/c mice with live rabies virus. *Virus Res.* 2018;248:39-43.
300. Roy A, Hooper DC. Lethal silver-haired bat rabies virus infection can be prevented by opening the blood-brain barrier. *J Virol.* 2007;81(15):7993-8.
301. Damodar T, Mani RS, Prathyusha PV. Utility of rabies neutralizing antibody detection in cerebrospinal fluid and serum for ante-mortem diagnosis of human rabies. *PLoS Negl Trop Dis.* 2019;13(1):e0007128.
302. Gnanadurai CW, Zhou M, He W, Leyson CM, Huang CT, Salyards G, et al. Presence of virus neutralizing antibodies in cerebral spinal fluid correlates with non-lethal rabies in dogs. *PLoS Negl Trop Dis.* 2013;7(9):e2375.
303. Dietzschold B, Kao M, Zheng YM, Chen ZY, Maul G, Fu ZF, et al. Delineation of putative mechanisms involved in antibody-mediated clearance of rabies virus from the central nervous system. *Proc Natl Acad Sci U S A.* 1992;89(15):7252-6.
304. Hooper DC, Roy A, Barkhouse DA, Li J, Kean RB. Rabies virus clearance from the central nervous system. *Adv Virus Res.* 2011;79:55-71.
305. Roy A, Phares TW, Koprowski H, Hooper DC. Failure to open the blood-brain barrier and deliver immune effectors to central nervous system tissues leads to the lethal outcome of silver-haired bat rabies virus infection. *J Virol.* 2007;81(3):1110-8.
306. Gnanadurai CW, Fu ZF. CXCL10 and blood-brain barrier modulation in rabies virus infection. *Oncotarget.* 2016;7(10):10694-5.
307. Wang ZW, Sarmiento L, Wang Y, Li XQ, Dhingra V, Tsegai T, et al. Attenuated rabies virus activates, while pathogenic rabies virus evades, the host innate immune responses in the central nervous system. *J Virol.* 2005;79(19):12554-65.
308. Baloul L, Camelo S, Lafon M. Up-regulation of Fas ligand (FasL) in the central nervous system: a mechanism of immune evasion by rabies virus. *J Neurovirol.* 2004;10(6):372-82.
309. Kojima D, Park CH, Satoh Y, Inoue S, Noguchi A, Oyamada T. Pathology of the spinal cord of C57BL/6J mice infected with rabies virus (CVS-11 strain). *J Vet Med Sci.* 2009;71(3):319-24.
310. Finke S, Cox JH, Conzelmann KK. Differential transcription attenuation of rabies virus genes by intergenic regions: generation of recombinant viruses overexpressing the polymerase gene. *J Virol.* 2000;74(16):7261-9.
311. Nikolic J, Civas A, Lama Z, Lagaudriere-Gesbert C, Blondel D. Rabies Virus Infection Induces the Formation of Stress Granules Closely Connected to the Viral Factories. *PLoS Pathog.* 2016;12(10):e1005942.
312. Prehaud C, Wolff N, Terrien E, Lafage M, Megret F, Babault N, et al. Attenuation of rabies virulence: takeover by the cytoplasmic domain of its envelope protein. *Sci Signal.* 2010;3(105):ra5.
313. Johnson N, Cunningham AF, Fooks AR. The immune response to rabies virus infection and vaccination. *Vaccine.* 2010;28(23):3896-901.
314. Grattan-Smith PJ, O'Regan WJ, Ellis PS, O'Flaherty SJ, McIntyre PB, Barnes CJ. Rabies. A second Australian case, with a long incubation period. *Med J Aust.* 1992;156(9):651-4.

315. Warrell DA. The clinical picture of rabies in man. *Trans R Soc Trop Med Hyg.* 1976;70(3):188-95.
316. Hemachuda T. Rabies. In: Roos KL, editor. *Central nervous system infectious diseases and therapy.* New York: Marcel Dekker, Incorporated; 1997.
317. Tesoriero C, Del Gallo F, Bentivoglio M. Sleep and brain infections. *Brain research bulletin.* 2019;145:59-74.
318. Gourmelon P, Briet D, Clarencon D, Court L, Tsiang H. Sleep alterations in experimental street rabies virus infection occur in the absence of major EEG abnormalities. *Brain Res.* 1991;554(1-2):159-65.
319. Dumb rabies. *Lancet.* 1978;2(8098):1031-2.
320. Mills RP, Swanepoel R, Hayes MM, Gelfand M. Dumb rabies: its development following vaccination in a subject with rabies. *Cent Afr J Med.* 1978;24(6):115-7.
321. Feasby T, Gilbert J, Brown W, Bolton C, Hahn A, Koopman W, et al. An acute axonal form of Guillain-Barré polyneuropathy. *Brain.* 1986;109(6):1115-26.
322. Hemachudha T, Griffin DE, Chen WW, Johnson RT. Immunologic studies of rabies vaccination-induced Guillain-Barre syndrome. *Neurology.* 1988;38(3):375-8.
323. Hemachudha T. Human rabies: clinical aspects, pathogenesis, and potential therapy. *Curr Top Microbiol Immunol.* 1994;187:121-43.
324. Hemachudha T, Phanuphak P, Sriwanthana B, Manutsathit S, Phanthumchinda K, Siriprasomsup W, et al. Immunologic study of human encephalitic and paralytic rabies. Preliminary report of 16 patients. *Am J Med.* 1988;84(4):673-7.
325. Hemachudha T, Panpanich T, Phanuphak P, Manatsathit S, Wilde H. Immune activation in human rabies. *Trans R Soc Trop Med Hyg.* 1993;87(1):106-8.
326. Healy DM, Brookes SM, Banyard AC, Nunez A, Cosby SL, Fooks AR. Pathobiology of rabies virus and the European bat lyssaviruses in experimentally infected mice. *Virus Res.* 2013;172(1-2):46-53.
327. Stamm DD, Kissling RE, Eidson ME. Experimental rabies infection in insectivorous bats. *J Infect Dis.* 1956;98(1):10-4.
328. Constantine DG. Transmission experiments with bat rabies isolates: bite transmission of rabies to foxes and coyote by free-tailed bats. *Am J Vet Res.* 1966;27(116):20-3.
329. Constantine DG, Woodall DF. Transmission experiments with bat rabies isolates: reactions of certain Carnivora, opossum, rodents, and bats to rabies virus of red bat origin when exposed by bat bite or by intramuscular inoculation. *Am J Vet Res.* 1966;27(116):24-32.
330. Constantine DG, Solomon GC, Woodall DF. Transmission experiments with bat rabies isolates: responses of certain carnivores and rodents to rabies viruses from four species of bats. *Am J Vet Res.* 1968;29(1):181-90.
331. Baer GM, Bales GL. Experimental rabies infection in the Mexican freetail bat. *J Infect Dis.* 1967;117(1):82-90.
332. Moreno JA, Baer GM. Experimental rabies in the vampire bat. *Am J Trop Med Hyg.* 1980;29(2):254-9.
333. Obregon-Morales C, Aguilar-Setien A, Perea Martinez L, Galvez-Romero G, Martinez-Martinez FO, Arechiga-Ceballos N. Experimental infection of *Artibeus intermedius* with a vampire bat rabies virus. *Comp Immunol Microbiol Infect Dis.* 2017;52:43-7.
334. Franka R, Johnson N, Muller T, Vos A, Neubert L, Freuling C, et al. Susceptibility of North American big brown bats (*Eptesicus fuscus*) to infection with European bat lyssavirus type 1. *J Gen Virol.* 2008;89(Pt 8):1998-2010.
335. Freuling C, Vos A, Johnson N, Kaipf I, Denzinger A, Neubert L, et al. Experimental infection of serotine bats (*Eptesicus serotinus*) with European bat lyssavirus type 1a. *J Gen Virol.* 2009;90(Pt 10):2493-502.
336. Johnson N, Vos A, Neubert L, Freuling C, Mansfield KL, Kaipf I, et al. Experimental study of European bat lyssavirus type-2 infection in Daubenton's bats (*Myotis daubentonii*). *J Gen Virol.* 2008;89(Pt 11):2662-72.

337. McCall BJ, Field HE, Smith GA, Storie GJ, Harrower BJ. Defining the risk of human exposure to Australian bat lyssavirus through potential non-bat animal infection. *Commun Dis Intell Q Rep.* 2005;29(2):202-5.
338. Kuzmin IV, Franka R, Rupprecht CE. Experimental infection of big brown bats (*Eptesicus fuscus*) with West Caucasian bat virus (WCBV). *Dev Biol (Basel).* 2008;131:327-37.
339. Suu-Ire R, Begeman L, Banyard AC, Breed AC, Drosten C, Eggerbauer E, et al. Pathogenesis of bat rabies in a natural reservoir: Comparative susceptibility of the straw-colored fruit bat (*Eidolon helvum*) to three strains of Lagos bat virus. *PLoS Negl Trop Dis.* 2018;12(3):e0006311.
340. Steece R, Altenbach JS. Prevalence of rabies specific antibodies in the Mexican free-tailed bat (*Tadarida brasiliensis mexicana*) at Lava Cave, New Mexico. *J Wildl Dis.* 1989;25(4):490-6.
341. Almeida MF, Martorelli LF, Aires CC, Sallum PC, Durigon EL, Massad E. Experimental rabies infection in haematophagous bats *Desmodus rotundus*. *Epidemiol Infect.* 2005;133(3):523-7.
342. Kuzmin IV, Botvinkin AD, Poleschuk EM, Orciari LA, Rupprecht CE. Bat rabies surveillance in the former Soviet Union. *Dev Biol (Basel).* 2006;125:273-82.
343. Kuzmin IV, Niezgoda M, Carroll DS, Keeler N, Hossain MJ, Breiman RF, et al. Lyssavirus surveillance in bats, Bangladesh. *Emerg Infect Dis.* 2006;12(3):486-8.
344. Steece RS, Calisher CH. Evidence for prenatal transfer of rabies virus in the Mexican free-tailed bat (*Tadarida brasiliensis Mexicana*). *J Wildl Dis.* 1989;25(3):329-34.
345. Benavides JA, Velasco-Villa A, Godino LC, Satheshkumar PS, Nino R, Rojas-Paniagua E, et al. Abortive vampire bat rabies infections in Peruvian peridomestic livestock. *PLOS Neglected Tropical Diseases.* 2020;14(6):e0008194.
346. Nagarajan T, Ertl HCJ. Chapter 14 - Human and animal vaccines. In: Fooks AR, Jackson AC, editors. *Rabies (Fourth Edition)*. Boston: Academic Press; 2020. p. 481-508.
347. Plotkin SA. Rabies vaccine prepared in human cell cultures: progress and perspectives. *Rev Infect Dis.* 1980;2(3):433-48.
348. Wiktor TJ, Fernandes MV, Koprowski H. Cultivation of Rabies Virus in Human Diploid Cell Strain Wi-38. *J Immunol.* 1964;93:353-66.
349. Barthe RFV. Laboratory techniques in rabies. WHO; 1996. p. 290-3.
350. Kessels JA, Recuenco S, Navarro-Vela AM, Deray R, Vigilato M, Ertl H, et al. Pre-exposure rabies prophylaxis: a systematic review. *Bull World Health Organ.* 2017;95(3):210-9C.
351. Rupprecht CE, Nagarajan T, Ertl H. Current Status and Development of Vaccines and Other Biologics for Human Rabies Prevention. *Expert Rev Vaccines.* 2016;15(6):731-49.
352. Quiambao BP, Dy-Tioco HZ, Dizon RM, Crisostomo ME, Teuwen DE. Rabies post-exposure prophylaxis with purified equine rabies immunoglobulin: one-year follow-up of patients with laboratory-confirmed category III rabies exposure in the Philippines. *Vaccine.* 2009;27(51):7162-6.
353. Organization WH. WHO expert consultation on rabies: second report: World Health Organisation; 2013.
354. Both L, Banyard AC, van Dolleweerd C, Horton DL, Ma JK, Fooks AR. Passive immunity in the prevention of rabies. *Lancet Infect Dis.* 2012;12(5):397-407.
355. Wilde H, Sirikawin S, Sabcharoen A, Kingnate D, Tantawichien T, Harischandra PA, et al. Failure of postexposure treatment of rabies in children. *Clin Infect Dis.* 1996;22(2):228-32.
356. Hemachudha T, Mitrabhakdi E, Wilde H, Vejabhuti A, Siripataravanit S, Kingnate D. Additional reports of failure to respond to treatment after rabies exposure in Thailand. *Clin Infect Dis.* 1999;28(1):143-4.
357. Montagnon B, Fanget B. Purified Vero cell vaccine for humans. Laboratory techniques in rabies Geneva: WHO. 1996:285-99.
358. Hu WT, Willoughby RE, Jr., Dhonau H, Mack KJ. Long-term follow-up after treatment of rabies by induction of coma. *N Engl J Med.* 2007;357(9):945-6.

359. Willoughby RE, Jr., Tieves KS, Hoffman GM, Ghanayem NS, Amlie-Lefond CM, Schwabe MJ, et al. Survival after treatment of rabies with induction of coma. *N Engl J Med*. 2005;352(24):2508-14.
360. Jackson AC. Current and future approaches to the therapy of human rabies. *Antiviral Res*. 2013;99(1):61-7.
361. Gilbert AT, Petersen BW, Recuenco S, Niezgoda M, Gomez J, Laguna-Torres VA, et al. Evidence of rabies virus exposure among humans in the Peruvian Amazon. *Am J Trop Med Hyg*. 2012;87(2):206-15.
362. Orr PH, Rubin MR, Aoki FY. Naturally acquired serum rabies neutralizing antibody in a Canadian Inuit population. *Arctic Med Res*. 1988;47 Suppl 1:699-700.
363. Follmann EH, Ritter DG, Beller M. Survey of fox trappers in northern Alaska for rabies antibody. *Epidemiol Infect*. 1994;113(1):137-41.
364. Lodmell DL. Genetic control of resistance to street rabies virus in mice. *J Exp Med*. 1983;157(2):451-60.
365. Lodmell DL, Chesebro B. Murine resistance to street rabies virus: genetic analysis by testing second-backcross progeny and verification of allelic resistance genes in SJL/J and CBA/J mice. *J Virol*. 1984;50(2):359-62.
366. Templeton JW, Holmberg C, Garber T, Sharp RM. Genetic control of serum neutralizing-antibody response to rabies vaccination and survival after a rabies challenge infection in mice. *J Virol*. 1986;59(1):98-102.
367. Klimpel GR. Immune defenses. *Medical Microbiology* 4th edition: University of Texas Medical Branch at Galveston; 1996.
368. Morimoto K, Hooper DC, Spitsin S, Koprowski H, Dietzschold B. Pathogenicity of different rabies virus variants inversely correlates with apoptosis and rabies virus glycoprotein expression in infected primary neuron cultures. *J Virol*. 1999;73(1):510-8.
369. Faber M, Pulmanusahakul R, Hodawadekar SS, Spitsin S, McGettigan JP, Schnell MJ, et al. Overexpression of the rabies virus glycoprotein results in enhancement of apoptosis and antiviral immune response. *J Virol*. 2002;76(7):3374-81.
370. Yoneyama M, Onomoto K, Jogi M, Akaboshi T, Fujita T. Viral RNA detection by RIG-I-like receptors. *Current opinion in immunology*. 2015;32:48-53.
371. Koraka P, Martina BEE, van den Ham H-J, Zaaraoui-Boutahar F, van Ijcken W, Roose J, et al. Analysis of Mouse Brain Transcriptome After Experimental Duvnaghe Virus Infection Shows Activation of Innate Immune Response and Pyroptotic Cell Death Pathway. *Frontiers in microbiology*. 2018;9:397-.
372. Zhang D, He F, Bi S, Guo H, Zhang B, Wu F, et al. Genome-Wide Transcriptional Profiling Reveals Two Distinct Outcomes in Central Nervous System Infections of Rabies Virus. *Front Microbiol*. 2016;7:751.
373. Benfield CTO, Smith SE, Wright E, Wash RS, Ferrara F, Temperton NJ, et al. Bat and pig IFN-induced transmembrane protein 3 restrict cell entry by influenza virus and lyssaviruses. *The Journal of general virology*. 2015;96(Pt 5):991-1005.
374. Pereira JM, Chin CR, Feeley EM, Brass AL. IFITMs restrict the replication of multiple pathogenic viruses. *J Mol Biol*. 2013;425(24):4937-55.
375. Amini-Bavil-Olyaei S, Choi YJ, Lee JH, Shi M, Huang IC, Farzan M, et al. The antiviral effector IFITM3 disrupts intracellular cholesterol homeostasis to block viral entry. *Cell Host Microbe*. 2013;13(4):452-64.
376. Smith S, Weston S, Kellam P, Marsh M. IFITM proteins-cellular inhibitors of viral entry. *Curr Opin Virol*. 2014;4:71-7.
377. El Asmi F, Brantis-de-Carvalho C, Blondel D, Chelbi-Alix M. Rhabdoviruses, Antiviral Defense, and SUMO Pathway. *Viruses*. 2018;10(12):686.
378. Hannoun Z, Maarifi G, Chelbi-Alix MK. The implication of SUMO in intrinsic and innate immunity. *Cytokine & Growth Factor Reviews*. 2016;29:3-16.

379. Maarifi G, Maroui MA, Dutrieux J, Dianoux L, Nisole S, Chelbi-Alix MK. Small ubiquitin-like modifier alters IFN response. *The Journal of Immunology*. 2015;1500035.
380. Geoffroy M-C, Hay RT. An additional role for SUMO in ubiquitin-mediated proteolysis. *Nature Reviews Molecular Cell Biology*. 2009;10(8):564.
381. Blondel D, Kheddache S, Lahaye X, Dianoux L, Chelbi-Alix MK. Resistance to rabies virus infection conferred by the PMLIV isoform. *Journal of virology*. 2010;84(20):10719-26.
382. Carlos F, Campagna M, García MA, Marcos-Villar L, Lang V, Baz-Martínez M, et al. Activation of the Double-Stranded RNA-Dependent Protein Kinase PKR by Sumo. *Journal of Biological Chemistry*. 2014:jbc. M114. 560961.
383. Horowitz A, Behrens RH, Okell L, Fooks AR, Riley EM. NK Cells as Effectors of Acquired Immune Responses: Effector CD4⁺ T Cell-Dependent Activation of NK Cells Following Vaccination. *The Journal of Immunology*. 2010;185(5):2808.
384. Fekadu M, Shaddock JH, Sanderlin DW, Smith JS. Efficacy of rabies vaccines against Duvenhage virus isolated from European house bats (*Eptesicus serotinus*), classic rabies and rabies-related viruses. *Vaccine*. 1988;6(6):533-9.
385. Brookes SM, Parsons G, Johnson N, McElhinney LM, Fooks AR. Rabies human diploid cell vaccine elicits cross-neutralising and cross-protecting immune responses against European and Australian bat lyssaviruses. *Vaccine*. 2005;23(32):4101-9.
386. Hanlon CA, Kuzmin IV, Blanton JD, Weldon WC, Manangan JS, Rupprecht CE. Efficacy of rabies biologics against new lyssaviruses from Eurasia. *Virus Research*. 2005;111(1):44-54.
387. Wright E, Temperton NJ, Marston DA, McElhinney LM, Fooks AR, Weiss RA. Investigating antibody neutralization of lyssaviruses using lentiviral pseudotypes: a cross-species comparison. *J Gen Virol*. 2008;89(Pt 9):2204-13.
388. Leslie MJ, Messenger S, Rohde RE, Smith J, Cheshier R, Hanlon C, et al. Bat-associated rabies virus in Skunks. *Emerg Infect Dis*. 2006;12(8):1274-7.
389. Daoust PY, Wandeler AI, Casey GA. Cluster of rabies cases of probable bat origin among red foxes in Prince Edward Island, Canada. *J Wildl Dis*. 1996;32(2):403-6.
390. Banyard AC, Evans JS, Luo TR, Fooks AR. Lyssaviruses and bats: emergence and zoonotic threat. *Viruses*. 2014;6(8):2974-90.
391. Weyer J, Kuzmin IV, Rupprecht CE, Nel LH. Cross-protective and cross-reactive immune responses to recombinant vaccinia viruses expressing full-length lyssavirus glycoprotein genes. *Epidemiol Infect*. 2008;136(5):670-8.
392. Blomer U, Naldini L, Verma IM, Trono D, Gage FH. Applications of gene therapy to the CNS. *Hum Mol Genet*. 1996;5 Spec No:1397-404.
393. Milone MC, O'Doherty U. Clinical use of lentiviral vectors. *Leukemia*. 2018;32(7):1529-41.
394. Wright E, McNabb S, Goddard T, Horton DL, Lembo T, Nel LH, et al. A robust lentiviral pseudotype neutralisation assay for in-field serosurveillance of rabies and lyssaviruses in Africa. *Vaccine*. 2009;27(51):7178-86.
395. Temperton NJ, Wright E. Retroviral pseudotypes. *eLS*. 2009.
396. Pekosz A, He B, Lamb RA. Reverse genetics of negative-strand RNA viruses: closing the circle. *Proc Natl Acad Sci U S A*. 1999;96(16):8804-6.
397. Goff SP, Berg P. Construction of hybrid viruses containing SV40 and lambda phage DNA segments and their propagation in cultured monkey cells. *Cell*. 1976;9(4 PT 2):695-705.
398. Racaniello VR, Baltimore D. Cloned poliovirus complementary DNA is infectious in mammalian cells. *Science*. 1981;214(4523):916-9.
399. Palese P. RNA virus vectors: Where are we and where do we need to go? *Proceedings of the National Academy of Sciences*. 1998;95(22):12750-2.
400. Brzozka K, Finke S, Conzelmann KK. Identification of the rabies virus alpha/beta interferon antagonist: phosphoprotein P interferes with phosphorylation of interferon regulatory factor 3. *J Virol*. 2005;79(12):7673-81.

401. Marschalek A, Drechsel L, Conzelmann KK. The importance of being short: the role of rabies virus phosphoprotein isoforms assessed by differential IRES translation initiation. *Eur J Cell Biol.* 2012;91(1):17-23.
402. Rieder M, Finke S, Conzelmann KK. Interferon in lyssavirus infection. *Berl Munch Tierarztl Wochenschr.* 2012;125(5-6):209-18.
403. Marston DA, McElhinney LM, Banyard AC, Horton DL, Núñez A, Koser ML, et al. Interspecies protein substitution to investigate the role of the lyssavirus glycoprotein. *The Journal of general virology.* 2013;94(Pt 2):284.
404. Marston DA, McElhinney LM, Ellis RJ, Horton DL, Wise EL, Leech SL, et al. Next generation sequencing of viral RNA genomes. *BMC Genomics.* 2013;14:444.
405. Heaton PR, Johnstone P, McElhinney LM, Cowley R, O'Sullivan E, Whitby JE. Heminested PCR assay for detection of six genotypes of rabies and rabies-related viruses. *J Clin Microbiol.* 1997;35(11):2762-6.
406. Wakeley PR, Johnson N, McElhinney LM, Marston D, Sawyer J, Fooks AR. Development of a real-time, TaqMan reverse transcription-PCR assay for detection and differentiation of lyssavirus genotypes 1, 5, and 6. *J Clin Microbiol.* 2005;43(6):2786-92.
407. Hayman DTS, Banyard AC, Wakeley PR, Harkess G, Marston D, Wood JLN, et al. A universal real-time assay for the detection of Lyssaviruses. *Journal of virological methods.* 2011;177(1):87-93.
408. Marston DA, Jennings DL, MacLaren NC, Dorey-Robinson D, Fooks AR, Banyard AC, et al. Pan-lyssavirus Real Time RT-PCR for Rabies Diagnosis. *J Vis Exp.* 2019(149).
409. McElhinney LM, Marston DA, Ellis RJ, Freuling CM, Müller TF, Fooks AR. Chapter Sixteen - Sanger Sequencing of Lyssaviruses. In: Rupprecht C, Nagarajan T, editors. *Current Laboratory Techniques in Rabies Diagnosis, Research and Prevention.* 1. Amsterdam: Academic Press; 2014. p. 159-70.
410. Marston DA, McElhinney LM, Wise E, Ellis RJ, Freuling CM, Müller TF, et al. Chapter Seventeen - Next Generation Sequencing of Lyssaviruses. In: Rupprecht C, Nagarajan T, editors. *Current Laboratory Techniques in Rabies Diagnosis, Research and Prevention.* 1. Amsterdam: Academic Press; 2014. p. 171-83.
411. Li H, Durbin R. Fast and accurate long-read alignment with Burrows–Wheeler transform. *Bioinformatics.* 2010;26(5):589-95.
412. Li H, Handsaker B, Wysoker A, Fennell T, Ruan J, Homer N, et al. The Sequence Alignment/Map format and SAMtools. *Bioinformatics (Oxford, England).* 2009;25(16):2078-9.
413. Shipley R, Wright E, Lean FZX, Selden D, Horton DL, Fooks AR, et al. Assessing Rabies Vaccine Protection against a Novel Lyssavirus, Kotalahti Bat Lyssavirus. *Viruses.* 2021;13(5).
414. Cliquet F, Aubert M, Sagne L. Development of a fluorescent antibody virus neutralisation test (FAVN test) for the quantitation of rabies-neutralising antibody. *J Immunol Methods.* 1998;212(1):79-87.
415. Sabeta C, Ngoepe E. Chapter Seven - Preparation of Fluorescent Antibody Conjugate in Goats. In: Rupprecht C, Nagarajan T, editors. *Current Laboratory Techniques in Rabies Diagnosis, Research and Prevention, Volume 2:* Academic Press; 2015. p. 69-81.
416. Faber M, Pulmanusahakul R, Nagao K, Prosnjak M, Rice AB, Koprowski H, et al. Identification of viral genomic elements responsible for rabies virus neuroinvasiveness. *Proc Natl Acad Sci U S A.* 2004;101(46):16328-32.
417. Aubert M. Methods for the calculation of titres. Meslin FX, Kaplan, M. M. & Koprowski, H., editor. Geneva: World Health Organisation; 1996.
418. Wiktor TJ, Aaslestad HG, Kaplan MM. Immunogenicity of rabies virus inactivated by - propiolactone, acetyleneimine, and ionizing irradiation. *Appl Microbiol.* 1972;23(5):914-8.
419. Robardet E, Picard-Meyer E, Andrieu S, Servat A, Cliquet F. International interlaboratory trials on rabies diagnosis: an overview of results and variation in reference diagnosis techniques (fluorescent antibody test, rabies tissue culture infection test, mouse inoculation test) and molecular biology techniques. *J Virol Methods.* 2011;177(1):15-25.

420. Percie du Sert N, Ahluwalia A, Alam S, Avey MT, Baker M, Browne WJ, et al. Reporting animal research: Explanation and elaboration for the ARRIVE guidelines 2.0. *PLOS Biology*. 2020;18(7):e3000411.
421. Brookes SM, Aegerter JN, Smith GC, Healy DM, Jolliffe TA, Swift SM, et al. European bat lyssavirus in Scottish bats. *Emerg Infect Dis*. 2005;11(4):572-8.
422. Cox R, Mykkeltvedt E, Robertson J, Haaheim L. Non-lethal viral challenge of influenza haemagglutinin and nucleoprotein DNA vaccinated mice results in reduced viral replication. *Scandinavian journal of immunology*. 2002;55(1):14-23.
423. Zufferey R, Nagy D, Mandel RJ, Naldini L, Trono D. Multiply attenuated lentiviral vector achieves efficient gene delivery in vivo. *Nature biotechnology*. 1997;15(9):871-5.
424. Schnell MJ, Mebatsion T, Conzelmann KK. Infectious rabies viruses from cloned cDNA. *EMBO J*. 1994;13(18):4195-203.
425. Schnell MJ, Foley HD, Siler CA, McGettigan JP, Dietzschold B, Pomerantz RJ. Recombinant rabies virus as potential live-viral vaccines for HIV-1. *Proc Natl Acad Sci U S A*. 2000;97(7):3544-9.
426. Buchholz UJ, Finke S, Conzelmann K-K. Generation of bovine respiratory syncytial virus (BRSV) from cDNA: BRSV NS2 is not essential for virus replication in tissue culture, and the human RSV leader region acts as a functional BRSV genome promoter. *Journal of virology*. 1999;73(1):251-9.
427. Mayes B, Rupprecht CE. Chapter Eight - Direct Fluorescent Antibody Test for Rabies Diagnosis. In: Rupprecht C, Nagarajan T, editors. *Current Laboratory Techniques in Rabies Diagnosis, Research and Prevention, Volume 2*: Academic Press; 2015. p. 83-92.
428. Hicks DJ, Nunez A, Healy DM, Brookes SM, Johnson N, Fooks AR. Comparative pathological study of the murine brain after experimental infection with classical rabies virus and European bat lyssaviruses. *J Comp Pathol*. 2009;140(2-3):113-26.
429. Tamura K, Stecher G, Peterson D, Filipinski A, Kumar S. MEGA6: molecular evolutionary genetics analysis version 6.0. *Molecular biology and evolution*. 2013;30(12):2725-9.
430. Rambaut A. FigTree-version 1.4. 3, a graphical viewer of phylogenetic trees. Computer program distributed by the author, website: <http://tree.bio.ed.ac.uk/software/figtree>. 2017.
431. Waterhouse A, Bertoni M, Bienert S, Studer G, Tauriello G, Gumienny R, et al. SWISS-MODEL: homology modelling of protein structures and complexes. *Nucleic Acids Res*. 2018;46(W1):W296-w303.
432. Schwede T, Kopp J, Guex N, Peitsch MC. SWISS-MODEL: an automated protein homology-modeling server. *Nucleic acids research*. 2003;31(13):3381-5.
433. Kiefer F, Arnold K, Künzli M, Bordoli L, Schwede T. The SWISS-MODEL Repository and associated resources. *Nucleic acids research*. 2009;37(suppl_1):D387-D92.
434. Schrödinger L. The PyMOL Molecular Graphics System, Version 2.3. 2019.
435. Smith DJ, Lapedes AS, de Jong JC, Bestebroer TM, Rimmelzwaan GF, Osterhaus ADME, et al. Mapping the Antigenic and Genetic Evolution of Influenza Virus. *Science*. 2004;305(5682):371-6.
436. Stading B, Ellison JA, Carson WC, Satheshkumar PS, Rocke TE, Osorio JE. Protection of bats (*Eptesicus fuscus*) against rabies following topical or oronasal exposure to a recombinant raccoon poxvirus vaccine. *PLoS Negl Trop Dis*. 2017;11(10):e0005958.
437. Tordo N, Bahloul C, Jacob Y, Jallet C, Perrin P, Badrane H. Rabies: epidemiological tendencies and control tools. *Dev Biol (Basel)*. 2006;125:3-13.
438. Organization WH. Rabies vaccines: WHO position paper, April 2018 - Recommendations. *Vaccine*. 2018;36(37):5500-3.
439. Dietzschold B, Rupprecht CE, Tollis M, Lafon M, Mattei J, Wiktor TJ, et al. Antigenic diversity of the glycoprotein and nucleocapsid proteins of rabies and rabies-related viruses: implications for epidemiology and control of rabies. *Rev Infect Dis*. 1988;10 Suppl 4:S785-98.

440. Servat A, Feyssaguet M, Blanchard I, Morize JL, Schereffer JL, Boue F, et al. A quantitative indirect ELISA to monitor the effectiveness of rabies vaccination in domestic and wild carnivores. *J Immunol Methods*. 2007;318(1-2):1-10.
441. Muller T, Selhorst T, Burow J, Schameitat A, Vos A. Cross reactive antigenicity in orally vaccinated foxes and raccoon dogs against European Bat Lyssavirus type 1 and 2. *Dev Biol (Basel)*. 2006;125:195-204.
442. Goldwasser RA, Kissling RE. Fluorescent antibody staining of street and fixed rabies virus antigens. *Proc Soc Exp Biol Med*. 1958;98(2):219-23.
443. Kuzmin IV, Orciari LA, Arai YT, Smith JS, Hanlon CA, Kameoka Y, et al. Bat lyssaviruses (Aravan and Khujand) from Central Asia: phylogenetic relationships according to N, P and G gene sequences. *Virus Res*. 2003;97(2):65-79.
444. Whitby JE, Heaton PR, Black EM, Wooldridge M, McElhinney LM, Johnstone P. First isolation of a rabies-related virus from a Daubenton's bat in the United Kingdom. *Vet Rec*. 2000;147(14):385-8.
445. Aubert M. Rabies in individual countries: France. *Rabies Bull Europe*. 1999;23(2):6.
446. Marston DA, Ellis RJ, Horton DL, Kuzmin IV, Wise EL, McElhinney LM, et al. Complete genome sequence of Ikoma lyssavirus. *J Virol*. 2012;86(18):10242-3.
447. Marston DA, Ellis RJ, Wise EL, Arechiga-Ceballos N, Freuling CM, Banyard AC, et al. Complete Genome Sequence of Lleida Bat Lyssavirus. *Genome Announc*. 2017;5(2).
448. Nokireki T, Jakava-Viljanen M, Virtala AM, Sihvonen L. Efficacy of rabies vaccines in dogs and cats and protection in a mouse model against European bat lyssavirus type 2. *Acta Vet Scand*. 2017;59(1):64.
449. Bahloul C, Jacob Y, Tordo N, Perrin P. DNA-based immunization for exploring the enlargement of immunological cross-reactivity against the lyssaviruses. *Vaccine*. 1998;16(4):417-25.
450. Ludi AB, Horton DL, Li Y, Mahapatra M, King DP, Knowles NJ, et al. Antigenic variation of foot-and-mouth disease virus serotype A. *The Journal of general virology*. 2014;95(Pt 2):384-92.
451. Organization WH. WHO Expert Committee on Rabies [meeting held in Geneva from 24 to 30 September 1991]: eighth report: World Health Organization; 1992.
452. Patel AC, Upmanyu V, Ramasamy S, Gupta PK, Singh R, Singh RP. Molecular and immunogenic characterization of BHK-21 cell line adapted CVS-11 strain of rabies virus and future prospect in vaccination strategy. *Virusdisease*. 2015;26(4):288-96.
453. Wild TF, Bijlenga G. A rabies virus persistent infection in BHK21 cells. *J Gen Virol*. 1981;57(Pt 1):169-77.
454. Moser LA, Boylan BT, Moreira FR, Myers LJ, Svenson EL, Fedorova NB, et al. Growth and adaptation of Zika virus in mammalian and mosquito cells. *PLoS neglected tropical diseases*. 2018;12(11):e0006880-e.
455. Morimoto K, Hooper DC, Carbaugh H, Fu ZF, Koprowski H, Dietzschold B. Rabies virus quasispecies: implications for pathogenesis. *Proc Natl Acad Sci U S A*. 1998;95(6):3152-6.
456. Bourhy H, Sureau P, Tordo N. From rabies to rabies-related viruses. *Vet Microbiol*. 1990;23(1-4):115-28.
457. Malerczyk C, Freuling C, Gniel D, Giesen A, Selhorst T, Muller T. Cross-neutralization of antibodies induced by vaccination with Purified Chick Embryo Cell Vaccine (PCECV) against different Lyssavirus species. *Hum Vaccin Immunother*. 2014;10(10):2799-804.
458. Malerczyk C, Selhorst T, Tordo N, Moore S, Muller T. Antibodies induced by vaccination with purified chick embryo cell culture vaccine (PCECV) cross-neutralize non-classical bat lyssavirus strains. *Vaccine*. 2009;27(39):5320-5.
459. Reading SA, Dimmock NJ. Neutralization of animal virus infectivity by antibody. *Archives of Virology*. 2007;152(6):1047-59.
460. Klasse P, Sattentau Q. Occupancy and mechanism in antibody-mediated neutralization of animal viruses. *Journal of General Virology*. 2002;83(9):2091-108.

461. Della-Porta A, Westaway E. A multi-hit model for the neutralization of animal viruses. *Journal of General Virology*. 1978;38(1):1-19.
462. Parren PW, Mondor I, Naniche D, Ditzel HJ, Klasse P, Burton DR, et al. Neutralization of human immunodeficiency virus type 1 by antibody to gp120 is determined primarily by occupancy of sites on the virion irrespective of epitope specificity. *Journal of Virology*. 1998;72(5):3512-9.
463. Dimmock NJ. Neutralization of animal viruses. 2012.
464. Sanders B, Koldijk M, Schuitemaker H. Inactivated Viral Vaccines. *Vaccine Analysis: Strategies, Principles, and Control*. 2014:45-80.
465. Colburn NH, Richardson R, Boutwell R. Studies of the reaction of β -propiolactone with deoxyguanosine and related compounds. *Biochemical pharmacology*. 1965;14(7):1113-8.
466. Maté U, Solomon JJ, Segal A. In vitro binding of β -propiolactone to calf thymus DNA and mouse liver DNA to form 1-(2-carboxyethyl) adenine. *Chemico-biological interactions*. 1977;18(3):327-36.
467. Roberts J, Warwick G. The reaction of beta-propiolactone with guanosine, deoxyguanylic acid and RNA. *Biochemical pharmacology*. 1963;12:1441-2.
468. Hemminki K. Reactions of β -propiolactone, β -butyrolactone and γ -butyrolactone with nucleic acids. *Chemico-biological interactions*. 1981;34(3):323-31.
469. Uittenbogaard JP, Zomer B, Hoogerhout P, Metz B. Reactions of β -propiolactone with nucleobase analogues, nucleosides, and peptides: Implications for the inactivation of viruses. *Journal of Biological Chemistry*. 2011;286(42):36198-214.
470. Herrera-Rodriguez J, Signorazzi A, Holtrop M, de Vries-Idema J, Huckriede A. Inactivated or damaged? Comparing the effect of inactivation methods on influenza virions to optimize vaccine production. *Vaccine*. 2019;37(12):1630-7.
471. De Benedictis P, Minola A, Rota Nodari E, Aiello R, Zecchin B, Salomoni A, et al. Development of broad-spectrum human monoclonal antibodies for rabies post-exposure prophylaxis. *EMBO Mol Med*. 2016;8(4):407-21.
472. Lodmell DL, Smith JS, Esposito JJ, Ewalt LC. Cross-protection of mice against a global spectrum of rabies virus variants. *J Virol*. 1995;69(8):4957-62.
473. Nel LH. Vaccines for lyssaviruses other than rabies. *Expert Rev Vaccines*. 2005;4(4):533-40.
474. Markotter W, Van Eeden C, Kuzmin IV, Rupprecht CE, Paweska JT, Swanepoel R, et al. Epidemiology and pathogenicity of African bat lyssaviruses. *Dev Biol (Basel)*. 2008;131:317-25.
475. Banyard AC, Fooks AR. The impact of novel lyssavirus discovery. *Microbiology Australia*. 2017;38(1):17-21.
476. Gibson DG, Young L, Chuang R-Y, Venter JC, Hutchison CA, Smith HO. Enzymatic assembly of DNA molecules up to several hundred kilobases. *Nature Methods*. 2009;6(5):343-5.
477. McGettigan JP, Foley HD, Belyakov IM, Berzofsky JA, Pomerantz RJ, Schnell MJ. Rabies virus-based vectors expressing human immunodeficiency virus type 1 (HIV-1) envelope protein induce a strong, cross-reactive cytotoxic T-lymphocyte response against envelope proteins from different HIV-1 isolates. *J Virol*. 2001;75(9):4430-4.
478. Wirblich C, Schnell MJ. Rabies virus (RV) glycoprotein expression levels are not critical for pathogenicity of RV. *J Virol*. 2011;85(2):697-704.
479. Pei J, Huang F, Wu Q, Luo Z, Zhang Y, Ruan J, et al. Codon optimization of G protein enhances rabies virus-induced humoral immunity. *J Gen Virol*. 2019;100(8):1222-33.
480. Luo J, Zhang Y, Zhang Q, Wu Y, Zhang B, Mo M, et al. The Deoptimization of Rabies Virus Matrix Protein Impacts Viral Transcription and Replication. *Viruses*. 2019;12(1).
481. Marosi A, Dufkova L, Forro B, Felde O, Erdelyi K, Sirmarova J, et al. Combination therapy of rabies-infected mice with inhibitors of pro-inflammatory host response, antiviral compounds and human rabies immunoglobulin. *Vaccine*. 2019;37(33):4724-35.

482. Jallet C, Jacob Y, Bahloul C, Drings A, Desmezieres E, Tordo N, et al. Chimeric lyssavirus glycoproteins with increased immunological potential. *J Virol*. 1999;73(1):225-33.
483. Fisher CR, Lowe DE, Smith TG, Yang Y, Hutson CL, Wirblich C, et al. Lyssavirus Vaccine with a Chimeric Glycoprotein Protects across Phylogroups. *Cell Reports*. 2020;32(3):107920.
484. Koprowski H. Laboratory techniques in rabies: vaccine for man prepared in human diploid cells. *Monogr Ser World Health Organ*. 1973(23):256-60.
485. Tao L, Ge J, Wang X, Zhai H, Hua T, Zhao B, et al. Molecular basis of neurovirulence of flury rabies virus vaccine strains: importance of the polymerase and the glycoprotein R333Q mutation. *J Virol*. 2010;84(17):8926-36.
486. Abreu-Mota T, Hagen KR, Cooper K, Jahrling PB, Tan G, Wirblich C, et al. Non-neutralizing antibodies elicited by recombinant Lassa-Rabies vaccine are critical for protection against Lassa fever. *Nat Commun*. 2018;9(1):4223.
487. Keshwara R, Hagen KR, Abreu-Mota T, Papaneri AB, Liu D, Wirblich C, et al. A Recombinant Rabies Virus Expressing the Marburg Virus Glycoprotein Is Dependent upon Antibody-Mediated Cellular Cytotoxicity for Protection against Marburg Virus Disease in a Murine Model. *J Virol*. 2019;93(6).
488. Willet M, Kurup D, Papaneri A, Wirblich C, Hooper JW, Kwilas SA, et al. Preclinical Development of Inactivated Rabies Virus-Based Polyvalent Vaccine Against Rabies and Filoviruses. *J Infect Dis*. 2015;212 Suppl 2:S414-24.
489. Kgaladi J, Faber M, Dietzschold B, Nel LH, Markotter W. Pathogenicity and Immunogenicity of Recombinant Rabies Viruses Expressing the Lagos Bat Virus Matrix and Glycoprotein: Perspectives for a Pan-Lyssavirus Vaccine. *Tropical Medicine and Infectious Disease*. 2017;2(3):37.
490. Dietzschold B, Gore M, Marchadier D, Niu HS, Bunschoten HM, Otvos L, Jr., et al. Structural and immunological characterization of a linear virus-neutralizing epitope of the rabies virus glycoprotein and its possible use in a synthetic vaccine. *J Virol*. 1990;64(8):3804-9.
491. Berman HM, Westbrook J, Feng Z, Gilliland G, Bhat TN, Weissig H, et al. The Protein Data Bank. *Nucleic Acids Research*. 2000;28(1):235-42.
492. Coll JM. The glycoprotein G of rhabdoviruses. *Archives of Virology*. 1995;140(5):827-51.
493. Healy D, Brookes S, Banyard A, Núñez A, Cosby S, Fooks A. Pathobiology of rabies virus and the European bat lyssaviruses in experimentally infected mice. *Virus research*. 2013;172(1-2):46-53.
494. Cliquet F, Verdier Y, Sagne L, Aubert M, Schereffer JL, Selve M, et al. Neutralising antibody titration in 25,000 sera of dogs and cats vaccinated against rabies in France, in the framework of the new regulations that offer an alternative to quarantine. *Rev Sci Tech*. 2003;22(3):857-66.
495. Nascimento Silva JR, Camacho LAB, Siqueira MM, Freire MdS, Castro YP, Maia MdLS, et al. Mutual interference on the immune response to yellow fever vaccine and a combined vaccine against measles, mumps and rubella. *Vaccine*. 2011;29(37):6327-34.
496. Dietzschold B, Wunner WH, Wiktor TJ, Lopes AD, Lafon M, Smith CL, et al. Characterization of an antigenic determinant of the glycoprotein that correlates with pathogenicity of rabies virus. *Proc Natl Acad Sci U S A*. 1983;80(1):70-4.
497. Ilina EN, Solopova ON, Balabashin DS, Larina MV, Aliev TK, Grebennikova TV, et al. Generation and Characterization of a Neutralizing Monoclonal Antibody Against Rabies Virus. *Russian Journal of Bioorganic Chemistry*. 2018;44(6):695-704.
498. Wunner WH, Conzelmann K-K. Chapter 2 - Rabies virus. In: Fooks AR, Jackson AC, editors. *Rabies (Fourth Edition)*. Boston: Academic Press; 2020. p. 43-81.
499. Shakin-Eshleman SH, Remaley AT, Eshleman JR, Wunner WH, Spitalnik SL. N-linked glycosylation of rabies virus glycoprotein. Individual sequons differ in their glycosylation efficiencies and influence on cell surface expression. *J Biol Chem*. 1992;267(15):10690-8.

500. Shakin-Eshleman SH, Wunner WH, Spitalnik SL. Efficiency of N-linked core glycosylation at asparagine-319 of rabies virus glycoprotein is altered by deletions C-terminal to the glycosylation sequon. *Biochemistry*. 1993;32(36):9465-72.
501. Kasturi L, Eshleman JR, Wunner WH, Shakin-Eshleman SH. The Hydroxy Amino Acid in an Asn-X-Ser/Thr Sequon Can Influence N-Linked Core Glycosylation Efficiency and the Level of Expression of a Cell Surface Glycoprotein *. *Journal of Biological Chemistry*. 1995;270(24):14756-61.
502. Dietzschold B, Wiktor TJ, Wunner WH, Varrichio A. Chemical and immunological analysis of the rabies soluble glycoprotein. *Virology*. 1983;124(2):330-7.
503. Wojczyk BS, Takahashi N, Levy MT, Andrews DW, Abrams WR, Wunner WH, et al. N-glycosylation at one rabies virus glycoprotein sequon influences N-glycan processing at a distant sequon on the same molecule. *Glycobiology*. 2005;15(6):655-66.
504. Badrane H, Tordo N. Host switching in Lyssavirus history from the Chiroptera to the Carnivora orders. *J Virol*. 2001;75(17):8096-104.
505. Liu H, Albina E, Gil P, Minet C, de Almeida RS. Two-plasmid system to increase the rescue efficiency of paramyxoviruses by reverse genetics: The example of rescuing Newcastle Disease Virus. *Virology*. 2017;509:42-51.
506. Celis E, Wiktor TJ, Dietzschold B, Koprowski H. Amplification of rabies virus-induced stimulation of human T-cell lines and clones by antigen-specific antibodies. *J Virol*. 1985;56(2):426-33.
507. Kawano H, Mifune K, Ohuchi M, Mannen K, Cho S, Hiramatsu K, et al. Protection against rabies in mice by a cytotoxic T cell clone recognizing the glycoprotein of rabies virus. *J Gen Virol*. 1990;71 (Pt 2):281-7.
508. Wilbur L. The NIH test for potency. *Laboratory techniques in rabies*. 1996:360-8.
509. Santra S, Liao H-X, Zhang R, Muldoon M, Watson S, Fischer W, et al. Mosaic vaccines elicit CD8+ T lymphocyte responses that confer enhanced immune coverage of diverse HIV strains in monkeys. *Nature Medicine*. 2010;16(3):324-8.
510. Calisher CH, Childs JE, Field HE, Holmes KV, Schountz T. Bats: important reservoir hosts of emerging viruses. *Clin Microbiol Rev*. 2006;19(3):531-45.
511. Irving AT, Ahn M, Goh G, Anderson DE, Wang L-F. Lessons from the host defences of bats, a unique viral reservoir. *Nature*. 2021;589(7842):363-70.
512. Dato VM, Campagnolo ER, Long J, Rupprecht CE. A Systematic Review of Human Bat Rabies Virus Variant Cases: Evaluating Unprotected Physical Contact with Claws and Teeth in Support of Accurate Risk Assessments. *PLoS One*. 2016;11(7):e0159443.
513. Liu Y, Li N, Zhang S, Zhang F, Lian H, Wang Y, et al. Analysis of the complete genome of the first Irkut virus isolate from China: comparison across the Lyssavirus genus. *Mol Phylogenet Evol*. 2013;69(3):687-93.
514. Iizuka K. Australian Bat Lyssavirus - Human fatality Promed mail2013 [Available from: <http://www.promedmail.org/direct.php?id=20130323.1600266>].
515. Regnault B, Evrard B, Plu I, Dacheux L, Troadec E, Cozette P, et al. First case of lethal encephalitis in Western Europe due to European bat lyssavirus type 1. *Clinical Infectious Diseases*. 2021.
516. Herzog M, Fritzell C, Lafage M, Montano Hirose JA, Scott-Algara D, Lafon M. T and B cell human responses to European bat lyssavirus after post-exposure rabies vaccination. *Clin Exp Immunol*. 1991;85(2):224-30.
517. Aubert MF. Practical significance of rabies antibodies in cats and dogs. *Rev Sci Tech*. 1992;11(3):735-60.
518. Zanetti CR, de Franco MT, Vassao RC, Pereira CA, Pereira OA. Failure of protection induced by a Brazilian vaccine against Brazilian wild rabies viruses. *Arch Virol*. 1998;143(9):1745-56.

519. Moore SM, Ricke TA, Davis RD, Briggs DJ. The influence of homologous vs. heterologous challenge virus strains on the serological test results of rabies virus neutralizing assays. *Biologicals*. 2005;33(4):269-76.
520. England PH. Rabies. 2012 [cited 25/05/2021]. In: The Green Book [Internet]. [cited 25/05/2021]. Available from: https://assets.publishing.service.gov.uk/government/uploads/system/uploads/attachment_data/file/723607/GreenBook_chapter_27_rabies.pdf.
521. van Thiel PP, de Bie RM, Eftimov F, Tepaske R, Zaaijer HL, van Doornum GJ, et al. Fatal human rabies due to Duvenhage virus from a bat in Kenya: failure of treatment with coma-induction, ketamine, and antiviral drugs. *PLoS Negl Trop Dis*. 2009;3(7):e428.
522. Ajjan N, Soulebot JP, Triaux R, Biron G. Intradermal immunization with rabies vaccine. Inactivated Wistar strain cultivated in human diploid cells. *JAMA*. 1980;244(22):2528-31.
523. Burridge MJ, Baer GM, Sumner JW, Sussman O. Intradermal immunization with human diploid cell rabies vaccine. Serological and clinical responses of persons with and without prior vaccination with duck embryo vaccine. *JAMA*. 1982;248(13):1611-4.
524. Holmes EC, Woelk CH, Kassir R, Bourhy H. Genetic constraints and the adaptive evolution of rabies virus in nature. *Virology*. 2002;292(2):247-57.
525. Davis PL, Bourhy H, Holmes EC. The evolutionary history and dynamics of bat rabies virus. *Infect Genet Evol*. 2006;6(6):464-73.
526. M  lade J, McCulloch S, Ramasindrazana B, Lagadec E, Turpin M, Pascalis H, et al. Serological Evidence of Lyssaviruses among Bats on Southwestern Indian Ocean Islands. *PLOS ONE*. 2016;11(8):e0160553.
527. Serra-Cobo J, Lopez-Roig M, Segui M, Sanchez LP, Nadal J, Borr  s M, et al. Ecological factors associated with European bat lyssavirus seroprevalence in spanish bats. *PLoS One*. 2013;8(5):e64467.
528. Sparrow E, Torvaldsen S, Newall AT, Wood JG, Sheikh M, Kieny MP, et al. Recent advances in the development of monoclonal antibodies for rabies post exposure prophylaxis: A review of the current status of the clinical development pipeline. *Vaccine*. 2019;37 Suppl 1:A132-A9.
529. Gogtay NJ, Munshi R, Ashwath Narayana DH, Mahendra BJ, Kshirsagar V, Gunale B, et al. Comparison of a Novel Human Rabies Monoclonal Antibody to Human Rabies Immunoglobulin for Postexposure Prophylaxis: A Phase 2/3, Randomized, Single-Blind, Noninferiority, Controlled Study. *Clin Infect Dis*. 2018;66(3):387-95.
530. Fritze CE, Anderson TR. Epitope tagging: General method for tracking recombinant proteins. In: Thorner J, Emr SD, Abelson JN, editors. *Methods in Enzymology*. 327: Academic Press; 2000. p. 3-16.
531. Lobbsta  l E, Reumers V, Ibrahimi A, Paesen K, Thiry I, Gijssbers R, et al. Immunohistochemical detection of transgene expression in the brain using small epitope tags. *BMC Biotechnology*. 2010;10(1):16.
532. Hannah BP, Heldwein EE, Bender FC, Cohen GH, Eisenberg RJ. Mutational evidence of internal fusion loops in herpes simplex virus glycoprotein B. *J Virol*. 2007;81(9):4858-65.
533. Morimoto K, Ni YJ, Kawai A. Syncytium formation is induced in the murine neuroblastoma cell cultures which produce pathogenic type G proteins of the rabies virus. *Virology*. 1992;189(1):203-16.
534. Nel LH, Niezgod   M, Hanlon CA, Morrill PA, Yager PA, Rupprecht CE. A comparison of DNA vaccines for the rabies-related virus, Mokola. *Vaccine*. 2003;21(19-20):2598-606.
535. Dacheux L, Larrous F, Mailles A, Boisseleau D, Delmas O, Biron C, et al. European bat Lyssavirus transmission among cats, Europe. *Emerg Infect Dis*. 2009;15(2):280-4.
536. Crick J, Tignor GH, Moreno K. A new isolate of Lagos bat virus from the Republic of South Africa. *Trans R Soc Trop Med Hyg*. 1982;76(2):211-3.
537. Inoue K, Shoji Y, Kurane I, Iijima T, Sakai T, Morimoto K. An improved method for recovering rabies virus from cloned cDNA. *J Virol Methods*. 2003;107(2):229-36.

- 538. Ito N, Takayama M, Yamada K, Sugiyama M, Minamoto N. Rescue of rabies virus from cloned cDNA and identification of the pathogenicity-related gene: glycoprotein gene is associated with virulence for adult mice. *J Virol*. 2001;75(19):9121-8.
- 539. Alberer M, Gnad-Vogt U, Hong HS, Mehr KT, Backert L, Finak G, et al. Safety and immunogenicity of a mRNA rabies vaccine in healthy adults: an open-label, non-randomised, prospective, first-in-human phase 1 clinical trial. *Lancet*. 2017;390(10101):1511-20.
- 540. Ertl HCJ. New Rabies Vaccines for Use in Humans. *Vaccines (Basel)*. 2019;7(2).
- 541. Bahloul C, Ahmed SB, B'Chir B I, Kharmachi H, Hayouni el A, Dellagi K. Post-exposure therapy in mice against experimental rabies: a single injection of DNA vaccine is as effective as five injections of cell culture-derived vaccine. *Vaccine*. 2003;22(2):177-84.
- 542. Wang C, Dulal P, Zhou X, Xiang Z, Goharriz H, Banyard A, et al. A simian-adenovirus-vectored rabies vaccine suitable for thermostabilisation and clinical development for low-cost single-dose pre-exposure prophylaxis. *PLoS Negl Trop Dis*. 2018;12(10):e0006870.
- 543. Xiang ZQ, Greenberg L, Ertl HC, Rupprecht CE. Protection of non-human primates against rabies with an adenovirus recombinant vaccine. *Virology*. 2014;450-451:243-9.

Appendix

Appendix 1: Reagents

A1.1. Tissue culture reagents

BHK-21 and BSR T7/5 Media

500 ml BHK-21 GMEM

25-50 ml heat inactivated FBS

50 ml Tryptose phosphate solution

5 ml penicillin/streptomycin solution to 100 U/ml penicillin and 100 µg/ml streptomycin

HEK 293T/17 Media

500 ml DMEM

50 ml heat inactivated FBS

15 ml D (+) glucose solution to 4 g/L

5 ml penicillin/streptomycin solution to 100 U/ml penicillin and 100 µl/ml streptomycin

Antibiotic Trypsin Versene (ATV):

450 ml sterile distilled water

50 ml Trypsin/versene 10X concentrate

5 ml Penicillin (100 U/ml)

Streptomycin (100 µg/ml)

Mycostatin (25 U/ml)

A1.2. Bacterial cell culture media

Luria –Bertaini (LB) Broth

10 g tryptone

5 g yeast extract

10 g sodium chloride (NaCl)

950 ml deionised water and autoclave to sterilise

Ampicillin or kanamycin to 100 mg/ml

LB Agar

10 g tryptone

5 g yeast extract

10 g NaCl

15 g melted agar

Deionised water to 1 l and autoclave to sterilise

Ampicillin or kanamycin to 100 mg/ml

A1.3. Molecular biological buffers

TAE Buffer (Tris-acetate EDTA) (50X)

242 g Tris base

57.1 g glacial acetic acid

100 ml 0.5 M EDTA

Distilled water to 1l and autoclave to sterilise

A1.4. Fluorescent mAb

Fujirebio fluorescein isothiocyanate conjugated (FITC) anti-rabies antibody:

Reconstituted with 5 ml of water and stored frozen in 1 ml aliquots

Or diluted (1/20) in PBS 0.1 M pH7.4

Filtered with a 0.45 µm syringe filter

Stored frozen at -20 °C

A1.5. Primers

Primer name	Forward/ Reverse	Sequence (5'-3')	Use	Target
1618	Reverse	GGTACCAAGCTTAAGTTTAAACG	Linearise pcDNA3.1(+)	pcDNA3.1(+)
1619	Forward	GAGCTCGGATCCACTAGTC		
1841	Forward	TCATGGTCATAGCTGTTTCCTGTGT GAAATTGTTATC	Linearise and exclude cSN G	cSN
1840	Reverse	TTTCACACAGGAAACAGCTATGACC ATGATTACGCC		
cSN fwd	Forward	GGACTGGCTAGCCTTTCAAC		
cSN rev	Reverse	CTTCCCGGGGTCTTTTG		
csn IKOV fwd	Forward	CTCAAAAGACCCCGGGAAAGATGG CTCAGTTGGTCACTTTG		
csn WCBV rev	Reverse	GTTGAAAGGCTAGCCAGTCCTTATT GGCAGTTTGTCCC	Gisbon assembly primers: Primers with incorporated overhangs complementary to cSN	IKOV G
csn LLEBV fwd	Forward	CTCAAAAGACCCCGGGAAAGATGG CTTACCAAGTAACC		WCBV G
csn IKOV rev	Reverse	GTTGAAAGGCTAGCCAGTCCTTAG AATGCAGAACTCTTG		LLEBV G
csn WCBV fwd	Forward	CTCAAAAGACCCCGGGAAAGATGG CTTCTACTTTGCG		IKOV G
csn LLEBV rev	Reverse	GTTGAAAGGCTAGCCAGTCCTTAG AGGTTTGTGGAGTTTTG		WCBV G
csn LBVD fwd	Forward	CTCAAAAGACCCCGGGAAAGATGA GTTACTCGATTTC AACAC		LLEBV G
csn RABV rev	Reverse	GTTGAAAGGCTAGCCAGTCCTCACA GTCTGGTCTCACC		LBV-D G
csn RABV fwd	Forward	CTCAAAAGACCCCGGGAAAGATGG TTCCTCAGGCTCTC		RABV G
csn LBVD rev	Reverse	GTTGAAAGGCTAGCCAGTCCTTAG GCATTTGAGGAGCC		RABV G
csn Mosaic All fwd	Forward	CTCAAAAGACCCCGGGAAAGATGA GTTACTCGATTTC AACAC		LBV-D G
csn Mosaic All rev	Reverse	GTTGAAAGGCTAGCCAGTCCTTAG GCATTTGAGGAGCC		Mosaic All G
csn Mosaic 1 and 2 fwd	Forward	CTCAAAAGACCCCGGGAAAGATGA GTTACTCGATTTC AACAC		Mosaic All G
csn Mosaic 1 and 2 rev	Reverse	GTTGAAAGGCTAGCCAGTCCTCACA GTCTGGTCTCACC		Mosaic 1 and 2 G
csn Mosaic 3 fwd	Forward	CTCAAAAGACCCCGGGAAAGATGG CTTACCAAGTAACC		Mosaic 1 and 2 G
csn Mosaic 3 rev	Reverse	GTTGAAAGGCTAGCCAGTCCTTATT GGCAGTTTGTCC		Mosaic 3 G
Mosaic 2 fwd	Forward	CTCAAAAGACCCCGGGAAAGATGA GTTACTCGATTTC AACAC		Mosaic 3 G
Mosaic 2 rev	Reverse	GTTGAAAGGCTAGCCAGTCCTTAG GCATTTGAGGAGCC		Mosaic 2 G
cSN G fwd	Forward	ATCCCTCAAAGACCCCG	Confirmatory primers used in PCR and Sanger sequencing	cSN
cSN G rev	Reverse	CGTTGAAAGGCTAGCCAG		cSN
LBVD/RABV middle G	Forward	CGAATCAACTAGTGAACCTGC		LBV-D/RABV G
RABV/LBVD middle G	Forward	CCC GATCAGTTGGTCAATGTGC		RABV/LBV-D G

IKOV/LLEBV middle G	Forward	GTTCCAGATCAGCCATGGTAAA		IKOV/LLEBV G
IKOV/WCBV middle G	Forward	GTTCCAGATCACAGCTGATCAA		IKOV/WCBV G
LLEBV/IKOV middle G	Forward	GTCCAAGATCTAAAATGGTGA		LLEBV/IKOV G
LLEBV/WCBV middle G	Forward	GTCCAAGATCTCAGCTGATCA		LLEBV/WCBV G
WCBV/IKOV middle G	Forward	GTTCTCCATCAAAAATGGTGA		WCBV/IKOV G
WCBV/LLEBV middle G	Forward	GTTCTCCATCAGCCATGGTAAA		WCBV/LLEBV G
Mosaic 3 middle G	Forward	CTGTTCAGATCAGTTAAAGG		Mosaic 3 G
Mosaic 1 and 2 middle G	Forward	TTTTACAGAACACTGAGAGG		Mosaic 1 and 2 G
Mosaic All middle G	Forward	CAGAGGTCATCCCACACA		Mosaic All G
JW12	Forward	ATGTAACACCYCTACAATG	RT/ PCR/ Real time PCR	All lyssavirus N
N1650146	Reverse	GCAGGGTAYTTRTACTCATA	RT/ PCR/ Real time PCR	All lyssavirus N
JW6UNI	Reverse	CARTTVGCRCACATYTTRTG	RT/ PCR/ Real time PCR	All lyssavirus N
BatRat beta- actin intronic	Forward	CGATGAAGATCAAGATCATTG	RT/ PCR/ Real time PCR	Multi species Beta Actin
BatRat beta- actin reverse	Reverse	AAGCATTTGCGGTGGAC	RT/ PCR/ Real time PCR	Multi species Beta Actin

Appendix 2: Cloning

A2.1. Cloning into cSN

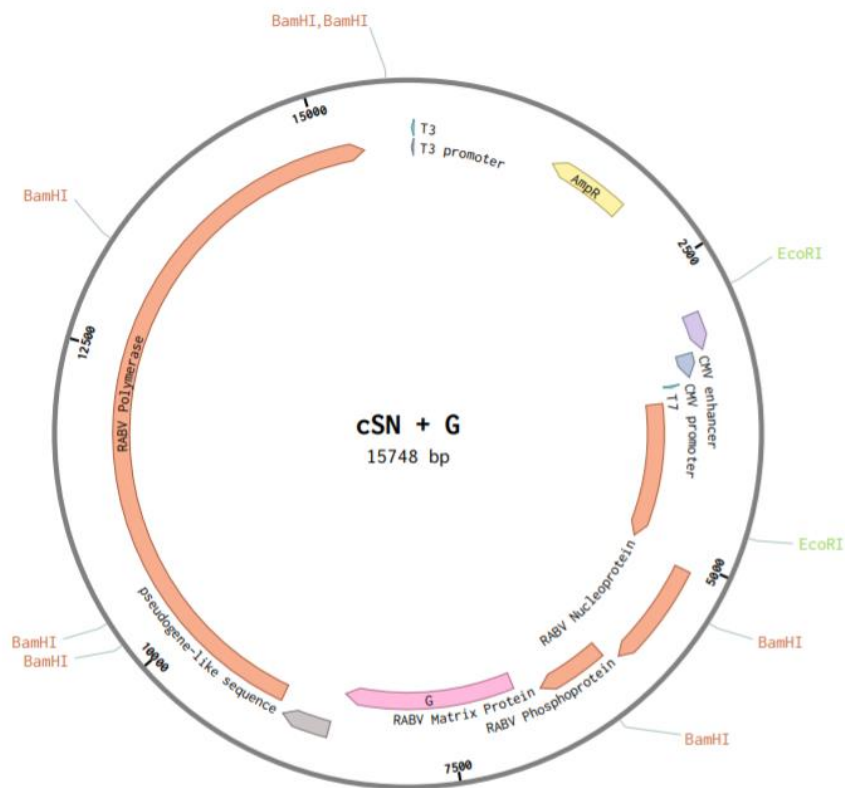


Figure A2.1: Cloning into cSN. The full length plasmid, cSN, and the proposed site for lyssavirus glycoprotein gene insertion, indicated by the pink G, in place of the homologous RABV G.

Appendix 3: Chimeric Glycoprotein

A3.1. Table of isolates used for generation of Mosaic 2 G.

Virus	Genbank Accession number
LBV	EF547432
	EF547431
	EF547425
	GU170202
	EF547433
	MH643893
	LN849915
	EU293108
	EF547423
	EF547429
	EF547422
	EF547428
	EF547421
	EF547430
	EF547426
	EF547427
MOKV	KF155005
	GQ473001
	EU293117
	EU293118
	GQ473002
	GQ473003
	GQ473004
	KF155006
	GQ500109
	GQ500110
	KF155008
	GQ500111
	GQ500112
	HQ266624
	KC218937
	GQ500108

A3.2. Chimeric Glycoprotein sequences

Chimeric Glycoprotein	Sequence (5'-3')
LBV-D/RABV	atgagttactcgatttcaacaccttttctgttcgtgtggctgcaatttcagttgcagacttccccctttacacaattcccgagaagatcgactcctggacgcctatagatatgatccatctgagttgtccaataacctttgtcaggggatgacgggtgc agcacatccacatccttcagttacgtggagctcaaaacagggtatctgactcatcagaaagtgtctgggttcacgtgtaccggggtcatcagtgaggctgttacatacacaaactttgtaggttatgtgacaaccacattaaaaggaagcatttcaag cccacggtctcagcctgtagagatgcatttctggaagatctcaggggatcctagatatgaagagttctgtcatacgccttaccctgacagtagttggttaagaacgggtcaccacaacaagggaatccttgcgtataatctccccagcattgtagag atggatataatagtagaactcttactctcctatgtttccacaggaaactgttccagattttatccatcagttccatcctgcgtaccaatcacgattacaccttgggttgcagaagattctaactaagtctcatttgtgacataatcgttactagcac aggtagaaaaagcaatgaacggctccaagatgtgtgggttcacagatgagaggggtttttacagaacactgagaggggctgtaaattgacgctctcgggaaaccagggtctaagactatatgtggaacatgggtatcctttacgcacgggaagt tcagtgtgtgtctcccgaatcaactagtgaaacctgcacgacttctcctcagacgaaattgagcaccttgtgtagaggagttggtcagggaagagagaggagtgctggatgcactagagtcctatgacaaccaagtcagtgagtttcagacgtc tcagtcatttaagaaaaactgtccctgggtttgaaaaagcatataccatattcaacaagacctgtgatggaagccgatgtcactacaagtcagtcagaacttggaatgagatcctccctcaaaagggtgtttaagagttggggggagggtgcacctc atgtgaacgggggtgttttcaatggtataatattaggacctgacggcaatgtcttaatcccagagatgcaatcatccctcctcagcaacatatggagttgttggaatcctcggttatcccttgtgcacccctggcagaccgtcgaccgttttcaag gacgggtgacgaggctgaggattttgtgaagttcaccttccgatgtgcacaatcagggtctcaggagttgacttgggtctcccgaactgggggaagtgtattactgagtgaggggccctgactgccttgatgttgataattttctgatgacatgttg tagaagagtcactcgatcagaacctacgcaacacaatctcagaggggacagggagggtgtcagtcactcccaaggcgggaagatcatatcttcatgggaatcacacaagagtgagggtgagaccagactgtga
RABV/LBV-D	atggttctcaggctctcctgtttgtacccctctggtttttccattgtgttttgggaaattccctatttacacgataccagacaagcttggctccctggagccgattgacatacatcacctcagctgccccaaacaatttggtagtgaggagcaaggatgc accaacctgtcagggttctcctacatggaacttaagtggatatactttagccataaaaaatgaacgggttcacttgcacaggcgttgtgacggaggctgaaacctactactaactcgttggttatgtcacaccagttcaaaagaaagcatttccgc ccaacaccagatgcatgtagagccgctacaactggaagatggcgggtgacccagatatgaagagtcctacacaatcgtacccgtactaccgtggcttgaactgtaaaaaaccaccaaggagtcctcgttatcatatctccaagtgtggcag atttggacccatagacagatcccttactcaggggtcttccctagcgggaagtgtcaggagtagcggtgtcttactactgtcctactaaccacgattacacatttggatgcccagagaatccgagactagggatgtcttgtgacatttttaccat agtagagggaagagagcatcaaaggagtgagacttgcggctttagatgaagaggcctataaagtctttaaaggagcatgcaaaactcaagttagtgaggatcttaggacttagacttatggatggaacatgggtcgcgatgcaaacatca aatgaaccaaaatggtgccctccgatcagttggtcaatgtgcataataacgtatcgtatgagcttgagcatctgattgtggatgaccttatcaaaaaagagaagcatgtttagataccctggaacaattctgatgttaagtcaattagtttcagg agactcagtcatttcagaaagttggtacctggatggaaggcttacaccatattaaacgggagcttgatggagacaaatgtccactacagaagggtggacaattggactgatcttaccatcgaaaggatgtctgaaagtgagggaacaaatgc cttgatccccataaaggagtttatttcaatggattattaagggtccgatggtcataattttaatcccagagatgcagtcgggatgtgtaaacagcatatagatcttctgaaggcagcggtttttccctccgtcaccctcttatagatcagagttctgtg ttcaaaaaagatggtgatgcagatgatttgttgatgttcacatgcggatgtaaacaaagttagatcggacatagatcagggttccatcactggggtctgttcatctgtaggggtgacagattggcgttttctgttctgatgtcttctttgtattt gttgaagagagtgaaaggggaaggcttactggggataggacggaccgctcatttagcattatcttcaatctcctcaatcaaaaccgaaagtgtgtcatcttgggagtcctacaagggtcctcaaatgcctaa
IKOV/LLEBV	atggctcagttggtcactttggtgctgaacggattgtcccttttgacagggccaggcatatttccaatgtatacaatccctgaagggtgggtccctggactccgattgattatctcatctgaagtgtcctgacaatacataactttgcagaagagggtcg caatgagggcagcaagggtgttacttagaactgaagccttcttctcctcaaaacaaagtacaggggatttacctgtacagggataatcaacatggcaccacatacaccaatttctgttggttatgtcaccaccacttttcagcggtccacttcac ccaaccagagggtgtgtcgaagctagagagtggaagaagggaagggaaccgaagatacgaagagtcattgaccactccttatcccactctaaatggttgagaacagtcacaacctccaaggatcatggctgatattggatcctgcagtggtt gagatggacatctacaacaagacaatgttttctcagtccttcggaatggatactgcaacttttctcagaaaaatccagattttgtgagacaaatcatcaaacctccatttggattccggaagatgagggacgagggaattacatgtgacatcttcaa gcgagtagctgtatattactgaaaaatggaagcaagtctgcggtttccaagatgaagaggattattcagaagcataaagggtgcatgcaaaatgataatctgtgaaagtctgggtccgactatatgatggacatgggtgtcttacaattctgt tgataacctcaggatgtgttccagatcagccatggttaaacatgcatacaacaaactggatgactagaagaagcagtcgtaagagatctgtaaagaagagagaagaatgtctcaatgcatttgaagagattattatacaaaatccatcagctt agaaaaatgagtcgttcagaaaaatggtcccaggttccgactcgtttacacgatgataaaacagacattgatggaggcacacgggactacaaatcagatcgaaactggtgagattcttctaccctatatgttattggttaaaggaaaatg ctacaagatcatgatggagtactgttcaatggaatctgaaggatcacagggaaggttctcatccctgaaatgcagtcctatctattacaggatcatttgaactcctgagatcaaacactataccatggaggcacccttagtgcactatccgat gatacagacccttctcagagactgctgagttcattcagttgcatatgagggtcctgcaaaagtcacttcagatatagatttggactttcttcttggaaagatacctcattttgtgtgcttcatattagggtgttgattcttgggttgaataaaa gtattcattcaagtgatcgggtgatgacaaaaaaagatctttaggagaagatgcaggacatccttcagatcctgtgatcagatctgtaggaggttaaccaattatcttgggagtcctacaaaaactccacaaaccttag
IKOV/WCBV	atggctcagttggtcactttggtgctgaacggattgtcccttttgacagggccaggcatatttccaatgtatacaatccctgaagggtgggtccctggactccgattgattatctcatctgaagtgtcctgacaatacataactttgcagaagagggtcg caatgagggcagcaagggtgttacttagaactgaaccttcttctcctcaaaacaaagtacagggatttacctgtacagggataatcaacatggcaccacatacaccaatttctgttggttatgtcaccaccacttttcagcggtccacttcac ccaaccagagggtgtgtcgaagctagagagtggaagaagggaagggaaccgaagatacgaagagtcattgaccactccttatcccactctaaatggttgagaacagtcacaacctccaaggatcatggctgatattggatcctgcagtggtt

gagatggacatctacaacaagacaatgttttccagtccttcggaatggatactgcaacttttccagaaaaatccagattttgtgagacaaatcatcaactccatttggattccggaagatgagggacgaggaattacatgtgacatcttcaa
 gcgagtactggtatattactgaaaaatggaagcaaagtcgtcggttttcaagatgaaagaggattattcagaagcataaaagggtgcatgcaaaatgataatctgtgaaagcttgggtccgactatatgatgggacatgggtgtcttacaattctgt
 tgataacctcaggatgtgtccagatcacagctgatcaacacgcacgacatcaaggtcgatgagctggagaatgctatagtttagacttgattaggaggagagaagaatgtcttgacaccctagaacaattttgatgtcaggatctgtgagtcaca
 ggaggctgagtcatttcagaaaagctgggtccaggatctgggaaggcttactcttatataaaacggcaccttaatggaatcagatgctcactacatcaaggtagagaattggtcagaggctatccacacaaaaggatgtctatggtcggggcacaatg
 ctatgagccagtcaatgatgtgtatttcaacgggatcattcgggattcaaataatcagatcttgatacctgagatcagtcagtcagtccttctcagagaacatgttgacctgttgaaaggctaataatagttccgttcaggcatccaatgttacttaggtcctca
 catctgacactgaagaagatatcgtcgagttgtcaaccctcatctccaagatacccagaagttgggtgcagatatggatctcgggttagcagactggaagagatatctactaattggatcttggccgtaggaggagtgtagcaatcttattcatcgg
 aacatgttgtctgagatgtagagcaggagagaacagaagaacaatccgatacataggtcattgtccatgacgtggtgttccataaagataaggataaagtgattactcttgggaatcttacaagggacaaactgcccaataa
 atggcttaccagaatgaaacccctattttgaacagctgtcttcttacttgacaggacatttttccctgtatactattcctgactctattgttcttggactcccatagattgtctcatctcaaatgtcctgataatgcctttatagtagatgagaactgcact
 gatcatggggagataaattattcagaattgaagccctattccattcccaaagcaaagttcctggattacatgtacaggaatagtgactcaggcggtagcctacaccaatttttaggttatgtctcaacaacatttcagagatcacattttgttccaa
 tccccgagagtgcagagctgcgcaagaatggaagagcaaagtgatccagatatgaagattctttacaaaatccctaccctgactcaaaatggccttagaacagtcactactaccagagaatctctgttatcatagaaccagcaatagctgagatg
 gatattctacaacaaaactatgttctctctgtcttctcaggcggtctgtgattctctcgagggaatcccgattattgtgaaacaagccactctgactcgtattggatgccatgaagaaagccgaggaataactgtgatataattcaatccagcac
 cgggagacttttcaaaaaagacgatcaggtttgtgggatacaagatgagagaggcatgttaagagcacgagaggggcatgaaatgacaatctgtggcaagtgcaggtgtccgcctttatgacggaacctggatttctacaatacaatcgacaa
 cctgaaagtgtgtccaagatctaaaatgggtgaacaaacacacagttaaatggataatagaagagtcattgtgagagatcttattaagaagcgtgaagagtgccatagatgctctagaagaagtcattgtgactagatctataagcttcagaaag
 ttgagtctctttagaaagcaagttccaggaagagggtatgtttacactatgataaacaatacaatgatggaggcaacagggcattataaatcagtggaactggagacagattctacctaaccaatctgccttatgtggagcgcaagtgtcatcc
 aggttatgatgggtgattatttaacggtatcataagagacagtagaggcaaaataactaattccagaaatgcaatcacatctactccgagaccatctggagttgtctcaagagaaatccattccctggagacacccctctgtgcactattctgaaatgg
 ggaagatggctcagatcttaccagcttctcagctatacataaaagacccctattgtctgttctgacatagatataggatttcttcatggaagaagtatttgatgattgtggggggagtggtgataggactaattgtcttctgttctgttctgtcaagtt
 gttgttagagtatgttatactgttaagaggaaaaggcttcgtgagggttctatgaatgagacatccagtggtccctgtcattcgggactcttggtgacaaaacagcttctgtgggaatcttacaagagttctgcattctag
 atggcttaccagaatgaaacccctattttgaacagctgtcttcttacttgacaggacatttttccctgtatactattcctgactctattgttcttggactcccatagattgtctcatctcaaatgtcctgataatgcctttatagtagatgagaactgcact
 gatcatggggagataaattattcagaattgaagccctattccattcccaaagcaaagttcctggattacatgtacaggaatagtgactcaggcggtagcctacaccaatttttaggttatgtctcaacaacatttcagagatcacattttgttccaa
 tccccgagagtgcagagctgcgcaagaatggaagagcaaagtgatccagatatgaagattctttacaaaatccctaccctgactcaaaatggccttagaacagtcactactaccagagaatctctgttatcatagaaccagcaatagctgagatg
 gatattctacaacaaaactatgttctctctgtcttctcaggcggtctgtgattctctcgagggaatcccgattattgtgaaacaagccactctgactcgtattggatgccatgaagaaagccgaggaataactgtgatataattcaatccagcac
 cgggagacttttcaaaaaagacgatcaggtttgtgggatacaagatgagagaggcatgttaagagcacgagaggggcatgaaatgacaatctgtggcaagtgcaggtgtccgcctttatgacggaacctggatttctacaatacaatcgacaa
 cctgaaagtgtgtccaagatctcagctgatcaacacgcacgacatcaaggtcgatgagctggagaatgctatagtttagacttgattaggaggagagaagaatgtcttgacaccctagaacaattttgatgtcaggatctgtgagtcacaggagg
 ctgagtcatttcagaagctggttccaggatctgggaaggcttactcttatataaaacggcaccttaatggaatcagatgctcactacatcaaggtagagaattggtcagaggctatccacacaaaaggatgtctatggtcgggggcaaatgctatga
 gccagtcaatgatgtgtatttcaacgggatcattcgggattcaaataatcagatcttgatacctgagatgcagtcagtcagtccttctcagagaacatgttgacctgttgaaaggctaataatagttccgttcaggcatccaatgttacttaggtcctcacatctg
 aactgaagaagatagctgtgagttgtcaacccctcatctccaagatacccagaagttgggtgcagatatggatctcgggttagcagactggaagagatatctactaattggatcttggccgttaggaggagtgtagcaatcttattcatcggaaacat
 gttgtctgagatgtagagcaggagagaacagaagaacaatccgatacataggtcattgtccatgacgtggtgttccataaagataaggataaagtgattacttcttgggaatcttacaagggacaaactgcccaataa
 atggcttctacttctgtggtgttgaacgggatctctatggttttcagtcagggtcttttccctttacactatccctgacatctgggacatggaccccatagatctaagtcaacctcactgccgaacaattttatactgatgcctcttattgtac
 aactgaacaaagcataacctacagaggtgaaggtcggatcatctgtgtcacaacaaatccccggattacatgtccggggtaagaactgaatctgtacatataccaactttgttggtatgtgactaccaggttcaagaaaaaacatttctctc
 ctaaatccagggactgtagagaggctatgagaggagaagaagcaggagatcctagatatgaagagtccttagccaccatcttgacaaacagtgagaaacagtgactacaacaaaggattcctgggtgatcatcgagccagtgtagtg
 gagttagatatatacaagaagtccttattcacctctttcaaggatggaacatgttcaaaaatctagaacatattccccctactgtccaaccaatcatgactcaccatttggatgagcagagagtgaaaacataagatctcctgtaatctgttttcac
 aagtagagggaactagtcaggaaacgcacatccactcgggattatcgtgagagagggtctgttagatcagttaaaggagcatgcaaaatatcaatatgcggtaggcagggaatccgttttagtggtggaactggatgtcttttagatactca
 gagtactacctgtgttctccatcaaaaatgggtgaacaaacacacagttaaatggataatagaagagtcattgtgagagatcttattaagaagcgtgaagagtgccatagatgctctagaagaagtcattgtgactagatctataagcttcag
 aaagttgagtcctttagaagcaagttccaggaagagggtatgtttacactatgataaacaatacaatgatggaggcaacagggcattataaatcagtggaactggacagacattctacctaaccaatctgccttatgttgagcggcgaagtgt
 catccaggttatgatggtgtattatttaacggtatcataagagacagtagaggcaaaataactaattccagaaatgcaatcacatctactccgagaccatctggagttgtctcaagagaaatccattccctggagacacccctctgtgcactattctgaa
 aatggggaagatggctcagatcttaccagcttctcagctatacataaaagacccctattgtctgtttctgacatagatataggatttcttcatggaagaagtatttgatgattgtggggggagtggtgataggactaattgtcttctgttctgtgtc
 aagttgtttagagtatgttatactgttaagaggaaaaggcttcgtgagggttctatgaatgagacatccagtggtccctgtcattcggactctggtgacaaaacagcttctgtgggaatcttacaagagttctgcattctag

LLEBV/IKOV

LLEBV/WCBV

WCBV/IKOV

WCBV/LLEBV	<p>atggcttctactttgctgttggtcttgaacgggacatctatggttttcagtcaggcttttccccctttacacatccctgaccatctgggacatggacccccatagatctaagtcaccttactgcccgaacaatctttatactgatgcctctattgtac aactgaacaaagcataacacacagagttgaaggctggatcatctgtgtcacaaaaatccccggatttacatgtacgggggtaagaactgaatctgtaacatataccaactttgttggtatgtgactaccacgttcaagaaaaacatttcttc ctaaatccagggactgtagagaggcgtatgagaggaagaaagcaggagatcctagatatgaagagcttttagccacccatatctgacaacagttggctgagaacagtgactacaacaaaggattcctgggtgatcatcgagccagtgtagtg gagtagatatatacaaaagtccttgtattcacctctttcaaggatggaaacatgttcaaaatctagaacatattccccctactgtccaaccaatcatgactccacatttggatgccagagagtgaaaacataagatctgcctgtaactgttttccac aagtagagggaactagtcaggaaacgcacatccactgcgggattatcgatgagagagggtgttcagatcagttaaaggagcatgcaaaatatcaatatcggttaggcagggaatccgttttagtgatggaaacttgatgtcttttagatactca gagtacttacctgtgttctccatcagccatggtaaacatgcatacaacaaactggatgcactagaagaagcagtcgtaagagatctgttaaagaagagagaagaatgtctcaatgcatttgaagagattattatacaaaattccatcagcttag aaaaatgagtctgttcagaaaaatgggtcccaggttccggactcgtttacacgatgataaacaagacattgatggaggcacacgggcactacaaatcagatcgaaactggctgagattcttctaccctatatgtctattgggtaaaggaaaaatgct atcaagatcatgatggagtactgttcaatggaaatcgtaaggatcacggaggaagggttctcatccctgaaatgcagtcctatctattacaggatcatttgaactcctgagatcaaacactataaccatggaggcacctcttagtcactatccggatg atacagacccctcttcagagactcgtgagttcattcagttgcataatgaggatcctgccaaagtcacttcagatatagatttggacttcttcttggaagagatacctcattttgttgcctcatattagggtctgttattcttgggtgttaataaag tattcattcaaagtgatcggtgatgacaaaaaaagatcttctaggagaagaatgcaggacatccttcagatcctgtgatcagatctgtaggaggtaaccaattatcttgggagcttcaaaaaactccacaaacctctag</p>
Mosaic 1 and 2	<p>atgagttactcgatttcaacaccttttctgttcgtgtggctgcaatttcagttgcagacttccccctttacacaattcccgagaagatcgactcctggacgcctatagatatgatccatctgagttgtccaaataaccttttgcaggggatgacgggtgc agcacatccacatccttcagttacgtggagctcaaaacagggtatctgactcatcagaagaatgtctgggttcacctgtaccggggtcatcagtgaggctgttacatacacaactttgtaggtatgtgacaaccacatttaaagggaagcatttcaag cccacggtctcagcctgtagagatgcatttcattggaagatctcaggggatcctagatatgaagagtctctacacaatccgtaccctgactaccgtggcttgaactgtaaaaaccaccaaggagctctcgttatcatatctcaagtggtgagatt tggaccatgatgacagatcccttactcgagggtcttccctagcgggaagtgtcaggagtagcgggtgtcttctactactgtccactaaccacgattacacatttggatgccgagaatccgagactagggatgtcttgtgacattttaccaatag tagagggaagagagatccaaagggaagtgcagacttccgcttcttagatgaagagggtctatataagttcttaaaaggagcatgcaaaactcaagttatgtggagtcttaggacttagactttagatggaacatgggtgcgagtcacaaatcaaa tgaaaccaaattgggtccctccgatcagttgggtgaacctgcacgacttctgcagacgaaattgagcaccttgtttagaggagttggtcaggaagagagaggagtgctggatgcactagagtcacatgacaaccaagtcagtgagttcaga cgttcagtcatttcagaaagttggtagcctggataggaagggttacaccatattaaacgggagcttgatggagacaaatgtccactcagaagggttggaacaattggactgatatcttaccatcgaaaaggatgtctgaaagtggggaaacaaatgcc ttgatccccataaaggagttatttcaatgggtattattaagggtccggatgggtcatattttaaattccagagatgcagtcgggcatgctgaaacagcatatagatcttctgaaggcagcggtttttccctccgtcacctcttatagatcagagttctgtgt tcaaaaaagatgggtgatgcagatgattttgtgatgttcacatgccgatgtaaacaagttagtagtcggacatagatctagggttccatcactggggtctgttattctgatagggtgacagattggcggttcttctgttgatgtcttctgtatttg ttgtaagagagtgaagagggaagggtactggggataggacggaccgtcattagcattatctcaatctctcaatcaaaaccgaaagtgggtcatcttgggagcttacaagggtcctcaaatgcctaa</p>
Mosaic 2	<p>atgagttactcgatttcaacaccttttctgttcgtgtggctgcaatttcagttgcagacttccccctttacacaattcccgagaagatcgactcctggacgcctatagatatgatccatctgagttgtccaaataaccttttgcaggggatgacgggtgc agcacatccacatccttcagttacgtggagctcaaaacagggtatctgactcatcagaagaatgtctgggttcacctgtaccggggtcatcagtgaggctgttacatacacaactttgtcgatatgtgacaaccacctttaaagggaacatttcaag ccgacggcattggcttcagagatccttatcattggaagatttctggggatccaaggtatgaggagctctccacacaccatatctgacaacagctgggttaggacagttaccacaaccaagaatctctgtgataatctctcaagcattgtagag atggatatataatagtagaactcttactctccatgtttccacagggaactgttccagatttatccatcagttccatcctgcgtaccaatcacgattacaccttgtgtgttcgagaagattctaacttaagtcatttgtgacatactgttactagcac aggtagaaaaagcaatgaacggctccaagatgtgtgggttcacagatgagaggggtttttacagaacactgagaggggctgtaaattgacgctctgcgggaacagggtttgaggttatttgatggcacatggatcttccaccgcccgggaagtc actacctgggtccttctaactcagtttagtaataattcacaacaataggatagatgaagttgagcatctgatttagaagatctcattcgaaaaagagaagcatgttagataccctggaaacaattctgatgtctaagtcaattagtttcaggagactc agtcatttcagaaagtgtgacttgatggaaggcttacctattttaaattgggagcttaattggaacaaatgtctactacaaaagagttgacaggtgggctggacatttgccttctaggggatgtctgaaagtgcgacaacagtgatggacc tgtcaaaagggtctcttcaacggaattatcaagggtccggatgggtcatattttaaattccagagatgcagtcagagcagctcaaacagcatatagatcttctgaaggcagcggtttttccctccgtcacctcttatagatcagagttctgtgttcaaa aaagatgggtgatgcagatgatttgttgatgttcacatgccgatgtaaacaaagttagtagtcggacatagatctagggttccatcactggggtctgttattctgatagggtgacagattggcggttcttctgttgatgtcttctgtatttgtgtaa gagagtgaaagggggaaggtctactgggtaggacgggaccgtcattagcattatctcaatctctcaatcaaaaccgaaagtgggtgtcatatgggagcttacaagggtcctcaaatgcctaa</p>
Mosaic 3	<p>atggcttaccagtaacccttatttgaacagcttcttcttacttgacaggacatttttccccctgtataacttctgactctatttggctcttggactcccatagatttgtctcatctcaaatgtcctgataatgcctttatagtagatgagaactgcact gatcatggggagataaattattcagaattgaagccttattccattcccaagcaaaagtctcgtgatttaccatgtacaggaatagtgcactcaggcggtgacctacaccaatttctgttggtatgtcaccaccattttcagcggtccacttcatccca accagagggtatgtcgtcaagctagagagtgaagaaggaaggggaccacagatacgaagagtcattgaccactcctatcccgactctaaatgggtgagaacagtcacaacctccaaggaaatcatggctgatattggatcctgcagtggttgaga tggacatctacaacaaaactatgttctcctgtcttctcaggcgggctctgtgatttctcaggggaatcccgattattgtgaaacaagccactcgtactcgtattggatgccagagagtgaaaacataagatctgcctgtaactgttttccacaagt agagggaactagtcaggaaccgcacatccactgcgggattatcgatgagagagggtcttcagatcagttaaaggagcatgcaaaatatcaatatgcggtaggcagggaatccgttttagtggaacttgatgtcttttagatactcagagt acttacctgtgttctccatcacagctgatcaacacgcacgacatcaaggtcgatgagctggagaatgctatagttttagacttgattaggaggagagaagaatgtctcaatgcatttgaagagattattatacaaaattccatcagctttagaaaaa tgagtctgttcagaaaaatgtccagggtccggactcgtttacacgatgataaacaatacaatgatggaggcaacagggcattataaatcagtggaataactggacagacattctactaaccacaaatctgccttatgggtggacggcaagtgatcca ggttatgatgggtattatttaacggtatcataagagacagtagaggcaaaataactaattccagaaatgcaatcacatctactccgagaccatctggagtgctcaagagaaatccattccctggagacaccccttctgtcactattctgaaaatggg</p>

Mosaic All
 gaagatggctcagatcttaccagcttctgctcagctatacataaaagaccctcatttctgtcttctgacatagatataggatttcttcatggaagaagtatttgatgattgtgggggagtggtgataggactaattgtcttctggttcttggtcaagttgt
 tgttttagagtattgtatactgttaagaggaaaaaggcttctgtgaggggttctatgaatgagacatccagtgccctgtcattcggacttctggtgacaaacagcttctggtggaatcttacaagggaacaaactgcccaataa
 atgagttactcgatttcaacaccttttctgttcgctgtggctgcaatttcagttgcagacttccccctttacatactccctgacctctgggacctggaccctcatagatctaagtcaccttactgcccgaacaatctttatactgatgcctcttattgtac
 aactgaacaaagcataacctacacagagttgaaggtcggatcatctgtgtcacaaaaatccccggattacatgtacaggaatagtgactcaggcggtgacctacaccaatttctggttattgtcacaccacgttcaagaaaaaacacttctctc
 ctaaatccagggactgtagagggcgtatgagaggaaagaaagcaggagatcctagatatgaagagctctgcatacgccttaccctgacagtagttggtaagaacggtcaccacaacaaaggaaatccttctgataatctccccagcattgtag
 agatggatataatagtagaactcttactctctatgtttccacaggaaactgttccagattttatccatcagttccatctgcgtaccaatcacgattacaccatttggatgccagagagtgaaaacataagatctgcctgtaatctgtttccaca
 gtagagggaagagagcatcaaaggagtgagacttggcgtttagatgaagaggcctataaagtctttaaaggagcatgaaaaatgataatctgtggaagtctgggtccgactatatgtggaacatgggtcgcgatgcaaacatca
 aatgaacaaaatggtgccctccgatcagttggtgaacctgcacgacttctgcgcagacgaaattgagcaccttgtttagaggagttggtcaggaagagagaggagtgctggatgcactagagtcctcatgacaaccaagtcagtgagttca
 gacgtctcagtcatttcagaaaagctggttccaggatctgggaaggcttactcttataaaacggcaccttaattggaatcagatgctcactacatcaaggtagagaattggtcagaggtcatccacacaaggatgttgaaagtggggaacaaatg
 ccttgatccccataaaggagtttattcaatggtattattaagggtccggatggatcatattttaatccagagatgcagtcagtccttctcagagaacatgttgacctgttgaaggctaataatagttccgttcaggatccaatgttacttaggtcctcac
 atctgacactgaagaagatatcgtcagttgtcaacctcatctccaagataccagaagtgggtgcagataggatctcgggttatcagactggaagagatacctcatttttggcttgcctcatattagggtgttgattcttgggttgtaataa
 gtattcattcaagtgatcgggtgatgacaaaaaaagatctttaggagaagatgcaggacatccttccagatcctgtgatcagatctgtaggaggtaaacattatcttgggagtcctacaagggtcctcaaatgcctaa
 atggttctcaggctctcgtttgtacccctctggttttccattgtgtttgggaaattccctatttacagataaccagacaagcttggctccctggagccgattgacatacatcactcagctgccccaaacatttggtagtgaggagcagcggtgc
 agcacatccatcctcagttacgtggagctcaaaacaggttatctgactcatcagaagtgtctgggttcacctgtaccggggtcatcagtgaggctgttacatacacaacattttaggttatgtgacaaccacatttaaagggaagcatttcaag
 cccacggctcagcctgtagagatgcatttcattggaagatctcaggggatcctagatatgaagagtcctgcatacgccttaccctgacagtagttggtaagaacggtcaccacaacaaaggaaatccttgcgtgataatctccccagcattgttagag
 atggatatatagtagaactcttactctctatgtttccacaggaaactgttccagattttatccatcagttccatcctgcgtaccaatcacgattacaccttgggtgccaagaagattctaacttaagtcctatttgcataatctggttactgcac
 aggtagaaaagcaatgaacggctccaagatgtgtgggttcacagatgagaggggtttttacagaacatgagaggggctgtaaattgacgctctcgcgggaaccagggtctaagactatagtggaacatgggttatcctttacacgacgggaagt
 tcatgtatggtgctccccgaatcaactagtcactgttgcctcagacgaaattgagcaccttgtttagaggagttggtcaggaagagagaggagtgctggatgcactagagtcctcatgacaaccaagtcagtgagtttcagacgtc
 tcagtcatttaaaaaactgtccctgggttggaaaagcataaccatattcaacaagaccttgatggaagccgatgctcactacaagtcagtcagaacttgaatgagatcctccctcaaaagggtgtttaagagtggggggaggtgcatcctc
 atgtgaacggggtgttttcaatggtataatattaggacctgacggcaatgtcttaatccagagatgcaatcatccctcctcagcaacatattggagtttgggaatcctcggttatccccctgtgcacccctggcagaccgtgcagcgttttcaag
 gacggtgacgaggctgaggattttgtgaagttcaccttccgatgtgcacaatcaggtctcaggagttgacttgggtctccgaactgggggaagtagtattactgagtgacggggcctgactgccttgatgttgataatttctgatgacatgttg
 tagaagagtcgaatcgcagacacacacatctcagagggacagggagggaggtgctagtcactccccaaagcgggaagatcatatcttcatgggaatcacacaagagtgggggtgagaccagactgtga
 atgagttactcgatttcaacaccttttctgttcgctgtggctgcaatttcagttgcagacttccccctttacacaattcccgagaagatcgactcctggagcgctatagatatgatccatctgagttgtccaataaccttttgcaggggatgaaggatgc
 accaactgtcagggttctcctacatggaacttaaaagttggatacatcttagccataaaaaatgaacgggttcaactgtcacaggcggtgtgacggaggctgaaacctactaactcgttgggtatgtcacaccacgttcaaaagaaagcatttccgc
 ccaacaccagatgcatgtagagccgctacaactggaagatggcgggtgacccagatatgaagagtcctcacacaatccgtaccctgactaccgctggcttgcgaactgaaaaaaccaaggagtcctcgttatcatatctccaagtgtggcag
 atttggaccatagacagatccctcactcaggggtcttccctagcgggaagtgtcaggagtagcggtgtcttactactgtctccactaaccacgattacaccatttggatgccgagaaatccgagactagggtgtcttgtgacattttaccaat
 agtagagggaagagagcatcaaaggagtgagacttgcggctttagatgaagaggcctataaagtctttaaaggagcatgcaaaactcaagttatgtggagttctaggacttagacttatggatggaacatgggtcgcgatgcaaacatca
 aatgaacaaaatggtgccctccgatcagttggtgaacctgcacaataaccgtatcgatgagcttgagcatctgattgtggatgaccttatcaaaaaagagaagcatgtttagataccctggaaacaattctgatgtctaagtcaattagtttcagg
 agactcagctatttcagaaaagttggtacctggatatgaaaaggcttacaccatattaaacgggagctttagggagacaaatgtccactacagaagggtggacaattggaactgatatcttaccatcgaaaggatgtctgaaagtggggaacaaatgc
 ctgatccccataaaaggagtttattcaatggtattattaagggtccggatggatcatattttaatccagagatgcagtcgggcatgctgaacacgcatatagatcttctgaaggcagcggttttccctccgtcacccctcttagatcagagttctgtg
 ttcaaaaaagatggtgatgagatgatttgttagtgttcacatgcccgtgtgaacaaagttagtatcggaatcagtagatctagggttccactcaggggtctgttctattctgatatagggtgacagtagtggcggttctgttctgtatgtcttctgtattt
 gttgtaagagagtgaaagggggaaggtctactgggtagtagcggaccgtcattagcattatcttcaatctctcaatcaaaaccgaaagtgtgtcatcttgggagtcctacaagggtcctcaaatgcctaa
 atgagttactcgatttcaacaccttttctgttcgctgtggctgcaatttcagttgcagacttccccctttacacaattcccgagaagatcgactcctggagcgctatagatatgatccatctgagttgtccaataaccttttgcaggggatgaaggatgc
 accaactgtcagggttctcctacatggaacttaaaagttggatacatcttagccataaaaaatgaacgggttcaactgtcacaggcggtgtgacggaggctgaaacctactaactcgttgggtatgtcacaccacgttcaaaagaaagcatttccgc
 ccaacaccagatgcatgtagagccgctacaactggaagatggcgggtgacccagatatgaagagtcctcacacaatccgtaccctgactaccgctggcttgcgaactgaaaaaaccaaggagtcctcgttatcatatctccaagtgtggcag
 atttggaccatagacagatccctcactcaggggtcttccctagcgggaagtgtcaggagtagcggtgtcttactactgtctccactaaccacgattacaccatttggatgccgagaaatccgagactagggtgtcttgtgacattttaccaat
 agtagagggaagagagcatcaaaggagtgagacttgcggctttagatgaagaggcctataaagtctttaaaggagcatgcaaaactcaagttatgtggagttctaggacttagacttatggatggaacatgggtcgcgatgcaaacatca
 aatgaacaaaatggtgccctccgatcagttggtgaacctgcacaataaccgtatcgatgagcttgagcatctgattgtggatgaccttatcaaaaaagagaagcatgtttagataccctggaaacaattctgatgtctaagtcaattagtttcagg

RBV/LBV-
 D/RBV
 atggttctcaggctctcgtttgtacccctctggttttccattgtgtttgggaaattccctatttacagataaccagacaagcttggctccctggagccgattgacatacatcactcagctgccccaaacatttggtagtgaggagcagcggtgc
 agcacatccatcctcagttacgtggagctcaaaacaggttatctgactcatcagaagtgtctgggttcacctgtaccggggtcatcagtgaggctgttacatacacaacattttaggttatgtgacaaccacatttaaagggaagcatttcaag
 cccacggctcagcctgtagagatgcatttcattggaagatctcaggggatcctagatatgaagagtcctgcatacgccttaccctgacagtagttggtaagaacggtcaccacaacaaaggaaatccttgcgtgataatctccccagcattgttagag
 atggatatatagtagaactcttactctctatgtttccacaggaaactgttccagattttatccatcagttccatcctgcgtaccaatcacgattacaccttgggtgccaagaagattctaacttaagtcctatttgcataatctggttactgcac
 aggtagaaaagcaatgaacggctccaagatgtgtgggttcacagatgagaggggtttttacagaacatgagaggggctgtaaattgacgctctcgcgggaaccagggtctaagactatagtggaacatgggttatcctttacacgacgggaagt
 tcatgtatggtgctccccgaatcaactagtcactgttgcctcagacgaaattgagcaccttgtttagaggagttggtcaggaagagagaggagtgctggatgcactagagtcctcatgacaaccaagtcagtgagtttcagacgtc
 tcagtcatttaaaaaactgtccctgggttggaaaagcataaccatattcaacaagaccttgatggaagccgatgctcactacaagtcagtcagaacttgaatgagatcctccctcaaaagggtgtttaagagtggggggaggtgcatcctc
 atgtgaacggggtgttttcaatggtataatattaggacctgacggcaatgtcttaatccagagatgcaatcatccctcctcagcaacatattggagtttgggaatcctcggttatccccctgtgcacccctggcagaccgtgcagcgttttcaag
 gacggtgacgaggctgaggattttgtgaagttcaccttccgatgtgcacaatcaggtctcaggagttgacttgggtctccgaactgggggaagtagtattactgagtgacggggcctgactgccttgatgttgataatttctgatgacatgttg
 tagaagagtcgaatcgcagacacacacatctcagagggacagggagggaggtgctagtcactccccaaagcgggaagatcatatcttcatgggaatcacacaagagtgggggtgagaccagactgtga
 atgagttactcgatttcaacaccttttctgttcgctgtggctgcaatttcagttgcagacttccccctttacacaattcccgagaagatcgactcctggagcgctatagatatgatccatctgagttgtccaataaccttttgcaggggatgaaggatgc
 accaactgtcagggttctcctacatggaacttaaaagttggatacatcttagccataaaaaatgaacgggttcaactgtcacaggcggtgtgacggaggctgaaacctactaactcgttgggtatgtcacaccacgttcaaaagaaagcatttccgc
 ccaacaccagatgcatgtagagccgctacaactggaagatggcgggtgacccagatatgaagagtcctcacacaatccgtaccctgactaccgctggcttgcgaactgaaaaaaccaaggagtcctcgttatcatatctccaagtgtggcag
 atttggaccatagacagatccctcactcaggggtcttccctagcgggaagtgtcaggagtagcggtgtcttactactgtctccactaaccacgattacaccatttggatgccgagaaatccgagactagggtgtcttgtgacattttaccaat
 agtagagggaagagagcatcaaaggagtgagacttgcggctttagatgaagaggcctataaagtctttaaaggagcatgcaaaactcaagttatgtggagttctaggacttagacttatggatggaacatgggtcgcgatgcaaacatca
 aatgaacaaaatggtgccctccgatcagttggtgaacctgcacaataaccgtatcgatgagcttgagcatctgattgtggatgaccttatcaaaaaagagaagcatgtttagataccctggaaacaattctgatgtctaagtcaattagtttcagg

LBV-
 D/RBV/LBV-
 D/RBV
 atgagttactcgatttcaacaccttttctgttcgctgtggctgcaatttcagttgcagacttccccctttacacaattcccgagaagatcgactcctggagcgctatagatatgatccatctgagttgtccaataaccttttgcaggggatgaaggatgc
 accaactgtcagggttctcctacatggaacttaaaagttggatacatcttagccataaaaaatgaacgggttcaactgtcacaggcggtgtgacggaggctgaaacctactaactcgttgggtatgtcacaccacgttcaaaagaaagcatttccgc
 ccaacaccagatgcatgtagagccgctacaactggaagatggcgggtgacccagatatgaagagtcctcacacaatccgtaccctgactaccgctggcttgcgaactgaaaaaaccaaggagtcctcgttatcatatctccaagtgtggcag
 atttggaccatagacagatccctcactcaggggtcttccctagcgggaagtgtcaggagtagcggtgtcttactactgtctccactaaccacgattacaccatttggatgccgagaaatccgagactagggtgtcttgtgacattttaccaat
 agtagagggaagagagcatcaaaggagtgagacttgcggctttagatgaagaggcctataaagtctttaaaggagcatgcaaaactcaagttatgtggagttctaggacttagacttatggatggaacatgggtcgcgatgcaaacatca
 aatgaacaaaatggtgccctccgatcagttggtgaacctgcacaataaccgtatcgatgagcttgagcatctgattgtggatgaccttatcaaaaaagagaagcatgtttagataccctggaaacaattctgatgtctaagtcaattagtttcagg

agactcagtcatttcagaaaagttggtacctggatatggaaaggcttacaccatattaacgggagcttgatggagacaaatgtccactacagaaggggtggacaattggactgatatcttaccatcgaaggatgtctgaaagtggggaacaaatgc
cttgatcccataaaggagtttatttcaatgggtattattaagggtccggatgggtcatatTTaatcccagagatgcagtcgggcatgctgaaacagcatatagatcttctgaaggcagcgggttttccctccgtcacccctttatagatcagagttctgtg
ttcaaaaaagatgggtgatgcagatgatttgttgatgttcacatgccggatgtaacaagttagtatcggacatagatctagggttccatcactggggtctgttcattctgataggggtgacagtattggcgtttctgttctgatatgtcttcttattt
gttgaagagagtgaatcgatcagaacctacgcaacacaatctcagagggacaggagggaggtgtcagtcactcccaagcggggaagatcatatcttcatgggaatcacacaagagtgggggtgagaccagactgtga

Appendix 4: Generic scoring system for Mice inoculated ic with lyssaviruses

Clinical Score	Clinical Signs
0	No effect
1	Ruffled fur Hunched back Paralysis in inoculated leg
2	Spasms (in certain strains) Affected gait (slow or circular movements)
3	Severe spasms (in certain strains)
4	Progressive paralysis
5	Prostration, permanent recumbency Death

Appendix 5: Papers published as part of this thesis



Review

Bats and Viruses: Emergence of Novel Lyssaviruses and Association of Bats with Viral Zoonoses in the EU

Rebecca Shipley ^{1,2}, Edward Wright ² , David Selden ¹, Guanghui Wu ¹, James Aegerter ³, Anthony R Fooks ^{1,4,5} and Ashley C Banyard ^{1,2,4,*}

¹ Wildlife Zoonoses and Vector-Borne Diseases Research Group, Animal and Plant Health Agency (APHA), Weybridge-London KT15 3NB, UK; Rebecca.Shipley@apha.gov.uk (R.S.); david.selden@apha.gov.uk (D.S.); guanghui.wu@apha.gov.uk (G.W.); tony.fooks@apha.gov.uk (A.R.F.)

² School of Life Sciences, University of Sussex, Falmer, Brighton BN1 9QG, UK; ew323@sussex.ac.uk

³ APHA—National Wildlife Management Centre, Wildlife Epidemiology and Modelling, Sand Hutton, York YO41 1LZ, UK; james.aegerter@apha.gov.uk

⁴ Institute for Infection and Immunity, St. George's Hospital Medical School, University of London, London SW17 0RE, UK

⁵ Department of Clinical Infection, Microbiology and Immunology, Institute of Infection and Global Health, University of Liverpool, Liverpool L69 7BE, UK

* Correspondence: ashley.banyard@apha.gov.uk; Tel.: +44-(0)-208-026-9463

Received: 15 January 2019; Accepted: 1 February 2019; Published: 7 February 2019



Abstract: Bats in the EU have been associated with several zoonotic viral pathogens of significance to both human and animal health. Virus discovery continues to expand the existing understating of virus classification, and the increased interest in bats globally as reservoirs or carriers of zoonotic agents has fuelled the continued detection and characterisation of new lyssaviruses and other viral zoonoses. Although the transmission of lyssaviruses from bat species to humans or terrestrial species appears rare, interest in these viruses remains, through their ability to cause the invariably fatal encephalitis—rabies. The association of bats with other viral zoonoses is also of great interest. Much of the EU is free of terrestrial rabies, but several bat species harbor lyssaviruses that remain a risk to human and animal health. Whilst the rabies virus is the main cause of rabies globally, novel related viruses continue to be discovered, predominantly in bat populations, that are of interest purely through their classification within the lyssavirus genus alongside the rabies virus. Although the rabies virus is principally transmitted from the bite of infected dogs, these related lyssaviruses are primarily transmitted to humans and terrestrial carnivores by bats. Even though reports of zoonotic viruses from bats within the EU are rare, to protect human and animal health, it is important characterise novel bat viruses for several reasons, namely: (i) to investigate the mechanisms for the maintenance, potential routes of transmission, and resulting clinical signs, if any, in their natural hosts; (ii) to investigate the ability of existing vaccines, where available, to protect against these viruses; (iii) to evaluate the potential for spill over and onward transmission of viral pathogens in novel terrestrial hosts. This review is an update on the current situation regarding zoonotic virus discovery within bats in the EU, and provides details of potential future mechanisms to control the threat from these deadly pathogens.

Keywords: rabies; lyssavirus; bats; emerging; novel; zoonoses

1. Introduction

The global discovery of lyssaviruses is of continued scientific interest and is of importance to both public and animal health. Lyssaviruses are known to cause fatal encephalitis, referred to as rabies. The term rabies has induced terror throughout human history, as the rabies virus (RABV)

is the only viral pathogen that is associated with 100% fatality following the onset of the clinical disease [1]. Whilst rabies is predominantly circulating within domestic and feral dog populations globally, the presence of lyssaviruses in bats is well established [2]. Historically, rabies' association with hematophagous bats (*Desmodus* sp., although primarily *Desmodus rotundus*) across the Caribbean, and Central and South America, has both embedded a fear of rabies into human populations, as well as driven an irrational and unjustified fear of bats across many cultures. Certainly, bat transmitted human RABV is rare, although in areas where terrestrial rabies has been eliminated, bat rabies remains a constant threat, as exemplified by continued human cases of bat rabies across North America [3]. In endemic areas, human infection with dog rabies results in thousands of human deaths annually. The estimates of human infection are thought to be conservative, because of inadequate diagnostic and reporting systems across Africa and Asia [4]. Wildlife species can also play an important role in the epidemiology of disease, although the paucity of data on wild animal populations, their distribution, and the generally sporadic interactions between different wildlife populations and domesticated carnivore species means that the role of wildlife and the epidemiology of the virus is often unclear. Still, the transmission of the virus between wildlife and domestic terrestrial carnivores is multidirectional, with incursions of domestic dog rabies into fox populations being reported [5].

The severity of disease caused by lyssaviruses means that the potential for cross species transmission events (CSTs) is of significance to human and animal populations [6]. For the rabies virus, spill over events are considered as those that result in dead-end infection, whilst CSTs result in the sustained onward transmission of the virus in the new host. Spill over from bats species appears common for RABV in the Americas, whilst events involving the other lyssaviruses across the Old World appear to be rare. Whilst spill over events for lyssaviruses have been reported, host switching events are far rarer and have only been described for RABV in the Americas [5,7–9]. The factors involved in CSTs with the sustained onward transmission of the virus remain undefined, and endeavours to identify specific amino acid substitutions facilitating virus adaptation to new host species have been, on the most part, unsuccessful. Kuzmin et al. (2012) observed that for sustainability within a bat population, a Serine at position 242 in the viral G protein appeared to predominate, and that contrastingly, an Alanine/Threonine substitution at position 242 appears to facilitate RABV sustainability within the carnivore population [10,11]. Intensive characterisation of the genetics within viral populations, including quasispecies, may elucidate the molecular mechanisms that facilitate lyssavirus adaption, however opportunities to genetically characterise such events are rare.

2. The Increasing Diversity of the Bat Lyssaviruses

Alongside RABV, which is both associated with the infection of terrestrial carnivore species and the chiroptera, fifteen other genetically-, and to some extent, antigenically-related viruses exist within the lyssavirus genus (Figure 1) [12]. Of these, 13 have been isolated from bat species, with the Mokola lyssavirus (MOKV) and Ikoma lyssavirus (IKOV) being the only two viruses that have no current association with bat species (Table 1). Whilst MOKV has been isolated on numerous occasions from rodent species [13,14], IKOV exists only as a single isolate from a rabid African civet (*Civetticus civetticus*) [15]. Enhanced surveillance activities are required in order to understand these isolations, and may not only inform on the natural reservoir host for these lyssaviruses, they may also facilitate the discovery and isolation of novel lyssaviruses from different hosts. A recently identified virus from Asia, named Taiwan Bat Lyssavirus (TBLV), is tentatively associated with the lyssavirus genus. Two separate isolations of TBLV have been reported from the Japanese house bat (*Pipistrellus abramus*) [16].

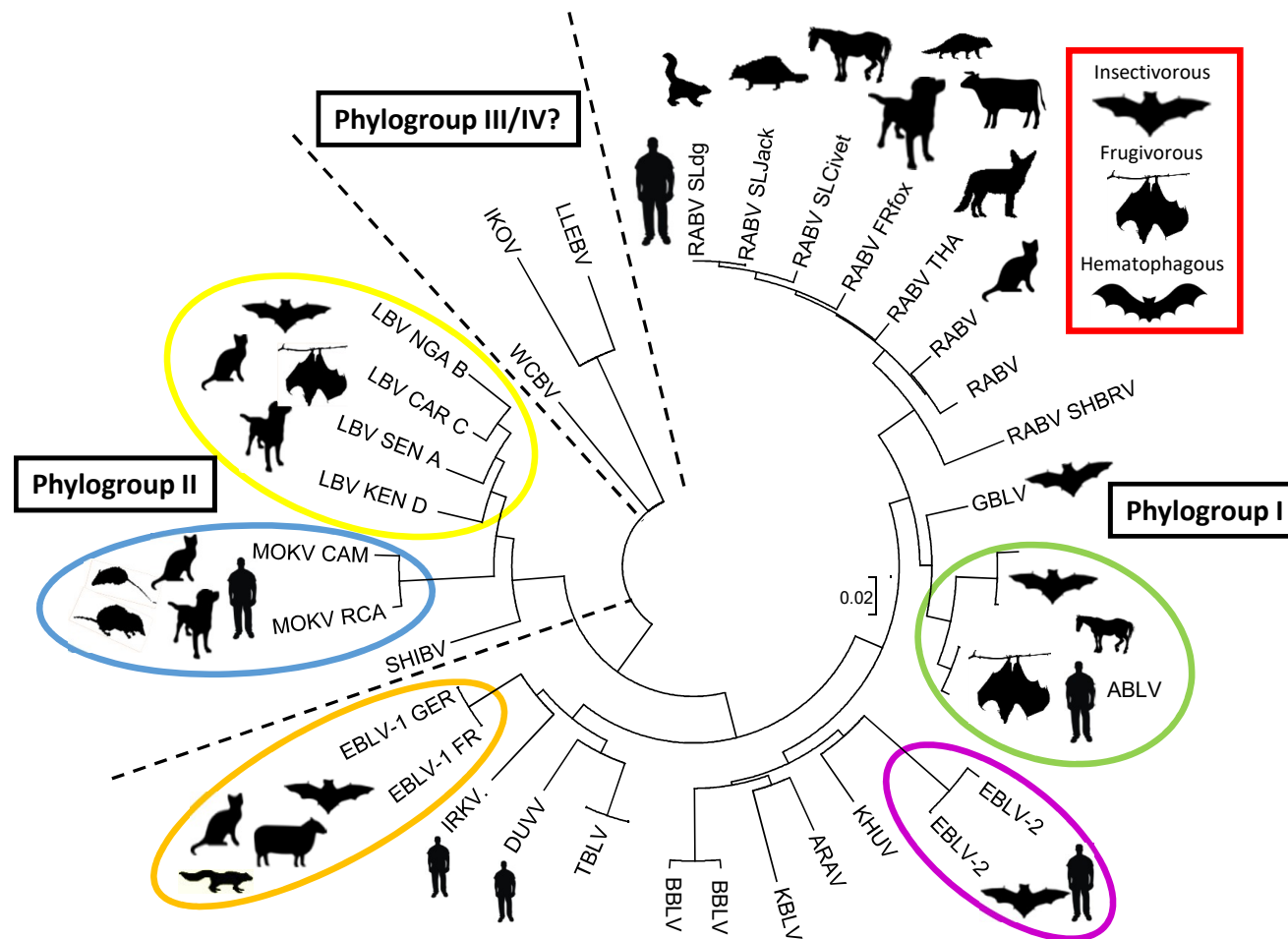


Figure 1. Phylogenetic relationships of the lyssaviruses. The phylogenetic tree is based on an alignment of a fragment of the lyssavirus nucleocapsid gene (450bp). The evolutionary history was inferred using the neighbor-joining method, with branch lengths in the same units as those of the evolutionary distances used to infer the phylogenetic tree. Evolutionary analyses were conducted using MEGA6.

Table 1. The association of the lyssavirus species with bats.

Lyssavirus Species	Common Bat Name	Bat Species Associated with Lyssavirus Infection	Countries Reporting Lyssavirus in Bats	Vaccine Protection Predicted?
Aravan lyssavirus (ARAV)	Lesser mouse-eared bat	<i>Myotis blythi</i>	Kyrgyzstan	Y
Australian bat lyssavirus (ABLV)	Black flying fox and related sp.	<i>Pteropus alecto</i>	Australia	Y
	Yellow-bellied sheath-tailed bat	<i>Saccolaimus flaviventris</i>		
Bokeloh bat lyssavirus (BBLV)	Natterer's bat	<i>Myotis nattereri</i>	Germany, France	Y
Duvenhage lyssavirus (DUVV)	Undefined	<i>Miniopterus sp.</i>	South Africa, Kenya	Y
	Egyptian slit-faced bat	<i>Nycteris thebaica</i>	Zimbabwe	
European bat 1 Lyssavirus (EBLV-1)	Serotine bat	<i>Eptesicus serotinus</i>	France, Germany, and Spain	Y
European bat 2 lyssavirus (EBLV-2)	Daubenton's bat	<i>Myotis daubentonii</i>	The Netherlands, Switzerland, UK, France, Germany, Luxembourg, and Finland	Y
Gannoruwa bat lyssavirus (GBLV)	Indian flying fox	<i>Pteropus medius</i>	Sri Lanka	Y
Ikoma lyssavirus (IKOV)	N/A	N/A	Tanzania	N
Irkut lyssavirus (IRKV)	Greater tube-nosed bat	<i>Murina leucogaster</i>	Russian Federation and China	Y
Kotolahti Bat Lyssavirus (KBLV)\$	Brandt's bat	<i>Myotis brandti</i>	Finland	Y
Khujand lyssavirus (KHUV)	Whiskered bat	<i>Myotis mystacinus</i>	Tajikistan	Y
Lagos bat lyssavirus (LBV)	Straw coloured fruit bat	<i>Eidolon helvum</i>	Nigeria, Senegal, Ghana, and Kenya	N
	Egyptian fruit bat	<i>Rousettus aegyptiacus</i>	France (ex-Togo or Egypt), and Kenya	
	Dwarf epaulet fruit bat	<i>Micropteropus pusillus</i>	Central African Republic	
	Gambian epauletted fruit bat	<i>Epomorphus gambianus</i>	Ghana	
	Buettikofer's epauletted fruit bat	<i>Epomops buettikoferi</i>	Ghana	
	Gambian slit-faced bat	<i>Nycteris gambiensis</i>	Guinea	
	Wahlberg's epauletted fruit bat	<i>Epomorphus wahlbergi</i>	South Africa	
Lleida bat lyssavirus (LLEBV)	Common bent-winged bat	<i>Miniopterus schreibersii</i>	Spain and France	N
Mokola Lyssavirus (MOKV)	N/A	N/A		N
Rabies lyssavirus (RABV)°	Big brown bat	<i>Eptesicus fuscus</i>	North and South America	Y
	Mexican/Brazilian free-tail bat	<i>Tadarida brasiliensis</i>		
	Silver-haired bat	<i>Lasiurus noctivagus</i>		
	Tri-coloured bat	<i>Perimyotis subflavus</i>		
	Vampire bat	<i>Desmodus rotundus</i>		
Shimoni bat lyssavirus (SHIBV)	Commerson's leaf-nosed bat	<i>Hipposideros commersoni</i>	Kenya	N
Taiwan bat lyssavirus (TBLV)\$	Japanese house bat	<i>Pipistrellus abramus</i>	Taiwan	Y
West Caucasian bat lyssavirus (WCBV)	Common bent-winged bat	<i>Miniopterus schreibersii</i>	Russian Federation and Kenya*	N

°: Only bat species most commonly associated with rabies virus infection are listed for clarity. \$: Awaiting official classification within the lyssavirus genus. *: Serological evidence alone.

Whilst the epidemiology of RABV is well defined, being present in terrestrial carnivores globally and bat species within the New World, the epidemiology of the other lyssaviruses is poorly understood, with only single isolates being available for several species (Table 1). However, from an epidemiological standpoint, other than RABV, all other lyssaviruses appear absent from the New World, being described solely within terrestrial or bat species across the Old World. Regardless, the paucity of the epidemiological data for the lyssaviruses may reflect fewer cases of infection with these viruses than

there are with RABV across human and animal populations, or, conversely, may be due to the inability of the existing diagnostic procedures used in endemic areas to differentiate between lyssavirus species. The fluorescent antibody test (FAT) is the most common diagnostic tool used for antigen detection, however it is unable to differentiate between the lyssavirus species. Laboratories in endemic areas do not generally have the capability, often through limitations in resources, to perform secondary confirmatory testing, such as PCR, and sequencing, so as to genetically type the virus to identify which lyssavirus is present in FAT positive samples [17]. The recent adoption of molecular tools for lyssavirus diagnosis by the World Organisation for Animal Health (OIE), will help to overcome this obstacle to virus identification; as more divergent lyssaviruses are discovered, the ability of commercial conjugates to detect them needs constant re-evaluation. Molecular differentiation will resolve the epidemiological status of each virus, and consequently, will help to understand the threats of each lyssavirus to animal and human populations [18].

Lyssaviruses in Europe were first reported in 1954 in Germany [19]. In 1955, a lyssavirus was isolated from insectivorous bats (*Nyctalus noctula*) from the FR Yugoslavia, which confirmed bat rabies [20]. Highly divergent lyssaviruses that reacted differently to monoclonal antibody panels when typed were initially discovered in 1956, originating with the description of the Lagos Bat virus in Africa. Prior to the advent of molecular testing, serological profiling using monoclonal antibodies was utilised to distinguish between lyssavirus species, and revealed virus isolates that were capable of causing rabies, but that reacted differently to defined panels of monoclonal antibodies [21]. The advancement of molecular methods, such as PCR and sequencing technologies, have superseded the antibody-based classification of new pathogens [22]. PCR and sequencing allow for the immediate genetic analysis of the suspect material, and their application to suspect material has led to the rapid typing of numerous novel lyssaviruses, initially often through genetic typing [23–26]. Although the true burden of novel lyssaviruses remains undefined, the potential for fatal infection following spill over events highlights the importance of the characterisation and classification of all lyssaviruses. The discovery of novel lyssaviruses has warranted a heightened interest in bats. As defined reservoirs of many zoonotic pathogens, the viruses harbored by bats are capable of causing explosive outbreaks of disease in human or animal populations following a cross species transmission event. In some areas, these transmission events have increased proportionally to the increased intrusion of human populations into areas of bat habitation [27], as well as the increasing popularity of leisure activities and occupations that involve entering habitats frequented by bats (e.g., caving and potholing).

The lyssavirus species have a distinct and unique epidemiology through their association with bats [28]. Classical RABV is present globally, being reported in terrestrial carnivores, herbivores, and across the New World within multiple bat species. Whilst terrestrial rabies has been largely eliminated in the Americas, it is still associated with the infection of insectivorous; hematophagous; and, to a lesser extent, frugivorous bats. Interestingly, of the 16 classified lyssaviruses, only classical RABV has been reported in the Americas, and the current bat population represents an omnipresent source of RABV infection, for which elimination options are very limited. Certainly, the potential for host switching events to occur into both animal and human populations persists with any resulting human fatalities being reported. In contrast to the situation across the Americas, classical RABV has never been detected in bats in the Old World [29], yet it exists in terrestrial carnivore populations globally. From a bat infection perspective, a further contrasting feature of RABV infection is the association with different bat hosts. Bat rabies in the New World has been detected in over 40 different bat species, although infection is most typically associated with a handful of chiropteran species. In contrast, the Old-World lyssaviruses appear to be most commonly associated with a single or restricted host bat reservoir species. For example, EBLV-1 is predominantly associated with *Eptesicus serotinus*; EBLV-2 with *Myotis daubentonii*, and so on. This species specific detection virus–host relationship has led to the suggestion of host restriction or co-evolution of pathogens with certain bat species, although evidence for either is scant. Further occasional cases of presumed spill over infection are reported in other species, although this appears to be rare (Table 2). EBLV-1 has been reported in sheep, cats, and a

stone marten, although onward transmission within the new host has not been demonstrated. With several bat lyssavirus species, the detection of only a handful of cases of each isolate, or in some cases, only a single isolation, precludes a thorough and accurate assessment of the viral epidemiology. The basis for the apparent abundance of bat lyssaviruses in the Old World, but only bat RABV in the New World, remains an enigma.

From a risk perspective, the known host ranges for lyssaviruses give an indication as to the areas where bat species can be found, and hence, a risk, albeit low, of human–bat interaction must exist. For the most commonly detected lyssaviruses, this range extends across much of the European Union (Figure 2). However, to date, only two human infections with bat lyssaviruses have been described within Europe, both involving fatalities associated with EBLV-2 (Table 2) [30–32].

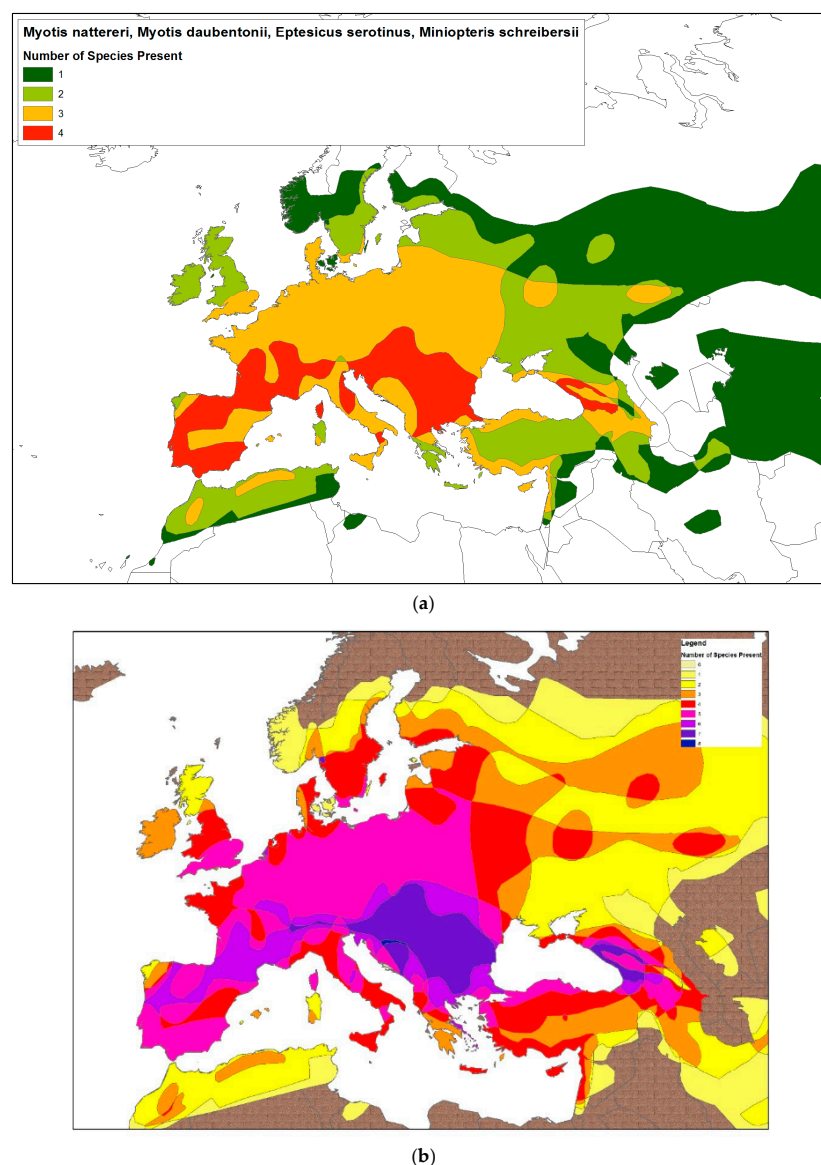


Figure 2. (a) Risk map for bat species most commonly reported as infected with lyssaviruses in the EU. Data includes ranges of *Eptesicus serotinus* (EBLV-1), *Myotis daubentonii* (EBLV-2), *Myotis nattereri* (BBLV), and *Miniopterus schreibersii* (LLEBV and WCBV). Data derived from IUCN (<https://www.iucn.org/>). (b) Risk map for all bat species associated with lyssavirus infection across Europe. Data includes ranges of *Eptesicus serotinus* (EBLV-1), *Myotis daubentonii* (EBLV-2), *Myotis nattereri* (BBLV) and *Miniopterus schreibersii* (LLEBV and WCBV), *Myotis mystacinus* (KHUV), *Myotis brandtii* (KBLV), *Myotis blythii* (ARAV), and *Murina leukogaster* (IRKV).

Table 2. Documented lyssavirus spill over events.

Continent	Lyssavirus Species	Country	Presumed Host Species	Spill over Species	Reference
Europe	EBLV-1	Germany	<i>Eptesicus serotinus</i>	Stone marten ×1	[33]
		Denmark	<i>Eptesicus serotinus</i>	Sheep ×4 (1998), 1 × (2002)	[34]
		France	<i>Eptesicus serotinus</i>	Cat ×1 (2003), 1 × Cat (2007)	[35]
		Germany	<i>Eptesicus serotinus</i>	Myotis myotis	[36]
			<i>Eptesicus serotinus</i>	Myotis daubentonii	
			<i>Eptesicus serotinus</i>	Nyctalus noctula	
			<i>Eptesicus serotinus</i>	Pipistrellus pipistrellus	
			<i>Eptesicus serotinus</i>	Pipistrellus nathusii	
			<i>Eptesicus serotinus</i>	Plecotus auritus	
			<i>Eptesicus serotinus</i>	Myotis nattereri	
			<i>Eptesicus serotinus</i>	Miniopterus schreibersii	
		Spain	<i>Eptesicus serotinus</i>	Rhinolophus ferrumequinum	[37]
			<i>Eptesicus serotinus</i>	Barbastella barbastellus	
			<i>Eptesicus serotinus</i>	Human	
	EBLV-2	Russia	<i>Eptesicus serotinus</i>	Human	[38]
		Finland	<i>Myotis daubentonii</i>	Human	[30]
		Scotland	<i>Myotis daubentonii</i>	Human	[32]
Oceania	ABLV	Australia	<i>Chalinolobus gouldii</i>	2× Horses	[39]
			<i>Saccolaimus flaviventris</i>	Human	[40]
			<i>Pteropus spp.</i>	Human	[41]
			<i>Pteropus spp.</i>	Human	[42]
			Unknown	Human	[43]
Africa	MOKV	Nigeria	Unknown	Human	[44]
			Unknown	Human	[45]
		Zimbabwe	Unknown	5 cats; 1 dog	[46]
			Unknown	1 cat	[47]
		South Africa	Unknown	Cat ×1 (1970); Cat ×1 (1995)	[48]
			Unknown	cat × 2 (1996), cat ×2 (1997), cat ×1 (1998)	[49]
			Unknown	1 cat	[50]
			Unknown	dog ×1 (2005), cat ×1 (2006), cat ×1 (2008)	[51]
			Unknown	cat ×2 (2012), cat ×1 (2014)	[13]
		Ethiopia	Unknown	1 cat	[52]
	DUVV	South Africa	<i>Microchiroptera</i>	Human	[53]
			<i>Microchiroptera</i>	Human	[54]
		Kenya	<i>Microchiroptera</i>	Human	[55]
	LBV	South Africa	<i>Epomophorus wahlbergi</i>	Cat	[56]
			<i>Epomophorus wahlbergi</i>	Mongoose	[57]
		Zimbabwe	<i>Epomophorus wahlbergi</i> / <i>Eidolon helvum</i>	Cat	[58]
		Ethiopia	<i>Epomophorus wahlbergi</i> / <i>Eidolon helvum</i>	Dog	[59]
Asia	IRKV	Siberia	<i>Murina leucogaster</i>	Human	[60]
		China	<i>Murina leucogaster</i>	Dog	[61]

3. The Association of Other Viral Zoonoses with European Bat Species

Published epidemiological studies have associated viral zoonoses with 45 different species of bat within European countries, which cluster within 5 families [60]. Of these 45 species, the majority (37) sit within the *Vespertilionidae*, which includes *Myotis*, *Eptesicus*, *Pipistrellus* and *Plecotus*. The *Vespertilionidae* is not only the largest family of bats in Europe but also the most geographically dispersed (Table 3).

Some Vespertilionids are found throughout Europe, for example *Myotis nattereri* and *Pipistrellus pipistrellus*, while others have restricted ranges, such as *Myotis punicus* and *Plecotus sardus*. Four other chiropteran families are represented in Europe, *Rhinolophidae*, *Miniopteridae*, *Molossidae* and *Pteropodidae*, with just single species representing the latter three families. Finally, all but one species recorded in Europe are insectivorous, with the Egyptian fruit bat (*Rousettus aegyptiacus*) as a frugivorous exception, found in Cyprus and southern Turkey [61,62].

Table 3. Association of non-lyssavirus zoonoses with bat species in the EU.

Family	Species Common Name	Species Latin Name	Association with Viral Pathogen?	References
Rhinolophidae	Blasius's horseshoe bat	<i>Rhinolophus blasii</i>	Coronaviruses	[63]
	Mediterranean horseshoe bat	<i>Rhinolophus euryale</i>	Coronaviruses	[63]
	Greater horseshoe bat	<i>Rhinolophus ferrumequinum</i>	Coronaviruses/Gammaherpesvirus/Adenovirus/Papillomaviruses	[37,63–65]
	Lesser horseshoe bat	<i>Rhinolophus hipposideros</i>	Coronaviruses/Orthoreovirus/Astrovirus	[66–69]
	Mehely's horseshoe bat	<i>Rhinolophus mehelyi</i>	Coronavirus	[63]
Vespertilionidae	Western Barbastelle bat	<i>Barbastella barbastellus</i>	Carmovirus	[70]
	Isabelline Serotine bat	<i>Eptesicus isabellinus</i>	Coronavirus	[71,72]
	Common Serotine	<i>Eptesicus serotinus</i>	Coronavirus/Herpesvirus/Papillomavirus	[36,73–77]
	Savi's pipistrelle	<i>Hypsugo savii</i>	Coronavirus	[67,78,79]
	Alcahoe whiskered bat	<i>Myotis alcathoe</i>	Paramyxovirus	[80]
	Bechstein's bat	<i>Myotis bechsteinii</i>	Astrovirus/Coronavirus/ Paramyxovirus	[81–83]
	Lesser mouse-eared bat	<i>Myotis blythii</i>	Coronavirus	[72,75,84]
	Long-fingered bat	<i>Myotis capaccinii</i>	Paramyxovirus	[80,85]
	Pond bat	<i>Myotis dasycneme</i>	Coronavirus	[83,86–88]
	Daubenton's bat	<i>Myotis daubentonii</i>	Atrovirus/Coronavirus/ Paramyxovirus	[63,80,81,83,85,87,89–92]
	Geoffroy's bat	<i>Myotis emarginatus</i>	Paramyxovirus/Coronavirus	[65]
	Greater mouse-eared bat	<i>Myotis myotis</i>	Coronavirus/Herpesvirus/Paramyxovirus	[72,73,80,93,94]
	Whiskered bat	<i>Myotis mystacinus</i>	Bunyavirus/Reovirus/ Paramyxovirus	[95–98]
	Natterer's bat	<i>Myotis nattereri</i>	Coronavirus/Herpesvirus	[94,99–101]
	Greater noctule bat	<i>Nyctalus lasiopterus</i>	Coronavirus	[72]
	Leisler's bat	<i>Nyctalus leisleri</i>	Coronavirus	[63]
	Common noctule	<i>Nyctalus noctula</i>	Hantavirus/Coronavirus/ Adenovirus	[67,102–104]
	Kuhl's pipistrelle	<i>Pipistrellus kuhlii</i>	Rhabdovirus/Coronavirus/ Bunyavirus/Reovirus	[79,105,106]
	Nathusius's pipistrelle	<i>Pipistrellus nathusii</i>	Adenovirus/Coronavirus/ Reovirus	[83,97,102,107]
	Common pipistrelle	<i>Pipistrellus pipistrellus</i>	Adenovirus/Coronavirus/ Herpesvirus/Paramyxovirus	[78,94,102,108–110]
	Pygmy pipistrelle	<i>Pipistrellus pygmaeus</i>	Astrovirus/Coronavirus	[111]
Miniopteridae	Brown long-eared bat	<i>Plecotus auritus</i>	Coronavirus/Astrovirus/ Herpesvirus/Reovirus	[81,94,101,102]
	Parti-coloured bat	<i>Vespertilio murinus</i>	Reovirus/Astrovirus	[68,69,112]
Molossidae	Schreiber's bat	<i>Miniopterus schreibersii</i>	Lloviu (filovirus)	[23,113]
Pteropodidae	European free-tailed bat	<i>Tadarida teniotis</i>	Mammalian orthoreovirus (reovirus)	[68,78]
Pteropodidae	Egyptian fruit bat	<i>Rousettus aegyptiacus</i>	Marburg and Ravn (filovirus)	[114,115]

The diversity observed in bat species across Europe also extends to the range of viruses that they have been shown to harbour. Many species have been reported antigen or antibody positive for lyssaviruses (Table 1). However the association of bats with other zoonoses is also of interest. The 2014 outbreak of Ebola in West Africa highlights the potential for bat pathogens to spill over into human populations. It is generally accepted that this outbreak initiated through human-bat

interaction, although some controversy surrounds this conclusion [116]. Regardless, the threat of bat viruses crossing the species barrier and entering human populations exists and must be considered a significant threat to public health in areas where bats and humans live in close proximity. Alongside the risk from lyssaviruses several other viruses of note have been identified in European bat species. Filoviruses represent one of the most feared viral families from the perspective of human health as infection has been sensationalised through films and books and explosive outbreaks have been recorded although the outbreaks themselves have often been self-limiting. Filoviruses can cause a lethal hemorrhagic fever in humans and nonhuman primates and the association with bats and other potential reservoir hosts remains undefined [117]. As with the lyssaviruses, the filovirus family is continually expanding with the discovery of novel isolates in different parts of the world [118]. Although primarily associated with primate infection, several bat species have been associated with filoviruses; with both the ebolavirus and marburgvirus genera reported as being associated with different bat species. For the ebolavirus genus the association is predominantly through the large fruit bat species (*Hypsignathus monstrosus*, *Epomops franqueti* and *Myonycteris torquata*) whilst Marburgvirus infection has been linked to both fruit bats (*Rousettus aegyptiacus*) and insectivorous bats (*Rhinolophus eloquens*, *Miniopterus inflatus* and *Miniopterus schreibersii*). The association of the latter species in Spain and Hungary with a novel ebolavirus, Lloviu virus (LLOV), led to a heightened awareness of bats as potential reservoirs of zoonoses [119]. Large insectivorous bat die off events have been reported historically in colonies of Schreiber's bats (*Miniopterus schreibersii*) in Spain, France and Portugal [120]. In Spain, these mortality events prompted investigation into the potential cause of the mortalities and although no causal relationship between filoviruses and the die off were established, the detection of LLOV in *Miniopterus schreibersii* is of potential concern to human and animal health. As described above, this species of bat has also been associated with the highly divergent Lleida bat lyssavirus and as such represents an important possible threat to human health as vaccines or antivirals specific for either infection do not exist; therefore, the consequences of any infection would be very serious. A further concern of filovirus infection of bats is the apparently asymptomatic nature of natural infection, which makes it difficult to identify the infected bats. Whilst bats are considered to be the reservoir host for lyssaviruses, infection will often result in the development of clinical disease and death. Lyssavirus natural infection is hard to define in terms of disease presentation but where experimental studies have been performed in bats, lyssavirus infection typically results in the development of rabies where intracranial inoculation is concerned but with either the development of disease or survivorship and seroconversion following inoculation by peripheral routes. Contrastingly, numerous experimental studies have demonstrated that bats experimentally infected with filoviruses remain healthy post infection but can shed viral products in fecal matter for several weeks [115,121,122]. Interestingly, LLOV was only detected in association with diseased bats with no virus, or viral products, being associated with healthy Schreiber's bats or co-roosting species. This is considered unusual as filovirus infection of other bat species is generally asymptomatic, so the isolation of virus from only diseased bats may indicate differences in pathogenicity for LLOV compared to other filovirus infections of bat. Certainly, the relationship between filovirus and bats requires further investigation as these viral pathogens pose potential threats to humans where interactions with bats occurs.

As well as lyssa- and filoviruses, bats within the EU have been also linked with coronavirus infection. Severe Acute Respiratory Syndrome Coronavirus (SARS-CoV) and Middle East Respiratory Syndrome Coronavirus (MERS-CoV) are coronaviruses capable of infecting humans resulting in a clinical disease of respiratory and gastrointestinal systems [123]. In animal reservoirs, coronavirus infection can result in respiratory, neurological or hepatic disease [124]. Since 2003, numerous novel coronavirus species have been isolated. Within the Alphacoronavirus and Betacoronavirus genera, nine of the 18 recognised viral species have been identified in bats [125]. Moreover, two high profile human disease outbreaks, Severe Acute Respiratory Syndrome (SARS) and Middle East Respiratory Syndrome (MERS) have been phylogenetically linked to a zoonotic viral origin in bats [126,127]. Most coronaviruses are associated with insectivorous bats (*Rhinolophus sinicus*, *Rhinolophus macrotis*,

Rhinolophus ferrumequinum, *Chaerephon plicata*, *Rhinolophus pusillus*, *Rhinolophus blasii*, *Tylonycteris pachypus*, *Pipistrellus abramus*, *Neoromica capensis*, *Vespertilio superans*) [126]. Bat-to-human transmission of coronaviruses is likely very rare, if it occurs at all, and it is more common for bats to infect another terrestrial animal which subsequently infects humans. After the discovery and characterisation of SARS-CoV circulating in masked palm civets sold at Chinese markets and then later in horseshoe bat populations (*Rhinolophus*) in China, it was suggested that bats were the primary reservoir and the civet infection was a result of a spill over event [128–132]. In addition to this, the initial detection of MERS-CoV in dromedary camels in Saudi Arabia suggested that camelids may be a reservoir host for this pathogen but subsequent studies have reported a single isolation from fecal matter from a *Taphozous perforatus* bat and a β -coronavirus, with 96.5% amino acid identity to the MERS-CoV, has been isolated from a *Nyctinomops laticaudatus* bat [127,133]. This warrants the speculation that either the MERS-CoV reservoir resides in a bat species and remains to be discovered, or that dromedary camels are the primary reservoir for MERS-CoV that originated following cross species transmission of a viral ancestor that once resided in a bat populations. The coronavirus surface-located trimeric spike glycoprotein (S) dictates the coronavirus host range as it specifically binds certain receptors for infection [134,135] and so studies surrounding receptor utilisation are warranted in determining any host restriction for these viruses. Rhinolophid bats in China have been described as hosts to many SARS-like coronaviruses, some of which are proposed to be the direct ancestors of SARS-CoV [136]. Each of these pathogens has the potential to cross the species barrier and cause disease outbreaks in terrestrial species, a process though to be driven by adaptation to the new host through genetic mutation [137]. Whilst many of the exact mechanisms required for a spill over event to occur are largely undefined, the S protein and host receptors are the logical starting point and key binding sites of the S protein and potential host receptors remain to be characterised for multiple pathogens. Certainly, identification of receptor binding domains may reveal host tropism patterns and enable evaluation of virus spill over potential.

Further to this, many other potentially highly pathogenic viruses, such as paramyxoviruses, bunyaviruses and hantaviruses, have been detected in European bats (Table 3). While similar viruses to these have previously been isolated across the globe and have shown to be a high risk to animal and human health, the precise risk posed by these novel viruses found in European bats is unknown. This is because for the majority of these viruses, detection is limited to nucleic acid or antibody detection with very little laboratory analysis having been performed.

4. Evolution of Viral Species within Bats

Surveillance programmes for bat lyssaviruses commonly report a diverse range of wild bat species apparently participating in the epizootiology of lyssaviruses. Spill over between ecologically distinct species appears to be common, with the divergence dates for viral clades often measured as evolutionarily recent events (i.e., <1000 years) [88,138–140]. The sheer diversity of bat species associated as potential reservoir hosts to different lyssavirus species suggests historic spill over events and the subsequent maintenance of disease in novel hosts. This would have ultimately promoted new disease reservoirs and the speciation of lyssaviruses. From a host perspective, factors such as the fundamental ecology of roost choice by individual temperate bats, which may fall within geographical locations consistent with what is now defined as the EU, have mediated intraspecific and interspecific transmission events.

The potential for virus transmission between bats requires close contact with lyssavirus transmission, likely requiring physical and direct contact, such as biting and scratching, in the absence of efficient aerosol spread. Away from their roosts, most temperate European species (i.e., insectivores in seasonal biomes) spend the majority of their time foraging and in flight. Most species appear to forage alone, and when foraging bats meet, interaction appears limited to chasing behavior and social calling. If in-flight contact does occur, significant injuries to delicate wings would probably be fatal. Additionally, the evidence suggests that lyssavirus excretion (and hence bat infectivity) is usually

associated with the final symptomatic stages of disease, and is often accompanied by ataxia and a flightless or moribund state, further reducing the likelihood that transmission occurs between bats in flight or in those that are away from roosts. The transmission of lyssaviruses within roosts therefore seems most likely, and with is what is known for the transmission of other viral pathogens, interactions within the roost structures would seem to be most favorable for disease transmission.

Historically, at the end of the last glacial maxima, the range of most European species is considered to have been constrained to multiple refugia around the Mediterranean basin and across to the Caucasus. At this time, northern Eurasia would presumably have been inhospitable to all bats. Both cave hibernator and tree hibernator bats (both classes of bats comprising species that use crevices and cavities for their nursery roosts) would have been competing for the same resource in the summer, across the same constrained landscape, so that direct interspecific contact, whilst infrequent, may have exceeded that which is documented today. In winter, the seasonal migration of cave hibernators would have resulted in interactions with cave specialists (a third class of bats that use caves for both nursery roosts and hibernation) to produce the substantial aggregations of many species. Today, tree hibernating bats will also periodically use caves (for either nursery sites or hibernacula in southern European countries), and it seems likely that this also occurred in the past. Thus, the whole European bat fauna may have frequently shared key sites in winter across the Mediterranean and Pannonian basins, as well as the Caucasus. Ancestral pathogens circulating in this environment would have benefited from the size and longevity of the colonies interacting in the most suitable caves, as well as the relatively frequent and prolonged opportunities for heterospecific transmission. However, an environment such as this would favor the most transmissible viruses, and these consequently would have become the most dominant/prevalent.

As the post glacial climate warmed across Europe, forested landscapes are thought to have extended northward, especially towards those forest communities of deciduous trees producing a diverse and abundant supply of cavities and crevices suitable for nursery sites for cave hibernating and tree hibernating species. This would have substantially extended the summer ranges of the tree roosting species, and whole populations of cave hibernators may have become disconnected from caves in their Mediterranean refugia, breeding in northern forests and hibernating in northern caves nearby. Cave specialists (including *M. myotis* and most *Rhinolophidae*) presumably remained fixed in their previous ranges, restricted to a range similar to that held today by other cave specialists such as *M. blythii*, *M. capaccinii*, and *Miniopterus schreibersii*. These changes in the abundance and distribution of tree roosting species may have driven opportunities for the diverse speciation of lyssaviruses across Europe, as distinct and discrete populations of some species emerged from their glacial refugia. Concomitantly, the dynamics of the cave specialists are proposed to have remained largely unchanged, and, as such, these cave dwelling species may have continued to circulate a common pool of ancestral lyssaviruses as well as other pathogens.

Finally, the present-day environment has been radically expanded and diversified by man to provide roost resources to all European bats. Mines and buildings have enriched the resources available to tree roosting species, as well as extending the geographical range of cave specialists. For the many tree roosting species that use buildings in the summer, it is not clear if the loss in the quantity of tree roosts following the reduction in the forested area is compensated for by their provision in buildings. For cave specialists, such as *M. myotis* and some *Rhinolophidae*, their exploitation of anthropogenic sites (buildings in summer, and local mines or caves in winter) has presumably led to a considerable northward extension of their ranges. As well as extending the sympatry of these expansive cave specialists with many tree roosting species, this process will have fragmented their populations, producing independent northern European populations, disconnected from their Mediterranean peers.

Buildings not only encourage heterospecific co-roosting in summer, when activity is much greater, but also facilitate “super roosts”, by presenting unnatural combinations of environmental qualities, such as size, as well as, occasionally, additional anthropogenic heat, enabling unnaturally large aggregations of many tree roosting species that would be impossible in natural sites. Virus

epizootiology would theoretically benefit from these increased opportunities for intra-specific and inter-specific transmission.

Lyssaviruses circulating in modern European bats may now have many new ways to spread and evolve, driven by the changes to the dynamics and interactions of their bat hosts. Cave specialists, and the viruses they have independently maintained in their perpetually large and aggregated Mediterranean populations, will have presumably been carried northward across substantially extended ranges, to mix with a diverse community of tree roosting species. As well as reacquainting populations of northern European tree roosting species with viruses they may not have seen for over 5000 years, this process also permits any viral pathogen that has co-evolved in a tree roosting species to move the other way into the more densely aggregated populations of cave specialists, although evidence of bat host switching is scant. Buildings, and the diversity of roost options offered, are the primary conduit for this potential interchange, bringing otherwise ecologically separate populations into close contact. Certainly, if the fragmentation of host bat populations promoted a sufficient evolutionary drift to produce antigenically distinct viruses, it can be imagined that this might lead to a substantial proliferation of disease, and perpetuate its spread to many new bat species. Antigenically similar viruses, even if they have co-evolved in separate cave hibernating species, may compete more directly for the new pool of hosts.

5. Bats and Their Role as a Reservoir for Viral Pathogens

Different chiropteran species are widely accepted as reservoir hosts for lyssaviruses and other viral pathogens, as described above. However, for the lyssaviruses, this interaction is poorly understood. Indeed, lyssaviruses and bats do not typically exhibit the classical symbiotic relationship expected of co-evolution, as the lyssavirus infection of bats is most commonly detected following the observation of clinical disease. This contrasts with other viral pathogens, for which bats are considered natural reservoirs, including filo- and henipa-viruses. Both the natural and experimental infection of bats with these other pathogens results in the shedding of the virus, often in the complete absence of clinical disease. Furthermore, evidence has shown that bats, and other mammals, are able to mount a sufficient immunological response following viral exposure, and successfully manage to clear the virus before the onset of clinical disease. For lyssaviruses, the repeated detection of healthy seropositive bats in different roost populations strongly suggests that exposure events can result in viral clearance, following the development of a localised and/or systemic immune response. Alongside this, recent studies have described serological positivity in unvaccinated humans within Amazonian populations [141]. Again, this suggests that lyssavirus exposure can result in clearance, most likely where detected, through the development of a humoral response. What drives this human exposure to RABV, however, is less clear with hunting of bats, as well as the feeding of vampire bats on humans being plausible exposure opportunities. Certainly, the structure of Amazonian populations, and the overlap in bat and human habitations, may facilitate the exposure to a lyssavirus, whether it be via bite or non-bite transmission. Also, the mechanisms involved in clinical disease manifestation following natural infection remain ill-defined, so the outcome of lyssavirus infection/exposure in bats versus another mammal cannot yet be accurately compared. It may be so that bats exhibit much longer incubation periods than other mammals, facilitating in the maintenance of the virus in bat populations. However, the lack of knowledge surrounding, specifically, the innate signalling mechanisms in bats following exposure, prohibits any understanding surrounding their status as the lyssavirus reservoir host. Related to this is the observation of clinical disease in a U.K. Daubenton's bat nine months following captive care [142]. This, again, demonstrates that these viruses can exist within bat species for long periods of time, before the development of clinical disease. How the virus is maintained and where the virus hides during prolonged periods post infection before the development of disease remains unknown.

6. Availability of Human Vaccines for Bat Pathogens

For lyssaviruses, the lack of vaccine protection against numerous divergent lyssaviruses has been previously defined. However, the continued emergence of novel lyssaviruses warrants the continued assessment of vaccine protection, as well as where human infection occurs and how the clinical disease develops, as there remains no cure for rabies. Human rabies vaccines have been available for decades, and following vaccination, it has long been established that a neutralising antibody titre over a defined threshold will protect individuals from the development of disease when infection with classical RABV occurs [143]. However, the protective cut-off for a serological neutralising antibody titre is poorly defined for many of the other lyssaviruses within the genus, and consequently, the discovery of novel viruses warrants an investigation on the efficacy of existing pre- and post-exposure preparations [144–150]. Although response to vaccines differs between individuals, it is widely accepted that a protective titre of 0.5 international units (IU)/ml is sufficient for protection against RABV [151]. Alongside RABV, the current vaccine protects against all phylogroup I lyssaviruses, namely: ARAV, ABLV, BBLV, DUVV, EBLV-1, EBLV-2, IRKV, KHUV, and GBLV, although the level of neutralising antibody required to protect is undefined. Evidence has shown, however, that a titre higher than 0.5IU/ml is required for protection for some phylogroup I lyssaviruses, indicating an increased antigenic distance of the vaccine strains to the circulating lyssaviruses [144] [146,149]. For more divergent lyssaviruses, such as those in phylogroup II and III, in vivo vaccination-challenge experiments have shown that the antibody response generated from the RABV vaccine is not sufficient for protection [17,147,150,152–154].

For other viral zoonoses of bat present within the EU there have been varying degrees of success in the development of vaccines. Following the 2014 Ebola outbreak, a vaccine based on vesicular stomatitis virus (VSV) expressing the surface glycoprotein of Zaire Ebola (EBOV), termed VSV-EBOV, was developed [155]. Clinical trials demonstrated 95–100% efficacy in generating a protective response against EBOV, making it the first filovirus vaccine in use [156]. However, as with the lyssaviruses, there is antigenic divergence across the filovirus family with six distinct species of ebolavirus being described and little is understood regarding any potential cross-protection afforded by the current vaccine. Further, two other genera are classified alongside the ebolaviruses within the filovirus family, Marburgviruses and Cuevavirus. Whilst a vaccine for Marburgviruses is not currently in use, studies have shown that, similar to EBOV, VSV expressing MARV glycoproteins is effective at generating a sufficient antibody titre for protection in non-human primates [157]. Of note, the VSV-MARV vaccine affords protection against Ravn virus (RAVV), a further novel lyssavirus [158].

The only currently available vaccine for coronaviruses is a canine vaccine although multiple studies are focused on creating vaccines for SARS-CoV and MERS-CoV. All coronavirus vaccine candidates are directed against the Spike protein (S protein), the most immunological component of coronaviruses. Both DNA vaccines and subunit viral vectored vaccines, such as Adenovirus, Venezuelan equine encephalitis virus and modified Vaccinia virus Ankara expressing the S protein, have been demonstrated provide a sufficient protective neutralising antibody response against MERS-CoV in a murine model [159]. Of note, the route of administration was a key determinant in the scale of the resulting antibody response with intranasal administration being the most effective method for both SARS-CoV and MERS-CoV protection as it stimulated significantly higher IgA antibody response than subcutaneous inoculation [160,161]. Clearly, vaccines for zoonotic viral pathogens of bats need further development.

7. Conclusions

Numerous viruses exist in European bat species, some of which currently no effective human or animal vaccines are available. Vaccination of bats, through their protected status in the EU is unlikely to ever be a viable option although developments in vaccine applications for chiroptera may have future applications in preventing the disease in wild bat populations [162]. For lyssaviruses, the OIE and WHO have targeted 2030 for the elimination of dog-mediated human rabies. It is possible

that should this be achieved, the spill over of bat lyssaviruses may become more evident and host switching events may occur with pathogens for which there is no vaccine protection. Certainly, the recent detection of highly divergent lyssaviruses (LLEBV) and filoviruses (LLOV) in bats across the EU poses potential the risk to human populations, especially as vaccines or antiviral drugs against these viruses do not exist. Further studies are required to understand: the mechanisms of both maintenance and transmission of viral pathogens within bat populations; the zoonotic potential of viral pathogens detected in bats; and the risk of host switching events that may impact on human and animal health.

Author Contributions: A.C.B. and A.R.F. conceptualized the review. A.C.B., R.S., J.A., G.W. and E.W. generated a draft of the review. All authors contributed to developing and finalizing the review and agreed on the final version of the manuscript.

Funding: A.C.B., D.S., G.W., and A.R.F. were part funded by the U.K. Department for Environment, Food, and Rural Affairs (Defra); the Scottish Government; and the Welsh Government, under project grants SV3500 and SE0431. R.S. is supported by a PhD studentship under Defra grant SE0431. A.B., D.S., G.W., and A.R.F. are part funded by the European Union's Horizon 2020 research and innovation program under RABYD-VAX grant agreement No. 733176.

Acknowledgments: We acknowledge Adam Ashton for creating the host range maps.

Conflicts of Interest: The authors declare no conflict of interest.

References

1. Fooks, A.R.; Banyard, A.C.; Horton, D.L.; Johnson, N.; McElhinney, L.M.; Jackson, A.C. Current status of rabies and prospects for elimination. *Lancet* **2014**, *384*, 1389–1399. [[CrossRef](#)]
2. Banyard, A.C.; Fooks, A.R. The impact of novel lyssavirus discovery. *Microbiol. Aust.* **2017**, *38*, 18–21. [[CrossRef](#)]
3. Dato, V.M.; Campagnolo, E.R.; Long, J.; Rupprecht, C.E. A Systematic Review of Human Bat Rabies Virus Variant Cases: Evaluating Unprotected Physical Contact with Claws and Teeth in Support of Accurate Risk Assessments. *PLoS ONE* **2016**, *11*, e0159443. [[CrossRef](#)] [[PubMed](#)]
4. Banyard, A.C.; Horton, D.; Freuling, C.; Müller, T.; Fooks, A.R. Control and prevention of canine rabies: The need for building laboratory based surveillance capacity. *Antivir. Res.* **2013**, *98*, 357–364. [[CrossRef](#)] [[PubMed](#)]
5. Marston, D.A.; Horton, D.L.; Nunez, J.; Ellis, R.J.; Orton, R.J.; Johnson, N.; Banyard, A.C.; McElhinney, L.M.; Freuling, C.M.; Firat, M.; et al. Genetic analysis of a rabies virus host shift event reveals within-host viral dynamics in a new host. *Virus Evol.* **2017**, *3*, vex038. [[CrossRef](#)] [[PubMed](#)]
6. Streicker, D.G.; Turmelle, A.S.; Vonhof, M.J.; Kuzmin, I.V.; McCracken, G.F.; Rupprecht, C.E. Host phylogeny constrains cross-species emergence and establishment of rabies virus in bats. *Science* **2010**, *329*, 676–679. [[CrossRef](#)] [[PubMed](#)]
7. Leslie, M.J.; Messenger, S.; Rohde, R.E.; Smith, J.; Cheshier, R.; Hanlon, C.; Rupprecht, C.E. Bat-associated rabies virus in Skunks. *Emerg. Infect. Dis.* **2006**, *12*, 1274–1277. [[CrossRef](#)] [[PubMed](#)]
8. Daoust, P.Y.; Wandeler, A.I.; Casey, G.A. Cluster of rabies cases of probable bat origin among red foxes in Prince Edward Island, Canada. *J. Wildl. Dis.* **1996**, *32*, 403–406. [[CrossRef](#)] [[PubMed](#)]
9. Wallace, R.M.; Gilbert, A.; Slate, D.; Chipman, R.; Singh, A.; Cassie, W.; Blanton, J.D. Right place, wrong species: A 20-year review of rabies virus cross species transmission among terrestrial mammals in the United States. *PLoS ONE* **2014**, *9*, e107539. [[CrossRef](#)] [[PubMed](#)]
10. Kuzmin, I.V.; Shi, M.; Orciari, L.A.; Yager, P.A.; Velasco-Villa, A.; Kuzmina, N.A.; Streicker, D.G.; Bergman, D.L.; Rupprecht, C.E. Molecular inferences suggest multiple host shifts of rabies viruses from bats to mesocarnivores in Arizona during 2001–2009. *PLoS Pathog.* **2012**, *8*, e1002786. [[CrossRef](#)] [[PubMed](#)]
11. Rupprecht, C.; Kuzmin, I.; Meslin, F. Lyssaviruses and rabies: Current conundrums, concerns, contradictions and controversies. *F1000Res* **2017**, *6*, 184. [[CrossRef](#)] [[PubMed](#)]
12. Fooks, A.R.; Cliquet, F.; Finke, S.; Freuling, C.; Hemachudha, T.; Mani, R.S.; Muller, T.; Nadin-Davis, S.; Picard-Meyer, E.; Wilde, H.; et al. Rabies. *Nat. Rev. Dis. Primers* **2017**, *3*, 17091. [[CrossRef](#)] [[PubMed](#)]
13. Coertse, J.; Markotter, W.; le Roux, K.; Stewart, D.; Sabeta, C.T.; Nel, L.H. New isolations of the rabies-related Mokola virus from South Africa. *BMC Vet. Res.* **2017**, *13*, 37. [[CrossRef](#)] [[PubMed](#)]

14. Markotter, W.; Kgaladi, J.; Nel, L.H.; Marston, D.; Wright, N.; Coertse, J.; Müller, T.F.; Sabeta, C.T.; Fooks, A.R.; Freuling, C.M. Diversity and Epidemiology of Mokola Virus. *PLoS Negl. Trop. Dis.* **2013**, *7*, e2511.
15. Marston, D.A.; Horton, D.L.; Ngeleja, C.; Hampson, K.; McElhinney, L.M.; Banyard, A.C.; Haydon, D.; Cleaveland, S.; Rupprecht, C.E.; Bigambo, M.; et al. Ikoma lyssavirus, highly divergent novel lyssavirus in an African civet. *Emerg. Infect. Dis.* **2012**, *18*, 664–667. [[CrossRef](#)] [[PubMed](#)]
16. Hu, S.C.; Hsu, C.L.; Lee, M.S.; Tu, Y.C.; Chang, J.C.; Wu, C.H.; Lee, S.H.; Ting, L.J.; Tsai, K.R.; Cheng, M.C.; et al. Lyssavirus in Japanese Pipistrelle, Taiwan. *Emerg. Infect. Dis.* **2018**, *24*, 782–785. [[CrossRef](#)] [[PubMed](#)]
17. Fooks, A.R. The challenge of new and emerging lyssaviruses. *Expert Rev. Vaccines* **2004**, *3*, 333–336. [[CrossRef](#)] [[PubMed](#)]
18. Banyard, A.C.; Evans, J.S.; Luo, T.R.; Fooks, A.R. Lyssaviruses and bats: Emergence and zoonotic threat. *Viruses* **2014**, *6*, 2974–2990. [[CrossRef](#)] [[PubMed](#)]
19. Schindler, R.; Denning, H.K.D. Untersuchungen über die Bedeutung der Fledermäuse für den gegenwärtigen Tollwut-Seuchenzug in Deutschland. *Monatsschrift für Tierheilkunde* **1958**, *10*, 169–177.
20. Jelesic, Z.; Nikolic, M. Isolation of rabies virus from insectivorous bats in Yugoslavia. *Bull. World Health Organ.* **1956**, *14*, 801–804. [[PubMed](#)]
21. King, A.A.; Haagsma, J.; Kappeler, A. Lyssavirus infections in European Bats. In *Historical Perspective of Rabies in Europe and the Mediterranean Basin*; King, A.A., Fooks, A.R., Aubert, M., Wandeler, A.I., Eds.; OIE: Paris, France, 2004; pp. 221–241.
22. Marston, D.A.; McElhinney, L.M.; Ellis, R.J.; Horton, D.L.; Wise, E.L.; Leech, S.L.; David, D.; de Lambellerie, X.; Fooks, A.R. Next Generation Sequencing of viral RNA genomes. *BMC Genom.* **2013**, *14*, 444. [[CrossRef](#)] [[PubMed](#)]
23. Arechiga Ceballos, N.; Vazquez Moron, S.; Berciano, J.M.; Nicolas, O.; Aznar Lopez, C.; Juste, J.; Rodriguez Nevado, C.; Aguilar Setien, A.; Echevarria, J.E. Novel lyssavirus in bat, Spain. *Emerg. Infect. Dis.* **2013**, *19*, 793–795. [[CrossRef](#)] [[PubMed](#)]
24. Gunawardena, P.S.; Marston, D.A.; Ellis, R.J.; Wise, E.L.; Karawita, A.C.; Breed, A.C.; McElhinney, L.M.; Johnson, N.; Banyard, A.C.; Fooks, A.R. Lyssavirus in Indian Flying Foxes, Sri Lanka. *Emerg. Infect. Dis.* **2016**, *22*, 1456–1459. [[CrossRef](#)] [[PubMed](#)]
25. Fooks, A.R.; McElhinney, L.M.; Horton, D.; Banyard, A.C.; Johnson, N.; Marston, D.; Freuling, C.; Hoffmann, B.; Tu, C.; Fehlnner-Gardiner, C.; et al. Molecular tools for rabies diagnosis in animals. In *Proceedings of the Compendium of the OIE Global Conference on Rabies Control*, Incheon-Seoul, Korea, 7–9 September 2011; OIE: Paris, France, 2012; pp. 75–85.
26. Nokireki, T.; Tammiranta, N.; Kokkonen, U.M.; Kantala, T.; Gadd, T. Tentative novel lyssavirus in a bat in Finland. *Transbound. Emerg. Dis.* **2018**, *65*, 593–596. [[CrossRef](#)] [[PubMed](#)]
27. Afelt, A.; Frutos, R.; Devaux, C. Bats, Coronaviruses, and Deforestation: Toward the Emergence of Novel Infectious Diseases? *Front. Microbiol.* **2018**, *9*, 702. [[CrossRef](#)] [[PubMed](#)]
28. Badrane, H.; Tordo, N. Host switching in Lyssavirus history from the Chiroptera to the Carnivora orders. *J. Virol.* **2001**, *75*, 8096–8104. [[CrossRef](#)] [[PubMed](#)]
29. Rupprecht, C.E.; Barrett, J.; Briggs, D.; Cliquet, F.; Fooks, A.R.; Lumlertdacha, B.; Meslin, F.X.; Muler, T.; Nel, L.H.; Schneider, C.; et al. Can rabies be eradicated? *Dev. Biol. (Basel)* **2008**, *131*, 95–121. [[PubMed](#)]
30. Lumio, J.; Hillbom, M.; Roine, R.; Ketonen, L.; Haltia, M.; Valle, M.; Neuvonen, E.; Lahdevirta, J. Human rabies of bat origin in Europe. *Lancet* **1986**, *1*, 378. [[CrossRef](#)]
31. Fooks, A.R.; Brookes, S.M.; Johnson, N.; McElhinney, L.M.; Hutson, A.M. European bat lyssaviruses: An emerging zoonosis. *Epidemiol. Infect.* **2003**, *131*, 1029–1039. [[CrossRef](#)] [[PubMed](#)]
32. Fooks, A.R.; McElhinney, L.M.; Pounder, D.J.; Finnegan, C.J.; Mansfield, K.; Johnson, N.; Brookes, S.M.; Parsons, G.; White, K.; McIntyre, P.G.; et al. Case report: Isolation of a European bat lyssavirus type 2a from a fatal human case of rabies encephalitis. *J. Med. Virol.* **2003**, *71*, 281–289. [[CrossRef](#)] [[PubMed](#)]
33. Muller, T.; Cox, J.; Peter, W.; Schafer, R.; Johnson, N.; McElhinney, L.M.; Geue, J.L.; Tjornehoj, K.; Fooks, A.R. Spill-over of European bat lyssavirus type 1 into a stone marten (*Martes foina*) in Germany. *J. Vet. Med. B Infect. Dis. Vet. Public Health* **2004**, *51*, 49–54. [[CrossRef](#)] [[PubMed](#)]
34. Tjornehoj, K.; Fooks, A.R.; Agerholm, J.S.; Ronsholt, L. Natural and experimental infection of sheep with European bat lyssavirus type-1 of Danish bat origin. *J. Comp. Pathol.* **2006**, *134*, 190–201. [[CrossRef](#)] [[PubMed](#)]

35. Dacheux, L.; Larrous, F.; Mailles, A.; Boisseleau, D.; Delmas, O.; Biron, C.; Bouchier, C.; Capek, I.; Muller, M.; Ilari, F.; et al. European bat Lyssavirus transmission among cats, Europe. *Emerg. Infect. Dis.* **2009**, *15*, 280–284. [[CrossRef](#)] [[PubMed](#)]
36. Muller, T.; Johnson, N.; Freuling, C.M.; Fooks, A.R.; Selhorst, T.; Vos, A. Epidemiology of bat rabies in Germany. *Arch. Virol.* **2007**, *152*, 273–288. [[CrossRef](#)] [[PubMed](#)]
37. Serra-Cobo, J.; Amengual, B.; Abellan, C.; Bourhy, H. European bat lyssavirus infection in Spanish bat populations. *Emerg. Infect. Dis.* **2002**, *8*, 413–420. [[CrossRef](#)] [[PubMed](#)]
38. Selimov, M.A.; Tatarov, A.G.; Botvinkin, A.D.; Klueva, E.V.; Kulikova, L.G.; Khismatullina, N.A. Rabies-related Yuli virus; identification with a panel of monoclonal antibodies. *Acta Virol.* **1989**, *33*, 542–546. [[PubMed](#)]
39. Annand, E.; Reid, P. Clinical review of two fatal equine cases of infection with the insectivorous bat strain of Australian bat lyssavirus. *Aust. Vet. J.* **2014**, *92*, 324–332. [[CrossRef](#)] [[PubMed](#)]
40. Samaratunga, H.; Searle, J.W.; Hudson, N. Non-rabies Lyssavirus human encephalitis from fruit bats: Australian bat Lyssavirus (pteropid Lyssavirus) infection. *Neuropathol. Appl. Neurobiol.* **1998**, *24*, 331–335. [[CrossRef](#)] [[PubMed](#)]
41. Hanna, J.N.; Carney, I.K.; Smith, G.A.; Tannenberg, A.E.; Deverill, J.E.; Botha, J.A.; Serafin, I.L.; Harrower, B.J.; Fitzpatrick, P.F.; Searle, J.W. Australian bat lyssavirus infection: A second human case, with a long incubation period. *Med. J. Aust.* **2000**, *172*, 597–599. [[PubMed](#)]
42. Iizuka, K. Australian Bat Lyssavirus—Human Fatality. Available online: <http://www.promedmail.org/direct.php?id=20130323.1600266> (accessed on 12 November 2018).
43. Familusi, J.B.; Moore, D.L. Isolation of a rabies related virus from the cerebrospinal fluid of a child with ‘aseptic meningitis’. *Afr. J. Med. Sci.* **1972**, *3*, 93–96. [[PubMed](#)]
44. Familusi, J.; Osunkoya, B.; Moore, D.; Kemp, G.; Fabiyi, A. A fatal human infection with Mokola virus. *Am. J. Trop. Med. Hyg.* **1972**, *21*, 959–963. [[CrossRef](#)] [[PubMed](#)]
45. Foggin, C.M. Atypical rabies virus in cats and a dog in Zimbabwe. *Vet. Rec.* **1982**, *110*, 338. [[CrossRef](#)] [[PubMed](#)]
46. Bingham, J.; Javangwe, S.; Sabeta, C.T.; Wandeler, A.I.; Nel, L.H. Report of isolations of unusual lyssaviruses (rabies and Mokola virus) identified retrospectively from Zimbabwe. *J. S. Afr. Vet. Assoc.* **2001**, *72*, 92–94. [[CrossRef](#)] [[PubMed](#)]
47. Meredith, C.D.; Nel, L.H.; von Teichman, B.F. Further isolation of Mokola virus in South Africa. *Vet. Rec.* **1996**, *138*, 119–120. [[PubMed](#)]
48. von Teichman, B.F.; de Koker, W.C.; Bosch, S.J.; Bishop, G.C.; Meredith, C.D.; Bingham, J. Mokola virus infection: Description of recent South African cases and a review of the virus epidemiology. *J. S. Afr. Vet. Assoc.* **1998**, *69*, 169–171. [[CrossRef](#)] [[PubMed](#)]
49. Sabeta, C.T.; Markotter, W.; Mohale, D.K.; Shumba, W.; Wandeler, A.I.; Nel, L.H. Mokola virus in domestic mammals, South Africa. *Emerg. Infect. Dis.* **2007**, *13*, 1371–1373. [[CrossRef](#)] [[PubMed](#)]
50. Sabeta, C.; Blumberg, L.; Miyen, J.; Mohale, D.; Shumba, W.; Wandeler, A. Mokola virus involved in a human contact (South Africa). *FEMS Immunol. Med. Microbiol.* **2010**, *58*, 85–90. [[CrossRef](#)] [[PubMed](#)]
51. Mebatsion, T.; Cox, J.H.; Frost, J.W. Isolation and characterization of 115 street rabies virus isolates from Ethiopia by using monoclonal antibodies: Identification of 2 isolates as Mokola and Lagos bat viruses. *J. Infect. Dis.* **1992**, *166*, 972–977. [[CrossRef](#)] [[PubMed](#)]
52. Tignor, G.H.; Murphy, F.A.; Clark, H.F.; Shope, R.E.; Madore, P.; Bauer, S.P.; Buckley, S.M.; Meredith, C.D. Duvenhage Virus: Morphological, Biochemical, Histopathological and Antigenic Relationships to the Rabies Serogroup. *J. Gen. Virol.* **1977**, *37*, 595–611. [[CrossRef](#)]
53. Paweska, J.T.; Blumberg, L.H.; Liebenberg, C.; Hewlett, R.H.; Grobbelaar, A.A.; Leman, P.A.; Croft, J.E.; Nel, L.H.; Nutt, L.; Swanepoel, R. Fatal human infection with rabies-related Duvenhage virus, South Africa. *Emerg. Infect. Dis.* **2006**, *12*, 1965–1967. [[CrossRef](#)] [[PubMed](#)]
54. van Thiel, P.P.; de Bie, R.M.; Eftimov, F.; Tepaske, R.; Zaaijer, H.L.; van Doornum, G.J.; Schutten, M.; Osterhaus, A.D.; Majoie, C.B.; Aronica, E.; et al. Fatal human rabies due to Duvenhage virus from a bat in Kenya: Failure of treatment with coma-induction, ketamine, and antiviral drugs. *PLoS Negl. Trop. Dis.* **2009**, *3*, e428. [[CrossRef](#)] [[PubMed](#)]
55. Crick, J.; Tignor, G.H.; Moreno, K. A new isolate of Lagos bat virus from the Republic of South Africa. *Trans. R. Soc. Trop. Med. Hyg.* **1982**, *76*, 211–213. [[CrossRef](#)]

56. Markotter, W.; Kuzmin, I.; Rupprecht, C.E.; Nel, L.H. Phylogeny of Lagos bat virus: Challenges for lyssavirus taxonomy. *Virus Res.* **2008**, *135*, 10–21. [[CrossRef](#)] [[PubMed](#)]
57. King, A.; Crick, J. Rabies-related viruses. In *Rabies*; Springer: Berlin, Germany, 1988; pp. 177–199.
58. Liu, Y.; Li, N.; Zhang, S.; Zhang, F.; Lian, H.; Wang, Y.; Zhang, J.; Hu, R. Analysis of the complete genome of the first Irkut virus isolate from China: Comparison across the Lyssavirus genus. *Mol. Phylogenet. Evol.* **2013**, *69*, 687–693. [[CrossRef](#)] [[PubMed](#)]
59. Chen, T.; Miao, F.M.; Liu, Y.; Zhang, S.F.; Zhang, F.; Li, N.; Hu, R.L. Possible Transmission of Irkut Virus from Dogs to Humans. *Biomed. Environ. Sci.* **2018**, *31*, 146–148. [[CrossRef](#)] [[PubMed](#)]
60. EUROBATS. *Action Plan for the Conservation of Bat Species in the European Union 2016–2021*; Inf.EUROBATS.AC21.5; EUROBATS: Bonn, Germany, 2006.
61. Benda, P.; Abi-Said, M.; Bartonička, T.; Bilgin, R.; Faizolahi, K.; Lučan, R.K.; NICOLAOU, H.; REITER, A.; SHOHDI, W.M.; Uhrin, M. *Rousettus aegyptiacus* (Pteropodidae) in the Palaearctic: List of records and revision of the distribution range. *Vespertilio* **2011**, *15*, 3–36.
62. Dietz, C.; Nill, D.; Von Helversen, O. *Bats of Britain, Europe and Northwest Africa*; A & C Black Publishers Ltd.: London, UK, 2009.
63. Drexler, J.F.; Gloza-Rausch, F.; Glende, J.; Corman, V.M.; Muth, D.; Goettsche, M.; Seebens, A.; Niedrig, M.; Pfefferle, S.; Yordanov, S.; et al. Genomic characterization of severe acute respiratory syndrome-related coronavirus in European bats and classification of coronaviruses based on partial RNA-dependent RNA polymerase gene sequences. *J. Virol.* **2010**, *84*, 11336–11349. [[CrossRef](#)] [[PubMed](#)]
64. Gouilh, M.A.; Puechmille, S.J.; Diancourt, L.; Vandenbogaert, M.; Serra-Cobo, J.; Roïg, M.L.; Brown, P.; Moutou, F.; Caro, V.; Vabret, A.; et al. SARS-CoV related Betacoronavirus and diverse Alphacoronavirus members found in western old-world. *Virology* **2018**, *517*, 88–97. [[CrossRef](#)] [[PubMed](#)]
65. Pauly, M.; Pir, J.B.; Loesch, C.; Sausy, A.; Snoeck, C.J.; Hubschen, J.M.; Muller, C.P. Novel Alphacoronaviruses and Paramyxoviruses Cocirculate with Type 1 and Severe Acute Respiratory System (SARS)-Related Betacoronaviruses in Synanthropic Bats of Luxembourg. *Appl. Environ. Microbiol.* **2017**, *83*, e01326–17. [[CrossRef](#)] [[PubMed](#)]
66. Rihtaric, D.; Hostnik, P.; Steyer, A.; Grom, J.; Toplak, I. Identification of SARS-like coronaviruses in horseshoe bats (*Rhinolophus hipposideros*) in Slovenia. *Arch. Virol.* **2010**, *155*, 507–514. [[CrossRef](#)] [[PubMed](#)]
67. Lelli, D.; Papetti, A.; Sabelli, C.; Rosti, E.; Moreno, A.; Boniotti, M.B. Detection of coronaviruses in bats of various species in Italy. *Viruses* **2013**, *5*, 2679–2689. [[CrossRef](#)] [[PubMed](#)]
68. Lelli, D.; Moreno, A.; Lavazza, A.; Bresaola, M.; Canelli, E.; Boniotti, M.B.; Cordioli, P. Identification of Mammalian orthoreovirus type 3 in Italian bats. *Zoonoses Public Health* **2013**, *60*, 84–92. [[CrossRef](#)] [[PubMed](#)]
69. Dufkova, L.; Strakova, P.; Sirmarova, J.; Salat, J.; Moutelikova, R.; Chrudimsky, T.; Bartonicka, T.; Nowotny, N.; Ruzek, D. Detection of Diverse Novel Bat Astrovirus Sequences in the Czech Republic. *Vector Borne Zoonotic Dis.* **2015**, *15*, 518–521. [[CrossRef](#)] [[PubMed](#)]
70. Kemenesi, G.; Foldes, F.; Zana, B.; Kurucz, K.; Estok, P.; Boldogh, S.; Gorfal, T.; Banyai, K.; Oldal, M.; Jakab, F. Genetic Characterization of Providence Virus Isolated from Bat Guano in Hungary. *Genome Announc.* **2016**, *4*, e00403–16. [[CrossRef](#)] [[PubMed](#)]
71. Vazquez-Moron, S.; Juste, J.; Ibanez, C.; Ruiz-Villamor, E.; Avellon, A.; Vera, M.; Echevarria, J.E. Endemic circulation of European bat lyssavirus type 1 in serotine bats, Spain. *Emerg. Infect. Dis.* **2008**, *14*, 1263–1266. [[CrossRef](#)] [[PubMed](#)]
72. Falcon, A.; Vazquez-Moron, S.; Casas, I.; Aznar, C.; Ruiz, G.; Pozo, F.; Perez-Brena, P.; Juste, J.; Ibanez, C.; Garin, I.; et al. Detection of alpha and betacoronaviruses in multiple Iberian bat species. *Arch. Virol.* **2011**, *156*, 1883–1890. [[CrossRef](#)] [[PubMed](#)]
73. Picard-Meyer, E.; Dubourg-Savage, M.J.; Arthur, L.; Barataud, M.; Becu, D.; Bracco, S.; Borel, C.; Larcher, G.; Meme-Lafond, B.; Moinet, M.; et al. Active surveillance of bat rabies in France: A 5-year study (2004–2009). *Vet. Microbiol.* **2011**, *151*, 390–395. [[CrossRef](#)] [[PubMed](#)]
74. Vazquez, S.; Ibanez, C.; Juste, J.; Echevarria, J.E. EBLV1 circulation in natural bat colonies of *Eptesicus serotinus*: A six year survey. *Dev. Biol. (Basel)* **2006**, *125*, 257–261. [[PubMed](#)]
75. De Benedictis, P.; Marciano, S.; Scaravelli, D.; Priori, P.; Zecchin, B.; Capua, I.; Monne, I.; Cattoli, G. Alpha and lineage C betaCoV infections in Italian bats. *Virus Genes* **2014**, *48*, 366–371. [[CrossRef](#)] [[PubMed](#)]
76. Molnar, V.; Janoska, M.; Harrach, B.; Glavits, R.; Palmai, N.; Rigo, D.; Sos, E.; Liptovszky, M. Detection of a novel bat gammaherpesvirus in Hungary. *Acta Vet. Hung.* **2008**, *56*, 529–538. [[CrossRef](#)] [[PubMed](#)]

77. Garcia-Perez, R.; Ibanez, C.; Godinez, J.M.; Arechiga, N.; Garin, I.; Perez-Suarez, G.; de Paz, O.; Juste, J.; Echevarria, J.E.; Bravo, I.G. Novel papillomaviruses in free-ranging Iberian bats: No virus-host co-evolution, no strict host specificity, and hints for recombination. *Genome Biol. Evol.* **2014**, *6*, 94–104. [[CrossRef](#)] [[PubMed](#)]
78. Lopez-Roig, M.; Bourhy, H.; Lavenir, R.; Serra-Cobo, J. Seroprevalence dynamics of European bat lyssavirus type 1 in a multispecies bat colony. *Viruses* **2014**, *6*, 3386–3399. [[CrossRef](#)] [[PubMed](#)]
79. Moreno, A.; Lelli, D.; de Sabato, L.; Zaccaria, G.; Boni, A.; Sozzi, E.; Prosperi, A.; Lavazza, A.; Cella, E.; Castrucci, M.R.; et al. Detection and full genome characterization of two beta CoV viruses related to Middle East respiratory syndrome from bats in Italy. *Virol. J.* **2017**, *14*, 239. [[CrossRef](#)] [[PubMed](#)]
80. Drexler, J.F.; Corman, V.M.; Muller, M.A.; Maganga, G.D.; Vallo, P.; Binger, T.; Gloza-Rausch, F.; Cottontail, V.M.; Rasche, A.; Yordanov, S.; et al. Bats host major mammalian paramyxoviruses. *Nat. Commun.* **2012**, *3*, 796. [[CrossRef](#)] [[PubMed](#)]
81. Kemenesi, G.; Dallos, B.; Gorfal, T.; Boldogh, S.; Estok, P.; Kurucz, K.; Oldal, M.; Nemeth, V.; Madai, M.; Banyai, K.; et al. Novel European lineages of bat astroviruses identified in Hungary. *Acta Virol.* **2014**, *58*, 95–98. [[CrossRef](#)] [[PubMed](#)]
82. Fischer, K.; Zeus, V.; Kwasnitschka, L.; Kerth, G.; Haase, M.; Groschup, M.H.; Balkema-Buschmann, A. Insectivorous bats carry host specific astroviruses and coronaviruses across different regions in Germany. *Infect. Genet. Evol.* **2016**, *37*, 108–116. [[CrossRef](#)] [[PubMed](#)]
83. Gloza-Rausch, F.; Ipsen, A.; Seebens, A.; Gottsche, M.; Panning, M.; Drexler, J.F.; Petersen, N.; Annan, A.; Grywna, K.; Muller, M.; et al. Detection and prevalence patterns of group I coronaviruses in bats, northern Germany. *Emerg. Infect. Dis.* **2008**, *14*, 626–631. [[CrossRef](#)] [[PubMed](#)]
84. Arai, Y.T.; Kuzmin, I.V.; Kameoka, Y.; Botvinkin, A.D. New lyssavirus genotype from the Lesser Mouse-eared Bat (*Myotis blythi*), Kyrgyzstan. *Emerg. Infect. Dis.* **2003**, *9*, 333–337. [[CrossRef](#)] [[PubMed](#)]
85. Serra-Cobo, J.; Lopez-Roig, M.; Segui, M.; Sanchez, L.P.; Nadal, J.; Borrás, M.; Lavenir, R.; Bourhy, H. Ecological factors associated with European bat lyssavirus seroprevalence in Spanish bats. *PLoS ONE* **2013**, *8*, e64467. [[CrossRef](#)] [[PubMed](#)]
86. Van der Poel, W.H.; Van der Heide, R.; Verstraten, E.R.; Takumi, K.; Lina, P.H.; Kramps, J.A. European bat lyssaviruses, The Netherlands. *Emerg. Infect. Dis.* **2005**, *11*, 1854–1859. [[CrossRef](#)] [[PubMed](#)]
87. Freuling, C.M.; Kliemt, J.; Schares, S.; Heidecke, D.; Driechciarz, R.; Schatz, J.; Muller, T. Detection of European bat lyssavirus 2 (EBLV-2) in a Daubenton's bat (*Myotis daubentonii*) from Magdeburg, Germany. *Berliner und Munchener Tierarztliche Wochenschrift* **2012**, *125*, 255–258. [[PubMed](#)]
88. Davis, P.L.; Holmes, E.C.; Larrous, F.; Van der Poel, W.H.; Tjornehoj, K.; Alonso, W.J.; Bourhy, H. Phylogeography, population dynamics, and molecular evolution of European bat lyssaviruses. *J. Virol.* **2005**, *79*, 10487–10497. [[CrossRef](#)] [[PubMed](#)]
89. Nokireki, T.; Sironen, T.; Smura, T.; Karkamo, V.; Sihvonen, L.; Gadd, T. Second case of European bat lyssavirus type 2 detected in a Daubenton's bat in Finland. *Acta Vet. Scand.* **2017**, *59*, 62. [[CrossRef](#)] [[PubMed](#)]
90. Moldal, T.; Vikoren, T.; Cliquet, F.; Marston, D.A.; van der Kooij, J.; Madslien, K.; Orpetveit, I. First detection of European bat lyssavirus type 2 (EBLV-2) in Norway. *BMC Vet. Res.* **2017**, *13*, 216. [[CrossRef](#)] [[PubMed](#)]
91. Hammarin, A.L.; Berndtsson, L.T.; Falk, K.; Nedinge, M.; Olsson, G.; Lundkvist, A. Lyssavirus-reactive antibodies in Swedish bats. *Infect. Ecol. Epidemiol.* **2016**, *6*, 31262. [[CrossRef](#)] [[PubMed](#)]
92. Harris, S.L.; Mansfield, K.; Marston, D.A.; Johnson, N.; Pajamo, K.; O'Brien, N.; Black, C.; McElhinney, L.M.; Fooks, A.R. Isolation of European bat lyssavirus type 2 from a Daubenton's bat (*Myotis daubentonii*) in Shropshire. *Vet. Rec.* **2007**, *161*, 384–386. [[CrossRef](#)] [[PubMed](#)]
93. Amengual, B.; Bourhy, H.; Lopez-Roig, M.; Serra-Cobo, J. Temporal dynamics of European bat Lyssavirus type 1 and survival of *Myotis myotis* bats in natural colonies. *PLoS ONE* **2007**, *2*, e566. [[CrossRef](#)] [[PubMed](#)]
94. Wibbelt, G.; Kurth, A.; Yasmum, N.; Bannert, M.; Nagel, S.; Nitsche, A.; Ehlers, B. Discovery of herpesviruses in bats. *J. Gen. Virol.* **2007**, *88*, 2651–2655. [[CrossRef](#)] [[PubMed](#)]
95. Kuzmin, I.V.; Orciari, L.A.; Arai, Y.T.; Smith, J.S.; Hanlon, C.A.; Kameoka, Y.; Rupprecht, C.E. Bat lyssaviruses (Aravan and Khujand) from Central Asia: Phylogenetic relationships according to N, P and G gene sequences. *Virus Res.* **2003**, *97*, 65–79. [[CrossRef](#)]
96. Dacheux, L.; Cervantes-Gonzalez, M.; Guigon, G.; Thiberge, J.M.; Vandenbogaert, M.; Maufrais, C.; Caro, V.; Bourhy, H. A preliminary study of viral metagenomics of French bat species in contact with humans: identification of new mammalian viruses. *PLoS ONE* **2014**, *9*, e87194. [[CrossRef](#)] [[PubMed](#)]

97. Kohl, C.; Lesnik, R.; Brinkmann, A.; Ebinger, A.; Radonic, A.; Nitsche, A.; Muhldorfer, K.; Wibbelt, G.; Kurth, A. Isolation and characterization of three mammalian orthoreoviruses from European bats. *PLoS ONE* **2012**, *7*, e43106. [[CrossRef](#)] [[PubMed](#)]
98. Kurth, A.; Kohl, C.; Brinkmann, A.; Ebinger, A.; Harper, J.A.; Wang, L.F.; Muhldorfer, K.; Wibbelt, G. Novel paramyxoviruses in free-ranging European bats. *PLoS ONE* **2012**, *7*, e38688. [[CrossRef](#)] [[PubMed](#)]
99. Picard-Meyer, E.; Servat, A.; Robardet, E.; Moinet, M.; Borel, C.; Cliquet, F. Isolation of Bokeloh bat lyssavirus in *Myotis nattereri* in France. *Arch. Virol.* **2013**, *158*, 2333–2340. [[CrossRef](#)] [[PubMed](#)]
100. Freuling, C.M.; Beer, M.; Conraths, F.J.; Finke, S.; Hoffmann, B.; Keller, B.; Kliemt, J.; Mettenleiter, T.C.; Muhlbach, E.; Teifke, J.P.; et al. Novel lyssavirus in Natterer's bat, Germany. *Emerg. Infect. Dis.* **2011**, *17*, 1519–1522. [[CrossRef](#)] [[PubMed](#)]
101. Rizzo, F.; Edenborough, K.M.; Toffoli, R.; Culasso, P.; Zoppi, S.; Dondo, A.; Robetto, S.; Rosati, S.; Lander, A.; Kurth, A.; et al. Coronavirus and paramyxovirus in bats from Northwest Italy. *BMC Vet. Res.* **2017**, *13*, 396. [[CrossRef](#)] [[PubMed](#)]
102. Schatz, J.; Freuling, C.M.; Auer, E.; Goharriz, H.; Harbusch, C.; Johnson, N.; Kaipf, I.; Mettenleiter, T.C.; Muhldorfer, K.; Muhle, R.U.; et al. Enhanced passive bat rabies surveillance in indigenous bat species from Germany—A retrospective study. *PLoS Negl. Trop. Dis.* **2014**, *8*, e2835. [[CrossRef](#)] [[PubMed](#)]
103. Strakova, P.; Dufkova, L.; Sirmarova, J.; Salat, J.; Bartonicka, T.; Klempa, B.; Pfaff, F.; Hoper, D.; Hoffmann, B.; Ulrich, R.G.; et al. Novel hantavirus identified in European bat species *Nyctalus noctula*. *Infect. Genet. Evol.* **2017**, *48*, 127–130. [[CrossRef](#)] [[PubMed](#)]
104. Janoska, M.; Vidovszky, M.; Molnar, V.; Liptovszky, M.; Harrach, B.; Benko, M. Novel adenoviruses and herpesviruses detected in bats. *Vet. J.* **2011**, *189*, 118–121. [[CrossRef](#)] [[PubMed](#)]
105. Lelli, D.; Prosperi, A.; Moreno, A.; Chiapponi, C.; Gibellini, A.M.; De Benedictis, P.; Leopardi, S.; Sozzi, E.; Lavazza, A. Isolation of a novel Rhabdovirus from an insectivorous bat (*Pipistrellus kuhlii*) in Italy. *Virol. J.* **2018**, *15*, 37. [[CrossRef](#)] [[PubMed](#)]
106. Verani, P.; Ciufolini, M.G.; Caciolli, S.; Renzi, A.; Nicoletti, L.; Sabatinelli, G.; Bartolozzi, D.; Volpi, G.; Amaducci, L.; Coluzzi, M.; et al. Ecology of viruses isolated from sand flies in Italy and characterized of a new Phlebovirus (*Arabia virus*). *Am. J. Trop. Med. Hyg.* **1988**, *38*, 433–439. [[CrossRef](#)] [[PubMed](#)]
107. Kohl, C.; Vidovszky, M.Z.; Muhldorfer, K.; Dabrowski, P.W.; Radonic, A.; Nitsche, A.; Wibbelt, G.; Kurth, A.; Harrach, B. Genome analysis of bat adenovirus 2: Indications of interspecies transmission. *J. Virol.* **2012**, *86*, 1888–1892. [[CrossRef](#)] [[PubMed](#)]
108. Eggerbauer, E.; Troupin, C.; Passior, K.; Pfaff, F.; Hoper, D.; Neubauer-Juric, A.; Haberl, S.; Bouchier, C.; Mettenleiter, T.C.; Bourhy, H.; et al. The Recently Discovered Bokeloh Bat Lyssavirus: Insights Into Its Genetic Heterogeneity and Spatial Distribution in Europe and the Population Genetics of Its Primary Host. *Adv. Virus Res.* **2017**, *99*, 199–232. [[CrossRef](#)] [[PubMed](#)]
109. Sonntag, M.; Muhldorfer, K.; Speck, S.; Wibbelt, G.; Kurth, A. New adenovirus in bats, Germany. *Emerg. Infect. Dis.* **2009**, *15*, 2052–2055. [[CrossRef](#)] [[PubMed](#)]
110. Reusken, C.B.; Lina, P.H.; Pielaat, A.; de Vries, A.; Dam-Deisz, C.; Adema, J.; Drexler, J.F.; Drosten, C.; Kooi, E.A. Circulation of group 2 coronaviruses in a bat species common to urban areas in Western Europe. *Vector Borne Zoonotic Dis.* **2010**, *10*, 785–791. [[CrossRef](#)] [[PubMed](#)]
111. Kemenesi, G.; Dallos, B.; Gorfal, T.; Boldogh, S.; Estok, P.; Kurucz, K.; Kutas, A.; Foldes, F.; Oldal, M.; Nemeth, V.; et al. Molecular survey of RNA viruses in Hungarian bats: Discovering novel astroviruses, coronaviruses, and caliciviruses. *Vector Borne Zoonotic Dis.* **2014**, *14*, 846–855. [[CrossRef](#)] [[PubMed](#)]
112. Selimov, M.A.; Smekhov, A.M.; Antonova, L.A.; Shablovskaya, E.A.; King, A.A.; Kulikova, L.G. New strains of rabies-related viruses isolated from bats in the Ukraine. *Acta Virol.* **1991**, *35*, 226–231. [[PubMed](#)]
113. Negredo, A.; Palacios, G.; Vazquez-Moron, S.; Gonzalez, F.; Dopazo, H.; Molero, F.; Juste, J.; Quetglas, J.; Savji, N.; de la Cruz Martinez, M.; et al. Discovery of an ebolavirus-like filovirus in europe. *PLoS Pathog.* **2011**, *7*, e1002304. [[CrossRef](#)] [[PubMed](#)]
114. Wellenberg, G.J.; Audry, L.; Ronsholt, L.; van der Poel, W.H.; Bruschke, C.J.; Bourhy, H. Presence of European bat lyssavirus RNAs in apparently healthy *Rousettus aegyptiacus* bats. *Arch. Virol.* **2002**, *147*, 349–361. [[CrossRef](#)] [[PubMed](#)]
115. Towner, J.S.; Amman, B.R.; Sealy, T.K.; Carroll, S.A.; Comer, J.A.; Kemp, A.; Swanepoel, R.; Paddock, C.D.; Balinandi, S.; Khristova, M.L.; et al. Isolation of genetically diverse Marburg viruses from Egyptian fruit bats. *PLoS Pathog.* **2009**, *5*, e1000536. [[CrossRef](#)] [[PubMed](#)]

116. Chowell, G.; Nishiura, H. Transmission dynamics and control of Ebola virus disease (EVD): A review. *BMC Med.* **2014**, *12*, 196. [[CrossRef](#)] [[PubMed](#)]
117. Messaoudi, I.; Amarasinghe, G.K.; Basler, C.F. Filovirus pathogenesis and immune evasion: Insights from Ebola virus and Marburg virus. *Nat. Rev. Microbiol.* **2015**, *13*, 663–676. [[CrossRef](#)] [[PubMed](#)]
118. Goldstein, T.; Anthony, S.J.; Gbakima, A.; Bird, B.H.; Bangura, J.; Tremeau-Bravard, A.; Belaganahalli, M.N.; Wells, H.L.; Dhanota, J.K.; Liang, E.; et al. The discovery of Bombali virus adds further support for bats as hosts of ebolaviruses. *Nat. Microbiol.* **2018**, *3*, 1084–1089. [[CrossRef](#)] [[PubMed](#)]
119. Kemenesi, G.; Kurucz, K.; Dallos, B.; Zana, B.; Földes, F.; Boldogh, S.; Görföl, T.; Carroll, M.W.; Jakab, F. Re-emergence of Llovio virus in *Miniopterus schreibersii* bats, Hungary, 2016. *Emerg. Microbes Infect.* **2018**, *7*, 66. [[CrossRef](#)] [[PubMed](#)]
120. Quetglas, J.; González, F.; Paz, Ó.D. Estudian la extraña mortandad de miles de murciélagos en cueva. *Quercus* **2003**, *203*, 50–51.
121. Leroy, E.M.; Kumulungui, B.; Pourrut, X.; Rouquet, P.; Hassanin, A.; Yaba, P.; Délicat, A.; Paweska, J.T.; Gonzalez, J.-P.; Swanepoel, R. Fruit bats as reservoirs of Ebola virus. *Nature* **2005**, *438*, 575–576. [[CrossRef](#)] [[PubMed](#)]
122. Swanepoel, R.; Leman, P.A.; Burt, F.J.; Zachariades, N.A.; Braack, L.; Ksiazek, T.G.; Rollin, P.E.; Zaki, S.R.; Peters, C.J. Experimental inoculation of plants and animals with Ebola virus. *Emerg. Infect. Dis.* **1996**, *2*, 321–325. [[CrossRef](#)] [[PubMed](#)]
123. Azhar, E.I.; Lanini, S.; Ippolito, G.; Zumla, A. The Middle East Respiratory Syndrome Coronavirus—A Continuing Risk to Global Health Security. *Adv. Exp. Med. Biol.* **2017**, *972*, 49–60. [[CrossRef](#)] [[PubMed](#)]
124. Poon, L.L.; Chu, D.K.; Chan, K.H.; Wong, O.K.; Ellis, T.M.; Leung, Y.H.; Lau, S.K.; Woo, P.C.; Suen, K.Y.; Yuen, K.Y.; et al. Identification of a novel coronavirus in bats. *J. Virol.* **2005**, *79*, 2001–2009. [[CrossRef](#)] [[PubMed](#)]
125. Lefkowitz, E.J.; Dempsey, D.M.; Hendrickson, R.C.; Orton, R.J.; Siddell, S.G.; Smith, D.B. Virus taxonomy: The database of the International Committee on Taxonomy of Viruses (ICTV). *Nucleic Acids Res.* **2018**, *46*, D708–D717. [[CrossRef](#)] [[PubMed](#)]
126. Hu, B.; Ge, X.; Wang, L.F.; Shi, Z. Bat origin of human coronaviruses. *Virol. J.* **2015**, *12*, 221. [[CrossRef](#)] [[PubMed](#)]
127. Memish, Z.A.; Mishra, N.; Olival, K.J.; Fagbo, S.F.; Kapoor, V.; Epstein, J.H.; Alhakeem, R.; Durosinioun, A.; Al Asmari, M.; Islam, A.; et al. Middle East respiratory syndrome coronavirus in bats, Saudi Arabia. *Emerg. Infect. Dis.* **2013**, *19*, 1819–1823. [[CrossRef](#)] [[PubMed](#)]
128. Guan, Y.; Zheng, B.J.; He, Y.Q.; Liu, X.L.; Zhuang, Z.X.; Cheung, C.L.; Luo, S.W.; Li, P.H.; Zhang, L.J.; Guan, Y.J.; et al. Isolation and characterization of viruses related to the SARS coronavirus from animals in southern China. *Science* **2003**, *302*, 276–278. [[CrossRef](#)] [[PubMed](#)]
129. Centers for Disease Control and Prevention (CDC). Prevalence of IgG antibody to SARS-associated coronavirus in animal traders—Guangdong Province, China, 2003. *MMWR Morb. Mortal. Wkly. Rep.* **2003**, *52*, 986–987.
130. Xu, H.F.; Wang, M.; Zhang, Z.B.; Zou, X.Z.; Gao, Y.; Liu, X.N.; Lu, E.J.; Pan, B.Y.; Wu, S.J.; Yu, S.Y. [An epidemiologic investigation on infection with severe acute respiratory syndrome coronavirus in wild animals traders in Guangzhou]. *Zhonghua Yu Fang Yi Xue Za Zhi* **2004**, *38*, 81–83. [[PubMed](#)]
131. Kan, B.; Wang, M.; Jing, H.; Xu, H.; Jiang, X.; Yan, M.; Liang, W.; Zheng, H.; Wan, K.; Liu, Q.; et al. Molecular evolution analysis and geographic investigation of severe acute respiratory syndrome coronavirus-like virus in palm civets at an animal market and on farms. *J. Virol.* **2005**, *79*, 11892–11900. [[CrossRef](#)] [[PubMed](#)]
132. Shi, Z.; Hu, Z. A review of studies on animal reservoirs of the SARS coronavirus. *Virus Res.* **2008**, *133*, 74–87. [[CrossRef](#)] [[PubMed](#)]
133. Anthony, S.J.; Ojeda-Flores, R.; Rico-Chávez, O.; Navarrete-Macias, I.; Zambrana-Torrel, C.M.; Rostal, M.K.; Epstein, J.H.; Tipps, T.; Liang, E.; Sanchez-Leon, M.; et al. Coronaviruses in bats from Mexico. *J. Gen. Virol.* **2013**, *94*, 1028–1038. [[CrossRef](#)] [[PubMed](#)]
134. Masters, P.S. The molecular biology of coronaviruses. *Adv. Virus Res.* **2006**, *66*, 193–292. [[CrossRef](#)] [[PubMed](#)]
135. Gallagher, T.M.; Buchmeier, M.J. Coronavirus spike proteins in viral entry and pathogenesis. *Virology* **2001**, *279*, 371–374. [[CrossRef](#)] [[PubMed](#)]
136. Li, W.; Shi, Z.; Yu, M.; Ren, W.; Smith, C.; Epstein, J.H.; Wang, H.; Crameri, G.; Hu, Z.; Zhang, H.; et al. Bats are natural reservoirs of SARS-like coronaviruses. *Science* **2005**, *310*, 676–679. [[CrossRef](#)] [[PubMed](#)]

137. Song, H.D.; Tu, C.C.; Zhang, G.W.; Wang, S.Y.; Zheng, K.; Lei, L.C.; Chen, Q.X.; Gao, Y.W.; Zhou, H.Q.; Xiang, H.; et al. Cross-host evolution of severe acute respiratory syndrome coronavirus in palm civet and human. *Proc. Natl. Acad. Sci. USA* **2005**, *102*, 2430–2435. [[CrossRef](#)] [[PubMed](#)]
138. Nadin-Davis, S.; Alnabelseya, N.; Knowles, M.K. The phylogeography of Myotis bat-associated rabies viruses across Canada. *PLoS Negl. Trop. Dis.* **2017**, *11*, e0005541. [[CrossRef](#)] [[PubMed](#)]
139. Hughes, G.J.; Orciari, L.A.; Rupprecht, C.E. Evolutionary timescale of rabies virus adaptation to North American bats inferred from the substitution rate of the nucleoprotein gene. *J. Gen. Virol.* **2005**, *86*, 1467–1474. [[CrossRef](#)] [[PubMed](#)]
140. Kuzmina, N.A.; Kuzmin, I.V.; Ellison, J.A.; Taylor, S.T.; Bergman, D.L.; Dew, B.; Rupprecht, C.E. A reassessment of the evolutionary timescale of bat rabies viruses based upon glycoprotein gene sequences. *Virus Genes* **2013**, *47*, 305–310. [[CrossRef](#)] [[PubMed](#)]
141. Gilbert, A.T.; Petersen, B.W.; Recuenco, S.; Niezgoda, M.; Gomez, J.; Laguna-Torres, V.A.; Rupprecht, C. Evidence of rabies virus exposure among humans in the Peruvian Amazon. *Am. J. Trop. Med. Hyg.* **2012**, *87*, 206–215. [[CrossRef](#)] [[PubMed](#)]
142. Pajamo, K.; Harkess, G.; Goddard, T.; Marston, D.; McElhinney, L.; Johnson, N.; Fooks, A.R. Isolation of European bat lyssavirus type 2 (EBLV-2) in a Daubenton's bat in the UK with a minimum incubation period of 9 months. *Rabies Bull. Eur.* **2008**, *32*, 6–7.
143. Warrell, M.J. Current rabies vaccines and prophylaxis schedules: Preventing rabies before and after exposure. *Travel Med. Infect. Dis.* **2012**, *10*, 1–15. [[CrossRef](#)] [[PubMed](#)]
144. Brookes, S.M.; Healy, D.M.; Fooks, A.R. Ability of rabies vaccine strains to elicit cross-neutralising antibodies. *Dev. Biol. (Basel)* **2006**, *125*, 185–193. [[PubMed](#)]
145. Brookes, S.M.; Parsons, G.; Johnson, N.; McElhinney, L.M.; Fooks, A.R. Rabies human diploid cell vaccine elicits cross-neutralising and cross-protecting immune responses against European and Australian bat lyssaviruses. *Vaccine* **2005**, *23*, 4101–4109. [[CrossRef](#)] [[PubMed](#)]
146. Hanlon, C.A.; Kuzmin, I.V.; Blanton, J.D.; Weldon, W.C.; Manangan, J.S.; Rupprecht, C.E. Efficacy of rabies biologics against new lyssaviruses from Eurasia. *Virus Res.* **2005**, *111*, 44–54. [[CrossRef](#)] [[PubMed](#)]
147. Evans, J.S.; Horton, D.L.; Easton, A.J.; Fooks, A.R.; Banyard, A.C. Rabies virus vaccines: Is there a need for a pan-lyssavirus vaccine? *Vaccine* **2012**, *30*, 7447–7454. [[CrossRef](#)] [[PubMed](#)]
148. Horton, D.L.; McElhinney, L.M.; Marston, D.A.; Wood, J.L.; Russell, C.A.; Lewis, N.; Kuzmin, I.V.; Fouchier, R.A.; Osterhaus, A.D.; Fooks, A.R.; et al. Quantifying antigenic relationships among the Lyssaviruses. *J. Virol.* **2010**, *84*, 11841–11848. [[CrossRef](#)] [[PubMed](#)]
149. Nolden, T.; Banyard, A.C.; Finke, S.; Fooks, A.R.; Hanke, D.; Hoper, D.; Horton, D.L.; Mettenleiter, T.C.; Muller, T.; Teifke, J.P.; et al. Comparative studies on the genetic, antigenic and pathogenic characteristics of Bokeloh bat lyssavirus. *J. Gen. Virol.* **2014**, *95*, 1647–1653. [[CrossRef](#)] [[PubMed](#)]
150. Badrane, H.; Bahloul, C.; Perrin, P.; Tordo, N. Evidence of two Lyssavirus phylogroups with distinct pathogenicity and immunogenicity. *J. Virol.* **2001**, *75*, 3268–3276. [[CrossRef](#)] [[PubMed](#)]
151. Moore, S.M.; Hanlon, C.A. Rabies-specific antibodies: Measuring surrogates of protection against a fatal disease. *PLoS Negl. Trop. Dis.* **2010**, *4*, e595. [[CrossRef](#)] [[PubMed](#)]
152. Horton, D.L.; Banyard, A.C.; Marston, D.A.; Wise, E.; Selden, D.; Nunez, A.; Hicks, D.; Lembo, T.; Cleaveland, S.; Peel, A.J.; et al. Antigenic and genetic characterization of a divergent African virus, Ikoma lyssavirus. *J. Gen. Virol.* **2014**, *95*, 1025–1032. [[CrossRef](#)] [[PubMed](#)]
153. Evans, J.S.; Selden, D.; Wu, G.; Wright, E.; Horton, D.L.; Fooks, A.R.; Banyard, A.C. Antigenic site changes in the rabies virus glycoprotein dictates functionality and neutralizing capability against divergent lyssaviruses. *J. Gen. Virol.* **2018**, *99*, 169–180. [[CrossRef](#)] [[PubMed](#)]
154. Kuzmin, I.V.; Niezgoda, M.; Franka, R.; Agwanda, B.; Markotter, W.; Beagley, J.C.; Urazova, O.Y.; Breiman, R.F.; Rupprecht, C.E. Possible emergence of West Caucasian bat virus in Africa. *Emerg. Infect. Dis.* **2008**, *14*, 1887–1889. [[CrossRef](#)] [[PubMed](#)]
155. Marzi, A.; Hanley, P.W.; Haddock, E.; Martellaro, C.; Kobinger, G.; Feldmann, H. Efficacy of Vesicular Stomatitis Virus-Ebola Virus Postexposure Treatment in Rhesus Macaques Infected With Ebola Virus Makona. *J. Infect. Dis.* **2016**, *214*, S360–S366. [[CrossRef](#)] [[PubMed](#)]






156. Henao-Restrepo, A.M.; Camacho, A.; Longini, I.M.; Watson, C.H.; Edmunds, W.J.; Egger, M.; Carroll, M.W.; Dean, N.E.; Diatta, I.; Doumbia, M.; et al. Efficacy and effectiveness of an rVSV-vectored vaccine in preventing Ebola virus disease: Final results from the Guinea ring vaccination, open-label, cluster-randomised trial (Ebola Ça Suffit!). *Lancet* **2017**, *389*, 505–518. [[CrossRef](#)]
157. Mire, C.E.; Geisbert, J.B.; Agans, K.N.; Satterfield, B.A.; Versteeg, K.M.; Fritz, E.A.; Feldmann, H.; Hensley, L.E.; Geisbert, T.W. Durability of a Vesicular Stomatitis Virus-Based Marburg Virus Vaccine in Nonhuman Primates. *PLoS ONE* **2014**, *9*, e94355. [[CrossRef](#)] [[PubMed](#)]
158. Kuhn, J.H.; Becker, S.; Ebihara, H.; Geisbert, T.W.; Johnson, K.M.; Kawaoka, Y.; Lipkin, W.I.; Negredo, A.I.; Netesov, S.V.; Nichol, S.T.; et al. Proposal for a revised taxonomy of the family Filoviridae: Classification, names of taxa and viruses, and virus abbreviations. *Arch. Virol.* **2010**, *155*, 2083–2103. [[CrossRef](#)] [[PubMed](#)]
159. Okba, N.M.A.; Raj, V.S.; Haagmans, B.L. Middle East respiratory syndrome coronavirus vaccines: Current status and novel approaches. *Curr. Opin. Virol.* **2017**, *23*, 49–58. [[CrossRef](#)] [[PubMed](#)]
160. Ma, C.; Li, Y.; Wang, L.; Zhao, G.; Tao, X.; Tseng, C.-T.K.; Zhou, Y.; Du, L.; Jiang, S. Intranasal vaccination with recombinant receptor-binding domain of MERS-CoV spike protein induces much stronger local mucosal immune responses than subcutaneous immunization: Implication for designing novel mucosal MERS vaccines. *Vaccine* **2014**, *32*, 2100–2108. [[CrossRef](#)] [[PubMed](#)]
161. Zhao, J.; Zhao, J.; Mangalam, A.K.; Channappanavar, R.; Fett, C.; Meyerholz, D.K.; Agnihothram, S.; Baric, R.S.; David, C.S.; Perlman, S. Airway Memory CD4+ T Cells Mediate Protective Immunity against Emerging Respiratory Coronaviruses. *Immunity* **2016**, *44*, 1379–1391. [[CrossRef](#)] [[PubMed](#)]
162. Stading, B.; Ellison, J.A.; Carson, W.C.; Satheshkumar, P.S.; Rocke, T.E.; Osorio, J.E. Protection of bats (*Eptesicus fuscus*) against rabies following topical or oronasal exposure to a recombinant raccoon poxvirus vaccine. *PLoS Negl. Trop. Dis.* **2017**, *11*, e0005958. [[CrossRef](#)] [[PubMed](#)]



© 2019 by the authors. Licensee MDPI, Basel, Switzerland. This article is an open access article distributed under the terms and conditions of the Creative Commons Attribution (CC BY) license (<http://creativecommons.org/licenses/by/4.0/>).

Article

Assessing Rabies Vaccine Protection against a Novel Lyssavirus, Kotalahti Bat Lyssavirus

Rebecca Shipley ^{1,2}, Edward Wright ² , Fabian Z. X. Lean ³ , David Selden ¹ , Daniel L. Horton ⁴, Anthony R. Fooks ^{1,5}  and Ashley C. Banyard ^{1,2,5,*} 

¹ Wildlife Zoonoses and Vector-Borne Diseases Research Group, Animal and Plant Health Agency (APHA), Weybridge, London KT15 3NB, UK; rebecca.shipley@apha.gov.uk (R.S.); david.selden@apha.gov.uk (D.S.); tony.fooks@apha.gov.uk (A.R.F.)

² School of Life Sciences, University of Sussex, Falmer, Brighton BN1 9QG, UK; ew323@sussex.ac.uk

³ Pathology Department, Animal and Plant Health Agency (APHA), New Haw, Addlestone KT15 3NB, UK; fabian.lean@apha.gov.uk

⁴ Department of Pathology and Infectious Diseases, School of Veterinary Medicine, University of Surrey, Guildford GU2 7XH, UK; d.horton@surrey.ac.uk

⁵ Institute for Infection and Immunity, St. George's Hospital Medical School, University of London, London SW17 0RE, UK

* Correspondence: ashley.banyard@apha.gov.uk; Tel.: +44-(0)-2080269463

Abstract: Rabies is a fatal encephalitis caused by an important group of viruses within the *Lyssavirus* genus. The prototype virus, rabies virus, is still the most commonly reported lyssavirus and causes approximately 59,000 human fatalities annually. The human and animal burden of the other lyssavirus species is undefined. The original reports for the novel lyssavirus, Kotalahti bat lyssavirus (KBLV), were based on the detection of viral RNA alone. In this report we describe the successful generation of a live recombinant virus, cSN-KBLV; where the full-length genome clone of RABV vaccine strain, SAD-B19, was constructed with the glycoprotein of KBLV. Subsequent in vitro characterisation of cSN-KBLV is described here. In addition, the ability of a human rabies vaccine to confer protective immunity in vivo following challenge with this recombinant virus was assessed. Naïve or vaccinated mice were infected intracerebrally with a dose of 100 focus-forming units/30 µL of cSN-KBLV; all naïve mice and 8% ($n = 1/12$) of the vaccinated mice succumbed to the challenge, whilst 92% ($n = 11/12$) of the vaccinated mice survived to the end of the experiment. This report provides strong evidence for cross-neutralisation and cross-protection of cSN-KBLV using purified Vero cell rabies vaccine.

Keywords: rabies; lyssavirus; Kotalahti bat lyssavirus; KBLV; bats; vaccine protection; neutralisation; emerging; novel; zoonoses



Citation: Shipley, R.; Wright, E.; Lean, F.Z.X.; Selden, D.; Horton, D.L.; Fooks, A.R.; Banyard, A.C. Assessing Rabies Vaccine Protection against a Novel Lyssavirus, Kotalahti Bat Lyssavirus. *Viruses* **2021**, *13*, 947. <https://doi.org/10.3390/v13050947>

Academic Editor: Laurent Dacheux

Received: 21 March 2021

Accepted: 12 May 2021

Published: 20 May 2021

Publisher's Note: MDPI stays neutral with regard to jurisdictional claims in published maps and institutional affiliations.



Copyright: © 2021 by the authors. Licensee MDPI, Basel, Switzerland. This article is an open access article distributed under the terms and conditions of the Creative Commons Attribution (CC BY) license (<https://creativecommons.org/licenses/by/4.0/>).

1. Introduction

Rabies is caused by viruses classified within the *Lyssavirus* genus, family Rhabdoviridae, order Mononegavirales [1]. These viruses are of importance to both human and animal health given the invariably fatal outcome from developing a neurological disease [2]. The genus *Lyssavirus* is divided into 17 species accepted by the International Committee on the Taxonomy of Viruses (ICTV) with two tentative novel lyssaviruses, Kotalahti bat lyssavirus (KBLV) and Matlo bat lyssavirus (MBLV), awaiting classification [3–5]. The ancestral lyssavirus reservoir host species is universally accepted as being members of the order Chiroptera with all but two lyssaviruses, Mokola and Ikoma lyssaviruses, having been detected in different bat species [6–8]. As well as lyssaviruses, bats have been associated as the host reservoir for an abundance of viruses, including coronaviruses (SARS and MERS viruses), filoviruses (Marburg virus and the newly discovered Mënglà virus), and Henipaviruses [9–11].

Within the *Lyssavirus* genus, the most broadly distributed and important to veterinary and public health is the rabies virus (RABV). Though this virus has largely been eliminated throughout western Europe, RABV is still the most commonly reported lyssavirus. RABV causes approximately 59,000 human deaths annually with the majority of these fatalities (>99%) being associated with dog-mediated transmission [12]. The human and animal burden of the other lyssaviruses, however, is largely undefined, with only 14 human lyssavirus-related deaths being reported [13,14]. This low number of reported cases may be because diagnostic capabilities often reliant on antigen detection or a clinical diagnosis, particularly in endemic areas, are unable to distinguish between different lyssavirus species [13,15].

The negative-stranded RNA lyssavirus genome consists of five genes that encode the nucleoprotein (N), phosphoprotein (P), matrix protein (M), glycoprotein (G), and viral RNA polymerase (L). Within the *Lyssavirus* genus, the species are genetically categorised according to the homology of nucleotide sequence encoding N and have been proposed to form distinct phylogroups following a combination of genetic and antigenic assessment [16,17]. Currently, rabies vaccines marketed for human use are based on whole inactivated RABV particles. It is understood that rabies vaccines confer protective immunity against phylogroup I lyssaviruses, which includes classical RABVs, Australian bat lyssavirus (ABLV), Aravan virus (ARAV), Bokeloh bat lyssavirus (BBLV), Duvenhage virus (DUVV), European bat lyssavirus type 1 (EBLV-1), European bat lyssavirus type 2 (EBLV-2), Gannoruwa bat lyssavirus (GBLV), Irkut virus (IRKV), and Khujand virus (KHUV) [18–20]. Certainly, studies undertaken have indicated that the level of protective immunity afforded by current vaccines against phylogroup I lyssaviruses correlate to the antibody titre level induced in the recipient of the vaccine. An antibody titre of 0.5 IU/mL is generally considered a conservative threshold above which protection from classical rabies virus strains is likely [21]. However, it has been suggested that a higher neutralising antibody titre is required to confer protection against non-RABV phylogroup I lyssaviruses [22]. Current evidence from an in vivo study suggested that an antibody titre of ≥ 10 IU/mL is required for protection against BBLV whilst in vitro ≥ 4.5 IU/mL is required for complete neutralisation of EBLV-1, EBLV-2, and ABLV [18,23]. Nevertheless, a defined cut-off for protection against non-RABV phylogroup I lyssaviruses remains to be established. Conversely, current RABV vaccines elicit no level of protective immunity against the more divergent lyssaviruses in phylogroup II, which includes Lagos bat virus (LBV Lineages A–D), Mokola virus (MOKV), and Shimon bat virus (SHIBV), as well as highly divergent viruses tentatively assigned to a third phylogroup, which includes Ikoma lyssavirus (IKOV), Lleida bat lyssavirus (LLEBV), and West Caucasian bat virus (WCBV) [24–26].

Whilst RABV is the most commonly reported lyssavirus in terrestrial species, the epidemiology of non-RABV lyssaviruses is less well understood. ARAV, KHUV, SHIBV, and IKOV, specifically, exist as single detections. Consequently, gaps in epidemiological distribution, host range, and ability to cross the species barrier remain. The continual discovery of novel lyssaviruses in bats has warranted an increasing interest in the degree of vaccine cross-protection afforded by rabies vaccines [13].

In 2017, nucleic acid from a novel lyssavirus, termed Kotalahti bat lyssavirus (KBLV), was discovered in a Brandt's bat (*Myotis brandtii*) in Kotalahti, Finland [27]. Attempts to isolate the virus were unsuccessful, likely because the bat was in a considerable stage of decomposition on arrival to the Finnish Food Safety Authority Evira [27]. Initial genetic assessment enabled amplification of a small fragment of the genome and sequencing of the nucleoprotein encoding gene demonstrated that KBLV was most closely related to KHUV (81%), followed by ARAV (79.7%), BBLV (79.5%), and EBLV-2 (79.4%), at the nucleotide level [27]. A follow-up investigation using deep sequencing successfully obtained the full KBLV genome sequence consisting of 11,878 nucleotides encoding for the five genes N, P, M, G, and L. Consequently, it was determined that KBLV is phylogenetically more closely related to EBLV-2 and clusters with KHUV and BBLV [4]. It was also determined that sera, derived from humans vaccinated against RABV, demonstrated cross-neutralising

activity against KBLV G pseudotyped RABV particles [4]. Despite the preliminary findings, attempts to isolate a live replication competent KBLV virus or recombinant virus were unsuccessful. This has prevented the *in vivo* evaluation of vaccine efficacy as well as full antigenic characterization.

The lyssavirus glycoprotein (G) is the only viral surface protein and is the sole target for neutralising antibodies [28]. Previous studies have utilised reverse genetics (RG) techniques to exchange G proteins derived from other lyssavirus species into a RABV vaccine RG backbone to enable assessment of vaccine protection against recombinant viruses [29–31].

The present study describes the development of a live recombinant RABV where the RABV G has been replaced by KBLV G. *In vitro* and *in vivo* studies were used to define the ability of vaccine-derived sera and vaccine-induced antibodies (anti-RABV) to neutralise and protect against a recombinant virus containing the KBLV G protein in a murine model.

2. Materials and Methods

2.1. Cells

BHK-21 (BHK) cells were propagated in Glasgow's modified Eagle's medium (GMEM; Gibco, Loughborough, UK) supplemented with 10% FBS, 100 U/mL penicillin, 100 µg/mL streptomycin and 25 U/mL mycostatin (Invitrogen, Paisley, UK). BSR-T7/5 cells (BHK-derived cells that stably express T7 RNA polymerase—a kind gift from Dr Stefan Finke, FLI, Greifswald, Germany) were propagated in Dulbecco's modified Eagle's medium (DMEM; Gibco) supplemented with 5–10% FBS, 100 U/mL penicillin, 100 µg/mL streptomycin, and 25 U/mL mycostatin (Invitrogen).

2.2. Full-Length Plasmid Construction

The cDNA clone of the SN strain of RABV (cSN) was derived from the SAD B19 cDNA clone as described previously [28,32,33]. Subsequently, cSN was used as a DNA backbone vector for the assembly of the recombinant virus by exchanging cSN RABV G with KBLV G through the process of Gibson assembly (New England Biolabs (NEB), Hitchin, UK) [34]. The KBLV G open reading frame (ORF) (European Nucleotide Archive accession no. PRJEB41152) was amplified with 20 bp overhangs directed at the 5' and 3' end of cSN using the Q5[®] Hot Start High-Fidelity 2X Master Mix (NEB) and the following primers: KBLVFwd (5'-CTCAAAAGACCCCGGGAAAGATGCCATTTCAAGCGGTTC-3') and KBLVRev (5'-GTTGAAAGGCTAGCCAGTCCCTAGGCCTGAGACTGATC-3'). The underlined sequences within the primers are the incorporated overhangs complementary to cSN. To generate a linear cSN lacking the RABV G, the following primers and the same PCR master mix were used: cSNFwd (5'-GGACTGGCTAGCCTTTCAAC-3') and cSNrev (5'-CTTTCCCGGGGTCTTTTG-3'). To confirm the presence of PCR amplicons of the appropriate size, reaction products were assessed via agarose gel electrophoresis. The insert and vector PCR products were purified using the Monarch[®] PCR & DNA Cleanup Kit (NEB). Dpn1 (NEB) digestion was performed on the purified PCR products to remove residual vector DNA prior to recombinant genome assembly of the insert (KBLV G) and vector (cSN) DNA using the NEBuilder[®] HiFi DNA Assembly Cloning Kit (NEB). Following transformation, plasmid propagation and plasmid harvest, plasmids were sequenced before virus rescue was attempted.

2.3. Virus Rescue and Titration

Virus rescue for cSN-KBLV was undertaken as described previously [30,31]. Briefly, BSR-T7/5 cells were seeded at 3×10^4 cells per well in a 96-well plate (Corning, High Wycombe, UK) 18 h before transfection and 200 ng of the full-length genome plasmid and 40 ng of each of three helper plasmids, encoding the RABV N, P, and L proteins, were transfected into cells using the FuGENE[®]6 Transfection Reagent (Promega, Southampton, UK). Transfected cells were then passaged with fresh BSR-T7/5 cells at a 1:1 ratio in a 12-well plate following a 72–96 h incubation at 37 °C. Further passage was undertaken, and cells were assessed for virus antigen as described previously [35]. Where virus antigen

was detected, supernatant was aspirated off and passaged further in BHK cells until 100% infection of the cell monolayer was achieved. Final stocks of cSN-KBLV were sequenced in their entirety using whole genome sequencing to confirm the expected sequence.

2.4. Virus Titration and Growth Kinetics

Virus titre was determined in triplicate in BHK cells as previously described [32]. Cells were seeded at 3×10^5 cells per well and infected with virus serially diluted 10-fold in a 96-well plate (Corning). Cells were fixed with 80% acetone and stained with FITC anti-rabies monoclonal globulin (Fujirebio, Tokyo, Japan) at 48 h post-infection (hpi). Fluorescent foci were counted and recorded as fluorescent focus forming units per mL (ffu/mL).

Virus growth for cSN-KBLV was assessed using a multistep growth curve in comparison with the parent virus cSN as described previously [30]. Cells were then infected with each virus at a multiplicity of infection (moi) of 0.1 and at set time points (0 h, 6 h, 12 h, 24 h, 48 h, 72 h, 96 h, 120 h) 150 μ L of media was removed and frozen at -80°C until required. After the course of the experiment, each of the time point aliquots were titrated in triplicate on fresh BHK cells as three independent titration experiments. Titres were compared using the Mann–Whitney test.

2.5. In Vitro Studies

To assess cross-neutralisation, a modified version of the fluorescent antibody virus neutralisation test (mFAVN) was used as described previously [36,37]. Excluding cSN-KBLV, a panel of 12 lyssaviruses (Table 1) and a panel of polyclonal antisera raised against 9 viruses was used to assess cross-neutralisation. Three RABV isolates were used for comparison; a wild or street RABV isolate (designated RABV in this study), the rabies challenge standard virus-11 isolate (designated CVS in this study), and the RABV parent virus isolate used as the backbone for cSN-KBLV (designated cSN in this study). Where standardised control sera were required, the following three RABV-specific polyclonal sera were used: WHO serum, OIE serum, and hyperimmune human sera from a Human diploid cell vaccine (HDCV) (Rabies Vaccine BP; Pasteur Merieux, Lyon, France) recipient. There are no internationally agreed cut-offs for interpreting neutralising antibody titres against lyssaviruses other than CVS. As a result, for mFAVN, a threshold (reciprocal titre of 1:16) was chosen by comparison with standard sera (0.5 IU/mL) that exhibits a similar titre against CVS.

Table 1. Virus panel used and stock titre.

Designation	Lyssavirus Species	Polyclonal Antisera Used in This Study	Stock Titre (ffu/mL)	RV Number *	Isolated from	Year	Country	Genbank Accession Code \$	Reference
RABV	RABV	Yes	1.6×10^5	RV437	Raccoon dog	-	Estonia	KF154997	[38]
CVS	RABV	No	4.3×10^6		Challenge virus standard-11 strain			EU352767	[39]
cSN	RABV	No	1.2×10^6		Recombinant virus; Street Alabama Dufferin (SADB19) backbone + SADB19 glycoprotein			M31046 ^	[40]
ABLV	ABLV	Yes	1.5×10^5	RV634	Bat	1996	Australia	AY062067 (G)	[41]
ARAV	ARAV	Yes	2.0×10^5	RV3379	Bat	1991	Kyrgyzstan	EF614259	[42]
BBLV	BBLV	Yes	2.5×10^6	RV2507	Bat	2009	Germany	JF311903	[43]
DUVV	DUVV	Yes	3.0×10^6	RV131	Bat	1986	Zimbabwe	GU936870 (G)	[37]
EBLV-1	EBLV-1	Yes	4.0×10^6	RV20	Bat	1986	Denmark	KF155003	[38]
EBLV-2	EBLV-2	Yes	4.3×10^4	RV628	Bat	1996	UK	KY688136	[44]
GBLV	GBLV	Yes	4.0×10^5	RV3267	Bat	2015	Sri Lanka	KU244267	[45]
IRKV	IRKV	No	1.8×10^5	RV3382	Bat	2002	Siberia	EF614260	[46]
KHUV	KHUV	Yes	5.0×10^4	RV3380	Bat	2001	Tajikistan	EF614261	[42]

Abbreviations: ABLV, Australian bat lyssavirus; ARAV, Aravan virus; BBLV, Bokeloh bat lyssavirus; DUVV, Duvenhage virus; EBLV, European bat lyssavirus; GBLV, Gannoruwa bat lyssavirus; IRKV, Irkut virus; KHUV, Khujand virus; RABV, rabies virus. * Animal and Plant Health Agency lab identification number. \$ Where full genome sequence accession numbers cannot be found, glycoprotein sequence accession numbers have been included instead and are highlighted by (G). ^ SADB19 GenBank accession number. - Data not known.

2.6. In Vivo Studies

All in vivo experimentation was undertaken in ACDP3/SAPO4 biocontainment facilities at the Animal and Plant Health Agency (APHA), Weybridge, UK, and complied with strict UK Home Office regulations under the Animals in Scientific Procedures Act (1986) and Home Office license PCA17EA73. Three-to-four-week-old female BALB/c mice were purchased from a commercial supplier (Charles River, Margate, UK). Mice ($n = 12$) were vaccinated with 0.5 mL of diluted human rabies vaccine VeroRab (Novartis, Surrey, UK) via the intraperitoneal (ip) route at days 0 and 7. Mock-vaccinated mice ($n = 8$) were inoculated with MEM alone via ip. At day 29 post-vaccination, both the vaccinated and mock-vaccinated mice were challenged intracranially (ic) with 100 ffu/30 μ L of cSN-KBLV. Following virus challenge, mice were observed twice daily for 22 days and clinical signs were scored using a scale of 0–5 (where 0, no effect; 1, hunched body/ruffled fur; 2, limb twitching; 3, hindquarter paralysis; 4, progressive paralysis; 5, terminal recumbency/death) [47]. The humane endpoint for termination was a clinical score of 1–2 where mice were bled under terminal anaesthesia followed by cervical dislocation. Kaplan–Meier survival curves and the log-rank Mantel–Cox test were used to analyse survivorship rates.

2.7. Virus Detection

A fluorescent antibody test (FAT) was undertaken as described previously [48]. Briefly, brain tissue was excised from the cerebellum and two impression smears were made on a microscope slide. Slides were left to air dry for 5 minutes at room temperature before being fixed in 99–100% acetone, washed, rinsed, and stained using FITC anti-rabies monoclonal globulin (Fujirebio, 800-092). Fluorescent green foci would indicate the presence of the N protein thereby indicating virus infection. Positive control material consisted of previously extracted CVS-infected mouse brain. Two mice from each group were tested.

Histopathology and immunohistochemistry were performed as described previously [49]. Mouse carcasses were fixed in 10% neutral buffered formalin for 2 weeks before being sectioned coronally and processed into paraffin tissue blocks. Serial sections of 4 μ m were prepared and stained with haematoxylin and eosin (H&E) for histopathology or immunohistochemistry for rabies virus nucleoprotein using a monoclonal antibody, mAb 5B12 (MyBioSource Inc., San Diego, CA, USA).

2.8. Molecular Analyses

A real-time SYBR based reverse transcription PCR (RT-PCR) assay (Bio-Rad, Hemel Hemstead, UK) was used to determine the presence or absence of lyssavirus RNA in the mouse samples. Nucleic acids were extracted from brain tissue using Trizol (Invitrogen) according to manufacturer's instructions. A SYBR real-time RT-PCR with N gene-specific primers and 1 μ g/ μ L of RNA was undertaken as described previously [50,51]. For semi-quantitative assessment of viral RNA, cDNA of CVS, at a known concentration (copies/g), was serially diluted from 10^{-1} to 10^{-8} in nuclease-free water and used alongside the mouse brain RNA extracts as a standard curve on the real-time RT-PCR assay. This standard curve was used to semi-quantitate the presence of viral RNA in each sample tested by comparison across Ct values. Amplification using beta actin-specific primers was used as a control for RNA extraction as described previously [51]. Two mice from each group were tested in triplicate.

2.9. Serology

The dorsal vein of each mouse was nicked and blood was collected in CB300 blood collection tubes with clotting activator (Sarstedt, Leicester, UK) at 21 days post-vaccination to assess seroconversion to the VeroRab vaccine. Each serum sample was tested with a standard fluorescent antibody virus neutralisation (FAVN) test as described previously [52]. At the termination of the experiment, mice were cardiac bled under terminal anaesthesia and sera were assessed by FAVN against CVS and modified FAVN against cSN-KBLV. Virus-

neutralising antibody titres were compared by two-way ANOVA and Tukey's multiple comparisons tests.

2.10. Antigenic Cartography

Lyssavirus antigenic maps were generated from the mFAVN data as described previously [37,53]. To optimise the relative positions of the viruses and sera on a map, metric and ordinal multidimensional scaling techniques were used. Where neutralisation occurred, each virus was positioned by multiple sera and vice versa. Hence, antisera with different neutralisation profiles to the homologous viruses could be in separate locations on the map but still contribute to the positioning of the viruses. Whilst resolution increased with each increasing dimension, 3D maps were used to determine antigenic distance and visualisation as the incremental increase in precision became negligible beyond three dimensions [37]. For highlighting antigenic clusters, 2D maps were included for clarity.

2.11. Phylogenetics

Phylograms were constructed in MEGA6 using the neighbour-joining (NJ) algorithm after sequences were aligned. The sequences were bootstrap re-sampled 1000 times to assess the robustness of each tree node. The evolutionary distances were computed using the maximum composite likelihood method and measured in the units of the number of base substitutions per site. The resulting tree was viewed in FigTree v1.4.2 (University of Edinburgh, Edinburgh, UK; <http://tree.bio.ed.ac.uk/software/figtree/> (accessed on 20 March 2021)).

3. Results

3.1. Virus Rescue and Titration

The cSN-KBLV virus was successfully rescued using RABV helper plasmids. After 5 passages, cSN-KBLV reached 100% infectivity whilst cSN only required 2 passages. Following the final passage to achieve 100% infectivity, the virus was harvested and subsequent whole genome sequencing confirmed 100% nucleotide identity to the original DNA cSN-KBLV clone (data not shown). Harvested virus was titrated in which the cSN-KBLV grew to a peak titre of 2.5×10^4 ffu/mL whilst the parent cSN strain grew to a peak titre of 1.6×10^6 ffu/mL. Both values, however, are comparable to similar studies using EBLV-1, EBLV-2 G, IKOV G, and WCBV G within a cSN vector [30,31].

3.2. Growth Kinetics

Due to the fact that the wildtype virus for KBLV had not been successfully isolated [4], the growth kinetics of cSN-KBLV were compared to that of cSN using multistep growth curves (Figure 1). By 24 hpi, both viruses were detected at around 10^3 ffu/mL. There was no statistically significant difference between the peak viral titres observed, however, cSN grew to the highest peak titre of 7.6×10^7 ffu/mL at around 96 hpi and cSN-KBLV grew to a peak titre of 1.55×10^7 ffu/mL at 72 hpi. The endpoint titres showed a significant difference between the two viruses with cSN-KBLV exhibiting a titre of 3.33×10^6 ffu/mL compared to cSN at 4.3×10^7 ffu/mL ($p < 0.001$).

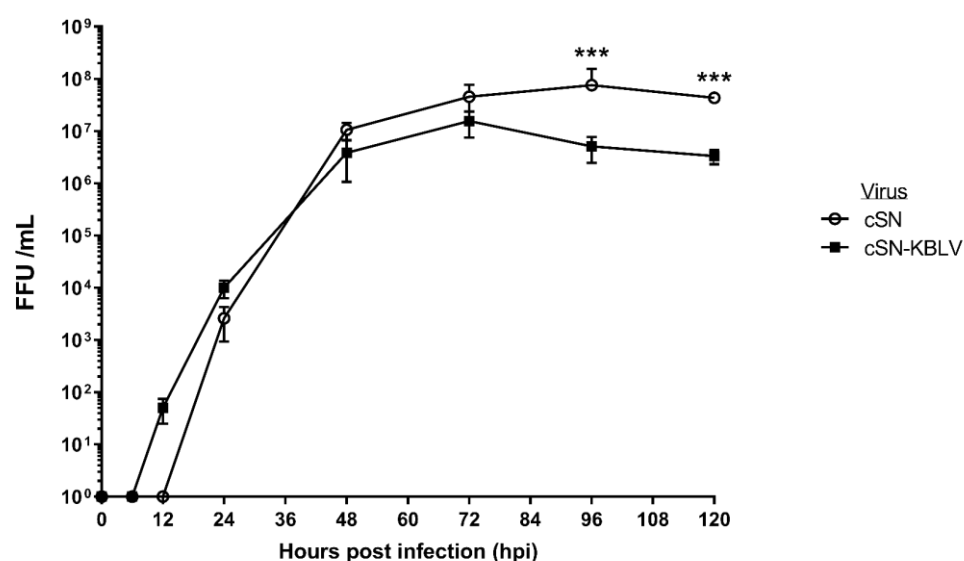


Figure 1. Growth kinetics of cSN-KBLV and the vaccine backbone, cSN, in vitro. For each virus, BHK-21 cells were infected with an MOI of 0.1 to produce a multiple-step growth curve over the course of 120 h. The test was performed in triplicate and the mean and standard deviation of the results plotted on a logarithmic scale. Asterisks indicate significant differences between the groups calculated using the Mann–Whitney test (** $p < 0.001$).

3.3. In Vitro Studies

Two experimental approaches were taken to assess cSN-KBLV antigenically: (i) to determine the titre of standard sera sufficient to neutralise cSN-KBLV over the 0.5 IU/mL value assigned as the cut-off for protection, and (ii) to evaluate for cross-neutralisation across the *lyssavirus* genus.

3.3.1. Assessment of cSN-KBLV Neutralisation Using Internationally Standardised Sera

A modified FAVN was used to test the comparative neutralisation of cSN-KBLV, cSN and CVS against increasing titres of two standard sera, OIE and WHO. Both the OIE and WHO sera were capable of neutralising all three viruses at 1 IU/mL and at 2.5 IU/mL, respectively (Figure 2). Both CVS and cSN were neutralised by both OIE and WHO sera with complete neutralisation at 0.5 IU/mL. Both serological standards demonstrated the lowest level of neutralising antibodies against cSN-KBLV as 1 IU/mL of OIE sera and 2.5 IU/mL of WHO sera were required to neutralise cSN-KBLV to above the 0.5 IU/mL threshold for WHO and OIE sera against CVS. Additionally, the trend in neutralising antibody levels differed between each of the standard sera used.

OIE sera consistently showed higher levels of neutralising antibodies than WHO sera when tested against each of the viruses, though the greatest difference was observed with cSN-KBLV. At 5 IU/mL, OIE sera showed almost a 10-fold increase in neutralising antibody titre against cSN-KBLV than the WHO sera, and almost double for CVS and cSN.

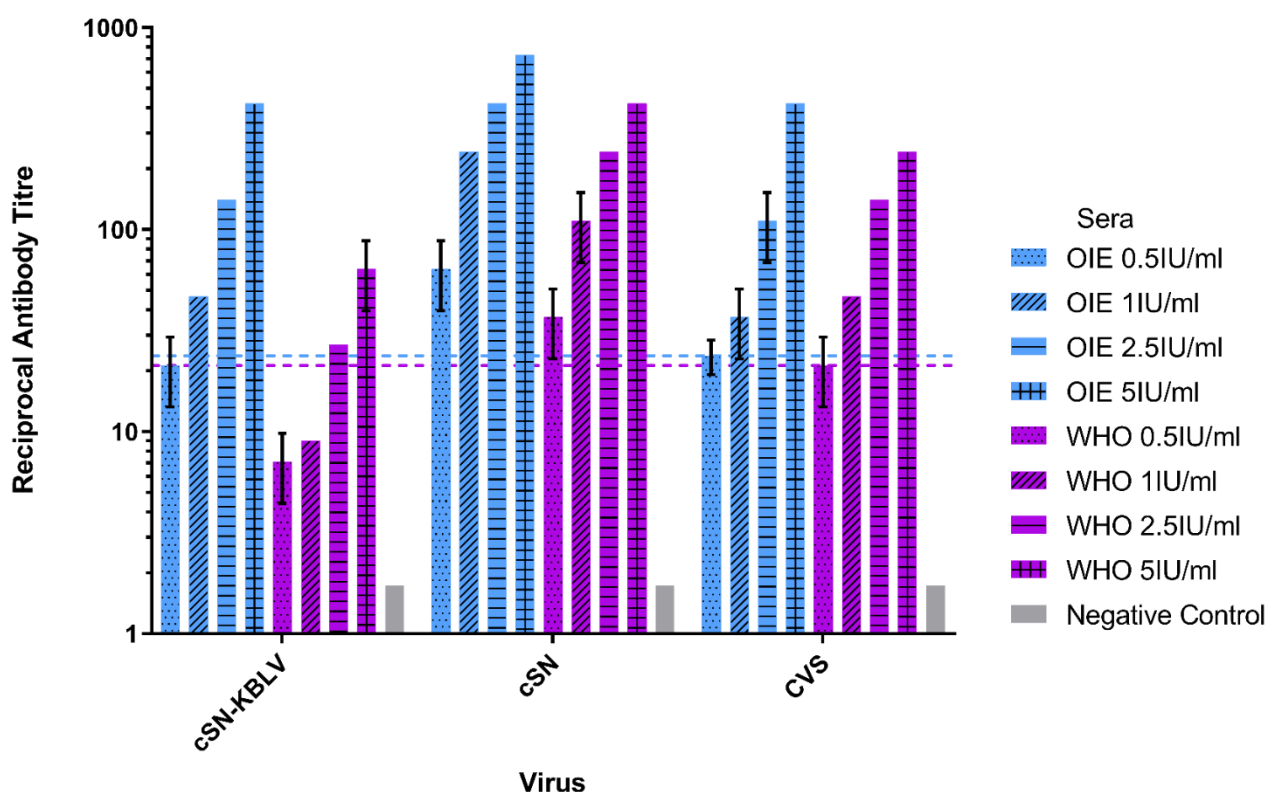


Figure 2. Neutralisation profiles of cSN-KBLV, cSN, and CVS against OIE and WHO standard sera using a modified fluorescent antibody virus neutralisation (mFAVN) test. The test was performed in triplicate and the mean and standard deviation of the results plotted on a logarithmic scale. The 0.5 IU/mL neutralisation cut-off is dictated by the serological standards against CVS (indicated by the coloured dashed lines—OIE = blue, WHO = purple).

3.3.2. Ability of Phylogroup I-Specific Sera to Neutralise cSN-KBLV

A mFAVN was used to assess cross-neutralisation of lyssavirus-specific sera against cSN-KBLV in addition to CVS and cSN as comparison (Figure 3). Varying levels of cross-neutralisation were observed with phylogroup I lyssavirus-specific sera described in Table 1. The virus cSN was most readily neutralised by the phylogroup I sera panel with seven lyssavirus-specific sera showing levels of neutralising antibodies above 0.5 IU/mL whereas cSN-KBLV and CVS were neutralised by five lyssavirus-specific sera. For cSN-KBLV, ARAV, BBLV, EBLV-1, EBLV-2, and GBLV-specific sera exhibited a titre of neutralising antibodies above the 0.5 IU/mL cut-off whilst ABLV, DUVV, KHUV, and RABV-specific sera did not. In addition, the ability of each sera to cross-neutralise each virus varied. For cSN-KBLV, EBLV-1-specific sera showed the highest titre of neutralising antibodies. BBLV-specific sera exhibited the greatest titre of neutralising antibodies against CVS. Specific sera for a wild/street RABV strain showed the highest titre of neutralising antibodies against cSN, closely followed by BBLV and EBLV-1. Interestingly, the wild/street RABV-specific sera were only capable of neutralising cSN, indicating possible antigenic divergence of wild/street strains to the cell culture-adapted CVS used regularly in diagnostic assays. Phylogroup II-specific sera were unable to neutralise all three viruses tested (data not shown) and IRKV-specific sera were unavailable.

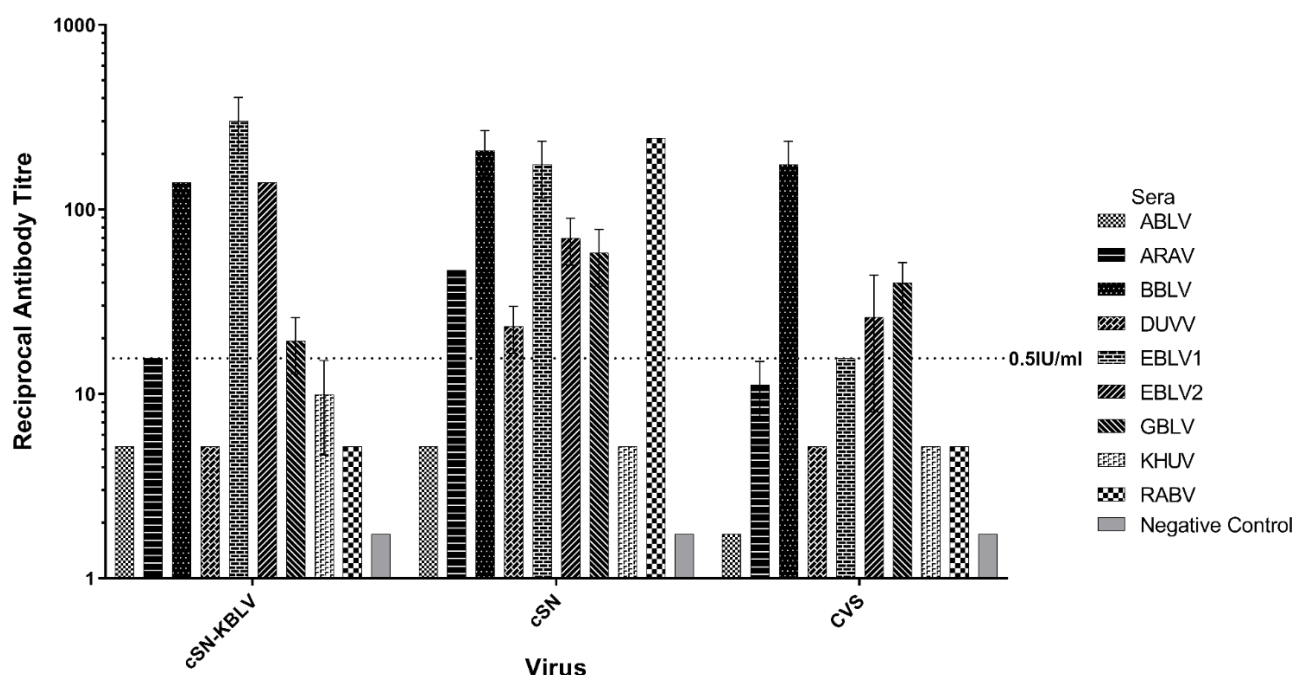


Figure 3. Cross-neutralisation profiles of each phylogroup I lyssavirus-specific sera using a mFAVN test. The test was performed in triplicate and the mean and standard deviation of the results plotted on a logarithmic scale. The 0.5 IU/mL neutralisation cut-off is dictated by the OIE sera against CVS (indicated by the dashed line). IRKV sera not shown.

3.3.3. Antigenic Cartography

Antigenic cartography was used to quantify antigenic relationships between phylogroup I viruses described in Table 1 and enable comparison to the evolutionary relationships facilitated via phylogenetic nucleotide analysis (Figure 4). Results showed cSN-KBLV was antigenically distinct from the other phylogroup I lyssaviruses, including the parent virus, cSN (Figure 4A,C,D). Based on the antigenic distances on the 3D map, cSN-KBLV is antigenically closest to cSN (1.00 AU), ARAV (1.21 AU), IRKV (1.45 AU), and EBLV-2 (1.65 AU). To further investigate the genetic basis of the antigenic distances, the evolutionary history of the glycoprotein nucleotide sequences of each phylogroup I lyssavirus was quantitatively inferred using the neighbour-joining method and the evolutionary distances were computed using the maximum composite likelihood (ML) method and displayed as a phylogenetic tree (Figure 4B). Based on the glycoprotein evolutionary distances, KBLV is most closely related to EBLV-2, KHUV, and BBLV. The correlation between antigenic distance and ML phylogenetic tree distance could be inferred by comparing the evolutionary and antigenic distances between cSN and each of the viruses. Based on this data, 1 AU was equal to an ML distance of 0.235 ($p = 0.007$) when RABV and CVS were excluded from the dataset. This was due to the fact that RABV G and CVS G are highly genetically similar to cSN G but are antigenically distinct, highlighting that it is not always possible to infer antigenic distance based on genetic data alone.

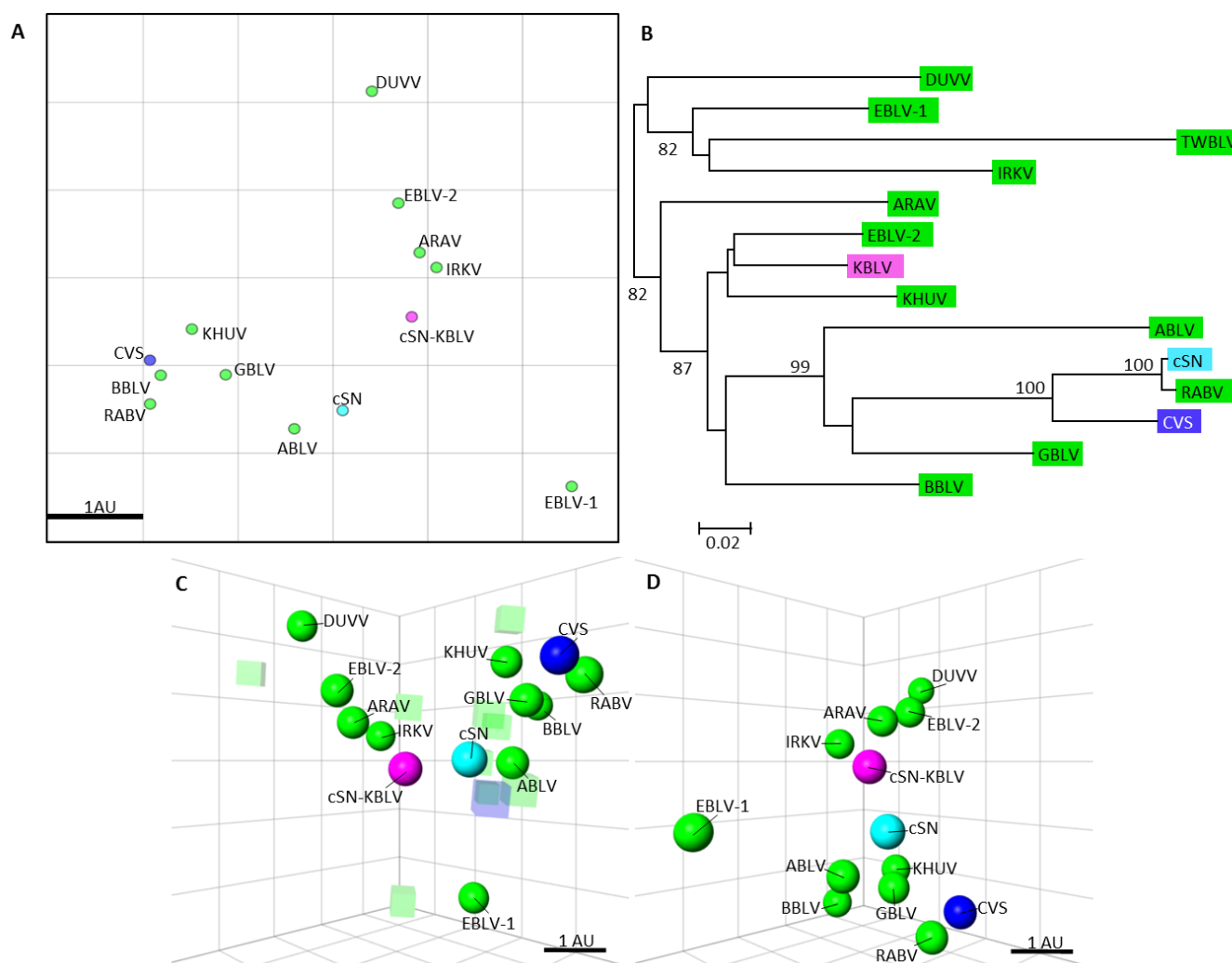


Figure 4. Phylogenetic tree showing the evolutionary distances of the phylogroup I lyssaviruses and antigenic cartography maps showing the antigenic distances of the phylogroup I lyssaviruses. **(A)** Two-dimensional antigenic map of Phylogroup I viruses, CVS, cSN, and cSN-KBLV. Phylogroup I lyssaviruses are coloured green, CVS coloured dark blue, cSN coloured light blue, and cSN-KBLV coloured magenta. Scale bar shows one antigenic unit with both horizontal and vertical axis representing antigenic distance so orientation within this map is free. **(B)** Phylogenetic tree of the glycoprotein nucleotide sequences. Viruses coloured as before. The evolutionary history was inferred using the neighbour-joining method and the evolutionary distances were computed using the maximum composite likelihood method and are in the units of the number of base substitutions per site. **(C)** Three-dimensional antigenic map of lyssaviruses and sera. Viruses (spheres, coloured as before) and sera (translucent-coloured boxes) are positioned such that the distance from each serum to each virus is determined by the neutralisation titre. Multidimensional scaling was used to position both sera and viruses relative to each other, so orientation of the map within the axes is free. Scale bar shows one antigenic unit (AU). **(D)** The same antigenic map rotated to a different orientation and sera removed for clarity.

3.4. In Vivo Vaccination Challenge Study

3.4.1. Vaccination and Survival

To assess the ability of vaccine-induced neutralising antibodies to protect mice from challenge with cSN-KBLV, mice were vaccinated as described and a standard FAVN test was used to determine serological response. All mice seroconverted to a titre above the internationally assigned cut-off for neutralisation of RABV, 0.5 IU/mL, with responses ranging from 0.87 IU/mL to 23.38 IU/mL 21 days after vaccination (Figure 5A). Mice were challenged via the ic route on day 29 post-vaccination with 100 ffu/30 μ L of cSN-KBLV

and clinical outcomes were compared to mock-vaccinated mice challenged with the same dose of cSN-KBLV. A statistically significant difference ($p < 0.001$) in survival was observed between the vaccinated and mock-vaccinated groups (Figure 5B). All mice in the mock-vaccinated group ($n = 8$) reached clinical endpoint by 7 days post-challenge, 1 day after onset of clinical disease. The first sign of clinical disease was ruffled fur. Subsequent clinical signs observed included piloerection, tail-biting, intermittent hyperactivity, and hunched stance. In the vaccinated group ($n = 12$), one mouse was terminated after developing score 2 clinical signs, which included an extreme hunched stance and limb twitching. The time from initiation of disease to termination in line with humane endpoints was protracted, however, with the mouse reaching clinical endpoint at day 13 post-challenge, 3 days after the onset of clinical disease. In addition, the vaccinated mouse that succumbed to infection had the lowest neutralising antibody titre of 0.87 IU/mL prior to challenge (indicated by ▼ on the graph). In contrast, all mice with virus-neutralising antibody titres of 1.5 IU/mL and above survived the challenge.

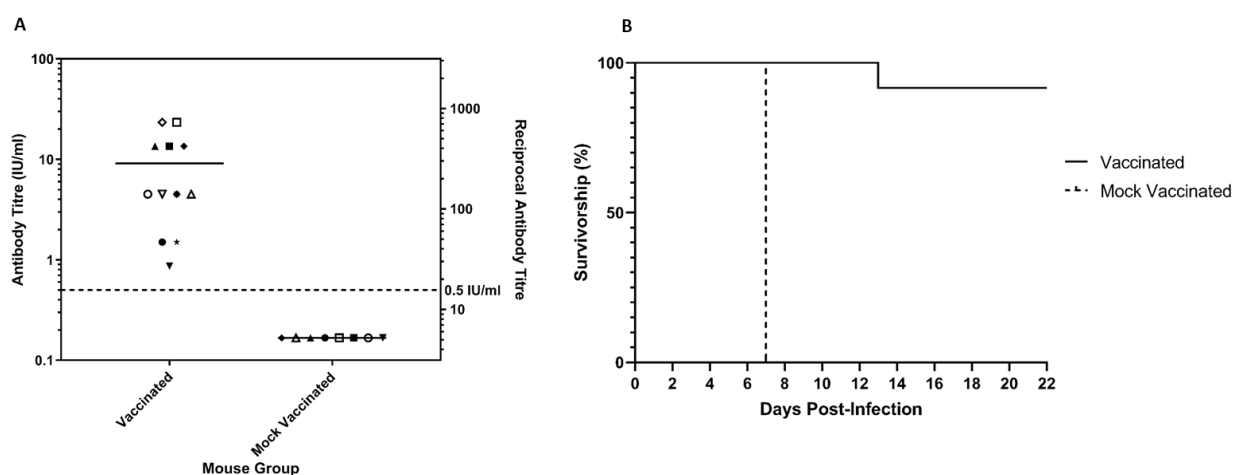


Figure 5. Seroconversion and survivorship of the animals. (A) Post-vaccination serology on day 21 for mice vaccinated with VeroRab and mice mock-vaccinated with MEM on days 0 and 7. All sera, each assigned a different symbol on the graph, were assessed for neutralising antibodies by FAVN and plotted on a logarithmic scale. The Y1 axis represents the antibody titre (IU/mL) and the Y2 axis represents the equivalent reciprocal antibody titre. (B) In vivo survivorship following intracranial inoculation with 100 ffu/30 µL of cSN-KBLV. Mice were vaccinated 28 days before challenge and day 0 on the graph refers to the day of challenge.

3.4.2. Serological Responses to Infection and Post-Vaccination Challenge

All animals that succumbed to clinical disease or survived until the end of the experiment were cardiac bled before being humanely terminated. Sera were assessed for seroconversion using both the standard FAVN against CVS and modified FAVN against cSN-KBLV. In the mock-vaccinated group ($n = 8$), 63% ($n = 5/8$) of the animals had an antibody response capable of neutralising cSN-KBLV using the modified FAVN. Of the mouse sera that exhibited neutralising antibodies against cSN-KBLV, the reciprocal titres ranged from 1/16 to 1/421. In contrast, no neutralising antibody against CVS was detected with the standard FAVN (Figure 6). Despite the difference in mean reciprocal titres against CVS in the standard FAVN ($1/4 \pm 1/2$) and cSN-KBLV in the modified FAVN ($1/87 \pm 1/134$), the difference was not statistically significant ($p = 0.066$).

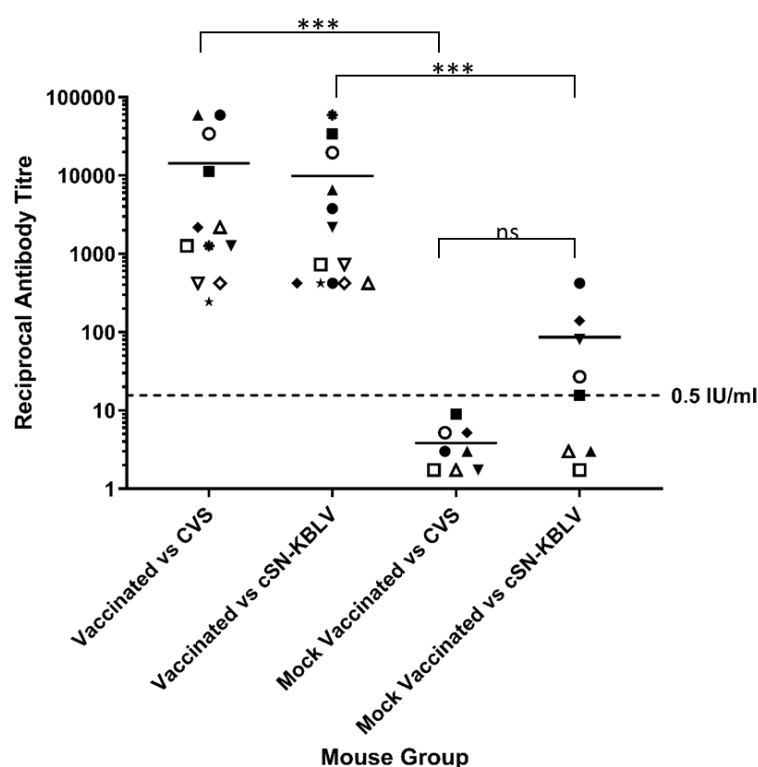


Figure 6. Assessment of serological status in mice following vaccination and challenge. The cSN-KBLV-challenged mice were serologically assessed against CVS and cSN-KBLV using FAVN and modified FAVN assays. Dotted line represents 0.5 IU/mL neutralisation cut-off dictated by OIE sera against CVS. Each symbol is representative of one animal. Scale is logarithmic. Asterisks indicate significant differences between the groups calculated using an ordinary two-way ANOVA and Tukey's multiple comparisons tests (** $p < 0.001$; ns is not significant).

For the vaccinated group, all surviving mice developed neutralising antibody titres. In the standard FAVN against CVS, sera showed neutralising antibody titres ranging from 1/243 to 1/59049. In the modified FAVN against cSN-KBLV, sera showed less variability with neutralising antibody titres ranging from 1/729 to 1/34092. On average, however, the titre of neutralising antibodies against CVS and cSN-KBLV were not significantly different.

When comparing the serology post-challenge to that following vaccination and prior to challenge (using the standard FAVN), the titre of neutralising antibodies in the vaccinated group increased 50-fold from an average reciprocal titre of 1/284 to 1/14400 (Figures 5 and 6).

Interestingly, the one mouse that succumbed to infection on day 13 post-infection showed high reciprocal titres of 1/1262 against CVS and 1/2187 against cSN-KBLV (as indicated by ▼ in both Figures 5A and 6). Despite this, sera from the vaccinated group show a statically significant difference in neutralising antibody titres against CVS and cSN-KBLV than the sera derived from the mock-vaccinated group ($p < 0.001$).

3.4.3. Histopathology and Immunohistochemistry

Of the mice that succumbed to cSN-KBLV, two were tested on the FAT and were positive for viral antigen. In contrast, of the mice that were vaccinated and survived challenge with cSN-KBLV, two were tested on the FAT and were all negative (data not shown). To demonstrate the pathogenicity of cSN-KBLV in the mouse model, naïve mice that succumbed to disease were evaluated by histopathology and immunohistochemistry. Infection of naïve mice with cSN-KBLV via the ic route resulted in mild to moderate, multifocal, neuronal necrosis in the cerebral cortex, thalamic (Figure 7A,B), and hippocampal regions (Figure 7C,D) of the forebrain with the association of high levels of viral antigen. Moderate to minimal amounts of virus antigen were also present multifocally within the

neuroparenchyma of the thalamus, cerebellum, and brain stem, and rare antigen labelling was detected in neuronal cell bodies within the spinal cord, but histological changes were not present in these areas.

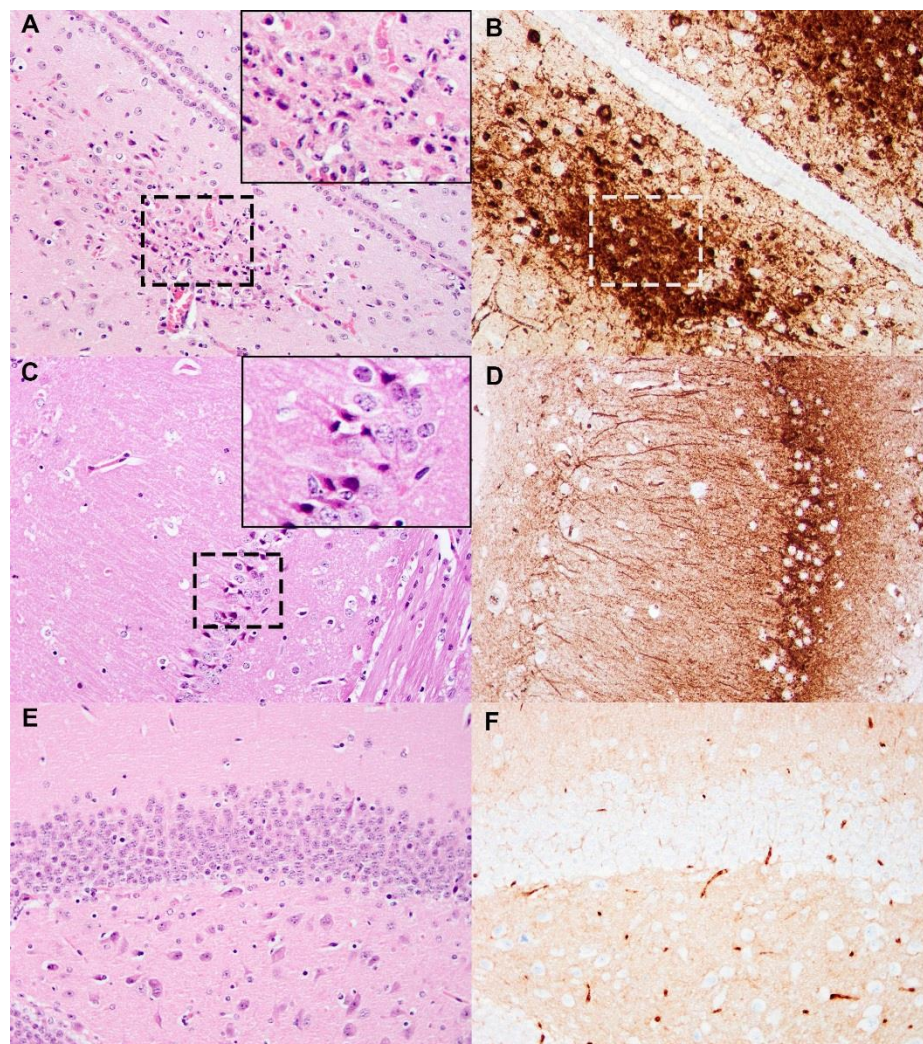


Figure 7. Histopathology and immunohistochemistry (IHC) against rabie nucleoprotein (N) on cSN-KBLV-infected and uninfected mouse brains. (A,B) A cSN-KBLV ic challenged mouse brain. Areas of neuronal necrosis with pyknotic nuclei and karyorrhectic cellular debris (outlined with black dashed-line box) observed in the thalamic region adjacent to the third ventricle (left, H&E stain) and serial-stained sections for N protein revealed abundant intralosomal virus antigens (right, IHC, white dashed line box for region of interest co-localised with H&E section). (C,D) A cSN-KBLV IC-challenged mouse brain. Areas of neuronal necrosis characterised by red, angular and shrunken neurons (outlined with dashed-line box) in the hippocampus (left, H&E) where IHC-stained serial tissue section revealed abundant intralosomal virus antigens (right, IHC). (E,F) Negative control. Representative sections showing no histological changes or virus antigens in the hippocampus. Images taken at 200x magnification. Insets show digitally magnified region of interest.

3.4.4. Real-Time RT-PCR

RNA extracts from the brains of two mice from each vaccine group were evaluated via SYBR real-time RT-PCR assay (Table 2). The mouse group showing the lowest mean Ct value, 19.05 ± 0.10 and 19.37 ± 0.11 , were the mice that succumbed to clinical disease in the cSN-KBLV-mock-vaccinated group, therefore indicating that this group had much higher viral RNA levels in the brain. The survivors of the vaccinated mouse group showed the highest mean Ct values with Ct values of 33.14 ± 0.53 and 36.06 ± 0.55 , indicating

that whilst clinical disease did not develop and FAT/IHC were negative, negligible viral RNA loads were still present in the brain at the time of termination. Based on the CVS cDNA standard curve, the cSN-KBLV-mock-vaccinated mouse group showed high copy numbers per gram (g) with 1.07×10^6 copies/g and 8.53×10^5 copies/g and the cSN-KBLV-vaccinated mice showed either an unquantifiable copy number or low copy number at 2.07×10^1 copies/g (Figure 8).

Table 2. Post-mortem molecular testing on the brains of two mice from each group.

Mouse Group	SYBR Real-Time RT-PCR Assay	
	Lyssavirus Nucleoprotein Ct-Value Mean \pm SD	β -Actin Ct-Value Mean \pm SD
cSN-KBLV-vaccinated	33.14 \pm 0.53	23.23 \pm 0.11
	36.06 \pm 0.55	23.87 \pm 0.12
cSN-KBLV-mock-vaccinated	19.37 \pm 0.11	21.93 \pm 0.08
	19.03 \pm 0.10	21.82 \pm 0.14

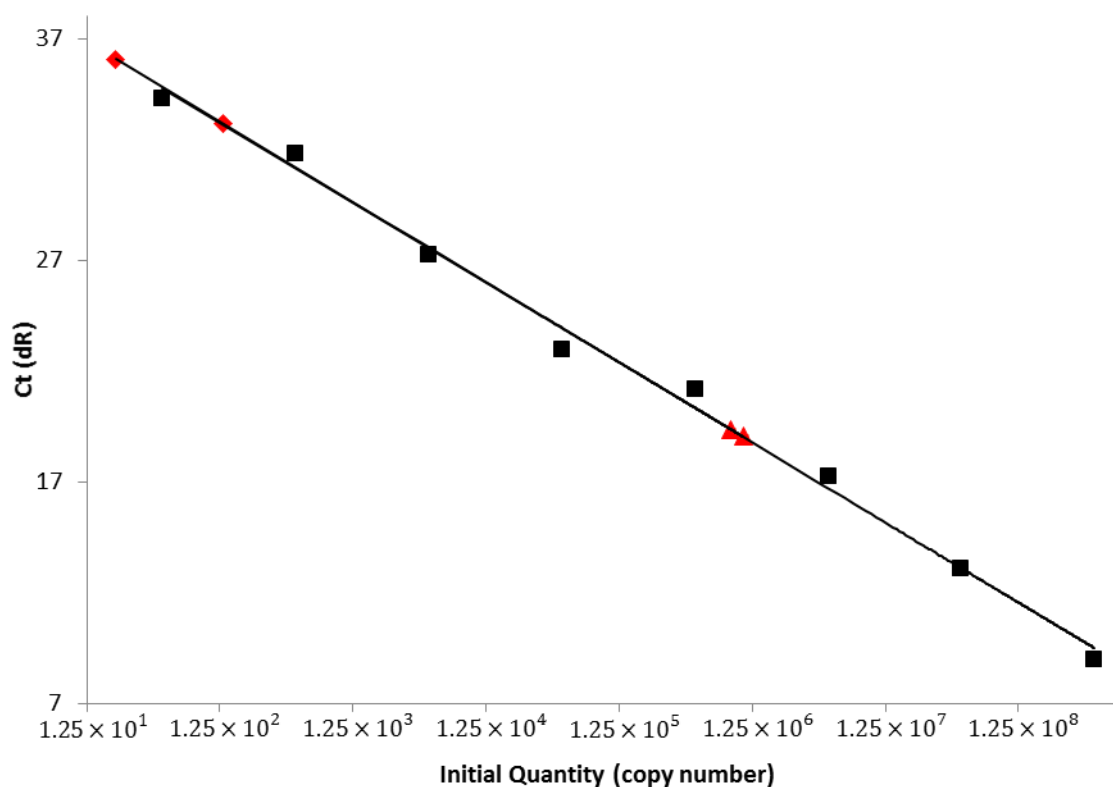


Figure 8. SYBR real-time RT-PCR specific to the lyssavirus nucleoprotein. Standard curve and standards are shown in black. SYBR sample values (indicated by the red symbols) plotted and interpolated using the standard curve regression line ($Y = -3.607 \times \text{LOG}(X) + 40.76$) ($R^2 = 0.995$; efficiency = 91%) and the mean Ct values. Triangles represent cSN-KBLV-mock-vaccinated mice and squares represent cSN-KBLV-vaccinated mice.

4. Discussion

Rabies, caused by lyssaviruses, remains a neglected tropical disease despite being a serious threat to human and animal health globally. For lyssaviruses, the zoonotic threat from bats exists and, alongside the emergence of other bat-borne zoonoses, has been heightened due to the ongoing encroachment of humans into more remote regions/ecosystems. Though the current rabies vaccines confer protection against phylogroup I lyssaviruses,

the discovery of novel lyssaviruses warrants investigation into vaccine efficacy as infection with lyssaviruses still results in a clinically incurable encephalitis.

KBLV has not been successfully isolated, nor has it been formally classified within the *lyssavirus* genus as a virus species despite being genetically related to other members of the genus. However, the availability of the KBLV genome enabled the synthesis of the recombinant virus expressing KBLV-G. In this study, the rescued virus was able to grow in both in vitro and in vivo conditions, demonstrating that the cSN backbone proteins were able to interact with the heterologous KBLV-G despite relatively low amino acid identity [4]. This further enabled in vitro cross-neutralisation assays and in vivo vaccination-challenge studies using the recombinant cSN-KBLV virus.

Growth kinetic assessment of this virus revealed that despite a successful virus rescue, endpoint titres achieved were significantly different with cSN-KBLV reaching a lower final titre compared to the parent cSN virus (Figure 1). However, the titre achieved was still higher than titres achieved in previous studies whereby more divergent glycoproteins were introduced into the same cSN backbone [31]. Decreased viral fitness of cSN-KBLV may be a result of cSN being more adapted to cell culture or a result of the parent virus (KBLV) being less able to replicate in cell culture models than the recombinant virus. This cannot be assessed as a wildtype virus isolate does not exist, although similar examples have been proposed previously. Certainly, wildtype EBLV-1 and -2 isolates grew to a lower titre than the recombinant cSN-EBLVs (referred to as cSN-1 and cSN-2), indicating that the low titres observed were not a result of the G-dependent processes such as receptor binding and viral entry but rather viral replication and assembly [30]. In a similar study, cSN expressing IKOV-G and WCBV-G have been shown to grow to viral titres around 10^5 – 10^6 , almost 2 log₁₀ lower than cSN-KBLV [31].

For the antigenic assessment of responses to viral glycoproteins in the absence of a wildtype isolate, cSN-KBLV was used. Previous studies and the data presented here reiterate that the viral G is the dominant target for neutralising antibodies and underscores the utility of recombinant vaccines for assessment where wildtype viruses are unavailable [30]. To assess the antigenicity of the KBLV-G protein, a mFAVN was undertaken with a panel of sera specific to different lyssavirus glycoproteins. Previous phylogenetic assessment determined that KBLV would be classified within phylogroup I given the nucleotide homology of 81%, 79.7%, 79.5%, and 79.4% with KHUV, ARAV, BBLV, and EBLV-2 N proteins, respectively [27]. It was concluded, following the analysis of the whole genome sequence in a second study, that KBLV is genetically most closely related to EBLV-2, KHUV, and BBLV [4]. In the neutralisation assays performed in this study, cSN-KBLV grouped within phylogroup I based on reactivity with phylogroup-specific sera with EBLV-1, BBLV, and EBLV-2-specific sera exhibited the highest titres of neutralising antibodies against cSN-KBLV (Figure 3).

Additionally, antigenic cartography was also used to quantitatively analyse antigenic data. Antigenic cartography involves geometric interpretation of binding assay data by assigning each antigen and serum a point on a 3D map such that the distance between the antigen and antiserum directly corresponds to the reciprocal titres in the cross-neutralisation assay [37]. Due to the extensive cross-neutralisation between phylogroup I species and the novel lyssavirus, cSN-KBLV, the location of these antigens on the map was fixed by multiple measurements to other antigens/antisera. Consequently, the resolution of the antigenic maps can be greater than the mFAVN assay resolution [53]. On the antigenic map, cSN-KBLV was closest to cSN, ARAV, IRKV, and EBLV-2 with antigenic distances of 1.00 AU, 1.21 AU, 1.45 AU, and 1.65 AU, respectively (Figure 4). These distances, however, must be interpreted with caution as the resolution of these antigenic maps in the average prediction error has been previously determined to be 1.22 (SE, 0.17) antigenic units in 3D [37].

Whilst EBLV-1-specific sera were most able to neutralise cSN-KBLV, being more potent than sera raised against EBLV-2, BBLV, and KHUV, this phenomenon was not visually translated in the antigenic maps with EBLV-1 showing an antigenic distance of 2.68 AU

from cSN-KBLV. Interestingly, cSN was antigenically distinct from RABV and CVS; this conflicts with the findings of previous studies where RABV strains were indistinguishable from cSN and ABLV [30,37]. However, a single wildtype RABV was used in this study (RV437) and further assessment against a panel of RABVs would be needed to reliably infer antigenic differences between KBLV and circulating street RABV strains. In addition, the inclusion of additional phylogroup I-specific sera in this study may have identified distinct antigenic differences between cSN, RABV, ABLV, and CVS. CVS and RABV appear to be antigenically distant in this study and a previous study [37], indicating antigenic divergence between street RABV strains and CVS regularly used in diagnostic assays. Furthermore, the use of serological data to measure antigenic differences in cross-neutralisation assays is limited by paradoxes or irregularities in the data, such as individual variations between sera raised against the same antigen or the difficulty of absolute quantification of sera raised against different isolates for different lyssavirus species [37].

Due to the close antigenic and genetic relationship to phylogroup I, specifically EBLV-2, EBLV-1, and BBLV, it was predicted that existing rabies vaccines would be able to afford protection against the KBLV [27]. It was reported that rabies vaccines protect against BBLV in vivo with an antibody titre of ≥ 10 IU/mL, suggested through in vivo murine studies as being required for protection, and EBLV-1 and EBLV-2 in vitro analyses have suggested that titres ≥ 4.5 IU/mL are required for neutralisation [18,36]. Additionally, in a previous study investigating KBLV, sera from human vaccinees could neutralise KBLV-G pseudotyped RABV particles, however, the sera exhibited a 1.8-fold lower titre of neutralising antibodies against KBLV than against CVS [4].

In the present study, in vitro neutralisation assays demonstrated that an antibody titre of 1.0 IU/mL of OIE sera or 2.5 IU/mL of WHO sera were sufficient for neutralisation of cSN-KBLV above the serological cut-off (Figure 2). In comparison to CVS, OIE standard sera showed 1.1-fold lower neutralisation activity against cSN-KBLV. The difference in the neutralising antibody titres against cSN and cSN-KBLV confirms that G is the dominant target for neutralising antibodies. These values, however, predict the antibody titre required for protection in vivo when using a standard challenge dose of 100 TCID₅₀/50 μ L.

Indeed, the in vivo vaccination-challenge experiments revealed that VeroRab, a commercially available rabies vaccine, afforded almost complete protection against intracranial challenge of cSN-KBLV (Figure 5B). One vaccinated mouse succumbed to infection at day 13 but interestingly demonstrated the lowest post-vaccination antibody response as assessed via FAVN at 0.87 IU/mL (Figure 5A). Whilst above the cut-off 0.5 IU/mL value, the nature of the “severe” virus challenge through the introduction of the virus intracranially may have been too invasive to prevent productive infection in this single animal. Regardless, with this sample size we can only speculate that for protection against KBLV a higher neutralising antibody titre may be needed than that required to give complete protection against RABV in this in vivo model, in which all mice with antibody titres above 1.5 IU/mL survived ic challenge [18,36,54]. Future work with larger sample sizes would need to be performed to address this conclusively.

Following in vivo assessment, post-mortem analyses revealed that, based on two mice from each group, the vaccinated mice that survived to the end of the experiment (22 days, $n = 11/12$) were negative for lyssavirus antigen in the brain by the gold standard FAT method but very low levels of viral RNA copies could be detected in the brain using SYBR real-time RT-PCR. The lethal outcome of infection with wildtype RABV likely involves multiple mechanisms whereby viral infection drives either evasion or delay of host-immune mechanisms [55]. Whilst undefined, it is likely that the RNA detected is remnant noninfectious viral RNA from the original infection, a phenomenon reported previously in survival from RABV challenge in the murine model [56]. The mock-vaccinated mice succumbed to infection and the two mice tested in this group were positive for lyssavirus antigen both in FAT and IHC assays. Further, mice that developed clinical disease had high levels of viral RNA in the brain, and the majority remained seronegative with only very low levels of neutralising antibodies being detected (Table 2, Figures 6 and 8).

Serological comparisons between the mock-vaccinated group and the vaccinated group revealed a significant difference in serological titre in both the challenge virus and vaccine virus (Figure 6). Additionally, serological comparison between the vaccinated mice post-vaccination and the same mice post-challenge revealed a 50-fold increase in neutralising antibody titre (Figures 5A and 6). These findings are consistent with the hypothesis that the vaccinated mice mount a successful humoral immune response to facilitate the clearance of infection earlier than the mock-vaccinated controls, leading to low viral RNA levels in the brain by the end of the experiment [57,58]. In addition to humoral immunity, whilst poorly defined, it is likely that the cellular immune response plays an important role in viral clearance in the CNS [58,59]. Certainly, previous studies have demonstrated enhanced innate immune responses following rabies vaccination, including host responses linked with elevated BBB permeability, which enables immune cell infiltration of the CNS [59,60].

In conclusion, a recombinant cSN-KBLV virus has been generated that has been used to demonstrate the efficacy of human rabies vaccines to protect against KBLV using the recombinant virus as a surrogate both in vitro and in vivo. Whilst genetically KBLV G is most closely related to that of EBLV-2, BBLV, KHUV, and EBLV-1, cross-neutralisation assays revealed that EBLV-1, BBLV, and EBLV-2 lyssavirus-specific sera showed the highest neutralising antibodies against cSN-KBLV and antigenic map data revealed that cSN-KBLV clusters with cSN, ARAV, EBLV-2, and IRKV. Furthermore, a neutralising antibody titre of 1.5 IU/mL or above was required for the protection in a murine model. As novel lyssaviruses continue to be described, contemporary assessment of vaccine protection and evaluation of both genetic and antigenic traits is necessary for the understanding of disease mitigation strategy.

Author Contributions: Conceptualisation: R.S. and A.C.B.; formal analysis: R.S.; investigation: R.S., F.Z.X.L., D.S., D.L.H.; writing—original draft, R.S., F.Z.X.L., A.C.B.; writing—review and editing: R.S., E.W., F.Z.X.L., D.S., D.L.H., A.R.F., A.C.B. All authors have read and agreed to the published version of the manuscript.

Funding: This study was supported by Defra, the Scottish Government and Welsh Government through grant SE0431 and by the European Union’s Horizon 2020 research and innovation program under RABYD-VAX grant agreement No. 733176. R.S. is supported by a PhD studentship under Defra grant SE0431.

Institutional Review Board Statement: All in vivo experimentation was undertaken in ACDP3/SAPO4 biocontainment facilities at the Animal and Plant Health Agency (APHA), Weybridge, UK, and complied with strict UK Home Office regulations under the Animals in Scientific Procedures Act (1986) and Home Office license PCA17EA73.

Data Availability Statement: Not applicable.

Acknowledgments: We would like to thank Alex Nunez for discussions on histopathology and Stuart Ackroyd for the technical support in the histology laboratory at APHA. We would also like to thank Hooman Goharriz and Leigh Thorne for their technical assistance.

Conflicts of Interest: The authors declare no conflict of interest.

References

1. Kuhn, J.H.; Adkins, S.; Alioto, D.; Alkhovsky, S.V.; Amarasinghe, G.K.; Anthony, S.J.; Avšič-Županc, T.; Ayllón, M.A.; Bahl, J.; Balkema-Buschmann, A.; et al. 2020 taxonomic update for phylum Negarnaviricota (Riboviria: Orthornavirae), including the large orders Bunyavirales and Mononegavirales. *Arch. Virol.* **2020**, *165*, 3023–3072. [[CrossRef](#)] [[PubMed](#)]
2. Rupprecht, C.; Kuzmin, I.; Meslin, F. Lyssaviruses and rabies: Current conundrums, concerns, contradictions and controversies. *F1000Research* **2017**, *6*, 184. [[CrossRef](#)]
3. Walker, P.J.; Siddell, S.G.; Lefkowitz, E.J.; Mushegian, A.R.; Adriaenssens, E.M.; Dempsey, D.M.; Dutilh, B.E.; Harrach, B.; Harrison, R.L.; Hendrickson, R.C.; et al. Changes to virus taxonomy and the Statutes ratified by the International Committee on Taxonomy of Viruses (2020). *Arch. Virol.* **2020**, *165*, 2737–2748. [[CrossRef](#)]

4. Calvelage, S.; Tammiranta, N.; Nokireki, T.; Gadd, T.; Eggerbauer, E.; Zaeck, L.M.; Potratz, M.; Wylezich, C.; Höper, D.; Müller, T.; et al. Genetic and Antigenetic Characterization of the Novel Kotalahti Bat Lyssavirus (KBLV). *Viruses* **2021**, *13*, 69. [\[CrossRef\]](#)
5. Coertse, J.; Grobler, C.S.; Sabeta, C.T.; Seamark, E.C.; Kearney, T.; Paweska, J.T.; Markotter, W. Lyssaviruses in Insectivorous Bats, South Africa, 2003–2018. *Emerg. Infect. Dis.* **2020**, *26*, 3056–3060. [\[CrossRef\]](#)
6. Marston, D.A.; Horton, D.L.; Ngeleja, C.; Hampson, K.; McElhinney, L.M.; Banyard, A.C.; Haydon, D.; Cleaveland, S.; Rupprecht, C.E.; Bigambo, M.; et al. Ikoma Lyssavirus, Highly Divergent Novel Lyssavirus in an African Civet. *Emerg. Infect. Dis.* **2012**, *18*, 664–667. [\[CrossRef\]](#) [\[PubMed\]](#)
7. Shope, R.E.; Murphy, F.A.; Harrison, A.K.; Causey, O.R.; Kemp, G.E.; Simpson, D.I.H.; Moore, D.L. Two African viruses serologically and morphologically related to rabies virus. *J. Virol.* **1970**, *6*, 690–692. [\[CrossRef\]](#) [\[PubMed\]](#)
8. Kgaladi, J.; Wright, N.; Coertse, J.; Markotter, W.; Marston, D.; Fooks, A.R.; Freuling, C.M.; Müller, T.F.; Sabeta, C.T.; Nel, L.H. Diversity and Epidemiology of Mokola Virus. *PLoS Negl. Trop. Dis.* **2013**, *7*, e2511. [\[CrossRef\]](#) [\[PubMed\]](#)
9. Luis, A.D.; Hayman, D.T.S.; O’Shea, T.J.; Cryan, P.M.; Gilbert, A.T.; Pulliam, J.R.C.; Mills, J.N.; Timonin, M.E.; Willis, C.K.R.; Cunningham, A.A.; et al. A comparison of bats and rodents as reservoirs of zoonotic viruses: Are bats special? *Proc. R. Soc. B Biol. Sci.* **2013**, *280*, 20122753. [\[CrossRef\]](#)
10. Zhou, P.; Yang, X.-L.; Wang, X.-G.; Hu, B.; Zhang, L.; Zhang, W.; Si, H.-R.; Zhu, Y.; Li, B.; Huang, C.-L.; et al. A pneumonia outbreak associated with a new coronavirus of probable bat origin. *Nature* **2020**, *579*, 270–273. [\[CrossRef\]](#)
11. Yang, X.L.; Tan, C.W.; Anderson, D.E.; Jiang, R.D.; Li, B.; Zhang, W.; Zhu, Y.; Lim, X.F.; Zhou, P.; Liu, X.L.; et al. Characterization of a filovirus (Mënglà virus) from Rousettus bats in China. *Nat. Microbiol.* **2019**, *4*, 390–395. [\[CrossRef\]](#) [\[PubMed\]](#)
12. Fooks, A.R.; Cliquet, F.; Finke, S.; Freuling, C.; Hemachudha, T.; Mani, R.S.; Muller, T.; Nadin-Davis, S.; Picard-Meyer, E.; Wilde, H.; et al. Rabies. *Nat. Rev. Dis. Primers* **2017**, *3*, 17091. [\[CrossRef\]](#) [\[PubMed\]](#)
13. Banyard, A.C.; Fooks, A.R. The impact of novel lyssavirus discovery. *Microbiol. Aust.* **2017**, *38*, 17–21. [\[CrossRef\]](#)
14. Freuling, C.M.; Klöss, D.; Schröder, R.; Kliemt, A.; Müller, T. The WHO Rabies Bulletin Europe: A key source of information on rabies and a pivotal tool for surveillance and epidemiology. *Rev. Sci. Tech.* **2012**, *3*, 799–807. [\[CrossRef\]](#) [\[PubMed\]](#)
15. Mani, R.S.; Anand, A.M.; Madhusudana, S.N. Human rabies in India: An audit from a rabies diagnostic laboratory. *Trop. Med. Int. Heal.* **2016**, *21*, 556–563. [\[CrossRef\]](#)
16. Fooks, A. The challenge of new and emerging lyssaviruses. *Expert Rev. Vaccines* **2004**, *3*, 333–336. [\[CrossRef\]](#)
17. Hayman, D.T.S.; Fooks, A.R.; Marston, D.A.; Garcia-R, J.C. The Global Phylogeography of Lyssaviruses—Challenging the ‘Out of Africa’ Hypothesis. *PLoS Negl. Trop. Dis.* **2016**, *10*, e0005266. [\[CrossRef\]](#)
18. Nolden, T.; Banyard, A.C.; Finke, S.; Fooks, A.R.; Hanke, D.; Höper, D.; Horton, D.L.; Mettenleiter, T.C.; Müller, T.; Teifke, J.P.; et al. Comparative studies on the genetic, antigenic and pathogenic characteristics of Bokeloh bat lyssavirus. *J. Gen. Virol.* **2014**, *95*, 1647–1653. [\[CrossRef\]](#)
19. Fekadu, M.; Shaddock, J.H.; Sanderlin, D.W.; Smith, J.S. Efficacy of rabies vaccines against Duvenhage virus isolated from European house bats (*Eptesicus serotinus*), classic rabies and rabies-related viruses. *Vaccine* **1988**, *6*, 533–539. [\[CrossRef\]](#)
20. Lefkowitz, E.J.; Dempsey, D.M.; Hendrickson, R.C.; Orton, R.J.; Siddell, S.G.; Smith, D.B. Virus taxonomy: The database of the International Committee on Taxonomy of Viruses (ICTV). *Nucleic Acids Res.* **2018**, *46*, D708–D717. [\[CrossRef\]](#)
21. Moore, S.M.; Hanlon, C.A. Rabies-specific antibodies: Measuring surrogates of protection against a fatal disease. *PLoS Negl. Trop. Dis.* **2010**, *4*, e595.
22. Malerczyk, C.; Freuling, C.; Gniel, D.; Giesen, A.; Selhorst, T.; Müller, T. Cross-neutralization of antibodies induced by vaccination with Purified Chick Embryo Cell Vaccine (PCECV) against different Lyssavirus species. *Hum. Vaccin Immunother.* **2014**, *10*, 2799–2804. [\[CrossRef\]](#) [\[PubMed\]](#)
23. Brookes, S.M.; Healy, D.M.; Fooks, A.R. Ability of rabies vaccine strains to elicit cross-neutralising antibodies. *Dev. Biol.* **2006**, *125*, 185–193.
24. Banyard, A.C.; Selden, D.; Wu, G.; Thorne, L.; Jennings, D.; Marston, D.; Finke, S.; Freuling, C.M.; Müller, T.; Echevarría, J.E.; et al. Isolation, antigenicity and immunogenicity of Lleida bat lyssavirus. *J. Gen. Virol.* **2018**, *99*, 1590–1599. [\[CrossRef\]](#)
25. Horton, D.L.; Banyard, A.C.; Marston, D.A.; Wise, E.; Selden, D.; Nunez, A.; Hicks, D.; Lembo, T.; Cleaveland, S.; Peel, A.J.; et al. Antigenic and genetic characterization of a divergent African virus, Ikoma lyssavirus. *J. Gen. Virol.* **2014**, *95*, 1025–1032. [\[CrossRef\]](#)
26. Badrane, H.; Bahloul, C.; Perrin, P.; Tordo, N. Evidence of Two Lyssavirus Phylogroups with Distinct Pathogenicity and Immunogenicity. *J. Virol.* **2001**, *75*, 3268–3276. [\[CrossRef\]](#)
27. Nokireki, T.; Tammiranta, N.; Kokkonen, U.-M.; Kantala, T.; Gadd, T. Tentative novel lyssavirus in a bat in Finland. *Transbound. Emerg. Dis.* **2018**, *65*, 593–596. [\[CrossRef\]](#)
28. Morimoto, K.; Foley, H.D.; Mcgettigan, J.P.; Schnell, M.J.; Dietzschold, B. Reinvestigation of the role of the rabies virus glycoprotein in viral pathogenesis using a reverse genetics approach. *J. NeuroVirology* **2000**, *6*, 373–381. [\[CrossRef\]](#)
29. Gaudin, Y.; Ruigrok, R.W.; Tuffereau, C.; Knossow, M.; Flamand, A. Rabies virus glycoprotein is a trimer. *Virology* **1992**, *187*, 627–632. [\[CrossRef\]](#)
30. Marston, D.A.; McElhinney, L.M.; Banyard, A.C.; Horton, D.L.; Núñez, A.; Koser, M.L.; Schnell, M.J.; Fooks, A.R. Interspecies protein substitution to investigate the role of the lyssavirus glycoprotein. *J. Gen. Virol.* **2013**, *94*, 284–292. [\[CrossRef\]](#)

31. Evans, J.S.; Wu, G.; Selden, D.; Buczkowski, H.; Thorne, L.; Fooks, A.R.; Banyard, A.C. Utilisation of Chimeric Lyssaviruses to Assess Vaccine Protection against Highly Divergent Lyssaviruses. *Viruses* **2018**, *10*, 130. [\[CrossRef\]](#)
32. Faber, M.; Pulmanausahakul, R.; Nagao, K.; Prosnjak, M.; Rice, A.B.; Koprowski, H.; Schnell, M.J.; Dietzschold, B. Identification of viral genomic elements responsible for rabies virus neuroinvasiveness. *Proc. Natl. Acad. Sci. USA* **2004**, *101*, 16328–16332. [\[CrossRef\]](#)
33. McGettigan, J.P.; Foley, H.D.; Belyakov, I.M.; Berzofsky, J.A.; Pomerantz, R.J.; Schnell, M.J. Rabies Virus-Based Vectors Expressing Human Immunodeficiency Virus Type 1 (HIV-1) Envelope Protein Induce a Strong, Cross-Reactive Cytotoxic T-Lymphocyte Response against Envelope Proteins from Different HIV-1 Isolates. *J. Virol.* **2001**, *75*, 4430–4434. [\[CrossRef\]](#) [\[PubMed\]](#)
34. Nikolic, J.; Le Bars, R.; Lama, Z.; Scrima, N.; Lagaudrière-Gesbert, C.; Gaudin, Y.; Blondel, D. Negri bodies are viral factories with properties of liquid organelles. *Nat. Commun.* **2017**, *8*, 58. [\[CrossRef\]](#) [\[PubMed\]](#)
35. Evans, J.S.; Selden, D.; Wu, G.; Wright, E.; Horton, D.L.; Fooks, A.R.; Banyard, A.C. Antigenic site changes in the rabies virus glycoprotein dictates functionality and neutralizing capability against divergent lyssaviruses. *J. Gen. Virol.* **2018**, *99*, 169–180. [\[CrossRef\]](#) [\[PubMed\]](#)
36. Brookes, S.M.; Parsons, G.; Johnson, N.; McElhinney, L.; Fooks, A. Rabies human diploid cell vaccine elicits cross-neutralising and cross-protecting immune responses against European and Australian bat lyssaviruses. *Vaccine* **2005**, *23*, 4101–4109. [\[CrossRef\]](#) [\[PubMed\]](#)
37. Horton, D.L.; McElhinney, L.M.; Marston, D.A.; Wood, J.L.N.; Russell, C.A.; Lewis, N.; Kuzmin, I.V.; Fouchier, R.A.M.; Osterhaus, A.D.M.E.; Fooks, A.R.; et al. Quantifying Antigenic Relationships among the Lyssaviruses. *J. Virol.* **2010**, *84*, 11841–11848. [\[CrossRef\]](#)
38. Marston, D.A.; McElhinney, L.M.; Ellis, R.J.; Horton, D.L.; Wise, E.L.; Leech, S.L.; David, D.; De Lamballerie, X.; Fooks, A.R. Next generation sequencing of viral RNA genomes. *BMC Genom.* **2013**, *14*, 1–12. [\[CrossRef\]](#)
39. Wright, E.; Temperton, N.J.; Marston, D.A.; McElhinney, L.M.; Fooks, A.R.; Weiss, R.A. Investigating antibody neutralization of lyssaviruses using lentiviral pseudotypes: A cross-species comparison. *J. Gen. Virol.* **2008**, *89*, 2204–2213. [\[CrossRef\]](#)
40. Schnell, M.; Mebatsion, T.; Conzelmann, K. Infectious rabies viruses from cloned cDNA. *EMBO J.* **1994**, *13*, 4195–4203. [\[CrossRef\]](#)
41. Johnson, N.; McElhinney, L.M.; Smith, J.; Lowings, P.; Fooks, A.R. Phylogenetic comparison of the genus Lyssavirus using distal coding sequences of the glycoprotein and nucleoprotein genes. *Arch. Virol.* **2002**, *147*, 2111–2123. [\[CrossRef\]](#) [\[PubMed\]](#)
42. Kuzmin, I.V.; Orciari, L.A.; Arai, Y.T.; Smith, J.S.; Hanlon, C.A.; Kameoka, Y.; Rupprecht, C.E. Bat lyssaviruses (Aravan and Khujand) from Central Asia: Phylogenetic relationships according to N, P and G gene sequences. *Virus Res.* **2003**, *97*, 65–79. [\[CrossRef\]](#)
43. Freuling, C.M.; Beer, M.; Conraths, F.J.; Finke, S.; Hoffmann, B.; Keller, B.; Kliemt, J.; Mettenleiter, T.C.; Mühlbach, E.; Teifke, J.P.; et al. Novel Lyssavirus in Natterer's Bat, Germany. *Emerg. Infect. Dis.* **2011**, *17*, 1519–1522. [\[CrossRef\]](#)
44. McElhinney, L.M.; Marston, D.A.; Wise, E.L.; Freuling, C.M.; Bourhy, H.; Zanoni, R.; Moldal, T.; Kooi, E.A.; Neubauer-Juric, A.; Nokireki, T.; et al. Molecular Epidemiology and Evolution of European Bat Lyssavirus 2. *Int. J. Mol. Sci.* **2018**, *19*, 156. [\[CrossRef\]](#) [\[PubMed\]](#)
45. Gunawardena, P.S.; Marston, D.A.; Ellis, R.J.; Wise, E.L.; Karawita, A.C.; Breed, A.C.; McElhinney, L.M.; Johnson, N.; Banyard, A.C.; Fooks, A.R. Lyssavirus in Indian Flying Foxes, Sri Lanka. *Emerg. Infect. Dis.* **2016**, *22*, 1456–1459. [\[CrossRef\]](#) [\[PubMed\]](#)
46. Kuzmin, I.V.; Hughes, G.J.; Botvinkin, A.D.; Orciari, L.A.; Rupprecht, C.E. Phylogenetic relationships of Irkut and West Caucasian bat viruses within the Lyssavirus genus and suggested quantitative criteria based on the N gene sequence for lyssavirus genotype definition. *Virus Res.* **2005**, *111*, 28–43. [\[CrossRef\]](#)
47. Healy, D.M.; Brookes, S.; Banyard, A.; Núñez, A.; Cosby, S.; Fooks, A. Pathobiology of rabies virus and the European bat lyssaviruses in experimentally infected mice. *Virus Res.* **2013**, *172*, 46–53. [\[CrossRef\]](#)
48. Dean, S. Rabies and quarantine. *Vet. Rec.* **1996**, *139*, 551.
49. Hicks, D.; Nuñez, A.; Healy, D.; Brookes, S.; Johnson, N.; Fooks, A. Comparative Pathological Study of the Murine Brain after Experimental Infection with Classical Rabies Virus and European Bat Lyssaviruses. *J. Comp. Pathol.* **2009**, *140*, 113–126. [\[CrossRef\]](#)
50. Hayman, D.T.; Banyard, A.C.; Wakeley, P.R.; Harkess, G.; Marston, D.; Wood, J.L.; Cunningham, A.A.; Fooks, A.R. A universal real-time assay for the detection of Lyssaviruses. *J. Virol. Methods* **2011**, *177*, 87–93. [\[CrossRef\]](#)
51. Marston, D.A.; Jennings, D.L.; MacLaren, N.C.; Dorey-Robinson, D.; Fooks, A.R.; Banyard, A.C.; McElhinney, L.M. Pan-lyssavirus Real Time RT-PCR for Rabies Diagnosis. *J. Vis. Exp.* **2019**, *2019*, 149. [\[CrossRef\]](#)
52. Cliquet, F.; Aubert, M.; Sagné, L. Development of a fluorescent antibody virus neutralisation test (FAVN test) for the quantitation of rabies-neutralising antibody. *J. Immunol. Methods* **1998**, *212*, 79–87. [\[CrossRef\]](#)
53. Smith, D.J.; Lapedes, A.S.; De Jong, J.C.; Bestebroer, T.M.; Rimmelzwaan, G.F.; Osterhaus, A.D.M.E.; Fouchier, R.A.M. Mapping the Antigenic and Genetic Evolution of Influenza Virus. *Science* **2004**, *305*, 371–376. [\[CrossRef\]](#) [\[PubMed\]](#)
54. Evans, J.S.; Horton, D.L.; Easton, A.J.; Fooks, A.R.; Banyard, A.C. Rabies virus vaccines: Is there a need for a pan-lyssavirus vaccine? *Vaccine* **2012**, *30*, 7447–7454. [\[CrossRef\]](#)
55. Katz, I.S.S.; Guedes, F.; Fernandes, E.R.; Silva, S.D.R. Immunological aspects of rabies: A literature review. *Arch. Virol.* **2017**, *162*, 3251–3268. [\[CrossRef\]](#)

-
56. Marosi, A.; Dufkova, L.; Forró, B.; Felde, O.; Erdélyi, K.; Širmarová, J.; Palus, M.; Hönig, V.; Salát, J.; Tikos, R.; et al. Combination therapy of rabies-infected mice with inhibitors of pro-inflammatory host response, antiviral compounds and human rabies immunoglobulin. *Vaccine* **2019**, *37*, 4724–4735. [[CrossRef](#)]
 57. Zhang, D.; He, F.; Bi, S.; Guo, H.; Zhang, B.; Wu, F.; Liang, J.; Yang, Y.; Tian, Q.; Ju, C.; et al. Genome-Wide Transcriptional Profiling Reveals Two Distinct Outcomes in Central Nervous System Infections of Rabies Virus. *Front. Microbiol.* **2016**, *7*, 751. [[CrossRef](#)] [[PubMed](#)]
 58. Hooper, D.C.; Morimoto, K.; Bette, M.; Weihe, E.; Koprowski, H.; Dietzschold, B. Collaboration of antibody and inflammation in clearance of rabies virus from the central nervous system. *J. Virol.* **1998**, *72*, 3711–3719. [[CrossRef](#)] [[PubMed](#)]
 59. Hooper, D.C.; Roy, A.; Barkhouse, D.A.; Li, J.; Kean, R.B. Rabies Virus Clearance from the Central Nervous System. *Adv. Virus Res.* **2011**, *79*, 55–71.
 60. Janewongwirot, P.; Jantarabenjakul, W.; Anugulruengkitt, S.; Anunsittichai, O.; Saengseesom, W.; Buranapraditkun, S.; Sophonphan, J.; Wacharachaisurapol, N.; Jitrungruengnij, N.; Pancharoen, C.; et al. A randomized open-label trial of 2-dose or 3-dose pre-exposure rabies prophylaxis among Thai children. *Vaccine* **2019**, *37*, 5307–5313. [[CrossRef](#)]

Commentary

Renewed Public Health Threat from Emerging Lyssaviruses

Anthony R. Fooks ^{1,*} , Rebecca Shipley ¹ , Wanda Markotter ² , Noël Tordo ³ , Conrad M. Freuling ⁴ , Thomas Müller ⁴ , Lorraine M. McElhinney ¹ , Ashley C. Banyard ¹  and Charles E. Rupprecht ⁵

- ¹ Animal and Plant Health Agency (APHA), WHO Collaborating Centre (Rabies)/OIE Reference Laboratory (Rabies), Weybridge KT15 3NB, UK; rebecca.shipley@apha.gov.uk (R.S.); Lorraine.McElhinney@apha.gov.uk (L.M.M.); ashley.banyard@apha.gov.uk (A.C.B.)
 - ² Centre for Viral Zoonoses, Department of Medical Virology, Faculty of Health Sciences, University of Pretoria, Pretoria 0001, South Africa; wanda.markotter@up.ac.za
 - ³ Institut Pasteur de Guinée, Route de Donka, Conakry BP 4416, Guinea; ntordo@pasteur.fr
 - ⁴ Friedrich-Loeffler-Institute (FLI), WHO Collaborating Centre for Rabies Surveillance and Research (Rabies)/OIE Reference Laboratory, 17493 Greifswald-Insel Riems, Germany; conrad.freuling@fli.de (C.M.F.); Thomas.Mueller@fli.de (T.M.)
 - ⁵ LYSSA LLC, Cumming, GA 30044, USA; charles_rupprecht@yahoo.com
- * Correspondence: Tony.Fooks@apha.gov.uk



Citation: Fooks, A.R.; Shipley, R.; Markotter, W.; Tordo, N.; Freuling, C.M.; Müller, T.; McElhinney, L.M.; Banyard, A.C.; Rupprecht, C.E. Renewed Public Health Threat from Emerging Lyssaviruses. *Viruses* **2021**, *13*, 1769. <https://doi.org/10.3390/v13091769>

Academic Editor: Laurent Dacheux

Received: 13 July 2021

Accepted: 31 August 2021

Published: 4 September 2021

Publisher's Note: MDPI stays neutral with regard to jurisdictional claims in published maps and institutional affiliations.



Copyright: © 2021 by the authors. Licensee MDPI, Basel, Switzerland. This article is an open access article distributed under the terms and conditions of the Creative Commons Attribution (CC BY) license (<https://creativecommons.org/licenses/by/4.0/>).

Abstract: Pathogen discovery contributes to our knowledge of bat-borne viruses and is linked to the heightened interest globally in bats as recognised reservoirs of zoonotic agents. The transmission of lyssaviruses from bats-to-humans, domestic animals, or other wildlife species is uncommon, but interest in these pathogens remains due to their ability to cause an acute, progressive, invariably fatal encephalitis in humans. Consequently, the detection and characterisation of bat lyssaviruses continues to expand our knowledge of their phylogroup definition, viral diversity, host species association, geographical distribution, evolution, mechanisms for perpetuation, and the potential routes of transmission. Although the opportunity for lyssavirus cross-species transmission seems rare, adaptation in a new host and the possibility of onward transmission to humans requires continued investigation. Considering the limited efficacy of available rabies biologicals it is important to further our understanding of protective immunity to minimize the threat from these pathogens to public health. Hence, in addition to increased surveillance, the development of a niche pan-lyssavirus vaccine or therapeutic biologics for post-exposure prophylaxis for use against genetically divergent lyssaviruses should be an international priority as these emerging lyssaviruses remain a concern for global public health.

Keywords: rabies; lyssavirus; bats; emerging; novel; encephalitis; prophylaxis; zoonoses

1. Introduction

Virus ‘hunting’ has stimulated the detection and characterisation of new lyssaviruses, most detected in chiropteran hosts [1] (1). Although cross-species transmission (CST) of lyssaviruses from bats-to-humans or any other mammalian species is rare [2–6] by comparison to the burden of canine rabies [7]. Interest in these RNA viruses remains high. All lyssaviruses cause clinical rabies and not a ‘rabies-like’ disease. Accurate estimates of human infection caused by lyssaviruses are imprecise, because of inadequate laboratory-based surveillance systems, mainly across Africa and Asia [8]. As is clear from the current COVID-19 pandemic, a more thorough understanding of bat ecology, immunology, and pathobiology will play an ever-increasing role in advancing our knowledge of the risks related to bat-transmitted diseases [9]. The paucity of relevant data, however, on bat populations, their distribution, relative abundance, and the sporadic interactions between bat populations and other taxa, such as carnivores, demonstrates that the role of bats and the epizootiology of host-virus dynamics are unclear. The extreme severity of disease caused by lyssaviruses means that the opportunity for CST is of major significance to

human and animal populations. For rabies virus (RABV), most CST events are considered a dead-end infection, with infrequent virus transmission from an infected host, such as rabid vampire bat infections of humans or livestock [8,10]. In contrast, viral host switching events can result in sustained onward transmission to a naive host [11]. Host switching of RABV from bats appear to be more frequent in the Americas [12–14], whilst events involving other Old World (Africa, Europe, and Asia, or Afro-Eurasia) lyssaviruses appear to be rare [4,15]. There are multiple factors, including ecological and virological impacts, involved in CST and eventual host switching events [16,17]. In either case, endeavours to identify specific amino acid substitutions facilitating viral adaptation to new host species have been, for the most part, unsuccessful [18].

2. The Increasing Diversity of Lyssaviruses

Lyssaviruses are classified in the family *Rhabdoviridae* and the order *Mononegavirales*. Within the *Lyssavirus* genus, there are 17 different viral species recognized by the International Committee on Taxonomy of Viruses [19]. Classified as separate entities according to their genomic sequences, these include: *Aravan lyssavirus* (ARAV); *Australian bat lyssavirus* (ABLV); *Bokeloh bat lyssavirus* (BBLV); *Duvenhage lyssavirus* (DUVV); *European bat 1 lyssavirus* (EBLV-1); *European bat 2 lyssavirus* (EBLV-2); *Gannoruwa bat lyssavirus* (GBLV); *Ikoma lyssavirus* (IKOV); *Irkut lyssavirus* (IRKV); *Khujand lyssavirus* (KHUV); *Lagos bat lyssavirus* (LBV); *Lleida bat lyssavirus* (LLEBV); *Mokola lyssavirus* (MOKV); *Rabies lyssavirus* (RABV); *Shimoni bat lyssavirus* (SHIBV); *Taiwan bat lyssavirus* (TWBLV); *West Caucasian bat lyssavirus* (WCBV). One further novel lyssavirus, *Kotalahti bat lyssavirus* (KBLV), which was detected in a Brandt's bat (*Myotis brandtii*) in Finland [20,21], and two sequences from a potentially novel lyssavirus, provisionally named Matlo bat lyssavirus (MBLV) [22,23], have been reported but remain as tentative species until fully characterised. Besides taxonomic classification into species, these viruses may also be grouped, according to genetics, using the nucleoprotein gene, phylogenetic, and antigenic data, into phylogroups [24]. At least two phylogroups can be identified by topological analysis of the phylogeny (Figure 1). The phylogroup I phylogenetic tree divides into two major branches, one of which is composed of the Palearctic and Indo-Malay regions (ARAV, BBLV, EBLV-2, KBLV, ABLV, GBLV, and KHUV); and another composed of EBLV-1, DUVV, IRKV, and TWBLV. Phylogroup II is composed of the African lyssaviruses, LBV, MOKV and SHIBV. The most genetically divergent lyssaviruses have been tentatively classified within a dispersed phylogroup III, subdivided in two branches gathering viruses isolated from Europe to Africa, consisting of species, WCBV-MBLV and IKOV-LLEBV, respectively. In terms of sequence identity, viruses classified into phylogroup II exhibit the highest average nucleotide sequence similarity of the glycoprotein gene at 71.5%, whilst viruses classified into phylogroup I exhibit an average nucleotide sequence similarity of 70.3%. Viruses tentatively classified into phylogroup III exhibit an average nucleotide sequence similarity of 58.2%, indicating divergence of these viruses. In relation to viruses classified into phylogroup I and II, phylogroup III viruses exhibit an average nucleotide sequence similarity of 54.1% and 54.5%, respectively. With similarity to the evolutionary and genetic data (Figure 1), the antigenic analyses have identified several antigenic groups, referred to as phylogroups (Figure 1). Differentiation into these phylogroups predicts the degree of cross protection afforded by available rabies vaccines based on RABV. Though immunological responses to vaccines differ between individuals, it is widely accepted that the conservative virus neutralising antibody (VNA) level equal to or greater than 0.5 international units (IU/mL) positively correlates with seroconversion after vaccination against RABV [25]. Besides RABV, licensed rabies vaccines appear to largely confer protective immunity against phylogroup I lyssaviruses [26,27], with the least potential against IRKV [26,28]. Altogether, the level of VNA required for protection is undefined for non-RABV lyssaviruses [29,30].

For more divergent lyssaviruses, in vivo vaccination-challenge experiments have shown that the VNA response generated from RABV vaccines is inadequate to protect against challenge [26,31,32]. Phylogroup II lyssaviruses include LBV (all lineages, A–D),

MOKV and SHIBV. Three further lyssaviruses, IKOV, LLEBV, and WCBV represent the most genetically and antigenically divergent lyssaviruses and these have been tentatively classified within a further phylogroup, phylogroup III (Figure 2). However, there appears to be limited cross neutralisation among these three viruses, and as such, they are unlikely to be antigenically categorised together in the same phylogroup. Phylogroup I viruses exhibit an average distance of 2 antigenic units (AU) to the SN strain, derived from the SAD B19 cDNA clone of RABV, equivalent to only a 4-fold difference in a VNA titre across multiple lyssavirus species [33]. In contrast, the highly genetically and antigenically divergent phylogroup III lyssaviruses demonstrate an average antigenic distance of 10 AU to the SN vaccine strain of RABV, equivalent to a 1024-fold difference in VNA titre (Figure 2).

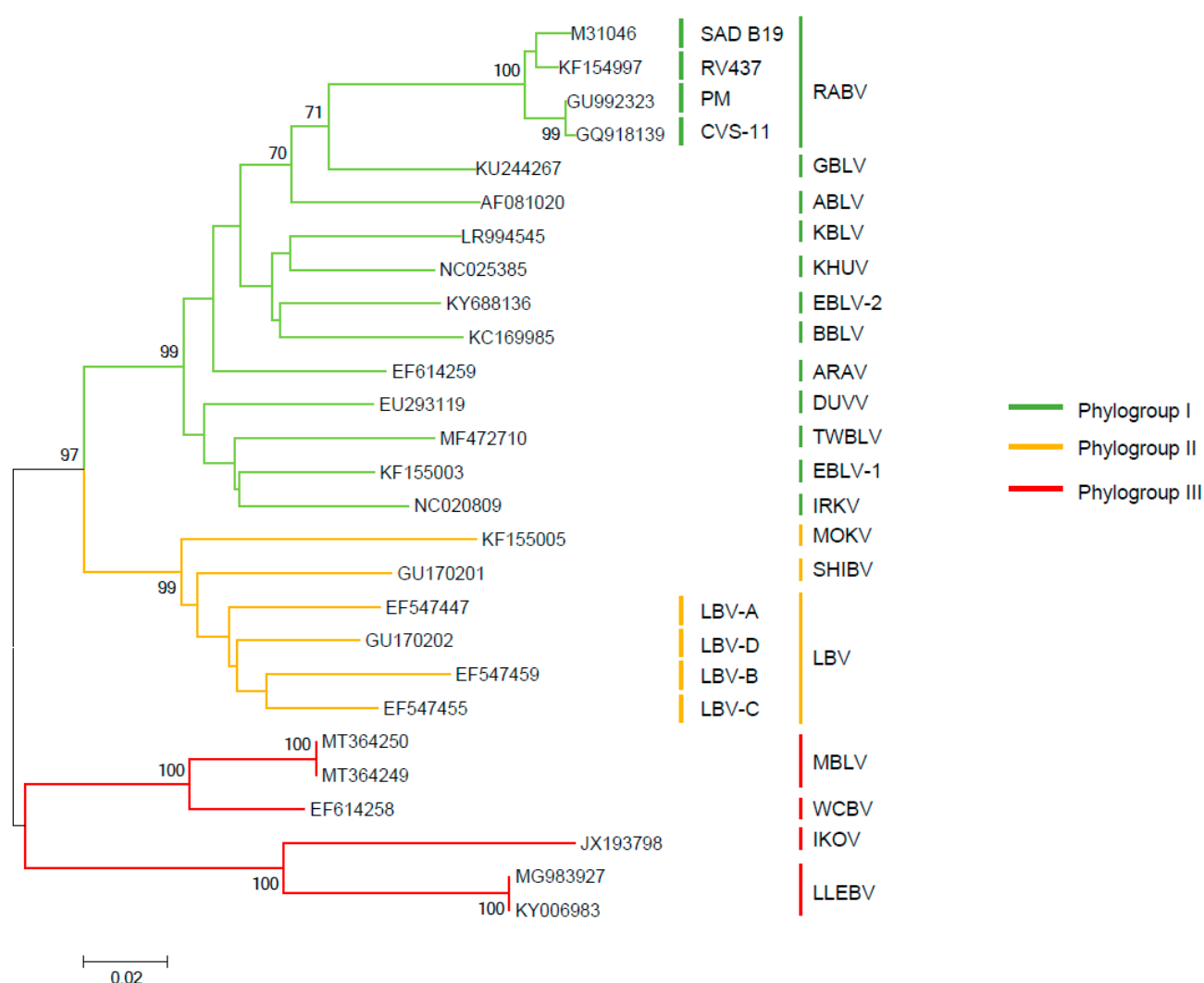


Figure 1. Phylogenetic reconstruction by inference of nucleoprotein gene sequences of lyssaviruses using the Neighbour-Joining method. The percentage of replicate trees in which the associated taxa clustered together in the bootstrap test (1000 replicates) are shown next to the branches. The GenBank accession numbers are indicated for each sequence. The evolutionary distances were computed using the Maximum Composite Likelihood method and are in the units of the number of base substitutions per site. Phylogenetic tree was generated in MEGA 6.

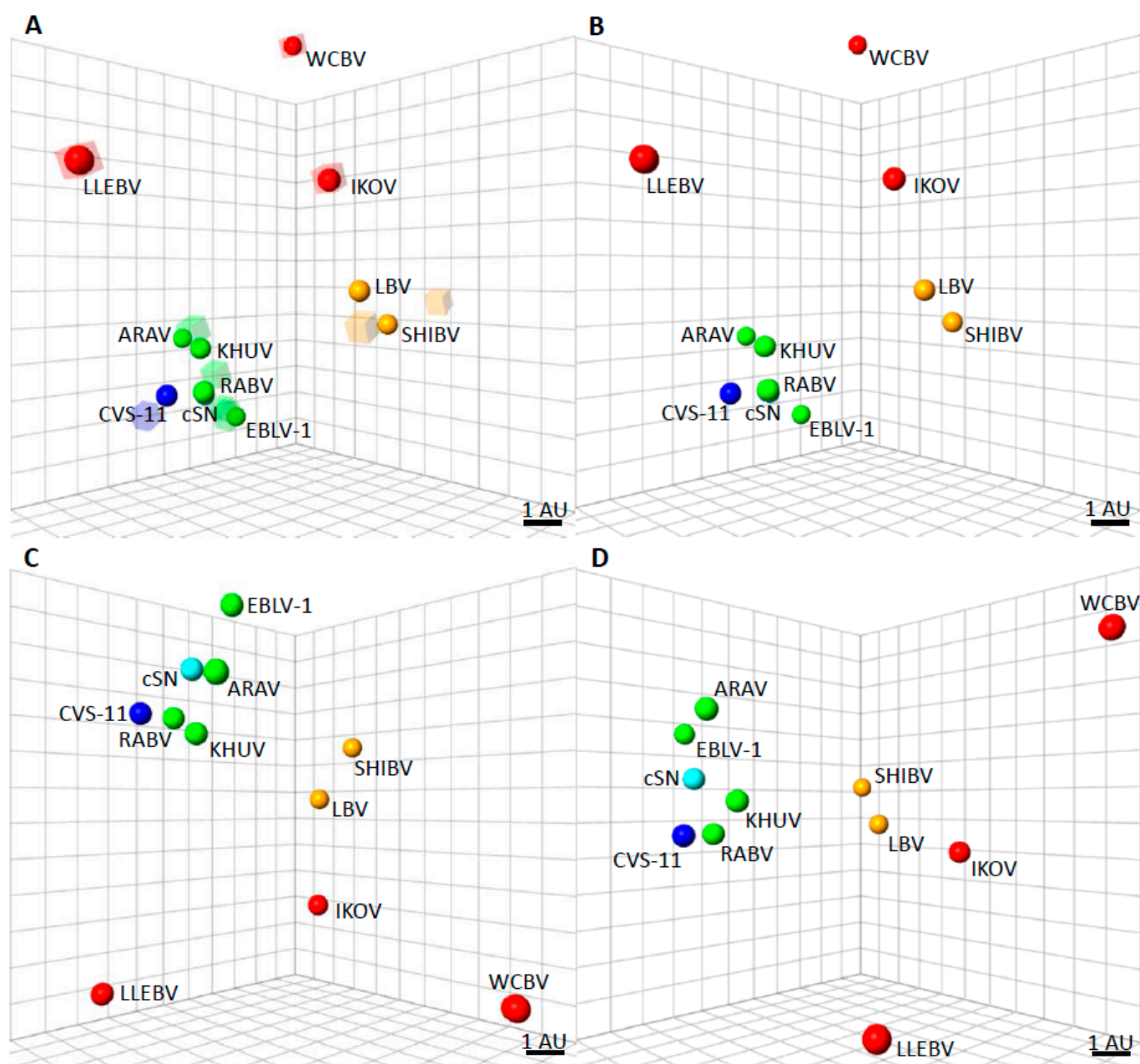


Figure 2. Antigenic cartography maps to show the antigenic distances of the lyssaviruses. **(A)** Three-dimensional antigenic map showing the antigenic relationship between lyssaviruses. Viruses (spheres) and sera (translucent coloured boxes) are positioned such that the distance from each serum to each virus is determined by the neutralisation titre. Multidimensional scaling is used to position both sera and viruses relative to each other, so orientation of the map within the axes is free. The scale bar represents 1 AU (antigenic unit), equivalent to a two-fold dilution in antibody titre. Phylogroup I lyssaviruses are coloured green, CVS-11 coloured dark blue [Challenge virus standard-11 strain of RABV, used routinely in diagnostic assays], cSN [cDNA clone of the SN strain of RABV derived from the RABV strain, SAD B19] coloured light blue, Phylogroup II lyssaviruses coloured orange, and Phylogroup III lyssaviruses coloured red. **(B)** Antigenic map with sera removed for clarity. **(C)** Antigenic map, rotated to a different orientation and sera removed for clarity. **(D)** Antigenic map, rotated to a different orientation and sera removed for clarity.

Lyssaviruses have a distinctive epidemiology through their evolutionary association with bats [12]. RABV is present globally, being reported in carnivores and multiple other mammalian species across the New World, within multiple bat taxa. Whilst canine rabies has been largely eliminated in the Americas, curiously, of the 17 recognized lyssaviruses, only RABV has been reported in the New World (representing the Americas), where it is

also identified within multiple bat taxa [8]. From a host-pathogen perspective, bat RABV in the New World has been associated with over 40 different species of insectivorous, hematophagous and frugivorous bats, including reservoirs among common genera, such as *Desmodus*, *Eptesicus*, *Lasiurus*, *Lasionycteris*, *Myotis*, *Perimyotis*, and *Tadarida* species, among others [2,5]. Hence, New World bat populations represent an omnipresent source of RABV infection for which elimination options remain unavailable. In contrast to the situation across the Americas, RABV has never been detected in bats in the Old World, yet the virus cycles among carnivores across much of the Old World [11,15,34]. This species-associated virus-host relationship of RABV has led to the suggestion of host restriction or co-evolution of pathogens with certain bat species (Table 1) [2,8]. However, there are partial exceptions to the rule. Detection of Old World lyssaviruses have been sporadic and opportunistic, complicating any inference on host species association and accurate distribution. For example, it remains enigmatic for WCBV and LLEBV appearing to occupy one and the same ecological niche, the Schreibers' long-fingered bat (*Miniopterus schreibersii*) in Europe, although detection of both viruses has been relatively rare. ABLV and LBV have been detected in different species of bats in Australia and Africa, respectively, with LBV demonstrating a higher genetic diversity than any other of the known Old World bat lyssaviruses [35,36].

The relative proportion of the bat population able to transmit a lyssavirus to other host species is considered less than 1% (data not shown). Consequently, only a small number of human rabies cases caused by Old World lyssaviruses have been recognized [37]. Such paucity of data on Old World lyssaviruses may reflect fewer cases of exposure in humans than there are with RABV in the New World across human and animal populations. However, the basis for this observation remains enigmatic.

Table 1. 21st century occurrence of the proposed 'phylogroup III' lyssavirus species.

Lyssavirus Species	Mammalian Isolate	Reservoir Species Associated with Lyssavirus Infection	Year of Isolation	Countries Reporting 'Phylogroup III' Lyssaviruses	Region
West Caucasian bat lyssavirus (WCBV)	Schreibers' long-fingered bat (also known as the common bent-wing bat)	<i>M. schreibersii</i>	2002	Russian Federation	Eurasia
Ikoma lyssavirus (IKOV)	African civet (<i>Civettictis civetta</i>)	* Not known	2009	Tanzania	East Africa
Lleida bat lyssavirus (LLEBV)	Schreibers' long-fingered bat	<i>M. schreibersii</i>	2011	Spain	Western Europe
Lleida bat lyssavirus (LLEBV)	Schreibers' long-fingered bat	<i>M. schreibersii</i>	2017	France	Western Europe
West Caucasian bat lyssavirus (WCBV)	Domestic cat (<i>Felis catus</i>)	Suspected <i>M. schreibersii</i> colonies near the house where the cat resided.	2020	Italy	Western Europe
Matlo bat lyssavirus (MBLV)	Natal long-fingered bat	<i>M. natalensis</i>	2015–2016	Republic of South Africa	Southern Africa

* Virus neutralizing antibodies detected from *Miniopterus* species bats in Kenya reported during 2006–2007 [38].

3. Are *Miniopterus* Species a Source of Genetically-Divergent Lyssaviruses?

More recently, there have been an increased number of reported cases and subsequently isolations of these most divergent and rare lyssaviruses. Retrospective characterization of laboratory samples from rabid animals indicated that such cases previously reported

as rabies positive were due to Old World lyssaviruses [37]. Where surveillance efforts are implemented, increased reports of known lyssaviruses will ultimately follow [22]. Historically, mass mortalities have been reported in colonies of *Miniopterus schreibersii* throughout Spain, France, and Portugal [39]. In Spain, these events prompted investigations into the potential cause of the mortalities, although no causal relationship between pathogens and the fatalities were established. This bat species has also been associated with the proposed highly divergent phylogroup III lyssaviruses (Table 1). In the past three years, divergent lyssaviruses have been described as exemplified below, not only broadening the potential lyssavirus species list but also expanding the geographical distribution of previous known species.

4. Lleida Bat Lyssavirus in France

Most cases of bat rabies in Europe are associated with EBLV-1 [40,41]. In Spain, LLEBV was first detected in 2011, only the second phylogroup III lyssavirus from the continent, after WCBV [32,42]. With the turn of the century, a passive surveillance network was initiated in France, with the objective of detecting lyssaviruses among indigenous bat species. In 2017, a dead adult male *M. schreibersii* was diagnosed as positive for lyssavirus antigen and molecular testing characterized the sample as LLEBV, more than 700 km from the original report of LLEBV in Spain [43]. The detection of one of the most genetically divergent lyssavirus species, LLEBV, in a dead *M. schreibersii* bat in France stimulated further interest in these highly divergent lyssaviruses. Brain samples were found positive for both viral antigens and nucleic acids and a virus isolate was recovered. The genome sequence had 99.7% nucleotide identity with the Spanish LLEBV [44,45].

5. West Caucasian Bat Virus in Italy

In 2020, rabies was confirmed in a two-year-old cat in the Arezzo region. The cat died four days after the demonstration of clinical disease. Diagnostic evaluation by antigen and PCR testing confirmed the presence of a lyssavirus. Sequencing of the virus from the cat showed 98.5% homology with WCBV, suggesting a nearby bat colony may have been the source of the virus. WCBV has previously been detected in *M. schreibersi* in the Caucasus Mountains of South Eastern Europe [42] and cross-reactive antibodies against WCBV were detected in *M. schreibersi* in Kenya [38].

6. Matlo Bat Lyssavirus in The Republic of South Africa

During an enhanced survey in insectivorous bats in South Africa between 2003 and 2018, a new lyssavirus, MBLV, was identified [22,23] in the brain of two *Miniopterus natalensis* bats. This lyssavirus is 78.9% related phylogenetically to WCBV (20) (Figure 1). It is supposed that the greatest diversity of lyssaviruses is associated principally with bats on the African continent [15]. Intrinsically, in terms of bat host associations all recent detections of highly divergent bat lyssaviruses were associated with the *Miniopterus* bat genera with more than 30 species named so far, which is omnipresent in the Old World.

7. Bat Host Associations

It is notable that all the recent detections of highly divergent bat lyssaviruses in bats were associated with the *Miniopterus* bat genera. These bats have a broad range, including much of southern Europe, Africa, southern and south-eastern Asia, northern and eastern Australia, as well as the Melanesian Islands [46]. Previous detections of bat lyssaviruses indicated a clear geographical separation of Old World lyssaviruses. The recent detection of WCBV in Italy highlights the broad geographical range of this virus in *Miniopterus*. Moreover, MBLV is a likely sub-lineage of WCBV, expanding the range of this lyssavirus species into Africa. With the isolation of both WCBV and LLEBV in *M. schreibersii*, questions of basic host susceptibility arise from more than one virus being associated with the same species. With the evidence from these more recent lyssavirus notifications, there is a suggestion for both geographical distribution as well as a compartmentalised co-evolution

of the bat species with association of a specific lyssavirus species. Regarding the latter, in fact, *Miniopterus* species are difficult to distinguish by external morphological features. This is particularly relevant in tropical regions of Africa where it is not yet possible to propose a clear taxonomy to prevailing species [47,48].

8. Availability of Vaccines for Bat Lyssaviruses

Continual recognition of novel emerging lyssaviruses warrants assessment of vaccine-derived cross reactivity. Modern human rabies vaccines and biologics have been available for decades. Following vaccination, a viral neutralising antibody titre above a defined threshold is considered a surrogate of efficacy for animal vaccination and also for humans at occupational risk of exposure to RABV [25]. However, this arbitrary cut off for a serological VNA titre is poorly defined for the other lyssaviruses. Certainly, reported variable efficacy of the WHO standard immune globulins and human sera from vaccinated personnel against more divergent phylogroup I viruses, such as DUVV and EBLV-1, and phylogroup II and III viruses suggests there is a cut-off threshold for antigenic relatedness for which human rabies vaccines will be ineffective [26,29–31]. Consequently, discovery of novel viruses warrants investigation on the safety, immunogenicity and efficacy of existing biologics, including the effectiveness of rabies immune globulin [25]. Detection of highly divergent lyssaviruses, LLEBV and WCBV in Europe and the putative MBLV in the Republic of South Africa, poses an increasing risk to human and animal populations alike, particularly if CST cases occur, especially as licensed biologics that have efficacy against these lyssavirus species do not exist. There are various avenues in how to overcome this limitation [49]. Current rabies vaccines are safe and, when administered properly, they are highly effective against RABV but lack efficacy against the highly divergent lyssavirus, particularly those lyssavirus species in phylogroup III. The surface glycoprotein G being the main immunogen for lyssaviruses, including a chimeric G protein RABV-MOKV or RABV-EBLV1 has shown that it is possible to enlarge the cross-neutralisation spectrum within the antigenic group I and between antigenic groups I and II, in the perspective of an anti-lyssavirus vaccine [50–53]. Therefore, new prototype vaccine candidates must have cost benefits, especially with broad immunologic and protective efficacy, as opposed to currently available vaccines, so these prototype vaccines will eventually enter clinical trials and become available on the global market [44,52].

9. Emerging Lyssaviruses

Although the number of reported historical human cases caused by a divergent lyssavirus is greater than 15 cases worldwide, this number is considered an underestimate due to underreporting and lower levels of typing of human rabies cases in the Old World, particularly in Africa. As long as biologics against these viruses are unavailable, reduction and prevention of exposure is the only available risk mitigating measure. Given the ongoing COVID-19 pandemic, there is an increased interest in zoonotic diseases and the availability of laboratory-based surveillance in support of national wildlife surveillance programmes. The development of surveillance programmes for detecting pathogens in wildlife offers an opportunity for future research on other viruses that may co-infect bats along with lyssaviruses and other emerging pathogens. Increased laboratory-based surveillance will support the discovery of novel lyssaviruses and will enhance knowledge on the distribution of recognised lyssaviruses. The increased use of pan-lyssavirus molecular tools and sequencing in routine diagnostic laboratories, as well as reduced reliance on RABV specific reagents, will also result in enhanced detection of non-RABV lyssaviruses in the future. Expanding this capacity worldwide may fill knowledge gaps and support the international health sectors in becoming more vigilant in recognising the risk of lyssaviruses to animal and human health.

10. Conclusions

In conclusion, further research under a ‘One Health’ programme is required to understand: the intraspecific mechanisms of perpetuation of viral pathogens within bat populations; the zoonotic potential of these viral pathogens detected in bats; the altered regional distribution of reservoirs such as bats, particularly as impacted by anthropological changes, habitat fragmentation and climate change; the risk of CST events that will impact both human and animal health.

Author Contributions: Conceptualization, A.R.F., T.M. and C.E.R.; Writing—Original Draft Preparation, A.R.F., R.S., A.C.B. and C.E.R.; Writing—Review & Editing, A.R.F., R.S., W.M., N.T., C.M.F., T.M., L.M.M., A.C.B. and C.E.R. All authors have read and agreed to the published version of the manuscript.

Funding: Members from APHA were supported by Defra, the Scottish Government and Welsh Government through grant SV3500 and by the European Union’s Horizon 2020 research and innovation program under RABYD-VAX grant agreement No. 733176. R.S. was supported by a PhD studentship under Defra grant SE0431. WM was supported by the South African Research Chair Initiative (of the Department of Science and Innovation and administered by the National Research Foundation of South Africa (UID: 98339). The authors’ thank Bernadette Abela-Ridder (World Health Organization, Geneva, Switzerland) for insightful ideas and encouragement.

Institutional Review Board Statement: Not applicable.

Informed Consent Statement: Not applicable.

Data Availability Statement: The data presented in this study are available on request from the corresponding author.

Conflicts of Interest: The sponsors had no role in the design, execution, interpretation, or writing of the study. The authors declare no conflict of interest.

References

1. Fooks, A.R.; Cliquet, F.; Finke, S.; Freuling, C.; Hemachudha, T.; Mani, R.S.; Müller, T.; Nadin-Davis, S.; Picard-Meyer, E.; Wilde, H.; et al. Rabies. *Nat. Rev. Dis. Primers* **2017**, *3*, 17091. [\[CrossRef\]](#)
2. Streicker, D.G.; Turmelle, A.S.; Vonhof, M.J.; Kuzmin, I.V.; McCracken, G.F.; Rupprecht, C.E. Host phylogeny constrains cross-species emergence and establishment of rabies virus in bats. *Science* **2010**, *329*, 676–679. [\[CrossRef\]](#) [\[PubMed\]](#)
3. Wallace, R.M.; Gilbert, A.; Slate, D.; Chipman, R.; Singh, A.; Cassie, W.; Blanton, J.D. Right place, wrong species: A 20-year review of rabies virus cross species transmission among terrestrial mammals in the United States. *PLoS ONE* **2014**, *9*, e107539. [\[CrossRef\]](#) [\[PubMed\]](#)
4. Marston, D.A.; Banyard, A.C.; McElhinney, L.M.; Freuling, C.M.; Finke, S.; de Lamballerie, X.; Muller, T.; Fooks, A.R. The lyssavirus host-specificity conundrum-rabies virus-the exception not the rule. *Curr. Opin. Virol.* **2018**, *28*, 68–73. [\[CrossRef\]](#)
5. Banyard, A.C.; Davis, A.; Gilbert, A.T.; Markotter, W. Bat rabies, Chapter 7. In *Rabies*, 4th ed.; Fooks, A.R., Jackson, A.C., Eds.; Academic Studies Press: Boston, MA, USA, 2020; pp. 231–276.
6. Regnault, B.; Evrard, B.; Plu, I.; Dacheux, L.; Troadec, E.; Cozette, P.; Chrétien, D.; Duchesne, M.; Vallat, J.-M.; Jamet, A.; et al. First Case of Lethal Encephalitis in Western Europe Due to European Bat Lyssavirus Type 1. *Clin. Infect. Dis.* **2021**. [\[CrossRef\]](#) [\[PubMed\]](#)
7. Hampson, K.; Coudeville, L.; Lembo, T.; Sambo, M.; Kieffer, A.; Attlan, M.; Barrat, J.; Blanton, J.D.; Briggs, D.J.; Cleaveland, S.; et al. Estimating the global burden of endemic canine rabies. *PLoS Negl. Trop. Dis.* **2015**, *9*, e0003709.
8. Rupprecht, C.E.; Kuzmin, I.; Meslin, F. Lyssaviruses and rabies: Current conundrums, concerns, contradictions and controversies. *F1000Research* **2017**, *6*, 184. [\[CrossRef\]](#)
9. Letko, M.; Seifert, S.N.; Olival, K.J.; Plowright, R.K.; Munster, V.J. Bat-borne virus diversity, spillover and emergence. *Nat. Rev. Microbiol.* **2020**, *18*, 461–471. [\[CrossRef\]](#) [\[PubMed\]](#)
10. Johnson, N.; Arechiga-Ceballos, N.; Aguilar-Setien, A. Vampire bat rabies: Ecology, epidemiology and control. *Viruses* **2014**, *6*, 1911–1928. [\[CrossRef\]](#)
11. Troupin, C.; Dacheux, L.; Tanguy, M.; Sabeta, C.; Blanc, H.; Bouchier, C.; Vignuzzi, M.; Duchene, S.; Holmes, E.; Bourhy, H. Large-Scale Phylogenomic Analysis Reveals the Complex Evolutionary History of Rabies Virus in Multiple Carnivore Hosts. *PLoS Pathog.* **2016**, *12*, e1006041. [\[CrossRef\]](#) [\[PubMed\]](#)
12. Badrane, H.; Tordo, N. Host switching in Lyssavirus history from the Chiroptera to the Carnivora orders. *J. Virol.* **2001**, *75*, 8096–104. [\[CrossRef\]](#) [\[PubMed\]](#)

13. Kuzmin, I.V.; Shi, M.; Orciari, L.A.; Yager, P.A.; Velasco-Villa, A.; Kuzmina, N.A.; Streicker, G.D.; Bergman, D.L.; Rupprecht, C.E. Molecular inferences suggest multiple host shifts of rabies viruses from bats to mesocarnivores in Arizona during 2001–2009. *PLoS Pathog.* **2012**, *8*, e1002786. [\[CrossRef\]](#)
14. Davis, R.; Nadin-Davis, S.A.; Moore, M.; Hanlon, C. Genetic characterization and phylogenetic analysis of skunk-associated rabies viruses in North America with special emphasis on the central plains. *Virus Res.* **2013**, *174*, 27–36. [\[CrossRef\]](#)
15. Hayman, D.T.S.; Fooks, A.R.; Marston, D.; Garcia-R, J.C. The Global Phylogeography of Lyssaviruses—Challenging the ‘Out of Africa’ Hypothesis. *PLoS Negl. Trop. Dis.* **2016**, *10*, e0005266. [\[CrossRef\]](#) [\[PubMed\]](#)
16. Mollentze, N.; Biek, R.; Streicker, D.G. The role of viral evolution in rabies host shifts and emergence. *Curr. Opin. Virol.* **2014**, *8*, 68–72. [\[CrossRef\]](#) [\[PubMed\]](#)
17. Mollentze, N.; Streicker, D.G.; Murcia, P.R.; Hampson, K.; Biek, R. Virulence mismatches in index hosts shape the outcomes of cross-species transmission. *Proc. Natl. Acad. Sci. USA* **2020**, *117*, 28859–28866. [\[CrossRef\]](#)
18. Bonnaud, E.M.; Troupin, C.; Dacheux, L.; Holmes, E.C.; Monchatre-Leroy, E.; Tanguy, M.; Bouchier, C.; Cliquet, F.; Barrat, J.; Bourhy, H. Comparison of intra- and inter-host genetic diversity in rabies virus during experimental cross-species transmission. *PLoS Pathog.* **2019**, *15*, e1007799. [\[CrossRef\]](#) [\[PubMed\]](#)
19. Walker, P.J.; Siddell, S.G.; Lefkowitz, E.J.; Mushegian, A.R.; Adriaenssens, E.M.; Dempsey, D.M.; Dutilh, B.E.; Harrach, B.; Harrison, R.L.; Hendrickson, R.C.; et al. Changes to virus taxonomy and the Statutes ratified by the International Committee on Taxonomy of Viruses (2020). *Arch. Virol.* **2020**, *165*, 2737–2748. [\[CrossRef\]](#)
20. Nokireki, T.; Tammiranta, N.; Kokkonen, U.-M.; Kantala, T.; Gadd, T. Tentative novel lyssavirus in a bat in Finland. *Transbound. Emerg. Dis.* **2018**, *65*, 593–596. [\[CrossRef\]](#)
21. Shipley, R.; Wright, E.; Lean, F.; Selden, D.; Horton, D.; Fooks, A.; Banyard, A. Assessing Rabies Vaccine Protection against a Novel Lyssavirus, Kotalahti Bat Lyssavirus. *Viruses* **2021**, *13*, 947. [\[CrossRef\]](#)
22. Coertse, J.; Grobler, C.S.; Sabeta, C.T.; Seamark, E.C.; Kearney, T.; Paweska, J.T.; Markotter, W. Lyssaviruses in Insectivorous Bats, South Africa, 2003–2018. *Emerg. Infect. Dis.* **2020**, *26*, 3056–3060. [\[CrossRef\]](#)
23. Grobler, C.S.; Coertse, J.; Markotter, W. Complete Genome Sequence of Matlo Bat Lyssavirus. *Microbiol. Resour. Announc.* **2021**, *10*, e00241-21. [\[CrossRef\]](#)
24. Badrane, H.; Bahloul, C.; Perrin, P.; Tordo, N. Evidence of Two Lyssavirus Phylogroups with Distinct Pathogenicity and Immunogenicity. *J. Virol.* **2001**, *75*, 3268–3276. [\[CrossRef\]](#) [\[PubMed\]](#)
25. World Health Organization. Rabies vaccines: WHO position paper, April 2018–Recommendations. *Vaccine* **2018**, *36*, 5500–5503. [\[CrossRef\]](#) [\[PubMed\]](#)
26. Hanlon, C.A.; Kuzmin, I.V.; Blanton, J.D.; Weldon, W.C.; Manangan, J.S.; Rupprecht, C.E. Efficacy of rabies biologics against new lyssaviruses from Eurasia. *Virus Res.* **2005**, *111*, 44–54. [\[CrossRef\]](#)
27. Brookes, S.; Parsons, G.; Johnson, N.; McElhinney, L.; Fooks, A. Rabies human diploid cell vaccine elicits cross-neutralising and cross-protecting immune responses against European and Australian bat lyssaviruses. *Vaccine* **2005**, *23*, 4101–4109. [\[CrossRef\]](#)
28. Liu, Y.; Chen, Q.; Zhang, F.; Zhang, S.; Li, N.; Lian, H.; Wang, Y.; Zhang, J.; Hu, R. Evaluation of Rabies Biologics against Irkut Virus Isolated in China. *J. Clin. Microbiol.* **2013**, *51*, 3499–3504. [\[CrossRef\]](#)
29. Malerczyk, C.; Freuling, C.; Gniel, D.; Giesen, A.; Selhorst, T.; Muller, T. Cross-neutralization of antibodies induced by vaccination with Purified Chick Embryo Cell Vaccine (PCECV) against different Lyssavirus species. *Hum. Vaccin. Immunother.* **2014**, *10*, 2799–2804. [\[CrossRef\]](#)
30. Malerczyk, C.; Selhorst, T.; Tordo, N.; Moore, S.; Muller, T. Antibodies induced by vaccination with purified chick embryo cell vaccine (PCECV) cross-neutralize non-classical bat lyssavirus strains. *Vaccine* **2009**, *27*, 5320–5325. [\[CrossRef\]](#)
31. Weyer, J.; Kuzmin, I.V.; Rupprecht, C.E.; Nel, L.H. Cross-protective and cross-reactive immune responses to recombinant vaccinia viruses expressing full-length lyssavirus glycoprotein genes. *Epidemiol. Infect.* **2008**, *136*, 670–678. [\[CrossRef\]](#) [\[PubMed\]](#)
32. Banyard, A.C.; Selden, D.; Wu, G.; Thorne, L.; Jennings, D.; Marston, D.; Finke, S.; Freuling, C.M.; Müller, T.; Echevarría, J.E.; et al. Isolation, antigenicity and immunogenicity of Lleida bat lyssavirus. *J. Gen. Virol.* **2018**, *99*, 1590–1599. [\[CrossRef\]](#)
33. Horton, D.L.; McElhinney, L.; Marston, D.; Wood, J.L.N.; Russell, C.; Lewis, N.; Kuzmin, I.V.; Fouchier, R.; Osterhaus, A.D.M.E.; Fooks, A.R.; et al. Quantifying Antigenic Relationships among the Lyssaviruses. *J. Virol.* **2010**, *84*, 11841–11848. [\[CrossRef\]](#)
34. Athingo, R.; Tenzin, T.; Shilongo, A.; Hikufe, E.; Shoombe, K.K.; Khaib, S.; Van Der Westhuizen, J.; Letshwenyo, M.; Torres, G.; Mettenleiter, T.C.; et al. Fighting Dog-Mediated Rabies in Namibia—Implementation of a Rabies Elimination Program in the Northern Communal Areas. *Trop. Med. Infect. Dis.* **2020**, *5*, 12. [\[CrossRef\]](#)
35. Coertse, J.; Geldenhuys, M.; le Roux, K.; Markotter, W. Lagos Bat Virus, an Under-Reported Rabies-Related Lyssavirus. *Viruses* **2021**, *13*, 576. [\[CrossRef\]](#) [\[PubMed\]](#)
36. Markotter, W.; Kuzmin, I.; Rupprecht, C.; Nel, L. Phylogeny of Lagos bat virus: Challenges for lyssavirus taxonomy. *Virus Res.* **2008**, *135*, 10–21. [\[CrossRef\]](#)
37. Coertse, J.; Markotter, W.; Le Roux, K.; Stewart, D.; Sabeta, C.T.; Nel, L.H. New isolations of the rabies-related Mokola virus from South Africa. *BMC Veter. Res.* **2016**, *13*, 37. [\[CrossRef\]](#)
38. Kuzmin, I.V.; Niezgod, M.; Franka, R.; Agwanda, B.; Markotter, W.; Beagley, J.C.; Urazova, O.Y.; Breiman, R.F.; Rupprecht, C.E. Possible emergence of West Caucasian bat virus in Africa. *Emerg. Infect. Dis.* **2008**, *14*, 1887. [\[CrossRef\]](#)
39. Quetglas, J.; González, F.; Paz, Ó.D. Estudian la extraña mortandad de miles de murciélagos en cueva. *Quercus* **2003**, *203*, 50.

40. Schatz, J.; Fooks, A.R.; McElhinney, L.; Horton, D.; Echevarría, J.E.; Vázquez-Morón, S.; Kooi, E.A.; Rasmussen, T.B.; Müller, T.; Freuling, C.M. Bat Rabies Surveillance in Europe. *Zoonoses Public Heal.* **2013**, *60*, 22–34. [[CrossRef](#)]
41. Troupin, C.; Picard-Meyer, E.; Dellicour, S.; Casademont, I.; Kergoat, L.; Lepelletier, A.; Dacheux, L.; Baele, G.; Monchâtre-Leroy, E.; Cliquet, F.; et al. Host Genetic Variation Does Not Determine Spatio-Temporal Patterns of European Bat 1 Lyssavirus. *Genome Biol. Evol.* **2017**, *9*, 3202–3213. [[CrossRef](#)] [[PubMed](#)]
42. Botvinkin, A.D.; Poleschuk, E.M.; Kuzmin, I.V.; Borisova, T.I.; Gazaryan, S.V.; Yager, P.; Rupprecht, C.E. Novel lyssaviruses isolated from bats in Russia. *Emerg. Infect. Dis.* **2003**, *9*, 1623. [[CrossRef](#)] [[PubMed](#)]
43. Picard-Meyer, E.; Beven, V.; Hirschaud, E.; Guillaume, C.; Larcher, G.; Robardet, E.; Servat, A.; Blanchard, Y.; Cliquet, F. Lleida Bat Lyssavirus isolation in *Miniopterus schreibersii* in France. *Zoonoses Public Health* **2019**, *66*, 254–258. [[CrossRef](#)] [[PubMed](#)]
44. Marston, D.; Ellis, R.J.; Wise, E.; Aréchiga-Ceballos, N.; Freuling, C.M.; Banyard, A.C.; McElhinney, L.M.; de Lamballerie, X.; Müller, T.; Fooks, A.R.; et al. Complete Genome Sequence of Lleida Bat Lyssavirus. *Genome Announc.* **2017**, *5*, e01427-16. [[CrossRef](#)] [[PubMed](#)]
45. Ceballos, N.A.; Moron, S.V.; Berciano, J.M.; Nicolas, O.; Lopez, C.A.; Juste, J.; Nevado, C.R.; Setién, Á.A.; Echevarría, J.E. Novel lyssavirus in bat, Spain. *Emerg. Infect. Dis.* **2013**, *19*, 793–795. [[CrossRef](#)]
46. Miller-Butterworth, C.M.; Murphy, W.J.; O'Brien, S.J.; Jacobs, D.; Springer, M.S.; Teeling, E.C. A Family Matter: Conclusive Resolution of the Taxonomic Position of the Long-Fingered Bats, *Miniopterus*. *Mol. Biol. Evol.* **2007**, *24*, 1553–1561. [[CrossRef](#)]
47. Miller-Butterworth, C.M.; Eick, G.; Jacobs, D.S.; Schoeman, M.C.; Harley, E.H. Genetic and phenotypic differences between South African long-fingered bats, with a global miniopterine phylogeny. *J. Mammal.* **2005**, *86*, 1121–1135. [[CrossRef](#)]
48. Goodman, S.M.; Ryan, K.E.; Maminirina, C.P.; Fahr, J.; Christidis, L.; Appleton, B. Specific Status of Populations on Madagascar Referred to *Miniopterus fraterculus* (Chiroptera: Vespertilionidae), with Description of a New Species. *J. Mammal.* **2007**, *88*, 1216–1229. [[CrossRef](#)]
49. Taylor, E.; Banyard, A.C.; Bourhy, H.; Cliquet, F.; Ertl, H.; Fehlnner-Gardiner, C.; Horton, D.L.; Mani, R.S.; Müller, T.; Rupprecht, C.E.; et al. Avoiding preventable deaths: The scourge of counterfeit rabies vaccines. *Vaccine* **2019**, *37*, 2285–2287. [[CrossRef](#)]
50. Bahloul, C.; Jacob, Y.; Tordo, N.; Perrin, P. DNA-based immunization for exploring the enlargement of immunological cross-reactivity against the lyssaviruses. *Vaccine* **1998**, *16*, 417–425. [[CrossRef](#)]
51. Jallet, C.; Jacob, Y.; Bahloul, C.; Drings, A.; Desmezières, E.; Tordo, N.; Perrin, P. Chimeric lyssavirus glycoproteins with increased immunological potential. *J. Virol.* **1999**, *73*, 225–233. [[CrossRef](#)] [[PubMed](#)]
52. Perrin, P.; Jacob, Y.; Desmézières, E.; Tordo, N. DNA-based immunisation against rabies and rabies-related viruses: Towards multivalent vaccines. *Dev. Biol.* **2000**, *104*, 151–157.
53. Fisher, C.R.; Lowe, D.E.; Smith, T.G.; Yang, Y.; Hutson, C.L.; Wirblich, C.; Cingolani, G.; Schnell, M.J. Lyssavirus Vaccine with a Chimeric Glycoprotein Protects across Phylogroups. *Cell Rep.* **2020**, *32*, 107920. [[CrossRef](#)] [[PubMed](#)]